EMERGING INFECTIOUS DISEASES®

CDC
CENTERS FOR DISEASE CONTROL AND PREVENTION

Antimicrobial Resistance

April 2018

Patricia Goslee, (b. 1960), *Water Prayer I*, 2005. Acrylic on canvas, 11 in × 17 in/28 cm × 43 cm. Digital image courtesy of the artist. Washington, DC, United State

EMERGING INFECTIOUS DISEASES®

Emerging Infectious Diseases is published monthly by the Centers for Disease Control and Prevention, 1600 Clifton Road, Mailstop D61, Atlanta, GA 30329-4027, USA. Telephone 404-639-1960, fax 404-639-1954, email eideditor@cdc.gov.

EMERGING INFECTIOUS DISEASES®

Antimicrobial Resistance

April 2018

On the Cover

Patricia Goslee, (b. 1960), Water Prayer I, 2005 (detail). Acrylic on canvas, 11 in × 17 in/28 cm × 43 cm. Digital image courtesy of the artist. Washington, DC, United States.

About the Cover p. 815

Synopses

Research

EMERGING INFECTIOUS DISEASES®
April 2018

Dispatches

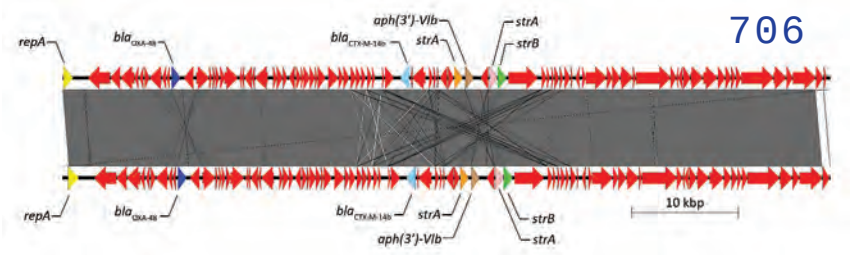

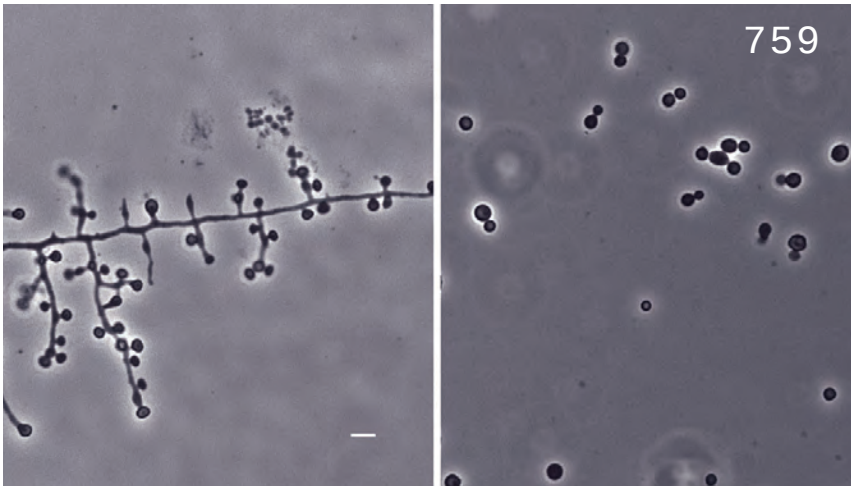

EMERGING INFECTIOUS DISEASES®
April 2018

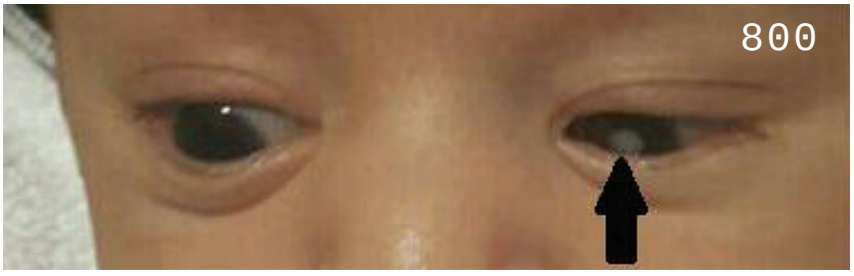

Research Letters

About the Cover

Etymologia

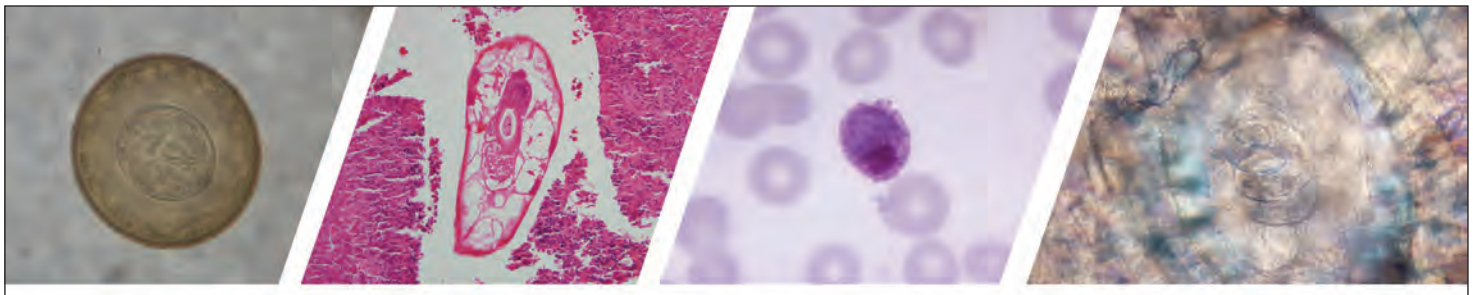

DPDx

Diagnostic Assistance and Training in Laboratory Identification of Parasites

A free service of CDC available to laboratorians, pathologists, and other health professionals in the United States and abroad

- Diagnosis from photographs of worms, histological sections, fecal, blood, and other specimen types
- Expert diagnostic review
- Formal diagnostic laboratory report
- Submission of samples via secure file share

Visit the DPDx website for information on laboratory diagnosis, geographic distribution, clinical features, parasite life cycles, and training via Monthly Case Studies of parasitic diseases.

www.cdc.gov/dpdx
dpdx@cdc.gov

U.S. Department of Health and Human Services
Centers for Disease Control and Prevention

CS272346-DE

Seroprevalence of Chikungunya Virus in 2 Urban Areas of Brazil 1 Year after Emergence

Juarez P. Dias, Maria da Conceição N. Costa, Gubio Soares Campos, Enny S. Paixão, Marcio S. Natividade, Florisneide R. Barreto, Martha Suely C. Itaparica, Cristina de Souza Borges Goes, Francisca L.S. Oliveira, Eloisa B. Santana, Neuza S.J. Silva, Carlos A.A. Brito, Laura C. Rodrigues, Silvia Inez Sardi, Ramon C. Saavedra, Maria Glória Teixeira

Chikungunya has had a substantial impact on public health because of the magnitude of its epidemics and its highly debilitating symptoms. We estimated the seroprevalence, proportion of symptomatic cases, and proportion of chronic form of disease after introduction of chikungunya virus (CHIKV) in 2 cities in Brazil. We conducted the population-based study through household interviews and serologic surveys during October–December 2015. In Feira de Santana, we conducted a serologic survey of 385 persons; 57.1% were CHIKV-positive. Among them, 32.7% reported symptoms, and 68.1% contracted chronic chikungunya disease. A similar survey in Riachão do Jacuípe included 446 persons; 45.7% were CHIKV-positive, 41.2% reported symptoms, and 75.0% contracted the chronic form. Our data confirm intense CHIKV transmission during the continuing epidemic. Chronic pain developed in a high proportion of patients. We recommend training health professionals in management of chronic pain, which will improve the quality of life of chikungunya-affected persons.

Chikungunya is an emerging mosquitoborne disease caused by an alphavirus (chikungunya virus; CHIKV) from the *Togaviridae* family (*1*). Reports of outbreaks of chikungunya were not frequent until the beginning of the 21st century; however, some serologic studies provided evidence that CHIKV had circulated in a sylvatic cycle in nonhuman primates (*2*). In 2004, an outbreak of chikungunya emerged in some Indian Ocean islands (Comoros, Seychelles, and Mauritius) (*2*) and later spread to Reunion Island; the 266,000 recorded cases represented an attack rate of 35% (*3*). In the following years, the disease circulated in Italy, France, and India (*3*), and in 2013 it was introduced in the Americas, causing an epidemic of nearly 2.6 million autochthonous cases in >40 countries from the southern United States to Argentina through December 2017 (*4*). Along with Zika and dengue viruses, chikungunya virus has become a substantial global public health threat, not only because of the high magnitude of the epidemics but also because it can produce highly debilitating clinical symptoms, including intense joint pain that can last for years (*2*).

Brazil confirmed autochthonous cases of chikungunya in 2014 simultaneously in 2 regions: Northern, in Oiapoque/Amazonas, caused by Asian genotype virus; and Northeast, in 2 cities (Feira de Santana and Riachão do Jacuípe-Bahia), caused by the East/Central/South African (ECSA) genotype (*5*,*6*). In 2015, there were 20,661 notified cases of this disease; 271,824 cases were notified in 2016 and 171,930 cases in 2017 through epidemiologic week 35. The disease has affected >50% (2,829/5,570) of Brazilian municipalities (*7*).

In the Americas, scientific investigation on CHIKV seroprevalence is scarce; to date, only 6 studies have been published. Three of the published studies involved blood donors; 1 in Puerto Rico, with seroprevalence of 23.5% (*8*); 1 in Guadeloupe, with 48.1% seroprevalence; and 1 in Martinique, with 41.9% seroprevalence (*9*). Another study used a convenience sample of a single laboratory of Saint Martin, whose seroprevalence was 16.9% (*10*), and the fifth used a sample from a small rural area population in Brazil, where seroprevalence was 20% (*11*). The only study in South America involving random sampling of urban population was in Nicaragua, where the seroprevalence was 32.8% (*12*). Thus, we consider it important to produce information on seroprevalence of CHIKV in urban areas of Brazil.

Author affiliations: Instituto de Saúde Coletiva, Rua Basílio da Gama, Salvador, Brazil (J.P. Dias, M.C.N. Costa, E.S. Paixão, M.S. Natividade, F.R. Barreto, M.S.C. Itaparica, M.G. Teixeira); Instituto de Ciências da Saúde, Av. Reitor Miguel Calmon, Salvador (G.S. Campos, S.I. Sardi); London School of Hygiene and Tropical Medicine, London, UK (E.S. Paixão, L.C. Rodrigues); Secretaria da Saúde de Salvador, Salvador (M.S.C. Itaparica); Faculdade de Tecnologia e Ciências, Av. Artêmia Pires Freitas, Sim, Brazil (C.S.B. Goes); Secretaria Municipal de Saúde de Feira de Santana, Feira de Santana, Brazil (F.L.S. Oliveira, E.B. Santana, N.S.J. Silva); Secretaria de Saúde do Estado da Bahia, Salvador (R.C. Saavedra); Universidade Federal de Pernambuco, Pernambuco, Brazil (C.A.A. Brito)

DOI: https://doi.org/10.3201/eid2404.171370

We estimated the seroprevalence of CHIKV 1 year after the introduction of the virus in the population of 2 urban areas in Brazil, Feira de Santana and Riachão do Jacuípe-Bahia, that are affected by the ECSA genotype. We further report the proportion of symptomatic cases of chikungunya and the proportion of patients that had the chronic form of disease.

Methods

Study Design and Participants

We conducted a cross-sectional population-based study through household interviews and serologic survey during November–December 2015, involving residents in delimited areas of 2 cities, Feira de Santana and Riachão do Jacuípe. These cities, which reported early epidemics of chikungunya in Brazil caused by ECSA genotype (*5*,*6*), are situated in Bahia state in northeastern Brazil (Figure 1), which has a hot, semiarid climate. In 2014, Feira de Santana had 612,000 inhabitants and a population density of 457.4 inhabitants/km^2; Riachão do Jacuípe had 35,322 inhabitants and a population density of 28.5 inhabitants/km^2 (*13*). These cities did not have *Aedes albopictus* mosquito infestations; the only vector present was *Ae. aegypti*. The mean of Premise Index (PI) of *Ae. aegypti* mosquitoes in 2014 was 1.1% in Feira de Santana and 2.0% in Riachão do Jacuípe, according to the records of the Vectors Control Program of the Health Department of Bahia State in Salvador, Bahia.

The study sampling frame was the general population of the 2 cities living in the epicenter area of the early chikungunya epidemics. To identify these epicenters, we georeferenced the cases of chikungunya notified to the Department of Health of the 2 municipalities, from epidemiologic week (EW) 32 of 2014 to EW 11 of 2015, using the geographic network of the cartographic base of each city. We then plotted the cases in the respective census tracts and estimated the kernel density (*14*) to delimit the census tracts that reported the highest number of cases (Figure 2).

Fieldworkers visited all households in the selected areas (areas with the highest density of cases, or hotspots). For the general population survey, we invited all household members who were ≥1 year of age to take part in the study and have a questionnaire answered if they had lived in the city for the last ≥6 months. We estimated the sample size for this survey as 296 persons in the delimited area of Feira de Santana and 295 in the delimited area in Riachão do Jacuípe, and estimated 30% seroprevalence, 95% confidence, and 80% power. The Research Ethics Committee of the Institute of Collective Health/Federal University of Bahia approved this study (no. 986.229 of 03/03/2015).

Procedures

For the general population survey, we conducted interviews using a semistructured questionnaire installed on tablets to register demographics, socioeconomics, household characteristics, and health status, especially self-reported chikungunya infection. We trained undergraduate students of health to visit all households in the area, explain the project objectives, and, when allowed, collect participants' signatures in the Free and Informed Consent Form (FICF) and carry out the interviews. For participants <18 years of age, we used the Term of Assent and a responsible adult signed the document.

After interviewing all residents in each house, we randomly selected 1 to participate in the serologic survey. This random sample was without replacement. Thereafter, a laboratory technician used a specific FICF and collected 5 mL of blood per venipuncture, in accordance with current biosafety standards, from consenting participants. Local laboratory staff separated the serum by centrifugation and conditioned it at –20°C. We transported the aliquots to the virology laboratory of the Federal University of Bahia/Institute of Health Sciences, where we processed these samples. We used ELISA (Euroimmun, Lübeck, Schleswig-Holstein, Germany) to identify specific antibodies against CHIKV IgM and IgG, according to the manufacturer's instructions (*15*). We considered any person with CHIKV IgM or IgG (or both) detected

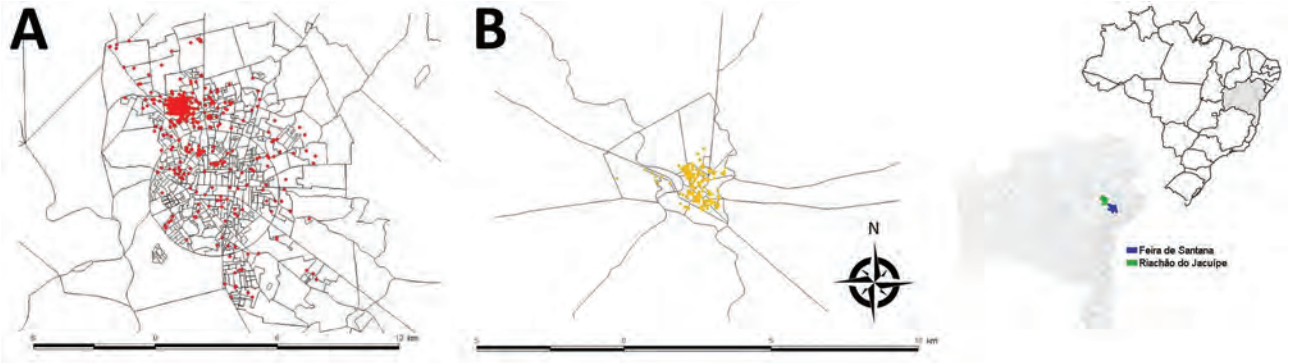

Figure 1. Notified cases of chikungunya georeferenced by household in Feira de Santana (A; n = 1,339), and Riachão do Jacuípe (B; n= 1,536), Bahia state, Brazil, during epidemiologic week 32 of 2014 through week 11 of 2015. Inset maps show locations of Feira de Santana and Riachão do Jacuípe in Bahia state and Bahia state in Brazil.

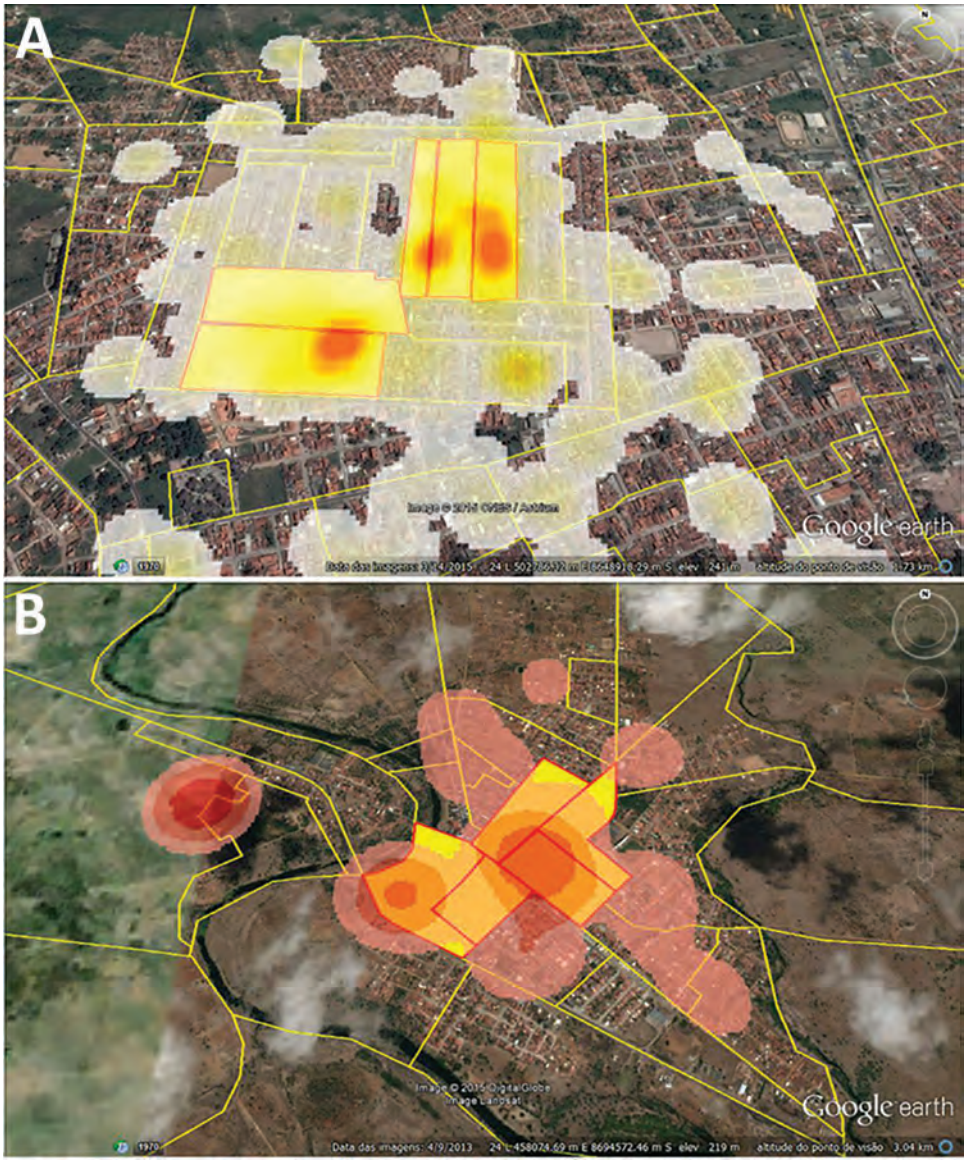

Figure 2. Density of notified cases of chikungunya by census tract in A) Feira de Santana and B) Riachão do Jacuípe, Bahia state, Brazil, during epidemiologic week 32 of 2014 through week 11 of 2015. Yellow shaded areas with red borders indicate the census tracts in which most cases were concentrated.

in the serum as CHIKV infected. The Euroimmun chikungunya IgM kit considers a ratio between the extinction value of the sample by the extinction value of the calibrator given within the kit. The lower detection limit of the CHIKV ELISA is ratio 0.05 IgM and 0.06 IgG. Samples with ratio <0.8 are considered negative, and those >1.1 are positive.

To calculate the proportion of symptomatic persons, we considered those who declared they have had chikungunya disease; those who reported fever and arthralgia as disease symptoms, at minimum, from August 2014 through the interview date; and those who had IgM- or IgG-positive tests. If the symptoms of joint pain, especially in extremities, had persisted for >3 months after the onset of the disease, we considered them in the chronic phase (*16*). We considered asymptomatic those who reported they had not had CHIKV infection but who had positive results for CHIKV IgM, IgG, or both.

Statistical Analysis

We analyzed the data using SPSS version 22 (https://www.ibm.com/analytics/data-science/predictive-analytics/spss-statistical-software). We reported the incidence of CHIKV infection (total and according to the variables of interest) as percentages with a 95% CI. We used the Pearson χ^2 test to assess statistically significant differences ($p<0.05$) for categorical variables.

Results

We georeferenced, by household, 1,339 cases of chikungunya in Feira de Santana and 1,536 in Riachão do Jacuípe (Figure 1) and identified the 5 census tracts with the highest density of cases of this disease during the epidemic in each city (Figure 2). The Municipal Department of Health of Feira de Santana registered 164 suspected cases of

chikungunya disease in the selected 5 census tracts in George Américo neighborhood, corresponding to incidence of 52.3 cases/1,000 inhabitants. In Riachão do Jacuípe, the Department of Health reported 697 suspected cases in Alto do Cemitério neighborhood, corresponding to incidence of 202.5 cases/1,000 inhabitants (Figure 3).

In the selected 5 census tracts of George Américo, there were 1,157 buildings (including uninhabited households and commercial spaces) and 3,135 inhabitants in a surface area of 0.283 km^2 (11,081.7 inhabitants/ km^2). During the survey, we visited 591 households and interviewed 1,858 persons. In the selected 5 census tracts of Alto do Cemitério, there were 1,122 buildings in total and 3,441 inhabitants in a surface area of 0.606 km^2 (1,454.9 inhabitants/km^2). In this area, we visited 659 households and interviewed 1,879 persons (Figure 3).

In George Américo, we invited 591 persons to be part of the serologic survey; 385 (65%) consented. We identified 220 (57.1%) persons, 80 male (36.4%) and 140 female (63.6%), who had CHIKV antibodies: 163 IgG, 25 IgM, and 32 both. In Alto do Cemitério, the consent rate was similar, 446/659 persons (67.7%). We identified 204 (45.7%) persons, 59 (28.9%) male and 145 (71%) female, who had CHIKV antibodies: 138 IgG, 38 IgM, and 28 both. We considered 9 participants in each city (18 total) as negative for CHIKV because their CHIKV ELISA ratio was 0.8–1.1 (Table; Figure 3). The difference in the seroprevalence rates of the 2 study areas was statistically significant (p = 0.001). The differences in distribution of seroprevalence by age group and sex between the study areas were not statistically significant.

Of the 220 persons with positive serologic test results in George Américo, 72 (32.7%) reported having been affected by chikungunya (Table). The rate of symptomatic CHIKV infections was significantly higher in women (54/140, 38.6%) than in men (18/80, 22.5%) (p = 0.015). For specific age groups, the difference was statistically significant (p<0.001); participants 40–59 years of age (32/69, 46.4%) and ≥60 years age (19/33, 57.6%) had the highest prevalence among those participants who reported symptoms. In Alto do Cemitério, the rate of symptomatic cases was 41.2% (84/204 participants) (Table). The prevalence of symptomatic cases in women (61/145, 42.1%) was also higher than in men (23/59, 39.0%), but the difference was not statistically significant (p = 0.755). For specific age groups, similar to George Américo, the difference was statistically significant (p<0.034); the 40–59-year (28/63, 44.4%) and ≥60-year (35/69, 50.7%) age groups had the highest prevalence among those participants who reported symptoms.

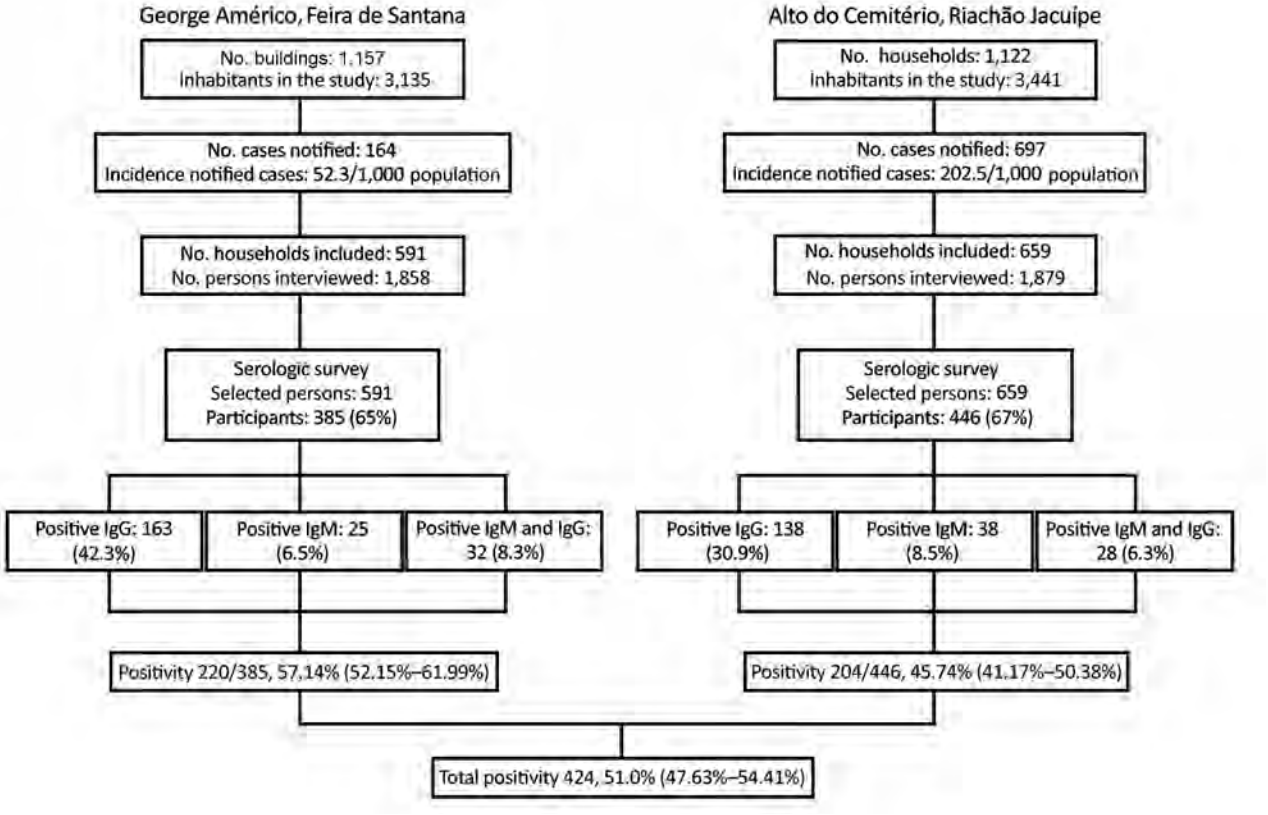

Figure 3. Flowchart of serologic survey of chikungunya in residents of George Américo, Feira de Santana, and Alto do Cemitério, Riachão de Jacuípe, in Bahia state, Brazil, 2015. Number ranges in paretheses indicate 95% CIs.

Table. Seroprevalence of CHIKV among survey participants reporting symptomatic, asymptomatic, and chronic infection, Bahia state, Brazil, 2015–2016*

Patient characteristics	George Américo, Feira de Santana			Alto do Cemitério, Riachão do Jacuípe		
	No. participants	No. positive	Prevalence, %	No. participants	No. positive	Prevalence, %
Age group, y†						
1–19	88	46	52.3	45	17	37.8
20–39	123	72	58.5	109	55	50.5
40–59	121	69	57.0	144	63	43.8
≥60	53	33	62.3	148	69	46.6
Total	385	220	57.1	446	204	45.7
Sex						
M	129	80	62.0	127	59	46.5
F	256	140	54.7	319	145	45.5
Total	385	220	57.1	446	204	45.7
Serologic results						
IgG	385	163	42.3	446	138	30.9
IgM	385	25	6.5	446	38	8.5
IgM and IgG	385	32	8.3	446	28	6.3
Total	385	220	57.1	446	204	45.7
Self-reported chikungunya infection						
Yes‡	220	72	32.7	204	84	41.2
No§	220	148	67.3	204	120	58.8
Total	220	220	100.0	204	204	100.0
Self-reported chronic form¶						
Yes	72	49	68.1	84	63	75.0
No	72	23	31.9	84	21	25.0
Total	72	72	100.0	84	84	100.0

*Selected area of each city. The difference in the seroprevalence rate of the 2 areas was statistically significant (p = 0.001). CHIKV, chikungunya virus.
†Children <1 y of age were not included in the study.
‡Attack rate of symptomatic CHIKV infection.
§Attack rate of asymptomatic CHIKV infection.
¶Percentage among positive symptomatic cases of CHIKV infection.

Among the cases of symptomatic CHIKV infection, the proportion of participants with symptoms that lasted >3 months (chronic chikungunya) was 49/72 (68.1%) in George Américo and 63/84 (75.0%) in Alto do Cemitério (Table). Considering the total number of study participants with positive serologic test results for CHIKV, the proportion of infected persons with long-term manifestations of the disease was 49/220 (22.2%) in George Américo and 63/204 (30.9%) in Alto do Cemitério. These proportions were 49/385 (12.7%) in George Américo and 63/446 (14.1%) in Alto do Cemitério when calculated for the whole study population in each area.

The rate of chronic forms of chikungunya disease among symptomatic participants with positive CHIKV serologic test results was higher in women than in men in both George Américo (40/54, 74.1% in women; 9/18, 50.0% in men) and Alto do Cemitério (54/61, 88.5% in women; 9/23, 39.1% in men). This difference was statistically different in Alto do Cemitério (p<0.001), whereas the p value was borderline in George Américo (p = 0.058). Regarding the age of the symptomatic persons with positive CHIKV serologic test results, we found no statistically significant difference in the rate of chronic form in both study areas.

Discussion

Our population-based seroprevalence study of CHIKV conducted in urban areas of 2 cities in Brazil where the ECSA (*5*,*6*) genotype recently emerged showed that >45% of the study population had CHIKV antibodies. The results of CHIKV serosurveys previously conducted in countries on different continents have varied from 10.2% to 75% seroprevalence (*17*,*18*), depending on the type of population studied and the time and intensity of the virus circulation. Our study revealed a higher incidence of this virus infection, more than double the values reported in studies previously published in the Americas (*8*–*11*), except for the serosurveys conducted in Guadeloupe and Martinique, which showed values similar to ours; however, only adults eligible for blood donation were included in the population of that study (*9*). Our study indicates that all age groups and genders were similarly exposed to CHIKV infection in both George Américo and Alto do Cemitério, as supported by the absence of significant difference in CHIKV seroprevalence across those groups.

We conducted our survey 1 year after the introduction of CHIKV in this area; the high incidence of infection suggests that the transmission of CHIKV was fast and intense. In addition, CHIKV circulation seems to have remained active, because CHIKV IgM was detected in >6% of the participants. However, some studies have shown that, unlike other arboviruses, CHIKV IgM may persist for prolonged periods: 12–13 months (*19*) or up to 3 years (*20*) postinfection. Moreover, CHIKV RNA was found in perivascular synovial macrophages in 1 patient 18 months after infection, suggesting that the virus may persist in organs or sites of immune privilege (*21*). Thus, late detection of

CHIKV IgM may represent prolonged viral circulation or the persistence of these antibodies in persons infected several months ago.

We cannot extrapolate our results for the entire population living in these 2 cities because the surveys took place in areas with the highest density of chikungunya cases during the first months of the epidemic, possibly constituting the diffusion poles of CHIKV. However, over time, other areas were becoming secondary sources of transmission, which resulted in the second epidemic wave, as other researchers have observed in Feira de Santana (*22*). It is possible that the mean seroprevalence of CHIKV in the populations of Feira de Santana and Riachão do Jacuípe has reached levels closer to those we found in the areas where most chikungunya cases were reported at the beginning of the epidemic. This same pattern of spread was observed after the emergence of dengue in urban spaces (*23*), evidencing once more the high vectorial capacity of the *Ae. aegypti* mosquitoes responsible for these epidemics (*5*).

The difference observed in the levels of seroprevalence between the 2 study areas may be due to different levels of vector infestation, human population density, or both. Data from the Brazilian Institute of Geography and Statistics show that the population density in the hotspots of Feira de Santana was 7 times higher than in the study area of Riachão do Jacuípe (*13*). However, the Premise Index recorded for *Ae. aegypti* mosquitoes in 2015 was lower in Feira de Santana than in Riachão do Jacuípe.

The wide range in CHIKV seroprevalence worldwide could be explained by many reasons, such as climatic factors, vector control measures applied before and during outbreaks that affect levels of *Ae. aegypti* infestation, the previous level of immunity of the population, and the strain and genotype of CHIKV. The CHIKV seroprevalence data in our study reflect levels that may be found in other big cities, because it was a population-based survey conducted in urban areas. The 3 surveys in the Caribbean (in Martinique, Guadeloupe, and Puerto Rico) used a convenience sample or were conducted in a rural community; low population density is not the most favorable environment for the proliferation of *Ae. aegypti* mosquitoes, which are adapted mostly to urban areas (*24*).

The proportion of symptomatic persons among those CHIKV positive in our study was similar to the proportion reported by Sissoko et al. (*25*) in Mayotte (37.2%). Our study revealed that the rate of symptomatic CHIKV infections was higher in the 40–59- and ≥60-year age groups, similar to the results of other studies. However, despite the higher rate of symptomatic CHIKV infections in women than in men, this difference was significant only in George Américo. It is possible this difference reflects the levels of prior prevalence of rheumatologic diseases in women in the 2 study populations.

The prevalence of long-term manifestations of CHIKV varies widely, ranging from 3% among pediatric patients <15 years of age (*26*) to 83% in a cohort of rheumatology patients (*27*). A recently published metaanalysis estimated that ≈50% of chikungunya patients have long-lasting related symptoms (*28*). In our study, the proportion of participants who had long-term manifestations of the disease among persons with positive serologic test results and who reported symptoms of chikungunya reached 68.1% in George Américo and 75.0% in Alto do Cemitério. Our results are similar to those obtained in a cohort of rheumatology patients in Reunion Island (France) (*27*), in which, 1 and 2 years after disease onset, ≈80% of patients had rheumatic manifestations associated with chikungunya. Our results also indicate that, 1 year after the beginning of the CHIKV outbreak, >12% of persons in our study populations in both cities suffered from joint pain that precluded the performance of many habitual activities, affected their quality of life, required medical care, and increased absenteeism at work. Some studies have shown that the chronic phase of chikungunya can last for >2 years (*27–30*). Thus, because of extremely debilitating symptoms during the acute phase of chikungunya disease, elevated attack rates, and the high proportion of patients who develop long-lasting symptoms, CHIKV outbreaks can have a substantial impact on the overall health of the population.

Our serologic survey has some limitations. First, we conducted it in the epicenters of the epidemic, so the results could be overestimated and cannot be extrapolated to the whole city. The fact that symptoms were self-reported is a potential source of bias, because participants may not accurately remember the symptoms of a disease that occurred 1 year earlier. In addition, we did not collect indicators of vector infestation in the 2 study areas. Despite these limitations, our investigation is a relevant study to understand the transmission of CHIKV of the ECSA genotype after its introduction into an urban population, in which the seroprevalence corresponds to the rate of infection attack.

This study revealed a worrying scenario that emerged after the introduction of CHIKV in Feira de Santana and Riachão do Jacuípe. The virus has spread almost completely through the cities (*22*,*31*,*32*), and at least one third of the infected persons had symptoms. In addition, there was a high frequency of the chronic form of chikungunya. These results reveal how much the emergence of CHIKV in these 2 cities has altered the health status of a relevant portion of the population, especially women. It is possible that this is the scenario in many urban centers in Brazil that have experienced epidemics of CHIKV infection. Studies have shown that several factors are strongly associated with risk of chronic chikungunya, including female sex, age >45 years, acute disease severity, and presence of anterior articular disease (*19*,*27*,*33*,*34*). Despite the evidence, there is still no

physiopathogenic explanation. However, because rheumatic diseases are more prevalent in women (*35*), it is plausible that CHIKV is a potential trigger for the onset or cornification of arthralgia in a group more susceptible to rheumatic diseases. Intense and disabling articular pain is a common symptom of CHIKV infection; this pain does not always respond to routine medical drugs and so requires specific and often long-term pharmacologic treatment. In chikungunya epidemic situations, the problems for patients do not end after the acute phase and decline of the transmission; a large proportion of those affected require continuous treatment and adequate pain management with drugs that can cause serious side effects, such as corticosteroids, opiates, and chemotherapeutics (*36*,*37*), to minimize suffering. These sequelae also influence individual and collective productive capacity and affect the public health sector and the economy. It is urgent to expand national and international research for developing technologies and strategies for increasing the effectiveness of vector control programs, for synthesizing antiviral drugs to mitigate the symptoms and chronic evolution of the disease, and, especially, for producing vaccines that can be used in populations vulnerable to CHIKV.

Secretaria Vigilância em Saúde/Fundo Nacional de Saúde/MoH Brazil provided financial support.

About the Author

Dr. Dias is a medical doctor who also holds a PhD in public health. He is currently an assistant professor at the School of Medicine and Public Health in Bahia and senior physician at Hospital Prof. Edgard Santos. His primary interest is vectorborne diseases.

References

1. Strauss JH, Strauss EG. The alphaviruses: gene expression, replication, and evolution. Microbiol Rev. 1994;58:491–562.
2. Burt FJ, Rolph MS, Rulli NE, Mahalingam S, Heise MT. Chikungunya: a re-emerging virus. Lancet. 2012;379:662–71. http://dx.doi.org/10.1016/S0140-6736(11)60281-X
3. Gérardin P, Guernier V, Perrau J, Fianu A, Le Roux K, Grivard P, et al. Estimating chikungunya prevalence in La Réunion Island outbreak by serosurveys: two methods for two critical times of the epidemic. BMC Infect Dis. 2008;8:99. http://dx.doi.org/10.1186/1471-2334-8-99
4. Pan American Health Organization. New cases of chikungunya in the Americas 2013–2017, per year and country [cited 2018 Feb 15]. http://ais.paho.org/phip/viz/ed_chikungunya_amro.asp
5. Teixeira MG, Andrade AM, Costa MC, Castro JN, Oliveira FL, Goes CS, et al. East/Central/South African genotype chikungunya virus, Brazil, 2014. Emerg Infect Dis. 2015;21:906–7. http://dx.doi.org/10.3201/eid2105.141727
6. Nunes MRT, Faria NR, de Vasconcelos JM, Golding N, Kraemer MU, de Oliveira LF, et al. Emergence and potential for spread of chikungunya virus in Brazil. BMC Med. 2015;13:102. http://dx.doi.org/10.1186/s12916-015-0348-x
7. Brasil. Ministério da Saúde. Secretaria de Vigilância da Saúde. Bol Epidemiol. 2017;48(3) [cited 2018 Feb 16]. http://portalarquivos.saude.gov.br/images/pdf/2017/abril/06/2017-002-Monitoramento-dos-casos-de-dengue–febre-de-chikungunya-e-febre-pelo-v–rus-Zika-ate-a-Semana-Epidemiologica-52–2016.pdf
8. Simmons G, Brès V, Lu K, Liss NM, Brambilla DJ, Ryff KR, et al. High incidence of chikungunya virus and frequency of viremic blood donations during epidemic, Puerto Rico, USA, 2014. Emerg Infect Dis. 2016;22:1221–8. http://dx.doi.org/10.3201/eid2207.160116
9. Gallian P, Leparc-Goffart I, Richard P, Maire F, Flusin O, Djoudi R, et al. Epidemiology of chikungunya virus outbreaks in Guadeloupe and Martinique, 2014: an observational study in volunteer blood donors. PLoS Negl Trop Dis. 2017;11:e0005254. http://dx.doi.org/10.1371/journal.pntd.0005254
10. Gay N, Rousset D, Huc P, Matheus S, Ledrans M, Rosine J, et al. Seroprevalence of Asian lineage chikungunya virus infection on Saint Martin Island, 7 months after the 2013 emergence. Am J Trop Med Hyg. 2016;94:393–6. http://dx.doi.org/10.4269/ajtmh.15-0308
11. Cunha RV, Trinta KS, Montalbano CA, Sucupira MV, de Lima MM, Marques E, et al. Seroprevalence of chikungunya virus in a rural community in Brazil. Version 2. PLoS Negl Trop Dis. 2017;11:e0005319. http://dx.doi.org/10.1371/journal.pntd.0005319
12. Ministerio del Poder Ciudadano para la Salud de Nicaragua. Seroprevalencia y tasa de ataque clínica por chikungunya en Nicaragua, 2014–2015 [Chikungunya seroprevalence and clinical case rate in Nicaragua, 2014–2015]. Rev Panam Salud Publica. 2017;41:e59.
13. Instituto Brasileiro de Geografia Estatística/IBGE. Estimativa populacional 2014 [cited 2018 Feb 12]. https://ww2.ibge.gov.br/home/estatistica/populacao/estimativa2014/estimativa_dou.shtm
14. Gatrell AC, Bailey TC. Interactive spatial data analysis in medical geography. Soc Sci Med. 1996;42:843–55. http://dx.doi.org/10.1016/0277-9536(95)00183-2
15. Prat CM, Flusin O, Panella A, Tenebray B, Lanciotti R, Leparc-Goffart I. Evaluation of commercially available serologic diagnostic tests for chikungunya virus. Emerg Infect Dis. 2014;20:2129–32. http://dx.doi.org/10.3201/eid2012.141269
16. Pan American Health Organization and Centers for Disease Control and Prevention. Preparación y respuesta ante la eventual introducción del virus chikungunya en las Américas. Washington: Organización Panamericana de la Salud; 2011.
17. Moro ML, Gagliotti C, Silvi G, Angelini R, Sambri V, Rezza G, et al.; Chikungunya Study Group. Chikungunya virus in north-eastern Italy: a seroprevalence survey. Am J Trop Med Hyg. 2010;82:508–11. http://dx.doi.org/10.4269/ajtmh.2010.09-0322
18. Sergon K, Njuguna C, Kalani R, Ofula V, Onyango C, Konongoi LS, et al. Seroprevalence of chikungunya virus (CHIKV) infection on Lamu Island, Kenya, October 2004. Am J Trop Med Hyg. 2008;78:333–7.
19. Moro ML, Grilli E, Corvetta A, Silvi G, Angelini R, Mascella F, et al.; Study Group "Infezioni da Chikungunya in Emilia-Romagna". Long-term chikungunya infection clinical manifestations after an outbreak in Italy: a prognostic cohort study. J Infect. 2012;65:165–72. http://dx.doi.org/10.1016/j.jinf.2012.04.005
20. Chaaithanya IK, Muruganandam N, Raghuraj U, Sugunan AP, Rajesh R, Anwesh M, et al. Chronic inflammatory arthritis with persisting bony erosions in patients following chikungunya infection. Indian J Med Res. 2014;140:142–5.
21. Hoarau J-J, Bandjee M-CJ, Trotot PK, Das T, Li-Pat-Yuen G, Dassa B, et al. Persistent chronic inflammation and infection by chikungunya arthritogenic alphavirus in spite of a robust host immune response. J Immunol. 2010;184:5914–592. http://dx.doi.org/10.4049/jimmunol.0900255
22. Rodrigues N F, Lourenço J, Cerqueira E M, Lima M M, Pybus O, Junior Alcantara C L. Epidemiology of chikungunya virus in Bahia, Brazil, 2014–2015. PLoS Curr. 2016; 8:1–7.
23. Barreto FR, Teixeira MG, Costa MC, Carvalho MS, Barreto ML. Spread pattern of the first dengue epidemic in the city of Salvador,

Brazil. BMC Public Health. 2008;8:51. http://dx.doi.org/ 10.1186/ 1471-2458-8-51
24. Gubler DJ. Dengue and dengue hemorrhagic fever: its history and resurgence as a global public health problem. In: Gubler DJ, Kuno G, editors. Dengue and dengue hemorrhagic fever. London; CAB International; 1997. p. 1–22.
25. Sissoko D, Moendandze A, Malvy D, Giry C, Ezzedine K, Solet JL, et al. Seroprevalence and risk factors of chikungunya virus infection in Mayotte, Indian Ocean, 2005–2006: a population-based survey. PLoS One. 2008;3:e3066. http://dx.doi.org/10.1371/journal.pone.0003066
26. Kumar A, Best C, Benskin G. Epidemiology, clinical and laboratory features and course of chikungunya among a cohort of children during the first Caribbean epidemic. J Trop Pediatr. 2017 Feb:63:43-49;63:43–9. http://dx.doi.org/10.1093/tropej/fmw051
27. Bouquillard E, Fianu A, Bangil M, Charlette N, Ribéra A, Michault A, et al. Rheumatic manifestations associated with chikungunya virus infection: a study of 307 patients with 32-month follow-up (RHUMATOCHIK study). Joint Bone Spine. 2017 [cited 2018 Feb 12]. https://doi.org/10.1016/j.jbspin.2017.01.014
28. Rodríguez-Morales AJ, Cardona-Ospina JA, Fernanda Urbano-Garzón S, Sebastian Hurtado-Zapata J. Prevalence of post-chikungunya infection chronic inflammatory arthritis: a systematic review and meta-analysis. Arthritis Care Res (Hoboken). 2016;68:1849–58. http://dx.doi.org/10.1002/acr.22900
29. Waymouth HE, Zoutman DE, Towheed TE. Chikungunya-related arthritis: case report and review of the literature. Semin Arthritis Rheum. 2013;43:273–8. http://dx.doi.org/10.1016/ j.semarthrit.2013.03.003
30. Marimoutou C, Vivier E, Oliver M, Boutin J-P, Simon F. Morbidity and impaired quality of life 30 months after chikungunya infection: comparative cohort of infected and uninfected French military policemen in Reunion Island. Medicine (Baltimore). 2012;91:212–9. http://dx.doi.org/10.1097/MD.0b013e318260b604
31. Feira de Santana. Secretaria Municipal de Saúde. Epidemiological situation of cases of chikungunya, dengue, Zika virus and micro-hydrocephalus [in Portuguese]. Bol Vig Epidemiol. 2017;4:1–2 [cited 2018 Feb 16]. http://www.feiradesantana.ba.gov.br/sms/arq/ Boletim_Epidemiologico.pdf
32. do Jacuípe R. Secretaria Municipal de Saúde. Informe Epidemiológico da febre chikungunya, dengue e DEI/Zika. Bol Vig Epidemiol. 2017;4:1–2.
33. Gérardin P, Fianu A, Michault A, Mussard C, Boussaïd K, Rollot O, et al. Predictors of chikungunya rheumatism: a prognostic survey ancillary to the TELECHIK cohort study. Arthritis Res Ther. 2013;15:R9. http://dx.doi.org/10.1186/ar4137
34. Essackjee K, Goorah S, Ramchurn SK, Cheeneebash J, Walker-Bone K. Prevalence of and risk factors for chronic arthralgia and rheumatoid-like polyarthritis more than 2 years after infection with chikungunya virus. Postgrad Med J. 2013;89:440–7. http://dx.doi.org/10.1136/postgradmedj-2012-131477
35. Hua C, Combe B. Chikungunya virus–associated disease. Curr Rheumatol Rep. 2017;19:69. http://dx.doi.org/10.1007/ s11926-017-0694-0
36. Javelle E, Ribera A, Degasne I, Gaüzère B-A, Marimoutou C, Simon F. Specific management of post-chikungunya rheumatic disorders: a retrospective study of 159 cases in Réunion Island from 2006–2012. PLoS Negl Trop Dis. 2015;9(3):e0003603. http://dx.doi.org/10.1371/journal.pntd.0003603
37. Brito CAA, Sohsten AK, Leitão CC, Brito RC, Valadares LD, Fonte CA, et al. Pharmacologic management of pain in patients with chikungunya: a guideline. Rev Soc Bras Med Trop. 2016;49:668–79. http://dx.doi.org/10.1590/0037-8682-0279-2016

Address for correspondence: Maria Glória Teixeira, Instituto de Saúde Coletiva, Universidade Federal da Bahia, Rua padre feijo, 29 Canela Salvador-Bahia 40.110-170, Brazil; email: magloria@ufba.br

Two Infants with Presumed Congenital Zika Syndrome, Brownsville, Texas, USA, 2016–2017

Ashley Howard,[1] John Visintine,[1] Jaime Fergie,[1,2] Miguel Deleon[1]

Since 2007, Zika virus has spread through the Pacific Islands and the Americas. Beginning in 2016, women in Brownsville, Texas, USA, were identified as possibly being exposed to Zika virus during pregnancy. We identified 18 pregnant women during 2016–2017 who had supportive serologic or molecular test results indicating Zika virus or flavivirus infection. Two infants were evaluated for congenital Zika syndrome after identification of prenatal microcephaly. Despite standard of care testing of mothers and neonates, comparative results were unreliable for mothers and infants, which highlights the need for clinical and epidemiologic evidence for an accurate diagnosis. A high index of suspicion for congenital Zika syndrome for at-risk populations is useful because of current limitations of testing.

Zika virus is an arbovirus and flavivirus transmitted by *Aedes aegypti* and *Ae. albopictus* mosquitoes, vectors that also transmit other arboviruses, such as dengue virus and chikungunya virus. Zika virus was discovered in the Zika Forest of Uganda in 1947 in rhesus and macaque monkey populations (http://www.who.int/emergencies/zika-virus/timeline/en/). Until 2007, only 14 cases of human infection were reported in Asia and Africa (*1*). However, outbreaks of infection with Zika virus occurred on Yap Island, Micronesia, in 2007 and in French Polynesia in 2013, affecting ≈31,000 persons (*2*). Zika has spread rapidly in the Americas since 2015 and has been associated with hundreds of confirmed microcephaly cases in Brazil, Colombia, and Puerto Rico (*2*–*7*). In April 2016, the Centers for Disease Control and Prevention (CDC) confirmed evidence that supported the causal relationship between Zika virus infection prenatally and microcephaly, in addition to other brain abnormalities, and described what has become known as congenital Zika syndrome (*2*,*8*–*11*).

In the United States since June 2017, there have been 5,335 travel-associated cases and 227 locally transmitted cases of infection with Zika virus in southern Florida and Brownsville, Texas (*4*). A total of 2,364 pregnant women (972 completed pregnancies) with laboratory evidence of Zika virus infection in the United States have been reported to CDC; the Zika-related birth defect risk among these women has been estimated to be 1 in 10 women (*12*,*13*). In November 2016, local transmission was confirmed by health authorities in Brownsville, and screening for Zika virus in asymptomatic pregnant patients and testing for Zika virus in symptomatic patients began (*14*,*15*). This screening was quickly followed in December 2016 by identification of pregnant women with supportive laboratory evidence of Zika virus infection in the Brownsville area.

Cases

Eighteen cases of possible Zika virus infection in pregnant women were identified by screening and testing of symptomatic patients living in Brownsville during December 2016–May 2017. Twelve case-patients had laboratory evidence of Zika virus infection: positive PCR results for serum (*8*), serum and urine (*3*), or placenta (*1*). One case-patient had plaque reduction neutralization test (PRNT) results consistent with recent Zika virus infection, and 5 case-patients had PRNT results consistent with recent flavivirus infection. Fifteen women had delivered their babies as of July 14, 2017; the remaining women had estimated dates of delivery through early 2018. Two pregnant women in this cohort had findings consistent with congenital Zika syndrome. Neonatal and infant follow-up is ongoing for women who delivered up to this point. We report the prenatal and neonatal outcomes for 2 infants who had congenital Zika syndrome.

Case-Patient 1

Case-patient 1 was born to a 23-year-old woman (G1P1) who spent the first 4 months of her pregnancy in Matamoros, Mexico. She received prenatal Zika testing while residing there, and results were negative. She moved to Brownsville, where she received prenatal care at 28 weeks' gestation. She was screened for Zika virus by serum IgM

Author affiliation: Driscoll Children's Hospital, Corpus Christi, Texas, USA

DOI: https://doi.org/10.3201/eid2404.171545

[1]All authors contributed equally to this article.

[2]Current affiliation: Texas A&M University College of Medicine, Bryan, Texas, USA.

testing; results were negative. She was referred for maternal fetal medicine at 36 weeks' gestation because of suspected microcephaly. The fetus was found to have microcephaly: head circumference (HC) 251 mm, which was 5 SD below the mean value. The mother denied having any symptoms of Zika virus infection (rash, fever, malaise, arthralgia, or conjunctivitis). At 37 weeks' gestation, transvaginal fetal neuroimaging was performed; results showed calcifications in the cortical white matter–gray matter junction, but no calcifications were observed in the thalami (Figure 1, panel C). On the basis of ultrasonographic findings, a maternal repeat Zika virus IgM test was performed and showed a positive result at 37 weeks' gestation. PRNT results were consistent with recent flavivirus infection (Zika and dengue PRNT titers >1,280) (*16*). A TORCH (toxoplasmosis, rubella cytomegalovirus, herpes simplex virus, and HIV) panel did not show evidence of recent infections, and results of a cell-free fetal DNA screening were negative.

An elective primary cesarean delivery was performed at 39 weeks' gestation. APGAR scores for the baby were 9 at 1 min and 9 at 5 min. At initial examination, the neonate had a vesicular generalized rash, overriding sutures, and microcephaly. The initial HC of the infant was 29 cm, which was 2.63 SD below the mean value for term male newborns. Birthweight was 2.62 kg (4.76 percentile), and birth length was 45 cm (3.2 percentile). On further examination, mild craniofacial disproportion with narrow and laterally depressed frontal bone and mild retrognathia was seen. No limb contractures were observed (Figure 1, panel A).

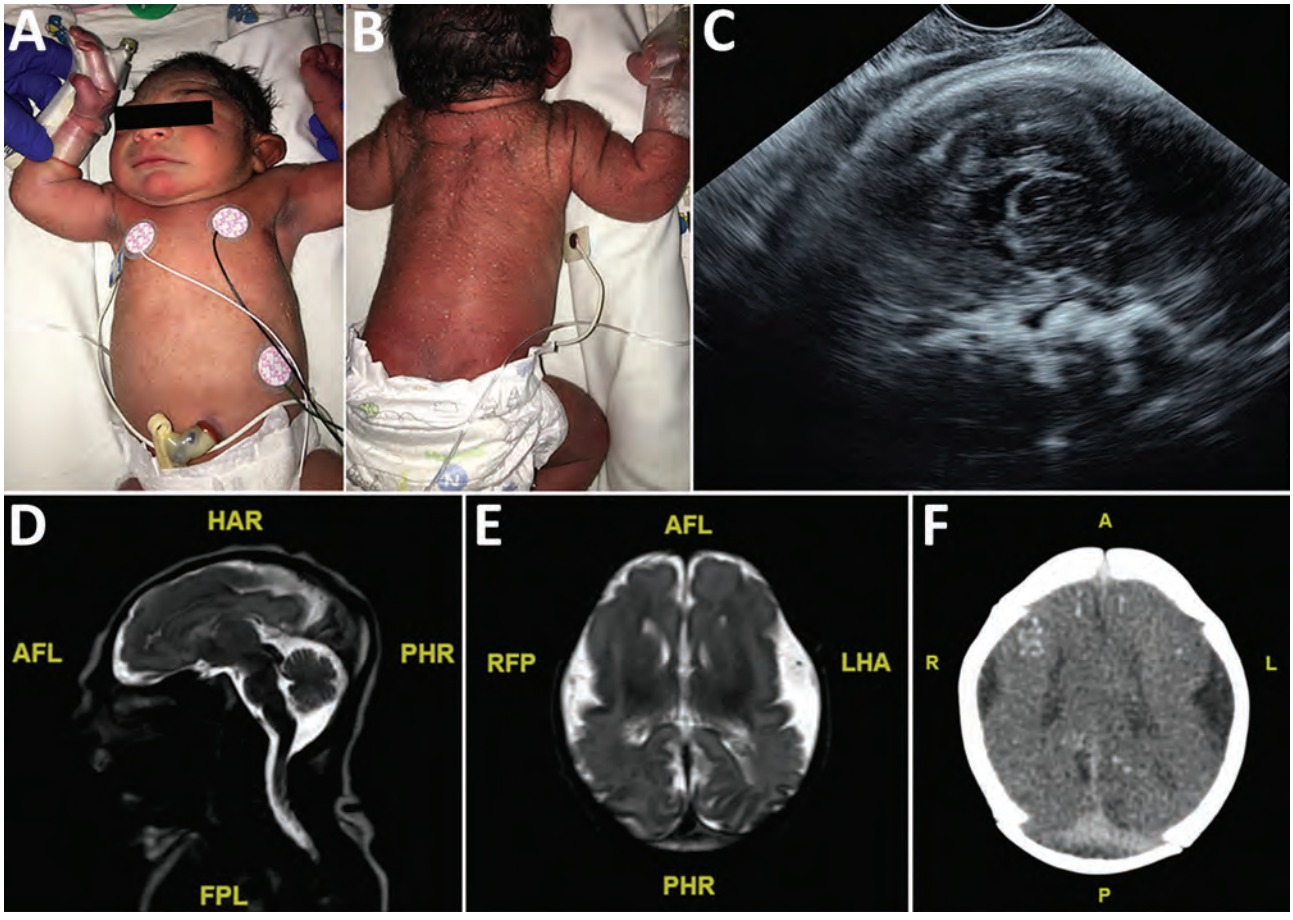

Figure 1. Term male infant (case-patient 1) with presumed congenital Zika syndrome, Brownsville, Texas, USA, 2016–2017. A) Microcephaly on the day of birth. Head circumference was 29 cm, which is 2.63 SDs below the mean value for term male newborns. Craniofacial abnormalities present are mild narrow and laterally depressed frontal bone and mild retrognathia. B) Generalized pustular melanosis rash. C) Prenatal transvaginal ultrasonographic (midsagittal plane) image at 37.2 weeks' gestation, showing calcifications at the gray matter–white matter junction. Head circumference was 251 mm. D) Sagittal T2 magnetic resonance image on day of life 1, showing severe microcephaly, frontal lobe polymicrogyria, and hypoplastic corpus callosum. E) Axial T2 magnetic resonance image on day of life 1, showing severely hypoplastic cerebral hemispheres and corpus callosum. Symmetric frontal lobe polymicrogyria and simplified gyral pattern in the occipital and temporal lobes are present. F) Axial computed tomography image on day of life 3, showing small bilateral brain hemispheres and hypogyration of the cerebral cortex. Areas of punctate calcification located at the subcortical and gray matter–white matter junctions of the frontal, parietal, and occipital lobes are present. A, anterior; AFL, anterior left; FPL, posterior left; HAR, anterior right; L, left; LHA, left anterior; P, posterior; PHR, posterior right; R, right; RFP, right posterior.

The newborn was transferred to the neonatal intensive care unit (NICU) at Driscoll Children's Hospital (Corpus Christi, TX, USA) on day 1 of life. Because of a generalized vesicular rash, concern for herpes simplex virus infection prompted treatment with acyclovir for the first 2 days of life. The rash was diagnosed as neonatal pustular melanosis; it faded by day 1 of life and disappeared by day 2 of life (Figure 1, panels A, B). Zika virus testing was performed on day 1 of life. Zika virus PCRs were performed for serum, urine, and cerebrospinal fluid (CSF); all results were negative. Zika virus IgM testing was ordered for serum and CSF, but the test for CSF was not performed by the state laboratory because of a negative PCR result for CSF. Serum was positive for Zika virus IgM, which is consistent with probable congenital Zika virus infection. Results of placental testing by reverse transcription PCR for the Zika virus nonstructural protein 5 gene were positive. Test results for dengue and chikungunya viruses were negative. Additional TORCH testing was performed, and results were negative for herpes simplex virus, cytomegalovirus, syphilis, HIV, *Toxoplasma* spp., and parvovirus.

The neonate passed the initial newborn hearing screen and had a pediatric ophthalmologic examination on day 1 of life, during which a small left subconjunctival hemorrhage was identified (*17*,*18*). Initial head ultrasonography on day 1 of life showed parietal calcifications and pachygyria. Follow-up magnetic resonance imaging showed frontal lobe polymicrogyria, bilateral dystrophic calcifications, and severe microcephaly (Figure 1, panels D, E). Computerized tomography was performed on day 3 of life for better characterization of calcifications and showed bilateral small brain hemispheres with hypogyration of the cerebral cortex. Areas of punctate calcification were observed at the subcortical and gray matter–white matter junctions of the frontal, parietal, and occipital lobes (Figure 1, panel F). A prominent occipital bone was observed with overlapping of the region of the lambdoid suture and prominent bony ridging at the region of the coronal sutures. Partial fusion of the inferior aspect of coronal sutures and asymmetric closure of the temporal sutures were also observed. There was no ventriculomegaly.

The infant was in the NICU for 9 days. During that time, the infant had poor feeding and required an orogastric tube to assist with feeds until day 7 of life. The CDC recommended electroencephalogram (EEG) testing because of new information concerning development of seizures in 30%–50% of infants with congenital Zika syndrome; the EEG result was unremarkable (*19*,*20*). Microarray and microcephaly gene panel were tested; all showed negative results. A screening echocardiogram showed results consistent with reference transitional neonatal cardiac changes. Results of thyroid function testing, complete blood count, and a comprehensive metabolic panel (CMP) were all within reference ranges.

The infant was discharged on day 9 of life. At discharge, he had an HC of 30 cm, which was 3.16 SD below the mean value for term male newborns with microcephaly.

Case-Patient 2

Case-patient 2 was born to an 18-year-old woman (G1P1) who lived in Brownsville. She reported weekly travel to Matamoros, Mexico, during the early stages of her pregnancy. She denied any viral symptoms of rash, fever, malaise, arthralgia, or conjunctivitis. She was screened by her obstetrician for Zika virus at 23 weeks' gestation by a PCR for serum; results were positive. Results were negative for a Zika virus PCR for urine and serum Zika virus IgM. At 28 weeks' gestation, fetal ultrasonography was performed for growth and anatomy evaluation. The fetus had microcephaly and was referred for maternal fetal medicine evaluation. The HC of the fetus was 203 mm at 29 weeks' gestation, which was 4–5 SD below the mean value. Coarse calcifications were observed in the basal ganglia and thalami by transabdominal and transvaginal fetal neuroimaging (Figure 2, panels C, D). The TORCH panel did not show evidence of recent infections.

A planned primary cesarean delivery was performed at 39 weeks' gestation. APGAR scores were 9 at 1 min and 9 at 5 min. At initial examination, the neonate had a prominent sagittal ridge, overriding sutures, and severe microcephaly (Figure 2, panel A). Initial head circumference was 26.5 cm, which was 6.23 SD below the mean value for term female newborns. Birthweight was 2.39 kg (2.21 percentile), and birth length was 41.5 cm (<0.01 percentile). Further examination showed excess scalp skin (Figure 2, panel B) and craniofacial disproportion with narrow and laterally depressed frontal bone (Figure 2, panel A). Upper limb contractures were also observed (Figure 2, panel A).

The patient was transferred to the NICU at Driscoll Children's Hospital on day 1 of life, and Zika virus testing was performed the same day. Results of Zika virus PCRs were negative for serum, urine, and CSF. IgM serum was negative for Zika virus. Testing for Zika virus IgM was ordered for serum and CSF, but the test for CSF was not performed by the state laboratory because of a negative PCR result for CSF. Test results were negative for dengue virus and chikungunya virus. Additional TORCH testing was performed, and results were negative for CMV, syphilis, HIV, *Toxoplasma* spp., and parvovirus. The infant passed the initial newborn hearing screen and had a pediatric ophthalmology examination performed on day 1 of life; no eye anomalies were identified (*17*,*18*).

Initial ultrasonography of the head on day 1 of life could not be completed because the anterior fontanelle was too small. Magnetic resonance imaging showed

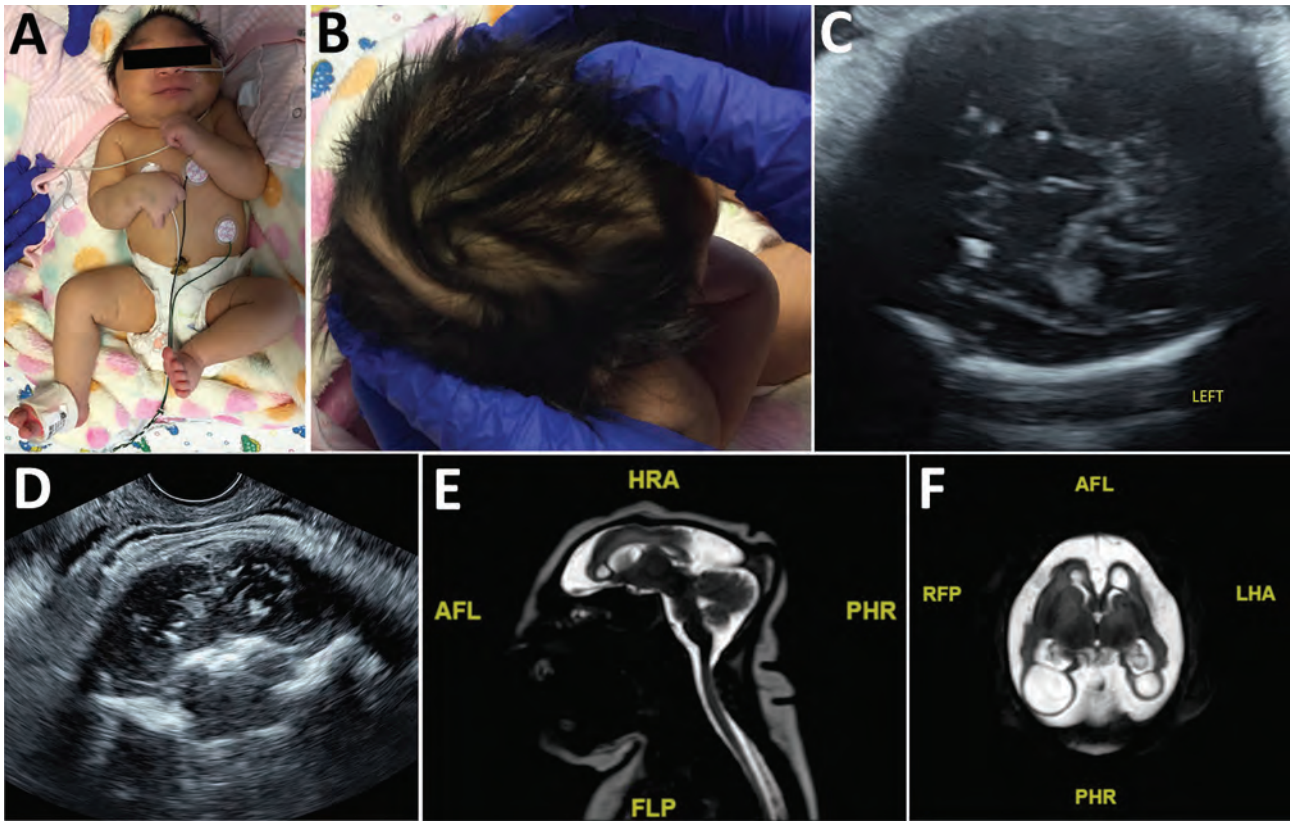

Figure 2. Term female infant (case-patient 2) with presumed congenital Zika syndrome, Brownsville, Texas, USA, 2016–2017. A) Microcephaly on the day of birth. Head circumference was 26.5 cm, which is 6.23 SDs below the mean value for term females. Craniofacial disproportion with narrow and laterally depressed frontal bone is seen. Upper wrist contractures are present, more apparent on the right, with ulnar deviation. B) Redundant scalp skin with multiple rugae. C) Transabdominal ultrasonography image of the axial transthalamic plane at 37 weeks' gestation, showing coarse bilateral calcifications in the thalami. D) Transvaginal ultrasonography image of the coronal section at 37 weeks' gestation, showing coarse calcifications in the thalami. E) Sagittal T2 turbo spin echo magnetic resonance image on day of birth, showing microcephaly, dysgenesis of the corpus callosum, and a small bilateral choroid plexus cyst. F) Axial T2 turbo spin echo magnetic resonance image on day of birth, showing microcephaly with enlarged extra-axial spaces and a smooth gyral pattern. Large bilateral posterior parietal and occipital lobe parenchymal cysts are present. AFL, anterior left; FLP, left posterior; HRA, right anterior; LHA, left anterior; PHR, posterior right; R, right; RFP, right posterior.

microcephaly with enlarged extraaxial spaces, large bilateral parenchymal cysts in the posterior parietal and occipital lobes, an overall smooth gyral pattern, dysgenesis of the corpus callosum, and 5 small bilateral choroid plexus cysts (Figure 2, panels E, F).

The infant was in the NICU for 28 days, during which daily examinations showed intermittent tremors, hypertonia, and an exaggerated Moro reflex. Upper bilateral wrists continued to be contracted in the flexed and ulnar deviated positions and required physical therapy intervention. The infant had to be fed by an orogastric tube because of poor feeding until she was able to be transitioned to ad libitum feeds on day 25 of life. Because of excessive irritability and crying, the infant was given phenobarbital on day 16 of life. In addition, an EEG was performed because of tremor activity; results were uneventful. Screening echocardiogram results were consistent with standard transitional neonatal cardiac changes. Abdominal ultrasonography was performed and results were unremarkable. Results were negative for a microarray and microcephaly gene panel testing. Results of thyroid function testing, complete blood count, and a comprehensive metabolic panel were all within reference ranges.

The infant was discharged on day 27 of life. She had an HC of 27 cm, which was 7.42 SD below the mean value for term females.

Discussion

Making a diagnosis of congenital Zika syndrome is challenging, despite testing and imaging available in a well-resourced area, such as the United States, which emphasizes the role of clinical and epidemiologic circumstances as critical pieces for a presumptive diagnosis. Diagnosis is needed not only epidemiologically, but also longitudinally

for follow-up of associated problems with congenital Zika virus infection, which have been reported as a constellation of malformations and clinical symptoms involving the brain, craniofacial defects, nervous system, eyes, and limbs (*3*,*5*–*9*,*12*,*19*–*24*).

Both infants reported in our case series had findings of congenital Zika syndrome (Figures 1, 2). Results of neuroimaging performed prenatally for both infants were consistent with the presence and degree of microcephaly observed postnatally (*25*). Calcifications identified prenatally in case-patient 1 had consistent postnatal distribution at the subcortical white matter–gray matter junction. Case-patient 2 had changes in the presence of calcifications seen during prenatal ultrasonography that were not present by postnatal imaging. In addition, prenatal diagnosis of arthrogryposis was not made because of spontaneous movement of all extremities on prenatal ultrasonographic images. This limitation illustrates that the spectrum of congenital Zika syndrome cannot be fully assessed until further postnatal assessment and highlights the need for advanced neuroimaging.

However, despite the neonatal diagnosis of congenital Zika syndrome, results for maternal testing were not consistent. The first case-patient had maternal laboratory findings of probable flavivirus infection that was not identified until the third trimester. The first IgM screening (at 28 weeks' gestation) might have shown a false-negative result, or the infection might have occurred later. However, even without definitive evidence of maternal Zika virus infection at the time of delivery, the neonate showed a positive result for Zika IgM in serum, and a subsequent placental test showed a positive result, which confirmed maternal infection.

Maternal diagnosis for case-patient 2 was confirmed with positive PCR results for serum at 23 weeks' gestation. However, despite this newborn displaying more severe features of congenital Zika syndrome postnatally (redundant scalp skin, bilateral upper arm arthrogryposis, smaller head size, and extrapyramidal symptoms), results of serum testing for Zika virus infection were negative.

In conclusion, results for these 2 case-patients indicate the complexity and challenges of screening and diagnostic testing for congenital Zika syndrome and illustrate the need for clinical findings and epidemiologic history. We advise a high index of suspicion for congenital Zika syndrome for at-risk populations on the basis of current limitations of testing.

About the Author

Dr. Howard is a physician and member of the South Texas Zika Task Force Team, Driscoll Children's Hospital, Corpus Christi, TX. Her primary research interests are congenital, arboviral, and emerging infections.

References

1. World Health Organization. Zika: the origin and spread of mosquito-borne virus, February 9, 2016 [cited 2016 Sep 12]. http://www.who.int/bulletin/online_first/16-171082/en/
2. Panchaud A, Stojanov M, Ammerdorffer A, Vouga M, Baud D. Emerging role of Zika virus in adverse fetal and neonatal outcomes. Clin Microbiol Rev. 2016;29:659–94. http://dx.doi.org/10.1128/CMR.00014-16
3. World Health Organization. Defining the syndrome associated with congenital Zika virus infection, June 2016 [cited 2016 Sep 12]. http://www.who.int/bulletin/volumes/94/6/16-176990/en/
4. Centers for Disease Control and Prevention. Cumulative Zika virus disease case in the United States, 2015–2017 [cited 2017 Aug 31]. https://www.cdc.gov/zika/reporting/case-counts.html
5. Cuevas EL, Tong VT, Rozo N, Valencia D, Pacheco O, Gilboa SM, et al. Preliminary report of microcephaly potentially associated with Zika virus infection during pregnancy–Colombia, January–November 2016. MMWR Morb Mortal Wkly Rep. 2016;65:1409–13. http://dx.doi.org/10.15585/mmwr.mm6549e1
6. Shapiro-Mendoza CK, Rice ME, Galang RR, Fulton AC, VanMaldeghem K, Prado MV, et al.; Zika Pregnancy and Infant Registries Working Group. Pregnancy outcomes after maternal Zika virus infection during pregnancy–US Territories, January 1, 2016–April 25, 2017. MMWR Morb Mortal Wkly Rep. 2017;66:615–21. http://dx.doi.org/10.15585/mmwr.mm6623e1
7. Brasil P, Pereira JP Jr, Moreira ME, Ribeiro Nogueira RM, Damasceno L, Wakimoto M, et al. Zika virus infection in pregnant women in Rio de Janeiro. N Engl J Med. 2016;375:2321–34. http://dx.doi.org/10.1056/NEJMoa1602412
8. Centers for Disease Control and Prevention. CDC concludes that Zika causes microcephaly and other birth defects [cited 2016 Sep 12]. http://www.cdc.gov/media/releases/2016/s0413-zika-microcephaly.html
9. Rasmussen SA, Jamieson DJ, Honein MA, Petersen LR. Zika virus and birth defects: reviewing the evidence for causality. N Engl J Med. 2016;374:1981–7. http://dx.doi.org/10.1056/NEJMsr1604338
10. Simeone RM, Shapiro-Mendoza CK, Meaney-Delman D, Petersen EE, Galang RR, Oduyebo T, et al.; Zika and Pregnancy Working Group. Possible Zika virus infection among pregnant women—United States and territories, May 2016. MMWR Morb Mortal Wkly Rep. 2016;65:514–9. http://dx.doi.org/10.15585/mmwr.mm6520e1
11. Meaney-Delman D, Hills SL, Williams C, Galang RR, Iyengar P, Hennenfent AK, et al. Zika virus infection among US pregnant travelers–August 2015–February 2016. MMWR Morb Mortal Wkly Rep. 2016;65:211–4. http://dx.doi.org/10.15585/mmwr.mm6508e1
12. Reynolds MR, Jones AM, Petersen EE, Lee EH, Rice ME, Bingham A, et al.; U.S. Zika Pregnancy Registry Collaboration. Vital signs: update on Zika virus–associated birth defects and evaluation of all US infants with congenital Zika virus exposure–US Zika pregnancy registry, 2016. MMWR Morb Mortal Wkly Rep. 2017;66:366–73. http://dx.doi.org/10.15585/mmwr.mm6613e1
13. Centers for Disease Control and Prevention. Pregnant women with any laboratory evidence of possible Zika virus infection in the United States and Territories, 2016–2017 [cited 2017 Aug 31]. https://www.cdc.gov/zika/geo/pregwomen-uscases.html
14. Honein MA, Dawson AL, Petersen EE, Jones AM, Lee EH, Yazdy MM, et al.; US Zika Pregnancy Registry Collaboration. Birth defects among fetuses and infants of US women with evidence of possible Zika virus infection during pregnancy. JAMA. 2017;317:59–68. http://dx.doi.org/10.1001/jama.2016.19006
15. Oduyebo T, Igbinosa I, Petersen EE, Polen KN, Pillai SK, Ailes EC, et al. Update: interim guidance for health care providers caring for pregnant women with possible Zika virus

exposure–United States, July 2016. MMWR Morb Mortal Wkly Rep. 2016;65:739–44. http://dx.doi.org/10.15585/mmwr.mm6529e1
16. Rabe IB, Staples JE, Villanueva J, Hummel KB, Johnson JA, Rose L, et al.; MTS. Interim guidance for interpretation of Zika virus antibody test results. MMWR Morb Mortal Wkly Rep. 2016;65:543–6. http://dx.doi.org/10.15585/mmwr.mm6521e1
17. Russell K, Oliver SE, Lewis L, Barfield WD, Cragan J, Meaney-Delman D, et al. Update: interim guidance for the evaluation and management of infants with possible congenital Zika virus infection–United States, August 2016. MMWR Morb Mortal Wkly Rep. 2016;65:870–8. http://dx.doi.org/10.15585/mmwr.mm6533e2
18. Ventura CV, Maia M, Travassos SB, Martins TT, Patriota F, Nunes ME, et al. Risk factors associated with the ophthalmoscopic findings identified in infants with presumed Zika virus congenital infection. JAMA Ophthalmol. 2016;134:912–8. http://dx.doi.org/10.1001/jamaophthalmol.2016.1784
19. Moura da Silva AA, Ganz JS, Sousa PD, Doriqui MJ, Ribeiro MR, Branco MD, et al. Early growth and neurologic outcomes of infants with probable congenital Zika virus syndrome. Emerg Infect Dis. 2016;22:1953–6. http://dx.doi.org/10.3201/eid2211.160956
20. Alves LV, Cruz DD, Linden AM, Falbo AR, Melo MJ, Paredes CE, et al. Epileptic seizures in children with congenital Zika virus syndrome. Revista Brasileira de Saude Materno Infantil. 2016;16 (Suppl 1):S27–S31.
21. Soares de Oliveira-Szejnfeld P, Levine D, Melo AS, Amorim MM, Batista AG, Chimelli L, et al. Congenital brain abnormalities and Zika virus: what the radiologist can expect to see prenatally and postnatally. Radiology. 2016;281:203–18. http://dx.doi.org/10.1148/radiol.2016161584
22. Del Campo M, Feitosa IM, Ribeiro EM, Horovitz DD, Pessoa AL, França GV, et al.; Zika Embryopathy Task Force-Brazilian Society of Medical Genetics ZETF-SBGM. The phenotypic spectrum of congenital Zika syndrome. Am J Med Genet A. 2017;173:841–57. http://dx.doi.org/10.1002/ajmg.a.38170
23. Eppes C, Rac M, Dunn J, Versalovic J, Murray KO, Suter MA, et al. Testing for Zika virus infection in pregnancy: key concepts to deal with an emerging epidemic. Am J Obstet Gynecol. 2017;216:209–25. http://dx.doi.org/10.1016/j.ajog.2017.01.020
24. Moore CA, Staples JE, Dobyns WB, Pessoa A, Ventura CV, Fonseca EB, et al. Characterizing the pattern of anomalies in congenital Zika syndrome for pediatric clinicians. JAMA Pediatr. 2017;171:288–95. http://dx.doi.org/10.1001/jamapediatrics.2016.3982
25. Chervenak FA, Rosenberg J, Brightman RC, Chitkara U, Jeanty P. A prospective study of the accuracy of ultrasound in predicting fetal microcephaly. Obstet Gynecol. 1987;69:908–10.

Address for correspondence: Ashley Howard, Driscoll Children's Hospital, 3533 S. Alameda St, Corpus Christi, TX 78411, USA; email: ashley.howard@dchstx.org

Reemergence of Intravenous Drug Use as Risk Factor for Candidemia, Massachusetts, USA

Nongnooch Poowanawittayakom, Anamika Dutta, Shannon Stock, Sunkaru Touray, Richard T. Ellison III, Stuart M. Levitz

Medscape EDUCATION ACTIVITY

JOINTLY ACCREDITED PROVIDER™ INTERPROFESSIONAL CONTINUING EDUCATION

In support of improving patient care, this activity has been planned and implemented by Medscape, LLC and Emerging Infectious Diseases. Medscape, LLC is jointly accredited by the Accreditation Council for Continuing Medical Education (ACCME), the Accreditation Council for Pharmacy Education (ACPE), and the American Nurses Credentialing Center (ANCC), to provide continuing education for the healthcare team.

Medscape, LLC designates this Journal-based CME activity for a maximum of 1.00 ***AMA PRA Category 1 Credit(s)™***. Physicians should claim only the credit commensurate with the extent of their participation in the activity.

All other clinicians completing this activity will be issued a certificate of participation. To participate in this journal CME activity: (1) review the learning objectives and author disclosures; (2) study the education content; (3) take the post-test with a 75% minimum passing score and complete the evaluation at http://www.medscape.org/journal/eid; and (4) view/print certificate. For CME questions, see page 817.

Release date: March 19, 2018; Expiration date: March 19, 2019

Learning Objectives

Upon completion of this activity, participants will be able to:

- Compare the clinical features of candidemia in patients with a history of intravenous drug use (IVDU) vs. patients without such a history, based on a case series from a tertiary care hospital in central Massachusetts
- Compare the microbiological features of candidemia in patients with a history of IVDU vs patients without such a history
- Determine the clinical implications of findings from this case series of patients with candidemia that is either associated or not associated with IVDU.

CME Editor

Deborah Wenger, MBA, Copyeditor, Emerging Infectious Diseases. *Disclosure: Deborah Wenger, MBA, has disclosed no relevant financial relationships.*

CME Author

Laurie Barclay, MD, freelance writer and reviewer, Medscape, LLC. *Disclosure: Laurie Barclay, MD, has disclosed the following relevant financial relationships: owns stock, stock options, or bonds from Alnylam; Biogen; Pfizer.*

Authors

Disclosures: ***Nongnooch Poowanawittayakom, MD; Anamika Dutta; Shannon Stock, PhD; Sunkaru Touray, MBChB, MSc;*** *and* ***Stuart M. Levitz, MD,*** *have disclosed no relevant financial relationships.* ***Richard T. Ellison III, MD,*** *has disclosed the following relevant financial relationships: served as an advisor or consultant for Philips Healthcare; received grants for clinical research from Philips Healthcare.*

The epidemic of illicit intravenous drug use (IVDU) in the United States has been accompanied by a surge in drug overdose deaths and infectious sequelae. *Candida albicans* infections were associated with injection of contaminated impure brown heroin in the 1970s–1990s; however, candidiasis accompanying IVDU became considerably rarer as the purity of the heroin supply increased. We reviewed cases of candidemia occurring over a recent 7-year period in persons ≥14 years of age at a tertiary care hospital in central Massachusetts. Of the 198 patients with candidemia, 24 cases occurred in patients with a history of IVDU. Compared with non-IVDU patients, those with a history of IVDU were more likely to have non-albicans *Candida*, be co-infected with hepatitis C, and have end-organ involvement, including endocarditis and osteomyelitis. Thus, IVDU appears to be reemerging as a risk factor for invasive candidiasis.

Author affiliations: University of Massachusetts Medical School, Worcester, Massachusetts, USA (N. Poowanawittayakom, S. Touray, R.T. Ellison III, S.M. Levitz); College of the Holy Cross, Worcester (A. Dutta, S. Stock)

DOI: https://doi.org/10.3201/eid2404.171807

Invasive fungal infections resulting from candidiasis are notable causes of illness and death in both adults and pediatric patients (*1*–*4*). *C. albicans* accounts for approximately half the cases of candidemia. For example, in a study of 2,019 candidemia cases during 2004–2008, *C. albicans* was responsible for 46% of the cases, followed by *C. glabrata* (26%), *C. parapsilosis* (16%), *C. tropicalis* (8%), and *C. krusei* (3%) (*1*). Risk factors for invasive *Candida* infections include immunocompromised status, central venous catheters, broad-spectrum antimicrobial drugs, kidney disease requiring dialysis, and genitourinary and gastrointestinal surgery or procedures (*5*).

Opioid addiction has emerged as an increasingly crucial public health problem in the United States. More than 50,000 persons died from drug overdoses in the United States in 2015, an increase of >500% since 1990 (*6*). Massachusetts has been one of the states hardest hit by this epidemic; an estimated 2,190 opioid-related deaths occurred in 2016, which is a ≈4-fold increase since 2010, when 560 such deaths occurred (*7*). In addition to deaths from overdoses, infectious sequelae from intravenous drug use (IVDU) commonly occur, including acute infections such as abscesses at injection sites and endocarditis and chronic infections such as HIV and hepatitis C.

During the 1970s–1990s, outbreaks were reported of *C. albicans* infections in intravenous drug users who used impure brown heroin (*8*,*9*). The source of the *Candida* was thought to be contaminated lemon juices used to dissolve the heroin (*10*–*12*). Clinical manifestations in the affected patients included nodular and pustular cutaneous lesions, chorioretinitis, and osteoarticular infection (*8*,*9*,*11*). After the 1990s, the general purity of heroin supplies increased, negating the need to use acidic sources such as lemon juice as solvents; thus, the problem of candidiasis associated with IVDU mostly disappeared. However, rare case reports of candidiasis syndromes associated with IVDU, such as endophthalmitis associated with injecting contaminated buprenorphine, continued to appear in the literature (*13*,*14*).

Recently, we noticed an apparent increase in cases of invasive candidiasis associated with IVDU at UMassMemorial Medical Center, Worcester, Massachusetts, USA. We therefore retrospectively reviewed all cases of candidemia seen at the hospital over a 7-year period. We compared cases in patients with a history of IVDU with those without such a history with regard to demographic, epidemiologic, clinical, laboratory, and microbiological features.

Methods

UMassMemorial Medical Center is a 781-bed academic medical center affiliated with the University of Massachusetts Medical School and located in central Massachusetts. The study was approved by the University of Massachusetts Medical School (UMMS) Institutional Review Board (IRB). Patients ≥14 years of age with a positive blood culture for *Candida* species during January 1, 2010–January 31, 2017, were included in the study. We excluded patients <14 years of age, as they were felt to be unlikely to have a history of IVDU. The protocol approved by the IRB also excluded the study of prisoners; however, none of the patients was excluded for this reason.

We identified cases of candidemia by a query of the hospital electronic medical records (EMRs) using Theradoc (Premier Inc., Charlotte, NC, USA). We then reviewed the EMRs of the patients with candidemia for any history of IVDU; we classified cases as IVDU and non-IVDU on the basis of this chart review. We included cases in the IVDU group if there was any history of IVDU, even if remote. We reviewed admission notes, infectious diseases consult notes, psychiatry consult notes, discharge notes, and toxicology screens. We then conducted a further review of the EMRs to extract data on the epidemiology, risk factors, clinical manifestations, microbiology, laboratory findings, and outcomes. The IRB protocol forbade contacting the patients directly.

We performed *Candida* speciation using standard techniques, including the Vitek 2-Yeast System, Vitek-MS, and API 20C (bioMérieux, Marcy l'Étoile, France). We compared the variables in the tables between the IVDU and non-IVDU populations using the Fisher exact test for categorical variables and the Wilcoxon rank sum test for continuous variables. These tests are nonparametric and avoid the need for large sample sizes. We defined statistical significance as a p value <0.05.

Results

Epidemiologic Data and Risk Factors

During January 1, 2010–January 31, 2017, a total of 198 patients had positive blood cultures for *Candida* species. Using the criteria noted in the previous section, we categorized 24 (12%) patients as being in the IVDU group and 174 (88%) patients in the non-IVDU group. Salient baseline characteristics of the study population are shown in Table 1. Patients in the IVDU group were significantly younger and more likely to have had a positive test for hepatitis C compared with patients in the non-IVDU group (p<0.001 for both variables). Although the numbers were small, a significantly higher percentage of patients in the IVDU group had prosthetic valves (p = 0.013). All 3 of the patients in the IVDU group with a prosthetic valve had valve replacement because of prior episodes of endocarditis. None of the other baseline characteristics we studied differed significantly between the groups. Only 1 patient had known HIV infection.

We compared the prevalence of many of the established risk factors for candidemia in IVDU and non-IVDU

Table 1. Baseline characteristics and risk factors for candidemia, categorized by IVDU and non-IVDU groups, among patients at a tertiary care hospital, Massachusetts, USA, 2010–2017*

Characteristics	IVDU	Non-IVDU	p value
No. patients	24	174	
Median age (IQR)	43.5 (14.8)	64.0 (19.0)	<0.001
Female sex†	6 (25.0)	70 (40.2)	0.183
Prosthetic valve	3 (12.5)	2 (1.2)	0.013
Hepatitis C	14 (58.3)	14 (8.1)	<0.001
HIV	0	1 (0.6)	1.00
History of malignancy	2 (8.3)	42 (24.1)	0.114
Diabetes	3 (12.5)	55 (31.6)	0.058
Systemic immunosuppression‡	3 (12.5)	28 (16.1)	1.00
Central intravenous line	9 (37.5)	67 (38.5)	1.00
History of broad-spectrum antimicrobial drug exposure§	4 (16.7)	27 (15.5)	1.00
Kidney disease, on dialysis	3 (12.5)	5 (2.9)	0.058
Genitourinary surgery/procedure§	0	14 (8.1)	0.226
Gastrointestinal surgery/procedure§	3 (12.5)	22 (12.6)	1.00

*Values are no. (%) patients except as indicated. IQR, interquartile range; IVDU, intravenous drug use.
†In all patients, gender and biological sex were identical.
‡Includes active chemotherapy, systemic corticosteroid use, and immunosuppression within 3 months before the onset of candidemia.
§ Procedure performed ≤30 days before onset of candidemia.

groups (Table 1). Although the differences were not statistically significant, patients in the non-IVDU group were more likely to have diabetes (31.6% v. 12.5%) and a history of malignancy (24.1% vs. 8.3%). We noted no significant differences between the 2 groups with regard to systemic immunosuppression, genitourinary procedures, kidney disease requiring dialysis, central intravenous lines, gastrointestinal surgery procedures, or history of broad-spectrum antimicrobial drug use.

Of the 24 cases of IVDU-associated candidemia recorded during the 7-year period of the study, only 2 occurred during the first 2 years. In contrast, 9 cases occurred in 2016, the last year of the study (Figure). The number of candidemia cases was not associated with diminished IVDU in the last 2 years of the study.

Features of Patients with Candidemia and History of IVDU

Details about the patients with a history of IVDU are provided in Table 2. Most of the patients gave a history of use of heroin, cocaine, or both. However, prescription opioids were also commonly found when toxicology screens were obtained.

Organ System Involvement

We determined the prevalence of brain abscesses, osteomyelitis, retinitis, skin lesions, septic emboli to the lungs, and endocarditis (Table 3). Although endocarditis and osteomyelitis were seen infrequently, the IVDU group had a significantly higher percentage of cases of these 2 diseases compared with the non-IVDU group.

Candida Species

C. albicans was isolated from the bloodstream in a significantly higher percentage of non-IVDU patients compared with IVDU patients (Table 4). In contrast, the percentage of *Candida* isolates identified as *C. parapsilosis* was significantly higher in the IVDU group. Other *Candida* species were isolated, mostly commonly *C. glabrata* and *C. tropicalis*, but their distribution was not significantly different between the IVDU and non-IVDU groups. Two patients in each group were co-infected with 2 *Candida* species.

Outcome Data

Mortality rates and length of hospitalization were lower in the IVDU group compared with the non-IVDU group (Table 5). However, the differences were not statistically significant.

Discussion

Our data establish that, in the setting of the ongoing opioid epidemic, candidemia appears to have emerged as a serious clinical problem in the IVDU population in central Massachusetts. Major differences appear, however, between the

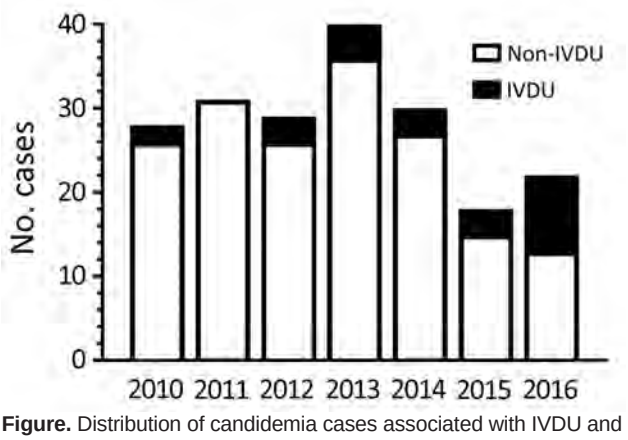

Figure. Distribution of candidemia cases associated with IVDU and non-IVDU by year at a tertiary care hospital, Massachusetts, USA, 2010–2017. Candidemia cases were divided into IVDU and non-IVDU groups and then plotted as a function of the year the patient had positive blood cultures for *Candida*. There were no positive blood cultures in January 2017, the last month of the study.

Table 2. Summary of characteristics of patients with candidemia and a history of IVDU admitted to a tertiary care hospital, Massachusetts, USA, 2010–2017*

Pt no.	Age, y/ sex	Date admitted	IVDU, by history	Toxicology screen	Last use, by history	*Candida* species	Vegetations on echo	Antifungal therapy (duration)	Outcome
1	32/M	2010 Jan	Heroin	Heroin, morphine, cocaine	5 d	*C. parapsilosis*	No	Fluc (14 d)	Cured
2	28/M	2010 Oct	Heroin	ND	6 mo	*C. parapsilosis*	No	Fluc (14 d)	Cured
3	52/F	2012 Jul	Heroin, cocaine	Opiates	NA	*C. glabrata*	No	MF (8 d) then fluc (20 d)	Cured
4	43/F	2012 Oct	Heroin	Cocaine, opiates†	1.5 d	*C. parapsilosis*	Yes (aortic, mitral)	None	Died
5	59/M	2012 Nov	Not documented	ND	30 y	*C. glabrata*	No	Fluc (14 d)	Died
6	54/M	2013 Mar	Heroin, cocaine	Methadone, opiates	2 y	*C. parapsilosis*	No	MF (3 d) then fluc (25 d)	Cured
7	43/F	2013 Apr	Heroin	ND	NA	*C. albicans*	No	MF (3 d) then fluc (25 d)	Cured
8	31/M	2013 Aug	Heroin	Opiates	2 y	*C. albicans*	No	MF (2 d) then fluc (12 d)	Cured
9	36/M	2013 Dec	Heroin	Oxycodone, hydromorphone	6 d	*C. glabrata, C. parapsilosis*	No	None	Lost to follow up
10	49 /F	2014 Jan	Unspecified narcotic	Opiates	NA	*C. glabrata*	No	MF (3 d)	Died
11	38/F	2014 Feb	Heroin	Oxycodone, oxymorphone	2 y	*C. albicans*	Possible (tricuspid on TTE, TEE negative)	Fluc (2 d) then MF (40 d)	Remission (had epidural abscess)
12	50/M	2014 Aug	Heroin	Morphine	6 mo	*C. tropicalis*	No	Fluc (14 d)	Cured
13	49/M	2015 Mar	Cocaine	ND	Unknown	*C. lipolytica*	No	Fluc (14 d)	Cured
14	22/M	2015 Jun	Heroin	Marijuana	Day admitted	*C. glabrata*	No	MF (3 d) then fluc (25 d)	Cured
15	53/M	2015 Sep	Cocaine	Cocaine	Remote	*C. tropicalis*	No	Fluc (2 d)	Died
16	31/F	2016 Jan	Cocaine	Morphine	NA	*C. tropicalis*	No	Fluc (14d)	Cured
17	37/M	2016 Feb	Heroin	ND	3 wk	*C. glabrata*	No	Fluc (14d)	Cured
18	35/M	2016 Mar	Heroin, Cocaine	Cocaine, opiates†	NA	*C. albicans*	No	MF (4 d) then fluc (24 d)	Cured
19	44/M	2016 Apr	Cocaine, heroin	Buprenorphine, norbuprenorphine	7 mo	*C. parapsilosis*	Yes (aortic)	Fluc (indefinite)	Remission follow up TTE after 3 mo: no vegetation
20	47/M	2016 Apr	Cocaine	ND	1 y	*C. albicans*	No	MF (6 d) then fluc (8d)	Cured
21	32/F	2016 May	Heroin	Methadone, oxycodone	2 wk	*C. albicans*	Yes (mitral)	AmpB (1 d) then fluc and vori (indefinite)‡	Remission follow up TTE after 3 mo: no vegetation
22	46/M	2016 May	Cocaine, heroin	ND	Day admitted	*C. glabrata*	No	Fluc (21 d)	Cured
23	40/M	2016 Jun	Heroin	Opiates	Day admitted	*C. albicans, C. glabrata*	No	MF (13 d) then fluc (1 d)	Cured
24	54/M	2016 Sep	Heroin	ND	1 mo	*C. parapsilosis*	Yes (aortic)	MF (5 d) then ampB and 5FC (5 d)	Died

*ampB, amphotericin B; 5FC, 5-flucytosine; echo, echocardiogram; fluc, fluconazole; IVDU, intravenous drug use; MF, micafungin; NA, not available; ND, not done; Pt, patient; TEE, transesophageal echocardiogram; TTE, transthoracic echocardiogram; vori, voriconazole.
†Positive toxicology screen was obtained during a previous admission.
‡Patient developed hypercalcemia after courses of fluconazole and treatment was changed to voriconazole.

cases reported in the literature that were associated with injection of brown heroin and the ones in this case series. Cutaneous, ocular, or osteoarticular involvement were commonly observed in the brown heroin users with candidiasis (*8*,*9*) but were rarely seen in the IVDU case-patients we report. In contrast, although all the cases in our study featured candidemia by definition, blood cultures were rarely positive for candidemia in the brown heroin cases.

As discussed earlier, in the brown heroin cases, the infections were linked to *C. albicans* contamination of

Table 3. Organ system involvement in patients with candidemia at a tertiary care hospital, Massachusetts, USA, 2010–2017*

Manifestation	No. (%) patients IVDU, n = 24	Non-IVDU, n = 174	p value
Endocarditis	4 (16.7)	5 (2.9)	0.014
Brain abscess	1 (4.2)	0	0.121
Septic emboli, lung	1 (4.2)	0	0.121
Retinitis	0	4 (2.3)	1.00
Osteomyelitis	2 (8.3)	0	0.014

*IVDU, intravenous drug use.

lemon juice used to solubilize the heroin; blood cultures, when positive, grew only *C. albicans* (*8*,*9*). In our case series, *C. albicans* was the third most common species, behind *C. glabrata* and *C. parapsilosis*. The finding of different species of *Candida* argues against a common source of infection. Rather, endogenous sources of *Candida* seem likely, because this fungus can colonize the skin and mouth; injection drug users may lick their needles before insertion into the skin. However, our IRB protocol did not permit us to interview subjects regarding injection habits or to culture their drugs and injection paraphernalia. Thus, the source of the *Candida* species isolated from the patients is speculative, and future studies are needed to address this question.

C. glabrata and *C. parapsilosis* are typically thought of as nosocomial pathogens, with spread of the pathogen facilitated by contaminated inanimate surfaces and person-to-person contact (*15*,*16*). However, both species can also be gut colonizers and commensals of human skin (*16*). *C. glabrata* is often resistant to fluconazole; a risk factor for infection with this species is prior receipt of fluconazole (*15*). However, none of our patients was known to have received fluconazole before contracting candidemia.

In our study, we found that the candidemia patients in the IVDU group were younger and more likely to be co-infected with hepatitis C than were patients in the non-IVDU group. This finding likely reflects the relatively young age of the IVDU population and the high prevalence of hepatitis C infection for this group (*17*). Even though more than half of the patients in the IVDU group were co-infected with hepatitis C, no patient had HIV infection. This finding is consistent with a 2012 report documenting declining rates of HIV infection and increasing rates of hepatitis C among injection drug users in Massachusetts (*18*).

In a recent multicenter study of >2,000 patients with candidemia, *C. albicans* was responsible for 46% of the cases, followed by *C. glabrata* (26%), *C. parapsilosis* (16%), *C. tropicalis* (8%), and *C. krusei* (3%) (*1*). In our study, the species distribution in the non-IVDU population with candidemia was very similar, with slightly more than half the cases attributable to *C. albicans* (Table 4). In contrast, only 7 (29%) of 24 candidemia cases in the IVDU population were caused by *C. albicans*, and 1 of those cases was a co-infection with *C. glabrata*. Perhaps reflecting these patients' younger age and fewer concurrent conditions, the mortality rate was lower for the IVDU population compared with the non-IVDU population, although the difference was not statistically significant. Nevertheless, 5 (21%) of 24 patients in the IVDU group died, emphasizing that candidemia in the IVDU population is a serious disease associated with a serious risk of death.

Table 4. *Candida* species isolated from blood of patients with candidemia at a tertiary care hospital, Massachusetts, USA, 2010–2017*

Organisms	No. (%) patients IVDU, n = 24	Non-IVDU, n = 174	p value
C. albicans	7 (29.2)†	93 (53.5)	0.03
C. glabrata	8 (33.3)	39 (22.4)	0.304
C. parapsilosis	8 (33.3)	25 (14.4)	0.036
C. tropicalis	3 (12.5)	13 (7.5)	0.419
C. dubliniensis	0	2 (1.2)	1.00
C. guilliermondii	0	1 (0.6)	1.00
C. krusei	0	1 (0.6)	1.00
C. lipolytica	0	1 (0.6)	1.00
C. kefyr	0	1 (0.6)	1.00
Co-infected	2 (8.3)	2 (1.2)	0.073

*IVDU, intravenous drug use.
†Percentages do not add up to 100% because patients co-infected with 2 species are counted twice.

Our retrospective study does not shed light on the optimal therapy for IVDU-associated candidemia. However, it seems reasonable to begin to treat patients with an echinocandin, according to the Infectious Diseases Society of America clinical practice guideline for the treatment of candidemia (*19*), pending identification and susceptibility testing of the isolate. One third of our IVDU-associated candidemia cases were caused by *C. glabrata* which, as noted earlier, is often resistant to fluconazole (*15*). In addition, the superiority of an echinocandin over fluconazole was demonstrated in a multicenter trial of patients with candidemia (*20*). However, a disadvantage of the echinocandins is their need to be given intravenously, a particular problem in the patient population with IVDU, because they may use intravenous lines for drug injection. In clinically stable patients with susceptible isolates and without endocarditis, transition to fluconazole can be considered when the patient is ready for discharge.

Several limitations should be taken into account when interpreting the data we present. The study was

Table 5. Outcomes of patients with candidemia, Massachusetts, USA, 2010–2017*

Outcome	IVDU, n = 24	Non-IVDU, n = 174	p value
Death, no. (%) patients	5 (20.8)	60 (34.5)	0.247
Median length of hospital stay (IQR), d	11 (17.5)	19 (27.5)	0.059

*IQR, interquartile range; IVDU, intravenous drug use.

retrospective, and because of our IRB protocol, we were not permitted to contact the patients directly to verify their histories or obtain additional information. Moreover, it is often difficult to obtain an accurate history of IVDU from patients. Thus, because it was not known whether the injection drug use was current or not, we cannot be certain that the IVDU contributed to the risk of developing candidemia. Indeed, it is possible that some of the patients were misclassified and there may be inaccuracies in variables such as when the patients last injected drugs and what drugs were injected. For this reason, when designing the study, we prospectively decided to include all patients with a history of IVDU, however remote, in the IVDU group. Second, although it is very likely that the trend toward increasing numbers of IVDU-associated candidemia is real, it is possible that the way IVDU is recorded has changed over the years because healthcare providers are now more attuned to the opioid epidemic and thus record the history of IVDU more often than they did in the past. Third, although the number of cases was relatively large, the study was not powered to detect differences in uncommon events between the IVDU and non-IVDU groups. In addition, multivariate analyses were not performed, so some statistically significant associations may be confounded. Fourth, there may have been a bias toward ordering certain tests, such as hepatitis C serology and echocardiography, in the IVDU-associated candidemia group. Finally, our study was a single-center study from a tertiary care institution. It remains to be seen whether candidemia in IVDU is mostly a local phenomenon peculiar to central Massachusetts or it is emerging at other medical centers in other geographic locations.

These limitations notwithstanding, our findings establish candidemia as an underappreciated outcome of the opioid epidemic gripping the United States. Moreover, we observed a marked increase in the number of cases during the last year of the study. Although this finding may reflect random variations, it is of concern that the problem may be worsening. In Worcester County, where UMassMemorial Hospital is located, the number of opioid-related overdose deaths increased every year during the 7-year study period, from 80 in 2010 to 251 in 2016 (*7*). Although many of the press reports surrounding illicit opioid use have centered on deaths from overdose, infections remain a serious cause of illness and death in persons with IVDU. Invasive candidiasis must be considered in the differential diagnosis of patients with infectious sequelae of IVDU.

Acknowledgments

We thank Deborah Mack for assistance with identifying candidemia patients in the database, and Jennifer Wang for helpful suggestions.

About the Author

Dr. Poowanawittayakom is an infectious diseases physician in Brockton, Massachusetts, USA, and is pursuing a master of public health degree at the University of Massachusetts. Her primary research interests are *Clostridium difficile* infections, fungal epidemiology, and viral hepatitis.

References

1. Horn DL, Neofytos D, Anaissie EJ, Fishman JA, Steinbach WJ, Olyaei AJ, et al. Epidemiology and outcomes of candidemia in 2019 patients: data from the Prospective Antifungal Therapy Alliance registry. Clin Infect Dis. 2009;48:1695–703. http://dx.doi.org/10.1086/599039
2. Chow JK, Golan Y, Ruthazer R, Karchmer AW, Carmeli Y, Lichtenberg DA, et al. Risk factors for albicans and non-albicans candidemia in the intensive care unit. Crit Care Med. 2008; 36:1993–8. http://dx.doi.org/10.1097/CCM.0b013e31816fc4cd
3. Playford EG, Marriott D, Nguyen Q, Chen S, Ellis D, Slavin M, et al. Candidemia in nonneutropenic critically ill patients: risk factors for non-albicans Candida spp. Crit Care Med. 2008; 36:2034–9. http://dx.doi.org/10.1097/CCM.0b013e3181760f42
4. Playford EG, Nimmo GR, Tilse M, Sorrell TC. Increasing incidence of candidaemia: long-term epidemiological trends, Queensland, Australia, 1999–2008. J Hosp Infect. 2010;76:46–51. http://dx.doi.org/10.1016/j.jhin.2010.01.022
5. Kullberg BJ, Arendrup MC. Invasive candidiasis. N Engl J Med. 2015;373:1445–56. http://dx.doi.org/10.1056/NEJMra1315399
6. Katz J. You draw it: just how bad is the drug overdose epidemic? 2017 [cited 2017 Sept 5]. https://www.nytimes.com/interactive/2017/04/14/upshot/drug-overdose-epidemic-you-draw-it.html?_r=0
7. Commonwealth of Massachusetts. Current opioid statistics. 2017 [cited 2018 Jan 9]. https://www.mass.gov/lists/current-opioid-statistics
8. Bisbe J, Miro JM, Latorre X, Moreno A, Mallolas J, Gatell JM, et al. Disseminated candidiasis in addicts who use brown heroin: report of 83 cases and review. Clin Infect Dis. 1992;15:910–23. http://dx.doi.org/10.1093/clind/15.6.910
9. Dupont B, Drouhet E. Cutaneous, ocular, and osteoarticular candidiasis in heroin addicts: new clinical and therapeutic aspects in 38 patients. J Infect Dis. 1985;152:577–91. http://dx.doi.org/10.1093/infdis/152.3.577
10. Miró JM, De La Bellacasa J, Odds FC, Gill BK, Bisbe J, Gatell JM, et al. Systemic candidiasis in Spanish heroin addicts: a possible source of infection. J Infect Dis. 1987;156:857–8. http://dx.doi.org/10.1093/infdis/156.5.857
11. Podzamczer D, Fernández-Viladrich P, Ribera M, Arruga J, de Celis G, Gudiol F. Systemic candidiasis in drug addicts. Eur J Clin Microbiol. 1985;4:509–12. http://dx.doi.org/10.1007/BF02014437
12. Shankland GS, Richardson MD, Dutton GN. Source of infection in candida endophthalmitis in drug addicts. Br Med J (Clin Res Ed). 1986;292:1106–7. http://dx.doi.org/10.1136/bmj.292.6528.1106-a
13. Cassoux N, Bodaghi B, Lehoang P, Edel Y. Presumed ocular candidiasis in drug misusers after intravenous use of oral high dose buprenorphine (Subutex). Br J Ophthalmol. 2002;86:940–1. http://dx.doi.org/10.1136/bjo.86.8.940
14. Aboltins CA, Allen P, Daffy JR. Fungal endophthalmitis in intravenous drug users injecting buprenorphine contaminated with oral Candida species. Med J Aust. 2005;182:427.
15. Rodrigues CF, Silva S, Henriques M. Candida glabrata: a review of its features and resistance. Eur J Clin Microbiol Infect Dis. 2014;33:673–88. http://dx.doi.org/10.1007/s10096-013-2009-3

16. Trofa D, Gácser A, Nosanchuk JD. Candida parapsilosis, an emerging fungal pathogen. Clin Microbiol Rev. 2008;21:606–25. http://dx.doi.org/10.1128/CMR.00013-08
17. Centers for Disease Control and Prevention. Viral hepatitis. Statistics and surveillance. 2017 [cited 2017 Sept 5]. https://www.cdc.gov/hepatitis/statistics/index.htm
18. Commonwealth of Massachusetts. Shifting epidemics. HIV and hepatitis C infection among injection drug users in Massachusetts. 2012 [cited 2017 Sept 5]. http://www.mass.gov/eohhs/docs/dph/aids/shifting-epidemics-report.doc
19. Pappas PG, Kauffman CA, Andes DR, Clancy CJ, Marr KA, Ostrosky-Zeichner L, et al. Clinical practice guideline for the management of candidiasis: 2016 update by the Infectious Diseases Society of America. Clin Infect Dis. 2016;62:409–17. http://dx.doi.org/10.1093/cid/civ1194
20. Reboli AC, Rotstein C, Pappas PG, Chapman SW, Kett DH, Kumar D, et al.; Anidulafungin Study Group. Anidulafungin versus fluconazole for invasive candidiasis. N Engl J Med. 2007;356:2472–82. http://dx.doi.org/10.1056/NEJMoa066906

Address for correspondence: Stuart M. Levitz, Department of Medicine, University of Massachusetts Medical School, 364 Plantation St, LRB317, Worcester, MA 01605, USA; email: stuart.levitz@umassmed.edu

Rickettsial Illnesses as Important Causes of Febrile Illness in Chittagong, Bangladesh

Hugh W. Kingston, Mosharraf Hossain, Stije Leopold, Tippawan Anantatat, Ampai Tanganuchitcharnchai, Ipsita Sinha, Katherine Plewes, Richard J. Maude, M.A. Hassan Chowdhury, Sujat Paul, Rabiul Alam Mohammed Erfan Uddin, Mohammed Abu Naser Siddiqui, Abu Shahed Zahed, Abdullah Abu Sayeed, Mohammed Habibur Rahman, Anupam Barua, Mohammed Jasim Uddin, Mohammed Abdus Sattar, Arjen M. Dondorp, Stuart D. Blacksell, Nicholas P.J. Day, Aniruddha Ghose, Amir Hossain, Daniel H. Paris

Medscape EDUCATION ACTIVITY

In support of improving patient care, this activity has been planned and implemented by Medscape, LLC and Emerging Infectious Diseases. Medscape, LLC is jointly accredited by the Accreditation Council for Continuing Medical Education (ACCME), the Accreditation Council for Pharmacy Education (ACPE), and the American Nurses Credentialing Center (ANCC), to provide continuing education for the healthcare team.

Medscape, LLC designates this Journal-based CME activity for a maximum of 1.00 ***AMA PRA Category 1 Credit(s)™***. Physicians should claim only the credit commensurate with the extent of their participation in the activity.

All other clinicians completing this activity will be issued a certificate of participation. To participate in this journal CME activity: (1) review the learning objectives and author disclosures; (2) study the education content; (3) take the post-test with a 75% minimum passing score and complete the evaluation at http://www.medscape.org/journal/eid; and (4) view/print certificate. For CME questions, see page 818.

Release date: March 16, 2018; Expiration date: March 16, 2019

Learning Objectives

Upon completion of this activity, participants will be able to:

- Distinguish common symptoms of rickettsial illness
- Evaluate the epidemiology of rickettsial illness in the current study
- Assess high-risk months for infection with scrub typhus in the current study
- Analyze the genotypes of *Orientia tsutsugamushi* isolated in the current study.

CME Editor

Jude Rutledge, BA, Technical Writer/Editor, Emerging Infectious Diseases. *Disclosure: Jude Rutledge has disclosed no relevant financial relationships.*

CME Author

Charles P. Vega, MD, FAAFP, Health Sciences Clinical Professor, University of California, Irvine, Department of Family Medicine; Associate Dean for Diversity and Inclusion, University of California, Irvine, School of Medicine; Executive Director, University of California, Irvine, Program in Medical Education for the Latino Community, Irvine, California. *Disclosure: Charles P. Vega, MD, FAAFP, has disclosed the following relevant financial relationships: served as an advisor or consultant for Johnson & Johnson Healthcare; served as a speaker or a member of a speakers bureau for Shire Pharmaceuticals.*

Authors

Disclosures: ***Hugh W. Kingston, BMBCh, PhD; Mosharraf Hossain, MBBS; Stije Leopold, MD; Tippawan Anantatat, MSc; Ampai Tanganuchitcharnchai, MSc; Ipsita Sinha, MBBS, MSc; Katherine Plewes, MD, DPhil; Richard J. Maude, MD, DPhil; M.A. Hassan Chowdhury, FCPS, FRCP, FACP, MD; Sujat Paul, FCPS, MBBS, MPhil; Rabiul Alam Md Erfan Uddin, MBBS, MCPS, FCPS; Md Abu Naser Siddiqui, MBBS, FCPS, MD; Abu Shahed Md Zahed, MBBS, FCPS; Abdullah Abu Sayeed, MD; Mohammed Habibur Rahman, MBBS, FCPS; Anupam Barua, MBBS, MD, FCPS; Md Jasim Uddin, FCPS, MD; Md Abdus Sattar, MBBS, FCPS; Arjen M. Dondorp, MD, PhD; Stuart D. Blacksell, BAppSc, MPH, PhD; Nicholas P.J. Day, DM; Aniruddha Ghose, MD, FCPS, MBBS; Amir Hossain, FCPS, MD;*** *and* ***Daniel H. Paris, MD, PhD,*** *have disclosed no relevant financial relationships.*

Author affiliations: Charles Darwin University, Casuarina, Northern Territory, Australia (H.W. Kingston); Mahidol University, Bangkok, Thailand (H.W. Kingston, S. Leopold, T. Anantatat, A. Tanganuchitcharnchai, I. Sinha, K. Plewes, R.J. Maude, A.M. Dondorp, S.D. Blacksell, N.P.J. Day, D.H. Paris); Chittagong Medical College Hospital, Chittagong, Bangladesh (M. Hossain, M.A.H. Chowdhury, S. Paul, R.A.M.E. Uddin, M.A.N. Siddiqui, A.S. Zahed, A.A. Sayeed, M.H. Rahman, A. Barua, M.J. Uddin, M.A. Sattar, A. Ghose, A. Hossain); Oxford University, Oxfordshire, UK (I. Sinha, R.J. Maude, A.M. Dondorp, S.D. Blacksell, N.P.J. Day, D.H. Paris); Harvard University, Boston, Massachusetts, USA (R.J. Maude); Swiss Tropical and Public Health Institute, Basel, Switzerland (D.H. Paris); University of Basel, Basel (D.H. Paris)

DOI: https://doi.org/10.3201/eid2404.170190

We conducted a yearlong prospective study of febrile patients admitted to a tertiary referral hospital in Chittagong, Bangladesh, to assess the proportion of patients with rickettsial illnesses and identify the causative pathogens, strain genotypes, and associated seasonality patterns. We diagnosed scrub typhus in 16.8% (70/416) and murine typhus in 5.8% (24/416) of patients; 2 patients had infections attributable to undifferentiated *Rickettsia* spp. and 2 had DNA sequence–confirmed *R. felis* infection. *Orientia tsutsugamushi* genotypes included Karp, Gilliam, Kato, and TA763-like strains, with a prominence of Karp-like strains. Scrub typhus admissions peaked in a biphasic pattern before and after the rainy season, whereas murine typhus more frequently occurred before the rainy season. Death occurred in 4% (18/416) of cases; case-fatality rates were 4% each for scrub typhus (3/70) and murine typhus (1/28). Overall, 23.1% (96/416) of patients had evidence of treatable rickettsial illnesses, providing important evidence toward optimizing empirical treatment strategies.

The prevalence, seasonality, and genotypes of tropical rickettsial illnesses in Bangladesh remain unknown. Scrub and murine typhus typically present as undifferentiated febrile illnesses and are insensitive to penicillins and cephalosporins, common antimicrobial drugs used empirically (*1*). Rickettsial illnesses are increasingly recognized as important causes of fever in adjacent countries in the region, including Thailand, Laos, and India (*2*–*5*). Therefore, determining whether rickettsial infections are widespread in Bangladesh, a low-income country with a population of ≈160 million, is of urgent public health interest.

Cross-sectional seroprevalence studies suggest that exposure to scrub typhus and murine typhus is common (*6*). In addition, given the substantial proportion of febrile patients from north-central Bangladesh with confirmed *R. felis* infection (*7*), further investigations regarding the clinical relevance of this pathogen are warranted.

Identification and characterization of circulating pathogens and strains is crucial for the development of diagnostics and vaccines (*8*). Strong seasonal trends might guide differential diagnostic considerations. Therefore, we conducted a year-long prospective study of febrile patients admitted to a tertiary referral hospital with a wide catchment area in southeast Bangladesh, aiming to assess the proportion of patients with rickettsial illnesses, identify the causative pathogens, strain genotypes, and the associated seasonality patterns.

Materials and Methods

We conducted our study at Chittagong Medical College Hospital (CMCH), Chittagong, Bangladesh, during August 2014–September 2015. We enrolled into the study all consenting patients ≥12 years old who were admitted with a febrile illness to the medical wards and referred to the hospital's malaria screening service with a history of fever for <3 weeks. Written informed consent was provided by all patients before inclusion in the study or by their relatives if the patient lacked capacity for providing consent. The study was approved by Chittagong Medical College ethics committee in Bangladesh and the Oxford Tropical Research Ethics Committee, United Kingdom.

We collected admission blood samples and convalescent-phase blood samples (taken 7–14 days apart, where possible) into EDTA tubes and separated the samples into packed cells and plasma before storage at -30°C. We subjected packed cell admission samples of all patients to DNA extraction for real-time PCR screening by using the 47-kDa *htra* gene–based assay for *Orientia* spp. and the 17-kDa gene–based assay for *Rickettsia* spp. We subsequently confirmed positive results by nested PCR (nPCR) assays with product sequencing. For *Orientia* spp., we targeted the 56-kDa and 47-kDa gene targets. For *Rickettsia* spp., we targeted 17-kDa and performed *ompB* real-time PCR and *gltA* nPCR, as previously described (*9*,*10*).

We aligned the resulting DNA sequences for construction of phylogenetic trees by using CLC Sequence Viewer 7.0.2 (http://www.clcbio.com). For serologic testing, all patient plasma samples underwent indirect immunofluorescence assays (IFA) by using slides from the Australian Rickettsial Reference Laboratory coated with *O. tsutsugamushi* (strains Karp, Kato, and Gilliam) for scrub typhus or *R. typhi* (Wilmington strain) for murine typhus. We used the following stringent diagnostic positivity criteria for scrub and murine typhus: a baseline IgM titer of ≥3,200 or a 4-fold rise to ≥3,200. In the absence of regional serologic positivity criteria for Bangladesh, we selected these cutoffs on the basis of experience from an area where scrub typhus is highly endemic (*11*). In suspected cases of *R. felis* infection, we conducted IFA by using dedicated IFA slides from the Australian Rickettsial Reference Laboratory. We conducted statistical analyses by using Stata 14 (StataCorp LLC, College Station, TX, USA).

Results

We screened 901 patients for enrollment; 794 patients met the enrollment criteria and, of these, 416 gave consent and were enrolled into the study. A total of 414 patient admission samples were available for PCR and 415 for serologic testing; 256/416 (62%) patients were followed up to provide paired samples. Of the enrolled patients, 16.8% (70/416) had a robust diagnosis of scrub typhus and 5.8% (24/416) of murine typhus by PCR, serologic testing, or both (Table). Two patients had evidence of both typhus group and scrub typhus infection, and 2 patients were found to have undifferentiated *Rickettsia* spp. infections. Samples from 2 patients were positive for *R. felis* (1 patient's blood was positive for *R. felis* by 17kDa nPCR and sequencing; the second patient was positive for *O. tsutsugamushi* by 47kDa and 56kDa nPCR and 56kDa gene sequencing from blood and eschar, but also had a superficial eschar swab positive for *R. felis* by 17kDa nPCR and sequencing, suggestive of scrub typhus infection with possible skin carriage of *R. felis* on the skin or eschar). Both of these patients with PCR evidence of *R. felis* infection were serologically negative (titer <1:10) by *R. felis*–specific IFA. In this prospective cohort of hospitalized febrile patients, 23.1% (96/416) of the fevers were attributable to rickettsial illnesses.

We plotted the geographic distribution of scrub typhus and murine typhus cases (Figure 1), reflecting the catchment area of the hospital in southeast Bangladesh. The case-patient with blood PCR positivity for *R. felis* was from urban Chittagong, whereas the case-patient with eschar swab positivity for *R. felis* and blood positivity for *O. tsutsugamushi* came from a rural area. Only 12% (8/67) of patients with scrub typhus came from urban areas, compared with 27% (84/310) of those without evidence of rickettsia ($p = 0.009$).

We observed 2 peaks of scrub typhus patient admissions during the study period, 1 in the cooler months of November and December, when 32/72 (44%) patients were found to be positive for scrub typhus, and the other before the rainy season in April and May, with 6/34 (18%) of cases. Murine typhus cases peaked in the months before the rainy season (Figure 2).

Among all patients with rickettsial illnesses, the most common complaints were headache, anorexia, and myalgia, whereas rash was only detected in 6/96 (6%) of patients. In

Table. Results of PCR and serologic tests for rickettsial illness among 416 patients, Chittagong Medical College Hospital, Chittagong, Bangladesh, August 2014–September 2015*

Organism and test type	No. positive/no. tested (%)
Orientia tsutsugamushi	70/416 (16.8)
Blood PCR, rPCR 47-kDa positive	45/414 (10.9)
nPCR 47 kDa positive	45/45 (100)
nPCR 56 kDa positive	45/45 (100)
Eschar swab, rPCR 47 kDa and n56kDa positive; crust (n = 1), swab (n = 3)	3/416 (0.7)
Indirect immunofluorescence assay	57/415 (13.7)
Admission titer ≥3,200	54/415 (13.0)
4-fold rise to ≥3,200	31/255 (12.1)
PCR+ and serology+, 32/70 (45.7% of ST positives)	32/413 (7.7)
PCR+ and serology–, 13/70 (18.6% ST positives)	13/413 (3.1)
PCR– and serology+, 25/70 (35.7% of ST positives)	25/413 (6.0)
Rickettsia spp.	29/416 (7.0)
Blood PCR, rPCR 17 kDa positive	23/414 (5.6)
nPCR 17 kDa positive	16/23 (69.6)
Rickettsia typhi, 24/29 (83.0%) of *Rickettsia* spp.	24/416 (5.8)
Blood PCR	17/414 (4.1)
rPCR *OmpB* positive	12/414 (2.9)
nPCR 17-kDa sequencing	15/16 (93.8)
Indirect immunofluorescence assay	15/415 (3.6)
Admission titer ≥3,200	11/415 (2.7)
4-fold rise to ≥3,200	5/255 (2.0)
PCR+ and serology+, 8/24 (33.3% of MT positives)	8/413 (1.9)
PCR+ and serology–, 9/24 (37.5% of MT positives)	9/413 (2.2)
PCR– and serology+, 7/24 (29.1% of MT positives)	7/413 (1.7)
Undifferentiated *Rickettsia* spp., 3/29 (10.3% of *Rickettsia* spp.)	3/416 (0.7)
rPCR 17-kDa positive, *ompB* negative	3/416 (0.7)
nPCR 17-kDa negative, *gltA* negative	3/416 (0.7)
MT serology negative	3/416 (0.7)
Rickettsia felis	2/416 (0.5)
Blood PCR, 17-kDa rPCR and nPCR	1/416 (0.2)
Eschar swab, 17-kDa rPCR and nPCR	1/416 (0.2)
All rickettsial illnesses†	96/416 (23.1)

*MT, murine typhus; nPCR, nested PCR; rPCR, real-time PCR; ST, scrub typhus.
†Twenty-nine patients had evidence of *Rickettsia* spp. Infection; 70 had evidence of *O. tsutsugamushi* infection. Because 2 case-patients had mixed blood *O. tsutsugamushi* and *Rickettsia* spp. infections and 1 case-patient with *O. tsutsugamushi* infection in addition to an eschar-positive swab for *R. felis*, the total number of rickettsial illness cases was 96.

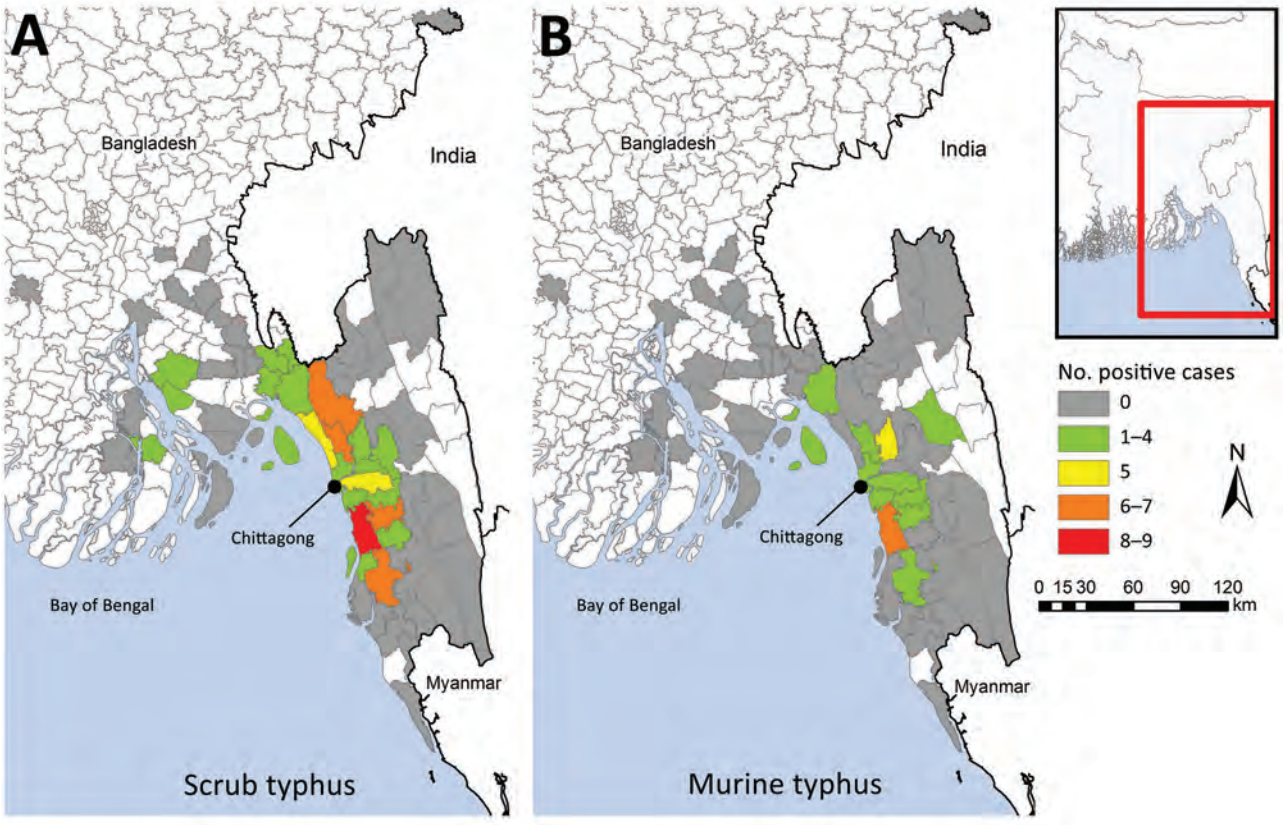

Figure 1. Geographic distribution of scrub typhus (A) and murine typhus (B) cases, Chittagong, Bangladesh, August 2014–September 2015. Inset shows location of enlarged area (red box).

scrub typhus cases, an eschar was found in only 3/70 (4%) of patients, despite training and use of a dedicated checklist for identifying eschars included in the clinical record form. The blood PCR–positive *R. felis* case (SW148) had a different manifestation than other rickettsioses: an itchy vesicular–petechial rash similar to spotted fever group rickettsioses that started periorally and distributed to the trunk and extremities. The patient reported contact with rats in the 3 weeks before illness onset. Overall, 4 deaths were attributable to typhus during this study (3/70 [4.3%] of the patients with scrub typhus and 1/28 [3.6%] patient in the murine typhus group). Of the rickettsia-negative case-patients, 14/320 (4.4%) died. All 3 of the patients with scrub typhus who died had clinical evidence of meningoencephalitis. At study enrollment, the first patient had a Glasgow Coma Scale of 7, severe respiratory distress, new atrial fibrillation with a rapid ventricular response, and hypotension with cold peripheries, consistent with septic shock. The second patient had impaired consciousness, meningism, dyspnea, chest pain, and cough. The third patient had a Glasgow Coma Scale of 12, with convulsions and a cough with severe respiratory distress. The patient with murine typhus who died had severe diarrhea, progressive impairment of consciousness, and renal failure.

Most 56-kDa gene sequences (cropped to ≈450 bp length) clustered with Karp and Karp-like sequences, previously described from Thailand (*12*), but we also observed a cluster of Gilliam-like strains. One sequence (SW275) grouped closely with the Thai animal TA763 strain and another (SW228) with the Kato reference strain (Figure 3). We found no evidence of substantial divergence from known *O. tsutsugamushi* strains or potential new *Orientia* species, and *Orientia chuto* sp. nov. from Dubai remains highly distinct in the 47-kDa gene sequence phylogenetic tree (online Technical Appendix Figure, https://wwwnc.cdc.gov/EID/article/24/4/17-0190-Techapp1.pdf) (*13,14*). Pairwise gene–gene sequence similarity values between *O. tsutsugamushi* samples from Bangladesh and reference strains (partial 56-kDa gene sequences) showed that the largest proportion of 56-kDa gene sequences were similar to the Karp reference strain or the Thai Karp-like strain UT76, followed by Gilliam (online Technical Appendix Table).

Most 17-kDa sequences (cropped to 314 bp) obtained from patient blood showed highest homologies to the *R. typhi* Wilmington strain, the TH1527 Thai strain from Chiangrai, and recently described strains from Laos and Yucatan, Mexico (GenBank accession nos. AE017197, CP003398,

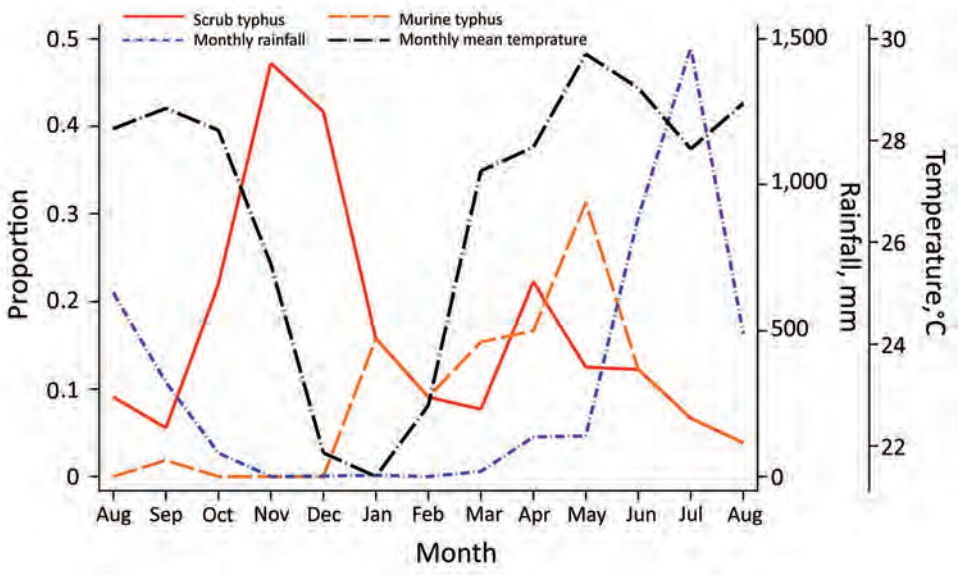

Figure 2. Seasonality of scrub typhus and murine typhus–related hospital admissions, Chittagong Medical College Hospital, Chittagong, Bangladesh, August 2014–September 2015. We observed a biphasic pattern in scrub typhus, with an increase of cases in the cooler months and a smaller peak before the rainy season.

KC283066, and JX198507, respectively). Two 17-kDa sequences from SW148 (blood) and SW211ES (eschar swab) showed 100% homologies with the previously sequenced *R. felis* strain URRWXCal2 and a recent isolate from cat fleas on opossums in Yucatan (GenBank accession numbers CP000053 and KR709306, respectively).

Discussion

Rickettsial illnesses are common causes of fever in hospitalized patients in southeastern Bangladesh. In total, 23% of all undifferentiated febrile case-patients recruited prospectively over a full calendar year were attributable to rickettsial illnesses, predominantly scrub typhus (16.8%) and murine typhus (5.8%). These febrile patients had disease severity that justified hospitalization and an overall mortality rate of 4.3% (18/417). The case-fatality rate for rickettsial illness was high (4% overall) and similar for each group (4.3% [3/70] for scrub typhus, 3.6% [1/28] for murine typhus, and 4.4% [14/320] for non–rickettsial fever).

The nonspecificity of clinical symptoms and lack of readily available accurate diagnostic tools continue to contribute to suboptimal recognition of these common infections. Less than half of the patients with scrub or murine typhus had evidence of positivity in both the PCR and serologic assays, confirming the importance of using both diagnostic modalities. In this study, nearly one quarter of hospitalized, febrile patients had easily treatable typhus cases, justifying consideration of the inclusion of doxycycline as part of the empirical treatment for febrile patients in this region; doxycycline is well-tolerated, inexpensive, and readily available in this setting. This study did not specifically target severe disease or vulnerable populations, but if extrapolation of data from recent reports in neighboring countries is valid, a high mortality rate associated with these groups can be assumed for both scrub and murine typhus. Further investigations in the region are urgently needed (*15*,*16*).

We observed a strong seasonal pattern in incidence, with an increase in scrub typhus cases before and at the end of the rainy season and a decrease in cases in the middle of the dry season, when the temperature fell (Figure 2). Nearly two thirds (64% [45/70]) of all scrub typhus cases occurred during October–December and in April, representing relevant periods of which clinicians should be aware. This biphasic pattern could be associated with reduced exposure by humans because of seasonal variation in their activities, a lower number of infected mites emerging from dry soil, or the transience of immune protection previously observed during multiple reexposures (*17*). The low frequency of eschars observed in scrub typhus patients in this study (4%), coupled with the high seroprevalence observed in the same region, probably reflects the presence of partial immune protection, which suggests continuous exposure in this population (*6*,*17*,*18*). Murine typhus cases peaked in the second half of the dry season, consistent with previously reported seasonality (*19*).

Despite multiple reports of serologic evidence for rickettsial illnesses in Bangladesh, no genotyping or molecular characterization of *Orientia* spp. and *Rickettsia* spp. has been performed to date. This step is an essential prerequisite to the development of rapid diagnostic tests and vaccines in disease-endemic areas. During World War II, the failed attempt to produce a scrub typhus vaccine in cotton rat lungs (termed Operation Tyburn) highlighted the importance of correctly identifying the circulating strains causing human disease. That vaccine, based on a clinically relevant strain identified in troops in the Burma Campaign

at Imphal, failed to protect troops when tested in Malaya, where different *Orientia* strains are present, and showed no evidence for cross-protection when tested during a large outbreak of scrub typhus (*20–22*).

A large, multicenter, high-quality *Orientia* genotyping effort in India recently reported a predominance of Kato-like strains in the south but a high proportion of Karp-like strains in the north (*2*). In our study, we found a spectrum of diverse *Orientia* strains, most of which were Karp-like strains, with Gilliam strains being common, and few samples representing TA763 and Kato-related *O. tsutsugamushi* strains (Figure 3). The dominance of Karp-like strains

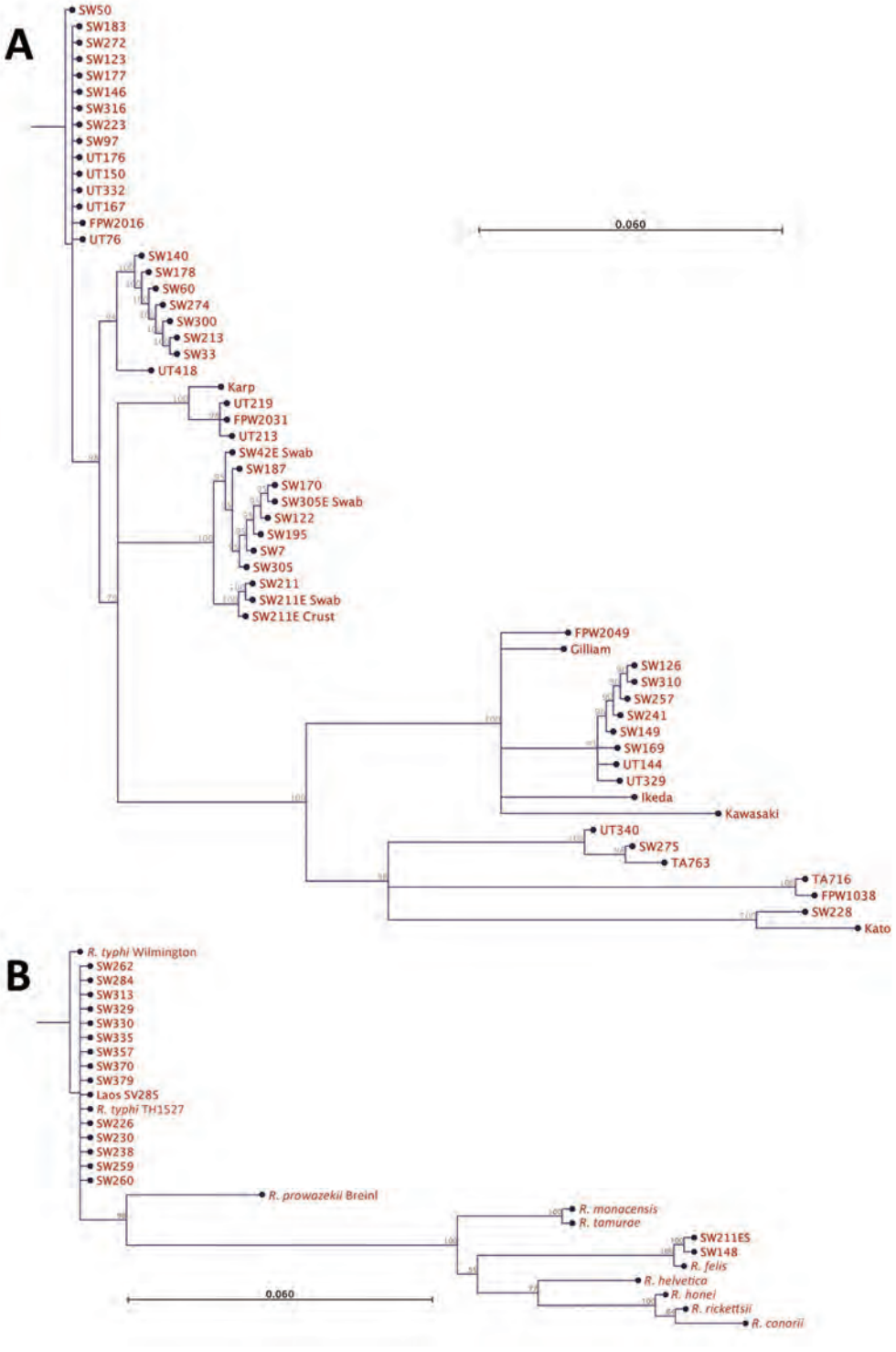

Figure 3. Phylogenetic analysis of pathogens contributing to rickettsial illnesses, Chittagong Medical College Hospital, Chittagong, Bangladesh, August 2014–September 2015. A) Phylogenetic dendrogram based on the nucleotide sequence of the partial open reading frame of the 56-kDa TSA gene (aligned and cropped to ≈450 bp), depicting *Orientia tsutsugamushi* strains in relationship with reference and other strains. *O. tsutsugamushi* genotypes in Bangladesh included Karp, Gilliam, Kato, and TA763 strains, with a predominance of Karp-like strains. B) *Rickettsia* spp. as characterized by 17-kDa gene sequencing (aligned and cropped to 314 bp). The predominant pathogen identified was *R. typhi*. Of note, 2 *R. felis* infection cases were identified, including 1 systemic bloodstream infection and 1 scrub typhus case with eschar swab positivity in patient no. SW211ES (online Technical Appendix Table, https://wwwnc.cdc.gov/EID/article/24/4/17-0190-Techapp1.pdf), whose blood specimen was negative for *R. felis*, suggesting possible skin colonization of *R. felis*. Scale bar indicates nucleotide substitutions per site; branches shorter than 0.002 are shown as having a length of 0.002.

along with frequent Gilliam strains matches well with genotypic findings from nearby populations in northeast India, Myanmar, and Thailand (*2*,*3*,*12*). These findings should inform the development of improved and more accurate rapid diagnostic tests, especially those using antigen-based assays (*23*). We saw no evidence for new or highly divergent strains on the basis of homologies of the more conserved 47kDa *htra* gene sequences, and *O. chuto* sp. nov. remains a distinct outlier (*14*; online Technical Appendix Figure).

This study also identified a large number of murine typhus cases, and the 17-kDa gene–derived *Rickettsia typhi* DNA sequences were remarkably similar to the Wilmington reference strain, the first human Thai isolate from 1965 in Chiangrai, Thailand (TH1527), and a recent case from Laos (SV285) (*24*). Despite the worldwide coastal distribution of murine typhus, as commonly described in various textbooks, little is known about the molecular epidemiology of this potentially severe disease.

The enigmatic role of *R. felis* in human disease is being unraveled, with emerging evidence indicating both pathogenic and opportunistic roles (*25*,*26*). The atypical symptoms of primary infection attributable to *R. felis*, the potential of mosquitoes as transmission vectors, and *R. felis* as a skin contaminant on healthy persons are intriguing recent findings (*27*,*28*). In our study, the blood-borne *R. felis* (SW148) was associated with an unusual papulo-vesicular skin rash. This finding is consistent with yaaf, a previously described vesicular fever representing primo-infection (*27*). A second case (SW211) in a patient with robust evidence of scrub typhus showed the presence of *R. felis* DNA in the superficial eschar swab only, possibly extending previous findings of *R. felis* as a skin contaminant in Africa to the continent of Asia (*29*). The recent evidence for *R. felis* playing a possible role in human disease and skin colonization in Laos and Bangladesh, along with widespread seroprevalence observed in cats and fleas, provide sufficient evidence to pursue investigations into the transmission of this pathogen and its maintenance in nature (*7*,*9*,*28*,*30*).

Limitations of this study include the fact that patients were enrolled from 1 hospital only, limiting the reports to the catchment area. However, this is a large single-study site, given that it is the main tertiary referral hospital for southern Bangladesh (Figure 1). A multicenter effort would provide a more representative range of genotypes across the country, as previously performed in India (*2*). In addition, being hospitalized, the patients in this study were more likely to have symptoms toward the more severe end of the clinical spectrum.

In summary, scrub and murine typhus are important infectious diseases contributing substantially to the burden of undifferentiated fever in Bangladesh. With a mortality rate of 4% each, these diseases clearly require more attention. Empiric treatment strategies should be adapted to cover these treatable rickettsial illnesses, and awareness among medical staff should be promoted regarding the diagnostic difficulties and seasonality of acute febrile illnesses. Studies assessing the prevalence of rickettsial illnesses should use both PCR and serologic testing to avoid missing cases and should cover 1 full calendar year to identify and adjust for seasonality. Further studies focusing on more in-depth assessment of transmission, incidence, and potential impact of these illnesses in Bangladesh are needed to increase awareness, improve empiric treatment strategies, and inform public health interventions aiming to reduce exposure.

Acknowledgments

We are grateful to the patients for their participation in this study.

This study was funded by the Wellcome Trust, London, UK. Wellcome Trust had no role in study design; in the collection, analysis, and interpretation of data; in the writing of the report; or in the decision to submit the paper for publication.

About the Author

Dr. Kingston graduated from medical school in 2007 and was a PhD student when this study was performed. His clinical research interests include the pathophysiology and treatment of severe malaria and typhus in resource-limited settings.

References

1. Paris DH, Day NPJ. Tropical rickettsial infections. In: Farrar J, Hotez PJ, Junghanss T, Kang G, Lalloo D, White NJ, editors. Manson's tropical diseases, 23 ed. Aalborg (Denmark): Elsevier Ltd.; 2013. p. 273–91. https://doi.org/10.1016/B978-0-7020-5101-2.00023-6
2. Varghese GM, Janardhanan J, Mahajan SK, Tariang D, Trowbridge P, Prakash JA, et al. Molecular epidemiology and genetic diversity of *Orientia tsutsugamushi* from patients with scrub typhus in 3 regions of India. Emerg Infect Dis. 2015;21:64–9. http://dx.doi.org/10.3201/eid2101.140580
3. Parola P, Miller RS, McDaniel P, Telford SR III, Rolain J-M, Wongsrichanalai C, et al. Emerging rickettsioses of the Thai–Myanmar border. Emerg Infect Dis. 2003;9:592–5. http://dx.doi.org/10.3201/eid0905.020511
4. Phongmany S, Rolain J-M, Phetsouvanh R, Blacksell SD, Soukkhaseum V, Rasachack B, et al. Rickettsial infections and fever, Vientiane, Laos. Emerg Infect Dis. 2006;12:256–62. http://dx.doi.org/10.3201/eid1202.050900
5. Chheng K, Carter MJ, Emary K, Chanpheaktra N, Moore CE, Stoesser N, et al. A prospective study of the causes of febrile illness requiring hospitalization in children in Cambodia. PLoS One. 2013;8:e60634. http://dx.doi.org/10.1371/journal.pone.0060634
6. Maude RR, Maude RJ, Ghose A, Amin MR, Islam MB, Ali M, et al. Serosurveillance of *Orientia tsutsugamushi* and *Rickettsia typhi* in Bangladesh. Am J Trop Med Hyg. 2014;91:580–3. http://dx.doi.org/10.4269/ajtmh.13-0570
7. Ferdouse F, Hossain MA, Paul SK, Ahmed S, Mahmud MC, Ahmed R, et al. *Rickettsia felis* infection among humans, Bangladesh, 2012–2013. Emerg Infect Dis. 2015;21:1483–5. http://dx.doi.org/10.3201/eid2108.150328

8. Paris DH, Shelite TR, Day NP, Walker DH. Unresolved problems related to scrub typhus: a seriously neglected life-threatening disease. Am J Trop Med Hyg. 2013;89:301–7. http://dx.doi.org/10.4269/ajtmh.13-0064
9. Dittrich S, Phommasone K, Anantatat T, Panyanivong P, Slesak G, Blacksell SD, et al. *Rickettsia felis* infections and comorbid conditions, Laos, 2003–2011. Emerg Infect Dis. 2014;20:1402–4. http://dx.doi.org/10.3201/eid2008.131308
10. Mayxay M, Castonguay-Vanier J, Chansamouth V, Dubot-Pérès A, Paris DH, Phetsouvanh R, et al. Causes of non-malarial fever in Laos: a prospective study. Lancet Glob Health. 2013;1:e46–54. http://dx.doi.org/10.1016/S2214-109X(13)70008-1
11. Lim C, Blacksell SD, Laongnualpanich A, Kantipong P, Day NPJ, Paris DH, et al. Optimal cutoff titers for indirect immunofluorescence assay for diagnosis of scrub typhus. J Clin Microbiol. 2015;53:3663–6. http://dx.doi.org/10.1128/JCM.01680-15
12. Blacksell SD, Luksameetanasan R, Kalambaheti T, Aukkanit N, Paris DH, McGready R, et al. Genetic typing of the 56-kDa type-specific antigen gene of contemporary *Orientia tsutsugamushi* isolates causing human scrub typhus at two sites in north-eastern and western Thailand. FEMS Immunol Med Microbiol. 2008;52:335–42. http://dx.doi.org/10.1111/j.1574-695X.2007.00375.x
13. Jiang J, Paris DH, Blacksell SD, Aukkanit N, Newton PN, Phetsouvanh R, et al. Diversity of the 47-kD HtrA nucleic acid and translated amino acid sequences from 17 recent human isolates of *Orientia.* Vector Borne Zoonotic Dis. 2013;13:367–75. http://dx.doi.org/10.1089/vbz.2012.1112
14. Izzard L, Fuller A, Blacksell SD, Paris DH, Richards AL, Aukkanit N, et al. Isolation of a novel *Orientia* species (*O. chuto* sp. nov.) from a patient infected in Dubai. J Clin Microbiol. 2010;48:4404–9. http://dx.doi.org/10.1128/JCM.01526-10
15. McGready R, Prakash JAJ, Benjamin SJ, Watthanaworawit W, Anantatat T, Tanganuchitcharnchai A, et al. Pregnancy outcome in relation to treatment of murine typhus and scrub typhus infection: a fever cohort and a case series analysis. PLoS Negl Trop Dis. 2014;8:e3327. http://dx.doi.org/10.1371/journal.pntd.0003327
16. Dittrich S, Rattanavong S, Lee SJ, Panyanivong P, Craig SB, Tulsiani SM, et al. *Orientia, Rickettsia,* and *Leptospira* pathogens as causes of CNS infections in Laos: a prospective study. Lancet Glob Health. 2015;3:e104–12. http://dx.doi.org/10.1016/S2214-109X(14)70289-X
17. Smadel JE, Ley HL Jr, Diercks FH, Paterson PY, Wisseman CL Jr, Traub R. Immunization against scrub typhus: duration of immunity in volunteers following combined living vaccine and chemoprophylaxis. Am J Trop Med Hyg. 1952;1:87–99. http://dx.doi.org/10.4269/ajtmh.1952.1.87
18. Paris DH, Chattopadhyay S, Jiang J, Nawtaisong P, Lee JS, Tan E, et al. A nonhuman primate scrub typhus model: protective immune responses induced by pKarp47 DNA vaccination in cynomolgus macaques. J Immunol. 2015;194:1702–16. http://dx.doi.org/10.4049/jimmunol.1402244
19. Civen R, Ngo V. Murine typhus: an unrecognized suburban vectorborne disease. Clin Infect Dis. 2008;46:913–8. http://dx.doi.org/10.1086/527443
20. Audy JR, Savoor SR. Typhus. In: Field JW, Green R, Byron FE, editors. The Institute for Medical Research 1900–1950, Jubilee Volume No. 25. Kuala Lumpur (Malaysia): Government Press; 1951.
21. Zarafonetis C, Baker M. Scrub typhus. In: Coates JB Jr, Havens WP Jr, eds. Internal medicine in World War II, volume 2: infectious diseases. Washington: Typhus Office of the Surgeon General, Department of the Army; 1963.
22. Kellaway CH. The Wellcome Research Institution. Proc R Soc Lond A Math Phys Sci. 1948;193:435–47. http://dx.doi.org/10.1098/rspa.1948.0055
23. Kingston HW, Blacksell SD, Tanganuchitcharnchai A, Laongnualpanich A, Basnyat B, Day NP, et al. Comparative accuracy of the InBios Scrub Typhus Detect IgM Rapid Test for the detection of IgM antibodies by using conventional serology. Clin Vaccine Immunol. 2015;22:1130–2. http://dx.doi.org/10.1128/CVI.00390-15
24. Phommasone K, Paris DH, Anantatat T, Castonguay-Vanier J, Keomany S, Souvannasing P, et al. Concurrent infection with murine typhus and scrub typhus in southern Laos—the mixed and the unmixed. PLoS Negl Trop Dis. 2013;7:e2163. http://dx.doi.org/10.1371/journal.pntd.0002163
25. Mediannikov O, Socolovschi C, Edouard S, Fenollar F, Mouffok N, Bassene H, et al. Common epidemiology of *Rickettsia felis* infection and malaria, Africa. Emerg Infect Dis. 2013;19:1775–83. http://dx.doi.org/10.3201/eid1911.130361
26. Angelakis E, Mediannikov O, Parola P, Raoult D. *Rickettsia felis*: the complex journey of an emergent human pathogen. Trends Parasitol. 2016;32:554–64. http://dx.doi.org/10.1016/j.pt.2016.04.009
27. Mediannikov O, Fenollar F, Bassene H, Tall A, Sokhna C, Trape JF, et al. Description of "yaaf", the vesicular fever caused by acute *Rickettsia felis* infection in Senegal. J Infect. 2013;66:536–40. http://dx.doi.org/10.1016/j.jinf.2012.10.005
28. Slesak G, Inthalath S, Dittrich S, Paris DH, Newton PN. Leeches as further potential vectors for rickettsial infections. Proc Natl Acad Sci U S A. 2015;112:E6593–4. http://dx.doi.org/10.1073/pnas.1515229112
29. Mediannikov O, Socolovschi C, Million M, Sokhna C, Bassene H, Diatta G, et al. Molecular identification of pathogenic bacteria in eschars from acute febrile patients, Senegal. Am J Trop Med Hyg. 2014;91:1015–9. http://dx.doi.org/10.4269/ajtmh.13-0629
30. Ahmed R, Paul SK, Hossain MA, Ahmed S, Mahmud MC, Nasreen SA, et al. Molecular detection of *Rickettsia felis* in humans, cats, and cat fleas in Bangladesh, 2013–2014. Vector Borne Zoonotic Dis. 2016;16:356–8. http://dx.doi.org/10.1089/vbz.2015.1886

Address for correspondence: Daniel H. Paris, Swiss Tropical and Public Health Institute, Socinstrasse 57, 4051, Basel, Switzerland; email: daniel.paris@swisstph.ch

Influence of Population Immunosuppression and Past Vaccination on Smallpox Reemergence

C. Raina MacIntyre, Valentina Costantino, Xin Chen, Eva Segelov, Abrar Ahmad Chughtai, Anthony Kelleher, Mohana Kunasekaran, John Michael Lane

We built a SEIR (susceptible, exposed, infected, recovered) model of smallpox transmission for New York, New York, USA, and Sydney, New South Wales, Australia, that accounted for age-specific population immunosuppression and residual vaccine immunity and conducted sensitivity analyses to estimate the effect these parameters might have on smallpox reemergence. At least 19% of New York's and 17% of Sydney's population are immunosuppressed. The highest smallpox infection rates were in persons 0–19 years of age, but the highest death rates were in those ≥45 years of age. Because of the low level of residual vaccine immunity, immunosuppression was more influential than vaccination on death and infection rates in our model. Despite widespread smallpox vaccination until 1980 in New York, smallpox outbreak severity appeared worse in New York than in Sydney. Immunosuppression is highly prevalent and should be considered in future smallpox outbreak models because excluding this factor probably underestimates death and infection rates.

Smallpox virus was eradicated in 1980 but remains a category A bioterrorism agent (*1*). The only official stocks of the virus are in the United States and Russia (*2*), but unofficial stocks could be present elsewhere. Advances in synthetic biology of poxviruses and availability of the full variola genome sequence make synthesis of smallpox virus in the laboratory possible (*3*). Smallpox could reemerge as a result of bioterrorism or a laboratory accident (*4*); thus, smallpox is a high priority for preparedness planning (*5*). Given that smallpox is eradicated, mathematical models enable researchers to predict the effects of a smallpox epidemic, but these predictions depend critically on the assumptions of the mathematical model.

Many researchers who have developed smallpox models have been optimistic about residual vaccine-induced immunity and assumed a case-fatality ratio (CFR) of 30%, whereas estimates of outbreaks in nonimmune populations suggest a CFR of 50%–70% (*6*). Given the absence of smallpox in the world for nearly 40 years and loss of immunologic boosting from wild-type infection, the CFR of an epidemic today might be higher.

The immunologic status of the population has also changed dramatically in the decades since smallpox eradication. A larger proportion of the population today is unvaccinated, and residual immunity in persons who were vaccinated before 1980 is waning (*7*). In addition, the prevalence of HIV, advances in transplantation, and therapies for cancer and many autoimmune conditions have resulted in unprecedented rates of immunosuppression (*8*). In 1980, when smallpox was eradicated, HIV had not yet manifested a high global burden of disease. Similarly, bone marrow transplantation was in its infancy, and heart–lung transplantations had not yet occurred. The fact that the proportion of unvaccinated and immunosuppressed persons in the population is increasing has not yet been adequately considered in estimations of the effect of reemergent smallpox.

Persons born after 1980 have no immunity to smallpox because they have never been exposed to wild-type virus or been vaccinated. For vaccinated cohorts, immunity wanes over time, and the highest protection is present during the first 5 years after vaccination, possibly waning to zero within 5–10 years (*9*). Furthermore, immunosenescence is a predictable, exponential decline in immune function that occurs after 50 years of age (*10*) and reduces the body's ability to fight infection and respond to vaccines (*11*). This phenomenon further adds to immunosuppression in countries with an aging population. The aim of this study was to estimate the effect of reemerging smallpox in New York, New York, USA, and Sydney, New South Wales,

Author affiliations: School of Public Health and Community Medicine, University of New South Wales, Sydney, New South Wales, Australia (C.R. MacIntyre, V. Costantino, X. Chen, A.A. Chughtai, M. Kunasekaran); Arizona State University, Phoenix, Arizona, USA (C.R. MacIntyre); Monash University and Monash Health, Melbourne, Victoria, Australia (E. Segelov); Kirby Institute, University of New South Wales, Sydney (A. Kelleher); Emory University, Atlanta, Georgia, USA (J.M. Lane)

DOI: https://doi.org/10.3201/eid2404.171233

Australia, 2 large cities with different vaccination histories for which estimates could be made on the population's immunologic status.

Methods

Population

We used Sydney's population in 2015 (*12*), which was estimated using data from the state of New South Wales (*13*). The New York population of the same year was derived from the relevant statistical collection (*14*). We divided both populations into 5-year age groups up through ages 80–84 years and combined the eldest (persons >84 years of age) into a single group (Figure 1, panel A). Each age group was divided into vaccinated and unvaccinated compartments, which were then further subdivided into 3 categories of immunity: immunocompetent, mildly immunosuppressed, and moderate-to-severely immunosuppressed. We assumed that immunosuppressed persons had no residual immunity from vaccination.

Immunosuppressed Population

We considered common types of immunosuppression estimated in an influenza study (*15*). We classified persons into 2 categories of immunosuppression: moderate to severe (called severe in our model) and mild. Severe immunosuppression was defined as a condition in which quantifiable data existed to demonstrate a risk for infection more than twice that of an immunocompetent person. This classification was left as a single category in the absence of reliable methodology to subdivide it. Mild immunosuppression was defined as a condition in which immunosuppression was documented but susceptibility to infection was estimated to be less than twice that of an immunocompetent host. For the analysis, persons with severe immunosuppression were assumed to have 2× and mild immunosuppression 1.5× the susceptibility to infection of a healthy person (*16*).

We sourced data for each city, and when only countrywide data were available, we attributed rates from the countrywide data set to the respective fraction of the population in the city. When age-specific immunosuppression prevalence data were not available, we used yearly age-specific incidence data instead to calculate prevalence age distribution (*17*,*18*).

We estimated the populations living with cancer (*17*,*19*), HIV (*20*,*21*), organ transplants (*22*,*23*), respiratory syndromes such as asthma (*24*,*25*) and chronic obstructive pulmonary disease (*26*,*27*), dialysis (*28*,*29*), and autoimmune diseases (*30*,*31*) and divided these populations into the 2 immunosuppression categories for each city (online Technical Appendix Table 1, https://wwwnc.cdc.gov/EID/article/24/4/17-1233-Techapp1.pdf). We acknowledge that many other diseases are associated with immunosuppression. Our method underestimates the amount of immunosuppression in the population.

Vaccine-Induced Residual Immunity

In the United States, including New York, widespread smallpox vaccination occurred until 1970 (*32*). In contrast, in the geographically isolated island continent of Australia, quarantine was used to protect the population because smallpox was never endemic (*32*). Widespread vaccination never occurred in Australia; only the armed forces and healthcare workers were vaccinated, which occurred until 1979, although reactive vaccination campaigns had been conducted during a smallpox outbreak in Sydney in 1917 (*33*).

For New York, we assumed 80% of the healthy population 40–69 years of age (born before 1975) were previously vaccinated. For Sydney, we estimated the proportion of persons vaccinated by estimating those born before 1980 in the following groups: healthcare workers in Sydney in 2015 (*34*), members of the defense forces, and migrants (>30% in the Sydney population) (*35*), who might have been vaccinated in their country of origin (≈80,000 persons). We estimated that, in Sydney, at most 30% of the total population born before 1980 (persons 35–69 years of age) had been vaccinated. On the basis of a mathematical model (*36*) that estimated waning immunity against severe smallpox as 1.41% per year after vaccination, we calculated the age-specific residual protection for vaccinated persons 40–69 years of age by multiplying that percentage by the number of years from vaccination and subtracting it from 100% starting protection.

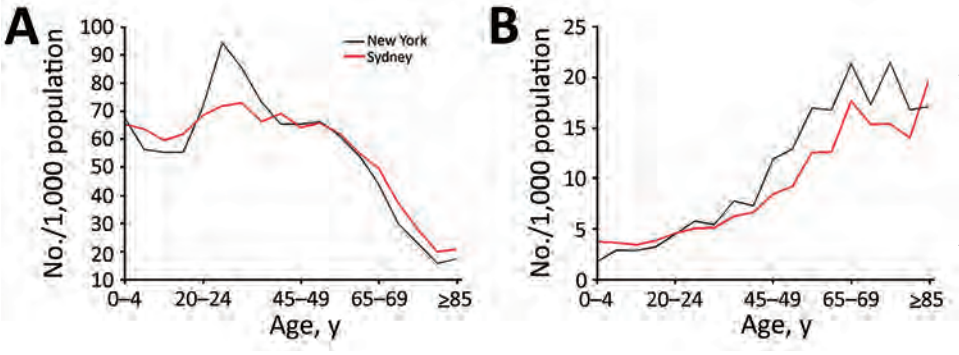

Figure 1. Characteristics of population used to model smallpox transmission, by age group, New York, NY, USA, and Sydney, New South Wales, Australia. Characteristics (e.g., size, age, immunosuppression rates) of populations from 2015 were used. A) Total population; B) immunosuppressed population.

Contact Mixing

In our model, we used the heterogeneous age-specific contact rates from the European mixing patterns study (*37*). We assumed that persons would greatly reduce their social contacts after becoming symptomatic with smallpox (*38*). To account for this change in social contact, we modified the normal contact matrix, multiplying the matrix by a factor ($0 < x < 1$) to reduce the number of contacts per day (*39*). Because of the lack of studies quantifying this reduction, we assumed x to be 0.5, as in a previous study (*39*). Considering severe smallpox types are more substantially prostrating, we applied the reduced contact matrix to hemorrhagic and flat smallpox infections from the first day of illness. For ordinary smallpox, we assumed the behavior change started on the second day and for vaccine-modified smallpox, on the third day.

Disease Types

We categorized smallpox disease into 4 different types defined by infectivity (R_0) and CFRs: hemorrhagic, flat, ordinary, and vaccine-modified. Age-specific and other model parameters (online Technical Appendix Table 2) as well as further model details are explained in the online Technical Appendix.

Smallpox Disease Type Distribution

We assumed infected persons had different probabilities of developing each disease type, depending on their age and immunologic status. The incidence of each disease type within each age group for healthy unvaccinated persons was drawn from historical outbreaks (*9*) (online Technical Appendix Table 3). For healthy unvaccinated persons, hemorrhagic smallpox ratios ranged from 7 cases/1,000 persons infected (in the 5–9-year age group) to 200 cases/1,000 persons infected (in the ≥85-year age group). Flat smallpox age-specific rates were lowest for the 10–14-year age group (30 cases/1,000 persons infected) and reached 180 cases/1,000 persons infected for the oldest age group. For the mildly immunocompromised population, we doubled the age-specific probability of hemorrhagic and flat smallpox. We assumed 100% of severely immunocompromised persons would develop hemorrhagic disease. We assumed the vaccinated subgroup had reduced susceptibility and rates of severe smallpox types. We estimated that 25.3% of vaccinated persons would get vaccine-modified smallpox (*9*). We applied a waning immunity function over time at a rate of 1.41% per year from vaccination (*36*) and assumed the rates of hemorrhagic and flat smallpox would increase with time from vaccination while rates of vaccine-modified smallpox would decrease with time from vaccination (online Technical Appendix Table 4).

Mathematical Model

We constructed a modified SEIR (susceptible, exposed, infected, recovered) model for smallpox transmission (online Technical Appendix Table 2). The population was divided into vaccinated and unvaccinated compartments, which were then further subdivided into 3 categories of immunity: immunocompetent, mildly immunosuppressed, and moderate-to-severely immunosuppressed. The model used ordinary differential equations to move populations into epidemiologic states related to their smallpox infectious status: susceptible, infected, prodromal, infectious, recovered, or dead. Once infected, populations were moved into the next state on the basis of disease duration rates. To obtain the age-specific force of infection (i.e., the rate at which susceptible persons acquire smallpox), we used the Euler approximation to make discrete contact rates, assuming the rates were proportional to the patterns observed in the United Kingdom. Then, to account for the different infectivity rates of different smallpox types, we estimated the transmission parameter β (i.e., the probability of getting infected from a contact) for each smallpox disease type to calculate the R_0 for hemorrhagic, flat, ordinary, and vaccine-modified smallpox. Finally, we multiplied the force of infection by a parameter (α_1, α_2, α_3, α_4; online Technical Appendix Table 2) to account for the different susceptibility levels of different populations.

The model ran for 100 simulated days. We assumed an attack in a crowded public space, such as an airport, and started the epidemic with 51 infected in New York and 29 in Sydney to reflect the same attack rate for each population. We assumed a dynamic population updated each day using the birth (*40*) and age-specific death rates (*41*,*42*) from 2014 for both cities.

Sensitivity Analysis

We conducted a sensitivity analysis on the assumption of waning immunity, reducing immunity by 0.7% per year (approximately half the value used in the base case scenario [i.e., the first scenario discussed]). We present results for 3 different assumptions about residual vaccine immunity: no residual immunity, base case immunity (1.41% waning immunity per year), and high residual immunity (0.7% waning immunity per year). We also conducted a sensitivity analysis to test the model outputs without considering population immunosuppression, which has been the approach in most past models (*43*).

Results

Population and Immunity Levels

We examined the population age distributions of New York and Sydney. Sydney has a higher percentage of persons <20 and >55 years of age than New York (Figure 1, panel A), whereas New York has a higher proportion of persons 20–39 years of age than Sydney. We estimated that 4.54% of New York's population and 3.76%

of Sydney's population are severely immunocompromised, 14.81% of New York's population and 12.95% of Sydney's population are mildly immunocompromised, 59.14% of New York's population and 72.56% of Sydney's population are healthy unvaccinated, and 21.51% of New York's population and 10.73% of Sydney's population are healthy vaccinated. Similar proportions of the 2 cities' populations (19% in New York and 17% in Sydney) are immunosuppressed (Figure 1, panel B). New York has a higher proportion of the population vaccinated (21%) than Sydney (10%).

Base Case Scenario

We analyzed age-specific infection (Figure 2, panel A) and death (Figure 2, panel B) rates using the base case scenario (medium immunity level) including the immunosuppressed population. Persons 5–19 years of age are at highest risk for smallpox infection in both cities (Figure 2, panel A). Although the proportion of persons infected in both cities is similar among the 0–19-year age groups, ≈25% more persons in New York than Sydney become infected among the 20–39-year age groups.

Cumulative deaths per 1,000 population increase with age starting with persons ≥20 years of age (Figure 2, panel B). Deaths peak in the 65–69-year age group in both cities, reaching 1.2 deaths/1,000 population for New York and 0.9 deaths/1,000 population for Sydney 60 days after the start of the outbreak; rates increase again in those ≥80 years of age. The New York population also has a smaller peak in deaths in the 35–39-year age group. Although the spread of infection is mostly driven by higher contact rates among persons of young age groups, the peaks in death reflect the distribution of the immunosuppressed population (Figure 1, panel B; Figure 2, panel B). The effect of residual immunity is more apparent in New York trends, which show a greater decrease in infections and cumulative deaths in the age groups that were previously vaccinated (40–65 years of age).

Looking at total rates over time, New York (Figure 3, panels A, C) and Sydney (Figure 3, panels B, D) have similar exponential growths of infection rates, with slightly higher trends for New York. The rate of infection reaches 0.094 infected/1,000 population for New York and 0.084 infected/1,000 population for Sydney 50 days after the smallpox introduction and increases to 0.496 infected/1,000 population for New York and 0.452 infected/1,000 population for Sydney by 70 days. The death rates are 0.028 deaths/1,000 population for New York and 0.025 deaths/1,000 population for Sydney after 50 days and reach 0.151 deaths/1,000 population for New York and 0.133 deaths/1,000 population for Sydney by 70 days.

Residual Immunity Analysis

Infection and death rate estimates for New York, where vaccine coverage is more than double that of Sydney, are more sensitive to assumptions of residual immunity. New York (Figure 3, panel A) has lower rates of infection than Sydney (Figure 3, panel B) only in the scenario of high residual immunity. At day 50 of the outbreak, rates are ≈15% (base case residual immunity) and 31% (high residual immunity) lower in New York and 10% (base case residual immunity) and 17% (high residual immunity) lower in Sydney with residual immunity than without residual immunity. Differences in infection and death rates among different residual immunity assumptions increased with time. Regarding the impact on age-specific rates in New York (Figure 4, panel A) and Sydney (Figure 4, panel B), the assumption of high residual immunity produced lower death rates for the older age groups.

Immunosuppression Analysis

Infection and death rates increase when including (vs. excluding) immunosuppression parameters in the model; greater differences are seen between New York's infection rates (Figure 3, panel C) and Sydney's infection rates (Figure 3, panel D). The difference in rates increases with time, reaching ≈20% in New York and 18% in Sydney at day 50 from the start of the outbreak and 28% for New York and 25% for Sydney at day 70. Although including immunosuppression estimates into the model produced similarly higher infection rates for each age group (less for the 0–4-year age group), differences in death rates increased with age (Figure 4).

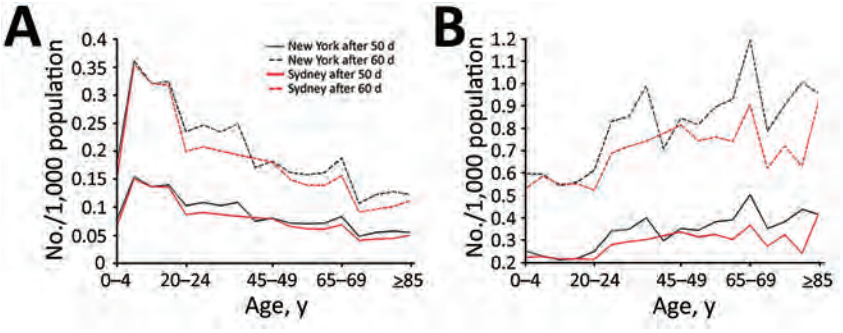

Figure 2. Smallpox infection and death rates of population for base case scenario and for scenario including immunosuppression in model, by age group, New York, NY, USA, and Sydney, New South Wales, Australia. Characteristics (e.g., size, age, immunosuppression rates) of populations from 2015 were used. A) Infection rate 50 and 60 days after start of smallpox outbreak; B) cumulative deaths in population 50 and 60 days after start of smallpox outbreak.

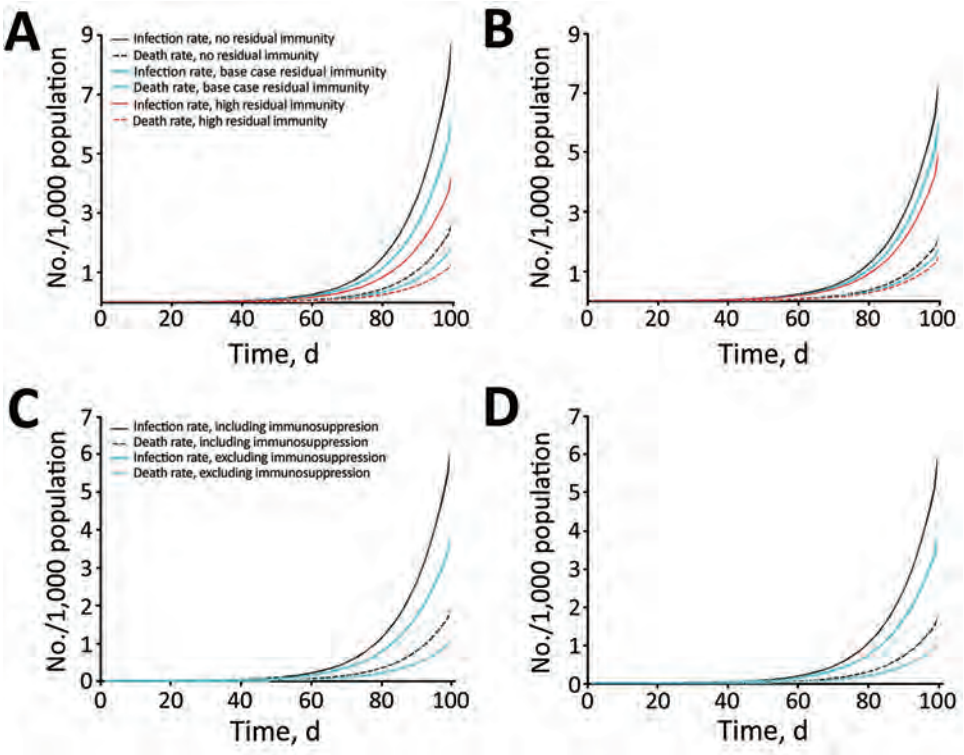

Figure 3. Smallpox infection and death rates over time considering different immunologic factors included in model, New York, NY, USA, and Sydney, Australia. Characteristics (e.g., size, age, immunosuppression rates) of populations from 2015 were used. A) Rates for New York, considering different levels (none, base case, and high) of residual vaccine immunity with the inclusion of immunosuppressed population. B) Rates for Sydney, considering different levels (none, base case, and high) of residual vaccine immunity with the inclusion of immunosuppressed population. C) Rates for New York, including and excluding immunosuppression with base case level of residual vaccine immunity. D) Rates for Sydney, including and excluding immunosuppression with base case level of residual vaccine immunity.

Discussion

With each passing year, population immunosuppression is a more influential determinant than residual vaccine immunity of the severity of a smallpox epidemic. Although the spread of disease is highest in younger age groups, driven mostly by their higher contact rates, higher death rates were seen in older populations, reflecting the prevalence of immunosuppression.

The differences between New York, which has high vaccination coverage (an estimated ≈22% of the population), and Sydney, which has low (≈10%) vaccination coverage, demonstrate that residual immunity assumptions are not as influential in Sydney as in New York. However, the consideration of population immunosuppression, from medical conditions to iatrogenic factors, strongly affects disease transmission and deaths in both cities. This large population subset must be considered when modeling the impact of any infectious disease outbreak. We estimated conservatively that almost 1 in 5 persons in New York and 1 in 6 persons in Sydney (and higher for the 60–64-year age group) are living with some degree of immunosuppression. Although New York has higher rates of immunosuppression for the 25–84-year age groups, Sydney has higher rates than New York for the youngest (0–19 years) and the oldest (≥85) populations.

Residual immunity affects age-specific infection and death rates, with both cities showing the highest infection rates for unvaccinated young persons 5–19 years of age. However, death rates rise after 40 years of age, despite higher vaccination coverage in this age group. For Sydney, even an assumption of higher immunity does not affect the infection or death rates greatly because of the low vaccine coverage before 1980. However, residual immunity becomes more influential if we use more optimistic assumptions of waning immunity. Note that persons who have been vaccinated would mount a more robust and rapid response to revaccination in the event of an outbreak and might be better protected after postexposure vaccination. Obtaining a vaccination history and checking for a consistent scar are necessary parts of outbreak management.

Although immunosuppression is a major determinant of the size and distribution of a smallpox outbreak, this fact should not be a major determinant of vaccination policy. Immunosuppression should continue to be an absolute contraindication for vaccination of persons who are not true contacts. Ensuring that persons with immunosuppression (including healthcare workers) avoid contact with persons with smallpox (if possible) should be a priority. Smallpox would always be more pathogenic than vaccinia virus, so any patient with a bona fide exposure to smallpox should be vaccinated with a fully potent vaccinia strain, such as ACAM2000 (*44*). If such patient develops a serious complication, such as eczema vaccinatum or progressive vaccinia, the patient can be treated with ST-246 (Siga Technologies, New York, NY, USA) (*45*).

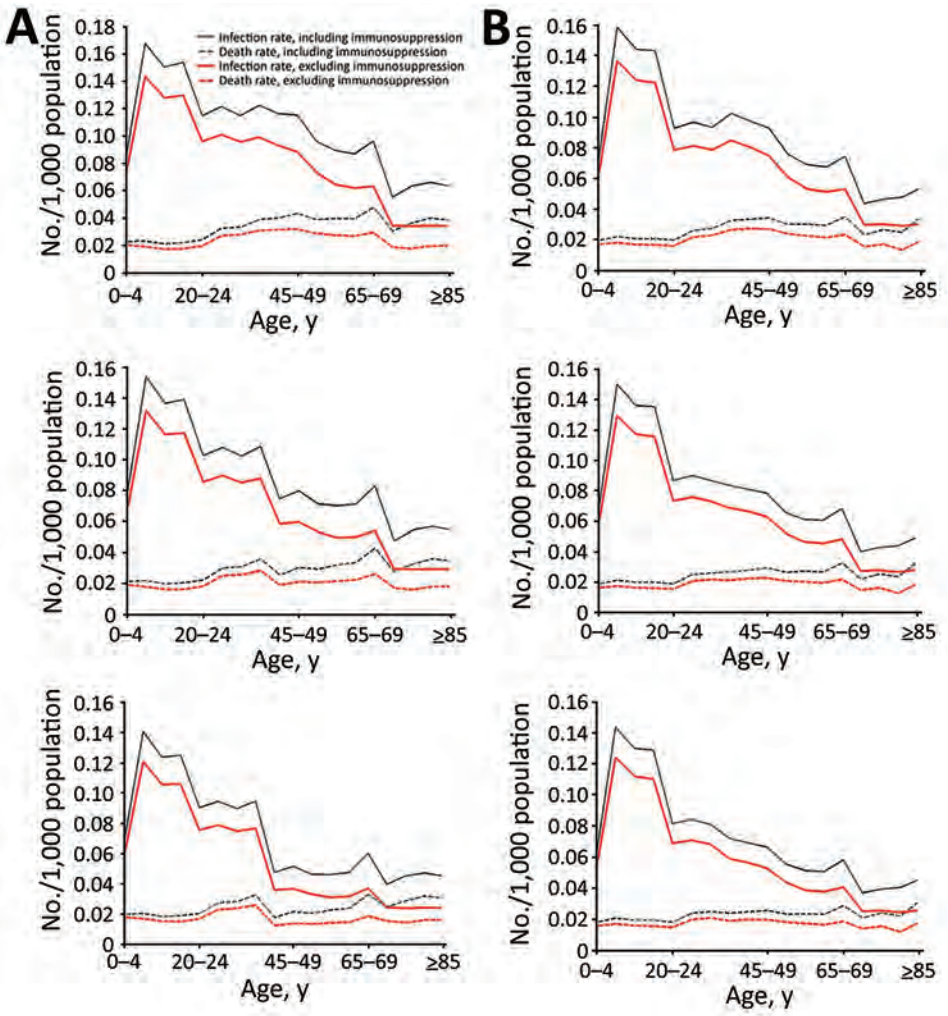

Figure 4. Smallpox infection and death rates with different levels of residual vaccine immunity including and excluding immunosuppression in model of smallpox transmission, by age group, New York, NY, USA, and Sydney, Australia. Characteristics (e.g., size, age, immunosuppression rates) of populations from 2015 were used. A) New York 50 days after start of smallpox outbreak with no (top), base case (middle), and high (bottom) residual vaccine immunity. B) Sydney 50 days after start of smallpox outbreak with no (top), base case (middle), and high (bottom) residual vaccine immunity.

Our study is subject to some limitations. We used an underestimate of immunosuppression; other conditions causing immunosuppression, such as diabetes, were not considered. We also used conservative estimates for the increased risk for infection in immunosuppressed persons and grouped persons with severe and moderate immunosuppression into single categories because of the absence of more specific data to categorize them further by degree of immunosuppression. The contact matrix we used was estimated in a study conducted in the United Kingdom in 2006, which might not necessarily reflect New York or Sydney social contact patterns (*37*). Furthermore, contacts with symptomatic infectious patients will probably drop to near zero once an outbreak has been confirmed and patients are well isolated, assuming adequate health system capacity for isolation and treatment of smallpox patients. The data in the model on age-specific rates of smallpox were obtained from hospitalized patients (*9*), which might overestimate the rates of severe disease in the model outputs.

The speed and vigor with which smallpox control efforts are implemented should be major aspects of control efforts and need to be tested in a model that accounts adequately for immunosuppression. Ensuring adequate hospital care and isolation facilities will also help in epidemic control. During the Ebola epidemic in West Africa, lack of beds resulted in widespread community transmission, and modeling showed that 70% of patients needed to be in treatment facilities to control the epidemic (*46*). The response to severe acute respiratory syndrome, with its rapid control despite the lack of a vaccine or antiviral agent, showed that patient isolation can be very successful (*47*). Experiences with severe acute respiratory syndrome, Ebola, and Middle East respiratory syncytial coronavirus also illustrate the heavy toll on healthcare workers (*48*), who should be assumed to be at high risk for infection in the event of a smallpox outbreak.

Given waning smallpox vaccine immunity (nearly 4 decades since eradication and a dwindling vaccinated population), the influence of population immunosuppression is

greater than that of residual vaccine immunity, yet has not been adequately considered in smallpox epidemic modeling. Advances in medicine and new endemic diseases, such as HIV, have resulted in almost 1 in 5 persons living with immunosuppression in large metropolitan cities. Immunosuppression must be considered in preparedness planning and poses a challenge for vaccination strategies during potential smallpox outbreaks.

About the Author

Dr. MacIntyre is professor of Infectious Diseases Epidemiology at the University of New South Wales, Sydney, and leads a research program on biosecurity, bioterrorism, and emerging infectious diseases, which are her primary research interests.

References

1. Centers for Disease Control and Prevention. General fact sheets on specific bioterrorism agents. 2017 May 9 [cited 2017 Jan 24]. https://emergency.cdc.gov/bioterrorism/factsheets.asp
2. Fenner F, Henderson DA, Arita I, Ježek Z, Ladnyi ID. Smallpox and its eradication. Geneva: World Health Organization; 1987.
3. Koblentz GD. The de novo synthesis of horsepox virus: implications for biosecurity and recommendations for preventing the reemergence of smallpox. Health Secur. 2017;15:620–8. http://dx.doi.org/10.1089/hs.2017.0061
4. MacIntyre CR. Biopreparedness in the age of genetically engineered pathogens and open access science: an urgent need for a paradigm shift. Mil Med. 2015;180:943–9. http://dx.doi.org/10.7205/MILMED-D-14-00482
5. MacIntyre CR, Seccull A, Lane JM, Plant A. Development of a risk-priority score for category A bioterrorism agents as an aid for public health policy. Mil Med. 2006;171:589–94. http://dx.doi.org/10.7205/MILMED.171.7.589
6. Gelfand HM, Posch J. The recent outbreak of smallpox in Meschede, West Germany. Am J Epidemiol. 1971;93:234–7. http://dx.doi.org/10.1093/oxfordjournals.aje.a121251
7. World Health Organization. Smallpox [cited 2017 Feb 28]. http://www.who.int/csr/disease/smallpox/en/
8. Parrino J, Graham BS. Smallpox vaccines: past, present, and future. J Allergy Clin Immunol. 2006;118:1320–6. http://dx.doi.org/10.1016/j.jaci.2006.09.037
9. Rao AR. Smallpox. Bombay (India): Kothari Book Depot; 1972.
10. Montecino-Rodriguez E, Berent-Maoz B, Dorshkind K. Causes, consequences, and reversal of immune system aging. J Clin Invest. 2013;123:958–65. http://dx.doi.org/10.1172/JCI64096
11. Raina MacIntyre C, Menzies R, Kpozehouen E, Chapman M, Travaglia J, Woodward M, et al. Equity in disease prevention: vaccines for the older adults—a national workshop, Australia 2014. Vaccine. 2016;34:5463–9. http://dx.doi.org/10.1016/j.vaccine.2016.09.039
12. Australian Bureau of Statistics. Australian demographic statistics. 2017 [cited 2018 Feb 8]. http://www.ausstats.abs.gov.au/ausstats/subscriber.nsf/0/0DEC5B368C5C2D72CA2581F5001011EB/$File/31010_jun 2017.pdf
13. Australian Bureau of Statistics. Australian historical population statistics, 2014. 2014 Sep 18 [cited 2017 Mar 14]. http://www.abs.gov.au/AUSSTATS/abs@.nsf/mf/3105.0.65.001
14. Baruch College. New York City (NYC) age and sex distribution—by county. 2015 [cited 2017 Mar 17]. http://www.baruch.cuny.edu/nycdata/population-geography/age_distribution.htm#
15. Kunisaki KM, Janoff EN. Influenza in immunosuppressed populations: a review of infection frequency, morbidity, mortality, and vaccine responses. Lancet Infect Dis. 2009;9:493–504. http://dx.doi.org/10.1016/S1473-3099(09)70175-6
16. Finin P, Kosaraju A, Rose E, Rubin H. The role of vaccination, antiorthopoxvirus drug, and social cooperativity in a mathematical model of smallpox control. Biosecur Bioterror. 2013;11:59–72. http://dx.doi.org/10.1089/bsp.2012.0037
17. Australian Government. Cancer in Australia statistics. 2017 [cited 2017 Feb 15]. https://canceraustralia.gov.au/affected-cancer/what-cancer/cancer-australia-statistics
18. New York State. Cancer incidence and mortality by age group, New York State, 2010–2014. 2016 [cited 2017 Mar 17]. https://www.health.ny.gov/statistics/cancer/registry/table6/tb6totalnys.htm
19. New York State, Department of Health. NYS cancer registry and cancer statistics. 2017 [cited 2018 Feb 8]. https://www.health.ny.gov/statistics/cancer/registry/
20. New South Wales Ministry of Health. NSW HIV strategy 2012–2015. 2015 [cited 2017 Feb 15]. http://www.health.nsw.gov.au/endinghiv/Documents/q4-2015-and-annual-hiv-data-report.pdf
21. Centers for Disease Control and Prevention. Diagnoses of HIV infection in the United States and dependent areas, 2015. HIV Surv Rep. 2015;27 [cited 2017 Mar 22]. https://www.cdc.gov/hiv/pdf/library/reports/surveillance/cdc-hiv-surveillance-report-2015-vol-27.pdf
22. New South Wales Ministry of Health. Increasing organ donation in NSW, government plan 2012. 2012 Aug [cited 2017 Feb 15]. http://www.health.nsw.gov.au/organdonation/Publications/increasing-organ-donation.pdf
23. United Network for Organ Sharing. Annual reports. A look back at UNOS' achievements. 2015 [cited 2017 Mar 16]. https://www.unos.org/about/annual-report/
24. Australian Institute of Health and Welfare. Who gets asthma? 2016 [cited 2017 Feb 15]. https://www.aihw.gov.au/reports/asthma-other-chronic-respiratory-conditions/asthma/contents/who-gets-asthma/
25. Centers for Disease Control and Prevention. Most recent asthma data. 2017 [cited 2017 Mar 16]. https://www.cdc.gov/asthma/most_recent_data.htm
26. Australian Institute of Health and Welfare. Chronic diseases data. 2016 [cited 2018 Feb 8]. https://www.aihw.gov.au/reports/life-expectancy-death/grim-books/contents/grim-books#page2
27. Centers for Disease Control and Prevention. Chronic obstructive pulmonary disease. COPD among adults in New York. 2012 [cited 2017 Mar 17]. https://www.cdc.gov/copd/maps/docs/pdf/NY_COPDFactSheet.pdf
28. McDonald S, Chang S, Excell L, editors. Australia and New Zealand dialysis and transplant registry. Adelaide (South Australia, Australia): The Queen Elizabeth Hospital; 2008.
29. Dialysis Patient Citizens. New York. 2015 [cited 2017 Mar 22]. http://www.dialysispatients.org/advocacy/state-resources/new-york
30. Australasian Society of Clinical Immunology and Allergy. Autoimmune diseases. 2017 [cited 2017 Mar 24]. https://www.allergy.org.au/patients/autoimmunity/autoimmune-diseases
31. Cooper GS, Bynum ML, Somers EC. Recent insights in the epidemiology of autoimmune diseases: improved prevalence estimates and understanding of clustering of diseases. J Autoimmun. 2009;33:197–207. http://dx.doi.org/10.1016/j.jaut.2009.09.008
32. Kennedy RB, Lane JM, Henderson DA, Poland GA. Smallpox and vaccinia. In: Plotkin SA, Orenstein WA, Offit PA, editors. Vaccines, 6th ed. Amsterdam: Elsevier Inc.; 2012. p. 718–45.
33. Australian Government Department of Health. Guidelines for smallpox outbreak, preparedness, response and management. 2004 [cited 2017 Apr 4]. http://www.health.gov.au/internet/main/publishing.nsf/content/health-pubhlth-publicat-document-metadata-smallpox.htm

34. Australian Institute of Health and Welfare. Australia's medical workforce 2012. 2014 Jan 24 [cited 2017 Apr 4]. https://www.aihw.gov.au/reports/workforce/medical-workforce-2012/contents/summary
35. Australian Bureau of Statistics. Migration, Australia, 2009–10. 2011 Jun 16 [cited 2017 Aug 3]. http://www.abs.gov.au/AUSSTATS/abs@.nsf/DetailsPage/3412.02009-10?OpenDocument
36. Eichner M. Analysis of historical data suggests long-lasting protective effects of smallpox vaccination. Am J Epidemiol. 2003;158:717–23. http://dx.doi.org/10.1093/aje/kwg225
37. Mossong J, Hens N, Jit M, Beutels P, Auranen K, Mikolajczyk R, et al. Social contacts and mixing patterns relevant to the spread of infectious diseases. PLoS Med. 2008;5:e74. http://dx.doi.org/10.1371/journal.pmed.0050074
38. Van Kerckhove K, Hens N, Edmunds WJ, Eames KTD. The impact of illness on social networks: implications for transmission and control of influenza. Am J Epidemiol. 2013;178:1655–62. http://dx.doi.org/10.1093/aje/kwt196
39. Del Valle SY, Hyman JM, Chitnis N. Mathematical models of contact patterns between age groups for predicting the spread of infectious diseases. Math Biosci Eng. 2013;10:1475–97. http://dx.doi.org/10.3934/mbe.2013.10.1475
40. Mundi I. Historical data graphs per year. 2015 Jun 30 [cited 2017 May 8]. http://www.indexmundi.com/g/g.aspx?v=25&c=as&l=en
41. Australian Bureau of Statistics. Deaths, year of occurrence, age at death, age-specific death rates, sex, states, territories and Australia. 2017 [cited 2017 May 8]. http://stat.data.abs.gov.au/Index.aspx?Queryid=457
42. Kochanek KD, Murphy SL, Xu J, Tejada-Vera B. Deaths: Final Data for 2014. Natl Vital Stat Rep. 2016;65:1–122.
43. Ren Y, Ordóñez F, Wu S. Optimal resource allocation response to a smallpox outbreak. Comput Ind Eng. 2013;66:325–37. http://dx.doi.org/10.1016/j.cie.2013.07.002
44. Berhanu A, King DS, Mosier S, Jordan R, Jones KF, Hruby DE, et al. Impact of ST-246® on ACAM2000™ smallpox vaccine reactogenicity, immunogenicity, and protective efficacy in immunodeficient mice. Vaccine. 2010;29:289–303. http://dx.doi.org/10.1016/j.vaccine.2010.10.039
45. Grosenbach DW, Jordan R, Hruby DE. Development of the small-molecule antiviral ST-246 as a smallpox therapeutic. Future Virol. 2011;6:653–71. http://dx.doi.org/10.2217/fvl.11.27
46. Meltzer MI, Atkins CY, Santibanez S, Knust B, Petersen BW, Ervin ED, et al.; Centers for Disease Control and Prevention. Estimating the future number of cases in the Ebola epidemic—Liberia and Sierra Leone, 2014–2015. MMWR Suppl. 2014;63:1–14.
47. Guan Y, Zheng BJ, He YQ, Liu XL, Zhuang ZX, Cheung CL, et al. Isolation and characterization of viruses related to the SARS coronavirus from animals in southern China. Science. 2003;302:276–8. http://dx.doi.org/10.1126/science.1087139
48. Heymann DL. Smallpox containment updated: considerations for the 21st century. Int J Infect Dis. 2004;8(Suppl 2):S15–20. http://dx.doi.org/10.1016/j.ijid.2004.09.005

Address for correspondence: Valentina Costantino, University of New South Wales Faculty of Science, SPHCM, Kensington Gate 9, Sydney, New South Wales 2052, Australia; email: v.costantino@unsw.edu.au

Emerging Coxsackievirus A6 Causing Hand, Foot and Mouth Disease, Vietnam

Nguyen To Anh, Le Nguyen Truc Nhu, Hoang Minh Tu Van, Nguyen Thi Thu Hong, Tran Tan Thanh, Vu Thi Ty Hang, Nguyen Thi Han Ny, Lam Anh Nguyet, Tran Thi Lan Phuong, Le Nguyen Thanh Nhan, Nguyen Thanh Hung, Truong Huu Khanh, Ha Manh Tuan, Ho Lu Viet, Nguyen Tran Nam, Do Chau Viet, Phan Tu Qui, Bridget Wills, Sarawathy Sabanathan, Nguyen Van Vinh Chau, Louise Thwaites, H. Rogier van Doorn, Guy Thwaites, Maia A. Rabaa, Le Van Tan

Hand, foot and mouth disease (HFMD) is a major public health issue in Asia and has global pandemic potential. Coxsackievirus A6 (CV-A6) was detected in 514/2,230 (23%) of HFMD patients admitted to 3 major hospitals in southern Vietnam during 2011–2015. Of these patients, 93 (18%) had severe HFMD. Phylogenetic analysis of 98 genome sequences revealed they belonged to cluster A and had been circulating in Vietnam for 2 years before emergence. CV-A6 movement among localities within Vietnam occurred frequently, whereas viral movement across international borders appeared rare. Skyline plots identified fluctuations in the relative genetic diversity of CV-A6 corresponding to large CV-A6–associated HFMD outbreaks worldwide. These data show that CV-A6 is an emerging pathogen and emphasize the necessity of active surveillance and understanding the mechanisms that shape the pathogen evolution and emergence, which is essential for development and implementation of intervention strategies.

Hand, foot and mouth disease (HFMD) is an emerging infection that has overwhelmed countries in the Asia–Pacific region over the past 2 decades. The outbreak in Sarawak, Malaysia, in 1997 caused 2,628 reported cases and 29 deaths and marked the start of explosive regional HFMD outbreaks in subsequent years. On average, >1 million cases have been recorded in China annually since 2008 (*1*). In Vietnam, the average annual incidence is ≈80,000 cases; an epidemic peak occurred during 2011–2012, resulting in >200,000 cases and >200 deaths (*2*).

HFMD is caused by enterovirus A (genus *Enterovirus*, family *Picornaviridae*), but the epidemic patterns until now have been punctuated by the frequent replacement of dominant pathogens between enterovirus serotypes over time. Enterovirus A71 (EV-A71) and coxsackievirus A16 (CV-A16) have been regarded as the major causes of HFMD (*3*). CV-A6 was isolated in the United States in 1949 (*4*) and has steadily become one of the main viruses causing HFMD outbreaks in Europe, America, and Asia, including China, Japan, Taiwan, and Thailand (*3*,*5*–*10*). Unlike EV-A71, for which the (sub)genogroup designation has been well established (*11*), but similar to other coxsackieviruses (CV-A16 and CV-A10), CV-A6 is arbitrarily divided into several phylogenetic clusters or lineages, from cluster A to F (*12*) or lineage A to E (E1 and E2) (*3*). Cluster A/lineage E2 is distributed worldwide and has frequently been detected in recent outbreaks. We use the term cluster in this article.

Despite the public health burden of HFMD, no antiviral drug has been clinically proven effective. A vaccine for EV-A71 has recently been licensed in China only (*13*), and CV-A16 vaccines (either monovalent or EV-A71/CV-A16 bivalent forms) are under development (*14*,*15*).

The emergence of CV-A6 has further challenged the development of intervention strategies, including vaccines, to reduce the burden of HFMD (*13*). It also emphasizes the need to better understand the molecular evolution of this emerging pathogen, which is essential for development of an effective CV-A6 vaccine in the future (*16*). However, few studies from endemic countries have documented the longitudinal evolution of CV-A6 (*5*,*17*–*19*). In this study, we applied next-generation sequencing to obtain whole-genome sequences for CV-A6 strains sampled from

Author affiliations: Oxford University Clinical Research Unit, Ho Chi Minh City, Vietnam (N.T. Anh, L.N.T. Nhu, H.M.T. Van, N.T.T. Hong, T.T. Thanh, V.T.T. Hang, N.T.H. Ny, L.A. Nguyet, B. Wills, S. Sabanathan, L. Thwaites, H.R. van Doorn, G. Thwaites, M.A. Rabaa, L.V. Tan); Hospital for Tropical Diseases, Ho Chi Minh City (T.T.L. Phuong, P.T. Qui, N.V.V. Chau); Children's Hospital 1, Ho Chi Minh City (L.N.T. Nhan, N.T. Hung, T.H. Khanh); Children's Hospital 2, Ho Chi Minh City (H.M. Tuan, H.L. Viet, N.T. Nam, D.C. Viet); University of Oxford, Oxford, United Kingdom (L. Thwaites, H.R. van Doorn, G. Thwaites, M.A. Rabaa)

DOI: https://doi.org/10.3201/eid2404.171298

primary, secondary, and tertiary referral hospitals in Ho Chi Minh City, Vietnam, during 2011–2015. To investigate the molecular evolution and recent spread of CV-A6, we performed phylogenetic and phylogeographic analysis on both a global scale and within the southern provinces of Vietnam.

Materials and Methods

Patients and Clinical Samples

We obtained the clinical samples used in this study from patients enrolled in an HFMD research program in which outpatients and inpatients with all severities of disease were recruited (*20*). During August 2011–June 2013, we carried out the research program at the pediatric intensive care unit (PICU) of the Hospital for Tropical Diseases in Ho Chi Minh City, Vietnam. This PICU admitted only patients with severe HFMD (the clinical grading system is described in the online Technical Appendix, https://wwwnc.cdc.gov/EID/article/24/4/17-1298-Techapp1.pdf). In the subsequent phase (July 2013–December 2015), we expanded patient enrollment to outpatient clinics, infectious disease wards, and PICUs in 3 major referral hospitals in Ho Chi Minh City (Children's Hospital 1, Children's Hospital 2, and Hospital for Tropical Diseases). We selected for analysis CV-A6–positive throat and rectal swab specimens with sufficient viral load (samples with real-time PCR crossing point values of ≤30 [*21*]) collected in viral transport medium from study participants. The real-time reverse transcription PCR (RT-PCR) methods used are described in the online Technical Appendix.

CV-A6 Whole-Genome Sequencing and Sequence Assembly

We performed whole-genome sequencing of CV-A6 on the selected swabs with sufficient viral load using a previously described MiSeq-based approach (*21*). In brief, we pretreated 110 μL of selected swab specimens in viral transport medium by a centrifugation step at 13,000 rpm for 10 min to remove host cells or large cellular components and followed this step with DNase treatment of the obtained supernatants. We then isolated viral nucleic acid (NA) using a QIAamp viral RNA kit (QIAGEN, Hilden, Germany) and recovered it in 50 μL of the elution buffer (provided with the kit). We subjected 10 μL of the isolated NA to cDNA synthesis using a Super Script III kit (Invitrogen, Carlsbad, CA, USA) and FR26RV-Endoh primer (*21*). We then converted the cDNA to double-stranded DNA using exo-Klenow (Invitrogen) and preamplified the cDNA using Platinum PCR supermix (Invitrogen) and FR20RV primer (*21*). We then purified the PCR product and subjected it to library preparation using a Nextera XT DNA sample preparation kit (Illumina, San Diego, CA, USA). Finally, we sequenced the product using MiSeq reagent kits (Illumina) in a MiSeq platform (Illumina) (*21*).

We performed whole-genome sequence assembly using the Geneious 8.1.5 software package (Biomatters, Auckland, New Zealand) with a reference-based mapping approach. This method involves the mapping of individual reads of each sample to a reference sequence and manual editing of the consensus.

Multiple Sequence Alignment, Recombination Detection, and Phylogenetic Analysis

We performed multiple sequence alignment using MUSCLE (multiple sequence comparison by log-expectation) (*22*), available in Geneious. For Vietnam sequences, we then calculated the percentages of sequence identities among them from the resulting multiple sequence alignment files using Geneious.

We inferred recombination using a combination of methods (Chimera, GENECONV, Maxchi, Bootscan, and Siscan) within RDP4 (Recombination Detection Program version 4) (*22*) using the default settings with recombination supported if >3 methods showed significant values ($p<0.05$) and reconfirmed findings by phylogenetic analysis. We then removed identified recombinants from further phylogenetic analysis.

To investigate the relationship between Vietnam CV-A6 strains and global strains downloaded from GenBank, we constructed maximum-likelihood trees for viral capsid protein 1 (VP1) and complete coding sequences (CDS) using IQ-TREE version 1.4.3 (*23*). The maximum likelihood phylogenetic analysis used the general time reversible (for CDS dataset) and Tamura-Nei 93 (for VP1 dataset) nucleotide substitution models with a gamma distributed among site rate variation (4 rate categories). We assessed support for individual nodes using a bootstrap procedure (10,000 replicates).

We analyzed the phylogeographic history of CV-A6 in Vietnam and worldwide using BEAST version 1.8.3 (https://github.com/beast-dev/beast-mcmc/releases/tag/v1.8.3). We performed this analysis for both complete CDS and VP1 sequences downloaded from GenBank (October 2016) and the sequences obtained from the present study. For GenBank sequences, we excluded all the partial sequences, identical sequences, sequences with internal gaps, recombinant sequences, and sequences without sampling dates or locations. We then performed regression analysis implemented in TempEst (https://academic.oup.com/ve/article/2/1/vew007/1753488) to further exclude sequences with insufficient temporal signals. For global strains, 170 VP1 and 52 complete CDS sequences from China, Finland, France, India, Japan, Spain, Taiwan, and the United Kingdom were included for analysis. For Vietnam sequences, we used 98 sequences. Southern provinces in Vietnam

from where the viruses were sampled were grouped into 3 discrete locations: Ho Chi Minh City (from where about half of the HFMD cases from Vietnam have been reported), southeast provinces (Long An, Can Tho, Tien Giang, Kien Giang, Dong Thap, and Hau Giang provinces), and Mekong Delta provinces (Tay Ninh, Dong Nai, Binh Duong, Binh Phuoc, Ba Ria, and Vung Tau provinces). Small sample sizes from individual provinces precluded phylogeographic analyses at a finer spatial scale.

For all analyses, we used the general time reversible (*24*) (for the CDS dataset) and Tamura-Nei 93 (*25*) (for the VP1 dataset) nucleotide substitution models with a gamma distributed among site rate variation (4 rate categories) (as indicated by IQ-TREE), the strict molecular clock model, and a Bayesian skyline plot (10 groups). We employed a Bayesian Markov chain Monte Carlo framework (available in BEAST) with 800 million steps and sampling every 80,000 steps. We assessed convergence using Tracer version 1.5 (http://tree.bio.ed.ac.uk/software/tracer/). We selected a burn-in threshold of 10% and accepted effective sample size values above 200. Maximum-clade credibility (MCC) trees were then summarized with TreeAnnotator (available in the BEAST package) and visualized in Figtree version 1.4.2 (http://tree.bio.ed.ac.uk/software/figtree).

To estimate the relative genetic diversity of CV-A6 over time, we analyzed CDS and VP1 sequences separately using the same Bayesian skyline method. We submitted the sequences of CV-A6 obtained in this study to the National Center for Biotechnology Information (GenBank accession nos. MF578282–MF578381).

Ethics Considerations

The study was approved by the corresponding institutional review board of the local hospitals in Vietnam where patients were enrolled: Children's Hospital 1, Ho Chi Minh City; Children's Hospital 2, Ho Chi Minh City; and Hospital for Tropical Diseases, Ho Chi Minh City. The study was also approved by the Oxford Tropical Research Ethics Committee and was performed in accordance with the ethics standards noted in the 1964 Declaration of Helsinki and its later amendments, or comparable ethics standards.

Results

Baseline Characteristics of Patients with CV-A6 Infections

During August 2011–December 2015, a total of 514 patients with HFMD had specimens that tested positive for CV-A6, accounting for 23% of the HFMD study participants who were enterovirus PCR positive (n = 2,230). We detected EV-A71 in 36% (812) of the patients, CV-A16 in 10% (240), and CV-A10 in 7% (164). Temporally, the detection rate of CV-A6 in HFMD patients increased from 6% in 2011 to 13% in 2012, 18% in 2013, 32% in 2014, and 29% in 2015 (Figure 1). Complete data on demographics and clinical grades were available from 510/514 CV-A6 infected patients (Table). Although CV-A6–associated HFMD was mostly mild, 93 (18%) patients had grade 2b1, 2b2, or 3 HFMD (i.e., severe HFMD), accounting for 76/76 (100%) of patients with CV-A6 who were enrolled in the first phase of the study and 17/434 (4%) of patients with CV-A6 who were enrolled in the second phase of the study.

CV-A6 Whole-Genome Sequences

From the 514 patients who had CV-A6, we subjected 131 swabs (97 throat swabs and 34 rectal swabs) with sufficient viral load to whole-genome sequencing. Of these, we successfully recovered 100 nearly complete or complete coding sequences (80%). We identified evidence of recombination in 2 CV-A6 sequences (data not shown) and removed these 2 sequences from subsequent phylogenetic analyses.

Phylogeny and Phylogeography

Phylogenetic analyses of 282 VP1 sequences of global strains, including 98 from Vietnam, showed that CV-A6 was grouped into 6 genetic clusters, in agreement with a previous report (*12*). All of the Vietnam CV-A6 isolates

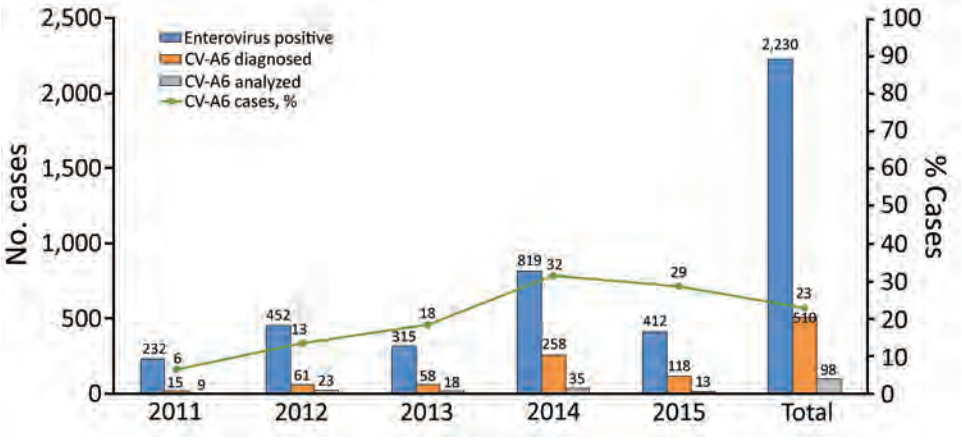

Figure 1. Temporal distribution of PCR-positive hand, foot and mouth disease cases and detection rates of CV-A6 during 2011–2015, Vietnam. CV, coxsackievirus.

Table. Demographics and clinical severity grades for patients with CV-A6–associated HFMD, Vietnam, 2011–2015*

Demographics	Total, n = 510	2011–2012, n = 76	2013–2015, n = 434	Group 1, patients with CDS included in analyses, n = 98	Group 2, patients excluded from phylogenetic analyses, n = 412
Sex					
M	330 (64.7)	50 (65.8)	280 (64.5)	68 (69.4)	262 (63.6)
F	180 (35.3)	26 (34.2)	154 (35.5)	30 (30.6)	150 (36.4)
Age, mo					
Median	16.07	15.23	16.18	15.52	16.17
IQR	11.57–22.46	9.83–24.74	11.85–22.43	10.68–24.48	11.71–22.41
Highest grade					
1	188 (36.8)	0	188 (43.3)	39 (39.8)	149 (36.1)
2a	229 (44.9)	0	229 (52.8)	26 (26.5)	203 (49.3)
2b1	81 (15.9)	68 (89.5)	13 (3.0)	30 (30.6)	51 (12.4)
2b2	5 (1.0)	2 (2.6)	3 (0.7)	1 (1.0)	4 (1.0)
3	7 (1.4)	6 (7.9)	1 (0.2)	2 (2.0)	5 (1.2)
Location					
HCMC	327 (64.1)	54 (71.1)	273 (62.9)	57 (58.2)	270 (65.5)
Mekong Delta†	89 (17.5)	17 (22.4)	72 (16.6)	21 (21.4)	68 (16.5)
Southeast‡	88 (17.3)	5 (6.6)	83 (19.1)	20 (20.4)	68 (16.5)
Others§	6 (1.1)	0	6 (1.4)	0	6 (1.5)

*Values are no. (%) patients except as indicated. CV, coxsackievirus; HCMC, Ho Chi Minh City; HFMD, hand, foot and mouth disease; IQR, interquartile range.
†Long An, Can Tho, Tien Giang, Kien Giang, Dong Thap, and Hau Giang provinces.
‡Tay Ninh, Dong Nai, Binh Duong, Binh Phuoc, Ba Ria, and Vung Tau provinces.
§Binh Thuan (n = 2), Hai Duong (n = 1), Quang Ngai (n = 1), Khanh Hoa (n = 1), and Thanh Hoa (n = 1).

belonged to cluster A (Figure 2), showing nucleotide identity of 91.8%–100% and amino acid identity of 98.6%–100%. This genogroup consists of viruses sampled from various geographic locations worldwide, whereas the CV-A6 strains from Vietnam fell within a viral lineage consisting of CV-A6 strains from China, India, Japan, Taiwan, and the United Kingdom.

Delineating the dispersal of an emerging pathogen between geographic locations and within endemic countries is critical for outbreak control. In-depth phylogeographic analysis for all 13 discrete provinces from where the patients came was uninformative because of the small sample sizes from some provinces. When we conducted the analysis for 3 main discrete geographic locations, the results revealed that CV-A6 spread widely within southern Vietnam during the sampling period (Figure 3, panel A; online Technical Appendix Figure 1, panel A). This finding is in contrast with what has been observed at the international level, at which movement of CV-A6 between endemic countries appears rare (Figure 3, panel B; online Technical Appendix Figure 1, panel B).

Estimation of the time to the most recent common ancestor in the phylogeny including only strains from Vietnam suggested that the CV-A6 lineage that circulated in Vietnam during this time period began circulating within the country by 2010. This estimation is consistent between VP1-based and complete CDS-based analyses, which show time to most recent common ancestor estimates of November 2010 (95% CI May 2010–March 2011) and May 2010 (95% CI February 2010–August 2010), respectively. These estimates suggest that CV-A6 was being transmitted in Vietnam for at least 2 years before becoming the dominant cause of HFMD in 2012. The nucleotide substitution rate of VP1 sequences was estimated to be 7.42×10^{-3} (95% CI 6.1126×10^{-3} to 8.722×10^{-3}) and the nucleotide substitution rate of complete CDS was estimated to be 4.556×10^{-3} (95% CI 4.209×10^{-3} to 4.913×10^{-3}) substitutions per site per year.

CV-A6 Demographics

Because of the relatively small number of CV-A6 whole genome sequences available in GenBank, we first assessed the global demographic history of the lineage using skyline plot analysis on VP1 sequences. The Bayesian VP1-based skyline plot of genogroup A viruses sampled across the world revealed fluctuations in the relative genetic diversity of CV-A6 from 2008 onward, especially during 2010–2012 (Figure 4, panel A), highlighting notable changes in viral diversity. This phenomenon coincided with CV-A6 outbreaks reported worldwide, including the 2008 Finland outbreak and major outbreaks affecting Asia, Europe, and the United States in subsequent years.

Bayesian skyline plot analysis for the CDS of the Vietnamese viruses alone did not suggest any major changes in relative genetic diversity during 2011–2015 compared with a global scale (Figure 4, panel B). Similar results were obtained when the analyses were done for VP1 sequences of the Vietnam strains and CDS of global strains (online Technical Appendix Figure 2).

Discussion

We report the evolutionary process of CV-A6 in Vietnam during 2011–2015. In addition, we summarize its detection rate in HFMD patients and associated demographics and

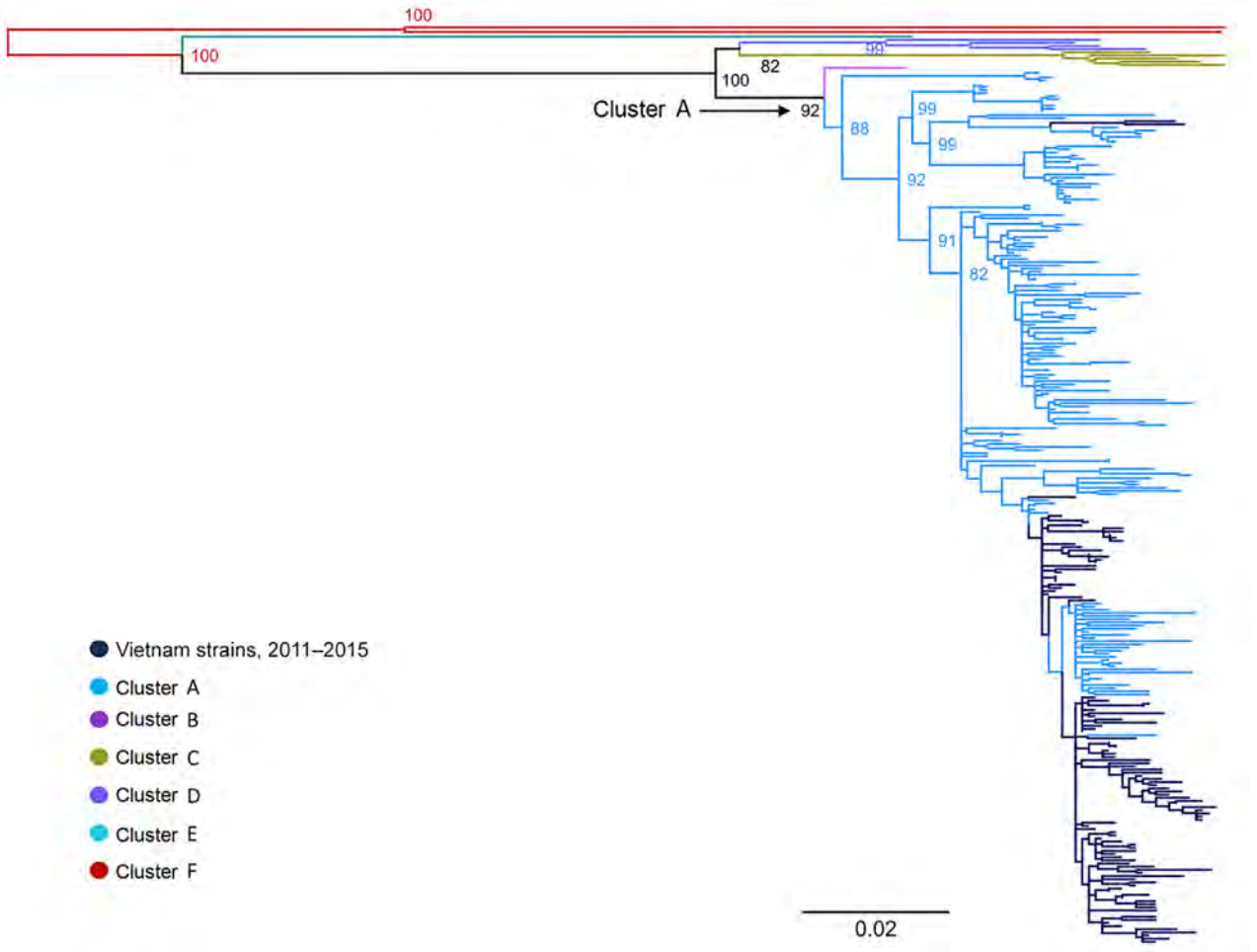

Figure 2. Maximum-likelihood tree of viral capsid protein 1 sequences of coxsackievirus A6 strains from Vietnam and worldwide. Branches are colored by cluster; cluster A, which includes the Vietnam strains, is indicated. Scale bar indicates nucleotide substitutions per site.

clinical outcomes. Of 510 patients with CV-A6 infection, 93 (18%) had severe HFMD (grade 2b1 or above). However, 18% should not be interpreted as the proportion of CV-A6 infections associated with severe disease because most severe cases (76/93 [82%]; Table) came from the first phase of the study, during which only patients with severe HFMD were enrolled. However, when patients with all severities of HFMD were enrolled in the second phase of the study, CV-A6–associated severe HFMD accounted for 4% (17/434; Table) of the total number of CV-A6 patients. This result is in accordance with previous reports showing that HFMD is a mild disease with sporadic severe cases and demonstrates the potential association of CV-A6 with severe HFMD (*26*).

Our analysis placed the Vietnam CV-A6 strains within cluster A of CV-A6. This cluster A includes viruses sampled from various countries worldwide, and has emerged only recently: in Finland in 2008, followed by France, the United Kingdom, and subsequently the United States and countries in Asia in subsequent years (*3*,*5*,*6*,*8*–*10*,*18*). Although this migration highlights the global dispersal of cluster A viruses, and their potential to cause outbreaks worldwide, phylogeographic analysis of global strains did not reveal a high frequency of CV-A6 movement between endemic countries. In contrast, viral transmission between geographic locations within southern Vietnam appeared frequently; Ho Chi Minh City is a likely source of viral circulation given the observed phylogeographic patterns, and transmission is highly connected with other endemic countries in the region and southern provinces in Vietnam through international and domestic transport. This observation is in agreement with previously observed patterns of EV-A71 transmission within and between endemic countries (*20*,*27*).

HFMD affects mostly young children, especially those <5 years of age, and humans are the only known natural host of HFMD-causing enteroviruses. It is therefore likely that human movement is critical to the transmission and spread of HFMD at both global and local scales. Although young children likely play a major role in local transmission

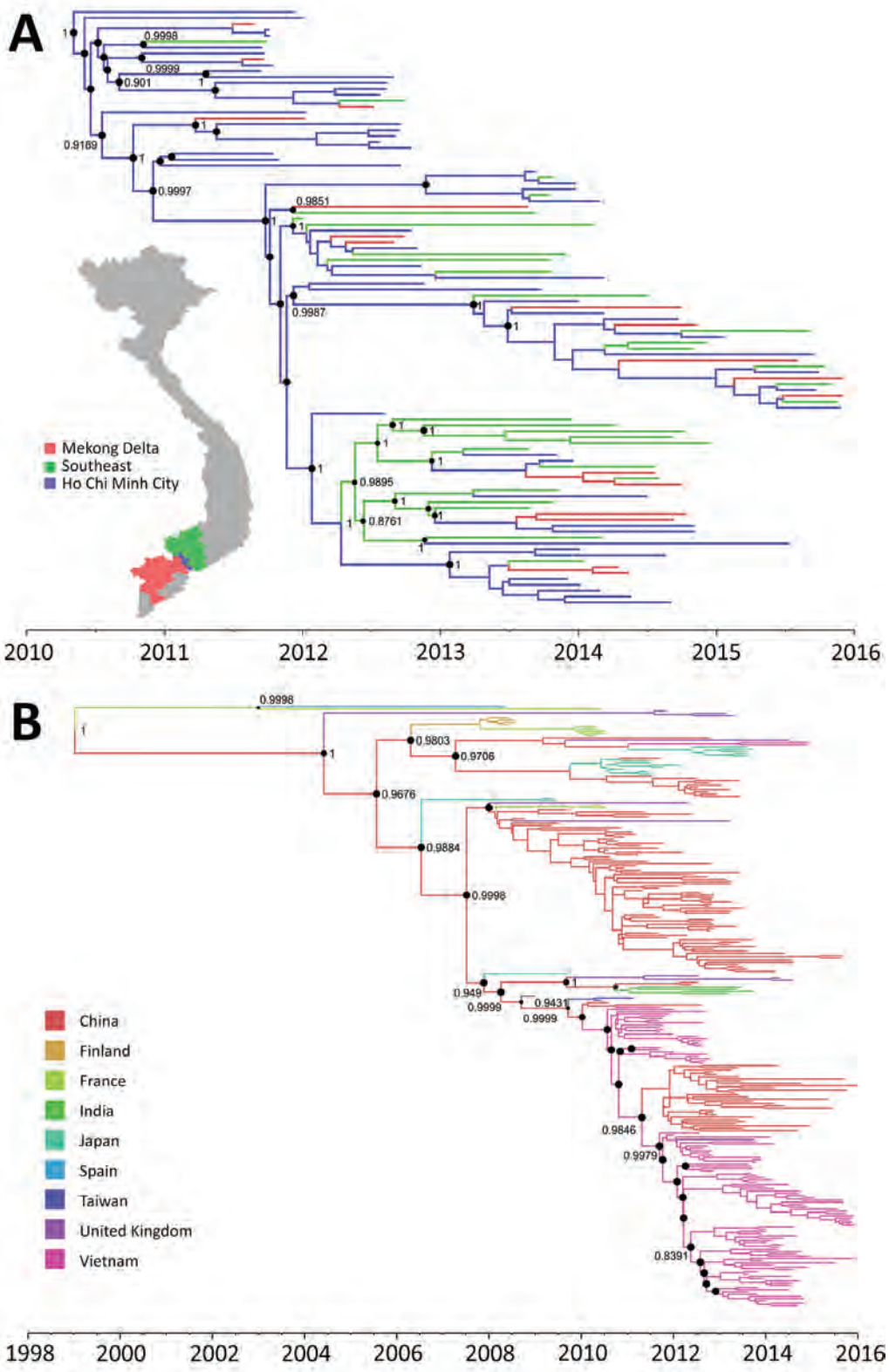

Figure 3. Maximum clade credibility trees illustrating the phylogeography of coxsackievirus A6. A) Complete coding sequence–based tree of Vietnam strains; B) viral capsid protein 1–based tree of global strains. Branches are color-coded according to location of sampling. Posterior probabilities ≥85% and state probabilities ≥75% (black circles) are indicated at all nodes. Map in panel A obtained from https://mapchart.net.

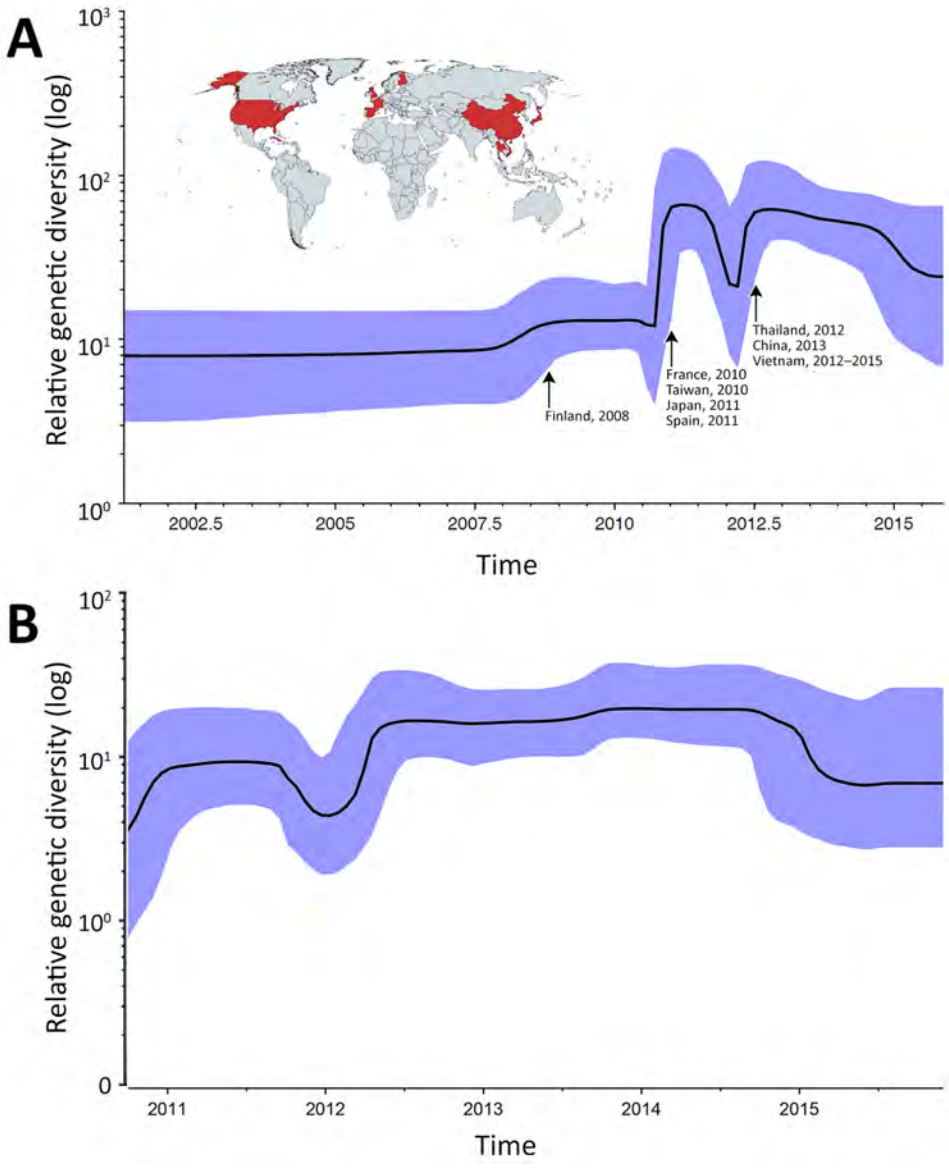

Figure 4. Skyline plots depicting the relative genetic diversity of CV-A6 over time. A) Result obtained from the analysis of viral capsid protein 1 sequences of global strains; B) result obtained from the analysis of complete coding sequences of Vietnam strains. Blue shading indicates 95% highest posterior density interlude. Arrows in panel A indicate worldwide CV-A6 outbreaks and associated fluctuations in relative genetic diversity; map (obtained from https://mapchart.net) illustrates the countries in which CV-A6–associated HFMD outbreaks have been recorded to date (*3*). No sequences from Cuba, Singapore, or the United States fulfilled the selection criteria for the skyline plot and phylogenetic analyses (see Methods section). CV, coxsackievirus.

of these pathogens, asymptomatic adults carrying HFMD-causing viruses have previously been reported (*28*); because adults are more likely to travel longer distances, they may play an integral role in the movement of these viruses across long distances.

Dating analysis based on VP1 and CDS consistently showed that CV-A6 had been circulating in Vietnam for 2 years before it emerged as a cause of illness in 2012 and subsequently become a dominant pathogen of HFMD. This finding parallels previous studies showing that emerging EV-A71 subgenogroups circulated cryptically for 2–3 years before emergence (*20*,*27*). Likewise, although our estimated evolutionary rates of CV-A6 were slightly different between VP1 and complete CDS, this finding is likely because CV-A6 VP1 is the main target of neutralizing antibody (*29*) and is therefore subjected to a higher selection pressure than other viral proteins. Still, our findings were within the ranges of previous estimations for emerging enteroviruses such as EV-A71 (*27*).

Skyline plots generated using global strains illustrate that CV-A6 cluster A maintained a relatively constant population size until 2010–2011, when a sharp increase in relative genetic diversity was detected along with outbreaks in several countries. Notably, although the most recent common ancestor for the Vietnam CV-A6 lineage is inferred to have existed during the first half of 2010, the first CV-A6 infections found in this study were in patients enrolled in September 2011. The skyline plot did not reveal major changes in terms of genetic diversity of the Vietnam CV-A6 strains during the study period, which may suggest that large-scale transmission occurred in the community for some months before its detection in hospitals.

The observed demographic features in this study should be interpreted with caution. For the Vietnam CV-A6 strains, the discordance between the fluctuating numbers of CV-A6 infections detected per year and the relatively constant demographic picture illustrated by the skyline plot may be the result of sampling bias inherent to the study, the initial focus of which was enrollment of patients with severe enough illness to go to the pediatric ICU; only later expansion included patients at outpatient facilities. Viruses of the family *Picornaviridae* (including CV-A6) are ubiquitous, and most infections are asymptomatic. It is therefore possible that the proportion of CV-A6 viruses detected during the first half of this study may have underestimated the overall epidemiologic burden of CV-A6 relative to other HFMD-causing enteroviruses during this time period because of the focus on severe cases, given that CV-A6 is proportionally less likely to cause severe disease than EV-A71. Likewise, for global strains, the skyline plot analysis in this study was in part based on publicly available CV-A6 sequences derived from studies across the world, of which most were from recent epidemic years (online Technical Appendix Figure 3); as such, the dramatic fluctuations in relative genetic diversity shown on the skyline plot in highly sampled epidemic years may be partly attributed to this sampling bias. However, the general trend toward increasing genetic diversity shown in the skyline plot during 2002–2015 would not be strongly affected by this bias and is likely to reflect a true increase in CV-A6 infections and genetic diversity during this period.

Together, these data emphasize the importance of active surveillance for molecular epidemiology of HFMD in disease-endemic countries. It is also critical to identify the underlying mechanisms that shape the evolutionary process and the emergence of new HFMD-causing enterovirus lineages in countries with high HFMD endemicity. Further research in these key areas would have profound implications for the development and implementation of HFMD vaccines. We hypothesize that population immunity and antigenic differences between circulating strains and emergent lineages are key drivers of the transmission dynamics and epidemiology of HFMD; therefore, studies to characterize cross-neutralization titers in serum samples of patients infected with common serotypes, including EV-A71, CV-A6, CV-A10, and CV-A16, to inform vaccine development are needed and ongoing.

Acknowledgments

We thank Le Kim Thanh for her logistic support. We are indebted to the patients and their parents for their participation in this study, and all the nursing and medical staff at the pediatric ICU, infectious disease wards, and outpatient clinics at Children's Hospital 1, Children's Hospital 2, and the Hospital for Tropical Diseases who provided care for the patients and helped collect clinical data.

This work was supported by the Wellcome Trust, UK (101104/Z/13/Z, 106680/B/14/Z, and 204904/Z/16/Z). The funding body did not have any influence on the study design, study conduct, preparation of the manuscript, or decision to publish.

About the Author

Ms. To Anh is a PhD candidate in life science at Open University, Milton Keynes, UK. Her research interests are virus discovery and evolution of emerging pathogens such as enteroviruses.

References

1. Xing W, Liao Q, Viboud C, Zhang J, Sun J, Wu JT, et al. Hand, foot, and mouth disease in China, 2008–12: an epidemiological study. Lancet Infect Dis. 2014;14:308–18. http://dx.doi.org/10.1016/S1473-3099(13)70342-6
2. Khanh TH, Sabanathan S, Thanh TT, Thoa PK, Thuong TC, Hang V, et al. Enterovirus 71-associated hand, foot, and mouth disease, southern Vietnam, 2011. Emerg Infect Dis. 2012;18:2002–5. http://dx.doi.org/10.3201/eid1812.120929
3. Bian L, Wang Y, Yao X, Mao Q, Xu M, Liang Z. Coxsackievirus A6: a new emerging pathogen causing hand, foot and mouth disease outbreaks worldwide. Expert Rev Anti Infect Ther. 2015;13:1061–71. http://dx.doi.org/10.1586/14787210.2015.1058156
4. Oberste MS, Peñaranda S, Maher K, Pallansch MA. Complete genome sequences of all members of the species human enterovirus A. J Gen Virol. 2004;85:1597–607. http://dx.doi.org/10.1099/vir.0.79789-0
5. Ogi M, Yano Y, Chikahira M, Takai D, Oshibe T, Arashiro T, et al. Characterization of genome sequences and clinical features of coxsackievirus A6 strains collected in Hyogo, Japan in 1999–2013. J Med Virol. 2017;89:1395–403. http://dx.doi.org/10.1002/jmv.24798
6. Puenpa J, Chieochansin T, Linsuwanon P, Korkong S, Thongkomplew S, Vichaiwattana P, et al. Hand, foot, and mouth disease caused by coxsackievirus A6, Thailand, 2012. Emerg Infect Dis. 2013;19:641–3. http://dx.doi.org/10.3201/eid1904.121666
7. He SZ, Chen MY, Xu XR, Yan Q, Niu JJ, Wu WH, et al. Epidemics and aetiology of hand, foot and mouth disease in Xiamen, China, from 2008 to 2015. Epidemiol Infect. 2017;145:1865–74. http://dx.doi.org/10.1017/S0950268817000309
8. Montes M, Artieda J, Piñeiro LD, Gastesi M, Diez-Nieves I, Cilla G. Hand, foot, and mouth disease outbreak and coxsackievirus A6, northern Spain, 2011. Emerg Infect Dis. 2013;19. http://dx.doi.org/10.3201/eid1904.121589
9. Fujimoto T, Iizuka S, Enomoto M, Abe K, Yamashita K, Hanaoka N, et al. Hand, foot, and mouth disease caused by coxsackievirus A6, Japan, 2011. Emerg Infect Dis. 2012;18:337–9. http://dx.doi.org/10.3201/eid1802.111147
10. Österback R, Vuorinen T, Linna M, Susi P, Hyypiä T, Waris M. Coxsackievirus A6 and hand, foot, and mouth disease, Finland. Emerg Infect Dis. 2009;15:1485–8. http://dx.doi.org/10.3201/eid1509.090438
11. Brown BA, Oberste MS, Alexander JP Jr, Kennett ML, Pallansch MA. Molecular epidemiology and evolution of enterovirus 71 strains isolated from 1970 to 1998. J Virol. 1999;73:9969–75.
12. Lu J, Zeng H, Zheng H, Yi L, Guo X, Liu L, et al. Hand, foot and mouth disease in Guangdong, China, in 2013: new trends in the continuing epidemic. Clin Microbiol Infect. 2014;20:O442–5. http://dx.doi.org/10.1111/1469-0691.12468
13. Mao Q, Wang Y, Bian L, Xu M, Liang Z. EV-A71 vaccine licensure: a first step for multivalent enterovirus vaccine to control HFMD and other severe diseases. Emerg Microbes Infect. 2016;5:e75. http://dx.doi.org/10.1038/emi.2016.73
14. Ku Z, Liu Q, Ye X, Cai Y, Wang X, Shi J, et al. A virus-like particle based bivalent vaccine confers dual protection against

enterovirus 71 and coxsackievirus A16 infections in mice. Vaccine. 2014;32:4296–303. http://dx.doi.org/10.1016/j.vaccine.2014.06.025
15. Li J, Liu G, Liu X, Yang J, Chang J, Zhang W, et al. Optimization and characterization of candidate strain for Coxsackievirus A16 inactivated vaccine. Viruses. 2015;7:3891–909. http://dx.doi.org/10.3390/v7072803
16. Caine EA, Fuchs J, Das SC, Partidos CD, Osorio JE. Efficacy of a trivalent hand, foot, and mouth disease vaccine against enterovirus 71 and coxsackieviruses A16 and A6 in mice. Viruses. 2015;7:5919–32. http://dx.doi.org/10.3390/v7112916
17. Puenpa J, Vongpunsawad S, Österback R, Waris M, Eriksson E, Albert J, et al. Molecular epidemiology and the evolution of human coxsackievirus A6. J Gen Virol. 2016;97:3225–31. http://dx.doi.org/10.1099/jgv.0.000619
18. Mirand A, le Sage FV, Pereira B, Cohen R, Levy C, Archimbaud C, et al. Ambulatory pediatric surveillance of hand, foot and mouth disease as signal of an outbreak of coxsackievirus A6 infections, France, 2014–2015. Emerg Infect Dis. 2016;22:1884–93. http://dx.doi.org/10.3201/eid2211.160590
19. Tan X, Li L, Zhang B, Jorba J, Su X, Ji T, et al. Molecular epidemiology of coxsackievirus A6 associated with outbreaks of hand, foot, and mouth disease in Tianjin, China, in 2013. Arch Virol. 2015;160:1097–104. http://dx.doi.org/10.1007/s00705-015-2340-3
20. Geoghegan JL, Tan V, Kühnert D, Halpin RA, Lin X, Simenauer A, et al. Phylodynamics of enterovirus A71-associated hand, foot, and mouth disease in Viet Nam. J Virol. 2015;89:8871–9. http://dx.doi.org/10.1128/JVI.00706-15
21. Nguyen AT, Tran TT, Hoang VM, Nghiem NM, Le NN, Le TT, et al. Development and evaluation of a non-ribosomal random PCR and next-generation sequencing based assay for detection and sequencing of hand, foot and mouth disease pathogens. Virol J. 2016;13:125. http://dx.doi.org/10.1186/s12985-016-0580-9
22. Edgar RC. MUSCLE: multiple sequence alignment with high accuracy and high throughput. Nucleic Acids Res. 2004;32:1792–7. http://dx.doi.org/10.1093/nar/gkh340
23. Nguyen LT, Schmidt HA, von Haeseler A, Minh BQ. IQ-TREE: a fast and effective stochastic algorithm for estimating maximum-likelihood phylogenies. Mol Biol Evol. 2015;32:268–74. http://dx.doi.org/10.1093/molbev/msu300
24. Lanave C, Preparata G, Sacone C, Serio G. A new method for calculating evolutionary substitution rates. J Mol Evol. 1984;20:86–93. http://dx.doi.org/10.1007/BF02101990
25. Tamura K, Nei M. Estimation of the number of nucleotide substitutions in the control region of mitochondrial DNA in humans and chimpanzees. Mol Biol Evol. 1993;10:512–26.
26. Yang F, Yuan J, Wang X, Li J, Du J, Su H, et al. Severe hand, foot, and mouth disease and coxsackievirus A6—Shenzhen, China. Clin Infect Dis. 2014;59:1504–5. http://dx.doi.org/10.1093/cid/ciu624
27. Tee KK, Lam TT, Chan YF, Bible JM, Kamarulzaman A, Tong CY, et al. Evolutionary genetics of human enterovirus 71: origin, population dynamics, natural selection, and seasonal periodicity of the VP1 gene. J Virol. 2010;84:3339–50. http://dx.doi.org/10.1128/JVI.01019-09
28. Chang LY, Tsao KC, Hsia SH, Shih SR, Huang CG, Chan WK, et al. Transmission and clinical features of enterovirus 71 infections in household contacts in Taiwan. JAMA. 2004;291:222–7. http://dx.doi.org/10.1001/jama.291.2.222
29. Xu L, Zheng Q, Li S, He M, Wu Y, Li Y, et al. Atomic structures of coxsackievirus A6 and its complex with a neutralizing antibody. Nat Commun. 2017;8:505. http://dx.doi.org/10.1038/s41467-017-00477-9

Address for correspondence: Le Van Tan, Oxford University Clinical Research Unit, Ho Chi Minh City, Vietnam; email: tanlv@oucru.org

Influenza A(H7N9) Virus Antibody Responses in Survivors 1 Year after Infection, China, 2017

Mai-Juan Ma,[1] Cheng Liu,[1] Meng-Na Wu, Teng Zhao, Guo-Lin Wang, Yang Yang, Hong-Jing Gu, Peng-Wei Cui, Yuan-Yuan Pang, Ya-Yun Tan, Hui Hang, Bao Lin, Jiang-Chun Qin, Li-Qun Fang, Wu-Chun Cao, Li-Ling Chen

Avian influenza A(H7N9) virus has caused 5 epidemic waves in China since its emergence in 2013. We investigated the dynamic changes of antibody response to this virus over 1 year postinfection in 25 patients in Suzhou City, Jiangsu Province, China, who had laboratory-confirmed infections during the fifth epidemic wave, October 1, 2016–February 14, 2017. Most survivors had relatively robust antibody responses that decreased but remained detectable at 1 year. Antibody response was variable; several survivors had low or undetectable antibody titers. Hemagglutination inhibition titer was ≥1:40 for <40% of the survivors. Measured in vitro in infected mice, hemagglutination inhibition titer predicted serum protective ability. Our findings provide a helpful serologic guideline for identifying subclinical infections and for developing effective vaccines and therapeutics to counter H7N9 virus infections.

The novel avian influenza A(H7N9) virus has caused 5 epidemic waves in China since its emergence in 2013. As of September 20, 2017, a total of 1,561 human cases were reported, with a case fatality rate of ≈39% (*1*). In particular, a substantial increase of 758 human cases was reported during the fifth epidemic, compared with the earlier 4 (*1*). Highly pathogenic H7N9 viruses emerged and infected both humans (*1*) and poultry (*2*) during the fifth epidemic. In addition, H7N9 virus readily obtained the 627K or 701N mutation in its polymerase basic (PB) 2 segment upon replication in ferrets (*3*), suggesting that the virus has pandemic potential and continues to pose grave risks to public health.

The H7N9 subtype has the highest risk score among the 12 novel influenza A viruses evaluated by the Centers for Disease Control and Prevention using the Influenza Risk Assessment Tool and is characterized as posing moderate- to high-potential pandemic risk (*4*). Apart from the ongoing monitoring of virologic and molecular characteristics of H7N9 viruses in poultry and humans, studies on the dynamic changes of antibody response in survivors are critical for serologic diagnosis, population-based seroepidemiologic surveys, and vaccine design and development. A few studies have investigated virus-specific antibody kinetics to the H7N9 virus in patients and their relationship with disease severity (*5*–*7*), but these studies were restricted to antibodies measured in the acute and convalescent phases. No follow-up studies have been done on dynamic antibody changes in survivors who had recovered from the disease. As a result, the long-term serologic response to H7N9 virus infections is poorly understood and remains of clinical interest. In our study, we investigated the long-term dynamic changes in antibody response in H7N9 survivors identified during the fifth epidemic in China and examined the relationship between antibody responses and clinical characteristics.

Materials and Methods

Study Design and Participants

During the fifth epidemic wave of the H7N9 virus (October 1, 2016–February 14, 2017), we conducted a longitudinal serologic survey on a cohort patient who had recovered from the disease in Suzhou, Jiangsu Province, China. We screened 34 patients who had laboratory-confirmed cases and were >18 years of age when they were discharged from the hospital (Figure 1). We enrolled 25 of these patients in our study after obtaining informed consent and prospectively followed them at ≈100, 200, and 300 days after symptom onset (Figure 1). In addition, we enrolled 10 control subjects who live in an area without known H7N9 virus detections, denied close contact with live poultry or live bird markets during the previous 12 months, and had no known diseases or conditions that would reduce their immune response.

Author affiliations: Beijing Institute of Microbiology and Epidemiology, Beijing, China (M.-J. Ma, M.-N. Wu, T. Zhao, G.-L. Wang, H.-J. Gu, L.-Q. Fang, W.-C. Cao); University of Florida, Gainesville, Florida, USA (Y. Yang); Suzhou Municipal Center for Disease Control and Prevention, Suzhou, China (C. Liu, P.-W. Cui, Y.-Y. Pang, Y.-Y. Tan, H. Hang, B. Lin, J.-C. Qin, L.-L. Chen)

DOI: https://doi.org/10.3201/eid2404.171995

[1]These authors contributed equally to this article.

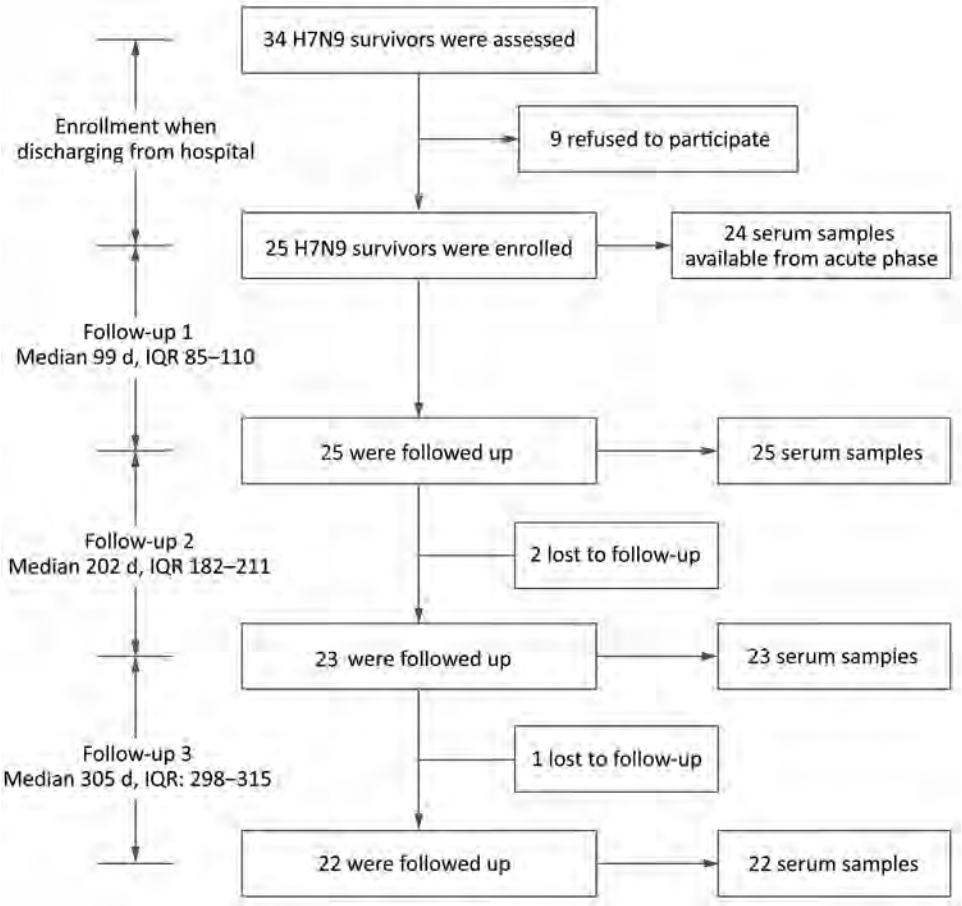

Figure 1. Schematic outline for study of influenza A(H7N9) virus antibody responses in survivors 1 year after infection, China, 2017. IQR, interquartile range.

We obtained written informed consent from all participants before conducting interviews and sample collection. The study protocol was approved by the Institutional Review Boards of Beijing Institute of Microbiology and Epidemiology and Suzhou Municipal Center for Disease Control and Prevention. The study was also approved by the Animal Care and Use Committee at the Academy of Military Medical Sciences.

Sampling and Data Collection

At patient enrollment, we used a comprehensive questionnaire to collect information about patients' demographic and clinical characteristics, history of exposure to poultry, and history of seasonal influenza vaccination. We included archived acute- or convalescent-phase serum samples from the participants in our study. At each of the 3 follow-up visits, we asked each participant to provide a 5-mL blood sample. We used a shorter questionnaire to collect information about demographic characteristics, recent history of exposure to poultry, and experience of influenza-like illness.

Serologic Testing

We measured serum hemagglutination inhibition (HI) antibody (*8*) by the HI assay; neutralizing antibody by the microneutralization (MN) assay (*9*); neuraminidase inhibition (NI) antibody by the enzyme-linked lectin assay (ELLA) (*10*); and IgG or IgA antibodies by ELISA (*5*). For HI, NI, and MN detection, we applied 2-fold serial dilutions of serum from 1:10 to 1:280. We defined the HI titer as the reciprocal of the highest serum dilution that completely inhibited hemagglutination; the NI titer as the reciprocal of highest serum dilution that exhibited 50% inhibition concentration (IC_{50}); and the MN titer as the reciprocal of the highest serum dilution that yielded ≥50% neutralization. For final titers <1:10 we assigned a value of 1:5 (seronegative). For IgG and IgA detection, we tested serum samples at a starting dilution of 1:50 with 2-fold serial dilutions to 1:12,800. The endpoint titer was the highest dilution giving an optical density at least twice that of background. The final titers <1:50 we assigned a value of 1:25. We used a human H7N9 isolate (A/Jiangsu/Wuxi05/2013) for the HI and MN assays. We used a genetic reassortant H6N9 virus, which contains the hemagglutinin gene of H6N1 virus A/Taiwan/1/2013, the neuraminidase gene of H7N9 virus A/Anhui/1/2013, and other internal genes of A/Puerto Rico/8/1934 H1N1, for ELLA. We used currently circulating human seasonal viruses (A/Shanghai/SWL1970/2015/H1N1 and A/Switzerland/

9715293/2013/H3N2) to examine the serum samples for cross-reacting antibodies with HI assay.

We defined a seroprotective threshold as an HI, NI, or MN antibody titer of 40. A titer of ≥1:40 of HI, NI, or MN antibody has been shown to protect against seasonal influenza viruses (*11*–*13*) and is considered protective against H7N9 infection in humans, but has not been proven so. There is no established correlation of protection for IgG and IgA titers for influenza virus infection, but any detectable antibody level is deemed protective. We set the cutoff value for IgG titer to 1:400 because the mean titer among control serum samples was 1:350.

Human Serum Passive Transfer and H7N9 Infection of Mice

We obtained 42 female 4-week-old specific pathogen-free BALB/c mice from the Laboratory Animal Center, Academy of Military Medical Sciences, Beijing, China. The mice weighed 13.3 ± 0.9 g. We injected 3 mice per group intravenously with 40 μL of human serum (2-fold serial HI titration ranged from 1:5 to 1:1,280) 12 hours before injecting them intranasally with 20 μL of 10 × 50% lethal dose of H7N9 virus. We gave an equal volume of healthy donor serum or phosphate-buffered saline to control mice. We observed the mice daily for signs of disease for ≤3 days. We conducted all work with the H7N9 virus in the Biosafety Level 3 laboratory of the State Key Laboratory of Pathogen and Biosecurity.

Antibody in Serum and Virus Titers in Lungs of Mice

We collected blood from the mice 12 hours after injection with human serum. Because we transferred only 40 μL serum to the mice and there was ≈30-fold dilution of >1 mL blood, we expected the HI titer in mice to be undetectable. Therefore, we used the ELISA method to measure IgG titers. To obtain virus titers, we harvested the lungs of 3 mice at 3 days after virus infection and homogenized them into 1.5 mL of Dulbecco's Modified Eagle Medium using a manual homogenizer. We aliquoted lung homogenates and kept them at –80°C. We determined the viral titer using the tissue culture infectious dosage on MDCK cells.

Statistical Analysis

We analyzed the antibody titers with $\log_{10}$-transformed geometric means and 95% CIs. We calculated the proportion of antibody titers equal to or greater than seroprotective threshold (HI, NI, and MN) or limit of detection and associated 95% CI. We used Mann-Whitney U test for testing the differences in antibody titers and χ^2 test and Fisher exact test for testing the differences in proportion of antibody titers above thresholds. All statistical tests were 2-sided with a significance level of 0.05. We conducted all statistical analyses using GraphPad Prism software (GraphPad Software, Inc., La Jolla, CA, USA).

Results

During October 1, 2016–February 14, 2017, we enrolled in our study 25 laboratory-confirmed H7N9 survivors from Suzhou, Jiangsu Province, China (Figure 1). Among these survivors, 17 were men and 8 were women; the median age was 59 years (range 49.5–66.5 years) (Table 1). All patients required hospitalization at 1–12 days after symptom onset. Most of the patients had severe illness and were admitted to the intensive care unit (ICU). Patients remained in the ICU for 7–30 days. Clinical symptoms included fever, cough, sore throat, fatigue, myalgia, chills, and dyspnea (Table 2). All patients received oseltamivir, and 21 received glucocorticoid for treatment. Laboratory tests at hospital admission showed that some patients had abnormal hepatic function. Most patients had low to medium viral load (online Technical Appendix Table 1, https://wwwnc.cdc.gov/EID/article/24/4/17-1995-Techapp1.pdf). In addition, H7N9 viruses isolated from 11/25 patients were of low pathogenicity and belonged to the Yangtze River Delta hemagglutinin lineages (online Technical Appendix Table 1). The radiographic findings included pneumonia, increased markings, fuzzy patch lesions, and patch effusion shadows in lungs (online Technical Appendix Table 2).

Table 3 shows the proportion of survivors with antibody titers equal to or greater than the seroprotective threshold (1:40 for HI, NI, and MN) or the minimum detection limit (1:400 for IgG and 1:50 for IgA) at each time point. Counting from the day of symptom onset, >90% of survivors had an HI titer ≥1:40 on day 100. This proportion reached 82.6% on day 200 but decreased to 36.4% on day 300. The overall patterns of the NI antibody titers were similar to the HI antibody titers, except that 63.6% of survivors had an NI titer ≥1:40 on day 300. Unlike the HI and NI antibody titers, the proportion of seroprotective MN (≈86%) and IgG (100%) titers remained steady over time. For IgA antibody titers, the seroprotective proportion decreased from 96% on day 100 to ≈60% on day 300, an absolute reduction of ≥30%.

The geometric mean titers (GMTs) of antibodies were plotted by the time points in Figure 2. Overall, ≈300 days after symptom onset, HI and NI GMTs substantially declined and were lower than the seroprotective threshold of 1:40 and the GMTs in the acute phase (Figure 2, panels A and B). In contrast, the MN GMTs increased over time, peaked on day 200, and then declined by day 300, yet remained considerably above the GMTs in the acute phase and the seroprotective threshold of 1:40 (Figure 2, panel C). Although we observed no substantial difference in GMTs across 3 follow-up time points, the MN GMTs on day 200 were relatively high, suggesting a possible delayed response after infection. IgG and IgA decreased gradually from day 100 to day 300 but remained higher than the limit of detection (Figure 2, panel D). However, IgG GMTs on

Table 1. Clinical characteristics of influenza A(H7N9) virus survivors, China, 2017*

Patient no.	Age, y/sex	Symptoms	Days to admission†	Hospitalization, d	ICU, d	Disease severity
1	89/M	Fever, cough, sore throat, fatigue, myalgia	6	18	16	Severe
2	32/M	Fever, cough, sore throat	12	22	12	Severe
3	41/F	Fever, cough, sore throat, fatigue	8	19	14	Severe
4	83/M	Fever, cough, fatigue	4	11	9	Severe
5	62/M	Fever, cough	7	12	12	Severe
6	71/M	Fever, cough	9	18	13	Severe
7	63/F	Fever, cough, fatigue	9	16	10	Severe
8	54/F	Fever, cough, sore throat	7	14	9	Severe
9	54/F	Fever, cough, fatigue	7	17	17	Mild
10	60/F	Fever, cough, fatigue, chills	7	28	23	Severe
11	28/F	Fever, cough, fatigue	7	16	11	Severe
12	63/M	Fever, cough	6	14	14	Severe
13	65/M	Fever, cough	5	19	0	Severe
14	35/M	Fever, cough, sore throat, fatigue	6	12	12	Severe
15	39/F	Fever, cough	7	19	19	Severe
16	57/M	Fever, cough	10	17	17	Severe
17	75/M	Fever, cough, fatigue	9	22	13	Severe
18	58/M	Fever, cough, myalgia	5	15	8	Mild
19	54/F	Fever, fatigue, myalgia	5	11	11	Severe
20	59/M	Fever, cough	5	21	7	Severe
21	68/M	Fever, cough, dyspnea	5	30	30	Severe
22	59/M	Fever, cough	7	22	22	Severe
23	45/M	Fever, cough	1	13	9	Severe
24	71/M	Fever, cough	2	73	NA	Severe
25	64/M	Fever, cough, sore throat	6	13	11	Mild

*ICU, intensive care unit; NA, not available.
†After symptom onset.

day 200 and day 300 were substantially higher than the IgG GMTs in the acute phase, whereas the IgA GMTs on day 200 and day 300 were similar to those in the acute phase. There were no detectable antibodies to the H7N9 virus in the control subjects, but GMT was 283.3 (titer ranged from 1:200 to 1:800) for IgG, suggesting a possible cross-reactivity between the H7N9 virus and other subtypes.

Approximately 300 days after symptom onset, nearly all survivors had a ≥4-fold decline in the HI titer compared with the titer on day 100, and 14 survivors had HI titers <1:40 (Tables 4, 5; Figure 2, panel A). Among these 14 survivors, 2 (patients 1 and 2) maintained low titers (1:10) throughout the study period, but 2 others (patients 4 and 25) had undetectable titers around day 300. The other 10 survivors had titers of 1:20. Twenty-one survivors had a ≥4-fold decrease of the NI titer ≈300 days after symptom onset, and 8 survivors (patients 1, 2, 4, 8, 11, 14, 22, and 25) had titers <1:40 (Tables 4, 5). Among these 8 survivors, the titer of patient 2 declined to seronegative on day 349, and others had titers ≤1:20 (Tables 4, 5; Figure 2, panel B). In contrast, the majority of survivors had a ≥2-fold increase in MN titer (9 survivors) or maintained MN titer (8 survivors) on day 200 in comparison to day 100 after symptom onset, followed by a decrease or a maintenance on day 300 (Figure 2, panel C; Tables 4 and 5). However, 6 survivors (patients 1, 2, 4, 8, 21, and 25) maintained low titers over the study period (Tables 4, 5; Figure 2, panel C), but none of them became seronegative. Although most of the survivors had a ≥4-fold decline in IgG titer over time, all survivors maintained detectable antibody titers ≥1:400 (Tables 4, 5; Figure 2, panel D). However, the overall response of IgA antibody was relatively weak, and 9 survivors (patients 1, 3, 4, 15, 18, 19, 21, 22, and 25) already had undetectable titer on day 200 (Tables 4, 5; Figure 2, panel E).

To further assess the physiologic contribution of the magnitude of the HI antibody titers, we transferred 40 μL convalescent-phase serum from individual patients to mice (online Technical Appendix Table 3). IgG titers in the serum samples of recipient mice correlated well with IgG, HI, and MN titers in the human serum samples, but we observed a better correlation for IgG titer in the human samples (Figure 3, panels A–D). Mouse IgG titers in the serum samples at the time of challenge correlated inversely with virus titers in the lung samples, confirming the importance of neutralizing antibodies assessed in laboratory analysis in virus clearance (Figure 3, panels E, F). These results also suggest that an IgG titer of >1:160 was required to reduce virus titers by 0.5 $\log_{10}$ in infected mice. Assuming that these numbers can be extrapolated to patients, transferring 40 μL of serum to a 13-g mouse is equivalent to transferring 210 mL of serum to a 70-kg patient (calculated per kilogram), thereby providing a potential guideline for its use in clinical settings.

The different types of antibody measures are significantly correlated with each other; we observed higher correlation between HI and NI and between NI and IgG at

Table 2. Underlying disease, complications, and treatment of influenza A(H7N9) virus survivors, China, 2017*

Patient no.	Underlying disease	Complications	Oxygen therapy	Mechanical ventilation	Days to antiviral treatment†	Oseltamivir	Glucocorticoid
1	HTN, DM	ARDS, RF	Yes	No	6	Yes	Yes
2	No	ARDS, RF	Yes	No	13	Yes	Yes
3	No	ARDS, RF	Yes	No	8	Yes	Yes
4	COPD, HTN	No	Yes	No	6	Yes	Yes
5	HTN	ARDS, RF	Yes	No	7	Yes	Yes
6	HTN, DM	ARDS, HI	Yes	No	14	Yes	No
7	No	ARDS	Yes	No	9	Yes	Yes
8	No	No	Yes	No	7	Yes	Yes
9	No	No	Yes	No	9	Yes	Yes
10	No	ARDS, RF, HI, RI	Yes	Yes	11	Yes	Yes
11	No	HI	Yes	No	7	Yes	Yes
12	No	No	Yes	No	8	Yes	No
13	No	No	Yes	No	8	Yes	Yes
14	No	No	Yes	No	6	Yes	Yes
15	No	HI	Yes	No	7	Yes	Yes
16	No	RF	Yes	No	13	Yes	No
17	No	ARDS	Yes	No	9	Yes	Yes
18	No	No	Yes	No	13	Yes	Yes
19	No	RF, HI	Yes	No	5	Yes	Yes
20	HTN	ARDS, RF, HI	Yes	Yes	11	Yes	Yes
21	HTN, DM, HL	ARDS, RF, HI	Yes	Yes	5	Yes	Yes
22	HTN	ARDS, RF, HI	Yes	No	7	Yes	Yes
23	HTN	No	Yes	No	6	Yes	NA
24	NA	NA	Yes	NA	1	Yes	NA
25	CHB	HI	Yes	No	9	Yes	Yes

*ARDS, acute respiratory distress syndrome; CB, chronic bronchitis; CHB, chronic hepatitis B infection; COPD, chronic obstructive pulmonary disease; DM, diabetes mellitus; HI, hepatic insufficiency; HL, hyperlipidemia; HTN, hypertension; NA, not available; RF, respiratory failure; RI, renal insufficiency.
†After admission.

R^2 >0.5 (online Technical Appendix Figure 1). We found no correlation between antibodies to the H7N9 virus and HI antibodies against seasonal H1N1 and H3N2 viruses (p>0.05) (online Technical Appendix Figure 2), indicating that there is no heterologous boost of antibodies against H7 by H3 or H1 hemagglutinin. The antibody responses did not vary by patient age, sex, presence of underlying conditions, time in ICU, ventilation, or disease severity.

Discussion

In our study, antibodies to H7N9 virus waned over time, but most survivors maintained detectable antibody titers ≈1 year after infection. However, >60% of survivors had an HI titer <1:40, which is potentially not seroprotective, ≈300 days after infection. Antibody responses were highly variable in survivors, and a few of them had weak antibody responses or had quickly waning antibody titers that were undetectable ≈1 year after infection despite their severity of infection. We also identified a threshold of IgG titer that was crucial to virus clearance in the animal model and could be useful in clinical settings.

HI antibodies induced by natural infection with the 2009 pandemic H1N1 virus persist at constant high titer (>1:40) for a minimum of 15 months (*14*). Additionally, the HI antibody against the H5N1 virus infection is reported to last even longer, at a stable titer (≥1:40) for nearly 5 years, although only a few survivors have been studied (*15*). In contrast, our study shows that only 36.4% of H7N9 survivors had HI titers ≥1:40 at ≈1 year after infection, although most survivors had detectable HI antibody titers. On the other hand, we observed relatively high MN antibody titers persisting over time in survivors, and these levels were sufficient to predict protection, based on the protection extrapolated from seasonal influenza. If we assume that MN antibody is truly a better correlate of protection than HI antibody and a titer of >1:40 is sufficient for protection, we could anticipate that most H7N9 survivors would remain protected against the H7N9 virus ≥1 year after infection.

Table 3. Proportion of influenza A(H7N9) virus survivors with titers at seroprotective levels at acute phase of infection and 3 follow-up points after infection, China, 2017*

Antibody	% Patients (95% CI)			
	Acute phase	Follow-up visit 1	Follow-up visit 2	Follow-up visit 3
HI	54.5 (32.2–75.6)	92.0 (74.0–99.0)	82.6 (61.2–95.0)	36.4 (17.2–59.3)
NI	50.0 (28.2–71.8)	96.0 (79.6–99.9)	91.3 (72.0–98.9)	63.6 (40.7–82.8)
MN	22.7 (7.8–45.4)	88.0 (68.8–97.5)	87.0 (66.4–97.2)	86.4 (65.1–97.1)
IgG	45.5 (24.4–67.8)	100 (86.3–100)	100 (85.2–100)	100 (84.6–100)
IgA	54.5 (32.2–75.6)	96.0 (79.6–99.9)	60.9 (38.5–80.3)	59.1 (36.4–79.3)

*Seroprotective levels for HI, NI, and MN titers, ≥1:40; IgG ≥1:400; or IgA ≥1:50. HI, hemagglutination inhibition; MN, microneutralization; NI, neuraminidase inhibition.

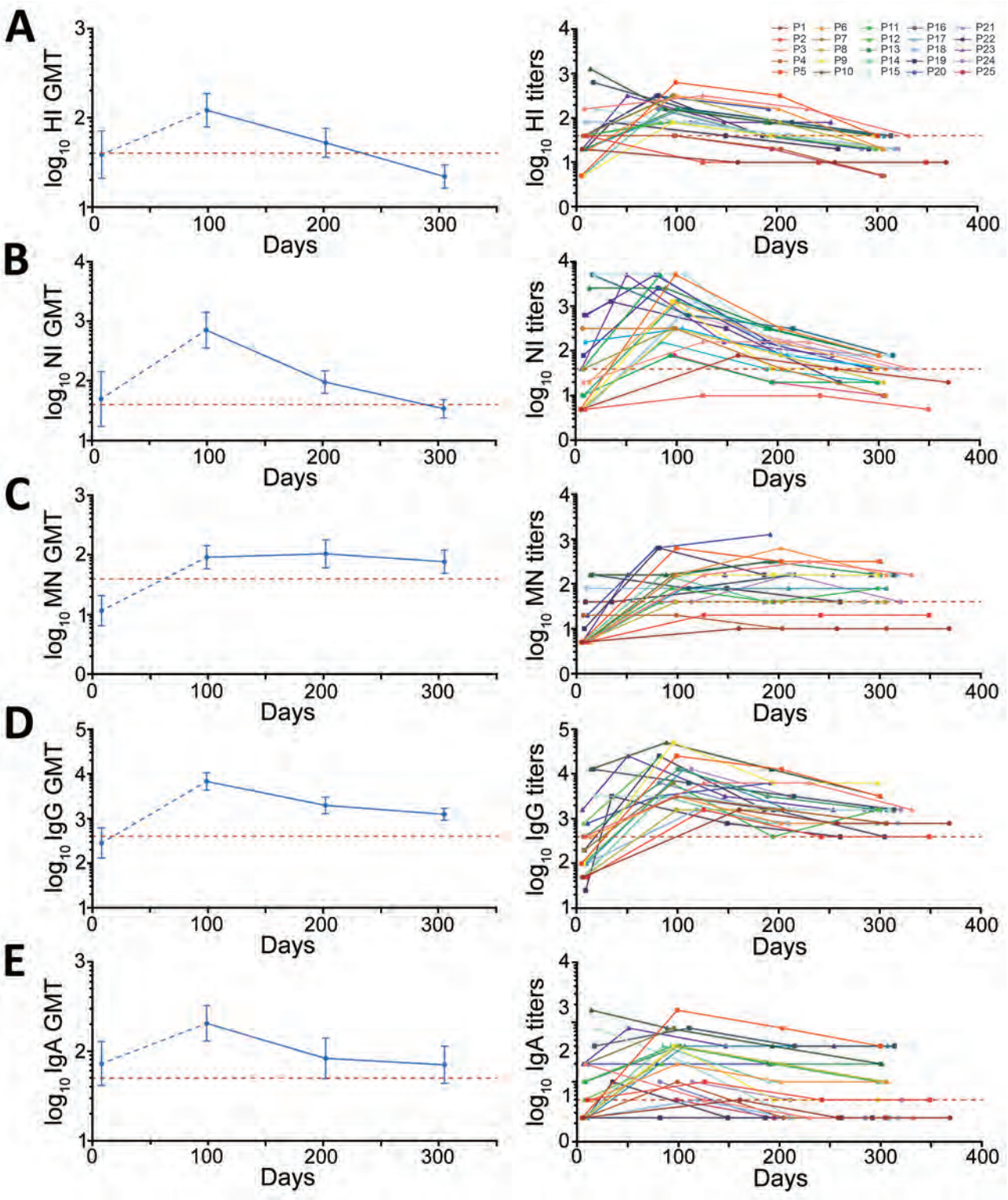

Figure 2. GMTs (left) and individual titers (right) of antibodies to influenza A(H7N9) virus in serum samples collected from survivors, China, 2017: A) HI, B) NI, C) MN, D) IgG, and E) IgA. Red dashed line indicates threshold for seroprotective titer (HI, NI, and MN = 1:40) or limited detection titer (IgG = 1:400; IgA = 1:50). Error bars indicate 95% CIs. GMT, geometric mean titer; HI, hemagglutination inhibition; MN, microneutralization; NI, neuraminidase inhibition; P, patient.

Table 4. Antibody titers in survivors of influenza A(H7N9) during the acute phase and at 3 follow-up points, China, 2017*

Patient no.	HI/NI/MN/IgG/IgA titers			
	Acute phase	Follow-up visit 1	Follow-up visit 2	Follow-up visit 3
1	20/5/5/50/25	10/80/10/1600/50	10/40/10/800/25	10/20/10/800/25
2	20/5/5/50/50	10/10/20/1600/100	10/10/20/400/50	10/5/20/400/50
3	160/20/5/400/200	320/160/160/6400/50	160/160/320/6400/25	40/40/160/1600/25
4	40/320/20/400/25	40/320/20/3200/100	20/40/10/1600/25	5/10/10/800/25
5	5/5/5/100/25	640/5120/640/25600/1600	320/320/320/12800/800	40/80/320/3200/400
6	20/20/5/400/50	320/1280/160/3200/200	160/160/640/800/100	20/40/160/800/100
7	40/40/5/200/200	320/320/160/6400/800	NA	NA
8	40/5/5/50/25	320/320/40/1600/400	80/80/40/1600/200	20/20/40/800/100
9	5/5/5/100/25	80/1280/160/51200/400	40/40/160/6400/50	40/40/160/6400/50
10	1280/2560/160/12800/1600	160/2560/160/51200/800	80/320/320/12800/400	40/80/320/3200/200
11	40/10/5/100/100	80/80/80/6400/400	40/20/40/400/200	20/20/80/1600/100
12	40/40/5/800/50	80/5120/40/25600/200	NA	NA
13	20/10/5/400/100	160/1280/160/12800/400	80/320/320/3200/200	40/80/160/1600/200
14	5/5/5/50/25	160/160/160/3200/400	40/40/40/800/100	20/20/40/800/100
15	160/5120/160/3200/800	80/5120/160/3200/200	40/80/160/1600/25	20/80/160/1600/25
16	640/5120/160/12800/400	160/640/80/6400/800	80/320/160/3200/400	40/80/160/1600/400
17	20/160/5/100/25	160/320/80/12800/400	80/80/80/1600/400	40/40/80/1600/400
18	80/5/80/100/25	80/1280/80/1600/50	40/80/160/800/25	20/40/160/800/25
19	40/80/10/200/25	320/2560/640/25600/25	40/160/160/1600/25	20/40/160/1600/25
20	40/640/20/800/200	320/5120/640/3200/200	160/160/1280/6400/200	NA
21	NA	160/5120/40/6400/100	40/160/40/1600/25	20/80/40/1600/25
22	20/640/40/25/25	80/1280/40/3200/100	40/320/80/800/25	20/20/40/400/25
23	20/40/5/1600/200	320/5120/160/25600/800	80/160/160/3200/400	80/80/160/1600/400
24	NA	80/640/40/12800/100	40/160/160/3200/50	20/40/40/1600/50
25	NA	40/80/40/3200/50	20/20/40/1600/25	5/10/40/400/25

*HI, hemagglutination inhibition; MN, microneutralization; NA, not available; NI, neuraminidase inhibition.

It has been observed that antibody responses in infections with H5N1 or 2009 pandemic H1N1 virus in which patients had mild or no symptoms waned faster than those in patients with severe influenza disease and decreased below the threshold of positivity within 1 year (*16*,*17*). Of all reported H7N9 cases, <10% were asymptomatic or mild (*18*–*20*), and our study included only 3 mildly symptomatic patients (patients 9, 18, and 25). These 3 patients maintained detectable NI, MN, and IgG antibodies, but patient 25 became seronegative for HI antibodies and IgA on or around day 305 after symptom onset. Meanwhile, several severely ill

Table 5. Change in antibody titers in survivors of influenza A(H7N9) at different follow-up points, China, 2017*

Patient no.	Change, -fold, HI/NI/MN/IgG/IgA	
	Follow-up visit 2 vs. follow-up visit 1	Follow-up visit 3 vs. follow-up visit 2
1	1/0.5/1/0.5/0.5	1/0.5/1/1/1
2	1/1/1/0.25/0.5	1/0.5/1/1/1
3	0.5/1/2/1/0.5	0.25/0.25/0.5/0.25/1
4	0.5/0.13/0.5/0.5/0.25	0.25/0.25/1/0.5/1
5	0.5/0.06/0.5/0.5/0.5	0.13/0.25/1/0.25/0.5
6	0.5/0.13/4/0.25/0.5	0.13/0.25/0.25/1/1
7	NA	NA
8	0.25/0.25/1/1/0.5	0.25/0.25/1/0.5/0.5
9	0.5/0.03/1/0.13/0.13	1/1/1/1/1
10	0.5/0.13/2/0.25/0.5	0.5/0.25/1/0.25/0.5
11	0.5/0.25/0.5/0.06/0.5	0.5/1/2/4/0.5
12	NA	NA
13	0.5/0.25/2/0.25/0.5	0.5/0.25/0.5/0.5/1
14	0.25/0.25/0.25/0.25/0.25	0.5/0.5/1/1/1
15	0.5/0.02/1/0.5/0.125	0.5/1/1/1/1
16	0.5/0.5/2/0.5/0.5	0.5/0.25/1/0.5/1
17	0.5/0.25/1/0.13/1	0.5/0.5/1/1/1
18	0.5/0.06/2/0.5/0.5	0.5/0.5/1/1/1
19	0.13/0.06/0.25/0.06/1	0.5/0.25/1/1/1
20	0.5/0.03/2/2/1	NA
21	0.25/0.03/1/0.25/0.25	0.5/0.5/1/1/1
22	0.5/0.25/2/0.25/0.25	0.5/0.06/0.5/0.5/1
23	0.25/0.03/1/0.13/0.5	1/0.5/1/0.5/1
24	0.5/0.25/4/0.25/0.5	0.5/0.25/0.25/0.5/1
25	0.5/0.25/1/0.5/0.5	0.25/0.5/1/0.25/1

*Change was calculated as ratio of titers. HI, hemagglutination inhibition; MN, microneutralization; NA, not available; NI, neuraminidase inhibition.

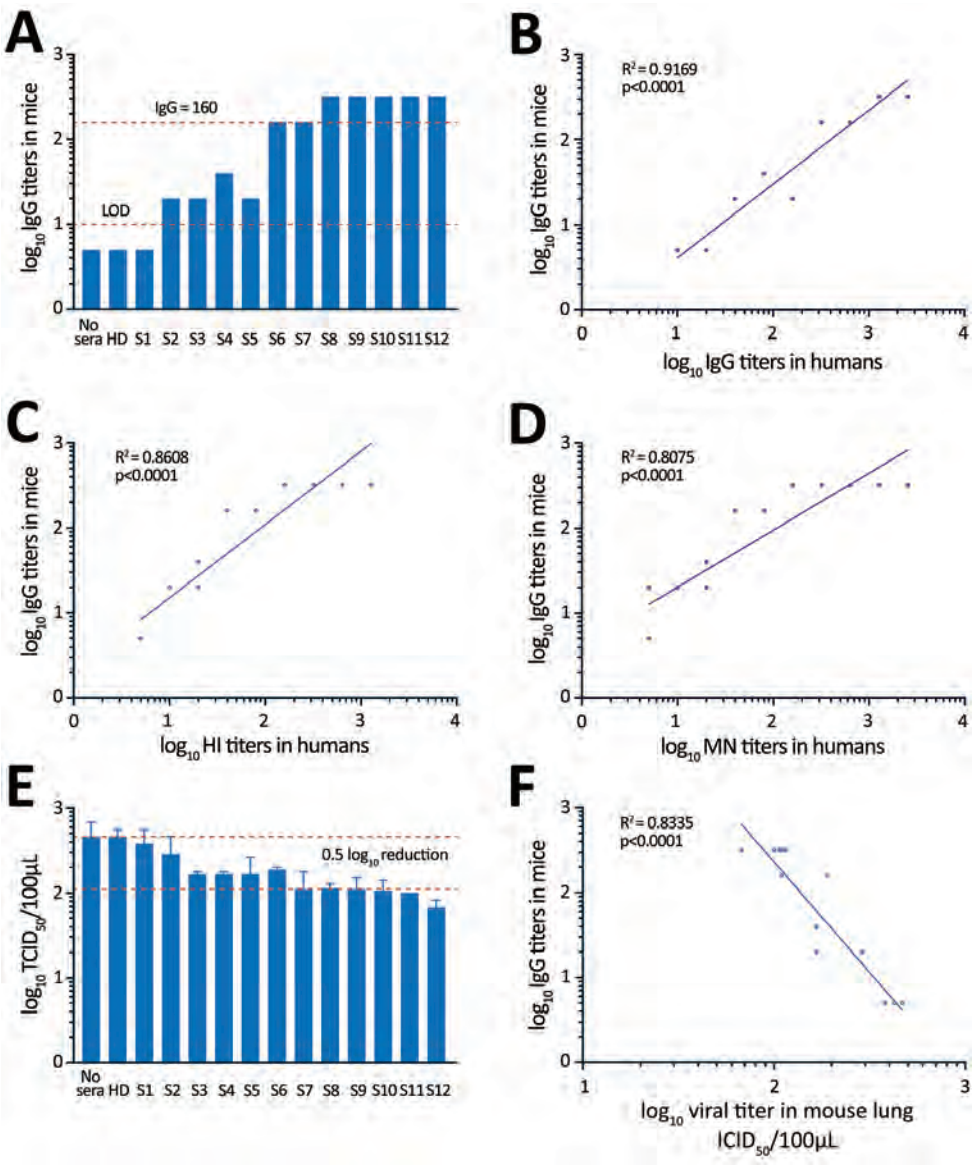

Figure 3. Testing of convalescent-phase serum transfer as potential protection against influenza A(H7N9) virus infection. Mice received 40 µL of patient serum intravenously 12 hours before H7N9 virus infection. A) IgG titers from mouse serum samples collected 1 h before infection. B–D) Relationships between IgG, HI, and MN titers in human serum and IgG titer in mouse recipients of transferred serum. E) Virus titers in homogenized mouse lungs at day 3 after infection (mean ± SE). F) Relationship between IgG titer in mouse serum samples and viral titers in mouse lung samples. HD, healthy donor; HI, hemagglutination inhibition; LOD, limit of detection; MN, microneutralization; S, serum; $TCID_{50}$, 50% tissue culture infectious dose.

patients had relatively weak antibody responses 100 days after symptom onset; in particular, patients 1, 2, and 4 either maintained low antibody titers over time or became seronegative at ≈1 year after symptom onset. Therefore, there was no clear association between disease severity and antibody response. Nevertheless, most patients in our study had severe symptoms, and so the findings may not be representative of mild cases or asymptomatic infections.

Previous seroepidemiological studies have identified the subclinical infections among both occupationally exposed workers and the general population, but the results varied (*21*–*29*). Similar to the problems with H5N1 infections in humans (*30*), the serologic threshold titer to recognize subclinical infections of the H7N9 virus is not yet established, which leads to difficulty in estimating the seroprevalence of subclinical infections. A major problem in identifying such a serologic threshold for seropositivity is the insufficient immunogenicity of the H7 hemagglutinin (*31*–*34*). Our results show that HI, NI, IgG, and IgA antibodies declined substantially over time. In particular, for HI antibody, >60% of survivors had a titer <1:40, and 2 of them became negative at ≈1 year after infection. Given the low magnitude in HI antibody response, the true incidence of H7N9 infection is likely to be underestimated if a titer of >1:40 is used as the serologic threshold for the HI assay in seroepidemiological studies. In our study, the level of MN antibody titer was relatively stable over time and correlated well with other types of antibodies; therefore, the MN antibody could be a more useful indicator than HI for determining the incidence of infection.

Convalescent plasma therapy has been considered as a treatment option for new and emerging infectious diseases for which effective drugs and vaccines are not readily available. Although the anti–influenza A virus drug oseltamivir appeared to be useful for the treatment of H7N9 infection, the ≈40% mortality rate still remains a challenge for clinical treatment, especially for severe cases who visit a hospital days past onset of their symptoms. Previous studies have shown that convalescent plasma treatment reduced the mortality rate of severe 2009 pandemic H1N1 infection (*35*) and benefited patients with severe H5N1 or H7N9 infections (*36*,*37*). Our results indicate that, despite substantially decreased HI antibody titers over time, most of the survivors still had a titer >1:40 ≈200 days after infection, and high antibody titers are likely for other antibodies from survivors' serum. The experimental results from our model using mice suggest that transferring 210 mL of serum with HI titer ≥1:80 to a 70-kg patient is a possible guideline for clinical treatment.

Our study had some limitations. First, our results need to be validated with larger numbers of survivors. We have thus far included 25 survivors, ≈3% of all reported H7N9 survivors in China. The small sample size limited our ability to analyze the antibody response stratified by patient age, sex, underlying condition, or disease severity. Second, we could not collect blood samples more frequently from the patients, especially between acute phase and ≈100 days after infection, which could have provided a more complete picture about the dynamics of antibody responses. Finally, we did not study the virus-specific memory T- and B-cell response because of constraints in logistics. Whether there are correlations between cellular immune responses and antibody responses needs further investigation.

In conclusion, our findings contribute to the understanding of individual immune responses to H7N9 virus infection and of population-based immunity in regions where H7N9 virus outbreaks have occurred. Our study provides a useful serologic guideline for developing effective vaccines and therapies to counter H7N9 virus infections.

Acknowledgments

We thank all patients for their participation in the study and the staff of the local Centers for Disease Control and Prevention whose collaboration made this study possible.

This study was supported by the National Natural Science Foundation of China (81773494, 81402730, and 81621005); Beijing Scientific and Technology Nova Program (Z171100001117088); China Mega-Project on Infectious Disease Prevention (2017ZX10303401-006); Suzhou Key Technology on Major and Infectious Diseases Prevention and Control (GWZX201502); and Suzhou Medical Key Subject (SZXK201516).

About the Author

Dr. Ma is a scientist at Beijing Institute of Microbiology and Epidemiology, Beijing, China. His research interests focus on molecular epidemiology and seroepidemiology of zoonotic influenza virus and zoonotic transmission of influenza between species.

References

1. Food and Agriculture Organization of the United Nations. H7N9 situation update. 2017 [cited 2018 Jan 31]. http://www.fao.org/ag/againfo/programmes/en/empres/h7n9/situation_update.html
2. World Organisation for Animal Health. OIE situation report for avian influenza. 2017 [cited 2017 May 9]. http://www.oie.int/fileadmin/Home/eng/Animal_Health_in_the_World/docs/pdf/OIE_AI_situation_report/OIE_SituationReport_AI__6_8May2017.pdf
3. Shi J, Deng G, Kong H, Gu C, Ma S, Yin X, et al. H7N9 virulent mutants detected in chickens in China pose an increased threat to humans. Cell Res. 2017;27:1409–21. http://dx.doi.org/10.1038/cr.2017.129
4. Centers for Disease Control and Prevention. Influenza risk assessment tool (IRAT). 2017 [cited 2018 Jan 31]. https://www.cdc.gov/flu/pandemic-resources/national-strategy/risk-assessment.htm
5. Guo L, Zhang X, Ren L, Yu X, Chen L, Zhou H, et al. Human antibody responses to avian influenza A(H7N9) virus, 2013. Emerg Infect Dis. 2014;20:192–200. http://dx.doi.org/10.3201/eid2002.131094
6. Zhang A, Huang Y, Tian D, Lau EH, Wan Y, Liu X, et al. Kinetics of serological responses in influenza A(H7N9)-infected patients correlate with clinical outcome in China, 2013. Euro Surveill. 2013;18:20657. http://dx.doi.org/10.2807/1560-7917.ES2013.18.50.20657
7. Huang R, Zhang L, Gu Q, Zhou YH, Hao Y, Zhang K, et al. Profiles of acute cytokine and antibody responses in patients infected with avian influenza A H7N9. PLoS One. 2014;9:e101788. http://dx.doi.org/10.1371/journal.pone.0101788
8. World Health Organization. Serological detection of avian influenza A(H7N9) virus infections by modified horse red blood cells haemagglutination-inhibition assay. 2013 [cited 2013 Dec 5]. http://www.who.int/influenza/gisrs_laboratory/cnic_serological_diagnosis_hai_a_h7n9_20131220.pdf
9. Rowe T, Abernathy RA, Hu-Primmer J, Thompson WW, Lu X, Lim W, et al. Detection of antibody to avian influenza A (H5N1) virus in human serum by using a combination of serologic assays. J Clin Microbiol. 1999;37:937–43.
10. Couzens L, Gao J, Westgeest K, Sandbulte M, Lugovtsev V, Fouchier R, et al. An optimized enzyme-linked lectin assay to measure influenza A virus neuraminidase inhibition antibody titers in human sera. J Virol Methods. 2014;210:7–14. http://dx.doi.org/10.1016/j.jviromet.2014.09.003
11. Hobson D, Curry RL, Beare AS, Ward-Gardner A. The role of serum haemagglutination-inhibiting antibody in protection against challenge infection with influenza A2 and B viruses. J Hyg (Lond). 1972;70:767–77. http://dx.doi.org/10.1017/S0022172400022610
12. Hannoun C, Megas F, Piercy J. Immunogenicity and protective efficacy of influenza vaccination. Virus Res. 2004;103:133–8. http://dx.doi.org/10.1016/j.virusres.2004.02.025
13. Coudeville L, Bailleux F, Riche B, Megas F, Andre P, Ecochard R. Relationship between haemagglutination-inhibiting antibody titres and clinical protection against influenza: development and application of a bayesian random-effects model. BMC Med Res Methodol. 2010;10:18. http://dx.doi.org/10.1186/1471-2288-10-18

14. Sridhar S, Begom S, Hoschler K, Bermingham A, Adamson W, Carman W, et al. Longevity and determinants of protective humoral immunity after pandemic influenza infection. Am J Respir Crit Care Med. 2015;191:325–32. http://dx.doi.org/10.1164/rccm.201410-1798OC
15. Kitphati R, Pooruk P, Lerdsamran H, Poosuwan S, Louisirirotchanakul S, Auewarakul P, et al. Kinetics and longevity of antibody response to influenza A H5N1 virus infection in humans. Clin Vaccine Immunol. 2009;16:978–81. http://dx.doi.org/10.1128/CVI.00062-09
16. Buchy P, Vong S, Chu S, Garcia JM, Hien TT, Hien VM, et al. Kinetics of neutralizing antibodies in patients naturally infected by H5N1 virus. PLoS One. 2010;5:e10864. http://dx.doi.org/10.1371/journal.pone.0010864
17. Bonduelle O, Carrat F, Luyt CE, Leport C, Mosnier A, Benhabiles N, et al. Characterization of pandemic influenza immune memory signature after vaccination or infection. J Clin Invest. 2014;124:3129–36. http://dx.doi.org/10.1172/JCI74565
18. Chen Z, Liu H, Lu J, Luo L, Li K, Liu Y, et al. Asymptomatic, mild, and severe influenza A(H7N9) virus infection in humans, Guangzhou, China. Emerg Infect Dis. 2014;20:1535–40. http://dx.doi.org/10.3201/eid2009.140424
19. Zeng X, Mai W, Shu B, Yi L, Lu J, Song T, et al. Mild influenza A/H7N9 infection among children in Guangdong Province. Pediatr Infect Dis J. 2015;34:104–7. http://dx.doi.org/10.1097/INF.0000000000000492
20. Wang X, Jiang H, Wu P, Uyeki TM, Feng L, Lai S, et al. Epidemiology of avian influenza A H7N9 virus in human beings across five epidemics in mainland China, 2013–17: an epidemiological study of laboratory-confirmed case series. Lancet Infect Dis. 2017;17:822–32. http://dx.doi.org/10.1016/S1473-3099(17)30323-7
21. Wang X, Fang S, Lu X, Xu C, Cowling BJ, Tang X, et al. Seroprevalence to avian influenza A(H7N9) virus among poultry workers and the general population in southern China: a longitudinal study. Clin Infect Dis. 2014;59:e76–83. http://dx.doi.org/10.1093/cid/ciu399
22. Yang P, Ma C, Cui S, Zhang D, Shi W, Pan Y, et al. Avian influenza A(H7N9) and (H5N1) infections among poultry and swine workers and the general population in Beijing, China, 2013–2015. Sci Rep. 2016;6:33877. http://dx.doi.org/10.1038/srep33877
23. Yang S, Chen Y, Cui D, Yao H, Lou J, Huo Z, et al. Avian-origin influenza A(H7N9) infection in influenza A(H7N9)-affected areas of China: a serological study. J Infect Dis. 2014;209:265–9. http://dx.doi.org/10.1093/infdis/jit430
24. Chen J, Ma J, White SK, Cao Z, Zhen Y, He S, et al. Live poultry market workers are susceptible to both avian and swine influenza viruses, Guangdong Province, China. Vet Microbiol. 2015;181:230–5. http://dx.doi.org/10.1016/j.vetmic.2015.09.016
25. Chen Z, Li K, Luo L, Lu E, Yuan J, Liu H, et al. Detection of avian influenza A(H7N9) virus from live poultry markets in Guangzhou, China: a surveillance report. PLoS One. 2014;9:e107266. http://dx.doi.org/10.1371/journal.pone.0107266
26. He F, Chen EF, Li FD, Wang XY, Wang XX, Lin JF. Human infection and environmental contamination with avian influenza A (H7N9) virus in Zhejiang Province, China: risk trend across the three waves of infection. BMC Public Health. 2015;15:931. http://dx.doi.org/10.1186/s12889-015-2278-0
27. Huang SY, Yang JR, Lin YJ, Yang CH, Cheng MC, Liu MT, et al. Serological comparison of antibodies to avian influenza viruses, subtypes H5N2, H6N1, H7N3, and H7N9 between poultry workers and non–poultry workers in Taiwan in 2012. Epidemiol Infect. 2015;143:2965–74. http://dx.doi.org/10.1017/S0950268815000394
28. Xiang N, Bai T, Kang K, Yuan H, Zhou S, Ren R, et al. Sero-epidemiologic study of influenza A(H7N9) infection among exposed populations, China 2013–2014. Influenza Other Respi Viruses. 2017;11:170–6. http://dx.doi.org/10.1111/irv.12435
29. Xu W, Lu L, Shen B, Li J, Xu J, Jiang S. Serological investigation of subclinical influenza A(H7H9) infection among healthcare and non–healthcare workers in Zhejiang Province, China. Clin Infect Dis. 2013;57:919–21. http://dx.doi.org/10.1093/cid/cit396
30. Morens DM. Editorial commentary: pandemic H5N1: receding risk or coming catastrophe? Clin Infect Dis. 2013;56:1213–5. http://dx.doi.org/10.1093/cid/cit051
31. Koopmans M, Wilbrink B, Conyn M, Natrop G, van der Nat H, Vennema H, et al. Transmission of H7N7 avian influenza A virus to human beings during a large outbreak in commercial poultry farms in the Netherlands. Lancet. 2004;363:587–93. http://dx.doi.org/10.1016/S0140-6736(04)15589-X
32. Du Ry van Beest Holle M, Meijer A, Koopmans M, de Jager CM. Human-to-human transmission of avian influenza A/H7N7, the Netherlands, 2003. Euro Surveill. 2005;10:264–8. http://dx.doi.org/10.2807/esm.10.12.00584-en
33. Meijer A, Bosman A, van de Kamp EE, Wilbrink B, Du Ry van Beest Holle M, Koopmans M. Measurement of antibodies to avian influenza virus A(H7N7) in humans by hemagglutination inhibition test. J Virol Methods. 2006;132:113–20. http://dx.doi.org/10.1016/j.jviromet.2005.10.001
34. Couch RB, Decker WK, Utama B, Atmar RL, Niño D, Feng JQ, et al. Evaluations for in vitro correlates of immunogenicity of inactivated influenza a H5, H7 and H9 vaccines in humans. PLoS One. 2012;7:e50830. http://dx.doi.org/10.1371/journal.pone.0050830
35. Hung IF, To KK, Lee CK, Lee KL, Chan K, Yan WW, et al. Convalescent plasma treatment reduced mortality in patients with severe pandemic influenza A (H1N1) 2009 virus infection. Clin Infect Dis. 2011;52:447–56. http://dx.doi.org/10.1093/cid/ciq106
36. Zhou B, Zhong N, Guan Y. Treatment with convalescent plasma for influenza A (H5N1) infection. N Engl J Med. 2007;357:1450–1. http://dx.doi.org/10.1056/NEJMc070359
37. Wu XX, Gao HN, Wu HB, Peng XM, Ou HL, Li LJ. Successful treatment of avian-origin influenza A (H7N9) infection using convalescent plasma. Int J Infect Dis. 2015;41:3–5. http://dx.doi.org/10.1016/j.ijid.2015.10.009

Address for correspondence: Wu-Chun Cao or Li-Qun Fang, State Key Laboratory of Pathogen and Biosecurity, Beijing Institute of Microbiology and Epidemiology, 20 Dongdajie, Beijing 100071, China; email: caowc@bmi.ac.cn or Fang_lq@163.com; Li-Ling Chen, Department of Infectious Diseases, Suzhou Municipal Center for Disease Control and Prevention, No. 72 Sanxiang Rd, Suzhou City, Jiangsu Province, China; email: liling_chen@163.com

Genomic Surveillance of 4CMenB Vaccine Antigenic Variants among Disease-Causing *Neisseria meningitidis* Isolates, United Kingdom, 2010–2016

Charlene M.C. Rodrigues, Jay Lucidarme, Ray Borrow, Andrew Smith, J. Claire Cameron, E. Richard Moxon, Martin C.J. Maiden

In September 2015, 4CMenB meningococcal vaccine was introduced into the United Kingdom infant immunization program without phase 3 trial information. Understanding the effect of this program requires enhanced surveillance of invasive meningococcal disease (IMD) *Neisseria meningitidis* isolates and comparison with prevaccination isolates. Bexsero Antigen Sequence Types (BASTs) were used to analyze whole-genome sequences of 3,073 prevaccine IMD *N. meningitidis* isolates obtained during 2010–2016. Isolates exhibited 803 BASTs among 31 clonal complexes. Frequencies of antigen peptide variants were factor H binding protein 1, 13.4%; Neisserial heparin-binding antigen 2, 13.8%; *Neisseria* adhesin A 8, 0.8%; and Porin A-VR2:P1.4,10.9%. In 2015–16, serogroup B isolates showed the highest proportion (35.7%) of exact matches to ≥1 Bexsero components. Serogroup W isolates showed the highest proportion (93.9%) of putatively cross-reactive variants of Bexsero antigens. Results highlighted the likely role of cross-reactive antigens. BAST surveillance of meningococcal whole-genome sequence data is rapid, scalable, and portable and enables international comparisons of isolates.

Neisseria meningitidis is an accidental human pathogen that is carried asymptomatically in the nasopharynx of 1%–40% of the population, depending on age and social behavior (*1*,*2*). In England and Wales, invasive meningococcal disease (IMD), comprising septicemia, meningitis, or both, develops in ≈2 persons/100,000 population/year (*3*). Patients might have nonspecific symptoms early in their illnesses, but their clinical conditions can deteriorate rapidly, with case-fatality rates of 5%–17% and physical and psychological sequelae in one third of survivors (*3*–*5*). Consequently, vaccination represents the optimal strategy for IMD prevention.

Meningococci are commonly characterized according to their expressed capsular polysaccharides, which define serogroups; 6 serogroups (A, B, C, W, X, and Y) cause most cases of IMD. The capsular antigens are major virulence factors, and efficacious A, C, W, and Y polysaccharide–based vaccines are used worldwide. However, serogroup B capsular polysaccharides are poorly immunogenic and share structural similarity to carbohydrates found in human tissues (*6*). The first serogroup B vaccines were derived from outer membrane vesicles (OMVs) for use in epidemics caused by single strains defined by genotype and Porin A (PorA) type (*7*). Genotype or clonal complex (CC), identified by multilocus sequence typing (MLST), groups related organisms and is useful for categorizing IMD phenotype, antimicrobial drug resistance, and vaccine antigens (*8*,*9*).

The United Kingdom and Ireland are among high-income countries with the highest incidence of IMD (*10*). The United Kingdom has low-incidence endemic disease and periods of hyperendemicity, which changes with frequency of hyperinvasive bacterial genotypes (*10*). Historically, endemic serogroup B IMD predominated and was caused by multiple CCs, especially hyperinvasive lineages CC41/44, CC269, CC213, and CC32 (*10*). In the 1990s, hyperendemic serogroup C IMD caused by CC11 (C:CC11) prompted introduction of infant meningococcal C conjugate vaccination and a catch-up campaign, which reduced disease incidence and carriage of C:CC11 (*11*). The United Kingdom experienced another period of hyperendemicity starting in 2012 with increasing incidence of W:CC11, lineage 11.1 meningococci, first identified in South America (*12*).

Author affiliations: University of Oxford, Oxford, UK (C.M.C. Rodrigues, E.R. Moxon, M.C.J. Maiden); Public Health England, Manchester, UK (J. Lucidarme, R. Borrow); Glasgow Royal Infirmary, Glasgow, Scotland, UK (A. Smith); University of Glasgow, Glasgow (A. Smith); Health Protection Scotland, Glasgow (J.C. Cameron)

DOI: https://doi.org/10.3201/eid2404.171480

The diversity of CCs responsible for IMD renders OMVs derived from a single CC insufficient to provide broad protection. Alternative vaccine candidates have been developed. These candidates are composed of subcapsular proteins prevalent among many *N. meningitidis* strains. However, their protective potential has been complicated by meningococcal diversity (*13*–*15*). Two vaccines were licensed in 2013: 4CMenB (Bexsero; GlaxoSmithKline, Brentford, UK) for infants in Europe and bivalent recombinant lipoprotein rLP2086 (Trumenba; Pfizer, New York, NY, USA) for persons 10–25 years of age in the United States (*16*–*18*). The 4CMenB vaccine contains multiple proteins: factor H binding protein (fHbp); Neisserial heparin-binding antigen (NHBA); *Neisseria* adhesin A (NadA); and PorA P1.7–2,4 from the New Zealand OMV vaccine (MeNZB) (*16*). The rLP2086 vaccine contains 2 fHbp variants, 1 each from subfamily A (A05) and subfamily B (B01) (*17*).

Bexsero was implemented into the United Kingdom immunization schedule on September 1, 2015, as a 2-dose priming course for infants at 2 and 4 months of age and a booster at 12 months of age, intended as an efficacious strategy for those at highest risk within the constraints of cost-effectiveness (*18*). As with previously licensed meningococcal vaccines, efficacy studies were precluded because of the rarity of IMD, and the Meningococcal Antigen Typing System (MATS) was developed, which estimated 73% (95% CI 57%–87%) vaccine coverage for UK isolates (*19*,*20*).

An appreciation of meningococcal antigenic diversity and persistence over time is required to determine the degree and longevity of coverage provided by protein vaccines. Real-time, continuous, and high-throughput methods are needed to identify characteristics of circulating meningococci on a national scale, especially the frequency distribution of vaccine antigens. This characterization can be performed rapidly and reproducibly by using whole-genome sequencing (WGS) of IMD *N. meningitidis* isolates, for which data are publicly available online in the PubMLST database (https://pubmlst.org/neisseria) (*21*).

A novel nomenclature, Bexsero Antigen Sequence Types (BASTs), was devised to describe Bexsero antigenic variants (*22*). There were strong, nonoverlapping associations between BAST and CC, with an estimated 58.3%–60.3% Bexsero coverage including the antigenic variants in Bexsero or cross-reactive variants (*22*). We cataloged genomic diversity of Bexsero vaccine antigens by using web-accessible platforms incorporating BAST. This study provides a reference point for changes in population structure of IMD-causing meningococci in the United Kingdom before introduction of Bexsero.

Materials and Methods

A total of 3,073 meningococci were isolated from culture-confirmed IMD cases in the United Kingdom during epidemiologic years (July 1–June 30) 2010–2016. For the purposes of this study, the prevaccine period includes 2015–16 because implementation of Bexsero started on September 1, 2015, and many infants were not fully vaccinated during the peak IMD season (December 2015–February 2016). The 3,073 isolates represented ≈55% of laboratory-confirmed cases of IMD (Table 1) because recovery of isolates reflects differential survival in artificial media, susceptibility to antimicrobial drugs given before venipuncture, or small-volume pediatric blood cultures.

Genomic Analysis

WGS was part of the Meningitis Research Foundation Meningococcus Genome Library initiative (*10*). Genomes were assembled by using Velvet and VelvetOptimiser, uploaded to the PubMLST database, and annotated by using *Neisseria* Sequence Typing Database numbers (NEIS) for all loci. Analysis was undertaken by using the gene-by-gene approach with the Bacterial Isolate Genome Sequence Database to determine sequence type (ST), CC, and strain designation (*21*,*23*). Each isolate had associated provenance and phenotype data, including year, serogroup, and region.

Table 1. Geographic distribution of culture-confirmed invasive meningococcal disease isolates that have undergone whole-genome sequencing, United Kingdom, 2010–2016*

	No. isolates by region†					No. laboratory-confirmed cases (% isolates)		Serogroup, no. isolates‡									
Year	1	2	3	4	Total	PHE	PHS	A	B	C	E	NG	W	W/Y	X	Y	Z
2010–11	464	37	36	13	550	1,009 (46.0)	76 (47.4)	1	423	13	1	5	27	2	1	76	1
2011–12	370	28	30	11	439	730 (50.7)	56 (53.6)	0	311	18	1	4	32	1	0	72	0
2012–13	415	29	34	13	491	769 (54.0)	66 (51.5)	0	325	29	0	7	51	1	0	78	0
2013–14	367	27	30	12	436	636 (57.7)	60 (50.0)	0	240	24	0	1	92	2	0	77	0
2014–15	483	19	55	15	572	724 (66.7)	65 (84.6)	0	283	23	0	5	172	2	0	87	0
2015–16	488	23	62	12	585	805 (60.6)	99 (62.6)	0	238	34	2	8	197	2	0	104	0
Total	2,587	163	247	76	3,073	4,673 (55.4)	442 (55.9)	1	1,820	141	4	30	571	10	1	494	1

*Laboratory-confirmed cases included culture-confirmed and PCR-confirmed cases. Data included in this study represented 55.4% of all laboratory-confirmed cases in England and 55.9% of those in Scotland. NG, nongroupable; PHE, Public Health England; PHS, Public Health Scotland.
†1, England; 2, Wales; 3, Scotland; 4, Northern Ireland.
‡W/Y serogroups were combined because of inconclusive serogrouping results.

We assigned BASTs as described (*22*). Nucleotide sequences of *fhbp*, *nhba*, *nadA*, and *porA* variable regions 1 and 2 (VR1 and VR2) were translated to deduce peptide sequences, and variant numbers were assigned by using established nomenclatures (*24–26*). Unique combinations of the 5 components were assigned a BAST number in order of discovery; BAST-1 corresponds to the vaccine constituents: fHbp 1, NHBA 2, NadA 8, and PorA 7–2,4 (*22*). Data were manually curated to confirm the absence of *fhbp*, *nhba*, *nadA*, and *porA*, and isolates were assigned peptide designation 0 (null). If nucleotide sequences contained a frameshift mutation, peptide designation 0 (null) was assigned. Peptide variants were not assigned if the complete gene was not available because of sequencing or assembly issues (*22*,*27*).

For assessment of Bexsero antigenic variants expected to be prevented by vaccination (coverage), we compared the genotypic profile (BAST) of isolates with those of vaccine antigenic variants. The term exact match indicates isolates having ≥1 of 4 Bexsero antigenic variants (fHbp 1, NHBA 2, NadA 8, and PorA-VR2:4). The term cross-reactive match indicates isolates having ≥1 variant that can potentially be recognized by Bexsero-induced antibodies, demonstrating a possible cross-protective immune response in humans.

These variants were previously identified by using MATS analysis, which at the time of writing, was the most extensively used method for assessing qualitative and quantitive differences in antigens (*20*,*28*,*29*). Variants were considered putatively cross-reactive; fHbp peptides 4, 13, 14, 15, 37, 232 and NadA variants 1 or 2/3. NadA peptides were included because of potential discrepancies between in vitro and in vivo NadA expression (*20*,*30*). Cross-reactive NHBA peptides were not included because of lack of data on the breadth of peptides covered by Bexsero. Genomic analysis has not been used to infer protein expression or immunologic cross-reactivity per se.

We performed all statistical analyses by using R software version 3.2.4 (https://www.r-project.org/). We calculated the Simpson index of diversity by using the Vegan package in R software to assess diversity of BAST; values closer to 1 indicated greater diversity.

Nomenclature of Antigenic Variants

There are 3 systems for classifying fHbp variants. The first system described 3 variants (1–3) on the basis of sequence similarity and cross-reactivity in serum bactericidal antibody (SBA) assays (*31*). The second system described 2 subfamilies, A and B (*32*). The third system, used in our study as part of the BAST scheme, assigned arbitrary numerical integers to unique deduced peptide sequences independent of variant/subfamily (*24*). NHBA peptide variants were assigned arbitrarily to unique peptide sequences. Updated nomenclature for NadA described 4 variants on the basis of peptide sequence homology: NadA-1, NadA-2/3, NadA-4/5, and NadA-6 (*26*). PorA nomenclature was based on nucleotide and peptide sequence homology and recognized the previous serologic classification: P1, followed by VR1 family-variant, and VR2 family-variant (e.g., P1.7–2,4) (*25*). All nomenclature is available in the PubMLST database.

Results

Distribution of Bexsero Vaccine Antigens

For 2,922 isolates (95.1%), MLST, which was deduced from WGS data, identifed 645 STs with 2,866 (93.3%) isolates assigned to 1 of 31 CCs. We found variation in CC distribution over the 6-year period, with a 10-fold increase in CC11 and decreases in CC41/44 (172 to 56, 50.0%) and CC269 (108 to 52, 51.8%), which accounted for most serogroup B isolates (Figure 1).

fHbp Peptide

An *fhbp* gene was present in 3,065 (99.7%) isolates, absent in 5 (1.6%), and not assigned in 3 (0.1%) because of incomplete sequence assembly. Across all serogroups, variant 2 fHbp peptides increased over the 6-year period, but most markedly in 2014–15 (313/572, 54.7%) and 2015–16 (347/585, 59.3%). From 2010–11 through 2012–13, variant 1 peptides predominated; from 2013–14 onwards, variant 2 peptides were more frequent than variant 1 peptides (Figure 2, panel A). Overall, there were 207 unique fHbp peptides in the collection: 109 variant 1, 43 variant 2, 54 variant 3, and 1 between variants 2 and 3.

Variant 1 peptides were present in 1,389 (45.3%) of 3,065 isolates, and 5 peptides accounted for 1,144 (82.4%) of 1,389 isolates: 4 (399, 28.7%), 13 (329, 23.7%), 15 (184, 13.2%), 14 (127, 9.1%), and 1 (105, 7.6%). The contribution of these 5 peptide variants among IMD *N. meningitidis* isolates decreased from 278 (50.5%) of 550 isolates in 2010–11 to 154 (26.3%) of 585 isolates in 2015–16. Peptide 4 was predominantly associated with B:CC41/44, whereas peptides 13 and 15 were mainly associated with B:CC269. Peptide 1, the variant in Bexsero, was present in 105 isolates, predominantly B:CC32, and decreased in incidence from 25 (4.5%) of 550 isolates in 2010–11 to 13 (2.2%) of 585 isolates in 2015–16.

Variant 2 peptides were present in 1,404 (45.8%) of 3,065 isolates; 6 peptides (22, 25, 19, 16, 21, and 24) accounted for 1,323 (94.2%) of 1,404 isolates. Peptide 22 (predominantly W:CC11) increased 13-fold from 15 isolates in 2010–11 to 198 isolates in 2015–16. Peptide 25, associated with Y:CC23, was consistently present through the period.

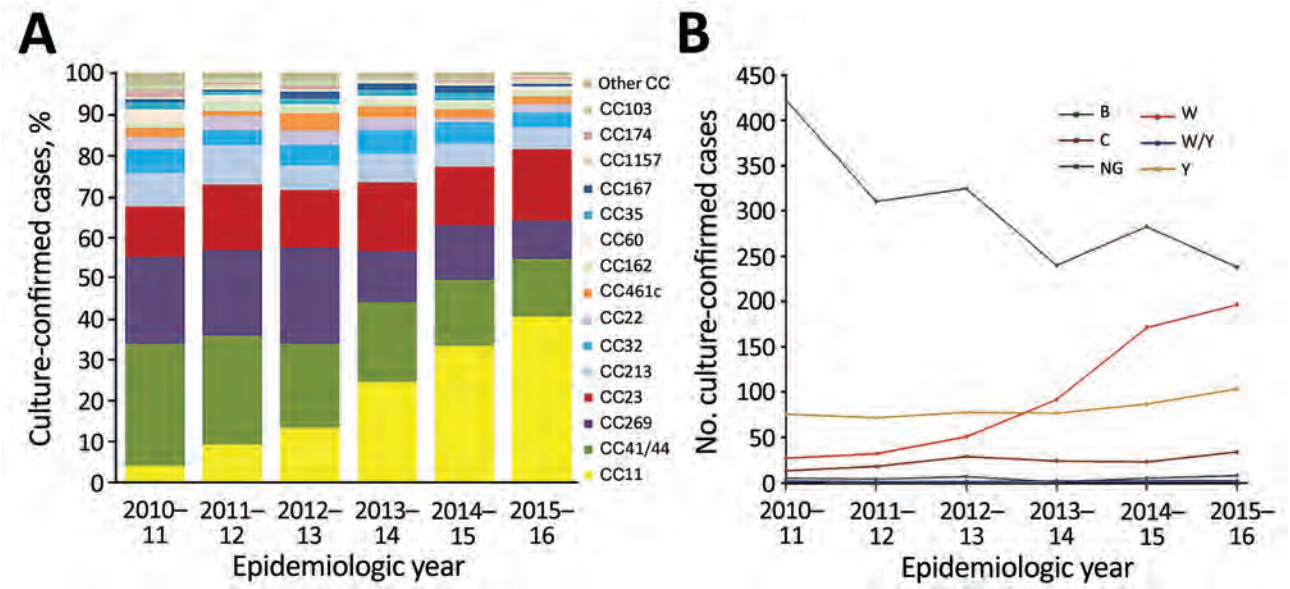

Figure 1. Clonal complex and serogroup distribution of invasive meningococcal disease isolates, United Kingdom, 2010–2016. A) Proportional contribution of each CC of disease-causing culture-confirmed meningococcal isolates by epidemiologic year. Other CC indicates CCs that were found in <20 isolates during the 6-year study period. B) Distribution of isolate serogroups by epidemiologic year. Serogroups shown had ≥10 isolates during the 6-year study period. Serogroups with ≤10 isolates (A, E, X, and Z) are shown in Table 1. CC, clonal complex; NG, nongroupable, W/Y, serogroups combined because of inconclusive serogrouping results.

Variant 3 peptides were present in 274 (8.9%) of 3,065 isolates. Peptides 45, 47, and 31 were the most frequently occurring (predominantly B:CC213 and B:CC461).

NHBA Peptide

The *nhba* gene was present in 2,986 (97.2%) isolates; 87 isolates were not assigned an allelic variant because of incomplete sequence assembly. There were 163 unique NHBA peptides, and 4 isolates were assigned null (0), considered unlikely to express functional proteins because of frameshift mutations in the *nhba* coding region. The most frequently occurring peptide was 29 (568/2,986, 19.0%), which increased 7-fold during the study period and was associated with W:CC11. The second most common was peptide 2, the variant in Bexsero, which decreased in incidence from 111 (20.2%) of 550 isolates in 2010–11 to 50 (8.5%) of 585 isolates in 2015–16; most (411/424) isolates belonged B:CC41/44. Other prevalent NHBA variants were 7, 17, 21, 20, and 18, which, with 29 and 2, accounted for 2,258 (75.6%) of 2,986 isolates (Figure 2, panel B).

NadA Peptide

We found 2,036 (66.3%) isolates in which *nadA* was absent, 34 (1.1%) with an insertion element, and 38 (1.2%) not assigned an allelic variant because of incomplete sequence assembly. A total of 2,128 (69.2%) isolates were assigned NadA peptide null (0) because of absence of *nadA* genes or presence of frameshift mutations or insertion elements disrupting the coding sequence. Of the prevalent CCs, NadA peptide was absent from all isolates belonging to CC41/44, CC23, CC22, CC162, CC35, CC167, CC103, and CC282. Of the 907 (29.5%) isolates with NadA peptides present, there were 135 (4.4%) NadA-1 variants, 592 (19.3%) NadA-2/3 variants, and 180 (5.9%) NadA-4/5 variants; there were no NadA-6 variants (Figure 2, panel C). The proportion of isolates with NadA peptides increased from 96 (17.5%) of 550 isolates in 2010–11 to 257 (43.9%) of 585 isolates in 2015–16. Among these isolates, there were 23 unique peptides. The most common, peptide 6 (NadA-2/3), increased from 14 (2.5%) of 550 isolates in 2010–11 to 187 (40.0%) of 585 isolates in 2015–16. Peptide 79 (NadA-4/5, contained a homopolymeric tract resulting in phase variation) was the second most common, designated as phase variable on, and occurred in 164 isolates, predominantly B:CC213. Peptide 8 (NadA-2/3), found in Bexsero, was present in 0.8% (26/3,073) of isolates (Y:CC174, B:CC269, B:CC60, B:CC18, A:CC5).

PorA Peptide

The *porA* gene was present in 3,011 (98.0%) of 3,073 isolates. For 54 isolates, no nucleotide sequence allele was assigned because of incomplete sequence assembly. For 3,064 (99.7%) isolates, predicted VR1 and VR2 peptides were obtained. PorA-VR2 variant 4 was found in 336 (10.9%) isolates, and showed decreasing incidence from 90

(16.5%) of 547 isolates in 2010–11 to 38 (6.5%) of 585 isolates in 2015–16. PorA-VR2 variant 4 containing isolates were predominantly B:CC41/44 (302/336, 89.9%) but also B:CC162, B:CC269, B:CC213, B:CC32, and B:CC60 and were associated with PorA-VR1 variants 7–2 (n = 330), 17 (n = 2), 12–3 (n = 2), 22 (n = 1), and 22–1 (n = 1) (Figure 2, panel D).

BAST

We determined 803 unique BASTs for 2,917 (94.9%) isolates. The ratio of BASTs per isolate was calculated by dividing the number of unique BASTs by the number of isolates. This ratio decreased from 0.416 in 2010–11 to 0.265 in 2015–16. The Simpson index of diversity ranged from 0.976 in 2010–11 to 0.902 in 2015–16 (Table 2). We

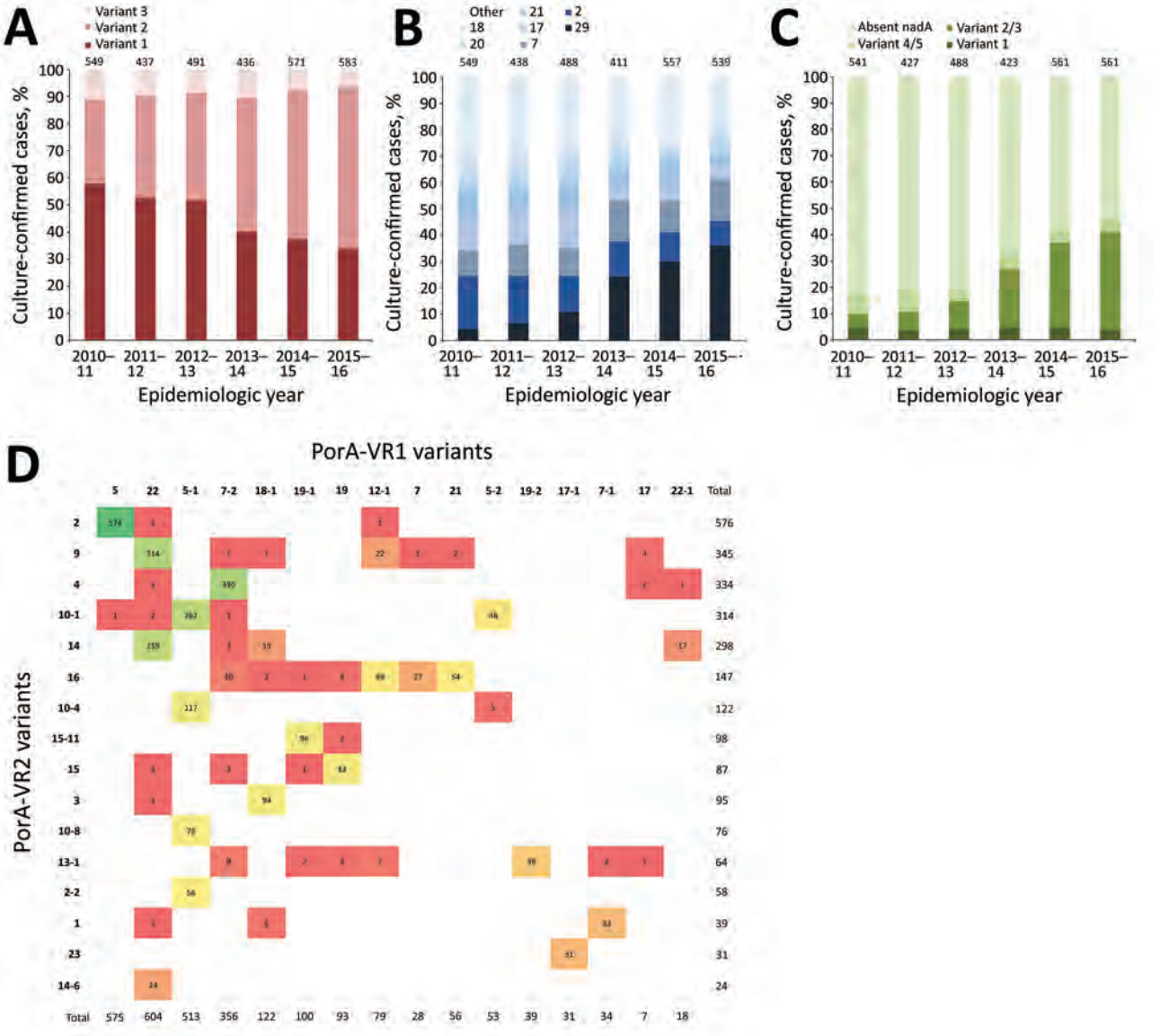

Figure 2. Distribution of 4CMenB vaccine antigenic variants among invasive meningococcal disease isolates, United Kingdom, 2010–2016. A) Proportion of isolates with fHbp variants 1, 2, and 3 by epidemiologic year. Peptide 1 is found in the Bexsero 4CMenB vaccine (GlaxoSmithKline, Bentford, UK), and cross-reactive variants included in this analysis are all variant 1 peptides. B) Proportion of isolates with the 7 most prevalent NHBA peptides by epidemiologic year; all other peptide variants are in "other." Peptide 2 is contained in Bexsero. C) Proportion of isolates with NadA variants 1, 2/3, and 4/5 by epidemiologic year; there were no isolates with NadA variant 6. Peptide 8 (variant 2/3) is contained in Bexsero. Values above columns indicate number of unique peptides. D) Frequency distribution of PorA-VR1 (horizontal axis) and PorA-VR2 (vertical axis) variants. Variants shown were those that had >20 isolates in the collection from the United Kingdom during 2010–2016. Bexsero contains the MeNZB OMV vaccine components, including variants PorA P1.7–2,4. Color scales show the frequency of isolates from highest (green) to lowest (red). fHbp, factor H binding protein; NadA, *Neisseria* adhesin A; NHBA, Neisserial heparin-binding antigen; OMV, outer membrane vesicles; PorA, porin A.

Table 2. Number of unique BASTs and measures of diversity among invasive meningococcal disease isolates, United Kingdom, 2010–2016*

Epidemiologic year	No. unique BASTs	No. isolates	No. BASTs/isolate	Simpson index of diversity
2010–11	229	550	0.416	0.976
2011–12	187	439	0.426	0.977
2012–13	226	491	0.460	0.976
2013–14	181	436	0.415	0.960
2014–15	199	572	0.348	0.924
2015–16	155	585	0.265	0.902
Total	803	3,073	0.261	0.963

*BASTs, Bexsero Antigen Sequence Types.

found strong, nonoverlapping association of BAST and CC (Figure 3). When we compared BAST prevalence pre-implementation (cases during July 1, 2010–September 1, 2015) and postimplementation (cases during September 1, 2015–June 30, 2016), we found statistically significant increases in BAST-2 (CC11), BAST-221 (CC23), BAST-232 (CC41/44), and BAST-8 (CC11) and a decrease in BAST-220 (CC41/44) (Figure 4).

BAST Distribution by Serogroup

Although Bexsero is licensed for serogroup B IMD, its components might be present on the surface of meningococci, independent of capsular type. Therefore, we analyzed distribution of Bexsero antigens by serogroup. Serogroup B isolates had the highest proportion of exact matches to ≥1 Bexsero antigen: 155 (36.6%) of 423 isolates in 2010–11 and 85 (35.7%) of 238 isolates in 2015–16, predominantly CC41/44. The proportion of isolates with exact or potentially cross-reactive antigens was 293 (69.3%) of 423 isolates in 2010–11 and 149 (62.6%) of 238 isolates in 2015–16 and represented CC269, CC41/44, CC32, CC213, CC60, CC1157, CC18, CC162, CC11, CC461, CC35, CC167, and CC254. The potentially cross-reactive variants included fHbp peptides 4, 13, 14, and 15 (956/1,144) and NadA peptide 1 (118/1,144).

For serogroup C, 8/141 isolates had ≥1 exact match to Bexsero components, but numbers varied each year depending on predominant CC. There were 2 (15.4%) of 13 matches to Bexsero components in 2010–11 and 3 (13.0%) of 23 matches to Bexsero components in 2014–15; isolates belonged to CC32. No isolates were exact matches in 2011–12 and 2015–16 (predominantly CC11). The proportion of isolates also having potentially cross-reactive antigens increased from 4 (30.8%) of 13 in 2010–11 to 25 (91.3%) of 34 in 2014–15. The antigenic variants were fHbp (50 isolates, predominantly peptide 13) and NadA (50 isolates, predominantly peptides 121, 127, and 1), largely reflecting secular changes in CC distribution with increases in CC11, CC269, CC32, and CC174.

Of 571 serogroup W isolates, 1 (0.2%) CC11 isolate was an exact match to Bexsero components (fHbp 1). When we included matches to potentially cross-reactive antigens, there were 14 (51.9%) of 27 isolates in 2010–11, which increased to 185 (93.9%) of 197 isolates in 2015–16. This increase was caused by NadA 6 in 500 (87.6%) of 571 isolates and fHbp 13 in 7 (1.2%) of 571 isolates, all of which belonged to lineage 11.1, W:CC11.

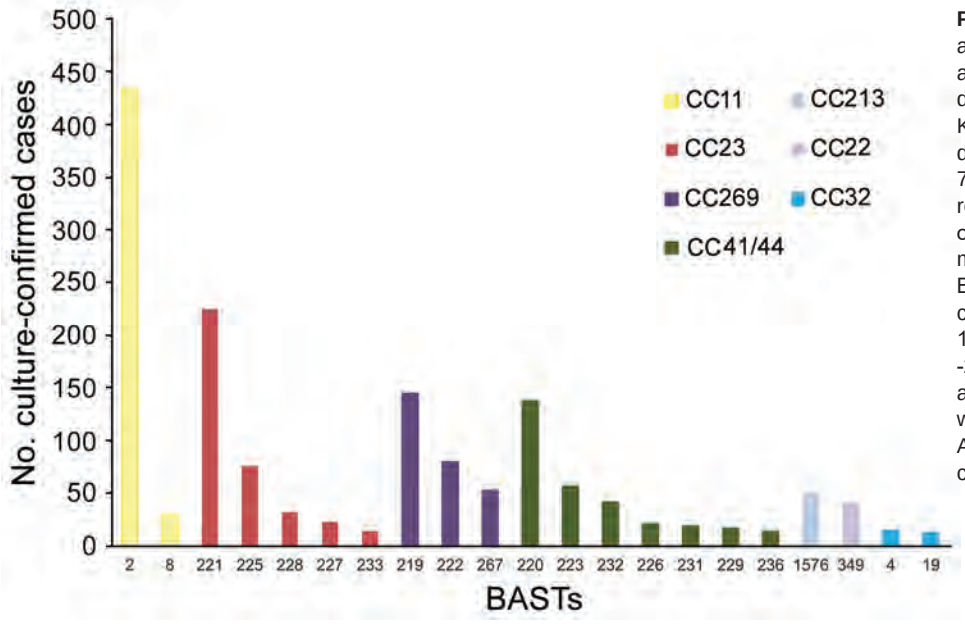

Figure 3. Nonoverlapping association of BAST and CC among invasive meningococcal disease isolates, United Kingdom, 2010–2016. Frequency distribution of BAST by CC for the 7 most frequently found CCs that represent 82.4% (2,533/3,073) of culture-confirmed invasive meningococcal disease isolates. BAST-220, -223, -4, and -19 contain an exact match with BAST-1. BAST-2, -8, -219, -222, -232, -226, -231, -229, and -236 contain a potentially cross-reactive match with BAST-1. BAST, Bexsero Antigen Sequence Type; CC, clonal complex.

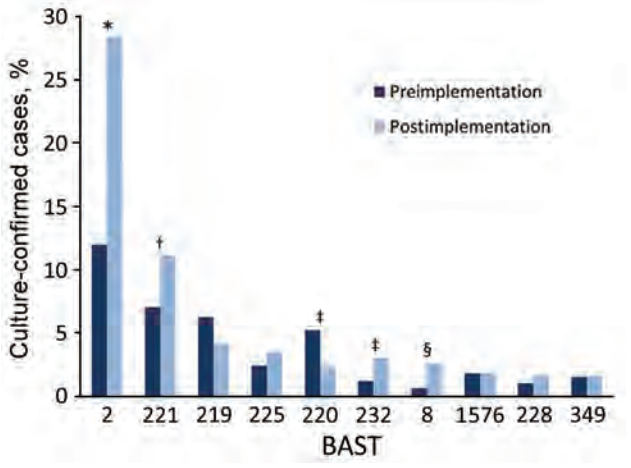

Figure 4. Changes in BAST prevalence before and after Bexsero implementation among invasive meningococcal disease isolates, United Kingdom, 2010–2016. Frequency of BASTs is shown for the period before implementation of Bexsero vaccine, July 2010–August 2015 (dark blue), and after implementation, September 2015–June 2016 (light blue). The most frequently occurring BASTs preimplementation were 2,¶ 221, 219,¶ 220,# 222,¶ 267, 225, 223,# 1576, and 349. The most frequent BASTs postimplementation were 2,¶ 221, 219,¶ 225, 220,# 232,¶ 8,¶ 1576, 228, and 349. *p<0.00001; †p<0.01; ‡p<0.05; §p<0001; ¶BAST contains a potentially cross-reactive match to BAST-1; #BAST contains an exact match to BAST-1. BASTs with significant changes preimplementation and postimplementation were BAST-2 (fHbp 22, NHBA 29, NadA 6, PorA-VR1:5, and PorA-VR2:2), p<0.00001; BAST-221 (25; 7; 0; 5–1; 10–1), p = 0.006; BAST-220 (4; 2; 0; 7–2; 4), p = 0.02; BAST-232 (4; 2; 0; 12–1; 16), p = 0.01; and BAST-8 (22; 29; 121; 5; 2), p = 0.0005. BAST, Bexsero Antigen Sequence Type.

Serogroup Y disease isolates showed exact matches to Bexsero components in 7 (9.2%) of 76 isolates in 2010–11, which decreased to 3 (2.9%) of 104 isolates in 2015–16. When potential cross-reactive antigens were included, matches ranged from 9 (11.8%) of 76 isolates in 2010–11 to 3 (2.9%) of 104 isolates in 2015–16 and represented CC174, CC23, CC22, and CC11.

Discussion

The requirement for vaccines to protect against serogroup B meningococci from multiple CCs led to development of multipeptide vaccines, such as 4CMenB (Bexsero) and bivalent rLP2086 (Trumenba) (*16*,*17*). Bexsero was introduced into the UK infant immunization schedule in September 2015, supported by data from the MATS assay that estimated 73% IMD *N. meningitidis* isolate coverage in England and Wales in 2007–08 (*20*).

We report a comprehensive evaluation of the frequency distribution of Bexsero antigen peptide variants in IMD *N. meningitidis* isolates, which used a national collection of WGS of culture-confirmed cases from 2010–2016. The frequency distribution of individual vaccine antigens was correlated with the distribution of meningococcal CCs in the United Kingdom over time. During 2010–2016, high diversity of 803 BASTs and 31 CCs emphasized the broad coverage required of peptide-based vaccines if they are to protect against endemic disease caused by multiple CCs. The most frequently occurring BASTs (20 representing 44.1% of serogroup B isolates) could provide useful information for future vaccine formulations.

Bexsero components correspond to BAST-1, fHbp 1, NHBA 2, NadA 8, PorA-VR1:7–2, and PorA-VR2:4. In this study, the incidence of individual BAST-1 antigens in serogroup B IMD cases in the United Kingdom during 2010–2016 was 5.4% (99/1,820) for fHbp, 23.0% (419/1,820) for NHBA, 0.3% (5/1,820) for NadA, and 18.4% (335/1,820) for PorA-VR2. Low levels of exact antigenic variants found in Bexsero imply that host immunogenicity to cross-reactive antigens would be necessary to provide the level of protection required by a national vaccination program, although this host response is also dependent on adequate protein expression, which cannot be determined solely from genomic analysis. In vitro studies comparing bactericidal killing of various fHbp variant 1 peptide–expressing meningococci (peptides 1, 2, 3, 4, 5, 10, 12, 13, 14, and 15) found cross-reactivity in postvaccination serum samples from adults, but functional activity in infants was limited to peptides 1 and 2 after immunization at 2, 4, and 6 months of age (*33*).

Surface protein expression is also a major determinant of bactericidal killing. For fHbp, when heterologous bactericidal activity was tested, mouse antisera to peptide 1 produced positive titers against closely related peptide 4 regardless of expression level. For more distantly related peptides, such as peptide 15, higher protein expression was required (*34*).

At the time of writing, the most extensive estimation of cross-reactivity data for Bexsero had been collected by using the MATS assay. This assay quantifies expression and antigenic similarities of fHbp, NHBA, and NadA by sandwich ELISA and identifies PorA serosubtype by sequencing for each isolate (*20*,*35*). During development, the antigen measurements for fHbp, NHBA, and NadA were correlated to bactericidal killing with relative potency (RP) against 57 reference isolates tested by an SBA assay, determining likelihood of bacterial killing. Isolates with PorA-VR P1.4 peptide were considered to be covered, without further serologic testing (*35*). Contemporaneous MATS estimate of coverage for IMD *N. meningitidis* isolates from the United Kingdom during 2014–15 was 66% (95% CI 52%–80%) (*28*). However, the presence, cross-reactivity, and expression levels of antigenic variants in meningococci alone does not directly measure their susceptibility to bactericidal killing, which is also dependent on host innate and adaptive immune responses, a function not measured by the

MATS assay. Therefore, this assay remains a surrogate for estimating functional activity against cross-reactive antigenic variants.

Among UK isolates we examined, the most frequent peptide variant 1 fHbp peptides were 4, 13, 15, 14, and 1. For most fHbp peptide 1 isolates tested by MATS, their RP lies above the positive bactericidal threshold (PBT), and these isolates are predicted to be killed by the pooled serum from Bexsero-vaccinated toddlers used in the assay (*20*). However, for other fHbp variant 1 peptides, there was marked variation in coverage estimates by MATS for isolates with the same peptide variant. Two MATS studies in Europe identified the RP for peptide 4 isolates to be most consistently above the PBT, but RP for peptide 13, 14, and 15 isolates spanned the PBT (*20*,*29*). The degree of protection afforded by Bexsero vaccination will be observed through postimplementation enhanced surveillance. With 2-dose vaccine uptake at 88.6%, early reports of vaccine efficacy were estimated to be 82.9% (95% CI 24.1%–95.2%) (*36*). If these high efficacy estimates, albeit with wide CIs, continue to show protection beyond that predicted by genotypic, phenotypic, or functional estimates, then synergistic activity or minor antigens might need to be considered, neither of which are quantified by MATS or BAST.

Coverage for nonserogroup B isolates by Bexsero-induced immunity was of special interest in the United Kingdom because of increasing IMD cases caused by W:CC11 from 2012, with severe and atypical IMD and high mortality rates (*37*). The principal change in this analysis was the increase of BAST-2 (22; 29; 6; 5; 2), a direct consequence of W:CC11 clonal expansion. Although conjugate ACWY vaccine was introduced in August 2015, it was targeted to teenagers, the age group with increased disease and highest risk for carriage (*38*). There is a paucity of supporting immunologic evidence for the role of Bexsero in protection against nonserogroup B isolates, but in a small case series of 6 W:CC11 isolates, all BAST-2, human SBA assay responses of $\geq$1:32 were observed by using pooled serum from infants vaccinated with 3 doses of Bexsero (*39*). Therefore, some protection might be provided to Bexsero-vaccinated infants and toddlers.

After implementation of Bexsero into the UK immunization schedule, long-term vaccine effectiveness will be established by enhanced IMD surveillance accompanied by characterization of meningococcal isolates (*36*). The methods used here are rapid, standardized, open-source, and readily applied to different settings (*22*,*40*). Use of WGS in the Meningitis Research Foundation Meningococcus Genome Library initiative in the United Kingdom to extract vaccine antigenic variant data enables rapid isolate characterization, surveillance of circulating meningococci, and monitoring of secular changes and the impact of all meningococcal vaccines in use (*10*,*22*). These data serve as a reference point against which effects of the national Bexsero program can be compared, and highlight reliance on cross-reactive variants to maintain effective protection. Finally, such data will be invaluable in development of novel vaccine formulations that ensure continued coverage.

Acknowledgments

We thank staff at all reference laboratories, in particular, Aiswarya Lekshmi, Tony Carr, Steve Gray, Kevin Scott, Roisin Ure, Diane Lindsay, and Barbara Denham, for their commitment to this study. This study used the Meningitis Research Foundation Meningococcus Genome Library (http://www.meningitis.org/research/genome), which was developed in a collaborative effort by Public Health England, the Wellcome Trust Sanger Institute, and the University of Oxford. It also used the Neisseria PubMLST website (http://pubmlst.org/neisseria/), developed by Keith Jolley and sited at the University of Oxford.

The Meningitis Research Foundation Meningococcus Genome Library is part of the *Neisseria* Sequence Typing database website developed by Keith Jolley and Martin Maiden and hosted by the University of Oxford and supported by the Wellcome Trust (grant 104992). C.M.C.R. (grant 109031/Z15/Z) and M.C.J.M. (grant 087622) were supported by the Wellcome Trust.

About the Author

Dr. Rodrigues is a clinician specializing in pediatric infectious diseases at the University of Oxford, Oxford, UK. Her research interests are the genomic epidemiology of meningococcal vaccine antigens.

References

1. MacLennan J, Kafatos G, Neal K, Andrews N, Cameron JC, Roberts R, et al.; United Kingdom Meningococcal Carriage Group. Social behavior and meningococcal carriage in British teenagers. Emerg Infect Dis. 2006;12:950–7. http://dx.doi.org/10.3201/eid1206.051297
2. Christensen H, May M, Bowen L, Hickman M, Trotter CL. Meningococcal carriage by age: a systematic review and meta-analysis. Lancet Infect Dis. 2010;10:853–61. http://dx.doi.org/10.1016/S1473-3099(10)70251-6
3. Ladhani SN, Flood JS, Ramsay ME, Campbell H, Gray SJ, Kaczmarski EB, et al. Invasive meningococcal disease in England and Wales: implications for the introduction of new vaccines. Vaccine. 2012;30:3710–6. http://dx.doi.org/10.1016/j.vaccine.2012.03.011
4. Viner RM, Booy R, Johnson H, Edmunds WJ, Hudson L, Bedford H, et al. Outcomes of invasive meningococcal serogroup B disease in children and adolescents (MOSAIC): a case-control study. Lancet Neurol. 2012;11:774–83. http://dx.doi.org/10.1016/S1474-4422(12)70180-1
5. Salisbury D, Ramsay MK. Immunisation against infectious disease. London: The Stationery Office; 2006.
6. Finne J, Leinonen M, Mäkelä PH. Antigenic similarities between brain components and bacteria causing meningitis: impli-

cations for vaccine development and pathogenesis. Lancet. 1983;2:355–7. http://dx.doi.org/10.1016/S0140-6736(83)90340-9
7. Holst J, Martin D, Arnold R, Huergo CC, Oster P, O'Hallahan J, et al. Properties and clinical performance of vaccines containing outer membrane vesicles from *Neisseria meningitidis.* Vaccine. 2009;27(Suppl 2):B3–12. http://dx.doi.org/10.1016/j.vaccine.2009.04.071
8. Maiden MC, Bygraves JA, Feil E, Morelli G, Russell JE, Urwin R, et al. Multilocus sequence typing: a portable approach to the identification of clones within populations of pathogenic microorganisms. Proc Natl Acad Sci U S A. 1998;95:3140–5. http://dx.doi.org/10.1073/pnas.95.6.3140
9. Jolley KA, Maiden MC. Using MLST to study bacterial variation: prospects in the genomic era. Future Microbiol. 2014;9:623–30. http://dx.doi.org/10.2217/fmb.14.24
10. Hill DMC, Lucidarme J, Gray SJ, Newbold LS, Ure R, Brehony C, et al. Genomic epidemiology of age-associated meningococcal lineages in national surveillance: an observational cohort study. Lancet Infect Dis. 2015;15:1420–8. http://dx.doi.org/10.1016/S1473-3099(15)00267-4
11. Maiden MC, Ibarz-Pavón AB, Urwin R, Gray SJ, Andrews NJ, Clarke SC, et al. Impact of meningococcal serogroup C conjugate vaccines on carriage and herd immunity. J Infect Dis. 2008;197:737–43. http://dx.doi.org/10.1086/527401
12. Lucidarme J, Hill DM, Bratcher HB, Gray SJ, du Plessis M, Tsang RS, et al. Genomic resolution of an aggressive, widespread, diverse and expanding meningococcal serogroup B, C and W lineage. J Infect. 2015;71:544–52. http://dx.doi.org/10.1016/j.jinf.2015.07.007
13. Gupta S, Maiden MCJ, Feavers IM, Nee S, May RM, Anderson RM. The maintenance of strain structure in populations of recombining infectious agents. Nat Med. 1996;2:437–42. http://dx.doi.org/10.1038/nm0496-437
14. Tan LKK, Carlone GM, Borrow R. Advances in the development of vaccines against *Neisseria meningitidis.* N Engl J Med. 2010;362:1511–20. http://dx.doi.org/10.1056/NEJMra0906357
15. Gupta S, Anderson RM. Population structure of pathogens: the role of immune selection. Parasitol Today. 1999;15:497–501. http://dx.doi.org/10.1016/S0169-4758(99)01559-8
16. Serruto D, Bottomley MJ, Ram S, Giuliani MM, Rappuoli R. The new multicomponent vaccine against meningococcal serogroup B, 4CMenB: immunological, functional and structural characterization of the antigens. Vaccine. 2012;30(Suppl 2):B87–97. http://dx.doi.org/10.1016/j.vaccine.2012.01.033
17. Jiang H-Q, Hoiseth SK, Harris SL, McNeil LK, Zhu D, Tan C, et al. Broad vaccine coverage predicted for a bivalent recombinant factor H binding protein based vaccine to prevent serogroup B meningococcal disease. Vaccine. 2010;28:6086–93. http://dx.doi.org/10.1016/j.vaccine.2010.06.083
18. Ladhani SN, Ramsay M, Borrow R, Riordan A, Watson JM, Pollard AJ. Enter B and W: two new meningococcal vaccine programmes launched. Arch Dis Child. 2016;101:91–5. http://dx.doi.org/10.1136/archdischild-2015-308928
19. Donnelly J, Medini D, Boccadifuoco G, Biolchi A, Ward J, Frasch C, et al. Qualitative and quantitative assessment of meningococcal antigens to evaluate the potential strain coverage of protein-based vaccines. Proc Natl Acad Sci U S A. 2010;107:19490–5. http://dx.doi.org/10.1073/pnas.1013758107
20. Vogel U, Taha MK, Vazquez JA, Findlow J, Claus H, Stefanelli P, et al. Predicted strain coverage of a meningococcal multicomponent vaccine (4CMenB) in Europe: a qualitative and quantitative assessment. Lancet Infect Dis. 2013;13:416–25. http://dx.doi.org/10.1016/S1473-3099(13)70006-9
21. Jolley KA, Maiden MC. BIGSdb: scalable analysis of bacterial genome variation at the population level. BMC Bioinformatics. 2010;11:595. http://dx.doi.org/10.1186/1471-2105-11-595
22. Brehony C, Rodrigues CMC, Borrow R, Smith A, Cunney R, Moxon ER, et al. Distribution of Bexsero® antigen sequence types (BASTs) in invasive meningococcal disease isolates: Implications for immunisation. Vaccine. 2016;34:4690–7. http://dx.doi.org/10.1016/j.vaccine.2016.08.015
23. Maiden MC, Jansen van Rensburg MJ, Bray JE, Earle SG, Ford SA, Jolley KA, et al. MLST revisited: the gene-by-gene approach to bacterial genomics. Nat Rev Microbiol. 2013;11:728–36. http://dx.doi.org/10.1038/nrmicro3093
24. Brehony C, Wilson DJ, Maiden MC. Variation of the factor H-binding protein of *Neisseria meningitidis.* Microbiology. 2009;155:4155–69. http://dx.doi.org/10.1099/mic.0.027995-0
25. Russell JE, Jolley KA, Feavers IM, Maiden MC, Suker J. PorA variable regions of *Neisseria meningitidis.* Emerg Infect Dis. 2004;10:674–8. http://dx.doi.org/10.3201/eid1004.030247
26. Bambini S, De Chiara M, Muzzi A, Mora M, Lucidarme J, Brehony C, et al. *Neisseria* adhesin A variation and revised nomenclature scheme. Clin Vaccine Immunol. 2014;21:966–71. http://dx.doi.org/10.1128/CVI.00825-13
27. Bratcher HB, Corton C, Jolley KA, Parkhill J, Maiden MC. A gene-by-gene population genomics platform: *de novo* assembly, annotation and genealogical analysis of 108 representative *Neisseria meningitidis* genomes. BMC Genomics. 2014;15:1138. http://dx.doi.org/10.1186/1471-2164-15-1138
28. Parikh SR, Newbold L, Slater S, Stella M, Moschioni M, Lucidarme J, et al. Meningococcal serogroup B strain coverage of the multicomponent 4CMenB vaccine with corresponding regional distribution and clinical characteristics in England, Wales, and Northern Ireland, 2007–08 and 2014–15: a qualitative and quantitative assessment. Lancet Infect Dis. 2017;17:754–62. http://dx.doi.org/10.1016/S1473-3099(17)30170-6
29. Abad R, Medina V, Stella M, Boccadifuoco G, Comanducci M, Bambini S, et al. Predicted strain coverage of a new meningococcal multicomponent vaccine (4CMenB) in Spain: analysis of the differences with other European countries. PLoS One. 2016;11:e0150721. http://dx.doi.org/10.1371/journal.pone.0150721
30. Fagnocchi L, Biolchi A, Ferlicca F, Boccadifuoco G, Brunelli B, Brier S, et al. Transcriptional regulation of the *nadA* gene in *Neisseria meningitidis* impacts the prediction of coverage of a multicomponent meningococcal serogroup B vaccine. Infect Immun. 2013;81:560–9. http://dx.doi.org/10.1128/IAI.01085-12
31. Masignani V, Comanducci M, Giuliani MM, Bambini S, Adu-Bobie J, Arico B, et al. Vaccination against *Neisseria meningitidis* using three variants of the lipoprotein GNA1870. J Exp Med. 2003;197:789–99. http://dx.doi.org/10.1084/jem.20021911
32. Fletcher LD, Bernfield L, Barniak V, Farley JE, Howell A, Knauf M, et al. Vaccine potential of the *Neisseria meningitidis* 2086 lipoprotein. Infect Immun. 2004;72:2088–100. http://dx.doi.org/10.1128/IAI.72.4.2088-2100.2004
33. Brunelli B, Del Tordello E, Palumbo E, Biolchi A, Bambini S, Comanducci M, et al. Influence of sequence variability on bactericidal activity sera induced by factor H binding protein variant 1.1. Vaccine. 2011;29:1072–81. http://dx.doi.org/10.1016/j.vaccine.2010.11.064
34. Biagini M, Spinsanti M, De Angelis G, Tomei S, Ferlenghi I, Scarselli M, et al. Expression of factor H binding protein in meningococcal strains can vary at least 15-fold and is genetically determined. Proc Natl Acad Sci U S A. 2016;113:2714–9. http://dx.doi.org/10.1073/pnas.1521142113
35. Medini D, Stella M, Wassil J. MATS: global coverage estimates for 4CMenB, a novel multicomponent meningococcal B vaccine. Vaccine. 2015;33:2629–36. http://dx.doi.org/10.1016/j.vaccine.2015.04.015

36. Parikh SR, Andrews NJ, Beebeejaun K, Campbell H, Ribeiro S, Ward C, et al. Effectiveness and impact of a reduced infant schedule of 4CMenB vaccine against group B meningococcal disease in England: a national observational cohort study. Lancet. 2016;388:2775–82. http://dx.doi.org/10.1016/S0140-6736(16)31921-3
37. Ladhani SN, Beebeejaun K, Lucidarme J, Campbell H, Gray S, Kaczmarski E, et al. Increase in endemic *Neisseria meningitidis* capsular group W sequence type 11 complex associated with severe invasive disease in England and Wales.Clin Infect Dis. 2015;60:578–85. http://dx.doi.org/10.1093/cid/ciu881
38. Campbell H, Saliba V, Borrow R, Ramsay M, Ladhani SN. Targeted vaccination of teenagers following continued rapid endemic expansion of a single meningococcal group W clone (sequence type 11 clonal complex), United Kingdom 2015. Euro Surveill. 2015;20:21188. http://dx.doi.org/10.2807/1560-7917.ES2015.20.28.21188
39. Ladhani SN, Giuliani MM, Biolchi A, Pizza M, Beebeejaun K, Lucidarme J, et al. Effectiveness of meningococcal B vaccine against endemic hypervirulent *Neisseria meningitidis* W strain, England. Emerg Infect Dis. 2016;22:309–11. http://dx.doi.org/10.3201/eid2202.150369
40. Mowlaboccus S, Perkins TT, Smith H, Sloots T, Tozer S, Prempeh LJ, et al. Temporal changes in BEXSERO® antigen sequence type associated with genetic lineages of *Neisseria meningitidis* over a 15-year period in Western Australia. PLoS One. 2016;11:e0158315. http://dx.doi.org/10.1371/journal.pone.0158315

Address for correspondence: Charlene M.C. Rodrigues, Department of Zoology, University of Oxford, Peter Medawar Bldg for Pathogen Research, South Parks Rd, Oxford OX1 3SY, UK; email: charlene.rodrigues@gtc.ox.ac.uk

Evolution of Sequence Type 4821 Clonal Complex Meningococcal Strains in China from Prequinolone to Quinolone Era, 1972–2013

Qinglan Guo,[1] Mustapha M. Mustapha,[1] Mingliang Chen, Di Qu, Xi Zhang, Min Chen, Yohei Doi, Minggui Wang, Lee H. Harrison

The expansion of hypervirulent sequence type 4821 clonal complex (CC4821) lineage *Neisseria meningitidis* bacteria has led to a shift in meningococcal disease epidemiology in China, from serogroup A (MenA) to MenC. Knowledge regarding the evolution and genetic origin of the emergent MenC strains is limited. In this study, we subjected 76 CC4821 isolates collected across China during 1972–1977 and 2005–2013 to phylogenetic analysis, traditional genotyping, or both. We show that successive recombination events within genes encoding surface antigens and acquisition of quinolone resistance mutations possibly played a role in the emergence of CC4821 as an epidemic clone in China. MenC and MenB CC4821 strains have spread across China and have been detected in several countries in different continents. Capsular switches involving serogroups B and C occurred among epidemic strains, raising concerns regarding possible increases in MenB disease, given that vaccines in use in China do not protect against MenB.

The incidence of meningococcal disease and *Neisseria meningitidis* strain distribution vary over time, within and between countries and regions (*1*). Six serogroups (A, B, C W, X, and Y) account for nearly all cases of invasive meningococcal disease (IMD) globally (*1*). Serogroup C (MenC) cases were rare in China until 2003–2005, when several MenC outbreaks were reported in Anhui Province (*2*–*4*). These outbreaks were caused by a previously unreported hypervirulent clonal complex (CC) 4821 lineage (*5*). A pharyngeal carriage survey and national public health surveillance during 2004–2005 identified CC4821 among sporadic IMD case-patients and asymptomatic carriers across 11 provinces, demonstrating the wide geographic distribution of CC4821 (*2*). During 2005–2012, MenC CC4821 became the leading cause of endemic meningococcal disease in China (*6*). Further analyses of historic isolate collections identified MenB and MenC CC4821 from carriage surveys in the 1970s (*2*,*7*). These studies demonstrated that CC4821 had been mostly associated with asymptomatic carriage over several decades before it emerged as a main cause of IMD (*2*,*7*,*8*). Also, our recent analyses of quinolone resistance among historic meningococcal isolate collections in China found a substantial temporal shift toward increased quinolone nonsusceptibility from the prequinolone era (before ≈1985) to the quinolone era (none versus >70%), particularly within hypervirulent CC4821 and CC5 lineages (*7*). Such findings support the hypothesis that quinolone resistance could have played a role in the emergence of MenC CC4821 outbreaks in China.

Meningococci have a dynamic genome that evolves rapidly through point mutations and frequent recombination. Such genetic changes give rise to strains with novel capsular or other major surface antigens that evade existing population immunity (*9*). A study by Zhu et al. found extensive genomic variation among 22 CC4821 invasive and carriage isolates from 12 provinces in China during 2005–2011 (*8*). In that study, CC4821 isolates belonged to 2 distinct phylogenetic groups, and results indicated that group 1, containing the epidemic reference strain 053442, might be more invasive than group 2 and that MenB and MenC coexisted within both groups 1 and 2 (*8*).

Our study describes phylogenetic relationships within a collection of historic and current isolates from Shanghai in the prequinolone and quinolone eras and explores how the isolates fit into the larger genetic profile of CC4821 from China (*8*). We aimed to shed light on the genomic factors underlying the abrupt transition of this lineage from a minority strain to a leading cause of endemic disease and outbreaks.

Author affiliations: Fudan University Huashan Hospital, Shanghai, China (Q. Guo, M. Wang); University of Pittsburgh School of Medicine, Pittsburgh, Pennsylvania, USA (M.M. Mustapha, Y. Doi, L.H. Harrison); Shanghai Municipal Center for Disease Control and Prevention, Shanghai (M. Chen, X. Zhang, M. Chen); Fudan University Shanghai Medical College, Shanghai (D. Qu)

DOI: https://doi.org/10.3201/eid2404.171744

[1]These authors contributed equally to this article.

Materials and Methods

Strain Selection and Molecular Typing

A total of 374 meningococcal isolates were collected from IMD case-patients, close contacts, and asymptomatic carriers during pharyngeal carriage surveys and routine, laboratory-based public health surveillance conducted during 1965–1985 and 2005–2013 (*7*). The interruption during 1986–2004 was because of the decreased incidence of meningococcal cases and the increased ability to identify *N. meningitidis* in hospitals, necessitating fewer isolates to be referred (*7*). In all, 52 CC4821 isolates were identified and underwent molecular characterization using traditional PCR sequencing of the *porA*, *porB*, *fetA*, *fHbp*, *nadA*, *nhba*, and *gyrA* genes and pulsed-field gel electrophoresis as described previously (*7*,*10*,*11*). We selected 8 of these 52 isolates, representing strains from different periods, serogroups, or pulsed-field gel electrophoresis groups, for whole-genome sequencing (WGS) and in-depth phylogenetic analysis. We downloaded assembled contiguous genome sequences (contigs) for 24 additional genome sequences from previous studies of CC4821 in China from GenBank (NM11003, accession no. NZ_ANBU00000000) (*5*,*8*). Therefore, a total of 32 whole-genome sequences underwent core genome phylogenetic analyses for this study (online Technical Appendix Table 1, https://wwwnc.cdc.gov/EID/article/24/4/17-1744-Techapp1.pdf).

Genome Sequencing and Assembly

We performed single molecule real-time sequencing (PacBio; Pacific Biosciences, Menlo Park, CA, USA) on 4 CC4821 isolates (NM040, NM062, NM205, and NM323) and sequenced the remaining 4 isolates (NM001, NM050, NM193, and NM313) by using Illumina HiSeq paired-end sequencing (Illumina, San Diego, CA, USA). We assembled PacBio genomes by using HGAP 4.0 (https://github.com/PacificBiosciences/Bioinformatics-Training/wiki/HGAP) and Illumina genomes by using SPAdes 3.7 (*12*). We annotated assembled contigs by using the Prokka v1.11 (*13*) pipeline and submitted them to the PubMLST *Neisseria* genome database (http://pubmlst.org/neisseria) with ID numbers 41414–41421, where allelic numbers were assigned to all identified genes (*14*).

Phylogenetic Analyses

We aligned assembled genomes (n = 32) and produced a core genome phylogenetic tree with 1,000 rapid bootstrap replicates by using RAxML and Mauve 2.3 as previously described (*15*–*17*). Serogroup A reference genome Z2491 was included as an outgroup (*18*). We aligned gene sequences selected for focused analyses with MEGA 5.2 (http://www.megasoftware.net) and constructed maximum-likelihood phylogenetic trees under the HKY model of evolution (*19*). We included comparison sequences from a global collection of 133 genomes from the PubMLST *Neisseria* genome database representing all major invasive disease lineages in some of these phylogenetic analyses as references.

Recombination

We assessed recombination by using ClonalFrameML and Gubbins (*20*,*21*). We then mapped the recombination to the CC4821 reference genome 053442 (online Technical Appendix).

Gene Content

We assessed gene content by using the Roary 3.6 ortholog clustering program (*22*), which identifies presence or absence of orthologous gene sequences using a cutoff of 90% sequence identity (–i = 90). We defined core genes as genes present in ≥90% of the genomes. When comparing the gene content of 2 groups of genomes, we defined a gene as specific to that group if it was present in ≥90% of the genomes in the group and in <20% of the genomes in the comparison group. We downloaded gene functional annotation from the COG database (*23*) and compared genes containing recombinant sequences with nonrecombinant ones based on the major COG classes (cellular processes and signaling, information storage and processing, metabolism, poorly characterized) using uncorrected χ^2 tests.

Results

Out of 52 Shanghai isolates, 18 (34%) were from 1972–1977 (3 IMD isolates and 15 asymptomatic carriage isolates), and the remaining 34 (23 IMD isolates, 6 isolates from close contacts, and 5 carriage isolates) were isolated during 2005–2013. Most (56%) Shanghai isolates were serogroup C, 42% were serogroup B, and 1 was nongroupable (online Technical Appendix Table 2).

Phylogenetic Analyses of CC4821 Isolates in China

We conducted comparative genome analyses for 8 isolates from Shanghai and 24 publicly available genomes from across China (Figure 1). Among the 8 newly sequenced isolates, 4 were from asymptomatic carriers from 1972–1977 (NM193, NM205, NM313, and NM323), 3 were IMD isolates from 2005–2011 (NM001, NM062, and NM040), and 1 was from an asymptomatic contact of a meningitis patient (NM050). The remaining 24 genome sequences included invasive and carriage CC4821 isolates from 12 provinces across China from 2004–2011, as characterized in previous studies (*4*,*8*). Overall, MenC represented 66% (21/32) of isolates that we analyzed, and the remaining 34% (11/32) belonged to MenB.

The core genome phylogenetic tree classified CC4821 into 2 distinct groups (Figure 1). Group 1 consisted of several isolates that were very closely related; this group con-

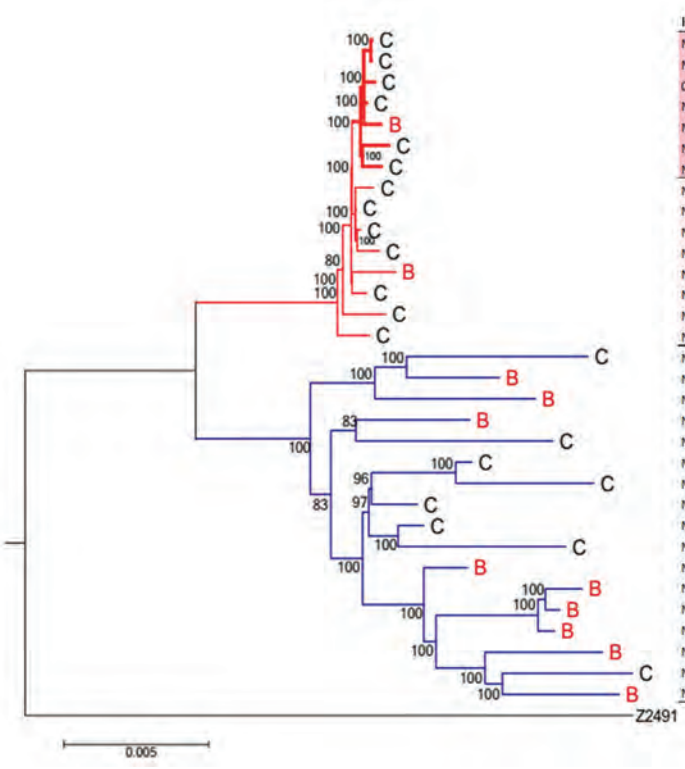

Isolate	Year	Sg	ST	CC	Province/ city	PorA_ VR1	PorA_ VR2	*gyrA allele*	Disease	
NM330505	2005	C	4821	4821	Zhejiang	7-2	14	71(T91I)	+	Epidemic clone
NM001	2005	C	4821	4821	Shanghai	7-2	14	71(T91I)	+	
053442	2004	C	4821	4821	Anhui	7-2	14	71(T91I)	+	
NM220601	2006	C	4821	4821	Jilin	7-2	14	71(T91I)	+	
NM341215	2011	B	4821	4821	Anhui	7-2	14	71(T91I)	+	
NM320501	2005	C	4820	4821	Jiangsu	7-2	14	71(T91I)	+	
NM062	2011	C	4821	4821	Shanghai	7-2	14	71(T91I)	+	
NM420718	2007	C	11920	4821	Hubei	12-1	16-8	71(T91I)	+	Group 1
NM11003	2011	C	4821	4821	Guangdong	12-1	16-8	71(T91I)	+	
NM100603	2005	C	4821	4821	Beijing	12-1	16-8	71(T91I)	+	
NM100601	2005	C	10737	4821	Beijing	12-1	16-8	71(T91I)	+	
NM440902	2008	B	4821	4821	Guangdong	20	23-1	71(T91I)	+	
NM320503	2005	C	4821	4821	Jiangsu	20	23-9	71(T91I)	+	
NM130803	2008	C	6928	4821	Hebei	20	23-1	71(T91I)		
NM131148	2011	C	9936	4821	Hebei	20	23-28	71(T91I)		
NM100572	2005	C	5610	4821	Beijing	20	23	12		Group 2
NM340552	2005	B	4897	4821	Anhui	21-2	28	12		
NM34173	2011	B	9477	4821	Guangxi	20	23-18	171(T91I)		
NM421007	2009	B	4821	4821	Hubei	12-11	16-8	12		
NM100514	2005	C	4832	4821	Beijing	20	23-1	203(T91I)		
NM193	1972	C	3436	4821	Shanghai	20-3	23-1	12		
NM440501	2005	C	4831	4821	Guangdong	20-3	23	12	+	
NM205	1973	C	4821	4821	Shanghai	20	23-2	4		
NM313	1977	C	4821	4821	Shanghai	20	23-1	12		
NM360624	2006	C	5473	4821	Jiangxi	UA	UA	114(T91I)		
NM323	1977	B	5798	4821	Shanghai	20	23	12		
NM040	2007	B	5798	4821	Shanghai	20	13-1	23	+	
NM311112	2011	B	5798	4821	Shanghai	20	13-1	12	+	
NM050	2009	B	5798	4821	Shanghai	20	13-2	71(T91I)		
NM100530	2005	B	5614	4821	Beijing	20-3	23	173(T91V)		
NM370601	2005	C	3200	4821	Shandong	20	23	UA(T91I)	+	
NM321114	2011	B	3200	4821	Jiangsu	20	23-3	175(T91I)	+	

Figure 1. Core genome phylogenetic tree showing relationships between *Neisseria meningitidis* serogroups C and B CC4821 strains, China, 1972–2011. The strains cluster within 1 of 2 distinct phylogenetic groups, group 1 and group 2. Within group 1 is an antigenically distinct clonal group (epidemic clone) containing outbreak-associated strains. Tree is rooted using serogroup A reference strain (Z2491) as an outgroup. Maximum-likelihood phylogenetic trees of aligned core genome sequences were generated under a general time reversible model of evolution with gamma rate heterogeneity, with 1,000 rapid bootstrap replicates represented as a percentage. Only node labels with >80% bootstrap support are shown. Strain type and date and place of isolation are shown; + indicates strains isolated from invasive disease cases. Resistant point mutations on the T91 position of *gyrA* gene are shown alongside data on *gyrA* allele designation. Scale bar represents total substitutions per site. CC, clonal complex; PorA VR, outer membrane protein PorA variable regions; Sg, serogroup; ST, sequence type.

tained 15 isolates from 2004 to 2011, and most were from IMD case-patients. In addition, the epidemic reference strain 053442 clustered with a small group of highly similar group 1 isolates. This subgroup is defined as the epidemic clone based on core genome phylogenetic analyses and antigen gene profile (described hereafter). A second more diverse phylogenetic group (group 2) consisted of isolates from Shanghai during 1972–1977 and more recent ones collected from 9 provinces during 2005–2011. In contrast to group 1, only 29% of group 2 isolates were from IMD case-patients (Figure 1). MenB was found in both groups and was interspersed with MenC genomes. Two of 11 MenB isolates belonged to group 1, the remainder to group 2 (Figure 1; online Technical Appendix Table 1).

Characterization of Antigen Gene Content

We examined 32 isolates that had undergone WGS to identify the major antigen gene (PorA VR1 and VR2, *porB*, FetA, *nhba*, and *fHbp*) alleles that corresponded to the epidemic strain, group 1 or group 2, as determined by the core genome phylogenetic analysis (Figures 1, 2; online Technical Appendix Table 1, Figures 1–5). *nadA* was missing in all CC4821 study genomes. Group 1 genomes had diverse *fHbp* and *porA* alleles. All 15 group 1 isolates contained the *porB* 3–48 and FetA F3–3 alleles, and *nhba* allele 124. The epidemic clone contained a few highly related *porA* alleles that all encoded unique, conserved *porA* variable regions (PorA VR1 and VR2: P1.7–2, 14). Group 2 isolates had the most antigen gene diversity, containing 5–12 different alleles for each antigen-encoding gene at the nucleotide level and no clear predominance of any single allelic profile. We observed little overlap between the antigen gene allelic profiles in groups 1 and 2. Only 2 of 13 group 1 alleles were also found in group 2. None of the antigen gene alleles found in the epidemic clone was present in group 2, suggesting that the epidemic clone had a nonoverlapping repertoire of antigens compared with historic and current group 2 isolates (Figure 2; online Technical Appendix Table 1, Figures 1–5). Group 2 was predominantly associated with PorA P1.20 variants (82%); PorB 3–229 (29%);

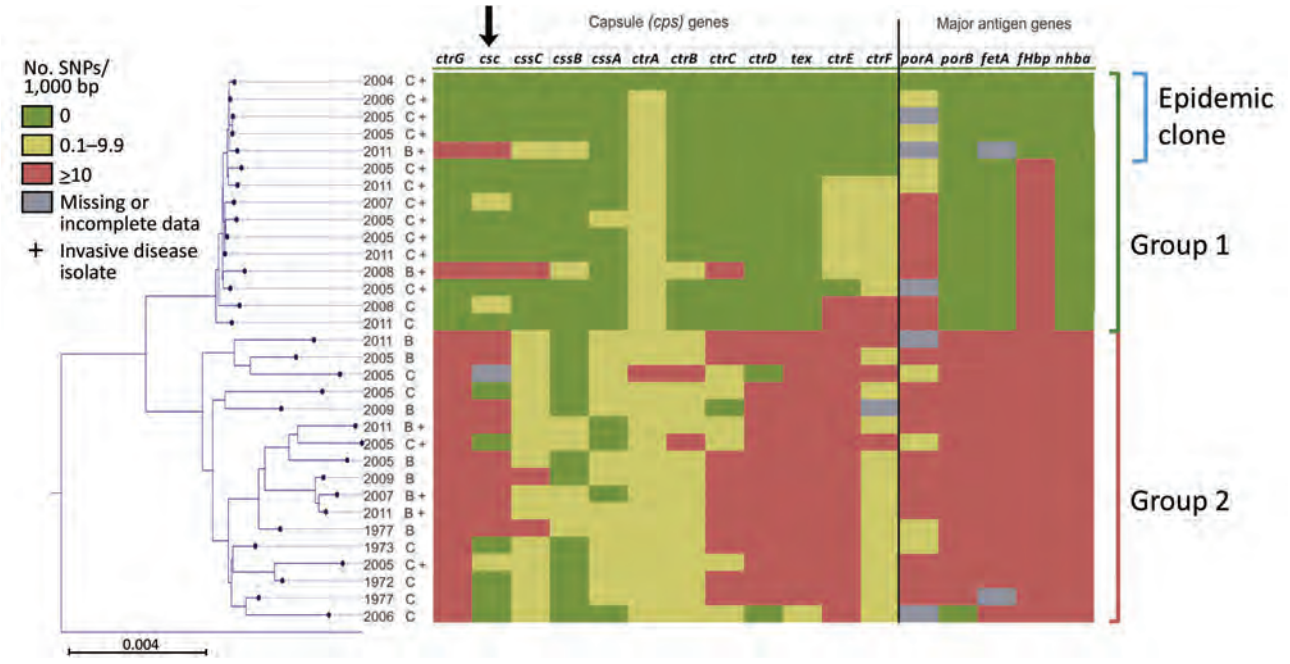

Figure 2. Genetic diversity within capsule and major antigen encoding genes among 32 *Neisseria meningitidis* clonal complex 4821 isolates, China, 1972–2011. Gene sequences from 32 clonal complex 4821 isolates were compared with the epidemic reference strain 053442 (the topmost isolate on the juxtaposed core genome phylogenetic tree). Scale bar represents total substitutions per site. SNP, single-nucleotide polymorphism.

FetA F3–9 (18%) and FetA F5–2 (18%); FHbp peptide 16 (65%); and *nhba* 553 (41%) (online Technical Appendix Table 1).

Recombination Events Separating Group 1 and Group 2 Isolates

We identified extensive recombination within CC4821 lineage, as detected by ClonalFrameML (*20*). The estimated rate of recombination relative to mutation (R/Θ) for the entire CC4821 core genome was 1.37 (95% CI 1.40–1.34), and the relative impact of recombination to mutation (r/m) was 20.83, indicating that ≈21 nt were acquired by recombination for every point mutation within the core genome of CC4821. Sublineage specific recombination rates (R/Θ) were 1.79 (95% CI 1.53–2.05) for group 1, 1.47 (95% CI 1.15–1.79) for group 2, and 0.5 (95% CI 0.26–0.75) for the epidemic clone.

A total of 46 recombination fragments containing 120 genes were mapped to the node that separated group 1 from group 2, indicating that these recombination events could be linked to the divergence of group 1 and 2 sublineages (online Technical Appendix Table 3). Sequence alignment and phylogenetic analysis confirmed that the 46 genomic loci represented regions of marked sequence divergence, presumably caused by homologous recombination within a common ancestral genome. These 120 recombinant genes belonged to diverse functional categories; metabolism was the overrepresented functional assignment (51/120 [42.5%]), compared with 28% of nonrecombinant genes ($p<0.001$ by χ^2 test). Proportions of other functional groups were similar between recombinant and nonrecombinant genes.

Recombination Events Unique to the Epidemic Clone

The epidemic clone diverged from group 1 through several additional recombination events, affecting 24 genes across 7 genomic loci (Table). These genomic loci included capsule translocation genes (*ctrE* and *ctrF*); major outer membrane protein (OMP) antigen genes *porA*, *porB*, and *fHbp*; *pts* genes involved in carbohydrate transport and metabolism; and the *tkl* locus encoding DNA polymerase and several metabolic enzymes.

Gene Content

We identified a total of 3,292 unique genes, of which 1,730 core genes were shared by most CC4821 genomes. Eleven genes were present in ≥90% of group 1 isolates but missing in most group 2 isolates. Genes that were predominantly found in group 1 included *lbpB* encoding lactoferrin binding protein B, *nhaP* encoding Na^+/K^+ antiporter, and genes encoding several putative enzymes and 4 hypothetical proteins whose functions are unknown (online Technical Appendix Table 4). These genes were spread across several locations on the reference genome 053442, suggesting that they were acquired separately rather than in a single event. The epidemic clone had no noticeable gene gain or loss compared with other group 1 isolates.

Table. Recombinant genes unique to the *Neisseria meningitidis* clonal complex 4821 epidemic clone, China, 1972–1977 and 2005–2013*

Gene ID	Gene name	Annotation
NMCC_0090	*ctrE*	Polysialic acid capsule modification protein LipA
NMCC_0091	*ctrF*	Polysialic acid capsule modification protein LipB
NMCC_0136		Putative RmuC-like protein
NMCC_0137		Putative metallo-dependent hydrolase
NMCC_0138		Putative periplasmic DNA ligase (polydeoxyribonucleotide synthase [ATP])
NMCC_0140	*ptsIIA*	Phosphotransferase system, enzyme IIA (protein IIA)
NMCC_0141	*ptsH*	Phosphocarrier protein HPr (phosphotransferase system, histidine-containing protein)
NMCC_0142	*ptsI*	Phosphoenolpyruvate-protein phosphotransferase (phosphotransferase system, enzyme I; protein I)
NMCC_0158	*porB*	Major outer-membrane protein P.IB (protein IB; PIB; porin)
NMCC_0350		Putative peptidase
NMCC_0351	*fHbp*	Factor H binding lipoprotein (lipoprotein GNA1870)
NMCC_0352	*fba*	Fructose-bisphosphate aldolase
NMCC_1338	*porA*	Major outer-membrane protein P.IA (protein IA; PIA; porin)
NMCC_1341	*greA*	Transcription elongation factor GreA (transcript cleavage factor GreA)
NMCC_1342	*aroA*	3-phosphoshikimate 1-carboxyvinyltransferase (5-enolpyruvylshikimate-3-phosphate synthase; EPSP synthase; EPSPS)
NMCC_1343		Conserved hypothetical lipoprotein
NMCC_1363		Putative DnaQ-like exonuclease
NMCC_1364		Arg tRNA
NMCC_1365		Glu tRNA
NMCC_1366		Putative dioxygenase
NMCC_1367		Conserved hypothetical membrane protein
NMCC_1368		Putative ferredoxin
NMCC_1370	*tkt*	Transketolase
NMCC_2038	*fmt*	Methionyl-tRNA formyltransferase

*Gene IDs correspond to the clonal complex 4821 reference genome 053442. ATP, adenosine triphosphate; EPSP, 5-enolpyruvylshikimate-3-phosphate; EPSPS, EPSP synthase; ID, identifier.

Capsular Gene *cps* Cluster

The *cps* cluster of *N. meningitidis* consists of 6 regions (D-A-C-E-D′-B) required for capsule biosynthesis (region A), transport (region C), and translocation (region B) (*24*). The group 1 isolates were characterized by a novel capsule region A (*ctrG4-cssE1-csc1-cssC3-cssB1-cssA3*), associated with region C (*ctrA5-ctrB1-ctrC4-ctrD1*) and region E (*tex-orf1-orf2*) (online Technical Appendix Table 1). Nine of 15 regions A-C-E identified among group 1 isolates were identical, and another 4 were almost identical (1-bp variation in *csc*, *cssA*, or *ctrA* over 14,489 bp). Only 2 diverged because of the allelic replacement containing the serogroup-specific polysialyltransferase gene (*csb*), resulting in capsular switches involving serogroups B and C (NM341215 and NM440902) (online Technical Appendix Table 2). Group 2 had substantial genetic diversity within the *cps* cluster, with no 2 isolates possessing an identical *cps* gene allelic profile (Figure 2).

Characterization of CC4821 Isolates from Shanghai

Our results classified 52 CC4821 isolates from Shanghai into epidemic clone or groups 1 and 2 on the basis of associated *porA*, *porB*, *fetA*, *fHbp*, and *nhba* antigen genes defined by WGS (Figure 1; online Technical Appendix Table 2). A substantial proportion of strains in Shanghai (23/52 [44%]) belonged to group 1, with 0–1 antigen gene differences (Figure 1; online Technical Appendix Table 2, Figures 1–5). Shanghai group 1 isolates were exclusively isolated during 2005–2013; were MenC (19/23), MenB (3/23), or nongroupable (1/23); and were isolated from IMD case-patients (18/23), close contacts of IMD case-patients (4/23), or an asymptomatic carrier (1/23). Within group 1, a total of 16 isolates (16/23 [70%]) contained PorA P1.7–2,14 and were consistent with the epidemic clone by all 5 antigen genes. Twenty-nine (29/52 [56%]) Shanghai isolates belonged to group 2 and differed from group 1 by 4–5 out of 5 antigen loci. Shanghai group 2 was dominated by carriage isolates (21/29 [72%]) from 1972–1977 and 2005–2013. MenB equaled or outnumbered MenC among historic (9/18 [50%]) and recent (10/11 [91%]) group 2 CC4821 isolates. MenB strains in group 1 possessed *fHbp* 498 or 22 encoding peptides 1.80 or 2.22 (subvariants belonging to FHbp variant group 1 or 2), as most (17/19 [89%]) of MenC epidemic clones did (online Technical Appendix Tables 1, 2).

All group 1 isolates contained fluoroquinolone-resistant *gyrA* allele 71 (corresponding to allele R1 in our previous study [*7*]), which was generated by a nonsynonymous mutation of fluoroquinolone-susceptible *gyrA* allele 12 (allele S1), creating an amino acid substitution of T91I. The *gyrA* allele 12/S1 was carried by 76% (22/29) of the group 2 strains (online Technical Appendix Table 2). In contrast, only 4 of 29 group 2 isolates from Shanghai and another 6 publicly available group 2 genomes contained resistant *gyrA* alleles, which were different from each other. Group 2 isolates with genotypic resistance to quinolones were

genetically highly diverse as evidenced by diverse sequence types, different antigen gene profiles, and expression of both MenB and MenC capsules. However, all quinolone-resistant isolates were from 2005–2013 (Figure 1; online Technical Appendix Tables 1, 2).

Discussion

This study presents detailed genomic analyses of the current major endemic meningococcal disease lineages in China, serogroups C and B CC4821. Phylogenetic analyses have suggested that the epidemic clone (corresponding to the epidemic China$^{CC4821\text{-}R1\text{-}C/B}$ clone described in our previous work [*7*)]) responsible for most recent CC4821 disease cases was nested within a distinct phylogenetic group (group 1), consistent with recent clonal expansion of a genetically distinct strain. In contrast, group 2 was temporally and genetically more diverse and accounted for a smaller proportion of IMD cases, as evidenced by the preponderance of asymptomatic carriage isolates within this group (*8*). Group 1 isolates were first identified during MenC outbreaks during 2003–2005, whereas group 2 isolates were mostly associated with carriage from the 1970s to 2013 (*7*).

This work adds to the description of CC4821 by a previous study (*8*) by demonstrating that, within group 1, a genetically distinct clone exists that shares the *porA* antigenic formula P1.7–2,14 and comprises strains associated with outbreaks and a large proportion of epidemic disease cases. This finding is in keeping with surveillance studies reporting MenC strains during 2005–2012 indicating that 55% of 238 confirmed meningococcal disease cases and 84% of 131 MenC strains belong to CC4821 with *porA* P1.7–2,14 (*6*), suggesting that the expansion of CC4821 was caused by clonal expansion of this antigenic type. Genomic analyses demonstrated that the epidemic CC4821 lineage had undergone 2 crucial genetic events compared with historic asymptomatic carriage isolates. First, CC4821 diverged into 2 major sublineages through extensive recombination events predominantly affecting genes involved in metabolic functions. Such extensive allelic exchanges might have enhanced the transmission fitness or the invasive potential within group 1. Second, a virulent, antigenically unique, epidemic strain emerged from within group 1 in a second set of more focused recombination events affecting major antigen genes, *porA, porB, fHbp*, capsule genes *ctrE* and *ctrF*, and several metabolic genes associated with oxidative phosphorylation and glycolytic processes. These genetic changes possibly account for the rapid dissemination and increased invasive potential of the epidemic clone.

This work also adds to the evidence that the emergence and persistence of virulent meningococcal strains occurs through the introduction of a novel antigenic variant in an immunologically naive population (*9*,*15*,*25*–*27*). In addition, even though a few major antigen gene repertoires mediate the microevolution of virulent meningococcal strains, a larger and more assorted number of metabolic genes might be involved in the divergence of sublineages. Additional research is needed to elucidate the intricate interactions between various metabolic pathways in the fitness and virulence potential of meningococci.

Selection pressure of fluoroquinolones might also affect the evolution and adaption of meningococcal strains, as evidenced by various resistant *gyrA* alleles recovered in many meningococcal lineages and singletons only in the quinolone era in China (*7*,*28*). All of the group 1 CC4821 strains contain *gyrA* allele 71/R1, in contrast to various resistant *gyrA* alleles in group 2, suggesting acquisition of this trait by group 1 at an early stage in evolution. The *gyrA* allele 71/R1 derived from *gyrA* allele 12/S1, which was possessed by most of the group 2 strains both in prequinolone and quinolone eras, indicating their common origin. The precise role of quinolone resistance in the emergence of the epidemic clone requires further study.

The relative rates and impact of recombination within the CC4821 lineage were considerably higher than previous estimates that examined recombination across 7 housekeeping genes (*29*–*31*). We identified 4,026 recombination events and 21 recombinant single-nucleotide polymorphisms (SNPs) for every point mutation within CC4821. Estimates of meningococcal recombination rates from whole-genome sequence data are limited. A study of MenA CC5 strains in Africa (*27*), an epidemic lineage notable for relatively low genetic diversity, found 34 recombinant sequences and 12 recombinant SNPs for every point mutation. A study of recombination rates within conserved multilocus sequence type loci among carriage isolates from the Czech Republic in 1993 found 6.2–16.8 SNPs caused by recombination for each point mutation (*29*). These data suggest that although homologous recombination is a shared mechanism for meningococcal strain emergence and persistence (*29*,*31*–*33*), the frequency and extent of recombination likely differs substantially between lineages.

High rates of recombination have led to multiple distinct capsular switch strains expressing group B and C capsule, as described in this study, and serogroup W (*8*,*34*). Both MenB and MenC were phylogenetically diverse and interspersed within both groups 1 and 2, suggesting multiple distinct capsular switches between these serogroups rather than clonal expansion of a single capsular switch strain (*35*,*36*). Moreover, recombination events that led to no apparent change in capsular phenotype were also prevalent.

Wide geographic and temporal spread of MenB strains in China is of concern given that vaccines currently in use do not protect against MenB disease. Furthermore, marked heterogeneity exists among both MenB and MenC strains within the gene encoding FHbp, a key component of MenB vaccines.

At the time of its emergence, CC4821 was confined to China and Taiwan (*37*). However, review of the PubMLST *Neisseria* genome database suggests a recent increase in the geographic spread of CC4821. CC4821 isolates were reported from a small number of asymptomatic carriers in Brazil (2014) (*38*,*39*) and Australia (2012–2017), as well as isolated disease cases and carriers from France (2009–2011), the United Kingdom (2011–2014), the United States (2007–2016), and India (2017) (*14*). A recent case report of a quinolone-resistant sequence type 4821 strain from Japan in a patient with no history of foreign travel also suggests local transmission of CC4821 in Japan (*40*). Global CC4821 carriage and IMD isolates on the PubMLST *Neisseria* database were antigenically diverse, containing PorA types associated with both group 1 and 2 strains, and expressed both serogroup C and B capsules. This finding suggests low-level dissemination of CC4821 strains with diverse virulence and antigenic types as opposed to clonal spread of a single epidemic strain. This pattern is in contrast to the pandemic spread of highly clonal serogroup A epidemic strains from China from the 1960s through the 1990s (*25*). Genome-based surveillance of these global CC4821 strains is needed to monitor the global spread of this clonal lineage.

Our study is limited by lack of isolates before the 1970s and during 1986–2004; isolates from those periods might have provided a clearer picture of the multiple evolutionary steps that led to the epidemic CC4821 clone. Also, the high frequency of recombination within capsular genes makes it difficult to accurately determine the direction of capsular switch.

In summary, we have presented detailed genomic analysis of a major hypervirulent meningococcal lineage associated with MenC and MenB in China and identified key genomic factors that might have led to the emergence and persistence of MenC in China. The potential emergence of MenB is of public health concern. Strengthened laboratory surveillance for disease cases and carefully planned carriage surveys are needed to monitor global trends, detect outbreaks, and inform immunization policies.

Acknowledgments

We thank Jane Marsh for providing thoughtful comments on an early draft of this manuscript.

This study made use of the PubMLST *Neisseria* genome database (http://pubmlst.org/neisseria), developed by Keith Jolley and hosted by the University of Oxford. The development of this site has been funded by the Wellcome Trust and European Union. This study also made use of the Meningitis Research Foundation Meningococcus Genome Library (http://www.meningitis.org/research/genome), developed by Public Health England, the Wellcome Trust Sanger Institute, and the University of Oxford as a collaboration. The project is funded by the Meningitis Research Foundation.

This work was supported by grants from the National Natural Science Foundation of China (81673479, 81120108024, and 81601801); the Shanghai Pujiang Program (16PJD010); the Shanghai Rising-Star Program (17QA1403100); the Shanghai Medical Health Plan for Outstanding Young Talents (2017YQ039); and the 4th Three-Year Action Plan for Public Health of Shanghai (GWTD2015S01).

About the Author

Dr. Guo is an associate professor in the Institute of Antibiotics, Huashan Hospital, Fudan University. Her research interests include mechanisms of antimicrobial resistance in clinical isolates.

References

1. Halperin SA, Bettinger JA, Greenwood B, Harrison LH, Jelfs J, Ladhani SN, et al. The changing and dynamic epidemiology of meningococcal disease. Vaccine. 2012;30(Suppl 2):B26–36. http://dx.doi.org/10.1016/j.vaccine.2011.12.032
2. Zhang X, Shao Z, Yang E, Xu L, Xu X, Li M, et al. Molecular characterization of serogroup C *Neisseria meningitidis* isolated in China. J Med Microbiol. 2007;56:1224–9. http://dx.doi.org/10.1099/jmm.0.47263-0
3. Ni JD, Jin YH, Dai B, Wang XP, Liu DQ, Chen X, et al. Recent epidemiological changes in meningococcal disease may be due to the displacement of serogroup A by serogroup C in Hefei City, China. Postgrad Med J. 2008;84:87–92. http://dx.doi.org/10.1136/pgmj.2007.065680
4. Shao Z, Li W, Ren J, Liang X, Xu L, Diao B, et al. Identification of a new *Neisseria meningitidis* serogroup C clone from Anhui Province, China. Lancet. 2006;367:419–23. http://dx.doi.org/10.1016/S0140-6736(06)68141-5
5. Peng J, Yang L, Yang F, Yang J, Yan Y, Nie H, et al. Characterization of ST-4821 complex, a unique *Neisseria meningitidis* clone. Genomics. 2008;91:78–87. http://dx.doi.org/10.1016/j.ygeno.2007.10.004
6. Zhou H, Shan X, Sun X, Xu L, Gao Y, Li M, et al. Clonal characteristics of invasive *Neisseria meningitidis* following initiation of an A + C vaccination program in China, 2005–2012. J Infect. 2015;70:37–43. http://dx.doi.org/10.1016/j.jinf.2014.07.022
7. Chen M, Guo Q, Wang Y, Zou Y, Wang G, Zhang X, et al. Shifts in the antibiotic susceptibility, serogroups, and clonal complexes of *Neisseria meningitidis* in Shanghai, China: a time trend analysis of the pre-quinolone and quinolone eras. PLoS Med. 2015;12:e1001838. http://dx.doi.org/10.1371/journal.pmed.1001838
8. Zhu B, Xu Z, Du P, Xu L, Sun X, Gao Y, et al. Sequence type 4821 clonal complex serogroup B *Neisseria meningitidis* in China, 1978–2013. Emerg Infect Dis. 2015;21:925–32. http://dx.doi.org/10.3201/eid2106.140687
9. Harrison LH, Jolley KA, Shutt KA, Marsh JW, O'Leary M, Sanza LT, et al.; Maryland Emerging Infections Program. Antigenic shift and increased incidence of meningococcal disease. J Infect Dis. 2006;193:1266–74. http://dx.doi.org/10.1086/501371
10. Thompson EA, Feavers IM, Maiden MC. Antigenic diversity of meningococcal enterobactin receptor FetA, a vaccine component. Microbiology. 2003;149:1849–58. http://dx.doi.org/10.1099/mic.0.26131-0
11. Urwin R, Fox AJ, Musilek M, Kriz P, Maiden MC. Heterogeneity of the PorB protein in serotype 22 *Neisseria meningitidis*. J Clin Microbiol. 1998;36:3680–2.

12. Bankevich A, Nurk S, Antipov D, Gurevich AA, Dvorkin M, Kulikov AS, et al. SPAdes: a new genome assembly algorithm and its applications to single-cell sequencing. J Comput Biol. 2012;19:455–77. http://dx.doi.org/10.1089/cmb.2012.0021
13. Seemann T. Prokka: rapid prokaryotic genome annotation. Bioinformatics. 2014;30:2068–9. http://dx.doi.org/10.1093/bioinformatics/btu153
14. Jolley KA, Maiden MC. BIGSdb: scalable analysis of bacterial genome variation at the population level. BMC Bioinformatics. 2010;11:595. http://dx.doi.org/10.1186/1471-2105-11-595
15. Mustapha MM, Marsh JW, Krauland MG, Fernandez JO, de Lemos APS, Dunning Hotopp JC, et al. Genomic epidemiology of hypervirulent serogroup W, ST-11 *Neisseria meningitidis.* EBioMedicine. 2015;2:1447–55. http://dx.doi.org/10.1016/j.ebiom.2015.09.007
16. Stamatakis A. RAxML version 8: a tool for phylogenetic analysis and post-analysis of large phylogenies. Bioinformatics. 2014;30:1312–3. http://dx.doi.org/10.1093/bioinformatics/btu033
17. Darling AE, Mau B, Perna NT. progressiveMauve: multiple genome alignment with gene gain, loss and rearrangement. PLoS One. 2010;5:e11147. http://dx.doi.org/10.1371/journal.pone.0011147
18. Parkhill J, Achtman M, James KD, Bentley SD, Churcher C, Klee SR, et al. Complete DNA sequence of a serogroup A strain of *Neisseria meningitidis* Z2491. Nature. 2000;404:502–6. http://dx.doi.org/10.1038/35006655
19. Tamura K, Peterson D, Peterson N, Stecher G, Nei M, Kumar S. MEGA5: molecular evolutionary genetics analysis using maximum likelihood, evolutionary distance, and maximum parsimony methods. Mol Biol Evol. 2011;28:2731–9. http://dx.doi.org/10.1093/molbev/msr121
20. Didelot X, Wilson DJ. ClonalFrameML: efficient inference of recombination in whole bacterial genomes. PLOS Comput Biol. 2015;11:e1004041. http://dx.doi.org/10.1371/journal.pcbi.1004041
21. Croucher NJ, Page AJ, Connor TR, Delaney AJ, Keane JA, Bentley SD, et al. Rapid phylogenetic analysis of large samples of recombinant bacterial whole genome sequences using Gubbins. Nucleic Acids Res. 2015;43:e15. http://dx.doi.org/10.1093/nar/gku1196
22. Page AJ, Cummins CA, Hunt M, Wong VK, Reuter S, Holden MT, et al. Roary: rapid large-scale prokaryote pan genome analysis. Bioinformatics. 2015;31:3691–3. http://dx.doi.org/10.1093/bioinformatics/btv421
23. Tatusov RL, Galperin MY, Natale DA, Koonin EV. The COG database: a tool for genome-scale analysis of protein functions and evolution. Nucleic Acids Res. 2000;28:33–6. http://dx.doi.org/10.1093/nar/28.1.33
24. Harrison OB, Claus H, Jiang Y, Bennett JS, Bratcher HB, Jolley KA, et al. Description and nomenclature of *Neisseria meningitidis* capsule locus. Emerg Infect Dis. 2013;19:566–73. http://dx.doi.org/10.3201/eid1904.111799
25. Zhu P, van der Ende A, Falush D, Brieske N, Morelli G, Linz B, et al. Fit genotypes and escape variants of subgroup III *Neisseria meningitidis* during three pandemics of epidemic meningitis. Proc Natl Acad Sci U S A. 2001;98:5234–9. http://dx.doi.org/10.1073/pnas.061386098
26. Taha MK, Giorgini D, Ducos-Galand M, Alonso JM. Continuing diversification of *Neisseria meningitidis* W135 as a primary cause of meningococcal disease after emergence of the serogroup in 2000. J Clin Microbiol. 2004;42:4158–63. http://dx.doi.org/10.1128/JCM.42.9.4158-4163.2004
27. Lamelas A, Harris SR, Röltgen K, Dangy JP, Hauser J, Kingsley RA, et al. Emergence of a new epidemic *Neisseria meningitidis* serogroup A clone in the African meningitis belt: high-resolution picture of genomic changes that mediate immune evasion. MBio. 2014;5:e01974–14. http://dx.doi.org/10.1128/mBio.01974-14
28. Zhu B, Fan Y, Xu Z, Xu L, Du P, Gao Y, et al. Genetic diversity and clonal characteristics of ciprofloxacin-resistant meningococcal strains in China. J Med Microbiol. 2014;63:1411–8. http://dx.doi.org/10.1099/jmm.0.078600-0
29. Jolley KA, Wilson DJ, Kriz P, McVean G, Maiden MC. The influence of mutation, recombination, population history, and selection on patterns of genetic diversity in *Neisseria meningitidis.* Mol Biol Evol. 2005;22:562–9. http://dx.doi.org/10.1093/molbev/msi041
30. Didelot X, Maiden MC. Impact of recombination on bacterial evolution. Trends Microbiol. 2010;18:315–22. http://dx.doi.org/10.1016/j.tim.2010.04.002
31. Vos M, Didelot X. A comparison of homologous recombination rates in bacteria and archaea. ISME J. 2009;3:199–208. http://dx.doi.org/10.1038/ismej.2008.93
32. Budroni S, Siena E, Dunning Hotopp JC, Seib KL, Serruto D, Nofroni C, et al. *Neisseria meningitidis* is structured in clades associated with restriction modification systems that modulate homologous recombination. Proc Natl Acad Sci U S A. 2011;108:4494–9. http://dx.doi.org/10.1073/pnas.1019751108
33. Kong Y, Ma JH, Warren K, Tsang RS, Low DE, Jamieson FB, et al. Homologous recombination drives both sequence diversity and gene content variation in *Neisseria meningitidis.* Genome Biol Evol. 2013;5:1611–27. http://dx.doi.org/10.1093/gbe/evt116
34. He B, Jia Z, Zhou H, Wang Y, Jiang X, Ma H, et al. CC4821 serogroup W meningococcal disease in China. Int J Infect Dis. 2014;29:113–4. http://dx.doi.org/10.1016/j.ijid.2014.08.022
35. Lucidarme J, Lekshmi A, Parikh SR, Bray JE, Hill DM, Bratcher HB, et al. Frequent capsule switching in 'ultra-virulent' meningococci: are we ready for a serogroup B ST-11 complex outbreak? J Infect. 2017;75:95–103. http://dx.doi.org/10.1016/j.jinf.2017.05.015
36. Mustapha MM, Marsh JW, Krauland MG, Fernandez JO, de Lemos AP, Dunning Hotopp JC, et al. Genomic investigation reveals highly conserved, mosaic, recombination events associated with capsular switching among invasive *Neisseria meningitidis* serogroup W sequence type (ST)-11 strains. Genome Biol Evol. 2016;8:2065–75. http://dx.doi.org/10.1093/gbe/evw122
37. Chiou CS, Liao JC, Liao TL, Li CC, Chou CY, Chang HL, et al. Molecular epidemiology and emergence of worldwide epidemic clones of *Neisseria meningitidis* in Taiwan. BMC Infect Dis. 2006;6:25. http://dx.doi.org/10.1186/1471-2334-6-25
38. Nunes AM, Ribeiro GS, Ferreira IE, Moura AR, Felzemburgh RD, de Lemos AP, et al. Meningococcal carriage among adolescents after mass meningococcal c conjugate vaccination campaigns in Salvador, Brazil. PLoS One. 2016;11:e0166475. http://dx.doi.org/10.1371/journal.pone.0166475
39. Moura ARSS, Kretz CB, Ferreira IE, Nunes AMPB, de Moraes JC, Reis MG, et al. Molecular characterization of *Neisseria meningitidis* isolates recovered from 11–19-year-old meningococcal carriers in Salvador, Brazil. PLoS One. 2017;12:e0185038. http://dx.doi.org/10.1371/journal.pone.0185038
40. Kawasaki Y, Matsubara K, Takahashi H, Morita M, Ohnishi M, Hori M, et al. Invasive meningococcal disease due to ciprofloxacin-resistant *Neisseria meningitidis* sequence type 4821: the first case in Japan. J Infect Chemother. 2017 Dec 7:S1341–321X(17)30274-X [Epub ahead of print].

Address for correspondence: Min Chen, Shanghai Municipal Center for Disease Control and Prevention, 1380 W ZhongShan Rd, Shanghai, China; email: chenmin@scdc.sh.cn; Yohei Doi, Division of Infectious Diseases, University of Pittsburgh School of Medicine, S829 Scaife Hall, 3550 Terrace St, Pittsburgh, PA 15261, USA; email: yod4@pitt.edu; Minggui Wang, Institute of Antibiotics, Huashan Hospital, Fudan University, 12 M Wulumuqi Rd, Shanghai 200040, China; email: mgwang@fudan.edu.cn

Avirulent *Bacillus anthracis* Strain with Molecular Assay Targets as Surrogate for Irradiation-Inactivated Virulent Spores

Roger D. Plaut, Andrea B. Staab, Mark A. Munson, Joan S. Gebhardt, Christopher P. Klimko, Avery V. Quirk, Christopher K. Cote, Tony L. Buhr, Rebecca D. Rossmaier, Robert C. Bernhards, Courtney E. Love, Kimberly L. Berk, Teresa G. Abshire, David A. Rozak, Linda C. Beck, Scott Stibitz, Bruce G. Goodwin, Michael A. Smith, Shanmuga Sozhamannan

The revelation in May 2015 of the shipment of γ irradiation–inactivated wild-type *Bacillus anthracis* spore preparations containing a small number of live spores raised concern about the safety and security of these materials. The finding also raised doubts about the validity of the protocols and procedures used to prepare them. Such inactivated reference materials were used as positive controls in assays to detect suspected *B. anthracis* in samples because live agent cannot be shipped for use in field settings, in improvement of currently deployed detection methods or development of new methods, or for quality assurance and training activities. Hence, risk-mitigated *B. anthracis* strains are needed to fulfill these requirements. We constructed a genetically inactivated or attenuated strain containing relevant molecular assay targets and tested to compare assay performance using this strain to the historical data obtained using irradiation-inactivated virulent spores.

Author affiliations: Food and Drug Administration, Silver Spring, Maryland, USA (R.D. Plaut, S. Stibitz); Naval Surface Warfare Center, Dahlgren, Virginia, USA (A.B. Staab, T.L. Buhr, L.C. Beck); Naval Medical Research Center, Fort Detrick, Maryland, USA (M.A. Munson, J.S. Gebhardt); US Army Medical Research Institute of Infectious Diseases, Fort Detrick (C.P. Klimko, A.V. Quirk, C.K. Cote, T.G. Abshire, D.A. Rozak); US Army Edgewood Chemical and Biological Center, Aberdeen Proving Ground, Maryland, USA (R.D. Rossmaier, R.C. Bernhards, C.E. Love, K.L. Berk); Defense Threat Reduction Agency, Fort Belvoir, Virginia, USA (R.C. Bernhards); Joint Research and Development, Inc., Stafford, Virginia, USA (C.E. Love, L.C. Beck); Defense Biological Product Assurance Office, Frederick, Maryland, USA (B.G. Goodwin, M.A. Smith, S. Sozhamannan); The Tauri Group, Inc., Alexandria, Virginia, USA (S. Sozhamannan)

DOI: https://doi.org/10.3201/eid2404.171646

An effective and constant real-time surveillance capability is crucial for protecting the public from biological threats. Biological threats can be intentional (e.g., resulting from biowarfare or bioterrorism) or unintentional (e.g., resulting from accidental release or emerging infectious diseases) (*1*,*2*). Early detection of a biological threat is critical not only for identifying the threat organism but also for implementing appropriate countermeasures to save and protect the victims and prevent further infection and for decontaminating and reclamating the affected environment and infrastructures.

The bedrock of successful biodetection platforms and sensors is use of well-characterized molecular assays, immunoassays, or other types of detection assays. Any assay development effort requires testing, evaluation, and validation of the assays with live or inactivated spiking materials in appropriate matrices relevant to the environments in which the assays are intended to be used (e.g., aerosol collection filters, soils, or clinical matrices). Distribution and use of select agents and toxins are restricted to facilities that have appropriate approval for storage and use of such materials in containment suites and are regulated by the Federal Select Agent Program of the Centers for Disease Control and Prevention (CDC; Atlanta, GA, USA) and the US Department of Agriculture Animal and Plant Health Inspection Service (Riverdale, MD, USA). For other facilities, inactivated select agents, including inactivated spores, historically were the source of reference materials. Many private and academic organizations, government agencies, and foreign government partners have used these materials for various activities, including quality control exercises and medical countermeasure research.

In May 2015, previously shipped irradiation-inactivated *B. anthracis* spore reference materials were found to contain a small number of live spores (*3*,*4*). The incomplete inactivation of the spores raised concern about the safety and security of these materials and doubts about the

validity of the protocols and procedures used to prepare them. After this revelation, the US Department of Defense (DoD) and Department of the Army took a series of measures that included review of existing processes and practices to prepare such reference materials (*5*); placement of a moratorium on shipping of inactivated *B. anthracis* and other select agents from DoD laboratories until further review (*6*); formation of an independent entity (BSAT Biorisk Program Office) to oversee all Biologic Select Agents and Toxins (BSAT) activities within DoD; and implementation of various recommendations of different committees established to evaluate BSAT risk mitigation strategies (*5*,*7*,*8*).

Currently, guidance for implementing the Secretary of the Army directive 2016-24 for the DoD BSAT biosafety program (*7*) has been drafted, with many new measures put in place for the safe handling of BSAT and BSAT-derived products within DoD laboratories and transfer and tracking of such materials across agencies and laboratories. One of the 3 key activities identified in this directive is to explore safer alternatives to BSAT, inactivated BSAT, and BSAT derivatives to reduce health and safety risks associated with BSAT production, handling, and distribution (*7*).

We describe the construction and characterization of a safer alternative to regulated *B. anthracis*: a genetically inactivated (rather than irradiation-inactivated) avirulent *B. anthracis* strain into which specific nucleic acid assay targets for pXO1 and pXO2 replicons have been introduced. The resulting recombinant strain substitutes for and reacts similarly to regulated *B. anthracis* in molecular testing, whereas currently excluded strains (such as Sterne) lack the pXO2 target (online Technical Appendix Figure 1, https://wwwnc.cdc.gov/EID/article/24/4/17-1646-Techapp1.pdf). The resulting recombinant strain can be used for testing PCRs used in many biodefense programs. Also, we demonstrate that these spores can be further inactivated by irradiation so they can be used even in a Biosafety Level (BSL) 1 setting.

Materials and Methods

Strains, Plasmids, and Primers

Escherichia coli and *B. anthracis* strains used in this study are listed in Table 1. The plasmids used in various cloning steps and the primers used for amplification, sequence verification, and diagnosis of constructs also are listed in Table 1.

Synthesis of a Recombinant Plasmid Carrying PCR Signatures

We synthesized the recombinant construct 4 cassette, containing 5 different PCR signatures, commercially (Blue Heron, LLC, Bothel, WA, USA) and cloned into pT7Blue (Novagen-MilliporeSigma, St. Louis, MO, USA). The cassette was sequence-verified and PCR-amplified from this plasmid. The PCR product and a *lef* deletion plasmid pRP1091 (*11*) were digested with *Xba*I, ligated, and transformed into TOP10 *E. coli* cells (Invitrogen). Successful cloning of the insert was confirmed by restriction enzyme digestion, PCR, and sequencing.

Construction of Tagged *B. anthracis* Sterne Triple Knockout Strain

We conducted transfer and integration of the cloned insert by allelic exchange as described previously (*11*) (online Technical Appendix Figure 2). We designated the final construct recombinant *B. anthracis* Surrogate with Assay Targets (rBaSwAT-BAP708), hereafter referred to as BAP708.

PCRs

Verification of Toxin Gene Deletions and Presence of Synthetic Cassette

We resuspended single colonies of the strains in 50 μL of PCR-Lyse (Epicentre) or Y-PER (Thermo Fisher Scientific, Waltham, MA, USA), vortexed, and incubated them at 99°C for 15 min. Five μL of each lysate was used as a template for PCR (50 cycles), with 2.5 μL of each 10 μM primer and 0.5 μL of Phusion polymerase (Thermo Fisher Scientific) in 50-μL reactions. Annealing temperatures were 49°C (primers RP214/RP215 [*lef*] and SS2166/SS2167 [*cya*]), 54°C (primers SS2168/SS2169 [*pagA*]), and 59°C (primers SS2164/SS2165 [*lef*]) (Table 1). Five μL of each PCR product was run on a 0.8% ethidium bromide agarose gel.

Verification of PCR Signature Sequences

We streaked *B. anthracis* strains on tryptic soy agar plates for isolation and incubated them overnight at 37°C before inoculating a colony from each strain into 15 mL of 3% brain heart infusion and incubating cultures with shaking (100 rpm) for 24 h at 37°C. We then centrifuged the entire culture to pellet the cells (room temperature, 10 min, 2,000 × *g*) and extracted DNA using the MoBio Ultraclean Microbial DNA Isolation Kit (QIAGEN Inc., Germantown, MD, USA) according to the manufacturer's recommended protocol; we eluted DNA in a volume of 200 μL. DNA concentration was determined using a NanoDrop (Thermo Fisher Scientific). We diluted extracts such that PCR reactions were performed starting with either 10 or 50 genomic copies. Various *B. anthracis*–specific PCRs were conducted on an ABI 7500 or 7900 instrument (*12*).

Animal Study to Evaluate Pathogenicity of the Recombinant Strain

We made spore preparations of various strains using published protocol (*13*,*14*). We infected female A/J mice (6–8 weeks old; Charles River, Frederick, MD, USA) subcutaneously with Sterne (34F2) and Sterne derivative spores

Table 1. Genotypic characteristics of *Escherichia coli* and *Bacillus anthracis* strains and plasmids and primers used to determine avirulent *B. anthracis* strain with molecular assay targets

Strain, plasmid, primer	Genotype	Reference/source
Strain		
DH5α	*F⁻ Φ80lacZΔM15 Δ(lacZYA-argF) U169 recA1 endA1 hsdR17(rk⁻, mk⁺) phoA supE44 thi-1 gyrA96 relA1 λ⁻*	Laboratory collection
SCS110	*rpsL thr leu endA thi-1 lacY galK galT ara tonA tsx dam dcm supE44 Δ(lac-proAB)*	Stratagene (La Jolla, CA, USA)
SM10	*thi thr leu tonA lacY supE recA::RP4–2-Tc::Mu KmR λpir*	(*9*)
S17.1	*hsdR pro recA, RP4–2 in chromosome, Km::Tn7 (Tc::Mu)*	(*9*)
DH5α/pSS1827	*F⁻ Φ80lacZΔM15 Δ(lacZYA-argF) U169 recA1 endA1 hsdR17(rk⁻, mk⁺) phoA supE44 thi-1 gyrA96 relA1 λ⁻, pSS1827 (Replicon fusion of pBR322 and pRK2013 at EcoRI and SalI sites)*	(*10*)
BA500	*B. anthracis* Sterne 34F2	Laboratory collection
BAP482	BA500 *Δcya* and *Δlef* (double toxin deletion)	(*11*)
BAP417	BA500 *Δcya, Δlef, and ΔpagA* (triple toxin deletion)	(*11*)
BAP708	BA417 with construct 4 (Signatures 1–5)	This study
Plasmid	Description	Source
pT7 Blue	Cloning vector	Novagen-MilliporeSigma, St. Louis, MO, USA
pT7 Blue::4	Construct 4 (Signatures 1–5)	This study
pRP1091	*Δlef* derivative of shuttle vector pRP1028	(*11*)
Primer	Sequence, 5′ → 3′	Application
RP411	TTTCACACAGGAAACAGCTATGACC	Amplify constructs
RP645	CCAGTCACGACGTTGTAAAACGAC	Amplify constructs
SS2178	GTAAATTATTTAGCAAGTAAATTTTGGTG	Sequence constructs
RP214	TATGGTCTCGGATCCTTTGGCTTTAACGAAATGTATGTGC	Diagnose, sequence *lef*
RP215	TATGGTCTCCGGCCGTTTCAGTTATTCATTCTGGATAGTC	Diagnose, sequence *lef*
SS2164	CACGAGAAGAGTATTTAAAGAAAATC	Diagnose *lef*
SS2165	AACTATAGGACAATATTCATTACCATG	Diagnose *lef*
SS2166	ATATCAAGTTTAATTGTTAAGTTTGAAGG	Diagnose *cya*
SS2167	CCCGCGGCCGCAACCAAATGGTTTTCATTTCTTAG	Diagnose *cya*
SS2168	CGCATATAAGCAAATACTTAATTGGTC	Diagnose *pagA*
SS2169	GGATAGGGTTTAACAACTTAATAATCCC	Diagnose *pagA*

and checked the mice daily for clinical signs. Animal research at the United States Army Medical Research Institute of Infectious Diseases was conducted under an animal use protocol approved by the Institute's Institutional Animal Care and Use Committee in compliance with the Animal Welfare Act, Public Health Service Policy, and other federal statutes and regulations relating to animals and experiments involving animals. The facility where this research was conducted is accredited by the Association for Assessment and Accreditation of Laboratory Animal Care International and adheres to principles stated in the Guide for the Care and Use of Laboratory Animals (https://grants.nih.gov/grants/olaw/Guide-for-the-Care-and-use-of-laboratory-animals.pdf).

Large-Scale Spore Preparation

We produced BAP708 spores according to the protocol described (online Technical Appendix) (*15*–*19*), and determined spore counts after heat inactivation to kill any viable vegetative bacteria. We assessed the quality of the spores (particle size and uniformity, diameter, and particle number) using a Coulter counter. In addition, we conducted phase contrast microscopy to examine the uniformity in size of spores and absence of spore clumps. Sporulation efficiency is the ratio of total CFUs before heat inactivation to CFUs after treating the culture at 65°C for 30 min.

Irradiation Inactivation of Spores and Postirradiation Sterility Testing

We irradiated 60 mL of the spores in a JL Shepperd-Model 109–68 Cobalt 60 instrument at a rate of 10,975 rads/min for a total of 456 min, with a final dose of ≈5 × 10^6 rads (50 KGreys). We tested complete inactivation and loss of viability of the spores using the recently established CDC-recommended protocol for select agent spores (*20*). We inoculated 6 mL (10%) of the inactivated spore preparation into 60 mL of Terrific broth and incubated at 37°C for 7 d, and plated 1.2 mL (200 μL × 6 plates; i.e., 2% of the culture volume) on Mueller-Hinton agar and incubated for an additional 7 d. No growth was found on any of the plates. We used positive (unirradiated BAP708) and negative (uninoculated broth of the same type and volume under test) controls to ensure the validity of the protocol.

Phage Sensitivity

We tested for phage sensitivity as described using the spot titer method (*21*). In brief, a bacterial lawn of test strains was prepared using log phase cultures and 10 μL of various

dilutions of phages AP50 and γ were spotted on the lawn and incubated overnight at 37°C.

Comparison of Assay Performance of BAP708 Spores to Historical Data from Irradiation-Inactivated Select Agent *B. anthracis* Spores

We prepared liquid and filter extracted samples according to established protocols using 2 separate aliquots of live and irradiation-inactivated BAP708 spore preparations. We diluted spore stock (≈2.0×10^{10} CFU/mL) in 1× phosphate-buffered saline to a spiking concentration of 2.0×10^{6} CFU/mL and either extracted the stock directly as liquid samples or spiked it onto quarter filters, allowed to it dry, and extracted it as filter samples. We used both clean and simulated dirty filters. We extracted samples in accordance with an established single-tube extraction protocol using Amicon Ultra –0.5 Centrifugal filter devices (MilliporeSigma). In brief, we extracted DNA by mechanical disruption using a bead beater (*22*) and size exclusion filtration and eluted results in a volume of 200 μL. We heat treated DNA extracts to inactivate any nuclease (65°C, 10 min) before use in PCR analysis. We used 5 μL of DNA in 5 different *B. anthracis*–specific real-time PCRs on the ABI 7500 or ABI 7900 platform (*12*).

Lateral Flow Immunoassay

We tested live and inactivated spores in a standard lateral flow immunoassay (LFI) that is designed to detect *B. anthracis* spores (S. Sozhamannan, unpub. data). We used 100 μL of spores in each test and quantified the intensities of test and control lines using a thin layer chromatography scanner and software for scanning LFIs (CAMAG-TLC-3). We plotted results as relative absorbance units versus concentration of spores, set the background threshold at 30 scanner units, and scored all results >30 units as positive. The measurements were done in quadruplicate, and the minimal spore concentration that crossed the threshold was reported as the limit of detection using each spore preparation.

Results

Rationale for Construction of Recombinant Strains with Assay Targets

Mitigating the risk associated with irradiation-inactivated wild-type *B. anthracis* strains, such as Ames, required use of avirulent, excluded strains as reference materials for detection/diagnostic assay developmental efforts. However, assay targets for virulent strains most often are located in genes that are absent in the excluded strains. *B. anthracis* detection relies on 3 specific markers, 1 each on the chromosome and the pXO1 and pXO2 replicons. Strains containing plasmid pXO2 are classified as select agents (*23*), and Sterne lacking pXO2 but carrying pXO1 can be pathogenic for some mice strains because of the presence of the toxin genes (*pagA*, *lef*, and *cya*) on pXO1 (*24*). Strains lacking either pXO1 or pXO2 lack target(s) for the missing plasmid and hence are of limited utility as reference materials. Therefore, we decided to construct recombinant strains carrying all 3 assay targets in the background of a highly attenuated excluded strain. We chose a Sterne derivative, designated ΔSterne triple knockout strain (BAP417), in which all 3 toxin genes have been deleted (online Technical Appendix Table) (*11*) and that lacks both pXO1 and pXO2 assay targets (Figure 1, panel A), as confirmed by whole-genome sequence analyses (Figure 2). In this strain, assay signatures for pXO1 and pXO2 plasmids were introduced into the ΔpXO1 backbone as described in Materials and Methods.

Synthesis of Assay Target Cassette and Transfer of the Cassette into *B. anthracis*

Of 4 constructs made, in synthetic construct 4 described here, 5 signatures (PCR targets; i.e., amplicon sequences, including primer and probe sequences) and 2 bar codes were embedded. The bar codes are unique for each construct and can be used to track the strain and distinguish it from the wild type. In addition, stop codons in all 3 open reading frames were placed on the 5′ and 3′ ends of the cassette to prevent any fortuitous translation of the inserts from read-through from neighboring transcriptional signals (Figure 1, panel C).

We conducted transfer of the cassettes onto *B. anthracis* ΔpXO1 as described previously (*11*). We determined the characteristics and predicted phenotypic properties of the resulting final scarless construct (Table 2). The deletion-insertion was verified by PCR (Figure 1, panels A, C) and further confirmed by whole-genome sequence analyses (Figure 2).

Characterization of the Recombinant Strain

We conducted a comprehensive phenotypic and genotypic characterization of the recombinant strain, BAP708, to establish its avirulent phenotype and the presence of assay targets for both molecular and immunoassays (Table 3). The characterization included basic microbiological tests, such as colony morphology on selective agar plates; biochemical and phage sensitivity tests; molecular assays, such as PCR; immunoassays, such as LFI; whole-genome sequencing; and animal lethality.

PCR Analyses of Toxin Gene Deletions and Presence of the Cloned Cassettes

We conducted PCRs to confirm the toxin gene deletions and the presence of the cassette in BAP708. We used primers flanking the toxin genes as well as the insertion site (*11*) to amplify the region. The double (*pagA*) and triple knockout strains showed the expected deletions, and BAP708 showed an increase in fragment size

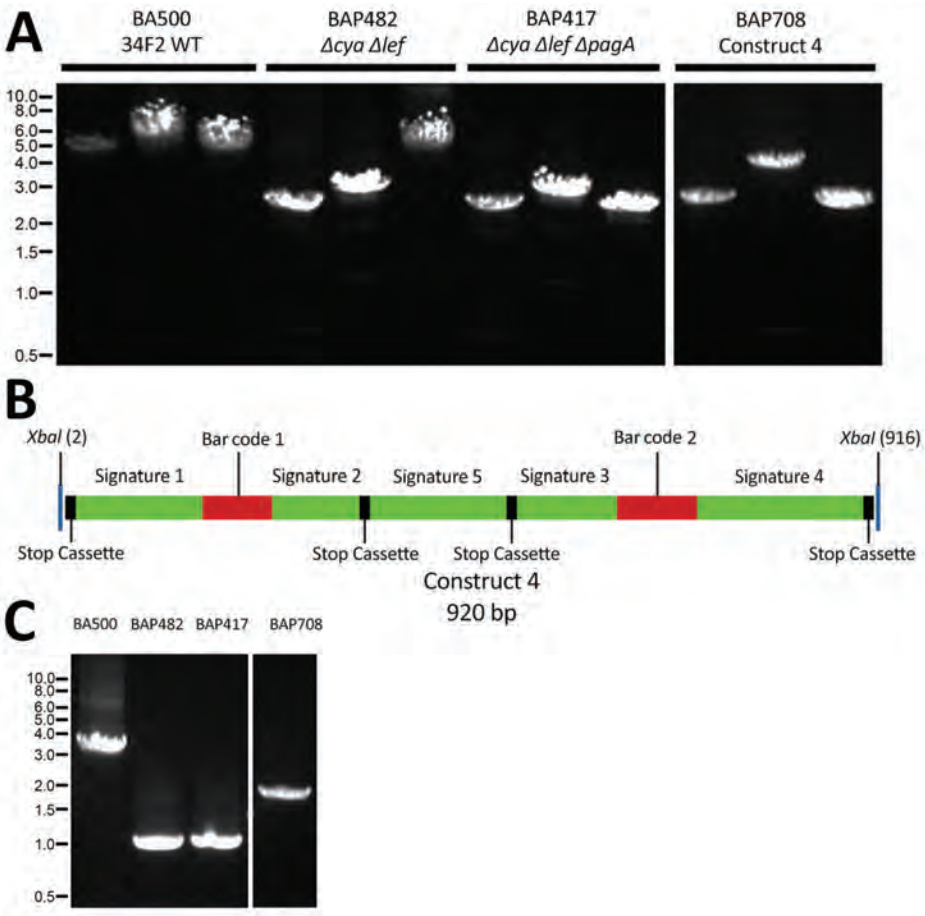

Figure 1. Verification of toxin gene deletions and the genetic structure of the construct 4 cassette in *Bacillus anthracis* surrogate strain. A) PCR verification of toxin gene deletions in BA500 (Sterne 34F2) derivatives. Single colonies were processed and used as templates for PCR with respective primers as described in Methods. For each strain, primers were used to amplify, from left to right, the regions of *cya* (SS2166/SS2167), *lef* (SS2164/SS2165), and *pagA* (SS2168/SS2169) on pXO1. B) Schematic representation of BAP708 (construct 4) cassette. Green bars represent the PCR signatures, red bars represent bar codes, and black boxes represent stop codons in all 3 open reading frames. *XbaI* sites at the ends of the cassette used in subcloning of the insert are marked. C) PCR verification of the presence of construct 4 synthetic sequence cassette in BAP708, using primers immediately flanking the *lef* deletion region (RP214 and RP215). Strains and PCR primers are listed in Table 1. Ladder indicates size in kbps. WT, wild-type.

corresponding to cassette insertion at the expected location (*lef*) (Figure 1, panels A, B). PCR products of expected sizes were obtained using DNA from the regulated strain *B. anthracis* Ames, whereas no products were obtained using DNA from *B. thuringiensis* Al Hakam, indicating absence of the toxin genes. In addition, a real-time PCR designed to distinguish this strain from wild-type virulent strains, such as Ames, detected BAP708 exclusively (data not shown).

Whole-Genome Sequencing and Analysis

We used Illumina next-generation sequencing technology to produce whole-genome sequences of various strains. Whole-genome sequences of the 3 parental strains have been deposited in GenBank under accession nos. BA500-NRIZ00000000, BA482-NRJA00000000, and BA417-NRJB00000000 (*27*). Analysis of the ΔpXO1 toxin region indicated that the triple knockout strain (BAP417) and its derivative (BAP708) lacked the

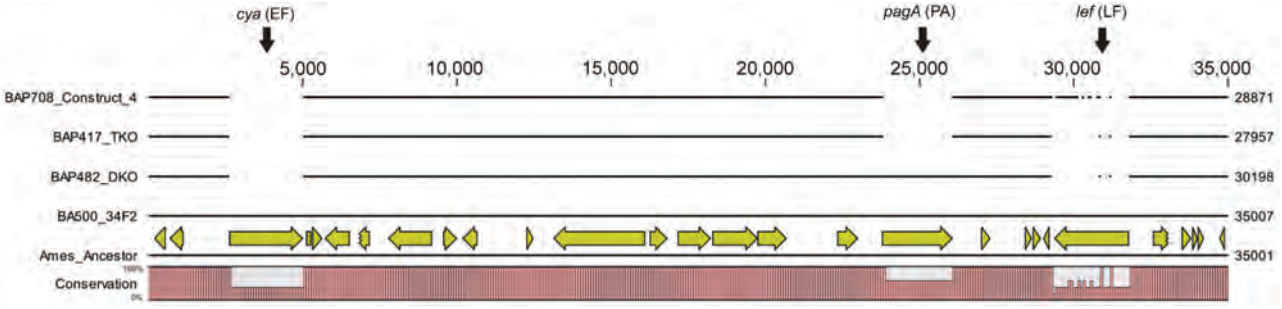

Figure 2. Whole-genome sequence verification of the deletion of toxin genes in *Bacillus anthracis* Sterne 34F2 derivatives. Comparative genomic view of the ≈35-kbp region of the pXO1 containing the toxin genes *cya*, *pagA,* and *lef* is shown. The bottom line indicates the sequence of Ames ancestor along with the annotations. Conservation of the same genetic structure in the grandparent strain BA500 is indicated. Deletions in the parent strains (DKO and TKO) and construct 4 are indicated by breaks in the lines and in the conservation percentage index at the bottom. DKO, double knockout; TKO, triple knockout.

pagA, *lef*, and *cya* genes that encode the 3 anthrax toxin subunits (Figure 2).

Sporulation

The infective form of *B. anthracis* is the spore, not the vegetative cell. Many detection/diagnostic assays target spore antigens (*28*). For immunoassays, the antigenic epitopes are most likely spore coat proteins, although there are immunoassays against anthrax toxin, which is produced by vegetative cells and secreted into the extracellular milieu (*29*). For nucleic acid–based tests, DNA extracted from spores is used as template to detect *B. anthracis*. Therefore, we assessed the spore-forming ability of BAP708. 34F2 and its derivative BAP708 produced spores efficiently (efficiencies ≈100% [Table 3]). The final titer for the BAP708 spore preparation was $\approx 1.5 \times 10^{10}$ spores/mL, and the particle size was 1.153 ± 0.122 μm. Sporulation results for regulated *B. anthracis* Ames strain and the negative control *B. thuringiensis* Al Hakam strain have been published and were normal (*16*,*25*).

Phage Sensitivity

One diagnostic test recommended by CDC for the suspected presence of *B. anthracis* in a sample is sensitivity of the bacterial isolate from the sample to γ phage. AP50c is another phage that can be used to verify *B. anthracis* (*30*). The recombinant strain, BAP708, exhibited sensitivity to both phages, as did the parent strains (Table 3), although they were less sensitive than other strains, such as Sterne 7702 (data not shown). In addition, bacteria in log phase were much more sensitive to infection by AP50c than were stationary phase cells (data not shown), which may be due to phase-dependent expression of the AP50c phage receptor, Sap (*31*,*32*). Regulated *B. anthracis* Ames strain was sensitive to both phages, and the negative control *B. thuringiensis* Al Hakam strain was resistant to both phages.

Molecular Assays

We assessed the performance of BAP708 in molecular assays (Table 4). Real-time PCRs using BAP708 and *B. anthracis* Ames produced expected results in accordance with the assay targets present or introduced into the strain, whereas assays using the negative control *B. thuringiensis* Al Hakam strain did not produce a positive amplification.

Validation of Avirulent Nature of Recombinant Strain

We inoculated female A/J mice (6–8 weeks old) subcutaneously with spores of Sterne (34F2) or its derivative. The 50% lethal dose (LD_{50}) in this model is 1.1×10^3 *B. anthracis* Sterne ($pXO1^+/pXO2^-$) spores (*33*), and the LD_{50} of fully virulent strains, such as Ames, and other species of *Bacillus,* such as *B. cereus* G9241, have been reported (*26*,*33*,*34*). The calculated delivered LD_{50} equivalents are as follows: BAP417, 109.7; BAP482, 152.7; BAP708, 106.1; and 34F2, 164.8. The animals were monitored daily for clinical signs for up to 14 days. Only the mice challenged with 34F2 showed any signs of disease; these mice succumbed to the infection or were euthanized after meeting early-endpoint criteria within 48 h (Figure 3). All animals in the other groups showed no signs of disease, indicating the avirulent nature of the toxin gene deletion derivatives.

Comparisons of Assay Performance of Recombinant Strain to Wild-Type and Inactivated Wild-Type Spores

We tested live and inactivated BAP708 spores for performance in immunoassays and PCRs to evaluate the effect of irradiation on assay targets. Unlike the near neighbor *B. thuringiensis* Al Hakam, BAP708 spores reacted positively in LFI, albeit weakly compared with historical reference materials, such as inactivated *B. anthracis* Ames (data not shown). PCR was done on DNA extracted in 2 different formats: liquid and spiked filter. All extracts reacted as expected in PCRs. These results were comparable to historical data obtained using irradiation-inactivated Ames spores. The inactivated *B. thuringiensis* Al Hakam spores treated and extracted similarly did not yield any positive results (Table 4).

Discussion

There are multiple instances of poor biosafety/biosecurity measures or laboratory accidents resulting in the release of harmful pathogens (*4*,*35*–*37*). These incidents underscore the

Table 2. Description of the DNA inserts in the recombinant *Bacillus anthracis* surrogate strain*

Replicon of assay target	WT gene	Size, bp	Assay	WT insert size, bp (%)†	Mutant insert size, bp‡	Predicted biological characteristic of recombinant product	Antimicrobial resistance/sensitivity of recombinant product
pXO2	*capA*	1,236	Signature 1	98 (7.9)	98	NC (Tox^-Cap^-)	Spc^S, Kan^S, Amp^S
pXO1	*pagA*	2,295	Signature 2	110 (4.8)	113	NC (Tox^-Cap^-)	Spc^S, Kan^S, Amp^S
pXO1	*pagA*	2,295	Signature 3	137 (6.0)	142	NC (Tox^-Cap^-)	Spc^S, Kan^S, Amp^S
pXO2	*capB*	1,395	Signature 4	182 (13.0)	186	NC (Tox^-Cap^-)	Spc^S, Kan^S, Amp^S
pXO1	*pagA*	2,295	Signature 5	153 (6.67)	NA	NC (Tox^-Cap^-)	Spc^S, Kan^S, Amp^S
Bar code 1	NS	78	NA	NA	NA	NA	NA
Bar code 2	NS	90	NA	NA	NA	NA	NA

*Amp, ampicillin; Cap^-, capsule negative; Kan, kanamycin; NA, not applicable; NC, no change from parent; NS, nonbiological, nonprotein-coding sequence; S, sensitive; Tox^-, protective antigen (PA), lethal factor (LF), and edema factor (EF) negative; Spc, spectinomycin; WT, wild-type.
†Percentage of the wild-type gene.
‡Contain unique restriction sites.

Table 3. Characterization of *Bacillus anthracis* surrogate strains*

		Summary of assays performed								
Strain	Inserts	WGS accession nos.	Toxin deletion PCR	Cassette PCR	Signature PCR†	Spore LFI	Phage test AP50	Phage test γ	Sporulation percentage	Animal model lethality
BA500	None	NRIZ00000000	WT	NI	ER	+	Sensitive	Sensitive	Normal (≈100%)	Lethal
BAP482	None	NRJA00000000	ED	NI	ER	+	Sensitive	Sensitive	Normal (≈100%)	Nonlethal
BAP417	None	NRJB00000000	ED	NI	ER	+	Sensitive	Sensitive	Normal (≈100%)	Nonlethal
BAP708	Signatures 1–5	Yes	ED	EI	ER	+	Sensitive	Sensitive	Normal (≈100%)	Nonlethal
Ames	None	CP009979–CP009981	WT	WT	ER	+	Sensitive	Sensitive	Normal (*25*) (≈100%)	Lethal (*24*)
B. thuringiensis Al Hakam	None	CP009645–CP009651	NP	NI	ER	–	Resistant	Resistant	Normal (*16*) (≈100%)	ND

*ED, expected deletion; EI, expected insert; ER, expected result; LFI, lateral flow immunoassay; ND, not done; NI, no insert; NP, no PCR product; WGS, whole-genome sequence; WT, wild-type; +, positive; –, negative.
†Results in Table 4.

lack of knowledge about factors influencing environmental survival of biological agents, the steps needed to ensure that established biosafety methods continue to work and meet expectations, and the need to acquire knowledge about how to recognize early any failure in established laboratory methods over time (*1*). We demonstrated an alternate approach that can potentially minimize risks associated with using BSATs and perhaps eliminate their use in some applications.

The need for BSATs and their derivatives for research and countermeasure development is inevitable. Guaranteeing inactivation of BSATs, especially spores, without adversely affecting their diagnostic and therapeutic targets can be problematic. However, the strategy described here of genetically inactivating the organism to mitigate the risk is a safer approach. In this study, we chose a *B. anthracis* strain that carries one of the virulence plasmids (pXO1) and removed the toxin genes from that plasmid to make it completely avirulent. Another option would have been to introduce pXO1 and pXO2 assay targets into the chromosome in a $pXO1^-$ and $pXO2^-$ background. However, the copy numbers of pXO1 and pXO2 have been determined to be slightly higher than that of the chromosome (1, 2, and 4 copies for the chromosome, pXO2, and pXO1 respectively) (*38*). To maintain a slightly higher copy number of the introduced plasmid assay targets, we introduced the assay targets into the ΔpXO1 backbone rather than into the chromosome in a strain lacking both pXO1 and pXO2. This way, assay results would be comparable in terms of copy numbers and cycle threshold values to historical assay data produced from a strain such as Ames.

In introducing the assay targets, neither full-length genes nor any antibacterial drug marker were introduced. Moreover, the surrogate strain is similar to virulent *B. anthracis* with respect to its utility as a reference material, except that it is risk-mitigated. In addition, unique bar codes

Table 4. Real-time PCR signature analyses in various *Bacillus anthracis* strains*

			Molecular assay result					
Strain	Material type	Insert	Chr	Sig 1	Sig 2	Sig 3	Sig 4	Sig 5
BA500	Vegetative cells†	None	+	–	+	+	–	+
BAP482	Vegetative cells†	None	+	–	+	+	–	+
BAP417	Vegetative cells†	None	+	–	–	–	–	–
BAP708	Vegetative cells†	Signatures 1–5	+	+	+	+	+	+
Ames‡	Vegetative cells†	Wild type	+	+	+	+	+	ND
B. thuringiensis Al Hakam	Vegetative cells†	None	–	–	–	–	–	ND
BAP708	Live spores-liquid extract	Signatures 1–5	+	+	+	+	+	ND
BAP708	Live spores-filter extract	Signatures 1–5	+	+	+	+	+	ND
BAP708	Inactivated spores-liquid extract	Signatures 1–5	+	+	+	+	+	ND
BAP708	Inactivated spores-filter extract	Signatures 1–5	+	+	+	+	+	ND
Ames‡	Inactivated spores-liquid extract	Wild type	+	+	+	+	+	ND
Ames‡	Inactivated spores-filter extract	Wild type	+	+	+	+	+	ND
B. thuringiensis Al Hakam	Live spores-liquid extract	None	–	–	–	–	–	ND
B. thuringiensis Al Hakam	Live spores-filter extract	None	–	–	–	–	–	ND

*Chr, chromosomal marker; ND, not done; Sig, signature; +, cycle threshold ≤35; –, cycle threshold >35.
†Genomic DNA extracted from vegetative cells was used as template for PCR (equivalent to 10 and 50 copies or 100 and 500 copies for *B. thuringiensis* Al Hakam).
‡Historical data.

have been introduced to distinguish the surrogate from the wild-type virulent agent and for forensic purposes.

The approach we describe can be easily adapted for other assay targets and applications. For example, genes encoding vaccine antigens, such as nonlethal variants of toxin genes, could be cloned and expressed in the recombinant strain. Because it is a platform technology, it would be relatively easy to construct strains for other assays by exchanging assay targets, which would also be safer and more cost-effective than handling BSATs and their derivatives. Noninfectious virus-like particles carrying assay targets could be created for BSL3 and BSL4 viral agents (*39*,*40*). The major disadvantage to this approach is that for every new assay signature/target, a new strain needs to be constructed, which may entail initial investment of time and funds to create the framework. Another disadvantage is that not all applications can be fulfilled by any 1 strain.

BSATs and inactivated BSATs pose risk and cost with respect to safety and security in production, validation, and shipping. Genetically inactivated and modified organisms provide almost the same level of assay capabilities as BSAT agents but with greatly reduced risk and cost. In addition, the recombinant construct described here is excluded from any regulatory concerns, such as need for exclusion from CDC select agent experiments, recombinant DNA advisory committee guidelines, or International Biological Weapons Convention regulations. Therefore, development of risk-mitigated solutions, such as the one we describe, can help minimize and perhaps prevent mishaps, such as the incident that came to light in 2015.

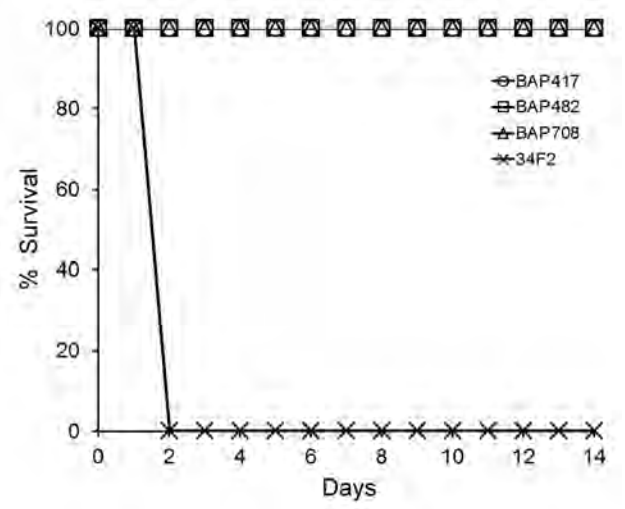

Figure 3. Role of *Bacillus anthracis* toxin components in lethality of Sterne strain 34F2 in female A/J mice and nonlethality of *B. anthracis* Sterne derivatives. Groups of mice were infected subcutaneously with *B. anthracis* spores of Sterne strain BA500 (34F2) or isogenic strains deficient for different toxin genes TKO-BAP417 (Δ*cya,* Δ*lef,* Δ*pagA*); DKO-BAP482 (Δ*cya,* Δ*lef*); BAP708-construct 4 (Δ*cya,* Δ*lef,* Δ*pagA*) plus insert. Fifty percent lethal dose equivalents ranged from ≈106 to 165. Based on a 1-sided Fisher exact test, p = 0.0003 for all groups (N = 10) versus the control 34F2 (N = 5) group.

Acknowledgments

We thank Amanda Horstman-Smith for many useful comments that improved the manuscript immensely, Carcie Graves for performing the LFI, and Tara Harvey and Jody Gostomski for help with PCRs.

The work was supported by funds from the Joint Program Executive Office for Chemical and Biological Defense.

About the Author

Dr. Plaut is a staff scientist at the Food and Drug Administration in Silver Spring, Maryland. His research interests include genetic regulation of virulence mechanisms of bacterial pathogens, such as *Staphylococcus aureus* and *Bacillus anthracis*, and development of allelic exchange systems for gram-positive bacteria.

References

1. Lieberman J, Ridge T, Shalala D, Daschle T, Greenwood J, Wainstein K. Blue Ribbon Study Panel on Biodefense Report: a national blueprint for biodefense: leadership and major reform needed to optimize efforts [cited 2015 Oct 28]. http://potomacinstitute.org/featured-news/1819-biodefense-blueprint-2
2. Imperiale MJ, Casadevall A. Bioterrorism: lessons learned since the anthrax mailings. MBio. 2011;2:e00232–11. http://dx.doi.org/10.1128/mBio.00232-11
3. Sozhamannan S, Smith M, Setlow P, Hanna PC. On the origin of live spores in gamma irradiated spore preparations a perfect example of Poisson distribution. ASM Microbe. 2016 Jan:4–5.
4. US Department of Defense. DoD launches review of lab procedures involving anthrax [cited 2015 May 29]. https://www.defense.gov/News/Article/Article/604749
5. US Department of Defense. Committee for Comprehensive Review of DoD Laboratory Procedures, Processes, and Protocols Associated with Inactivating *Bacillus anthracis* Spores. Review committee report: inadvertent shipment of live *Bacillus anthracis* spores by DoD [cited 2017 Aug 26]. https://www.defense.gov/Portals/1/features/2015/0615_lab-stats/Review-Committee-Report-Final.pdf
6. Secretary of the Army. Memorandum: immediate safety review and extension of moratorium. 2015 Sep 2 [cited 2017 Aug 26]. https://www.defense.gov/Portals/1/Documents/BSAT_Safety_Review_directive.pdf
7. Secretary of the Army. Memorandum: Army Directive 2016-24 (Department of Defense Biological Select Agent and Toxins Biosafety Program). 2016 Jul 25 [cited 2017 Aug 26]. http://armypubs.army.mil/epubs/DR_pubs/DR_a/pdf/web/Army%20Directive%202016-24%20Final.pdf
8. Deputy Secretary of Defense. Implementation of the recommendations in the comprehensive review report: inadvertent shipment of live *Bacillus anthracis* (anthrax) spores by Department of Defense. 2015 Jul 23 [cited 2017 Aug 26]. https://www.defense.gov/Portals/1/features/2015/0615_lab-stats/docs/DSD-Memo-Implementation-of-Recommendations-in-Comprehensive-Review-Report.pdf
9. Simon R, Priefer U, Puhler A. A broad host range mobilization system for in vivo genetic-engineering: transposon mutagenesis in gram-negative bacteria. Nat Biotech. 1983;1:784–91. http://dx.doi.org/10.1038/nbt1183-784

10. Stibitz S, Carbonetti NH. Hfr mapping of mutations in *Bordetella pertussis* that define a genetic locus involved in virulence gene regulation. J Bacteriol. 1994;176:7260–6. http://dx.doi.org/10.1128/jb.176.23.7260-7266.1994
11. Plaut RD, Stibitz S. Improvements to a markerless allelic exchange system for *Bacillus anthracis*. PLoS One. 2015;10:e0142758. http://dx.doi.org/10.1371/journal.pone.0142758
12. Hoffmaster AR, Meyer RF, Bowen MD, Marston CK, Weyant RS, Thurman K, et al. Evaluation and validation of a real-time polymerase chain reaction assay for rapid identification of *Bacillus anthracis*. Emerg Infect Dis. 2002;8:1178–82. http://dx.doi.org/10.3201/eid0810.020393
13. Nicholson W, Setlow P. Molecular biological methods for *Bacillus*. New York: John Wiley; 1990.
14. Thomas D, Naughton J, Cote C, Welkos S, Manchester M, Young JA. Delayed toxicity associated with soluble anthrax toxin receptor decoy-Ig fusion protein treatment. PLoS One. 2012;7:e34611. http://dx.doi.org/10.1371/journal.pone.0034611
15. Atrih A, Foster SJ. Analysis of the role of bacterial endospore cortex structure in resistance properties and demonstration of its conservation amongst species. J Appl Microbiol. 2001;91:364–72. http://dx.doi.org/10.1046/j.1365-2672.2001.01394.x
16. Buhr TL, Young AA, Minter ZA, Wells CM, McPherson DC, Hooban CL, et al. Test method development to evaluate hot, humid air decontamination of materials contaminated with *Bacillus anthracis* ΔSterne and *B. thuringiensis* Al Hakam spores. J Appl Microbiol. 2012;113:1037–51. http://dx.doi.org/10.1111/j.1365-2672.2012.05423.x
17. Gladstone GP, Fildes P. A simple culture medium for general use without meat extract or peptone. Br J Exp Pathol. 1940;21:161–73.
18. Camp DW, Montgomery NK. How good labs can get wrong results—keys to accurate and reproducible quantitation of *Bacillus anthracis* spore sampling or extraction efficiency. Presented at: Third National Conference on Environmental Sampling and Detection for Biol-Threat Agents. Las Vegas, NV, USA; 2008 Dec 2–4.
19. Buhr TL, Wells CM, Young AA, Minter ZA, Johnson CA, Payne AN, et al. Decontamination of materials contaminated with *Bacillus anthracis* and *Bacillus thuringiensis* Al Hakam spores using PES-Solid, a solid source of peracetic acid. J Appl Microbiol. 2013;115:398–408. http://dx.doi.org/10.1111/jam.12253
20. Federal Select Agent Program. Revised FSAP policy statement: inactivated *Bacillus anthracis* and *Bacillus cereus* biovar *anthracis*. August 14, 2017 [cited 2017 Aug 26]. https://www.selectagents.gov/policystatement_bacillus.html
21. Bishop-Lilly KA, Plaut RD, Chen PE, Akmal A, Willner KM, Butani A, et al. Whole genome sequencing of phage resistant *Bacillus anthracis* mutants reveals an essential role for cell surface anchoring protein CsaB in phage AP50c adsorption. Virol J. 2012;9:246. http://dx.doi.org/10.1186/1743-422X-9-246
22. BSP- Biol Spec products. Mini-Bead Beater-8- Preparation of sample [cited 2017 Nov 21]. https://biospec.com/instructions/minibeadbeater_8
23. Centers for Disease Control and Prevention. Federal Select Agent Program: select agents and toxins list. 2017 [cited 2017 Aug 24]. https://www.selectagents.gov/SelectAgentsandToxinsList.html
24. Loving CL, Khurana T, Osorio M, Lee GM, Kelly VK, Stibitz S, et al. Role of anthrax toxins in dissemination, disease progression, and induction of protective adaptive immunity in the mouse aerosol challenge model. Infect Immun. 2009;77:255–65. http://dx.doi.org/10.1128/IAI.00633-08
25. Buhr TL, Young AA, Minter ZA, Wells CM, Shegogue DA. Decontamination of a hard surface contaminated with *Bacillus anthracis* ΔSterne and *B. anthracis* Ames spores using electrochemically generated liquid-phase chlorine dioxide (eClO2). J Appl Microbiol. 2011;111:1057–64. http://dx.doi.org/10.1111/j.1365-2672.2011.05122.x
26. Lyons CR, Lovchik J, Hutt J, Lipscomb MF, Wang E, Heninger S, et al. Murine model of pulmonary anthrax: kinetics of dissemination, histopathology, and mouse strain susceptibility. Infect Immun. 2004;72:4801–9. http://dx.doi.org/10.1128/IAI.72.8.4801-4809.2004
27. Staab A, Plaut RD, Pratt C, Lovett SP, Wiley MR, Biggs TD, et al. Whole-genome sequences of variants of *Bacillus anthracis* Sterne and their toxin gene deletion mutants. Genome Announc. 2017;5:e01231–17. http://dx.doi.org/10.1128/genomeA.01231-17
28. Waller DF, Hew BE, Holdaway C, Jen M, Peckham GD. Rapid detection of *Bacillus anthracis* spores using immunomagnetic separation and amperometry. Biosensors (Basel). 2016;6:E61. http://dx.doi.org/10.3390/bios6040061
29. Biagini RE, Sammons DL, Smith JP, MacKenzie BA, Striley CA, Snawder JE, et al. Rapid, sensitive, and specific lateral-flow immunochromatographic device to measure anti-anthrax protective antigen immunoglobulin G in serum and whole blood. Clin Vaccine Immunol. 2006;13:541–6. http://dx.doi.org/10.1128/CVI.13.5.541-546.2006
30. Sozhamannan S, McKinstry M, Lentz SM, Jalasvuori M, McAfee F, Smith A, et al. Molecular characterization of a variant of *Bacillus anthracis*–specific phage AP50 with improved bacteriolytic activity. Appl Environ Microbiol. 2008;74:6792–6. http://dx.doi.org/10.1128/AEM.01124-08
31. Mignot T, Mesnage S, Couture-Tosi E, Mock M, Fouet A. Developmental switch of S-layer protein synthesis in *Bacillus anthracis*. Mol Microbiol. 2002;43:1615–27. http://dx.doi.org/10.1046/j.1365-2958.2002.02852.x
32. Plaut RD, Beaber JW, Zemansky J, Kaur AP, George M, Biswas B, et al. Genetic evidence for the involvement of the S-layer protein gene sap and the sporulation genes *spo0A*, *spo0B*, and *spo0F* in phage AP50c infection of *Bacillus anthracis*. J Bacteriol. 2014;196:1143–54. http://dx.doi.org/10.1128/JB.00739-13
33. Welkos SL, Keener TJ, Gibbs PH. Differences in susceptibility of inbred mice to *Bacillus anthracis*. Infect Immun. 1986;51:795–800.
34. Wilson MK, Vergis JM, Alem F, Palmer JR, Keane-Myers AM, Brahmbhatt TN, et al. *Bacillus cereus* G9241 makes anthrax toxin and capsule like highly virulent *B. anthracis* Ames but behaves like attenuated toxigenic nonencapsulated *B. anthracis* Sterne in rabbits and mice. Infect Immun. 2011;79:3012–9. http://dx.doi.org/10.1128/IAI.00205-11
35. Meselson M, Guillemin J, Hugh-Jones M, Langmuir A, Popova I, Shelokov A, et al. The Sverdlovsk anthrax outbreak of 1979. Science. 1994;266:1202–8. http://dx.doi.org/10.1126/science.7973702
36. Centers for Disease Control and Prevention. Conclusion of select agent inquiry into *Burkholderia pseudomallei* release at Tulane National Primate Research Center. 2015 Mar 13 [cited 2017 Aug 26]. http://www.cdc.gov/media/releases/2015/s0313-burkholderia-pseudomallei.html
37. US Department of Justice. Amerithrax investigative summary. 2010 Feb 19 [cited 2017 Aug 26]. www.justice.gov/amerithrax/docs/amx-investigative-summary.pdf
38. Straub T, Baird C, Bartholomew RA, Colburn H, Seiner D, Victry K, et al. Estimated copy number of *Bacillus anthracis* plasmids pXO1 and pXO2 using digital PCR. J Microbiol Methods. 2013;92:9–10. http://dx.doi.org/10.1016/j.mimet.2012.10.013
39. Noda T, Sagara H, Suzuki E, Takada A, Kida H, Kawaoka Y. Ebola virus VP40 drives the formation of virus-like filamentous particles along with GP. J Virol. 2002;76:4855–65. http://dx.doi.org/10.1128/JVI.76.10.4855-4865.2002
40. Warfield KL, Swenson DL, Demmin G, Bavari S. Filovirus-like particles as vaccines and discovery tools. Expert Rev Vaccines. 2005;4:429–40. http://dx.doi.org/10.1586/14760584.4.3.429

Address for correspondence: Shanmuga Sozhamannan, The Tauri Group Supporting Defense Biological Product Assurance Office JPM Guardian, 110 Thomas Johnson Dr, Ste 250, Frederick, MD 21702, USA; email: shanmuga.sozhamannan.ctr@mail.mil

Phenotypic and Genotypic Characterization of *Enterobacteriaceae* Producing Oxacillinase-48–Like Carbapenemases, United States

Joseph D. Lutgring, Wenming Zhu, Tom J.B. de Man, Johannetsy J. Avillan, Karen F. Anderson, David R. Lonsway, Lori A. Rowe, Dhwani Batra, J. Kamile Rasheed, Brandi M. Limbago

Oxacillinase (OXA)–48–like carbapenemases remain relatively uncommon in the United States. We performed phenotypic and genotypic characterization of 30 *Enterobacteriaceae* producing OXA-48–like carbapenemases that were recovered from patients during 2010–2014. Isolates were collected from 12 states and not associated with outbreaks, although we could not exclude limited local transmission. The alleles β-lactamase OXA-181 ($bla_{OXA-181}$) (43%), $bla_{OXA-232}$ (33%), and bla_{OXA-48} (23%) were found. All isolates were resistant to ertapenem and showed positive results for the ertapenem and meropenem modified Hodge test and the modified carbapenem inactivation method; 73% showed a positive result for the Carba Nordmann–Poirel test. Whole-genome sequencing identified extended-spectrum β-lactamase genes in 93% of isolates. In all $bla_{OXA-232}$ isolates, the gene was on a ColKP3 plasmid. A total of 12 of 13 isolates harboring $bla_{OXA-181}$ contained the insertion sequence ΔIS*Ecp1*. In all isolates with bla_{OXA-48}, the gene was located on a TN*1999* transposon; these isolates also carried IncL/M plasmids.

The prevalence of carbapenem-resistant *Enterobacteriaceae* (CRE) has been increasing in the United States since 2000 (*1*,*2*). This finding is problematic because treatment options for CRE infection are limited, and these infections are associated with a higher mortality rate than are infections with carbapenem-susceptible *Enterobacteriaceae* (*3*). *Enterobacteriaceae* might be resistant to carbapenems by a variety of mechanisms, the most concerning of which is production of carbapenemases (*4*). Although the *Klebsiella pneumoniae* carbapenemase is the most common carbapenemase reported in the United States, there have been reports of several other carbapenemases including the metallo-β-lactamases and, more recently, oxacillinase (OXA)–48–like carbapenemases (*1*,*5*–*10*).

OXA-48 is a member of the ambler class D β-lactamase family, first described in a *K. pneumoniae* isolate from Turkey in 2004 (*11*). The OXA-48 enzyme hydrolyzes penicillins efficiently, carbapenems slowly, and extended-spectrum cephalosporins poorly; it is not inhibited by tazobactam, sulbactam, or clavulanic acid (*12*). Since the initial report, OXA-48 has established reservoirs in Turkey, the Middle East, countries in North Africa, and throughout Europe (*12*). These reservoirs have been reported in multiple *Enterobacteriaceae* species in addition to *K. pneumoniae*, including *Citrobacter freundii*, *Enterobacter cloacae*, *Escherichia coli*, *K. oxytoca*, *Serratia marcescens*, and *Providencia rettgeri* (*12*). In addition to OXA-48, several variants with similar enzymatic profiles have been described, including OXA-162, -181, -204, -232, -244, -245, -370, -436, -438, and -484; each variant differs from OXA-48 by only a few amino acids (*12*–*16*). Other variants that do not hydrolyze carbapenems have also been described, including OXA-163, -247, and -405 (*13*,*17*,*18*).

The first description of isolates with β-lactamase OXA-48–like (bla_{OXA-48}–like) genes in the United States was from a surveillance study in 2013, which incidentally reported 2 *K. pneumoniae* isolates (*6*). This description was followed shortly afterward by a report of 2 clinical *K. pneumoniae* isolates with bla_{OXA-48}–like genes in patients from 1 institution in Virginia who had traveled internationally (*7*). More recently, CRE with $bla_{OXA-232}$ genes have been isolated in the United States (*8*). The Centers for Disease Control and Prevention (CDC) has collected multiple isolates harboring bla_{OXA-48}–like genes from patients in the United States (*19*). We report the genotypic and phenotypic characterization of those isolates.

Author affiliations: Emory University School of Medicine, Atlanta, Georgia, USA (J.D. Lutgring); Centers for Disease Control and Prevention, Atlanta (J.D. Lutgring, W. Zhu, T.J.B. de Man, J.J. Avillan, K.F. Anderson, D.R. Lonsway, L.A. Rowe, D. Batra, J.K. Rasheed, B.M. Limbago)

DOI: https://doi.org/10.3201/eid2404.171377

Materials and Methods

Collection of Isolates

Isolates are submitted to CDC for antimicrobial susceptibility testing (AST) for many reasons, including outbreak response, AST confirmation, and surveillance studies. Surveillance studies include the Multi-Site Gram-Negative Surveillance Initiative, which is part of the Emerging Infections Program, and the Sentinel Study (*5*,*20*). All *Enterobacteriaceae* isolates received for AST at CDC during June 1, 2010–October 31, 2012, with reduced susceptibility to carbapenems (MIC ≥1 μg/mL for any carbapenem), a positive modified Hodge test result, and a PCR-negative result for *bla K. pneumoniae* carbapenemase were retrospectively screened for $bla_{\text{OXA-48}}$–like genes (n = 115). During November 1, 2012–September 30, 2014, all *Enterobacteriaceae* received at CDC were routinely tested for $bla_{\text{OXA-48}}$–like genes by real-time PCR (n = 1,399). Submitting institutions were characterized by state and US Department of Health and Human Services (HHS) region (https://www.hhs.gov/ash/about-ash/regional-offices/index.html).

Phenotypic Characterization of Isolates

We performed reference broth microdilution AST on all isolates by using in-house prepared frozen panels that included carbapenems, cephalosporins, aztreonam, penicillins, quinolones, trimethoprim/sulfamethoxazole, aminoglycosides, chloramphenicol, tetracyclines, tigecycline, polymyxin B, and colistin (*21*,*22*). The modified Hodge test, Carba Nordmann–Poirel test, and the modified carbapenem inactivation method (mCIM) were performed on all $bla_{\text{OXA-48}}$–like isolates according to Clinical and Laboratory Standards Institute guidelines (*22*). We confirmed species identification by using the Biotyper 3.1 MALDI System (Bruker Daltronics, Billerica, MA, USA).

Genotypic Characterization of Isolates

The PCR for $bla_{\text{OXA-48}}$–like genes was developed at CDC and detects $bla_{\text{OXA-48}}$, $bla_{\text{OXA-162}}$, $bla_{\text{OXA-163}}$, $bla_{\text{OXA-181}}$, $bla_{\text{OXA-204}}$, $bla_{\text{OXA-232}}$, $bla_{\text{OXA-244}}$, $bla_{\text{OXA-245}}$, $bla_{\text{OXA-247}}$, $bla_{\text{OXA-370}}$, $bla_{\text{OXA-405}}$, $bla_{\text{OXA-438}}$, $bla_{\text{OXA-484}}$, and $bla_{\text{OXA-505}}$ by using 2 sets of $bla_{\text{OXA-48}}$–like primers/probes and a bacterial 16S rRNA gene as an endogenous control for lysate validation and PCR amplification (Table 1). We extracted DNA by using the thermal/sodium hydroxide method for preparation of bacterial cell lysates (*23*). Cycling conditions were a 3-min enzyme activation step at 95°C, followed by 40 cycles for 3 s at 95°C, and a final step for 30 s at 60°C (*24*).We characterized all isolates positive for $bla_{\text{OXA-48}}$–like genes by using whole-genome sequencing (WGS). We extracted DNA by using the Maxwell 16 Cell Low Elution Volume DNA Purification Kit (Promega, Madison, WI, USA) and fragmented input genomic DNA (gDNA) with an absorbance ratio of 1.8–2.0 to ≈800 bp by using an ultrasonic fragmentation system (Covaris, Woburn, MA, USA). We prepared libraries by using the Ovation Ultralow DR Multiplex System 1-96 Kit (Nugen Technologies, Inc., San Carlos, CA, USA), then multiplexed, and sequenced with MiSeq V2.0 (Illumina, San Diego, CA, USA). We filtered raw Illumina sequencing reads for quality (average ≥Q20) and discarded trimmed reads <50 bp from the dataset by using SolexaQA version 3.1 (*25*). We then assembled clean reads into contigs by using SPAdes version 3.1.0 and 4 k-mer sizes (k = 41, 79, 85, and 97) (*26*). Afterward, we mapped trimmed reads back to each assembled genome by using the Burrows-Wheeler Alignment tool for minor contig error correction (*27*).

We randomly selected *K. pneumoniae* isolates 1, 11, and 23, encoding $bla_{\text{OXA-181}}$, $bla_{\text{OXA-232}}$, and $bla_{\text{OXA-48}}$, respectively, as internal reference strains and sequenced them by using Single Molecule Real-Time Technology (Pacific Biosciences, Menlo Park, CA, USA) in addition to Illumina sequencing (Table 2). We extracted and purified gDNA by using the MasterPure Complete DNA and RNA Kit (Epicenter, Madison, WI, USA), according to the manufacturer's recommended protocol. We generated 10-kb libraries by using the SMRTbell Template Prep Kit 1.0 (Pacific Biosciences) and sequenced libraries by using C4v2 Chemistry on the RSII Instrument (Pacific Biosciences). We assembled data by using Hierarchical Genome-Assembly Process

Table 1. Sequences of primers and probes used for identification of *Enterobacteriaceae* isolates with β-lactamase OXA-48–like carbapenemases, United States*

Primers and probes	Sequence, 5′→3′
16S rRNA, forward primer	TGG AGC ATG TGG TTT AAT TCG A
16S rRNA, reverse primer	TGC GGG ACT TAA CCC AAC A
16S rRNA, probe (CY5)	CY5-CA CGA GCT GAC GAC ARC CAT GCA-BHQ
OXA-48, forward 180	ACG GGC GAA CCA AGC AT
OXA-48, reverse 239	GCG ATC AAG CTA TTG GGA ATT T
OXA-48, probe 199	FAM-TT ACC CGC ATC TAC C-BHQ
OXA-48, forward 722	TGC CCA CAT CGG ATG GTT
OXA-48, reverse 781	CCT GTT TGA GCA CTT CTT TTG TGA
OXA-48, probe 741	AG GGC TGC GCC AAG
OXA-48 F1	ATG CGT GTR TTA GCC TTA TC
OXA-48 R1	CTA KGG AAT WAT YTT YTC CTG

*OXA, oxacillinase.

Table 2. Phenotypic and genotypic characterization of *Enterobacteriaceae* harboring β-lactamase OXA-48–like carbapenemase, United States*

Isolate no.	Species	Year	Source	HHS region†	MHT MEM	mCIM	Carba NP	ST	OXA allele	NDM allele	ESBLs
1	*Klebsiella pneumoniae*	2010	Urine	9	+	+	+	ST34	181	None	CTX-M-15
2	*K. pneumoniae*	2011	Urine	9	+	+	+	ST34	181	None	CTX-M-15
3	*K. pneumoniae*	2011	Urine	9	+	+	+	ST34	181	None	CTX-M-15
4	*K. pneumoniae*	2011	Urine	9	+	+	+	ST34	181	None	CTX-M-15
5	*K. pneumoniae*	2011	Respiratory	9	+	+	+	ST34	181	None	CTX-M-15
6	*K. ozaenae*	2011	Respiratory	9	+	+	+	None	181	None	CTX-M-15
7	*K. pneumoniae*	2011	Wound	10	+	+	+	ST14	232	None	CTX-M-15
8	*K. pneumoniae*	2012	Peritoneal fluid	3	+	+	–	ST43	181	None	CTX-M-15
9	*K. pneumoniae*	2012	Urine	5	+	+	+	ST14	232	1	CTX-M-15
10	*K. pneumoniae*	2012	Rectal swab	5	+	+	+	ST14	232	1	CTX-M-15
11	*K. pneumoniae*	2013	Urine	3	+	+	+	ST14	232	1	CTX-M-15
12	*K. pneumoniae*	2013	Respiratory	3	+	+	+	ST14	232	1	CTX-M-15
13	*K. pneumoniae*	2013	Respiratory	5	+	+	Ind	ST147	181	None	CTX-M-15
14	*Enterobacter aerogenes*	2013	Peritoneal fluid	3	+	+	+	None	48	None	None
15	*K. pneumoniae*	2013	Urine	6	+	+	–	ST16	232	None	CTX-M-15
16	*K. pneumoniae*	2013	Urine	6	+	+	–	ST16	232	None	CTX-M-15
17	*K. pneumoniae*	2013	Urine	6	+	+	Ind	ST16	232	None	CTX-M-15
18	*K. pneumoniae*	2013	Urine	5	+	+	+	ST14	232	None	CTX-M-15
19	*K. pneumoniae*	2013	Respiratory	5	+	+	Ind	ST43	181	None	CTX-M-15
20	*K. pneumoniae*	2013	Respiratory	5	+	+	+	ST43	181	None	CTX-M-15
21	*K. pneumoniae*	2013	Urine	5	+	+	+	ST15	48	None	CTX-M-15
22	*K. pneumoniae*	2014	Respiratory	1	+	+	+	ST437	232	5	CTX-M-15, SHV-12
23	*K. pneumoniae*	2014	Respiratory	5	+	+	+	ST14	48	None	CTX-M-14b, CTX-M-15
24	*Escherichia coli*	2014	Urine	2	+	+	–	None	181	None	None
25	*K. pneumoniae*	2014	Urine	2	+	+	+	ST36	48	None	None
26	*K. pneumoniae*	2013	Urine	9	+	+	+	ST34	181	None	CTX-M-15
27	*K. pneumoniae*	2013	Urine	9	+	+	Ind	ST34	181	None	CTX-M-15
28	*K. pneumoniae*	2014	Respiratory	4	+	+	+	ST101	48	None	CTX-M-15
29	*K. pneumoniae*	2014	Respiratory	4	+	+	+	ST101	48	None	CTX-M-15
30	*K. pneumoniae*	2014	Unknown	4	+	+	+	ST101	48	None	CTX-M-15

*ESBLs, extended-spectrum β-lactamases; HHS, Health and Human Services; Ind, indeterminate; mCIM, modified carbapenem inactivation method; MEM, meropenem; MHT, modified Hodge test; NDM, New Delhi metallo-β-lactamase gene; NP, Nordmann–Poirel; OXA, oxacillinase; ST, sequence type (by multilocus sequence typing); –, negative; +, positive.
†HHS regions: 1, Connecticut, Maine, Massachusetts, New Hampshire, Rhode Island, Vermont; 2, New Jersey, New York; 3, Delaware, District of Columbia, Maryland, Pennsylvania, Virginia, West Virginia; 4, Alabama, Florida, Georgia, Kentucky, Mississippi, North Carolina, South Carolina, Tennessee; 5, Illinois, Indiana, Michigan, Minnesota, Ohio, Wisconsin; 6, Arkansas, Louisiana, New Mexico, Oklahoma, Texas; 7, Iowa, Kansas, Missouri, Nebraska; 8, Colorado, Montana, North Dakota, South Dakota, Utah, Wyoming; 9, Arizona, California, Hawaii, Nevada; 10, Alaska, Idaho, Oregon, Washington.

version 3.0 (Pacific Biosciences) and generated clean consensus sequences by using Quiver (*28*).

We deposited all raw sequencing reads, Pacific Biosciences assemblies, and MIC results in GenBank under BioProject PRJNA296771. We determined multilocus sequence types for each specimen by mapping clean Illumina reads to allele sequences (http://www.pubmlst.org) by using SRST2 software (*29*). We described antimicrobial resistance genotype profiles from assembled Illumina and Pacific Biosciences contigs by using SSTAR V1.0 (*30*) in combination with the ARG-ANNOT (*31*) and ResFinder (*32*) repositories.

We used the PlasmidFinder database (http://www.genomicepidemiology.org/) to detect plasmid replicon sequences among Illumina and Pacific Biosciences contigs to estimate the plasmid composition of each isolate (*33*). In addition, we predicted insertion sequences that might be associated with spread of antimicrobial resistance genes by using ISfinder (*34*). For isolates with $bla_{\text{OXA-48}}$, we estimated the copy number of IS*1R* insertion sequences for determining Tn*1999* variants by using blastn (https://blast.ncbi.nlm.nih.gov/Blast.cgi) and SPAdes K-mer coverage output (*26*,*34*–*36*). The clonality of our plasmids was also assessed, as was the location of $bla_{\text{OXA-48}}$–like genes (online Technical Appendix, https://wwwnc.cdc.gov/EID/article/24/4/17-1377-Techapp1.pdf). Because of a cluster of isolates from 1 state in this study, a phylogenetic tree and single-nucleotide polymorphism (SNP) tree matrix were produced by using RAxML version 8 (*37*) (online Technical Appendix).

Transformation Experiments

We randomly transformed 10 selected isolates (3 with $bla_{\text{OXA-48}}$, 4 with $bla_{\text{OXA-181}}$, and 3 with $bla_{\text{OXA-232}}$) for

transformation experiments to better characterize plasmids harboring bla_{OXA-48}–like genes. We subcultured parent isolates on trypticase soy agar containing 5% sheep blood, placed them in 50 mL of tryptic soy broth containing ertapenem (1 μg/mL), and incubated them overnight at 35°C. We extracted plasmid DNA by using Plasmid Midi Kits (QIAGEN, Valencia, CA, USA), according to the manufacturer's protocol. We digested intact plasmid DNA and gDNA with *Hin*dIII (New England Biolabs, Ipswich, MA, USA) and separated this DNA by electrophoresis on a 0.9% agarose gel.

We transformed 500 ng of plasmid DNA from each isolate into *E. coli* DH10B cells (Invitrogen, Carlsbad, CA, USA) by electroporation and incubated at 35°C for 2 h. Potential transformants were plated on Luria–Bertani agar containing ertapenem (1 μg/mL) and incubated overnight at 35°C. Four colonies from each transformant plate were screened for bla_{OXA-48}–like genes by using PCR. Transformant plasmid DNA was digested and separated by gel electrophoresis along with digested parent plasmid DNA to ensure that transformant plasmids were also present in parental cells.

We characterized confirmed transformants by using AST, the modified Hodge test, and WGS with MiSeq V2.0 (Illumina), as described previously. Trimmed reads from transformants were mapped to the genome sequence of *E. coli* K12, substrain DH10B (GenBank accession no. NC_010473.1), by using Bowtie 2 software (*38*,*39*). Unmapped reads were extracted by using bam2fastq (https://gsl.hudsonalpha.org/information/software/bam2fastq) and were considered to represent plasmid DNA harboring bla_{OXA-48}–like genes (https://gsl.hudsonalpha.org/information/software/bam2fastq). We subsequently assembled these unmapped reads by using SPAdes software and screened generated contigs for antimicrobial drug resistance genes by using SSTAR V1.0 and for plasmid replicon sequences by using the PlasmidFinder database (*26*,*30*,*33*).

Results

Epidemiology of Isolates

We included all 30 US isolates in our collection that were positive for a bla_{OXA-48}–like carbapenemase gene in this study. Isolates were submitted from patients in 12 states representing 8 HHS regions: one from region 1, two from region 2, four from region 3, three from region 4, eight from region 5, three from region 6, eight from region 9, and one from region 10. *K. pneumoniae* predominated (n = 27, 90%), although single isolates of *K. ozaenae*, *Enterobacter aerogenes*, and *E. coli* (n = 1 each, 3%) were also found. Isolates were collected from a variety of sources: urine (n = 15, 50%), respiratory samples (n = 10, 33%), peritoneal fluids (n = 2, 7%), wounds (n = 1, 3%), rectal swab specimens (n = 1, 3%), and unknown sources (n = 1, 3%) (Table 2).

Phenotypic Characterization of Isolates

All submitted isolates with a bla_{OXA-48}–like carbapenemase gene showed resistance to ertapenem and all penicillins tested (including those with β-lactamase inhibitors). Most showed intermediate resistance or resistance to imipenem (n = 30, 100%), meropenem (n = 28, 93%), doripenem (n = 28, 93%), ceftriaxone (n = 29, 97%), ceftazidime (n = 27, 90%), and cefepime (n = 28, 93%). In addition, all isolates had a colistin MIC ≤2 μg/mL (Table 3). Results for the ertapenem modified Hodge test, meropenem modified Hodge test, and mCIM were positive for all isolates harboring bla_{OXA-48}–like genes. The Carba Nordmann–Poirel test result was positive for 73% of isolates, indeterminate in 13%, and negative in 13% (Table 2).

Transformation Experiments

We purified plasmid DNA from 10 isolates (3 with bla_{OXA-48}, 4 with $bla_{OXA-181}$, and 3 with $bla_{OXA-232}$) for transformation into *E. coli* DH10B. Transformants were obtained for each preparation from strains harboring bla_{OXA-48} and $bla_{OXA-232}$, as confirmed by PCR and phenotypic and genotypic characterization of each transformant (Table 4). Transformation was unsuccessful for all DNA preparations from strains with $bla_{OXA-181}$ (isolates 1, 2, 26, and 27).

When we compared transformants with parent strains, most of which harbored multiple plasmids and numerous resistance genes, transformants were confirmed to carry only 1 plasmid and typically showed greater susceptibility to extended-spectrum cephalosporins but retained resistance to ≥1 carbapenem. As confirmed by WGS, we found that ESBL genes were not typically present on the same plasmid as bla_{OXA-48}–like genes; only 1 transformant (23T) carried a plasmid harboring $bla_{CTX-M-14b}$ on the IncL/M plasmid carrying bla_{OXA-48}. Similar to the parent strain, strain 23T showed increased MICs to cephalosporins and carbapenems, although the carbapenem MICs were lower than both the parent strain and other transformants carrying only an OXA-48–like carbapenemase (Table 4). None of the plasmids harboring bla_{OXA-48}–like genes encoded additional carbapenemases.

Genotypic Characterization of Isolates

We confirmed by using WGS the presence of bla_{OXA-48}–like genes in every isolate, including the alleles bla_{OXA-48} (n = 7, 23%), $bla_{OXA-181}$ (43%), and $bla_{OXA-232}$ (33%). The gene bla_{NDM} was identified in 5 isolates with $bla_{OXA-232}$. Nearly all isolates (93%) contained >1 ESBL gene, including bla_{SHV-12}, $bla_{CTX-M-14b}$, and $bla_{CTX-M-15}$ (Table 2). We also found aminoglycoside, fluoroquinolone, sulfonamide, trimethoprim, tetracycline, chloramphenicol, macrolide, and fosfomycin resistance genes. Multilocus sequence typing of 27 *K. pneumoniae* isolates showed ST34 (n = 7), ST14 (n = 7), ST16 (n = 3), ST43 (n = 3), and ST101 (n = 3) to be most common in this collection (Table 2).

Table 3. MIC results for *Enterobacteriaceae* harboring β-lactamase oxacillinase-48–like carbapenemases, United States*

Isolate no.	Species	Drug, MIC, μg/mL											
		ETP	MEM	IMP	DOR	TZP	CRO	CAZ	FEP	CIP	COL	TIG	AMK
1	*Klebsiella pneumoniae*	>4	4	4	4	>128	>32	>32	>32	>8	<0.25	2	4
2	*K. pneumoniae*	>8	4	2	4	>128	>32	>128	>32	>8	<0.5	2	>64
3	*K. pneumoniae*	>8	4	2	4	>128	>32	>128	>32	>8	1	1	>64
4	*K. pneumoniae*	8	2	4	2	>128	>32	>128	>32	>8	0.5	<0.5	>64
5	*K. pneumoniae*	8	2	2	2	>128	>32	>128	>32	>8	0.5	<0.5	>64
6	*K. ozaenae*	>8	4	4	4	>128	>32	>128	>32	>8	0.5	1	>64
7	*K. pneumoniae*	>8	>8	4	>8	>128	>32	>128	>32	>8	1	4	32
8	*K. pneumoniae*	>8	8	4	8	>128	>32	>128	>32	>8	0.5	1	16
9	*K. pneumoniae*	>8	>8	>64	>8	>128	>32	>128	>32	>8	0.5	2	>64
10	*K. pneumoniae*	>8	>8	64	>8	>128	>32	>128	>32	>8	1	2	>64
11	*K. pneumoniae*	>8	>8	64	>8	>128	>32	>128	>32	>8	0.5	2	>64
12	*K. pneumoniae*	>8	>8	>64	>8	>128	>32	>128	>32	>8	0.5	2	>64
13	*K. pneumoniae*	>8	>8	4	8	>128	>32	128	>32	>8	0.5	4	>64
14	*Enterobacter aerogenes*	2	2	4	2	>128	<1	<1	1	<0.25	0.5	<0.5	<1
15	*K. pneumoniae*	>8	>8	8	>8	>128	>32	>128	>32	>8	0.5	4	>64
16	*K. pneumoniae*	>8	>8	8	>8	>128	>32	>128	>32	>8	0.5	4	>64
17	*K. pneumoniae*	>8	>8	2	8	>128	>32	>128	>32	>8	0.5	4	>64
18	*K. pneumoniae*	>8	>8	64	>8	>128	>32	>128	>32	>8	0.5	2	>64
19	*K. pneumoniae*	>8	>8	8	>8	>128	>32	>128	>32	>8	2	1	<1
20	*K. pneumoniae*	>8	>8	8	>8	>128	>32	>128	>32	>8	2	1	<1
21	*K. pneumoniae*	2	0.25	2	0.5	>128	>32	64	>32	>8	0.5	1	>64
22	*K. pneumoniae*	>8	>8	32	>8	>128	>32	>128	>32	>8	0.5	4	>64
23	*K. pneumoniae*	>8	4	4	4	>128	>32	128	>32	>8	0.5	4	64
24	*Escherichia coli*	4	0.5	2	0.5	>128	8	2	8	>8	0.5	<0.5	2
25	*K. pneumoniae*	>8	8	4	8	>128	2	<1	2	<0.25	1	<0.5	<1
26	*K. pneumoniae*	>8	8	4	8	>128	>32	>128	>32	>8	0.5	1	>64
27	*K. pneumoniae*	>8	2	2	2	>128	>32	128	>32	>8	0.5	4	<1
28	*K. pneumoniae*	>8	>8	4	>8	>128	>32	>128	>32	>8	1	1	8
29	*K. pneumoniae*	>8	>8	32	>8	>128	>32	>128	>32	>8	0.5	<0.5	8
30	*K. pneumoniae*	>8	>8	8	>8	>128	>32	>128	>32	>8	0.5	1	8

*Not all drugs tested are listed. *bla*, β-lactamase; AMK, amikacin; CAZ, ceftazidime; CIP, ciprofloxacin; COL, colistin; CRO, ceftriaxone; DOR, doripenem; ETP, ertapenem; FEP, cefepime; IMP, imipenem; MEM, meropenem; TIG, tigecycline; TZP, piperacillin/tazobactam.

Isolates 1, 11, and 23 (carrying $bla_{\text{OXA-181}}$, $bla_{\text{OXA-232}}$, and $bla_{\text{OXA-48}}$, respectively) were randomly chosen for Pacific Biosciences WGS in addition to Illumina WGS. Isolate 1 had 2 plasmids and encoded 20 antimicrobial drug resistance genes, including 3 chromosomal copies of the ESBL CTX-M-15; $bla_{\text{OXA-181}}$ was also chromosomally located, with an upstream ΔIS*Ecp1* insertion sequence. The ΔIS*Ecp1* insertion sequence has been described elsewhere (*40*–*42*). Isolate 11 had 4 plasmids and encoded 34 antimicrobial drug resistance genes, including plasmid-mediated $bla_{\text{CTX-M-15}}$ and $bla_{\text{NDM-1}}$ genes. The $bla_{\text{OXA-232}}$ allele in isolate 11 was found on a ColKP3 plasmid (plasmid size 6,139 bp, G + C content 52.17%); upstream of $bla_{\text{OXA-232}}$, there was a ΔIS*Ecp1* insertion sequence. The sequence

Table 4. Plasmid transformation of *Enterobacteriaceae* producing OXA-48–like carbapenemases, United States*

Isolate no.†	MIC, μg/mL					MHT MEM	OXA allele	Plasmid replicon type	ESBL CTX-M
	ETP	MEM	CRO	TZP	AMK				
R	≤0.12	≤0.12	≤1	≤4	≤1	–			
7	>8	>8	>32	>128	32	+	232	ColKP3, IncR, IncFIB(pQIL)	15
7T	>8	4	≤1	>128	≤1	+	232	ColKP3	
9	>8	>8	>32	>128	>64	+	232	ColKP3, IncR, IncHI1B, IncFIB(K)	15
9T	>8	8	≤1	>128	≤1	+	232	ColKP3	
11	>8	>8	>32	>128	>64	+	232	ColKP3, IncR, IncHI1B, IncFIB(K)	15
11T	>8	8	≤1	>128	≤1	+	232	ColKP3	
23	>8	4	>32	>128	64	+	48	IncL/M	14b, 15
23T	4	1	>32	>128	16	+	48	IncL/M	14b
25	>8	8	2	>128	≤1	+	48	IncL/M	
25T	>8	8	≤1	>128	≤1	+	48	IncL/M	
28	>8	>8	>32	>128	8	+	48	IncL/M, IncR, ColRNAI	
28T	>8	8	≤1	128	≤1	+	48	IncL/M	

*AMK, amikacin; CRO, ceftriaxone; ESBL, extended-spectrum β-lactamase; ETP, ertapenem; MEM, meropenem; MHT, modified Hodge test; OXA, oxacillinase; R, recipient strain before transformation (*Escherichia coli* DH10B); T, transformant; TZP, piperacillin/tazobactam; –, negative; +, positive.
†Isolates 1, 2, 26, and 27 did not have any transformants.

of this plasmid (pColKP3_DHQP1300920) has been deposited in GenBank under accession no. CP016920.1. pColKP3_DHQP1300920 was most similar to a ColKP3 plasmid previously deposited under GenBank accession no. JX423831 (100% query coverage, 99% sequence similarity) (Figure 1) (*43*).

Isolate 23 had 3 plasmids and encoded 16 antimicrobial drug resistance genes, including 2 ESBLs (plasmid-mediated CTX-M-14b and CTX-M-15). $bla_{\text{OXA-48}}$ was present on an IncL/M plasmid (plasmid size 72,093 bp, G + C content 50.55%). This plasmid contained 89 open reading frames, including those for several antimicrobial drug resistance genes ($bla_{\text{CTX-M-14b}}$, [streptomycin] *strA, strB,* and [aminoglycoside] *aph(3')-VIb*), in addition to $bla_{\text{OXA-48}}$, which appears to have been inserted into the plasmid by transposon Tn*1999.2* (GenBank accession no. JN714122). The sequence of this plasmid (pIncL_M_DHQP1400954) has been deposited in GenBank under accession no. CP016927.1. This plasmid, pIncL_M_DHQP1400954, was most similar to pOXA48-Pm (GenBank accession no. KP025948) (95% query coverage, 99% sequence similarity) (Figure 2) (*44*).

We identified no SNPs when we compared Illumina and Pacific Biosciences genome sequences for the same isolate for isolates 1, 11, and 23. This finding indicates that Pacific Biosciences sequences can be used as a mapping reference. We compared Illumina sequence data for the remaining clinical isolates, which were not subjected to Pacific Biosciences sequencing, against the Pacific Biosciences genomes according to $bla_{\text{OXA-48}}$–like allele. For all 10 isolates containing $bla_{\text{OXA-232}}$, the gene was co-located with the ColKP3 replicon gene and a ΔIS*Ecp1* upstream insertion sequence (upstream of $bla_{\text{OXA-232}}$) on an ≈6 kb contig. Pacific Biosciences sequence analysis of isolate 23 confirmed the presence of $bla_{\text{OXA-48}}$ on transposon Tn*1999.2*; $bla_{\text{OXA-48}}$ was found on a variant of transposon Tn*1999* in all instances. In 3 isolates (23, 28, and 29), coverage of the IS*1R* insertion sequence was similar to the overall assembly coverage suggestive of the Tn*1999.2* variant identified in isolate 23 by Pacific Biosciences sequencing. However, in 4 isolates (14, 21, 25, and 30), coverage of the IS*1R* insertion sequence was much higher than the overall assembly coverage, indicating multiple occurrences of this locus, suggestive of a different Tn*1999* variant. Of the 13 isolates containing $bla_{\text{OXA-181}}$, 12 had an upstream insertion sequence ΔIS*Ecp1*. In isolate 1, which was sequenced by using Pacific Biosciences technology, $bla_{\text{OXA-181}}$ was confirmed as being chromosomally located. Finally, given the geographic association of several isolates carrying $bla_{\text{OXA-181}}$, we created a phylogenetic tree and SNP matrix table for the 7 *K. pneumoniae* isolates from 1 state in HHS region 9 (Table 5; Figure 3).

Discussion

The increasing prevalence of CRE in the United States poses a challenge to patients, clinicians, and public health. The diversity of carbapenemases, including the OXA-48–like enzymes reported in this study, is an ongoing diagnostic challenge to clinical microbiology laboratories because of the variety of phenotypes displayed by isolates producing different, and sometimes multiple, carbapenemases. OXA-48 has been described as the phantom menace because of its subtle phenotype in the absence of co-resistance mechanisms (*12*).

In this study, all isolates with $bla_{\text{OXA-48}}$–like genes showed resistance to ertapenem, and most showed intermediate resistance or resistance to meropenem, ceftriaxone, ceftazidime, and cefepime. Three tests for carbapenemase production were performed on the isolates in this study. The modified Hodge test, performed for ertapenem or meropenem, and the mCIM showed positive results for all isolates with $bla_{\text{OXA-48-}}$like genes. The Carba Nordmann–Poirel test showed positive results for 73% of all isolates, which is consistent with other studies that have shown that this test had a sensitivity of 72%–76% for OXA-48–like carbapenemase producers (*45,46*). All isolates in this study would be identified as CRE by the current CDC and Council of State and Territorial

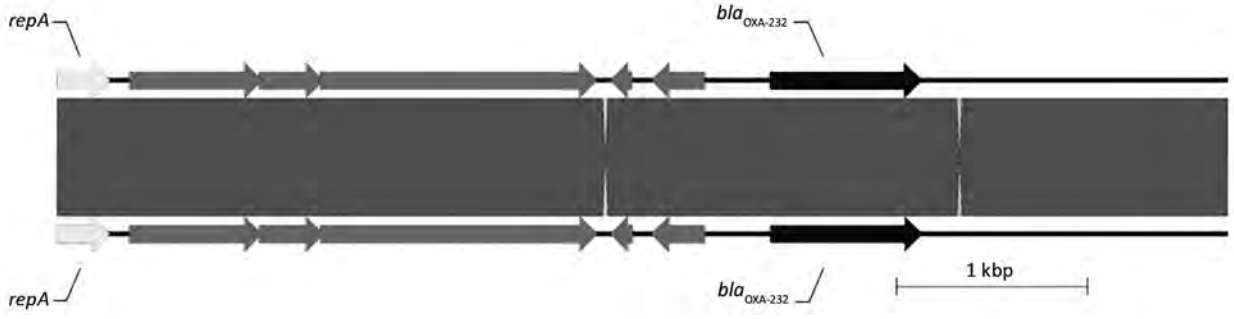

Figure 1. Sequence structure of 2 β-lactamase OXA-232 ($bla_{\text{OXA-232}}$) plasmids tested during phenotypic and genotypic characterization of *Enterobacteriaceae* producing OXA-48–like carbapenemases, United States. Top plasmid is from isolate 11 in this study (pColKP3_DHQP1300920) (6,139 bp), and bottom plasmid is from Potron et al. (*43*) (GenBank accession no. JX423831). Arrows indicate direction of transcription. Unlabeled arrows indicate other genes. OXA, oxacillinase; *repA*, COLe type replicase.

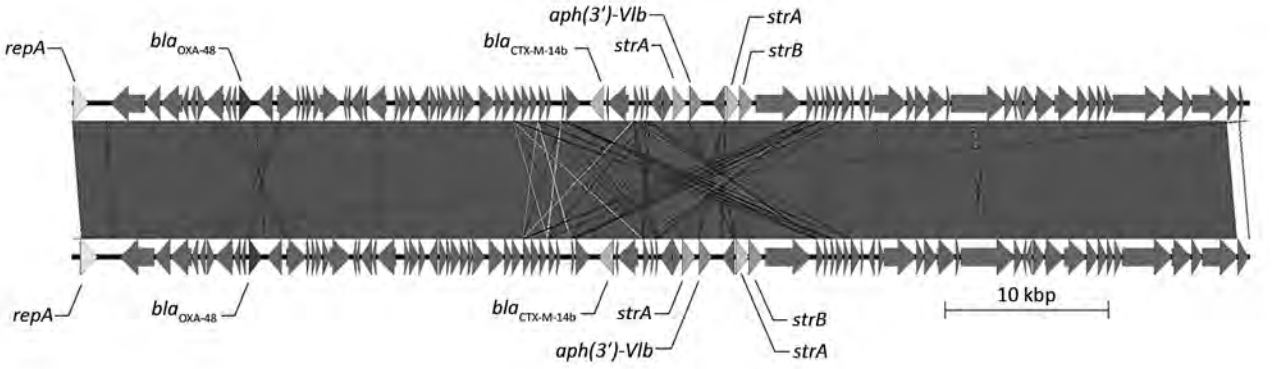

Figure 2. Sequence structure of 2 β-lactamase OXA-48 (bla_{OXA-48}) plasmids tested during phenotypic and genotypic characterization of *Enterobacteriaceae* producing OXA-48–like carbapenemases, United States. Top plasmid is from isolate 23 in this study (pIncL_M_DHQP1400954) (72,093 bp), and bottom plasmid is from Chen et al. (*44*) (GenBank accession no. KP025948). Arrows indicate direction of transcription. Unlabeled arrows indicate other genes. Gray area indicates regions of homology, white lines indicate nonhomologous regions, and dark gray lines indicate inversions. *aph*, aminoglycoside; OXA, oxacillinase; *repA*, IncL/M type replicase; *str*, streptomycin.

Epidemiologists definitions (https://www.cdc.gov/hai/organisms/cre/definition.html) (*47*).

The 10 isolates that harbored $bla_{OXA-232}$ were all found on a small ColKP3 plasmid, and this association has been reported by Potron et al. (*43*). Likewise, the 7 isolates producing OXA-48 carried bla_{OXA-48} on a similar genetic environment to those reported (*44*,*48*,*49*). Isolate 23, which was sequenced by using Illumina and Pacific Biosciences technology, harbored bla_{OXA-48} on an IncL/M plasmid. The other 6 isolates, which were sequenced only by using Illumina technology, all had the IncL/M replicon gene. In addition, bla_{OXA-48} was always associated with a variant of transposon TN*1999*, as discerned on the basis of the copy number of IS*1R* insertion sequences (*36*). Because these IS*1R* sequences are identical and duplicated, Illumina technology often fails to assemble these as separate loci but instead produces a single locus with high coverage. Comparing coverage of the IS*1R* insertion sequence to the overall coverage of the assembly sequence enabled us to estimate the presence of the TN*1999* variant by using isolate 23 as the reference. In 12 of 13 isolates with $bla_{OXA-181}$, we found an upstream ΔIS*Ecp1* element inserted upstream of the $bla_{OXA-181}$ cassette. $bla_{OXA-181}$ is often associated with IS*Ecp1*, which might facilitate its spread (*50*).

The transformation experiment helped to clarify our understanding of the plasmids harboring bla_{OXA-48}–like genes. Transformation experiments were successful for each of the parent strains carrying bla_{OXA-48} or $bla_{OXA-232}$. Carbapenem and penicillin MICs were not different between the parent and transformant, but transformant MICs were comparatively lower for cephalosporins and aminoglycosides. This finding supports the genotypic data, which indicated that ESBL genes and other β-lactamase genes did not cotransfer with the plasmid encoding bla_{OXA-48}–like genes. One transformant (23T) did not have decreased cephalosporin MICs when compared with its parental strain, which is consistent with Pacific Biosciences sequencing of this isolate, which showed $bla_{CTX-M-14b}$ to be on the same IncL/M plasmid as bla_{OXA-48}. The unsuccessful transformation attempts of $bla_{OXA-181}$–containing strains 1, 2, 26, and 27 were explained by WGS evidence that $bla_{OXA-181}$ was chromosomally located in isolate 1.

We also detected a possible reservoir of isolates with bla_{OXA-48}–like genes in the United States. Among the 13 isolates with $bla_{OXA-181}$, 8 were from 1 state in HHS region 9 and contained $bla_{CTX-M-15}$, bla_{SHV-26}, and *ampH*. Seven of these isolates were *K. pneumoniae* belonging to ST34, and 5 were collected during June 2010–May 2011 (Tables 2, 5; Figure 3).

Table 5. SNP matrix for 7 *Klebsiella pneumoniae* isolates with β-lactamase oxacillinase-181–like carbapenemases from HHS region 9, United States*

	Isolate no.						
Isolate no.	26	27	4	5	1	2	3
26	0	31	33	17	32	27	28
27	31	0	27	15	28	23	26
4	33	27	0	6	13	10	8
5	17	15	6	0	5	3	1
1	32	28	13	5	0	7	9
2	27	23	10	3	7	0	6
3	28	26	8	1	9	6	0

*Genetic diversity ranged from 1 to 33 high-quality SNPs that were called in an ≈5-Mb core genome, which equals ≈90% of the reference genome size (isolate 1 sequenced by using Pacific Biosciences [Menlo Park, CA, USA] technology). *bla*, β-lactamase; HHS, Health and Human Services; SNP, single-nucleotide polymorphism.

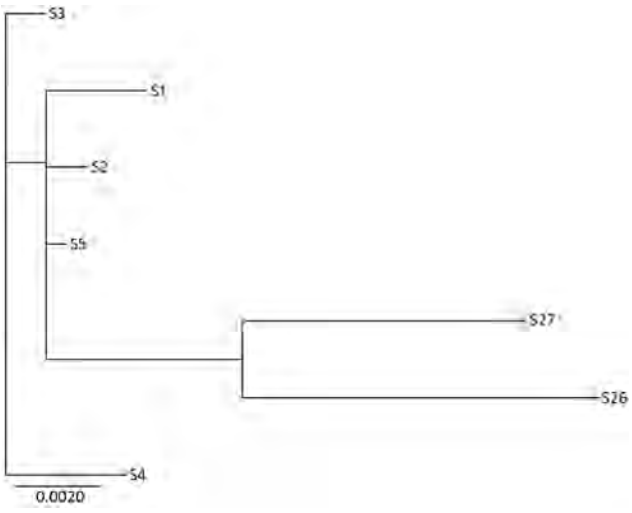

Figure 3. Phylogenetic tree of 7 sequence type 34 *Klebsiella pneumoniae* isolates tested during phenotypic and genotypic characterization of *Enterobacteriaceae* producing oxacillinase-48–like carbapenemases, United States. Genetic diversity ranged from 1 to 33 high-quality single-nucleotide polymorphisms that were called in an ≈5 Mb core genome, which equals ≈90% of the reference genome size (isolate 1 sequenced by using Pacific Biosciences [Menlo Park, CA, USA] technology). Scale bar indicates nucleotide substitutions per site.

This study had several limitations. The collection of isolates in this study might not be representative of all isolates with $bla_{\text{OXA-48}}$–like genes in the United States. There is also a reporting bias because only isolates sent to CDC were included. CDC receives isolates as part of outbreak investigations, surveillance studies, and to confirm AST results, but there is no national requirement to submit carbapenemase-producing isolates. Thus, unusually resistant isolates are more likely to be sent to the CDC and included in this study. Also, no prevalence rates of *Enterobacteriaceae* with $bla_{\text{OXA-48}}$–like genes in the United States can be inferred because there is not an evaluable denominator. In addition, almost all the isolates we studied were clinical isolates; colonizing isolates might have different phenotypic characteristics.

Another limitation is that the 10 isolates selected for the transformation experiment and the 3 isolates selected for Pacific Biosciences sequencing might not have been representative of the other isolates in this collection. Ideally, all isolates would have been sequenced by using Pacific Biosciences technology and been a part of the transformation experiment, but this testing was not performed because of limited resources. In addition, the decisions regarding which isolates to select for transformation experiments and sequencing by using Pacific Biosciences technology were made before WGS was complete. In retrospect, it would have been better to select $bla_{\text{OXA-181}}$ isolates that were hypothesized to be on a plasmid for the transformation experiment; instead, chromosomal $bla_{\text{OXA-181}}$ isolates were selected. Thus, the $bla_{\text{OXA-181}}$ gene loci for the isolates in this study are inconclusive.

In summary, the continued increase of CRE in the United States is a major problem, and the increasing prevalence of OXA-48–like carbapenemases is also concerning. We found *Enterobacteriaceae* in the United States with $bla_{\text{OXA-48}}$–like genes on similar mobile genetic elements to those described elsewhere and that displayed relatively resistant AST profiles. The first step in continued detection of CRE producing these and other carbapenemases is identifying all carbapenem resistance among *Enterobacteriaceae*, including resistance to ertapenem. Future prospective investigations are needed to determine the true prevalence of OXA-48–like carbapenemases in the United States.

This study was supported by the Advanced Molecular Detection Program at CDC.

About the Author

Dr. Lutgring is an assistant professor of medicine at Emory University School of Medicine, Atlanta, GA. His primary research interest is the molecular mechanisms of antimicrobial resistance in gram-negative bacteria.

References

1. Gupta N, Limbago BM, Patel JB, Kallen AJ. Carbapenem-resistant *Enterobacteriaceae*: epidemiology and prevention. Clin Infect Dis. 2011;53:60–7. http://dx.doi.org/10.1093/cid/cir202
2. Centers for Disease Control and Prevention. Vital signs: carbapenem-resistant Enterobacteriaceae. MMWR Morb Mortal Wkly Rep. 2013;62:165–70.
3. Patel G, Huprikar S, Factor SH, Jenkins SG, Calfee DP. Outcomes of carbapenem-resistant *Klebsiella pneumoniae* infection and the impact of antimicrobial and adjunctive therapies. Infect Control Hosp Epidemiol. 2008;29:1099–106. http://dx.doi.org/10.1086/592412
4. Walther-Rasmussen J, Høiby N. Class A carbapenemases. J Antimicrob Chemother. 2007;60:470–82. http://dx.doi.org/10.1093/jac/dkm226
5. Guh AY, Bulens SN, Mu Y, Jacob JT, Reno J, Scott J, et al. Epidemiology of carbapenem-resistant Enterobacteriaceae in 7 US communities, 2012–2013. JAMA. 2015;314:1479–87. http://dx.doi.org/10.1001/jama.2015.12480
6. Lascols C, Peirano G, Hackel M, Laupland KB, Pitout JD. Surveillance and molecular epidemiology of *Klebsiella pneumoniae* isolates that produce carbapenemases: first report of OXA-48-like enzymes in North America. Antimicrob Agents Chemother. 2013;57:130–6. http://dx.doi.org/10.1128/AAC.01686-12
7. Mathers AJ, Hazen KC, Carroll J, Yeh AJ, Cox HL, Bonomo RA, et al. First clinical cases of OXA-48-producing carbapenem-resistant *Klebsiella pneumoniae* in the United States: the "menace" arrives in the new world. J Clin Microbiol. 2013;51:680–3. http://dx.doi.org/10.1128/JCM.02580-12
8. Doi Y, O'Hara JA, Lando JF, Querry AM, Townsend BM, Pasculle AW, et al. Co-production of NDM-1 and OXA-232 by *Klebsiella pneumoniae.* Emerg Infect Dis. 2014;20:163–5. http://dx.doi.org/10.3201/eid2001.130904

9. Yang S, Hemarajata P, Hindler J, Li F, Adisetiyo H, Aldrovandi G, et al. Evolution and transmission of carbapenem-resistant *Klebsiella pneumoniae* expressing the $bla_{OXA-232}$ gene during an institutional outbreak associated with endoscopic retrograde cholangiopancreatography. Clin Infect Dis. 2017;64:894–901. http://dx.doi.org/10.1093/cid/ciw876
10. Rojas LJ, Hujer AM, Rudin SD, Wright MS, Domitrovic TN, Marshall SH, et al. NDM-5 and OXA-181 beta-lactamases, a significant threat continues to spread in the Americas. Antimicrob Agents Chemother. 2017;61:e00454–17. http://dx.doi.org/10.1128/AAC.00454-17
11. Poirel L, Héritier C, Tolün V, Nordmann P. Emergence of oxacillinase-mediated resistance to imipenem in *Klebsiella pneumoniae*. Antimicrob Agents Chemother. 2004;48:15–22. http://dx.doi.org/10.1128/AAC.48.1.15-22.2004
12. Poirel L, Potron A, Nordmann P. OXA-48-like carbapenemases: the phantom menace. J Antimicrob Chemother. 2012;67:1597–606. http://dx.doi.org/10.1093/jac/dks121
13. Oteo J, Hernández JM, Espasa M, Fleites A, Sáez D, Bautista V, et al. Emergence of OXA-48-producing *Klebsiella pneumoniae* and the novel carbapenemases OXA-244 and OXA-245 in Spain. J Antimicrob Chemother. 2013;68:317–21. http://dx.doi.org/10.1093/jac/dks383
14. Sampaio JL, Ribeiro VB, Campos JC, Rozales FP, Magagnin CM, Falci DR, et al. Detection of OXA-370, an OXA-48-related class D β-lactamase, in *Enterobacter hormaechei* from Brazil. Antimicrob Agents Chemother. 2014;58:3566–7. http://dx.doi.org/10.1128/AAC.02510-13
15. Meunier D, Vickers A, Pike R, Hill RL, Woodford N, Hopkins KL. Evaluation of the K-SeT R.E.S.I.S.T. immunochromatographic assay for the rapid detection of KPC and OXA-48-like carbapenemases. J Antimicrob Chemother. 2016;71:2357–9. http://dx.doi.org/10.1093/jac/dkw113
16. Pasteran F, Denorme L, Ote I, Gomez S, De Belder D, Glupczynski Y, et al. Rapid identification of OXA-48 and OXA-163 subfamilies in carbapenem-resistant gram-negative bacilli with a novel immunochromatographic lateral flow assay. J Clin Microbiol. 2016;54:2832–6. http://dx.doi.org/10.1128/JCM.01175-16
17. Dortet L, Naas T. Noncarbapenemase OXA-48 variants (OXA-163 and OXA-405) falsely detected as carbapenemases by the β Carba test. J Clin Microbiol. 2017;55:654–5. http://dx.doi.org/10.1128/JCM.02086-16
18. Gomez S, Pasteran F, Faccone D, Bettiol M, Veliz O, De Belder D, et al. Intrapatient emergence of OXA-247: a novel carbapenemase found in a patient previously infected with OXA-163-producing *Klebsiella pneumoniae*. Clin Microbiol Infect. 2013;19:E233–5. http://dx.doi.org/10.1111/1469-0691.12142
19. Lyman M, Walters M, Lonsway D, Rasheed K, Limbago B, Kallen A. Notes from the field: carbapenem-resistant Enterobacteriaceae producing OXA-48-like carbapenemases—United States, 2010–2015. MMWR Morb Mortal Wkly Rep. 2015;64:1315–6. http://dx.doi.org/10.15585/mmwr.mm6447a3
20. Lascols C, Bonaparte S, Lonsway D, Johnson K, Robinson G, Rasheed K, et al. Snapshot of beta-lactam resistance in *Enterobacteriaceae* in the United States. Poster 1051. In: Abstracts of the 25th European Congress of Clinical Microbiology and Infectious Diseases, Copenhagen, Denmark, April 25–28, 2015. Abstract 1051 [cited 2018 Jan 26] https://www.escmid.org/dates_events/calendar/calendar_event/cal/2015/04/25/event/tx_cal_phpicalendar/25th_European_Congress_of_Clinical_Microbriology_and_Infectious_Diseases_ECCMID_2015/?tx_cal_controller%5Blastview%5D=view-search_event%7Cpage_id-130&cHash=fc21e6af2b4d39892216b2e8d30f0936
21. Clinical and Laboratory Standards Institute. Methods for dilution antimicrobial susceptibility tests for bacteria that grow aerobically: approved standard. 10th ed. (M07-A10). Wayne (PA): The Institute; 2015.
22. Clinical and Laboratory Standards Institute. Performance standards for antimicrobial susceptibility testing: twenty-seventh informational supplement. (M100-S27). Wayne (PA): The Institute; 2017.
23. Conrad S, Oethinger M, Kaifel K, Klotz G, Marre R, Kern WV. *gyrA* mutations in high-level fluoroquinolone-resistant clinical isolates of *Escherichia coli*. J Antimicrob Chemother. 1996;38:443–55. http://dx.doi.org/10.1093/jac/38.3.443
24. Kitchel B, Zhu W, Travis T, Limbago BM, Rasheed JK. Detection and evaluation of OXA-48 like carbapenemases by real-time PCR. Poster D-1139. In: Abstracts of the 53rd Interscience Conference on Antimicrobial Agents and Chemotherapy, Denver, Colorado, September 10–13, 2013 cited 2018 Jan 26]. https://www.medscape.com/viewcollection/32893
25. Cox MP, Peterson DA, Biggs PJ, Solexa QA. SolexaQA: at-a-glance quality assessment of Illumina second-generation sequencing data. BMC Bioinformatics. 2010;11:485. http://dx.doi.org/10.1186/1471-2105-11-485
26. Bankevich A, Nurk S, Antipov D, Gurevich AA, Dvorkin M, Kulikov AS, et al. SPAdes: a new genome assembly algorithm and its applications to single-cell sequencing. J Comput Biol. 2012;19:455–77. http://dx.doi.org/10.1089/cmb.2012.0021
27. Li H, Durbin R. Fast and accurate long-read alignment with Burrows-Wheeler transform. Bioinformatics. 2010;26:589–95. http://dx.doi.org/10.1093/bioinformatics/btp698
28. Chin CS, Alexander DH, Marks P, Klammer AA, Drake J, Heiner C, et al. Nonhybrid, finished microbial genome assemblies from long-read SMRT sequencing data. Nat Methods. 2013;10:563–9. http://dx.doi.org/10.1038/nmeth.2474
29. Inouye M, Dashnow H, Raven LA, Schultz MB, Pope BJ, Tomita T, et al. SRST2: Rapid genomic surveillance for public health and hospital microbiology labs. Genome Med. 2014;6:90. http://dx.doi.org/10.1186/s13073-014-0090-6
30. de Man TJ, Limbago BM. SSTAR: a stand-alone easy-to-use antimicrobial resistance gene predictor. mSphere. 2016;1:pii: e00050-25. http://dx.doi.org/10.1128/mSphere.00050-15 PMID: 27303709.
31. Gupta SK, Padmanabhan BR, Diene SM, Lopez-Rojas R, Kempf M, Landraud L, et al. ARG-ANNOT, a new bioinformatic tool to discover antibiotic resistance genes in bacterial genomes. Antimicrob Agents Chemother. 2014;58:212–20. http://dx.doi.org/10.1128/AAC.01310-13
32. Zankari E, Hasman H, Cosentino S, Vestergaard M, Rasmussen S, Lund O, et al. Identification of acquired antimicrobial resistance genes. J Antimicrob Chemother. 2012;67:2640–4. http://dx.doi.org/10.1093/jac/dks261
33. Carattoli A, Zankari E, García-Fernández A, Voldby Larsen M, Lund O, Villa L, et al. In silico detection and typing of plasmids using PlasmidFinder and plasmid multilocus sequence typing. Antimicrob Agents Chemother. 2014;58:3895–903. http://dx.doi.org/10.1128/AAC.02412-14
34. Siguier P, Perochon J, Lestrade L, Mahillon J, Chandler M. ISfinder: the reference centre for bacterial insertion sequences. Nucleic Acids Res. 2006;34:D32–6. http://dx.doi.org/10.1093/nar/gkj014
35. Potron A, Nordmann P, Rondinaud E, Jaureguy F, Poirel L. A mosaic transposon encoding OXA-48 and CTX-M-15: towards pan-resistance. J Antimicrob Chemother. 2013;68:476–7. http://dx.doi.org/10.1093/jac/dks397
36. Altschul SF, Gish W, Miller W, Myers EW, Lipman DJ. Basic local alignment search tool. J Mol Biol. 1990;215:403–10. http://dx.doi.org/10.1016/S0022-2836(05)80360-2
37. Stamatakis A. RAxML version 8: a tool for phylogenetic analysis and post-analysis of large phylogenies. Bioinformatics. 2014;30:1312–3. http://dx.doi.org/10.1093/bioinformatics/btu033

38. Durfee T, Nelson R, Baldwin S, Plunkett G III, Burland V, Mau B, et al. The complete genome sequence of *Escherichia coli* DH10B: insights into the biology of a laboratory workhorse. J Bacteriol. 2008;190:2597–606. http://dx.doi.org/10.1128/JB.01695-07
39. Langmead B, Salzberg SL. Fast gapped-read alignment with Bowtie 2. Nat Methods. 2012;9:357–9. http://dx.doi.org/10.1038/nmeth.1923
40. Karim A, Poirel L, Nagarajan S, Nordmann P. Plasmid-mediated extended-spectrum beta-lactamase (CTX-M-3 like) from India and gene association with insertion sequence ISEcp1. FEMS Microbiol Lett. 2001;201:237–41.
41. McGann P, Snesrud E, Ong AC, Appalla L, Koren M, Kwak YI, et al. War wound treatment complications due to transfer of an IncN plasmid harboring $bla_{OXA-181}$ from *Morganella morganii* to CTX-M-27-producing sequence type 131 *Escherichia coli*. Antimicrob Agents Chemother. 2015;59:3556–62. http://dx.doi.org/10.1128/AAC.04442-14
42. Potron A, Nordmann P, Lafeuille E, Al Maskari Z, Al Rashdi F, Poirel L. Characterization of OXA-181, a carbapenem-hydrolyzing class D beta-lactamase from *Klebsiella pneumoniae*. Antimicrob Agents Chemother. 2011;55:4896–9. http://dx.doi.org/10.1128/AAC.00481-11
43. Potron A, Rondinaud E, Poirel L, Belmonte O, Boyer S, Camiade S, et al. Genetic and biochemical characterisation of OXA-232, a carbapenem-hydrolysing class D β-lactamase from Enterobacteriaceae. Int J Antimicrob Agents. 2013;41:325–9. http://dx.doi.org/10.1016/j.ijantimicag.2012.11.007
44. Chen L, Al Laham N, Chavda KD, Mediavilla JR, Jacobs MR, Bonomo RA, et al. First report of an OXA-48-producing multidrug-resistant *Proteus mirabilis* strain from Gaza, Palestine. Antimicrob Agents Chemother. 2015;59:4305–7. http://dx.doi.org/10.1128/AAC.00565-15
45. Papagiannitsis CC, Študentová V, Izdebski R, Oikonomou O, Pfeifer Y, Petinaki E, et al. Matrix-assisted laser desorption ionization-time of flight mass spectrometry meropenem hydrolysis assay with NH4HCO3, a reliable tool for direct detection of carbapenemase activity. J Clin Microbiol. 2015;53:1731–5. http://dx.doi.org/10.1128/JCM.03094-14
46. Tijet N, Boyd D, Patel SN, Mulvey MR, Melano RG. Evaluation of the Carba NP test for rapid detection of carbapenemase-producing *Enterobacteriaceae* and *Pseudomonas aeruginosa*. Antimicrob Agents Chemother. 2013;57:4578–80. http://dx.doi.org/10.1128/AAC.00878-13
47. Chea N, Bulens SN, Kongphet-Tran T, Lynfield R, Shaw KM, Vagnone PS, et al. Improved phenotype-based definition for identifying carbapenemase producers among carbapenem-resistant *Enterobacteriaceae*. Emerg Infect Dis. 2015;21:1611–6. http://dx.doi.org/10.3201/eid2109.150198
48. Carrër A, Poirel L, Eraksoy H, Cagatay AA, Badur S, Nordmann P. Spread of OXA-48-positive carbapenem-resistant *Klebsiella pneumoniae* isolates in Istanbul, Turkey. Antimicrob Agents Chemother. 2008;52:2950–4. http://dx.doi.org/10.1128/AAC.01672-07
49. Poirel L, Bonnin RA, Nordmann P. Genetic features of the widespread plasmid coding for the carbapenemase OXA-48. Antimicrob Agents Chemother. 2012;56:559–62. http://dx.doi.org/10.1128/AAC.05289-11
50. Villa L, Carattoli A, Nordmann P, Carta C, Poirel L. Complete sequence of the IncT-type plasmid pT-OXA-181 carrying the blaOXA-181 carbapenemase gene from *Citrobacter freundii*. Antimicrob Agents Chemother. 2013;57:1965–7. http://dx.doi.org/10.1128/AAC.01297-12

Address for correspondence: Joseph D. Lutgring, Department of Medicine, Division of Infectious Diseases, Emory University School of Medicine, 1648 Pierce Dr NE, Atlanta, GA 30307, USA; email: joseph.lutgring@emory.edu

etymologia

TEM

Joaquim Ruiz

In 1965, the transferability of ampicillin resistance was reported, and the plasmid-encoded mechanism of resistance for 2 *Salmonella* sp. isolates from the United Kingdom and 1 *Escherichia coli* isolate from Greece was determined. Resistance (R) factors from *Salmonella* sp. isolates were designated R1818 and R7268 (R7268 encoding the current TEM-1). The *E. coli* isolate and its plasmid were named TEM (encoding the current TEM-2) because the isolate was recovered from a feces culture of an Athenian patient named Temoniera in 1963.

β-lactam resistance is a problem worldwide; >2,000 β-lactamases are currently identified. Of these β-lactamases, >200 enzymes are classified within TEM family, including extended-spectrum β-lactamases (ESBLs). However, the original TEM-1 and TEM-2 hydrolyze only penicillin derivatives.

Sources

1. Ambler RP, Scott GK. Partial amino acid sequence of penicillinase coded by *Escherichia coli* plasmid R6K. Proc Natl Acad Sci U S A. 1978;75:3732–6. http://dx.doi.org/10.1073/pnas.75.8.3732
2. Anderson ES, Datta N. Resistance to penicillins and its transfer in *Enterobacteriaceae*. Lancet. 1965;1:407–9. http://dx.doi.org/10.1016/S0140-6736(65)90004-8
3. Bonomo RA. β-lactamases: a focus on current challenges. Cold Spring Harb Perspect Med. 2017;7:a025239. http://dx.doi.org/10.1101/cshperspect.a025239
4. Bush K, Jacoby GA, Medeiros AA. A functional classification scheme for beta-lactamases and its correlation with molecular structure. Antimicrob Agents Chemother. 1995;39:1211–33. http://dx.doi.org/10.1128/AAC.39.6.1211
5. Datta N, Kontomichalou P. Penicillinase synthesis controlled by infectious R factors in *Enterobacteriaceae*. Nature. 1965;208:239–41. http://dx.doi.org/10.1038/208239a0
6. Kontomichalou P. Studies on resistance transfer factors. Pathol Microbiol (Basel). 1967;30:71–93.
7. Medeiros AA. β-lactamases. Br Med Bull. 1984;40:18–27. http://dx.doi.org/10.1093/oxfordjournals.bmb.a071942
8. Sutcliffe JG. Nucleotide sequence of the ampicillin resistance gene of *Escherichia coli* plasmid pBR322. Proc Natl Acad Sci U S A. 1978;75:3737–41. http://dx.doi.org/10.1073/pnas.75.8.3737

Address for correspondence: Joaquim Ruiz, PO Box 16, 08214 Badia del Valles, Spain; email: joruiz.trabajo@gmail.com

DOI: https://doi.org/10.3201/eid2404.ET2404

Bacterial Infections in Neonates, Madagascar, 2012–2014

Bich-Tram Huynh, Elsa Kermorvant-Duchemin, Perlinot Herindrainy, Michael Padget, Feno Manitra Jacob Rakotoarimanana, Herisoa Feno, Elisoa Hariniaina-Ratsima, Tanjona Raheliarivao, Awa Ndir, Sophie Goyet, Patrice Piola, Frederique Randrianirina, Benoit Garin, Jean-Marc Collard, Didier Guillemot, Elisabeth Delarocque-Astagneau[1]

Severe bacterial infections are a leading cause of death among neonates in low-income countries, which harbor several factors leading to emergence and spread of multidrug-resistant bacteria. Low-income countries should prioritize interventions to decrease neonatal infections; however, data are scarce, specifically from the community. To assess incidence, etiologies, and antimicrobial drug–resistance patterns of neonatal infections, during 2012–2014, we conducted a community-based prospective investigation of 981 newborns in rural and urban areas of Madagascar. The incidence of culture-confirmed severe neonatal infections was high: 17.7 cases/1,000 live births. Most (75%) occurred during the first week of life. The most common (81%) bacteria isolated were gram-negative. The incidence rate for multidrug-resistant neonatal infection was 7.7 cases/1,000 live births. In Madagascar, interventions to improve prevention, early diagnosis, and management of bacterial infections in neonates should be prioritized.

Most deaths of children <5 years of age (6.3 million in 2013) still occur in low-income countries; a leading cause is infectious disease (*1*). In these countries, deaths of neonates are particularly concerning; in 2013, there were 20 deaths/1,000 live births, 23% directly attributable to severe infections (*1*–*3*). Each year in low-income countries, 7 million possible (clinical signs with no bacteriological documentation) severe neonatal bacterial infections occur (*4*,*5*). In these countries, multiple factors lead to enhanced emergence and spread of drug-resistant bacteria (e.g., antimicrobial drug misuse, poor quality or counterfeit drugs, and substandard hygiene and living conditions) (*6*,*7*). This phenomenon involves gram-positive (*Staphylococcus aureus* and *Streptococcus pneumoniae*) and gram-negative (*Haemophilus influenzae*, *Enterobacteriaceae*) bacteria (*8*). These pathogens, especially those acquired in hospitals, are becoming increasingly resistant to multiple drugs; for most populations in these settings, the antimicrobial drugs required to treat these infections are not affordable (*9*).

Because few data on the burden of invasive bacterial infections and resistance patterns in low-income countries are available, we do not have an accurate picture of their true burden among the youngest children. Indeed, most studies of antimicrobial drug resistance in neonates were conducted >10 years ago. Data about antimicrobial drug resistance were sparse and often relied on few isolates; no clear conclusions have been made with regard to *Enterobacteriaceae* resistance to third-generation cephalosporins (6%–97% of infections) or methicillin resistance among *S. aureus* (0–67%) (*10*,*11*). Moreover, data regarding infections occurring in the community, which may differ from those in hospitalized persons, are especially lacking. To our knowledge, incidence rates for severe resistant infections in neonates have not been estimated (*10*,*11*).

In low-income countries, investment and mobilization to control neonatal infections and antimicrobial drug resistance remain extremely low. As long as the real burden of these events remains unknown, the scope for public health decision-making will be limited (*10*,*12*). Therefore, to assess incidence, etiologies, and antimicrobial drug–resistance patterns of neonatal infections, we conducted a prospective study of a cohort of 981 newborns enrolled at birth in rural and urban communities in Madagascar, one of the poorest countries in the world, where the mortality rate for neonates is high (*13*).

Methods

This study was part of the Bacterial Infections and Antimicrobial Drug Resistant Diseases among Young Children

Author affiliations: Institut Pasteur, Paris, France (B.-T. Huynh, M. Padget, D. Guillemot, E. Delarocque-Astagneau); Assistance Publique–Hôpitaux de Paris Hôpital Universitaire Necker-Enfants Malades and Université Paris Descartes, Paris (E. Kermorvant-Duchemin); Institut Pasteur de Madagascar, Antananarivo, Madagascar (P. Herindrainy, F.M.J. Rakotoarimanana, H. Feno, E. Hariniaina-Ratsima, T. Raheliarivao, P. Piola, F. Randrianirina, B. Garin, J.-M. Collard); Institut Pasteur de Dakar, Dakar, Senegal (A. Ndir); Institut Pasteur du Cambodge, Phnom Penh, Cambodia (S. Goyet)

DOI: https://doi.org/10.3201/eid2404.161977

[1]On behalf of the BIRDY project group. Members of the group are listed at the end of this article.

in Low-Income Countries (BIRDY project, http://www.birdyprogram.org). The BIRDY project investigates and responds to consequences of bacterial sepsis and antimicrobial drug resistance in children <2 years of age (protocol in online Technical Appendix, https://wwwnc.cdc.gov/EID/article/24/4/16-1977-Techapp1.pdf). The study was authorized by the Institut Pasteur in Paris and by the Ethics Committee in Madagascar. Informed consent was obtained for all participants.

Study Areas and Study Population

The study population included all neonates born in 3 districts (Avaradoha, Besarety, and Soavinadriana) of Antananarivo (the capital of Madagascar, with a catchment area population of 14,997 and 4,128 women of childbearing age) and those of the rural city of Moramanga (catchment area population of 17,159 and 3,795 women of childbearing age) (Figure 1). These areas were chosen because their populations, from poor to extremely poor, were representative of the general population.

Recruitment

Before Birth

We exhaustively identified pregnant women within the study areas during their routine third trimester antenatal visit and pre-enrolled those who met the following criteria: routine residence in the study area with no plan to move away during the follow-up period and no opposition to the research being conducted or to the collection of biological samples (online Technical Appendix). We actively monitored preincluded women to ensure enrollment of their neonates at birth. At the time of preinclusion or at delivery, a vaginal swab sample was collected from the pregnant women to detect group B *Streptococcus* (GBS).

At Birth

To ensure the exhaustiveness of live-birth recruitment, all newborns were eligible at birth, even if their mothers had not been pre-enrolled. Neonate inclusion criteria were similar to preinclusion criteria of pregnant women: neonates born to parents living in the study area with no plan to move during the follow-up period; those whose legal guardians were informed and had no objection to the study procedures and collection of biological samples; and those for whom written consent was obtained from at least 1 legal guardian.

We collected fecal samples from the mothers perinatally to test for extended-spectrum β-lactamase (ESBL)–producing *Enterobacteriaceae*. We also collected the mothers' sociodemographic, medical, and obstetric characteristics; delivery information; and the neonates' anthropometric measurements and Apgar scores.

Figure 1. Locations of Antananarivo and Moramanga in Madagascar.

The neonates were examined at birth, and risk factors for infection (online Technical Appendix) were assessed. The presence of risk factors for infection led immediately to collection of a placental biopsy sample and collection of gastric fluid (before the first feeding), deep auditory canal samples, and anal swab samples from the neonate to document perinatal bacterial colonization. We then referred neonates with suspected infection to a participating hospital for evaluation. When indicated, antimicrobial drugs were empirically administered according to the World Health Organization (WHO) criteria. For these neonates, we obtained blood samples and lumbar puncture samples (if indicated) beforehand (*14*).

Follow-Up Evaluations

We actively and prospectively followed up on all neonates during their first month of life. To detect early signs of

infection, we arranged for home visits to be conducted twice during the first week of life, beginning within 3 days after delivery. Routine checkups were then conducted weekly during the first month. We conducted active monitoring to minimize the number of missed or uncharacterized suspected infections and to obtain anthropometric measurements. Throughout follow-up, we asked mothers to contact an investigator whenever the child had a fever or showed signs suggestive of infection (online Technical Appendix). If that occurred, the child was evaluated by a physician. When indicated, we collected samples including blood cultures according to the protocol and recorded clinical presentation, final diagnosis, and collected samples.

We adapted clinical criteria for infection and flow charts for bacterial sampling from WHO recommendations (online Technical Appendix). Decisions regarding antimicrobial drug treatments were left to the attending physicians to decide according to local protocols.

Bacteriology Analyses

All samples were transported within hours to Institut Pasteur in Madagascar for analysis. Specimen sampling, bacterial isolation, and species identification were performed according to the procedures recommended by the French Society for Microbiology (*15*). Antimicrobial susceptibilities were determined by use of the disk-diffusion method, according to the recommendations of the French Society for Microbiology (online Technical Appendix) (*15*). Suspected ESBL-producing *Enterobacteriaciae* were confirmed by use of the double-disk synergy test. *Escherichia coli* ATCC 25922 was used for quality control strains.

Classification Procedures

All cases for whom clinical or biological criteria for bacterial infection occurred during the neonatal period (including biological markers of infection based on C-reactive protein or complete blood count when available) were reviewed by an epidemiologist, a neonatologist, and a microbiologist to classify them and exclude nonsevere cases and contaminants. We defined severe bacterial infection as 1) presence of clinical signs of sepsis according to the WHO guidelines (online Technical Appendix) and 2) a positive culture from blood or cerebrospinal fluid or urine (bacterial and leukocyte counts $\geq 10^5$ and 10^4, respectively) or umbilical purulent discharge in case of omphalitis-associated sepsis. We defined 3 periods: very early (0–3 days), early (0–6 days), and late (7–30 days). We considered multidrug-resistant infections to be those caused by pathogens resistant to ≥1 agent in ≥3 antibacterial categories (*16*).

Statistical Analyses

For our analyses, we used Stata version 12 (StataCorp, LLC, College Station, TX, USA). We used descriptive statistics (e.g., proportions, means, and SDs) to summarize characteristics of mothers and neonates. We compared differences in proportions and means by using the χ^2 and Student *t* tests, respectively. $p<0.05$ was considered significant. We calculated the person-time (no. days followed until event [infection]) and then estimated the incidence of culture-confirmed severe neonatal infections per 1,000 live births. We calculated 95% CIs for all rates.

Results

Characteristics of Mothers and Neonates

From September 2012 through October 2014, we approached 1,030 pregnant women, of whom 54 refused to be included and 976 were enrolled (Table 1; Figure 2); of those included, 393 (40.3%) were from the urban site and 583 (59.7%) from the rural site. On average, the women were 26.1 years of age (range 14–48 years of age) and 33.7% were primigravidae. A total of 351 (37%) women gave birth at home. At delivery, 981 live neonates were included; mean ± SD birth weight was 2,952.6 ± 504.4 g; of these neonates, 161 (16%) were premature (<37 weeks' gestation).

Incidence of Neonatal Infections

A total of 16 neonates were classified as having culture-confirmed severe infection (online Technical Appendix). Of these, 12 (75%) infections occurred during the first week of life. The incidence rates were 17.7 (95% CI 10.8–28.9) culture-confirmed cases of severe neonatal infection and 13.3 (95% CI 7.5–23.4) culture-confirmed cases of early-onset severe neonatal infections per 1,000 live births. The incidence rates for culture-confirmed severe neonatal infections were 14.8 (95% CI 7.4–29.5)/1,000 live births in rural sites and 22.2 (95% CI 11.1–44.4)/1,000 live births in urban sites. The incidence rates for culture-confirmed severe neonatal infections were 15.6 (95% CI 7.0–34.6)/1,000 live births at home and 19.4 (95% CI 10.4–36.0)/1,000 live births at healthcare facilities. Final clinical diagnoses were sepsis for 13 and meningitis for 3 neonates.

Samples and Pathogens

We cultured 144 blood (including 65 [45.1%] at birth), 79 urine, and 7 cerebrospinal fluid samples from neonates with clinical signs of infection (Table 2). Among blood samples, results of 9 (6.3%) were positive and 8 (5.5%) others were considered to be contaminated. Among urine samples, results were positive for 39 (49.4%), of which 3 were associated with severe neonatal infection. One (14.3%) cerebrospinal fluid sample was culture-positive for *Pasteurella* spp., and 2 (28.6%) others grew gram-negative bacteria that could not be further identified. Gram-negative rods were detected in 13 (81.2%) samples from the 16 neonates

Table 1. Characteristics of mothers and neonates enrolled in study of bacterial infections in neonates, Antananarivo and Moramanga, Madagascar, 2012–2014

Characteristic	Urban site, no. (%)	Rural site, no. (%)	p value
Pregnant women*†			
Parity			
Primigravida	144 (37)	185 (32)	>0.99
Multigravida	249 (63)	398 (68)	
Education			
None or primary	119 (30)	145 (25)	<0.001
Partial secondary	171 (44)	334 (57)	
Completed secondary or university	103 (26)	104 (18)	
No. antenatal visits at enrollment			
0–1	45 (11)	47 (8)	0.01
2–4	239 (61)	408 (70)	
>4	109 (28)	128 (22)	
Neonates‡			
M	215 (55)	277 (47)	0.03
F	179 (45)	310 (53)	
Premature, <37 wk of gestation	77 (19)	84 (14)	0.6
Risk factors for infection at delivery			
Fetid amniotic fluid	39 (9.9)	42 (7.1)	0.13
Prolonged membrane rupture	13 (3.3)	15 (2.6)	
Maternal fever at delivery	5 (1.2)	9 (1.5)	
Difficult birth	25 (6.3)	56 (9.5)	

*Mean (± SD, minimum–maximum) age of urban mothers 25.8 (6.7, 14.3–43.5) years and of rural mothers 26.2 (6.5, 14.3–48.1) years; p = 0.4.
†Total = 976 pregnant women (393 urban and 583 rural), including 17 who had twin pregnancies and 12 who had stillbirths.
‡Total = 981 (394 urban and 587 rural). Mean (± SD) weights of 954 neonates at delivery were 2,921 (±515.9) g for urban and 2,973 (± 495.7) g for rural sites; p = 0.12.

with culture-confirmed severe infections; the most prevalent pathogen was *Klebsiella* spp.

Antibacterial Resistance

Among the 11 samples with gram-negative rods that could be tested for antimicrobial drug susceptibility, more than half showed resistance to cefotaxime (6/10) and more than one third were resistant to gentamicin (4/10) and ciprofloxacin (4/11) (online Technical Appendix Table 2). Among the 14 isolates for which antimicrobial drug resistance data were available, 5 isolates were resistant to ciprofloxacin and 9 were resistant to co-trimoxazole. Of the 6 *Klebsiella* spp. isolates, 4 were ESBL producers. The isolated *Staphylococcus epidermidis* strain was resistant to methicillin.

A total of 11 isolates were resistant to ≥1 antimicrobial drug of the combination recommended by WHO for cases of neonatal sepsis (ampicillin and gentamicin); 4 were resistant to both drugs. The incidence rates for severe neonatal infection resistant to 1 drug recommended by WHO was 7.7 (95% CI 3.7–16.2) cases/1,000 live births and to both drugs was 4.4 (95% CI 1.6–11.7) cases/1,000 live births. Seven isolates were multidrug resistant, and the incidence rate for multidrug-resistant severe neonatal infection was 7.7 (95% CI 3.7–16.2) cases/1,000 live births.

Clinical Outcomes

In total, 19 neonates, including 2 sets of twins and 1 other twin, died during the follow-up period. Four died at home with no etiology documented, 3 deaths were the direct consequence of severe prematurity, 1 was caused by birth injury, and 1 was caused by neonatal tetanus. The 10 remaining infants who died showed clinical signs of severe infection; no blood cultures could be performed before death. Six neonates were premature. All deliveries took place in healthcare facilities, except for 1, which occurred at home. The mother of a pair of twins was positive for vaginal carriage of GBS. A total of 4 neonates received a combination of gentamicin and a third-generation cephalosporin, and 5 received penicillin in addition to the 2 other drugs. All neonatal deaths except 1 occurred in the first week of life. None of the 16 neonates with a culture-confirmed severe infection died.

Discussion

Incidence of culture-confirmed severe neonatal infections in a community-based cohort of neonates in Madagascar was high (17.7 cases/1,000 live births). These infections are usually difficult to document, especially where women frequently deliver their babies at home, because neonates may show few symptoms before the infections progress rapidly. By using active community recruitment and follow-up, we were able to identify severe neonatal bacterial infections, including those with very early onset. Also, performing blood cultures before initiating antimicrobial drug therapy increased the likelihood of identifying a pathogen.

In low-income countries, incidence estimates for severe neonatal infections are few and the available data are heterogeneous (*10*). On the basis of community recruitment, Darmstadt et al. estimated an incidence rate of confirmed severe neonatal infection of 2.9 (95% CI 1.9–4.2)/1,000 live births almost 10 years ago in Bangladesh; this rate is much lower than the one we found (*17*).

However, the findings of Darmstadt et al. may be underestimated because of delayed care seeking and a shorter active surveillance period.

Our incidence estimate is lower than the 44.8 early-onset infections/1,000 live births found by Turner et al. on the Thailand–Myanmar border; their estimate was based on a clinical definition of infections and was thus possibly overestimated (*18*). Also, our incidence risk (1.6%, 16/981) is lower than the pooled incidence risk for possible severe bacterial infection (7.6%) estimated by Seale et al. in a metaanalysis of 22 studies (*5*). However, the designs of the studies contributing to the Seale analysis varied widely. Our community-based study with pre-enrollment of pregnant women before delivery is likely to reflect a higher ascertainment.

The bacterial isolation rate in blood culture is low (≈10%) for infected neonates in high-income and low-income countries (*19*). Blood cultures require that trained staff collect these samples before any antimicrobial drug use is initiated. These practices are not routine in low-income countries, and some highly suspected infections could not be bacteriologically confirmed, even in the setting of our research protocol, which included continuous training. However elevated, the incidence rate of confirmed severe infections may therefore be underestimated in our study.

As a comparison, in 2008, the United States reported 0.77 early-onset infections/1,000 live births (*20*). Although most studies in high-resource settings focus on the early neonatal period and are not population based, our results clearly suggest a much higher burden of neonatal infections in Madagascar than in high-income countries.

Most (75%) neonatal infections occurred during the first week after birth, most during the first 3 days. This finding confirms that community-based active surveillance in the very early period of life is crucial for capturing infections in neonates (*4*). This result also points out the value of reinforcing interventions and research programs targeting the perinatal period.

Gram-negative bacteria were predominant; the most prevalent pathogen isolated was *Klebsiella* spp. In a review of studies reporting the etiology of serious bacterial infections in community settings, Zaidi et al. found that *Klebsiella* spp., *E. coli*, and *S. aureus* were the most prevalent bacteria isolated during the first week of life (*21–25*). In our study, *S. aureus* was not predominant. It is possible that healthcare workers caring for mothers and neonates in our study were more prone to use clean birth kits distributed by the BIRDY program and to follow good hygiene practices, potentially minimizing horizontal transmission of *S. aureus* to newborns.

The overall burden of GBS infection in the developing world is not clear; incidence ranges from 0.3 to 0.6 infections/1,000 live births (*26*). Our study identified no GBS infections. One possible explanation for this low incidence is that several early-onset GBS infections may have not been identified because of rapid death (*27*). However, this hypothesis is unlikely because we performed close and active surveillance directly after birth and no deaths occurred during the very short period between delivery and neonate enrollment. However, we cannot exclude the possibility that GBS might have been responsible for some cases of infection that could not be bacteriologically confirmed for neonates with clinical signs of sepsis, including some who died. In the context of GBS vaccine development, if confirmed, this low incidence may bring into question the potential cost-effectiveness of maternal vaccination in low-income countries.

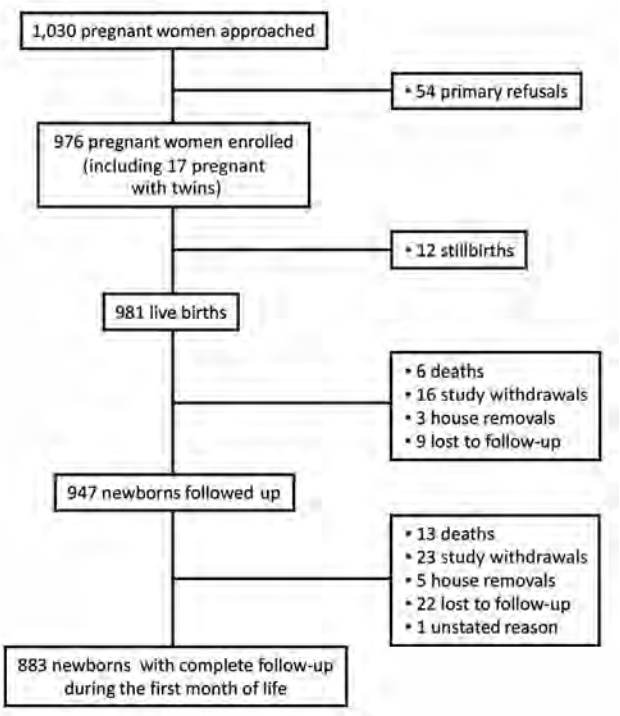

Figure 2. Flowchart for study of bacterial infections in neonates, Antananarivo and Moramanga, Madagascar, 2012–2014.

We found that the proportion of multidrug-resistant infections was significant (50%, 7/14); 28.6% (4/14) of *Enterobacteriaceae* were ESBL producers, and 1 of the 2 *Staphylococcus* spp. isolates was resistant to methicillin. One striking result of our study, however, is the relatively low incidence of antimicrobial drug–resistant infections (≈7.7 infections/1,000 live births). We found no carbapenemase-producing *Enterobacteriaceae*. In most published studies, assessment of antimicrobial drug resistance at the community level is based on the proportion of resistant infections at hospital admission, which may lead to biased conclusions because of variability in care access

Table 2. Pathogens isolated and characteristics of neonates with culture-confirmed severe infections, Antananarivo and Moramanga, Madagascar, 2012–2014*

Pathogen	No. isolates	Neonate age at infection, d				Sample type, no.	Place of birth		Premature		Site	
		0–3	4–6	7–13	14–30		Home	HCF	No	Yes	Urban	Rural
Gram-positive												
Staphylococcus aureus	1				1	Blood, 1	1			1	1	
S. epidermidis	1				1	Blood, 1	1			1	1	
Streptococcus pneumoniae	1				1	Blood, 1	1		1		1	
Gram-negative												
Klebsisella pneumoniae	4	1	3			Blood, 2; urine, 2	1	3	4		1	3
K. oxytoca	2	1	1			Blood, 1; urine, 1		2	2		2	
Escherichia coli	2	2				Blood, 2	1	1	1	1		2
Enterobacter cloacae	1	1				Blood, 1	1		1	1		1
Acinetobacter baumanii	1	1				Umbilical, 1		1	1			1
Pasteurella spp.	1				1	Spinal tap, 1		1	1			1
Gram-negative staining†	2	2				Spinal tap, 2		2	2	2		2

*HCF, healthcare facility.
†Pathogens identified by staining as gram-negative but could not be cultured and, therefore, were not further identified.

and case severity. Our results enabled a more complete picture of this issue and suggest that multidrug-resistant infections in the community may be less problematic than previously estimated.

Nevertheless, more than three quarters (11/14) of the pathogens we isolated were resistant to at least 1 antimicrobial drug recommended by WHO, including 4 isolates resistant to both recommended drugs (*14*). These findings are consistent with those of several studies conducted in hospital or community settings, which also highlight reduced susceptibility to at least 1 antimicrobial drug recommended for empirical treatment (resistance ranging from 43% to 97%) (*19*,*22*,*28*). In contrast, we observed that the most frequent attitude of physicians in Madagascar was to prescribe 3 antimicrobial drugs, including ampicillin, a third-generation cephalosporin, and gentamicin, when invasive bacterial neonatal infection was suspected. The use of large and unnecessarily broad-spectrum therapy may contribute to increased rates of antimicrobial drug resistance. The development of rapid diagnostic tests to identify pathogens and their antimicrobial drug susceptibility may therefore prevent unnecessary use of broad-spectrum antimicrobial drugs.

Our study has some limitations. We cannot exclude the possibility that 4 pathogens, including one ESBL-producing *Enterobacteriaceae*, which we documented in the community, might have been acquired in the hospital because the infections occurred after 48 hours in neonates born in a healthcare facility. However, no hospitalization during pregnancy was recorded for the mothers of any of these 4 neonates. Also, because the neonates were enrolled in a research study, their standard of care might have been higher, including better hand hygiene, than that for most of the population. This Hawthorne effect might have induced bias in our results, such as an underestimation of *Staphylococcus*-associated infections (*29*). We also probably changed the evolution of these severe bacterial infections by improving early diagnosis and providing better care. These actions might have helped avoid deaths of neonates, which would otherwise have occurred, and contributed to our underestimation of case-fatality ratio.

In conclusion, incidence of bacterial infections among neonates in a community-based cohort in Madagascar was high, although incidence of multidrug-resistant bacterial infections was relatively low. Most of these infections occurred during the first week of life. Our findings suggest that public health measures to decrease deaths from severe bacterial infection among neonates should focus on improving prevention, early diagnosis, and management of infections and prioritizing intervention strategies according to successes with vaccines, clean deliveries, and care of neonates. Current knowledge gaps, including those associated with local burden, bacterial etiology, and antimicrobial drug resistance profiles of severe bacterial infections in low-income countries, prevent us from having a clear picture of the situation. Recently, several international bodies called for global action to combat antimicrobial drug resistance, deemed a "global health security threat" (*11*,*30*). Although antimicrobial drug resistance is a real threat, more community data are clearly needed in countries with limited resources so they can select and prioritize effective preventive and treatment strategies to tackle bacterial infections in neonates.

Acknowledgments

We are grateful to all the mothers and their newborns for their participation. We thank all physicians, laboratory staff, field interviewers, and community workers for their involvement in this project.

We thank all collaborators of the BIRDY project: Laurence Borand, Thida Chon, Agathe De Lauzanne, Alexandra Kerleguer, Siyin Lach, Veronique Ngo, Arnaud Tarantola, Sok Touch, Zo Zafitsara Andrianirina, Muriel Vray, Vincent Richard, Abdoulaye Seck, Raymond Bercion, Amy Gassama Sow, Jean Baptiste Diouf, Pape Samba Dieye, Balla Sy, Bouya Ndao, Maud Seguy, and Laurence Watier.

This work was supported by the Department of International Cooperation of the Principality of Monaco.

About the Author

Dr. Huynh is a medical epidemiologist at Institut Pasteur. Her interests lie in applied public health research, and her main research topics focus on maternal and child health in low-income countries, specifically, the causes and consequences of malaria during pregnancy in sub-Saharan Africa, infections in neonates, and antimicrobial resistance in low-income countries.

References

1. UNICEF. Levels & trends in child mortality [cited 2014 Dec 31]. https://www.unicef.org/media/files/Levels_and_Trends_in_Child_Mortality_2014.pdf
2. Liu L, Oza S, Hogan D, Perin J, Rudan I, Lawn JE, et al. Global, regional, and national causes of child mortality in 2000–13, with projections to inform post-2015 priorities: an updated systematic analysis. Lancet. 2015;385:430–40. http://dx.doi.org/10.1016/S0140-6736(14)61698-6
3. Wang H, Naghavi M, Allen C, Barber RM, Bhutta ZA, Carter A, et al.; GBD 2015 Mortality and Causes of Death Collaborators. Global, regional, and national life expectancy, all-cause mortality, and cause-specific mortality for 249 causes of death, 1980–2015: a systematic analysis for the Global Burden of Disease Study 2015. Lancet. 2016;388:1459–544. http://dx.doi.org/10.1016/S0140-6736(16)31012-1
4. Lawn JE, Cousens S, Zupan J. 4 million neonatal deaths: when? Where? Why? Lancet (London, England). 2005;365:891–900. http://dx.doi.org/10.1016/S0140-6736(05)71048-5
5. Seale AC, Blencowe H, Manu AA, Nair H, Bahl R, Qazi SA, et al.; pSBI Investigator Group. Estimates of possible severe bacterial infection in neonates in sub-Saharan Africa, south Asia, and Latin America for 2012: a systematic review and meta-analysis. Lancet Infect Dis. 2014;14:731–41. http://dx.doi.org/10.1016/S1473-3099(14)70804-7
6. Kelesidis T, Kelesidis I, Rafailidis PI, Falagas ME. Counterfeit or substandard antimicrobial drugs: a review of the scientific evidence. J Antimicrob Chemother. 2007;60:214–36. http://dx.doi.org/10.1093/jac/dkm109
7. Okeke IN, Lamikanra A, Edelman R. Socioeconomic and behavioral factors leading to acquired bacterial resistance to antibiotics in developing countries. Emerg Infect Dis. 1999; 5:18–27. http://dx.doi.org/10.3201/eid0501.990103
8. Okeke IN, Laxminarayan R, Bhutta ZA, Duse AG, Jenkins P, O'Brien TF, et al. Antimicrobial resistance in developing countries. Part I: recent trends and current status. Lancet Infect Dis. 2005;5:481–93. http://dx.doi.org/10.1016/S1473-3099(05)70189-4
9. Laxminarayan R, Duse A, Wattal C, Zaidi AK, Wertheim HF, Sumpradit N, et al. Antibiotic resistance–the need for global solutions. Lancet Infect Dis. 2013;13:1057–98. http://dx.doi.org/10.1016/S1473-3099(13)70318-9
10. Huynh BT, Padget M, Garin B, Herindrainy P, Kermorvant-Duchemin E, Watier L, et al. Burden of bacterial resistance among neonatal infections in low income countries: how convincing is the epidemiological evidence? BMC Infect Dis. 2015;15:127. http://dx.doi.org/10.1186/s12879-015-0843-x
11. World Health Organization. Antimicrobial resistance, global report on surveillance [cited 2014 Dec 31]. http://apps.who.int/iris/bitstream/10665/112642/1/9789241564748_eng.pdf
12. Seale AC, Head MG, Fitchett EJ, Vergnano S, Saha SK, Heath PT, et al.; SPRING. Neonatal infection: a major burden with minimal funding. Lancet Glob Health. 2015;3:e669–70. http://dx.doi.org/10.1016/S2214-109X(15)00204-1
13. UNICEF/World Bank. Levels and trends in child mortality [cited 2014 Dec 31]. https://www.unicef.org/media/files/Levels_and_Trends_in_Child_Mortality_2014.pdf
14. World Health Organization. Pocket book of hospital care for children–guidelines for the management of common illnesses with limited resources [cited 2013 Dec 31]. http://apps.who.int/iris/bitstream/10665/81170/1/9789241548373_eng.pdf
15. French Society for Microbiology. Référentiel en microbiologie médicale. 5th edition. Paris: The Society; 2015.
16. Magiorakos AP, Srinivasan A, Carey RB, Carmeli Y, Falagas ME, Giske CG, et al. Multidrug-resistant, extensively drug-resistant and pandrug-resistant bacteria: an international expert proposal for interim standard definitions for acquired resistance. Clin Microbiol Infect. 2012;18:268–81.
17. Darmstadt GL, Saha SK, Choi Y, El Arifeen S, Ahmed NU, Bari S, et al.; Bangladesh Projahnmo-2 (Mirzapur) Study Group. Population-based incidence and etiology of community-acquired neonatal bacteremia in Mirzapur, Bangladesh: an observational study. J Infect Dis. 2009;200:906–15. http://dx.doi.org/10.1086/605473
18. Turner C, Turner P, Hoogenboom G, Aye Mya Thein N, McGready R, Phakaudom K, et al. A three year descriptive study of early onset neonatal sepsis in a refugee population on the Thailand Myanmar border. BMC Infect Dis. 2013;13:601. http://dx.doi.org/10.1186/1471-2334-13-601
19. Hamer DH, Darmstadt GL, Carlin JB, Zaidi AK, Yeboah-Antwi K, Saha SK, et al.; Young Infants Clinical Signs Study Group. Etiology of bacteremia in young infants in six countries. Pediatr Infect Dis J. 2015;34:e1–8. http://dx.doi.org/10.1097/INF.0000000000000549
20. Weston EJ, Pondo T, Lewis MM, Martell-Cleary P, Morin C, Jewell B, et al. The burden of invasive early-onset neonatal sepsis in the United States, 2005–2008. Pediatr Infect Dis J. 2011;30:937–41. http://dx.doi.org/10.1097/INF.0b013e318223bad2
21. Aiken AM, Mturi N, Njuguna P, Mohammed S, Berkley JA, Mwangi I, et al.; Kilifi Bacteraemia Surveillance Group. Risk and causes of paediatric hospital-acquired bacteraemia in Kilifi District Hospital, Kenya: a prospective cohort study. Lancet. 2011;378:2021–7. http://dx.doi.org/10.1016/S0140-6736(11)61622-X
22. Downie L, Armiento R, Subhi R, Kelly J, Clifford V, Duke T. Community-acquired neonatal and infant sepsis in developing countries: efficacy of WHO's currently recommended antibiotics—systematic review and meta-analysis. Arch Dis Child. 2013; 98:146–54. http://dx.doi.org/10.1136/archdischild-2012-302033
23. Seale AC, Mwaniki M, Newton CR, Berkley JA. Maternal and early onset neonatal bacterial sepsis: burden and strategies for prevention in sub-Saharan Africa. Lancet Infect Dis. 2009;9:428–38. http://dx.doi.org/10.1016/S1473-3099(09)70172-0
24. Vergnano S, Sharland M, Kazembe P, Mwansambo C, Heath PT. Neonatal sepsis: an international perspective. Arch Dis Child Fetal Neonatal Ed. 2005;90:F220–4. http://dx.doi.org/10.1136/adc.2002.022863
25. Zaidi AK, Thaver D, Ali SA, Khan TA. Pathogens associated with sepsis in newborns and young infants in developing countries.

Pediatr Infect Dis J. 2009;28(Suppl):S10–8. http://dx.doi.org/10.1097/INF.0b013e3181958769
26. Dagnew AF, Cunnington MC, Dube Q, Edwards MS, French N, Heyderman RS, et al. Variation in reported neonatal group B streptococcal disease incidence in developing countries. Clin Infect Dis. 2012;55:91–102. http://dx.doi.org/10.1093/cid/cis395
27. Edmond KM, Kortsalioudaki C, Scott S, Schrag SJ, Zaidi AK, Cousens S, et al. Group B streptococcal disease in infants aged younger than 3 months: systematic review and meta-analysis. Lancet. 2012;379:547–56. http://dx.doi.org/10.1016/S0140-6736(11)61651-6
28. Zaidi AK, Huskins WC, Thaver D, Bhutta ZA, Abbas Z, Goldmann DA. Hospital-acquired neonatal infections in developing countries. Lancet. 2005;365:1175–88. http://dx.doi.org/10.1016/S0140-6736(05)71881-X
29. McCambridge J, Witton J, Elbourne DR. Systematic review of the Hawthorne effect: new concepts are needed to study research participation effects. J Clin Epidemiol. 2014;67:267–77. http://dx.doi.org/10.1016/j.jclinepi.2013.08.015
30. The Review on Antimicrobial Resistance. Antimicrobial resistance: tackling a crisis for the health and wealth of nations [cited 2014 Dec 31]. https://amr-review.org/sites/default/files/AMR%20Review%20Paper%20-%20Tackling%20a%20crisis%20for%20the%20health%20and%20wealth%20of%20nations_1.pdf

Address for correspondence: Bich-Tram Huynh, Institut Pasteur, 25 Rue du Docteur Roux, Paris, Île-de-France 75015, France; email: bich-tram.huynh@pasteur.fr

Artemisinin-Resistant *Plasmodium falciparum* with High Survival Rates, Uganda, 2014–2016

Mie Ikeda, Megumi Kaneko, Shin-Ichiro Tachibana, Betty Balikagala, Miki Sakurai-Yatsushiro, Shouki Yatsushiro, Nobuyuki Takahashi, Masato Yamauchi, Makoto Sekihara, Muneaki Hashimoto,[1] Osbert T. Katuro,[2] Alex Olia,[3] Paul S. Obwoya, Mary A. Auma, Denis A. Anywar, Emmanuel I. Odongo-Aginya, Joseph Okello-Onen,[4] Makoto Hirai, Jun Ohashi, Nirianne M.Q. Palacpac, Masatoshi Kataoka, Takafumi Tsuboi, Eisaku Kimura, Toshihiro Horii, Toshihiro Mita

Because ≈90% of malaria cases occur in Africa, emergence of artemisinin-resistant *Plasmodium falciparum* in Africa poses a serious public health threat. To assess emergence of artemisinin-resistant parasites in Uganda during 2014–2016, we used the recently developed ex vivo ring-stage survival assay, which estimates ring-stage–specific *P. falciparum* susceptibility to artemisinin. We conducted 4 cross-sectional surveys to assess artemisinin sensitivity in Gulu, Uganda. Among 194 isolates, survival rates (ratio of viable drug-exposed parasites to drug-nonexposed controls) were high (≥10%) for 4 isolates. Similar rates have been closely associated with delayed parasite clearance after drug treatment and are considered to be a proxy for the artemisinin-resistant phenotype. Of these, the *PfKelch13* mutation was observed in only 1 isolate, A675V. Population genetics analysis suggested that these possibly artemisinin-resistant isolates originated in Africa. Large-scale surveillance of possibly artemisinin-resistant parasites in Africa would provide useful information about treatment outcomes and help regional malaria control.

Despite reports of decreasing incidence and deaths from malaria, this disease remains a global health problem; in 2016, an estimated 216 million new cases and 445,000 deaths occurred (*1*). One of the main causes for the reduction of the malaria burden is the global deployment of artemisinin-based combination therapies as a first-line treatment (*1*). However, since first reported in 2007–2008 (*2*), artemisinin-resistant *Plasmodium falciparum* parasites have spread into the Greater Mekong Subregion of Southeast Asia (*3*,*4*). In western Cambodia, recent increases in the prevalence of piperaquine-resistant parasites have further reduced effectiveness of dihydroartemisinin/piperaquine (*5*).

Until now, there was no clear evidence for the emergence of *P. falciparum* artemisinin-resistant isolates in Africa (*6*). The standard for monitoring the emergence of artemisinin resistance has been the effectiveness of artemisinin-based combination therapies. In high-transmission regions, as in many parts of Africa where most persons have some immunity to malaria, partially immune persons may, however, experience some response to drug treatment even if they are infected by drug-resistant parasites (*7*,*8*). Interpretations of drug effectiveness could also be made difficult with the widely used ex vivo conventional drug-susceptibility assay (*3*,*9*,*10*) because reduced susceptibility to artemisinin is limited to the very narrow early ring stage of the parasites (*10*–*12*).

The recently developed ring-stage survival assay (RSA) can evaluate ring-stage–specific reduction of artemisinin susceptibility (*12*). In this assay, ring-stage parasites are exposed to 700 nmol/L of dihydroartemisinin for 6 h and then cultured for 66 h in the absence of the drug.

Author affiliations: Juntendo University School of Medicine, Tokyo, Japan (M. Ikeda, M. Kaneko, S.-I. Tachibana, M. Yamauchi, M. Sekihara, M. Hashimoto, M. Hirai, T. Mita); Ehime University, Matsuyama, Japan (B. Balikagala, T. Tsuboi); Tokyo Women's Medical University, Tokyo (M. Sakurai-Yatsushiro, N. Takahashi); National Institute of Advanced Industrial Science and Technology, Kagawa, Japan (S. Yatsushiro, M. Kataoka); Med Biotech Laboratories, Kampala, Uganda (O.T. Katuro); Gulu University, Gulu, Uganda (A. Olia, D.A. Anywar, E.I. Odongo-Aginya, J. Okello-Onen); St. Mary's Hospital Lacor, Gulu (P.S. Obwoya, M.A. Auma); The University of Tokyo, Tokyo (J. Ohashi); Osaka University, Osaka, Japan (N.M.Q. Palacpac, E. Kimura, T. Horii)

DOI: https://doi.org/10.3201/eid2404.170141

[1]Current affiliation: National Institute of Advanced Industrial Science and Technology, Kagawa, Japan.

[2]Current affiliation: Mildmay Uganda-KAMPALA, Kampala, Uganda.

[3]Current affiliation: Gunma University, Gunma, Japan.

[4]Deceased.

Levels of artemisinin susceptibility are estimated according to the survival rate (i.e., the ratio of viable parasites exposed to 700 nmol/L dihydroartemisinin to parasites cultured simultaneously in drug-free medium). In a study of isolates from 31 persons in Cambodia, all isolates classified as artemisinin resistant by ex vivo conventional assay (having parasite clearance half-lives >5 h after artemisinin treatment [*4*,*13*]) also had an ex vivo survival rate >10% by RSA (*12*).

In Africa, few attempts have been made to detect artemisinin-resistant parasites by using ex vivo RSA. So far, only 2 studies have been reported, both of which showed the absence of *P. falciparum* isolates with survival rates ≥10% (*14*,*15*). Close monitoring is nevertheless valuable because parasites resistant to all widely used antimalarial drugs (chloroquine [*16*], pyrimethamine [*17*], and sulfadoxine [*18*]) have migrated from Southeast Asia to sub-Saharan Africa. Also reported in Africa is indigenous emergence of parasites, albeit all of minor lineages, resistant to these antimalarial drugs (*19*,*20*).

During 2014–2016, to assess artemisinin sensitivity in Gulu, northern Uganda, we performed 4 cross-sectional surveys. We evaluated the emergence of artemisinin resistance by using 3 methods: ex vivo RSA for dihydroartemisinin; conventional ex vivo drug susceptibility assay; and genotyping of *PfKelch13*, the gene responsible for artemisinin resistance in Southeast Asia (*21*–*24*).

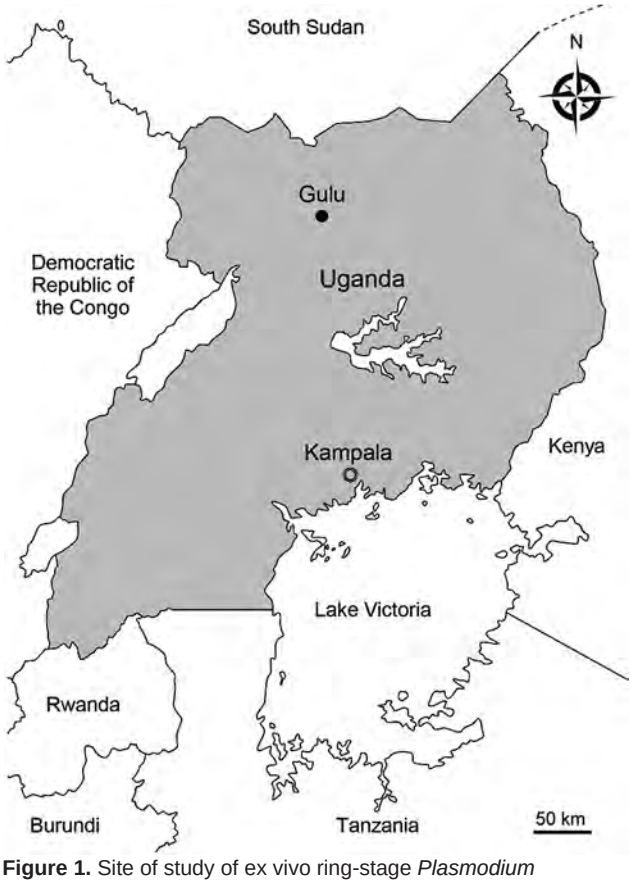

Figure 1. Site of study of ex vivo ring-stage *Plasmodium falciparum* survival rates, Gulu (black circle), northern Uganda, 2014–2016.

Materials and Methods

Study Site, Design, and Patients

During 2014–2016, we conducted 4 cross-sectional surveys in Gulu, northern Uganda (Figure 1). In this region, malaria transmission is high; estimated prevalence is ≈60%. Each year, weak seasonal fluctuation is observed; peaks occur in May and October. All 4 surveys were performed during peak malaria seasons: October–November 2014, May–June 2015, October–November 2015, and June–July 2016. The major mosquito vector in this region is *Anopheles funestus* (*25*), and the entomological inoculation rate was estimated at ≥100 infective mosquito bites/person/year (*26*). Since 2004, artemether/lumefantrine has been used as a first-line treatment for uncomplicated malaria (*27*). Persons who visited St. Mary's Hospital Lacor, Gulu, Uganda, with signs and symptoms suggestive of malaria were screened by microscopic examination of Giemsa-stained blood smears. We enrolled those with *P. falciparum* monoinfection (parasitemia ≥0.1%) if written informed consent was obtained from a parent/guardian (for patients <7 years of age), from a parent/guardian and from the patient (for patients 7–17 years of age), or from adult patients (≥18 years of age). Ethics approval for the study was obtained from the Lacor Hospital Institutional Research and Ethics Committee (LH 021/09/13), the Ugandan National Council for Science and Technology (HS 1395), and the institutional review board at Juntendo University in Tokyo, Japan (2014168).

Ex Vivo RSA

We performed the ex vivo RSA as described previously, with some modifications (*12*,*28*). In brief, 1 mL of venous blood was immediately transferred to the hospital laboratory. After plasma removal, erythrocyte pellets were washed 3 times in RPMI-1640 (Thermo Fisher Scientific, Waltham, MA, USA) with 100 μg/mL gentamicin. Washed infected erythrocytes were suspended in RPMI-1640, 25 mM HEPES (4-[2-hydroxyethyl]-1-piperazineethanesulfonic acid), 2 mM L-glutamine supplemented with 100 μg/mL gentamicin and heat-inactivated 10% serum type AB from Japanese volunteers, and stored at 4°C before initiation of the ex vivo RSA. All procedures were performed within 4 h after blood collection.

The next morning, 100 μL/well of parasite culture mixture adjusted to 2% hematocrit was dispensed with 700 nmol/L dihydroartemisinin (Tokyo Chemical Industry Co. Ltd, Tokyo, Japan). As nonexposed control, 0.1% DMSO (dimethyl sulfoxide) was used. Parasitemia >1%

was adjusted to 1% by adding uninfected O-type erythrocytes. Cultures were incubated in a gas atmosphere with 5% CO_2 and 5% O_2 by using the AnaeroPack malaria culture system (Mitsubishi Gas Chemical Co. Inc., Tokyo, Japan). After 6 h of exposure to dihydroartemisinin, pellets were washed 3 times in RPMI-1640 with gentamicin, resuspended in fresh culture medium, and incubated for another 66 h. Assays were performed in duplicate for all samples except those obtained October–November 2014 because of insufficient sample volume.

At the end of the culture period, by counting 20,000 erythrocytes and using thin blood smears, 2 investigators independently determined the number of viable parasites with normal morphologic appearance that developed into ring stages, trophozoites, and schizonts. Parasites that appeared pyknotic were considered to be dead (*28*,*29*). When the proportion of viable parasites in the nonexposed culture at 72 h was higher than the initial parasitemia at 0 h, the samples were considered to be interpretable (*29*). The investigators calculated survival rates as the ratios of parasites in exposed and nonexposed cultures (*12*); if the survival rates calculated by 2 researchers differed by >50%, a third researcher assessed the slides. Based on previous comparative studies of ex vivo RSA and in vivo drug susceptibility tests (*12*), the cutoff for a high survival rate by RSA was ≥10%. This cutoff has 89% sensitivity and 91% specificity in predicting parasites likely to have >5 h of clearance half-life after artemisinin treatment. As a reference for ex vivo RSA, we used laboratory-adapted artemisinin-susceptible (3D7) and artemisinin-resistant clones (MRA-1236 and MRA-1240) (*12*). The *P. falciparum* artemisinin-resistant strains IPC 3445 Pailin Cambodia 2010 (MRA-1236) and IPC 5202 Battanbang Cambodia 2011 (MRA-1240) were contributed by Didier Ménard and provided by the Malaria Research and Reference Reagent Resource Center (part of BEI Resources, National Institute of Allergy and Infectious Diseases, National Institutes of Health, Rockville, MD, USA).

Ex Vivo Conventional Drug-Susceptibility Assay

For each sample, 100 μL of parasite culture with parasitemia adjusted to 0.05% at 2.5% hematocrit was pipetted per well into predosed culture plates and incubated under the same conditions as the ex vivo RSA for 72 h. Wells A–H were dosed with 0 (control), 0.25, 0.5, 1, 2, 4, 8, or 16 nmol/L of dihydroartemisinin, respectively. Samples were then frozen (–20°C overnight) and thawed until complete hemolysis was obtained. We assessed parasite growth by using an ELISA that quantifies parasite histidine-rich protein 2, as reported previously (*30*). We established the effective concentration of dihydroartemisinin needed to inhibit growth of *P. falciparum* by 50% (IC_{50}) by nonlinear regression in the online ICEstimator software (http://www.antimalarial-icestimator.net) (*31*).

Genotyping

We extracted parasite DNA from blood-spotted filter paper (ET31CHR; Whatman Limited, Kent, UK) by using QIAcube (QIAGEN, Hilden, Germany). The sequence of 6 propeller domains in *PfKelch13* was determined as previously reported (*32*). From isolates showing high RSA rates of survival, we determined the following 6 mutations suggested as background genetic changes for artemisinin resistance as described (*32*,*33*): D193Y in ferredoxin (*fd*), T484I in multidrug resistance protein 2 (*mdr2*), V127M in apicoplast ribosomal protein S10 (*arps10*), I356T in chloroquine resistance transporter (*crt*), V1157L in protein phosphatase (*pph*), and C1484F in phosphoinositide-binding protein (*pibp*). Samples with minor peaks ≥50% the height of the major peak were considered mixed genotypes.

Whole-Genome Sequencing and Variant Detection

For 3 isolates with high survival rates by RSA, we extracted genomic DNA from leukocyte-removed blood with Acrodisc filters (Pall Corporation, New York, NY, USA) by using a QIAamp DNA Blood Mini Kit (QIAGEN). We prepared DNA libraries by using a TruSeq DNA PCR-Free Library Preparation Kit (Illumina, San Diego, CA, USA) after amplification of the genomic DNA with an Illustra GenomiPhi DNA Amplification Kit (GE Healthcare, Chicago, IL, USA) or without genome amplification with a Nextera XT DNA Sample Prep Kit (Illumina). We obtained ≈1–1.5 Gb of data per sample, consisting of paired-end reads 100 or 150 bp long by using Illumina instruments (Miseq and Hiseq2000). Data are available at the DDBJ Sequence Read Archive (http://trace.ddbj.nig.ac.jp/dra/index.html) under accession nos. DRA005346, DRA005347, and DRA005348.

For comparative analyses, we obtained raw sequence data (fastq files) of 31 *P. falciparum* isolates from various regions in Asia (n = 19) and Africa (n = 12) from the Short Read Archive at the National Center for Biotechnology Information (https://www.ncbi.nlm.nih.gov/sra) (online Technical Appendix Table 1, https://wwwnc.cdc.gov/EID/article/24/4/17-0141-Techapp1.pdf). Among 19 isolates from Asia, 6 harbored mutant alleles in *PfKelch13*. We mapped all short-read data onto the 3D7 reference genome (National Center for Biotechnology Information BioProject ID PRJNA148) by using CLC Genomics Workbench software (QIAGEN) with default parameters. We then used the resulting files for detecting single-nucleotide polymorphisms (SNPs) by using the Basic Variant Detection program in CLC Genomics Workbench. SNPs were called at all genomic positions with >80% frequency of >10 reads support.

Population Genetic Analyses

To clarify lineages of isolates exhibiting high rates of survival according to RSA, we performed principal component analysis and STRUCTURE analysis (*34*). SNPs with minor allele frequency >25% were used after standardization. For principal component analysis, we used BellCurve for Excel (Social Survey Research Information Co., Ltd, Tokyo, Japan). We used STRUCTURE 2.3.3 to assign individual isolates from all populations to 2 clusters (i.e., K = 2). For each run, a burn-in period of 10,000 steps was followed by 10,000 iterations under the admixture model and the assumption of uncorrelated haplotype frequencies among populations.

Results

Ex Vivo RSA

In the ex vivo RSA study, we enrolled 249 patients (Table 1). Most patients were children; median age was 3 years. Fever ≥37.5°C was reported for 83% of patients. Other signs and symptoms were present for 7%–22% of enrolled patients. Examination of blood smears and species-specific PCR revealed that all blood samples contained monoinfections with *P. falciparum*.

We obtained successful ex vivo RSA results for dihydroartemisinin for 194 (77.9%) patients. Unsuccessful results were mostly caused by insufficient parasite growth (n = 28) or inability to count 20,000 erythrocytes because of low-quality blood smears and limited amounts of blood (n = 27). We found no significant differences for patient background characteristics or parasitemia in all enrolled and ex vivo RSA–successful patients (Table 1; online Technical Appendix Table 2). Artemisinin-susceptible laboratory clone 3D7 showed no parasites at 700 nmol/L, whereas artemisinin-resistant laboratory clones MRA-1236 and MRA-1240 showed survival rates (± SEM) of >10% (14.3 ± 0.5% and 27.0 ± 2.7%, respectively) (Table 2).

Among the study samples, 4 (2.1%) were classified as having high parasite survival rates by RSA; mean survival rates (± SEM) ranged from 13.3% ± 1.5% (isolate H2) to 34.3% (isolate H1) (Figure 2, Table 2). We assayed all except 1 isolate (H1) in duplicate. We observed these resistant isolates in all sampling periods except October–November 2015. One isolate (H1) had higher survival rates (34.3%) than the 2 artemisinin-resistant laboratory clones from Cambodia (MRA-1236 and MRA-1240). Developmental stages of the parasites at enrollment were microscopically determined (online Technical Appendix Figure). In the 3 isolates with high survival rates by RSA, proportions of early ring-stage parasites at enrollment were high (72%–98%) (online Technical Appendix Table 3), except for 1 isolate (H3), which had a lower proportion of early ring-stage parasites. For parasites with survival rates ≈10% (I1, I5, and I7), early ring-stage parasites were ≈51.9%–57.7% and the rest were late ring-stage parasites. These observations show that the developmental stages of the parasite before start of the RSA was not biased or skewed so as to influence RSA results. In fact, survival rates of samples with an almost 50:50 ratio of parasites in early and late stages might be underestimated because susceptibility to artemisinin occurs only during the early ring stage (*10–12*).

Table 1. Baseline characteristics of patients enrolled in study of *Plasmodium falciparum* ex vivo RSA survival rates, Uganda, 2014–2016*

Characteristics	Enrolled	RSA results obtained
No. patients	249	194
2014 Oct	16	15
2015 May	74	43
2015 Oct	63	51
2016 June	96	85
Sex, no. patients		
M	126	92
F	123	102
Age, y		
Median (IQR)	3.0 (2.0–4.5)	2.9 (2.0–4.4)
Fever ≥37.5°C		
No. (%) patients	207 (83)	177 (92)
Median (IQR) body temperature, °C	39 (38.0–39.4)	39 (38.3–39.5)
Signs and symptoms, % patients		
Cough	22	29
Vomiting	21	25
Abdominal pain	11	21
Headache	10	19
Diarrhea	7	10
Convulsion	7	8
Day 0 parasitemia, median (IQR), %	1.71 (0.17–4.13)	1.95 (0.85–4)

*IQR, interquartile range; RSA, ring-stage survival assay.

Table 2. Characteristics of *Plasmodium falciparum* isolates with high ex vivo ring-stage survival rates and patients enrolled in study of *Plasmodium falciparum* survival rates, Uganda, 2014–2016*

Sample name	Patient age, y	Patient sex	Signs and symptoms	Day 0 parasitemia, %	Early ring-stage parasites at day 0, %	Mean parasite survival rate, %, ± SEM
H1	3.0	M	Fever, headache, cough	0.85	80.4	34.3
H2	2.0	M	Fever	15.0	98.2	13.3 ± 1.5
H3	3.2	M	Fever	0.76	51.9	18.9 ± 0.9
H4	4.5	F	Fever	2.56	72.0	18.1 ± 1.4
3D7	NA	NA	NA	NA	NA	0 ± 0
MRA-1236	NA	NA	NA	NA	NA	14.3 ± 0.5
MRA-1240	NA	NA	NA	NA	NA	27.0 ± 2.7

*Survival rate, parasitemia at 700 nmol/L dihydroartemisinin exposed/parasitemia at 0 nmol/L control × 100; mean value ± SEM in 2 (H2, H3, and H4) and 3 (3D7, MRA-1236, and MRA-1240) independent trials. Day 0, day of enrollment. NA, not applicable.

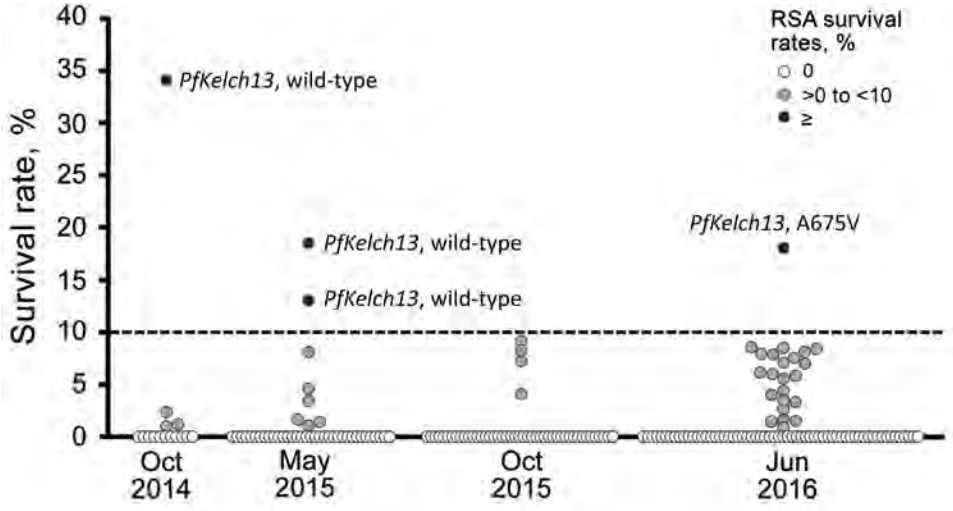

Figure 2. Distribution of ex vivo ring-stage *Plasmodium falciparum* survival rates, by RSA during each study period, 2014–2016. Susceptibility to dihydroartemisinin was determined by using ex vivo RSA survival rates. Survival rate was calculated as follows: (parasitemia at 700 nmol/L dihydroartemisinin exposed/parasitemia at 0 nmol/L control) × 100. Broken line indicates the cutoff value for what we consider to be high ex vivo RSA survival rates (≥10%). RSA, ring-stage survival assay.

Conventional Ex Vivo Drug Susceptibility Assay for Dihydroartemisinin

We performed a conventional ex vivo dihydroartemisinin-susceptibility assay in all but 1 survey (June–July 2016) and successfully determined ex vivo RSA and conventional ex vivo IC_{50} values for 93 patients (Figure 3). IC_{50} values were not correlated with survival rates by RSA. Geometric mean IC_{50} for isolates with high survival rates by RSA (3.3 nmol/L) were similar to those for the artemisinin-susceptible isolates (2.25 nmol/L).

Genotypes of *PfKelch13* and Potential Background Mutations

Only 5 (2.6%) isolates (C469Y, M472V, A621S, V666I, A675V) harbored nonsynonymous mutations at propeller domains in *PfKelch13*, all of which were observed as singletons (online Technical Appendix Table 4). Among 4 parasites with high survival rates by RSA, 1 harbored the A675V mutation and the other 3 harbored the wild-type allele (Figure 2). We observed no background genetic changes for artemisinin resistance (D193Y in *fd*, T484I in *mdr2*, V127M in *arps10*, I356T in *crt*, V1157L in *pph*, and C1484F in *pibp*; data not shown).

Lineages of Parasites with High Survival Rates by RSA

To clarify whether parasites with high survival rates by RSA indigenously originated in Africa or migrated from Southeast Asia, we performed principal component and STRUCTURE analyses. Whole-genome sequences were determined for all except 1 (H1) parasite isolate with a high survival rate by RSA. As reference, we used 31 *P. falciparum* isolates with origins from Asia or Africa. High-quality whole-genome sequence data enabled identification of 174,266 SNPs, of which 168,908 were biallelic SNPs. Among these, we used 14,341 SNPs with minor allele frequency >25% for the analyses. In principal component analysis, the first principal component clearly separated isolates from Africa from those from Southeast Asia (Figure 4, panel A). All 7 reference isolates harboring mutant *PfKelch13* were located in the cluster from Southeast Asia. In contrast, all 3 isolates from Uganda with high survival rates by RSA were inside the cluster from Africa. STRUCTURE analysis also clarified the distinct population structure of isolates from Southeast Asia compared with all isolates from Africa, including the 3 isolates with high survival rates by RSA (Figure 4, panel B).

Discussion

Emergence and spread of artemisinin-resistant *P. falciparum* outside the Greater Mekong Subregion pose a serious public health threat, especially in sub-Saharan Africa, the region that in 2015 accounted for 90% of global malaria cases and 92% of malaria deaths (*35*). The recently developed ex vivo RSA found that 4 (2.1%) isolates from Uganda showed high (>10%) survival rates, levels of which are reported to be closely associated with slow-clearing *P. falciparum* infections (*12*). Among these, mutation in *PfKelch13* was observed in only 1 isolate. Population genetic analysis with whole-genome sequences demonstrated that these isolates belong to the cluster from Africa, suggesting an indigenous origin rather than migration from Southeast Asia.

So far, 2 ex vivo RSA results have been reported in sub-Saharan Africa: in Cameroon (*15*) and in Kampala, Uganda, ≈300 km from our study site (*14*). Neither study found isolates with high survival rates. In our analysis, 4 (2.1%) isolates had survival rates >10%. In addition, 3 (1.5%) isolates with survival rates of ≈10% had lower proportions of early ring-stage parasites (51.9%–57.7%) at patient enrollment. Because artemisinin resistance is known to be confined to the early ring stage (*10–12*), the observed survival rate for these isolates might be underestimated. For our analysis, we

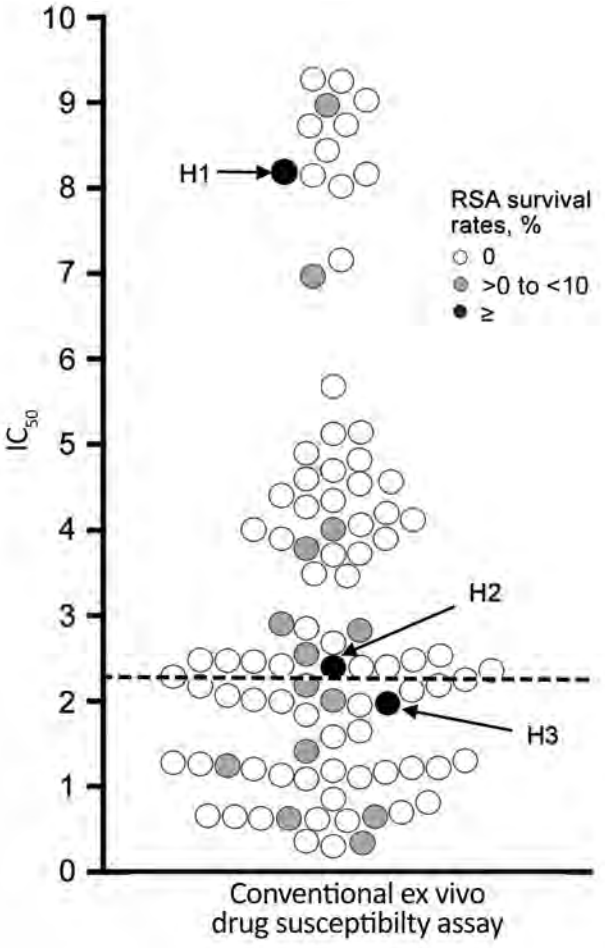

Figure 3. Distribution of IC_{50} of *Plasmodium falciparum* values by dihydroartemisinin in conventional ex vivo drug susceptibility assay. IC_{50} values to dihydroartemisinin in conventional ex vivo drug susceptibility assay are plotted. Geometric mean IC_{50} values in isolates with survival rates of 0, >0 to <10%, and ≥10% (high RSA survival) were 3.0 nmol/L (n = 74), 1.9 nmol/L (n = 14), and 3.3 nmol/L (n = 3), respectively. In the conventional ex vivo drug susceptibility assay, replication of parasites was monitored after continuous exposure to dihydroartemisinin for 72 h. Dashed line indicates geometric mean IC_{50} value of all isolates (2.25 nmol/L). IC_{50}, concentration needed to inhibit 50% growth; RSA, ring-stage survival assay.

assumed that an overall 2%–4% of isolates had artemisinin-resistant potential. Since the discovery of *PfKelch13* as an artemisinin-resistant responsible gene in 2013 (*21*), numerous molecular epidemiologic studies identified >200 mutations in this gene (*4*,*35*,*36*). The correlation with clinical and laboratory artemisinin resistance in 6 mutations (N458Y, Y493H, R539T, I543T, R561H, C580Y) has been validated (*37*). In our study, 1 isolate with a high survival rate by RSA harbored a mutation allele in *PfKelch13* (A675V). This mutation is reported to have a level of parasite clearance half-life similar to that of the most prevalent C580Y mutation (*4*,*38*) and has thus been regarded as candidate artemisinin-related mutation (*37*). The allele is distributed in Southeast Asia (Thailand–Myanmar border) and sub-Saharan Africa (Democratic Republic of the Congo and Rwanda) (*4*,*38*–*40*). However, our population genomic analysis revealed that this isolate belongs to African lineage, suggesting that artemisinin-resistant migration of A675V from Southeast Asia to Africa is less likely than the indigenous emergence of this mutation in Africa.

Three other isolates with high survival rates by RSA harbored a wild-type allele in *PfKelch13*. A similar finding in Cambodia has been recently reported (*41*). The parasiticidal mechanism of artemisinin is known to result from induction of highly reactive carbon-centered radicals that inactivate multiple crucial proteins (*42*). To combat this effect, resistant parasites are believed to enhance the oxidative stress response, altering the cell cycle (*29*,*36*,*39*,*43*–*45*). Recent population transcriptome analyses that used 1,043 clinical *P. falciparum* isolates obtained directly from patients with acute falciparum malaria demonstrated associations between *PfKelch13* mutations and upregulation of unfolded protein response, one of the stress response systems, and PI3K/PI3P/AKT pathways (*46*). One possible hypothesis to explain the absence of a *PfKelch13* mutation in the ex vivo RSA artemisinin-resistant isolates is the activation of alternate pathways by yet unknown mechanism(s).

Witkowski et al. showed a strong correlation between ex vivo RSA survival rates and in vivo parasite clearance half-lives in Cambodia (*12*). When the ex vivo RSA survival rate cutoff of 10% is applied to their study, 29 of 30 infections are accurately identified as artemisinin resistant and artemisinin susceptible (*12*). This cutoff point produced 89% sensitivity and 91% specificity for in vivo artemisinin resistance in the parasites from Cambodia (*12*). However, a similar correlation study is lacking for isolates from Africa. Because many factors such as levels of host immunity and pharmacokinetics could complicate drug clinical effectiveness, further correlation of ex vivo RSA and in vivo studies is strongly required in the various malaria-endemic regions with different population ethnicities and malaria ecologies.

Our study has several limitations. Parasites were not cryopreserved; thus, survival rate was not reconfirmed by in vitro RSA with culture-adapted parasites. Reconfirmation was not performed because of the difficulties in logistics and cryopreservation of natural parasites at our field site and transportation to our laboratory. However, we performed ex vivo RSA duplicate (except during October–November 2014), enabling confirmation via independently performed assays. In addition, we did not obtain clinical confirmation of artemisinin resistance for all 4 isolates with high survival rates by RSA because clinical study in 2014 was performed only during October–November, and only in 9 random isolates was artemether/lumefantrine treatment efficacy assessed.

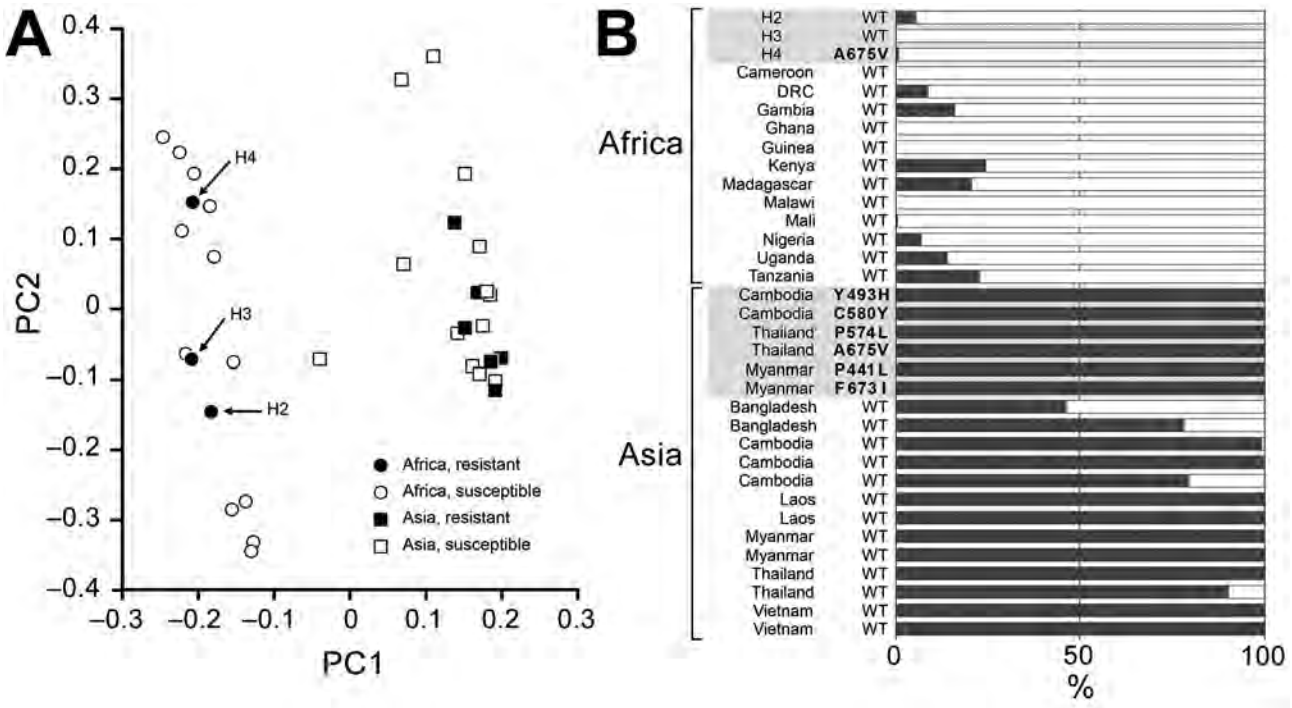

Figure 4. Potential lineage of ring-stage *Plasmodium falciparum* isolates with high survival rates according to ring-stage assay (RSA) in Uganda. Principal component analysis (A) and STRUCTURE (*34*) analysis (B) suggested an indigenous emergence of parasites with high survival rates by RSA (H2, H3, and H4) in Africa. *P. falciparum* isolates (n = 31) that originated from Asia (n = 19), including 6 isolates with *PfKelch13* mutation, or from Africa (n = 12) were obtained from Sequence Read Archive in National Center for Biotechnology Information (https://www.ncbi.nlm.nih.gov/sra). DRC, Democratic Republic of the Congo; PC1, first principal component; PC2, second principal component; WT, wild-type.

In the conventional ex vivo artemisinin susceptibility assay, parasites are exposed to dihydroartemisinin for 48–72 h, affecting trophozoite and schizont stages. Strictly, therefore, this assay theoretically underestimates the level of artemisinin resistance. Using ex vivo assays, we found that the mean IC_{50} in isolates with high survival rates by RSA was similar to that for those isolates characterized as having low survival rates or those that are completely susceptible (showed no survival by RSA). This finding was similar to previous field observations in Cambodia, where a lack of correlation was found between ex vivo survival rates by RSA and IC_{50}s to dihydroartemisinin in conventional ex vivo drug susceptibility assay (*12*), supporting the notion that conventional ex vivo assays may not be useful for properly distinguishing isolates with decreased artemisinin susceptibility in the field.

In conclusion, our analysis has revealed the potential emergence of *P. falciparum* with high survival rates by RSA in Uganda. One of these parasites harbored a *PfKelch13* A675V mutation. Because ≈90% of malaria cases occur in Africa (*35*), emergence and spread of artemisinin resistance impose substantial obstacles for effective malaria control and the approach toward elimination. It is thus imperative to perform further intensive surveillance for artemisinin resistance in various malaria-endemic regions in Africa and to elucidate genetic changes that confer resistance to artemisinin in parasites in Africa. Use of ex vivo RSA would help solve these challenges.

Acknowledgments

We thank the many doctors, nurses, and laboratory technicians at St. Mary's Hospital Lacor, who greatly contributed to the hospital survey. We also thank Sakurako Emoto, Keishi Fukuhara, Nagamasa Kano, Akimasa Maeta, Akihiro Kosuge, Azusa Takahashi, Koji Ijichi, Ryoichi Matsubara, Kouki Soda, and Sachifumi Sakamoto for their support in the field.

This publication uses data from the MalariaGEN *Plasmodium falciparum* Community Project as described in Genomic Epidemiology of Artemisinin-Resistant Malaria, eLife, 2016 (http://dx.doi.org/10.7554/eLife.08714). This work was supported by Grants-in-aid for Scientific Research (Ministry of Education, Culture, Sports, Science, and Technology of Japan) to T.M. and by funds for Integrated Promotion of Social System Reform and Research and Development (Ministry of Education, Culture, Sports, Science, and Technology of Japan), and grants from the Translational Research Network program (Japan Agency for Medical Research and Development) and the Global Health Innovative Technology Fund (G2013-105) to T.H.

About the Author

Dr. Ikeda is a postdoctoral student at the Department of Tropical Medicine and Parasitology, Juntendo University. Her research interest includes epidemiology of drug-resistant malaria.

References

1. World Health Organization. World malaria report 2017. Geneva: The Organization; 2017.
2. Noedl H, Se Y, Schaecher K, Smith BL, Socheat D, Fukuda MM; Artemisinin Resistance in Cambodia 1 (ARC1) Study Consortium. Evidence of artemisinin-resistant malaria in western Cambodia. N Engl J Med. 2008;359:2619–20. http://dx.doi.org/10.1056/NEJMc0805011
3. Dondorp AM, Nosten F, Yi P, Das D, Phyo AP, Tarning J, et al. Artemisinin resistance in *Plasmodium falciparum* malaria. N Engl J Med. 2009;361:455–67. http://dx.doi.org/10.1056/NEJMoa0808859
4. Ashley EA, Dhorda M, Fairhurst RM, Amaratunga C, Lim P, Suon S, et al.; Tracking Resistance to Artemisinin Collaboration (TRAC). Spread of artemisinin resistance in *Plasmodium falciparum* malaria. N Engl J Med. 2014;371:411–23. http://dx.doi.org/10.1056/NEJMoa1314981
5. Amaratunga C, Lim P, Suon S, Sreng S, Mao S, Sopha C, et al. Dihydroartemisinin-piperaquine resistance in *Plasmodium falciparum* malaria in Cambodia: a multisite prospective cohort study. Lancet Infect Dis. 2016;16:357–65. http://dx.doi.org/10.1016/S1473-3099(15)00487-9
6. World Health Organization. World malaria report 2015. Geneva: The Organization; 2015.
7. Rogerson SJ, Wijesinghe RS, Meshnick SR. Host immunity as a determinant of treatment outcome in *Plasmodium falciparum* malaria. Lancet Infect Dis. 2010;10:51–9. http://dx.doi.org/10.1016/S1473-3099(09)70322-6
8. Lopera-Mesa TM, Doumbia S, Chiang S, Zeituni AE, Konate DS, Doumbouya M, et al. *Plasmodium falciparum* clearance rates in response to artesunate in Malian children with malaria: effect of acquired immunity. J Infect Dis. 2013;207:1655–63. http://dx.doi.org/10.1093/infdis/jit082
9. Amaratunga C, Sreng S, Suon S, Phelps ES, Stepniewska K, Lim P, et al. Artemisinin-resistant *Plasmodium falciparum* in Pursat Province, western Cambodia: a parasite clearance rate study. Lancet Infect Dis. 2012;12:851–8. http://dx.doi.org/10.1016/S1473-3099(12)70181-0
10. Klonis N, Xie SC, McCaw JM, Crespo-Ortiz MP, Zaloumis SG, Simpson JA, et al. Altered temporal response of malaria parasites determines differential sensitivity to artemisinin. Proc Natl Acad Sci U S A. 2013;110:5157–62. http://dx.doi.org/10.1073/pnas.1217452110
11. Witkowski B, Lelièvre J, Barragán MJ, Laurent V, Su XZ, Berry A, et al. Increased tolerance to artemisinin in *Plasmodium falciparum* is mediated by a quiescence mechanism. Antimicrob Agents Chemother. 2010;54:1872–7. http://dx.doi.org/10.1128/AAC.01636-09
12. Witkowski B, Amaratunga C, Khim N, Sreng S, Chim P, Kim S, et al. Novel phenotypic assays for the detection of artemisinin-resistant *Plasmodium falciparum* malaria in Cambodia: in-vitro and ex-vivo drug-response studies. Lancet Infect Dis. 2013;13:1043–9. http://dx.doi.org/10.1016/S1473-3099(13)70252-4
13. Phyo AP, Nkhoma S, Stepniewska K, Ashley EA, Nair S, McGready R, et al. Emergence of artemisinin-resistant malaria on the western border of Thailand: a longitudinal study. Lancet. 2012;379:1960–6. http://dx.doi.org/10.1016/S0140-6736(12)60484-X
14. Cooper RA, Conrad MD, Watson QD, Huezo SJ, Ninsiima H, Tumwebaze P, et al. Lack of artemisinin resistance in *Plasmodium falciparum* in Uganda based on parasitological and molecular assays. Antimicrob Agents Chemother. 2015;59:5061–4. http://dx.doi.org/10.1128/AAC.00921-15
15. Menard S, Tchoufack JN, Maffo CN, Nsango SE, Iriart X, Abate L, et al. Insight into k13-propeller gene polymorphism and ex vivo DHA-response profiles from Cameroonian isolates. Malar J. 2016;15:572. http://dx.doi.org/10.1186/s12936-016-1622-x
16. Wootton JC, Feng X, Ferdig MT, Cooper RA, Mu J, Baruch DI, et al. Genetic diversity and chloroquine selective sweeps in *Plasmodium falciparum*. Nature. 2002;418:320–3. http://dx.doi.org/10.1038/nature00813
17. Roper C, Pearce R, Nair S, Sharp B, Nosten F, Anderson T. Intercontinental spread of pyrimethamine-resistant malaria. Science. 2004;305:1124. http://dx.doi.org/10.1126/science.1098876
18. Mita T, Venkatesan M, Ohashi J, Culleton R, Takahashi N, Tsukahara T, et al. Limited geographical origin and global spread of sulfadoxine-resistant *dhps* alleles in *Plasmodium falciparum* populations. J Infect Dis. 2011;204:1980–8. http://dx.doi.org/10.1093/infdis/jir664
19. McCollum AM, Poe AC, Hamel M, Huber C, Zhou Z, Shi YP, et al. Antifolate resistance in *Plasmodium falciparum*: multiple origins and identification of novel *dhfr* alleles. J Infect Dis. 2006;194:189–97. http://dx.doi.org/10.1086/504687
20. Mita T, Tanabe K, Takahashi N, Culleton R, Ndounga M, Dzodzomenyo M, et al. Indigenous evolution of *Plasmodium falciparum* pyrimethamine resistance multiple times in Africa. J Antimicrob Chemother. 2009;63:252–5. http://dx.doi.org/10.1093/jac/dkn482
21. Ariey F, Witkowski B, Amaratunga C, Beghain J, Langlois AC, Khim N, et al. A molecular marker of artemisinin-resistant *Plasmodium falciparum* malaria. Nature. 2014;505:50–5. http://dx.doi.org/10.1038/nature12876
22. Ghorbal M, Gorman M, Macpherson CR, Martins RM, Scherf A, Lopez-Rubio JJ. Genome editing in the human malaria parasite *Plasmodium falciparum* using the CRISPR-Cas9 system. Nat Biotechnol. 2014;32:819–21. http://dx.doi.org/10.1038/nbt.2925
23. Straimer J, Gnädig NF, Witkowski B, Amaratunga C, Duru V, Ramadani AP, et al. K13-propeller mutations confer artemisinin resistance in *Plasmodium falciparum* clinical isolates. Science. 2015;347:428–31. http://dx.doi.org/10.1126/science.1260867
24. Ménard D, Khim N, Beghain J, Adegnika AA, Shafiul-Alam M, Amodu O, et al.; KARMA Consortium. A worldwide map of *Plasmodium falciparum* K13-propeller polymorphisms. N Engl J Med. 2016;374:2453–64. http://dx.doi.org/10.1056/NEJMoa1513137
25. Okello PE, Van Bortel W, Byaruhanga AM, Correwyn A, Roelants P, Talisuna A, et al. Variation in malaria transmission intensity in seven sites throughout Uganda. Am J Trop Med Hyg. 2006;75:219–25.
26. Uganda Bureau of Statistics. Malaria Indicator Survey 2009 [cited 2017 Dec 15]. https://dhsprogram.com/pubs/pdf/MIS6/MIS6.pdf
27. Yeka A, Gasasira A, Mpimbaza A, Achan J, Nankabirwa J, Nsobya S, et al. Malaria in Uganda: challenges to control on the long road to elimination: I. Epidemiology and current control efforts. Acta Trop. 2012;121:184–95. http://dx.doi.org/10.1016/j.actatropica.2011.03.004
28. Witkowski B, Menard D, Amaratunga C, Fairhurst RM. Ring-stage survival assays (RSA) to evaluate the in-vitro and ex-vivo susceptibility of *Plasmodium falciparum* to artemisinins [cited 2017 Dec 15]. http://www.wwarn.org/sites/default/files/attachments/procedures/INV10-Standard-Operating-Procedure-Ring-Stage-Survival-Assays-v1.2.pdf
29. Dogovski C, Xie SC, Burgio G, Bridgford J, Mok S, McCaw JM, et al. Targeting the cell stress response of *Plasmodium falciparum* to overcome artemisinin resistance. PLoS Biol. 2015;13:e1002132. http://dx.doi.org/10.1371/journal.pbio.1002132
30. Noedl H, Wernsdorfer WH, Miller RS, Wongsrichanalai C. Histidine-rich protein II: a novel approach to malaria drug

sensitivity testing. Antimicrob Agents Chemother. 2002;46:1658–64. http://dx.doi.org/10.1128/AAC.46.6.1658-1664.2002
31. Le Nagard H, Vincent C, Mentré F, Le Bras J. Online analysis of in vitro resistance to antimalarial drugs through nonlinear regression. Comput Methods Programs Biomed. 2011;104:10–8. http://dx.doi.org/10.1016/j.cmpb.2010.08.003
32. Balikagala B, Mita T, Ikeda M, Sakurai M, Yatsushiro S, Takahashi N, et al. Absence of in vivo selection for K13 mutations after artemether-lumefantrine treatment in Uganda. Malar J. 2017;16:23. http://dx.doi.org/10.1186/s12936-016-1663-1
33. Miotto O, Amato R, Ashley EA, MacInnis B, Almagro-Garcia J, Amaratunga C, et al. Genetic architecture of artemisinin-resistant *Plasmodium falciparum*. Nat Genet. 2015;47:226–34. http://dx.doi.org/10.1038/ng.3189
34. Pritchard JK, Stephens M, Donnelly P. Inference of population structure using multilocus genotype data. Genetics. 2000; 155:945–59.
35. World Health Organization. World malaria report 2016. Geneva: The Organization; 2016.
36. Fairhurst RM, Dondorp AM. Artemisinin-resistant *Plasmodium falciparum* malaria. Microbiol Spectr. 2016;4.
37. World Health Organization. Artemisinin and artemisinin-based combination therapy resistance. Status report. Geneva: The Organization; 2016.
38. Boullé M, Witkowski B, Duru V, Sriprawat K, Nair SK, McDew-White M, et al. Artemisinin-resistant *Plasmodium falciparum* K13 mutant alleles, Thailand–Myanmar border. Emerg Infect Dis. 2016;22:1503–5. http://dx.doi.org/10.3201/eid2208.160004
39. Hott A, Casandra D, Sparks KN, Morton LC, Castanares GG, Rutter A, et al. Artemisinin-resistant *Plasmodium falciparum* parasites exhibit altered patterns of development in infected erythrocytes. Antimicrob Agents Chemother. 2015;59:3156–67. http://dx.doi.org/10.1128/AAC.00197-15
40. Tacoli C, Gai PP, Bayingana C, Sifft K, Geus D, Ndoli J, et al. Artemisinin resistance-associated K13 polymorphisms of *Plasmodium falciparum* in southern Rwanda, 2010–2015. Am J Trop Med Hyg. 2016;95:1090–3. http://dx.doi.org/10.4269/ajtmh.16-0483
41. Mukherjee A, Bopp S, Magistrado P, Wong W, Daniels R, Demas A, et al. Artemisinin resistance without *pfkelch13* mutations in *Plasmodium falciparum* isolates from Cambodia. Malar J. 2017;16:195. http://dx.doi.org/10.1186/s12936-017-1845-5
42. O'Neill PM, Barton VE, Ward SA. The molecular mechanism of action of artemisinin—the debate continues. Molecules. 2010;15:1705–21. http://dx.doi.org/10.3390/molecules15031705
43. Mbengue A, Bhattacharjee S, Pandharkar T, Liu H, Estiu G, Stahelin RV, et al. A molecular mechanism of artemisinin resistance in *Plasmodium falciparum* malaria. Nature. 2015;520:683–7. http://dx.doi.org/10.1038/nature14412
44. Mita T, Tachibana S, Hashimoto M, Hirai M. *Plasmodium falciparum kelch 13*: a potential molecular marker for tackling artemisinin-resistant malaria parasites. Expert Rev Anti Infect Ther. 2016;14:125–35. http://dx.doi.org/10.1586/14787210.2016.1106938
45. Paloque L, Ramadani AP, Mercereau-Puijalon O, Augereau JM, Benoit-Vical F. *Plasmodium falciparum*: multifaceted resistance to artemisinins. Malar J. 2016;15:149. http://dx.doi.org/10.1186/s12936-016-1206-9
46. Mok S, Ashley EA, Ferreira PE, Zhu L, Lin Z, Yeo T, et al. Population transcriptomics of human malaria parasites reveals the mechanism of artemisinin resistance. Science. 2015;347:431–5. http://dx.doi.org/10.1126/science.1260403

Address for correspondence: Toshihiro Mita, Juntendo University School of Medicine, Department of Tropical Medicine and Parasitology, 2-1-1 Hongo, Bunkyo-ku, Tokyo, 113-0033, Japan; email: tmita@juntendo.ac.jp

Carbapenem-Nonsusceptible *Acinetobacter baumannii*, 8 US Metropolitan Areas, 2012–2015

Sandra N. Bulens, Sarah H. Yi, Maroya S. Walters, Jesse T. Jacob, Chris Bower, Jessica Reno, Lucy Wilson, Elisabeth Vaeth, Wendy Bamberg, Sarah J. Janelle, Ruth Lynfield, Paula Snippes Vagnone, Kristin Shaw, Marion Kainer, Daniel Muleta, Jacqueline Mounsey, Ghinwa Dumyati, Cathleen Concannon, Zintars Beldavs, P. Maureen Cassidy, Erin C. Phipps, Nicole Kenslow, Emily B. Hancock, Alexander J. Kallen

In healthcare settings, *Acinetobacter* spp. bacteria commonly demonstrate antimicrobial resistance, making them a major treatment challenge. Nearly half of *Acinetobacter* organisms from clinical cultures in the United States are nonsusceptible to carbapenem antimicrobial drugs. During 2012–2015, we conducted laboratory- and population-based surveillance in selected metropolitan areas in Colorado, Georgia, Maryland, Minnesota, New Mexico, New York, Oregon, and Tennessee to determine the incidence of carbapenem-nonsusceptible *A. baumannii* cultured from urine or normally sterile sites and to describe the demographic and clinical characteristics of patients and cases. We identified 621 cases in 537 patients; crude annual incidence was 1.2 cases/100,000 persons. Among 598 cases for which complete data were available, 528 (88.3%) occurred among patients with exposure to a healthcare facility during the preceding year; 506 (84.6%) patients had an indwelling device. Although incidence was lower than for other healthcare-associated pathogens, cases were associated with substantial illness and death.

Author affiliations: Centers for Disease Control and Prevention, Atlanta, Georgia, USA (S.N. Bulens, S.H. Yi, M.S. Walters, A.J. Kallen); Emory University School of Medicine, Atlanta (J.T. Jacob); Georgia Emerging Infections Program, Atlanta (J.T. Jacob, C. Bower, J. Reno); Atlanta Veterans Affairs Medical Center, Decatur, Georgia, USA (C. Bower, J. Reno); Atlanta Research and Education Foundation, Decatur (C. Bower, J. Reno); Maryland Department of Health and Mental Hygiene, Baltimore, Maryland, USA (L. Wilson, E. Vaeth); Colorado Department of Public Health and Environment, Denver, Colorado, USA (W. Bamberg, S.J. Janelle); Minnesota Department of Health, St. Paul, Minnesota, USA (R. Lynfield, P.S. Vagnone, K. Shaw); Tennessee Department of Public Health, Nashville, Tennessee, USA (M. Kainer, D. Muleta, J. Mounsey); New York Rochester Emerging Infections Program at the University of Rochester Medical Center, Rochester, New York, USA (G. Dumyati, C. Concannon); Oregon Health Authority, Portland, Oregon, USA (Z. Beldavs, P.M. Cassidy); University of New Mexico, Albuquerque, New Mexico, USA (E.C. Phipps, N. Kenslow, E.B. Hancock)

DOI: https://doi.org/10.3201/eid2404.171461

The bacterium *Acinetobacter baumannii* is a recognized cause of healthcare-associated illness, including pneumonia, bacteremia, and urinary tract infections (UTIs) (*1–3*). *Acinetobacter* isolates often demonstrate resistance to multiple classes of antimicrobial drugs, leading to treatment challenges. A Centers for Disease Control and Prevention (CDC) report, Antimicrobial Resistance Threats in the United States, 2013, highlighted multidrug-resistant *Acinetobacter* as a serious threat that causes ≈7,000 infections and ≈500 deaths in the United States each year (*4*).

Carbapenems are often used to treat multidrug-resistant bacterial infections, such as those caused by *Acinetobacter* spp. Nearly half of *Acinetobacter* strains isolated from persons with healthcare-associated infections reported to the CDC National Healthcare Safety Network in 2014 were carbapenem-nonsusceptible (*5*). Infections with carbapenem-resistant *A. baumannii* have been associated with death rates as high as 52% (*6–10*).

Preventing the transmission of resistant organisms, including carbapenem-resistant *A. baumannii*, is a major public health priority (*11*). To identify opportunities for prevention, the Emerging Infections Program (EIP) conducts population- and laboratory-based surveillance for carbapenem-nonsusceptible *A. baumannii* in 8 US metropolitan areas through its Multi-site Gram-negative Surveillance Initiative (MuGSI). Our objective was to describe the epidemiology and estimate the crude population-based incidence of carbapenem-nonsusceptible *A. baumannii* during the first 4 years of surveillance.

Methods

Surveillance Catchment Area

Surveillance was population-based and conducted in 3 metropolitan areas in 2012: Atlanta, Georgia (estimated

population 3,991,607); Minneapolis and St. Paul, Minnesota (1,761,282); and Portland, Oregon (1,766,135). Four more metropolitan areas were added in 2013: Denver, Colorado (2,694,886); Baltimore, Maryland (1,934,018); Albuquerque, New Mexico (676,685); and Rochester, New York (749,600). One other site, Nashville, Tennessee (1,653,871), was added in 2014. The total population under surveillance in 2015 was ≈15.2 million, which included 31 counties in the identified metropolitan areas (*12*). The project comprised cases for which samples were collected for culture of carbapenem-nonsusceptible *A. baumannii* during January 1, 2012–December 31, 2015.

Case Definition and Epidemiologic Classification

We defined a case as the first isolation of carbapenem-nonsusceptible *A. baumannii* complex in a 30-day period from a normally sterile body site or urine specimen of a surveillance catchment area resident. Carbapenem nonsusceptibility was based on antimicrobial drug susceptibility test results generated by the local clinical laboratory's primary testing method and 2012 Clinical and Laboratory Standards Institute interpretive criteria for meropenem and imipenem nonsusceptibility (MIC ≥2 μg/mL) (*13*). For doripenem, nonsusceptibility was defined using the 2012 Food and Drug Administration's breakpoint (MIC >1 μg/mL) (https://druginserts.com/lib/rx/meds/doribax/page/3/). Most clinical laboratories in the EIP catchment area used automated testing instruments for primary antimicrobial susceptibility testing (*14*). Respiratory cultures, although clinically important for carbapenem-nonsusceptible *A. baumannii*, were not included as part of this surveillance.

We considered a sample collected for initial culture to be hospital-collected if it was collected in a short-stay acute-care hospital inpatient setting. We considered a sample to be other healthcare–collected if it was collected in any of the following settings: long-term care facility ([LTCF]; i.e., nursing home, skilled nursing facility, inpatient hospice, or physical rehabilitation facility); long-term acute-care hospital (LTACH); dialysis center; outpatient care center (i.e., outpatient surgery center, urgent care, private doctor's office/clinic); or the emergency department or observation units in an acute-care hospital.

Case Identification and Data Collection

To identify cases, we actively collected reports of all carbapenem-nonsusceptible *A. baumannii* isolates from clinical laboratories serving the catchment areas. We reviewed the patient address that accompanied the isolate to determine whether the patient resided in the surveillance catchment area. We abstracted inpatient and outpatient medical records using a standardized case report form. Information collected was patient demographics, location of sample collection, healthcare exposures, types of infection diagnosed, underlying conditions, and patient outcomes. Death was determined at discharge if the sample had been collected from a hospital inpatient; 30 days after the sample collection date if the sample was collected in an outpatient dialysis center, LTCF, or LTACH; and on the date of visit if the sample was collected in an outpatient setting. We calculated a Charlson Comorbidity Index score on the basis of underlying conditions abstracted from the medical record (*15*,*16*). We collected additional data elements if the sample was urine: method of urine collection, colony count of organisms isolated from the urine sample, and signs and symptoms documented in the medical record during the 2 calendar days before through the 2 calendar days after sample collection. We distinguished UTIs from colonization on the basis of the following criteria: 1) urine sample positive for $\geq 10^5$ CFU/mL carbapenem-nonsusceptible *A. baumannii*; and 2) signs or symptoms consistent with UTI documented in the medical record during the 2 calendar days before through the 2 calendar days after sample collection. We further categorized UTIs as catheter-associated if a urinary catheter was in place in the 2 days before sample collection and if the case-defining sample was a catheter urine specimen for the same organism.

Statistics

To compare incidence between sites and over time, we linked annual case counts reported by each EIP surveillance site with annual US Census population counts for the corresponding counties. We also stratified counts from both data sources and linked them by age, sex, and race to enable adjustment of potential confounding factors. We imputed cases with missing values for race in accordance with the distribution of known race among patients by age category. Incidence rates, calculated from case counts, were expressed as number of infections per 100,000 population, and precision was quantified using 95% CIs assuming a Poisson distribution (*17*). We compared stratified rates for each site to the combined EIP population using standardized incidence ratios, an indirect method of rate standardization appropriate for small event counts. The combined EIP population served as the standard population. We calculated exact Poisson confidence intervals around the standardized incidence ratios using a formula relating the χ^2 and Poisson distributions (*18*) and calculated p values using Miettinen's modification for Mid-P exact test for counts ≤100 and Byar's approximation of the Poisson method for counts >100 (*19*). We calculated adjusted incidence rates by multiplying the site-specific standardized incidence ratios adjusted for age, sex, and race by the crude incidence rate of the standard population (*20*). We assessed change in incidence over time

using incidence rate ratios (IRRs) obtained from a Poisson regression model adjusting for site, age, race, and sex with 2013 as the reference year. We limited analysis to sites contributing data annually during 2013–2015 (i.e., we excluded Tennessee data).

Analyses were conducted to describe patients' healthcare exposures, outcomes, demographic information, and antimicrobial drug susceptibility information for cases and for unique patients. Patients with complete case report form data as of August 26, 2016, were included in analyses of healthcare exposures and demographic and clinical characteristics and outcomes, and all cases (some patients contributed multiple cases to the analysis) were included in the antimicrobial drug susceptibility analysis. We calculated p values for comparison of categorical variables using the χ^2 test or the Fisher exact test when cell size was <5. Data management and analyses were conducted using SAS version 9.4 (SAS Institute Inc., Cary, NC, USA).

Ethics Review

Human subjects advisors in CDC's National Center for Emerging and Zoonotic Infectious Diseases determined the EIP's MuGSI to be a nonresearch activity; therefore, CDC institutional review board review was not required. This study also underwent ethics review at each of the participating EIP sites and was either approved with waiver of informed consent or deemed a nonresearch activity.

Results

Incidence Rates, Standardized Infection Rate Ratios, and Trends

The overall crude incidence rate was 1.2 (95% CI 1.1–1.3)/100,000 persons for 2012–2015 (Table 1). Crude incidence rates varied by EIP site during the 4-year period; the highest rates occurred in Maryland. Standardized incidence ratios were significantly higher than expected for Maryland (p = 0.00) and Georgia (p = 0.001) and significantly lower than expected for Colorado (p = 0.000), Minnesota (p = 0.000), New Mexico (p = 0.000), New York (p = 0.000), Oregon (p = 0.000), and Tennessee (p = 0.041) (Table 1). When we accounted for age, sex, race, and site, among the 7 sites that participated during 2013–2015, the adjusted IRRs did not differ (0.83 [95% CI 0.67–1.03]; p = 0.09). In 2014, the adjusted IRR decreased 24% from that of 2013 (0.76 [95% CI 0.61–0.95]; p = 0.02). During the surveillance period, 1 facility accounted for much of the decrease from 2013 to 2014, consistent with resolution of an outbreak. When we removed this facility from this temporal analysis, the change from 2013 to 2014 was no longer significant (adjusted IRR 0.82 [95% CI 0.66–1.03]; p = 0.09).

Cases and Patients

A total of 621 carbapenem-nonsusceptible *A. baumannii* cases from 537 unique patients were reported during the study period. Most cases occurred in Georgia (300 [48.3%]), followed by Maryland (236 [38.0%]), Minnesota (26 [4.2%]), Colorado (26 [4.2%]), and Tennessee (19 [3.1%]). New York, Oregon, and New Mexico reported 8, 4, and 2 cases, respectively. Of the 537 patients, 119 (22.2%) had ≥2 carbapenem-nonsusceptible *A. baumannii* cultures; these repeat positives accounted for 203 of all cases during the 4-year surveillance period (range 2–8 cultures/patient).

Among the 513 patients with complete case report form data, 178 (34.7%) were female, and median age was 58.6 years (range 0–102 years). Information about underlying conditions was available for 512 patients. The median Charlson Comorbidity Index score was 2.9 (range 0–13). Sixteen (3.1%) patients had no identified underlying conditions at the time of sample collection. The following underlying conditions were reported in ≥25% of patients: neurologic problems (277 [54.0%]), decubitus or pressure ulcers (275 [53.6%]), diabetes (216 [42.1%]), and chronic pulmonary disease (139 [27.1%]).

Table 1. Case counts and incidence of carbapenem-nonsusceptiable *Acinetobacter baumannii* in Emerging Infections Program sites, United States, 2012–2015*

Area	No. cases, N = 621				Crude annual incidence rates‡ (95% CI)				aSIR§ (95% CI)	aIR§ for all years
	2012†	2013	2014	2015	2012†	2013	2014	2015		
CO	ND	11	7	8	ND	0.4 (0.2–0.8)	0.3 (0.1–0.6)	0.3 (0.1–0.6)	0.4 (0.3–0.6)	0.4
GA	111	78	47	64	2.9 (2.4–3.5)	2.0 (1.6–2.5)	1.2 (0.9–1.5)	1.6 (1.2–2.1)	1.2 (1.1–1.4)	1.2
MD	ND	77	81	78	ND	4.0 (3.2–5.0)	4.2 (3.3–5.2)	4.0 (3.2–5.0)	2.5 (2.2–2.9)	3.0
MN	2	10	7	7	0.12 (0–0.4)	0.6 (0.3–1.1)	0.4 (0.2–0.8)	0.4 (0.2–0.8)	0.4 (0.2–0.5)	0.4
NM	ND	0	1	1	ND	0 (0–0.4)	0.2 (0–0.8)	0.2 (0–0.8)	0.1 (0–0.4)	0.1
NY	ND	4	1	3	ND	0.5 (0.2–1.4)	0.1 (0–0.7)	0.4 (0.1–1.2)	0.3 (0.1–0.6)	0.4
OR	0	4	0	0	0 (0–0.2)	0.2 (0.1–0.6)	0 (0–0.2)	0 (0–0.2)	0.1 (0–0.1)	0.1
TN	ND	ND	12	7	ND	ND	0.7 (0.4–1.3)	0.4 (0.2–0.9)	0.6 (0.4–1.0)	0.7
Total	113	184	156	168	1.6 (1.3–1.9)	1.4 (1.2–1.6)	1.0 (0.9–1.2)	1.1 (0.9–1.3)	ND	ND

*The study areas were Denver, CO; Atlanta, GA; Baltimore, MD; Minneapolis/Saint Paul, MN; Albuquerque, NM; Rochester, NY; Portland, OR; Nashville, TN. aIR, annual incidence rate; aSIR, adjusted standardized incidence ratio; ND, no data available.
†Only 3 Emerging Infections Program sites participated in 2012.
‡Per 100,000 population.
§Adjusted for age, race, and sex.

Most of the 598 cases were based on isolation of carbapenem-nonsusceptible *A. baumannii* from urine (429 [71.7%]), followed by blood (157 [26.3%]). Other sterile sites from which carbapenem-nonsusceptible *A. baumannii* was isolated were bone (8 [1.3%]), joint/synovial fluid (2 [0.3%]), peritoneal fluid (2 [0.3%]), pleural fluid (1 [0.2%]), and other normally sterile sites (3 [0.5%]). For 4 cases, both blood and urine samples were collected on same date, and both grew carbapenem-nonsusceptible *A. baumannii*.

For most (503 [84.1%]) cases, at least 1 type of infection was associated with the carbapenem-nonsusceptible *A. baumannii* from the sample collected. Among those, UTI was the most common infection type reported (328 [65.2%]), followed by bacteremia (158 [31.4%]), septic shock (55 [10.9%]), and pneumonia (33 [6.6%]). For most (403 [80.1%]) cases, only 1 infection type was reported; 100 (19.9%) had ≥2 types of infection.

Of the infections in the 429 cases for which carbapenem-nonsusceptible *A. baumannii* was isolated from urine, 115 (26.8%) met criteria for a UTI based on our definition. Of these, fever was the only symptom reported in 76 (66%) cases. A provider documented UTI in the medical record for 328 (76.5%) cases; of these, only 96 (29.3%) met the criteria for a UTI based on our definition.

Of the 598 cases, 228 (38.1%) were identified from cultures of hospital-collected samples. Of these, 85 (14.2%) samples were collected in the intensive care unit (ICU), and 148 (24.8%) were collected >3 days after hospital admission. The median time between admission and sample collection was 7 days (range 0–341 days). The remaining 370 (61.9%) samples were collected outside of the acute-care hospital setting (other healthcare–collected): 210 (35.1%) in the emergency department of an acute-care hospital, 101 (16.9%) in an LTCF, 31 (5.2%) in an LTACH, and 28 (4.7%) in an outpatient setting (e.g., private doctors' offices or clinics). Of the 210 cases with samples collected in an emergency department, 177 (84.2%) were subsequently admitted to the acute-care hospital.

Previous Healthcare Exposure

For nearly all cases (590 [98.7%]), healthcare exposure in the year before sample collection or an indwelling device around the time of sample collection was documented (Table 2). Admission to a short-stay acute-care hospital (469 [78.4%] patients) or LTCF (360 [60.2%]) were the most frequent healthcare exposures documented. Additionally, 14.0% of cases occurred in patients admitted to an LTACH. Among the 506 (84.6%) cases for which an indwelling device was documented in the 2 days before specimen collection, a urinary catheter (399 [66.7%]) was the most common device. For 8 (<1%) cases, healthcare exposure during the previous year was not identified; of these, 2 case-patients traveled internationally in the 2 months before sample collection.

Outcomes of Cases

For 449 (75.1%) cases, patients were hospitalized at the time of or within 30 days after sample collection (Table 3). Of these cases, 168 (37.4%) patients were admitted to the ICU on the day of or within 7 days after sample collection. Death was assessed at different time points depending on where the patient was treated. The overall death rate of 17.9% (106/594 cases) was significantly higher for cases for which carbapenem-nonsusceptible *A. baumannii* was isolated from a sterile site than for those for which carbapenem-nonsusceptible *A. baumannii* was isolated only from urine (41.3% vs 8.3%; p<0.0001). Among case-patients who died, carbapenem-nonsusceptible *A. baumannii* was isolated within 7 days of death for 61.3% (65/106).

Antimicrobial Drug Susceptibilities

Antimicrobial drug susceptibility information from local clinical laboratories was available for all 621 cases (Table 4). Most isolates were susceptible to at least 1 aminoglycoside (72.9%). Isolates from urine samples were significantly more likely than those from sterile site samples to be susceptible to fluoroquinolones (4.6% vs. 0.6%; p = 0.02);

Table 2. Previous healthcare exposures among 598 carbapenem-nonsusceptible *Acinetobacter baumannii* cases in Emerging Infections Program sites, United States, 2012–2015*

Healthcare exposure	No. (%)
Healthcare facility exposure in the year before sample collection†	528 (88.3)
Previous acute care hospitalization	469 (78.4)
Residence in long-term care facility	360 (60.2)
Inpatient or outpatient surgery	199 (33.3)
Admission to long-term acute care hospital‡	73 (14.0)
Current hemodialysis treatment	66 (11.0)
Any indwelling device in place in the 2 calendar days before sample collection	506 (84.6)
Urinary catheter	399 (66.7)
Central venous catheter	222 (37.1)
Other§	269 (45.0)
No healthcare exposure	8 (1.3)

*The study areas were Denver, CO; Atlanta, GA; Baltimore, MD; Minneapolis/Saint Paul, MN; Albuquerque, NM; Rochester, NY; Portland, OR; Nashville, TN.
†Sum of subcategory percentages >100 due to patients with multiple healthcare exposures in year before case.
‡2013–2015 cases only.
§Other indwelling devices: endotracheal or nasotracheal tube, tracheostomy, gastrostomy tube, nephrostomy tube, nasogastric tube.

Table 3. Outcomes for 598 *Acinetobacter baumannii* cases in Emerging Infections Program sites, United States, 2012–2015*

Outcome	No. (%)
Hospitalized at, or within 30 d after, date of specimen collection, n = 598	449 (75.1)
Admission to intensive care unit on day of or within 7 d after sample collection, n = 449	168 (37.4)
Discharge location after acute care hospitalization among patients who survived, n = 356†	
Long-term care facility	187 (52.5)
Private residence	131 (36.8)
Long-term acute care hospital	34 (9.6)
Other	1 (0.3)
Died,‡ n = 594	106 (17.9)
Among cases with a sterile site culture, n = 172§	71 (41.3)
Among cases with a positive urine culture, n = 422§	35 (8.3)

*The study areas were Denver, CO; Atlanta, GA; Baltimore, MD; Minneapolis/Saint Paul, MN, Albuquerque, NM; Rochester, NY; Portland, OR; Nashville, TN.
†Three case-patients were discharged to unknown locations.
‡Death was determined at discharge for hospital inpatients; 30 d after sample collection for case-patients identified in outpatient dialysis, long-term care, and long-term acute care hospitals; and at evaluation for outpatients. For 4 case-patients, outcome was unknown. The 1 patient who had a blood sample and a urine sample was counted in the "sterile site culture" category.
§Significant difference in death by specimen source (p<0.0001).

susceptibilities based on specimen source did not differ significantly for other antimicrobial drugs.

Discussion

Data from population-based surveillance covering 8 geographically diverse metropolitan areas in the United States show that the overall incidence of carbapenem-nonsusceptible *A. baumannii* infection during 2012–2015 was low (1.2 cases/100,000 persons). Cases occurred almost exclusively in patients who stayed overnight in healthcare facilities or had indwelling devices. The crude mortality rate was 17.9%, approximately double that for patients with carbapenem-resistant *Enterobacteriaceae* (CRE) from the same catchment areas (*21*). For most cases, samples for culture were collected outside of short-stay acute-care hospitals, indicating that efforts to prevent transmission should include a variety of healthcare settings. These unique data, which include clinical data and isolate reports from a variety of healthcare settings and patients, highlight potential opportunities to reduce transmission.

The incidence rates for carbapenem-nonsusceptible *A. baumannii* are lower than those reported from the identical EIP catchment areas for CRE (2.93 cases/100,000 population) (*21*) and substantially lower than rates reported from EIP for invasive methicillin-resistant *Staphylococcus aureus* (25.1/100,000) (*22*) and for *Clostridium difficile* (141.77/100,000) infections (*23*). The reasons for the lower incidence of carbapenem-nonsusceptible *A. baumannii* in this population than for other healthcare-associated pathogens are not clear but might be related to the low virulence of carbapenem-nonsusceptible *A. baumannii* (*2*) and the lack of dominant, well-adapted clones capable of spreading easily from person to person or within healthcare environments in our specific surveillance areas (*1*,*2*,*24*). However, because this surveillance is population-based, we were unable to measure the incidence of carbapenem-nonsusceptible *A. baumannii* within individual healthcare facilities, where it could be substantial.

Nearly all incident carbapenem-nonsusceptible *A. baumannii* cases were healthcare-associated; the most common exposures were admission to a short-stay acute-care hospital or residence in an LTCF during the previous year or the presence of an indwelling device. Similarly, Zeana et al. found multidrug-resistant phenotypes only among the hospital strains of *A. baumannii* collected from 2 US hospitals and from the community (*25*). Our findings support current recommendations to focus on preventing *A. baumannii* transmission in long-term care and acute-care hospital settings (*26*). In addition, the large proportion of patients transferred to LTCFs (60.2%) highlights the critical need for reporting patient multidrug-resistant organism status at interfacility transfer to ensure no gaps exist in the application of appropriate precautions. We observed substantial heterogeneity in adjusted incidence rates among EIP sites: a 20-fold difference between the site with the highest incidence (Maryland, 2.29 cases/100,000 persons) and the site with the lowest incidence (Oregon, 0.07/100,000). Similar geographic heterogeneity has been described with CRE (*21*) and might reflect several factors, including the underlying resistance mechanisms present or circulating among organisms in a specific location, length of time the organisms have been present in the region, and the implementation of infection control interventions to control spread.

Yearly adjusted incidence rates did not change significantly during 2013–2015 in the EIP surveillance catchment area. Although not always concordant with changes in incidence rates, the percentage of *Acinetobacter* spp. resistant to a carbapenem from healthcare-associated infections reported to the National Healthcare Safety Network decreased slightly from 2011 to 2014; in 2014, the percentage of *Acinetobacter* spp. nonsusceptible to a carbapenem was 50%, compared with 58% in 2011 (*5*,*27*). By contrast, before 2012, multiple US reports documented increases in resistant *Acinetobacter* (*28–30*). In a small study of clinical isolates conducted in Detroit during 2003–2008,

Table 4. Antimicrobial susceptibility of 621 carbapenem-nonsusceptible *Acinetobacter baumannii* isolates reported by local clinical laboratories in Emerging Infections Program sites, United States, 2012–2015*

Antimicrobial agent	No. susceptible isolates/no. isolates tested (%)			p value†
	Total (%)	Sterile site cultures, n = 173	Urine cultures, n = 425	
Any aminoglycoside‡	421/577 (72.9)	123/166 (74.1)	298/411 (72.5)	0.70
Tobramycin	308/541 (56.9)	92/158 (58.2)	216/383 (56.4)	0.70
Amikacin	254/416 (61.1)	71/121 (58.7)	183/295 (62.0)	0.52
Gentamicin	175/571 (30.7)	49/163 (30.1)	126/408 (30.9)	0.85
Any fluoroquinolone‡	20/575 (3.5)	1/164 (0.6)	19/411 (4.6)	0.02
Levofloxacin	15/432 (3.5)	1/120 (0.8)	14/312 (4.5)	0.08
Ciprofloxacin	10/522 (1.9)	1/145 (0.7)	9/377 (2.4)	0.30
Any extended-spectrum β-lactam‡	114/577 (19.8)	27/165 (16.4)	87/412 (21.1)	0.20
Ceftazidime	72/447 (16.1)	17/129 (13.2)	55/318 (17.3)	0.28
Cefepime	68/562 (12.1)	18/161 (11.2)	50/401 (12.5)	0.67
Piperacillin/tazobactam	4/113 (3.5)	1/37 (2.7)	3/76 (1.9)	>0.99
Other				
Ampicillin/sulbactam	180/498 (36.1)	47/146 (32.2)	133/352 (37.8)	0.24
Colistin	114/122 (93.4)	36/39 (92.3)	78/83 (94.0)	0.73
Trimethoprim/sulfamethoxazole	83/483 (17.2)	26/142 (18.3)	57/341 (16.7)	0.67
Tigecycline	74/120 (61.7)	27/40 (67.5)	47/80 (58.8)	0.35

*The study areas were Denver, CO; Atlanta, GA; Baltimore, MD; Minneapolis/Saint Paul, MN, Albuquerque, NM; Rochester, NY; Portland, OR; Nashville, TN.
†The χ^2 test or Fisher exact test was used to test the null hypothesis "carbapenem-nonsusceptible *A. baumannii* isolates antimicrobial susceptibility did not differ for sterile site vs. urine cultures." Fisher exact test was used when >1 cell size was <5.
‡Includes the antimicrobial drugs listed below.

the total number of patients with *A. baumannii* increased from 1.7/1,000 patient days in 2003 to 3.7/1,000 patient days in 2008; among these same patients the percentage of *Acinetobacter* isolates that were susceptible to imipenem decreased from 99% in 2003 to 42% in 2008 (*29*). In another US study of susceptibility results from hospital clinical microbiology laboratories contributing data to the Eurofins laboratory testing network across the United States, the percentage of *A. baumannii* isolates that were resistant to carbapenems increased from 21% in 2003–2005 to 48% in 2009–2012 (*30*). The relatively small number of cases and relatively short interval in our evaluation preclude us from identifying a clear trend in disease; additional years of surveillance data are needed to clarify these trends and the factors contributing to resistance and incidence differences across geographic regions.

Antimicrobial drug susceptibility testing performed at local laboratories demonstrated high levels of resistance to other antimicrobial drugs in addition to carbapenems. Most isolates were also nonsusceptible to cephalosporins, fluoroquinolones, trimethoprim/sulfamethoxazole, ampicillin/sulbactam, and piperacillin/tazobactam. Most remained susceptible to at least 1 aminoglycoside and, for the subset for which a result was available, to colistin and tigecycline. The 3 drug classes to which most isolates were susceptible can be associated with substantial toxicities or treatment failure (*29*) and are generally considered second-line agents for treatment. Although we did not collect data on carbapenem-nonsusceptible *A. baumannii* infection treatment and were unable to determine the proportion of deaths attributable to *Acinetobacter* infection, the limited availability of drugs to which carbapenem-nonsusceptible *A. baumannii* isolates were susceptible could have contributed to the overall death rate of 41% for cases for which carbapenem-nonsusceptible *A. baumannii* was isolated from a sterile site.

Our findings are subject to several limitations. First, because not all local clinical laboratories serving the catchment area participated during the entire period, these results underestimate the true incidence of carbapenem-nonsusceptible *A. baumannii*, particularly among specific populations, such as dialysis patients and LTCF residents. Second, although *Acinetobacter* can be isolated from sputum and other nonsterile sites, these sources were not included in the surveillance, which resulted in an underestimation of the total number of cases. Third, we did not collect carbapenem-nonsusceptible *A. baumannii* isolates and therefore were unable to describe resistance mechanisms. A better understanding of these mechanisms could inform prevention and control strategies. Going forward, isolate collection through CDC's Antimicrobial Resistance Laboratory Network will help to define *Acinetobacter* resistance mechanisms in the United States. Fourth, although 15 million persons live in the areas under surveillance, the data demonstrate considerable geographic heterogeneity; therefore the results of this analysis might not be generalizable to all areas of the United States. Fifth, use of the population of the catchment area is an imperfect denominator to represent the burden of disease attributable to a pathogen largely concentrated within selected healthcare facilities. Sixth, data were retrospectively abstracted from medical records, and the quality and completeness of such records can vary among healthcare systems and facility types, resulting in underreporting of some data elements. Finally, our incidence

case definition was based on a 30-day period; extending the interval between incident cases or excluding recurrent cases would have resulted in a lower incidence rate.

In summary, we present population-based carbapenem-nonsusceptible *A. baumannii* incidence rates in the United States and provide additional information about the epidemiology of carbapenem-nonsusceptible *A. baumannii*. These data, along with data from the National Healthcare Safety Network, provide early evidence that carbapenem resistance among *A. baumannii* isolates might have plateaued, although additional years of surveillance in both systems are needed to confirm this observation. Despite a currently low population-based incidence, the medical complexity of carbapenem-nonsusceptible *A. baumannii* patients, along with treatment challenges posed by high levels of resistance to noncarbapenem antimicrobial drugs and high death rates, highlight the need for additional work in healthcare settings to contain carbapenem-nonsusceptible *A. baumannii* spread.

Acknowledgments

We thank the MuGSI Information Technology Team, especially Tonya Habersham, Joseph Dunlap, and Christopher Jason Hall, for providing us with the MuGSI Data Management System. We also acknowledge Shelley Magill for her leadership of the Healthcare-Associated Infections Community Interface program and editorial assistance; Isaac See for his scientific input; Shirley Zhang, Ruby Phelps, David G. Kleinbaum, andYi Mu for their assistance with data management and statistical analysis; and Taylor Chambers, Sarah Harb, Stepy Thomas, Jane Harper, and Annastasia Gross for assistance with data collection in the field.

The Healthcare-Associated Infections Community Interface MuGSI program is supported through CDC's cooperative agreement, CDC-RFA-CK17-1701.

About the Author

Ms. Bulens is a health scientist in the Division of Healthcare Quality Promotion, National Center for Emerging and Zoonotic Infectious Diseases, CDC. Her research interests include surveillance for carbapenem-resistant *Acinetobacter baumannii* and other carbapenem-resistant gram-negative bacteria.

References

1. Peleg AY, Seifert H, Paterson DL. *Acinetobacter baumannii*: emergence of a successful pathogen. Clin Microbiol Rev. 2008;21:538–82. http://dx.doi.org/10.1128/CMR.00058-07
2. Pogue JM, Mann T, Barber KE, Kaye KS. Carbapenem-resistant *Acinetobacter baumannii*: epidemiology, surveillance and management. Expert Rev Anti Infect Ther. 2013;11:383–93. http://dx.doi.org/10.1586/eri.13.14
3. Towner KJ. Acinetobacter: an old friend, but a new enemy. J Hosp Infect. 2009;73:355–63. http://dx.doi.org/10.1016/j.jhin.2009.03.032
4. Centers for Disease Control and Prevention. Antibiotic resistance threats in the United States, 2013 [cited 2017 Apr 24]. https://www.cdc.gov/drugresistance/threat-report-2013/pdf/ar-threats-2013-508.pdf
5. Centers for Disease Control and Prevention. CDC's antibiotic resistance patient safety atlas [cited 2017 Apr 24]. https://gis.cdc.gov/grasp/PSA/MapView.html
6. Falagas ME, Bliziotis IA, Siempos II. Attributable mortality of *Acinetobacter baumannii* infections in critically ill patients: a systematic review of matched cohort and case-control studies. Crit Care. 2006;10:R48. http://dx.doi.org/10.1186/cc4869
7. Falagas ME, Rafailidis PI. Attributable mortality of *Acinetobacter baumannii*: no longer a controversial issue. Crit Care. 2007;11:134. http://dx.doi.org/10.1186/cc5911
8. Grupper M, Sprecher H, Mashiach T, Finkelstein R. Attributable mortality of nosocomial *Acinetobacter* bacteremia. Infect Control Hosp Epidemiol. 2007;28:293–8. http://dx.doi.org/10.1086/512629
9. Sunenshine RH, Wright MO, Maragakis LL, Harris AD, Song X, Hebden J, et al. Multidrug-resistant *Acinetobacter* infection mortality rate and length of hospitalization. Emerg Infect Dis. 2007;13:97–103. http://dx.doi.org/10.3201/eid1301.060716
10. Nutman A, Glick R, Temkin E, Hoshen M, Edgar R, Braun T, et al. A case–control study to identify predictors of 14-day mortality following carbapenem-resistant *Acinetobacter baumannii* bacteraemia. Clin Microbiol Infect. 2014;20:O1028–34. http://dx.doi.org/10.1111/1469-0691.12716
11. Office of the Assistant Secretary for Health. Presidential Advisory Council on Combating Antibiotic-Resistant Bacteria [cited 2017 Jul 27]. https://www.hhs.gov/ash/advisory-committees/paccarb/about-paccarb/index.html
12. US Census Bureau. 2015 Population estimates [cited 2016 Jun 27]. http://quickfacts.census.gov/qfd/index.html
13. Clinical and Laboratory Standards Institute. Performance standards for antimicrobial susceptibility testing: twenty-second informational supplement (M100–S22). Wayne (PA): The Institute; 2012.
14. Reno J, Schenck C, Scott J, Clark LA, Wang YF, Ray S, et al. Querying automated antibiotic susceptibility testing instruments: a novel population-based active surveillance method for multidrug-resistant gram-negative bacilli. Infect Control Hosp Epidemiol. 2014;35:336–41.http://dx.doi.org/10.1086/675608
15. McGregor JC, Kim PW, Perencevich EN, Bradham DD, Furuno JP, Kaye KS, et al. Utility of the Chronic Disease Score and Charlson Comorbidity Index as comorbidity measures for use in epidemiologic studies of antibiotic-resistant organisms. Am J Epidemiol. 2005;161:483–93. http://dx.doi.org/10.1093/aje/kwi068
16. McGregor JC, Perencevich EN, Furuno JP, Langenberg P, Flannery K, Zhu J, et al. Comorbidity risk-adjustment measures were developed and validated for studies of antibiotic-resistant infections. J Clin Epidemiol. 2006;59:1266–73. http://dx.doi.org/10.1016/j.jclinepi.2006.01.016
17. Daly L. Simple SAS macros for the calculation of exact binomial and Poisson confidence limits. Comput Biol Med. 1992;22:351–61. http://dx.doi.org/10.1016/0010-4825(92)90023-G
18. Dobson AJ, Kuulasmaa K, Eberle E, Scherer J. Confidence intervals for weighted sums of Poisson parameters. Stat Med. 1991;10:457–62. http://dx.doi.org/10.1002/sim.4780100317
19. Rothman KJ, Boice JD. Exact Testing and Estimation Program 15: exact (and approximate) confidence limits for a proportion. In: Epidemiologic analysis with a programmable calculator. Bethesda (MD): National Institutes of Health; 1979. p. 31–32 [cited 2017 Feb 27]. http://www.epi.msu.edu/janthony/Epidemiologic%20Analysis%20with%20a%20Programmable%20Calculator.pdf
20. Schoenbach VJ. Standardization of rates and ratios [cited 2017 Mar 7]. http://www.epidemiolog.net/evolving/Standardization.pdf

21. Guh AY, Bulens SN, Mu Y, Jacob JT, Reno J, Scott J, et al. Epidemiology of carbapenem-resistant *Enterobacteriaceae* in 7 US communities, 2012–2013. JAMA. 2015;314:1479–87. http://dx.doi.org/10.1001/jama.2015.12480
22. Dantes R, Mu Y, Belflower R, Aragon D, Dumyati G, Harrison LH, et al.; Emerging Infections Program—Active Bacterial Core Surveillance MRSA Surveillance Investigators. National burden of invasive methicillin-resistant *Staphylococcus aureus* infections, United States, 2011. JAMA Intern Med. 2013;173:1970–8.
23. Centers for Disease Control and Prevention. 2013 annual report for the Emerging Infections Program for *Clostridium difficile* infection [cited 2017 Apr 24]. https://www.cdc.gov/hai/eip/pdf/cdiff/2013-annual-report.pdf
24. Munoz-Price LS, Arheart K, Nordmann P, Boulanger AE, Cleary T, Alvarez R, et al. Eighteen years of experience with *Acinetobacter baumannii* in a tertiary care hospital. Crit Care Med. 2013;41:2733–42. http://dx.doi.org/10.1097/CCM.0b013e318298a541
25. Zeana C, Larson E, Sahni J, Bayuga SJ, Wu F, Della-Latta P. The epidemiology of multidrug-resistant *Acinetobacter baumannii*: does the community represent a reservoir? Infect Control Hosp Epidemiol. 2003;24:275–9. http://dx.doi.org/10.1086/502209
26. Slayton RB, Toth D, Lee BY, Tanner W, Bartsch SM, Khader K, et al.; Centers for Disease Control and Prevention. Vital signs: estimated effects of a coordinated approach for action to reduce antibiotic-resistant infections in health care facilities—United States. MMWR Morb Mortal Wkly Rep. 2015;64:826–31. http://dx.doi.org/10.15585/mmwr.mm6430a4
27. Weiner LM, Webb AK, Limbago B, Dudeck MA, Patel J, Kallen AJ, et al. Antimicrobial-resistant pathogens associated with healthcare-associated infections: summary of data reported to the National Healthcare Safety Network at the Centers for Disease Control and Prevention, 2011–2014. Infect Control Hosp Epidemiol. 2016;37:1288–301. http://dx.doi.org/10.1017/ice.2016.174
28. Sievert DM, Ricks P, Edwards JR, Schneider A, Patel J, Srinivasan A, et al.; National Healthcare Safety Network (NHSN) Team and Participating NHSN Facilities. Antimicrobial-resistant pathogens associated with healthcare-associated infections: summary of data reported to the National Healthcare Safety Network at the Centers for Disease Control and Prevention, 2009—2010. Infect Control Hosp Epidemiol. 2013;34:1–14. http://dx.doi.org/ 10.1086/668770
29. Reddy T, Chopra T, Marchaim D, Pogue JM, Alangaden G, Salimnia H, et al. Trends in antimicrobial resistance of *Acinetobacter baumannii* isolates from a metropolitan Detroit health system. Antimicrob Agents Chemother. 2010;54:2235–8. http://dx.doi.org/10.1128/AAC.01665-09
30. Zilberberg MD, Kollef MH, Shorr AF. Secular trends in *Acinetobacter baumannii* resistance in respiratory and blood stream specimens in the United States, 2003 to 2012: a survey study. J Hosp Med. 2016;11:21–6. http://dx.doi.org/10.1002/jhm.2477

Address for correspondence: Sandra N. Bulens, Centers for Disease Control and Prevention, 1600 Clifton Rd NE, Mailstop A16, Atlanta, GA, 30329-4027, USA; email: zgf6@cdc.gov

Cooperative Recognition of Internationally Disseminated Ceftriaxone-Resistant *Neisseria gonorrhoeae* Strain

Monica M. Lahra, Irene Martin, Walter Demczuk, Amy V. Jennison, Ken-Ichi Lee, Shu-Ichi Nakayama, Brigitte Lefebvre, Jean Longtin, Alison Ward, Michael R. Mulvey, Teodora Wi, Makoto Ohnishi, David Whiley

Ceftriaxone remains a first-line treatment for patients infected by *Neisseria gonorrhoeae* in most settings. We investigated the possible spread of a ceftriaxone-resistant FC428 *N. gonorrhoeae* clone in Japan after recent isolation of similar strains in Denmark (GK124) and Canada (47707). We report 2 instances of the FC428 clone in Australia in heterosexual men traveling from Asia. Our bioinformatic analyses included core single-nucleotide variation phylogeny and in silico molecular typing; phylogenetic analysis showed close genetic relatedness among all 5 isolates. Results showed multilocus sequence type 1903; *N. gonorrhoeae* sequence typing for antimicrobial resistance (NG-STAR) 233; and harboring of mosaic *penA* allele encoding alterations A311V and T483S (*penA*-60.001), associated with ceftriaxone resistance. Our results provide further evidence of international transmission of ceftriaxone-resistant *N. gonorrhoeae*. We recommend increasing awareness of international spread of this drug-resistant strain, strengthening surveillance to include identifying treatment failures and contacts, and strengthening international sharing of data.

Author affiliations: World Health Organization, Sydney, New South Wales, Australia (M.M. Lahra); University of New South Wales School of Medical Sciences, Sydney (M.M. Lahra); Public Health Agency of Canada, Winnipeg, Manitoba, Canada (I. Martin, W. Demczuk, M.R. Mulvey); Health Support Queensland, Brisbane, Queensland, Australia (A.V. Jennison); National Institute of Infectious Diseases, Tokyo, Japan (K.-I. Lee, S.-I. Nakayama, M. Ohnishi); Institut National de Sante Publique Québec, Ste-Anne-de-Bellevue, Quebec, Canada (B. Lefebvre, J. Longtin); Royal Adelaide Hospital, Adelaide, South Australia, Australia (A. Ward); World Health Organization, Geneva, Switzerland (T. Wi); National Institute of Infectious Diseases, Tokyo (M. Ohnishi); The University of Queensland Faculty of Medicine, Brisbane (D. Whiley)

DOI: https://doi.org/10.3201/eid2404.171873

Ceftriaxone is among the last remaining recommended therapies for treating *Neisseria gonorrhoeae* infections and is used in many countries around the world as part of a dual therapy with azithromycin. Cephalosporin resistance in *N. gonorrhoeae* has been associated with modifications of the *penA* gene, which encodes penicillin-binding protein 2 (PBP2), a target for β-lactam antimicrobial drugs (*1*). During 2009–2015, several ceftriaxone-resistant (MIC 0.5–4 mg/L) *N. gonorrhoeae* strains were reported: in 2009, H041 in Japan (*2*); in 2010, F89 in France (*3*); in 2011, F89 in Spain (*4*); in 2013, A8806 in Australia (*5*); in 2014, GU140106 in Japan (*6*); and in 2015, FC428 and FC460 in Japan (*7*). However, until 2017, all of these strains were considered to have occurred sporadically because, except for limited transmission of F89 among persons in France and Spain during 2010–2011, there had been no reports of sustained transmission of these strains identified nationally or internationally. In 2017, this changed, substantiated by independent reports from Canada (*8*) and Denmark (*9*) of gonococcal isolates that had substantive similarity to the previously described FC428 strain in Japan.

The first reported case of the FC428 ceftriaxone-resistant *N. gonorrhoeae* strain was in Japan during January 2015 in a heterosexual man in his twenties who had urethritis (*7*). The FC428 isolate was resistant to ceftriaxone (MIC 0.5 mg/L), cefixime (MIC 1 mg/L), and ciprofloxacin (MIC >32 mg/L); susceptible to spectinomycin (MIC 8 mg/L) and azithromycin (MIC 0.25 mg/L); and, unlike all previously described ceftriaxone-resistant strains, a penicillinase-producing *N. gonorrhoeae* (PPNG; MIC ≥32 mg/L) bacterium. The patient was treated successfully with a single dose of spectinomycin 2 g intramuscularly (IM); however, a second isolate with an identical susceptibility profile (FC460) was subsequently cultured from the same patient 3 months later, suggesting reinfection by a separate contact.

In Canada, during January 2017, a gonococcal isolate (47707) (*8*) of similar susceptibility to the first reported case

(including ceftriaxone-resistant MIC 1 mg/L and PPNG; Table 1 [*10*]) was isolated from a sample collected from a 23-year-old woman. This patient had no history of travel, but her male partner, who had been treated empirically and had no culture results available, reported sexual contact during travel in China and Thailand during the fall of 2016. She was successfully treated with combination therapy of a single dose each of cefixime (800 mg orally) and azithromycin (1 g orally) and an additional dose 13 days later of azithromycin (2 g orally). The strain from Denmark (GK124) was also isolated in January 2017, had a similar susceptibility profile to FC428, and was obtained from a heterosexual man in his twenties who had reported unprotected sexual contact with women from Denmark, China, and Australia (*9*). The patient was successfully treated with single doses of ceftriaxone (0.5 g IM) and azithromycin (2 g orally). Here, we report additional FC-428–like cases among persons in Australia, providing further evidence of the sustained international transmission of a ceftriaxone-resistant *N. gonorrhoeae* strain.

Methods

We confirmed *N. gonorrhoeae* isolates by using matrix-assisted laser desorption/ionization time-of-flight mass spectrometry (Bruker Daltonics, Melbourne, Victoria, Australia; bioMérieux, Brisbane, Queensland, Australia). We determined antimicrobial susceptibilities of *N. gonorrhoeae* to ceftriaxone, penicillin, tetracycline, azithromycin, gentamicin, and ciprofloxacin by using Etest (bioMérieux) and spectinomycin by using the agar dilution method (*11*). We interpreted MIC on the basis of interpretive criteria from the Clinical and Laboratory and Standards Institute (*12*): penicillin resistance (MIC ≥2.0 mg/L); tetracycline resistance (MIC ≥2.0 mg/L); ciprofloxacin resistance (MIC ≥1.0 mg/L); and spectinomycin resistance (MIC ≥128.0 mg/L). Because the Clinical and Laboratory Standards Institute does not have an azithromycin breakpoint, and ceftriaxone breakpoints only state susceptibility (≤0.25 mg/L), we used the European Committee on Antimicrobial Susceptibility Testing (*13*) breakpoints for ceftriaxone resistance (MIC>0.12 mg/L) and azithromycin resistance (MIC>0.5 mg/L). β-lactamase production was analyzed by using nitrocefin (Thermo-Fisher Scientific, Melbourne, Victoria, Australia). We subcultured isolates on GC agar base with Vitox Supplement (Thermo-Fisher Scientific) and incubated for 24 h at 35°C in a 5% CO_2 atmosphere with or without antimicrobial drugs and stored in Tryptone (Thermo-Fisher Scientific) soya broth with 10% glycerol at –80°C.

Genomic Analyses

We put each isolate from Japan and Australia through DNA extraction, library preparation, and sequencing (Illumina, San Diego, CA, USA). From the strains from Japan, FC428 and FC460, we extracted DNA samples with the DNeasy Blood & Tissue Kit (QIAGEN, Tokyo, Japan). We created multiplexed libraries with Nextera XT DNA sample prep kit (Illumina) and generated paired-end 300-bp indexed reads on the Illumina MiSeq platform (Illumina) yielding 6,121,575 reads/genome and genome coverage of 845× for FC428 and 1,272,909 reads/genome and genome coverage of 845× for FC460.

Table 1. Phenotypic and molecular characterization of ceftriaxone-resistant *Neisseria gonorrhoeae**

Isolate ID	Year	Country (ref)	MIC, mg/L									MLST	*porB*	*tbpB*	NG-MAST	*penA*	NG-STAR
			CEF	CFM	SPX	TET	CIP	AZM	GEN	PCN	β-lac, PPNG						
FC428	2015	Japan (*7*)	0.5	1	8	0.5	>32	0.25	8	≥32	+	1903	1053	21	3435	60.001	233
FC460	2015	Japan (*7*)	0.5	1	8	0.5	>32	0.25	8	≥32	+	1903	1053	21	3435	60.001	233
GK124	2017	DEN (*9*)	0.5	1	8	NA	>32	0.5	NA	>256	NA	1903	1053	33	1614	NA	NA
47707	2017	Canada (*8*)	1	2	16	4	32	0.5	8	≥256	+	1903	1053	33	1614	60.001	233
A7846	2017	AUS (This study)	0.5	NA	8	2	>32	0.25	4	≥32	+	1903	1053	33	1614	60.001	233
A7536	2017	AUS (This study)	0.5	NA	8	4	>32	0.25	4	≥32	+	1903	9300	21	15925	60.001	233
F89	2010	France (*3,10*)	1	2	16	4	>32	1	8	1	–	1901	908	110	1407	42.001	16
A8806	2013	AUS (*5,10*)	0.5	2	16	4	>32	1	4	2	–	7363	1059	10	4015	64.001	227
H041	2009	Japan (*2*)	2	4	16	2	>32	0.5	4	4	–	7363	2594	10	4220	37.001	226

*AUS, Australia; AZM, azithromycin; β-lac, β-lactamase; CEF, ceftriaxone; CFM, cefixime; CIP, ciprofloxacin; DEN, Denmark; GEN, gentamicin; MLST, multilocus sequence type; NG-MAST, *Neisseria gonorrhoeae* multi-antigen sequence type; NG-STAR, *Neisseria gonorrhoeae* sequence type for antimicrobial resistance; NA, not available; PCN, penicillin; PPNG, penicillinase-producing *N. gonorrhoeae*; ref, reference; SPX, spectinomycin; TET, tetracycline; +, positive; –, negative.

To analyze the strains from Australia, A7536 and A7846, we extracted DNA on the QIAsymphony SP (QIAGEN) by using the DSP DNA Mini Kit (QIAGEN). We prepared the libraries according to manufacturer instructions for the Nextera XT library preparation kit (Illumina) and sequenced on the NextSeq 500 (Illumina) by using the NextSeq 500 Mid Output V2 kit (Illumina). Sequencing generated 6,763,774 reads and genome coverage of 361× for A7536 and 3,672,072 reads and genome coverage of 202× for A7846.

We then provided sequencing data to the Canadian National Microbiology Laboratory, where bioinformatic analyses were performed as previously described (*14*). Quality reads were assembled by using SPAdes (*15*) (http://bioinf.spbau.ru/spades) and annotated with Prokka (*16*) (https://github.com/tseemann/prokka), and produced an average of 86 contigs per isolate, an average contig length of 26,276 nt, and an average N50 length of 68,884 nt. Quality metrics for whole-genome sequencing (WGS) are shown in online Technical Appendix Table 1 (https://wwwnc.cdc.gov/EID/article/24/4/17-1873-Techapp1.pdf). A core single-nucleotide variation (SNV) phylogeny was created by mapping reads to FA1090 (GenBank accession no. NC_002946.2) by using a custom Galaxy SNVPhyl workflow (*17*). Repetitive and highly recombinant regions with >2 SNVs per 500 nt were removed from the analysis. The percentage of valid and included positions in the core genome was 97.6%; 567 sites were used to generate the phylogeny. We used a metaalignment of informative core SNV positions to create a maximum-likelihood phylogenetic tree for A7536, A7846, FC428, FC460, and 47707 (Figure). The H041, F89, and A8806 ceftriaxone-resistant strains (available in the World Health Organization [WHO] reference panel as WHO-X, WHO-Y, and WHO-Z, respectively) (*10*) were included for comparison. WGS read data for A7536, A7846, FC428, and FC460 are available under BioProject PRJNA416507, and previously reported 47707 was submitted under BioProject PRJNA415047 (*8*) .

We implemented *N. gonorrhoeae* multiantigen sequence typing (NG-MAST) (*18*), multilocus sequence typing (MLST) (*19*), and *N. gonorrhoeae* sequence typing for antimicrobial resistance (NG-STAR) (*20*) by using gene sequences extracted in silico from WGS data. We submitted the sequences to the NG-MAST (http://www.ng-mast.net/), *Neisseria* MLST (http://pubmlst.org/neisseria/), and NG-STAR (https://ngstar.canada.ca) databases to determine respective sequence types. Sequence data for the GK124 strain (*9*) were not available for these analyses; however, a summary of the documented susceptibility and MLST and NG-MAST data is provided (Table 1).

Results

Case Histories and Isolate Details

The first documented case-patient in Australia was a man in his forties who was visiting from the Philippines. He went to a sexual health clinic in Adelaide in April 2017 reporting urethral discharge and dysuria. He reported recent heterosexual contact with multiple female sex workers in Cambodia and the Philippines; it was unclear where the infection was acquired. An *N. gonorrhoeae* isolate (A7846) of similar susceptibility to FC428 (showing the characteristic ceftriaxone resistance and PPNG; Table 1) was cultured. The patient was treated with a 1-time dose combination therapy of ceftriaxone (500 mg IM) and azithromycin

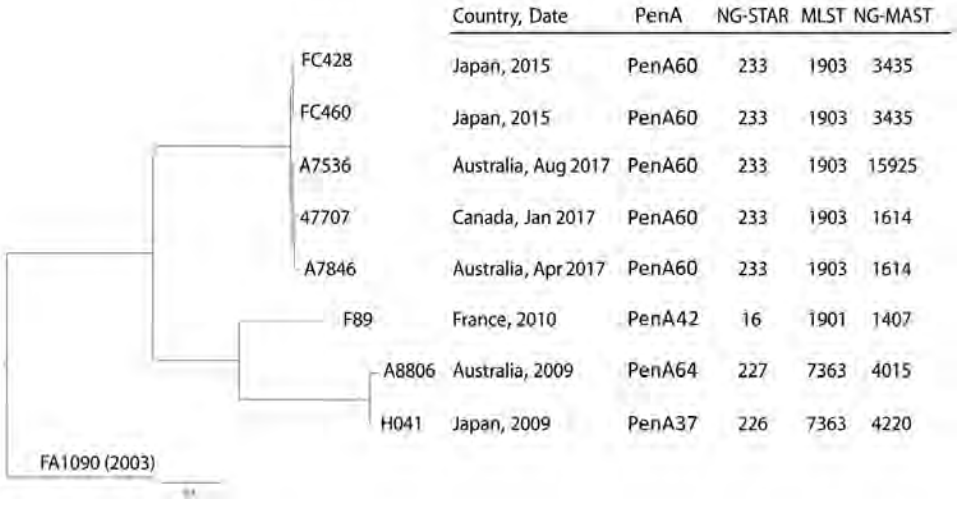

Figure. Core single-nucleotide variation (SNV) phylogenetic tree of ceftriaxone-resistant *Neisseria gonorrhoeae* isolates. The maximum-likelihood phylogenetic tree is rooted on the reference genome of *N. gonorrhoeae* FA1090 (GenBank accession no. NC_002946.2). Isolates are indicated by country and year. Strains F89, A8806, and H041 (World Health Organization [WHO] reference panel WHO-Y, WHO-Z, and WHO-X, respectively) are previously reported ceftriaxone-resistant reference strains (*10*). Scale bar indicates estimated evolutionary divergence between isolates on the basis of average genetic distance between strains (estimated number of substitutions in the sample/total number of high-quality SNVs). MLST, multilocus sequence type; NG-MAST, *Neisseria gonorrhoeae* multiantigen sequence type; NG-STAR, *Neisseria gonorrhoeae* sequence type for antimicrobial resistance; PenA, penicillin-binding protein 2.

(1 g orally). A test result 7 days after treatment was negative for *N. gonorrhoeae*.

A second case-patient in Australia was a man visiting from China. He was in his early 40s and described symptoms of urethral discharge and dysuria to a general practitioner in Sydney in August 2017. He reported heterosexual contact in China, but none in Australia. An isolate (A7536) of similar susceptibility to FC428 (ceftriaxone-resistant and PPNG; Table 1) was cultured. The patient was treated with a 1-time dose combination therapy of ceftriaxone (500 mg IM) and azithromycin (1 g orally); he returned to China shortly thereafter. Attending physicians advised him to return to follow up for test of cure and to trace contacts, but follow-up was not confirmed.

Core SNV phylogenetic analysis results (Figure) showed a close genetic relatedness among the FC428, FC460, 47707, A7536, and A7846 isolates. These isolates were distinct from the other previously described F89, A8806, and H041 ceftriaxone-resistant strains; the 2 groups of isolates were separated from each other by an average of 292 core SNVs. We detected no SNVs in the 2 isolates from Japan (FC428, FC460 collected from the same patient 3 months apart). For other isolates, 12 SNVs separated FC428 from both 47707 and A7536; 17 SNVs separated FC428 and A7846 (47707, A7536, and A7846 shared 8 identical SNVs); 8 SNVs separated 47707 and A7536; 5 SNVs separated 47707 and A7846; and 11 SNVs separated A7536 and A7846 (online Technical Appendix Table 2).

Molecular typing of FC428, FC460, 47707, A7536, and A7846 from the WGS showed an identical MLST of ST1903, which was also reported for GK124 from Denmark (*9*) (Table 1). We observed different NG-MAST: ST3435 for FC428 and FC460; ST1614 for 47707, A7846, and GK124; and ST15925 for A7536. FC428, FC460, 47707, A7536, and A7846 were of the same NG-STAR, ST233, which was characterized by a mosaic *penA*-60.001 allele that had only been reported previously for FC428 and 47707 (*8*). This allele encodes key alterations A311V and T483S in PBP2 (Table 2; also observed for GK124) that are linked to ceftriaxone resistance, some of which are also present among the previously described ceftriaxone-resistant strains (Table 2 [*1*]). We observed additional resistance mutations for FC428, FC460, 47707, A7536, and A7846 by using the NG-STAR designations, including the previously described alleles *mtrR*-1 (promoter-35A deletion); *porB*-8 (PorB G120K, PorB A121D); *ponA*-1 (PonA L421P); *gyrA*-7 (GyrA S91F, GyrA D95A); and *parC*-3 (ParC S87R).

Discussion

The recent reports of the *N. gonorrhoeae* FC428 clonal strain in Denmark, Canada, and now Australia provide new evidence that there is sustained international transmission of a ceftriaxone-resistant *N. gonorrhoeae* strain. This strain appears to have been circulating globally for ≥2 years. Thus, it is highly likely this strain is prevalent elsewhere, possibly in Asia, but undetected. There are serious gaps in *N. gonorrhoeae* antimicrobial resistance surveillance worldwide (*21*), and we estimate that samples from as few as 0.1% of the estimated 80 million cases of *N. gonorrhoeae* reported globally each year (*22*) are tested for antimicrobial resistance. Therefore, there are many opportunities for such strains to avoid detection.

Fortunately, the ceftriaxone MICs of the FC428 clonal strain remain lower than the H041 strain from Japan (MIC 2 mg/L) (*2*), and further, the FC428 strain does not exhibit resistance to azithromycin (Table 1). Therefore, treatment failure is arguably less likely against FC428 infections than in H041 and F89 infections, particularly when using ceftriaxone and azithromycin dual therapy; treatment failure was not observed in our study. Nevertheless, previous pharmacodynamic analyses indicate that ceftriaxone MICs of 0.5–1.0 mg/L can result in treatment failures with ceftriaxone 250 mg monotherapy and even (albeit to a lesser extent) when 1.0 g doses are used (*23*). As such, a dissemination of the FC428 clone could offset dual therapy guidelines because azithromycin resistance is being increasingly reported (*24*,*25*).

Table 2. PenA types identified in ceftriaxone-resistant *Neisseria gonorrhoeae* strains*

PenA type	Strain ID	Amino acid position in PenA protein (*2*,*18*)
		3471111122222222222333333333333333333333333333444444444444444444455555555555555555
		5100046700001367889111222222333344444577778880001113445666667788800111134445555567 7
		0140312344029581126346789012512356346783691470238488235690314625136732360236775 6
		↑ ↑ ↑
0	M32091	MCAKDDVNYGEDQQAADRRAIVAGTDLNERLQPSPR.SRGAEFEITLNRRPAVLQIFESRENPTTAFANVAAHGGAPPKII.A
37	H041	....E.ASHAGEE..VEKQVMPS.V.TTDTFL.ATQ.TMTPK.DVSV.K..VEVKVIA.KKEASI.LVY...N.ST.VQVVNV
42	F89	....E.ASHAGEE..VEKQ.MTS.V.ATDTFLSATQ.TMTPK.DV..S.QKVEVKVIA.KKEA..PLVY...N.S.....
60	FC428/ FC460/ A7536/ A7846/ 47707	..................VMTS.V.PTDTFL.ATQ.TMTPK.DV..S.QKVEVKVIA.KKEASI.LVY...N.ST.VQVVNV
64	A8806	....E.ASHAGEE......VMTS.V.PTDTFL.ATQ.TMTPK.DV..S.QKVEVKVIA.KKEASI.LVY...N.ST.VQVVNV

*Arrows indicate key amino acid positions associated with high-level β-lactam resistance. PenA, penicillin-binding protein 2.

The cases of *N. gonorrhoeae* described here and the circumstances under which these analyses took place are also a timely reminder of the need for international collaboration in addressing the overall *N. gonorrhoeae* problem and highlight the benefits of rapid access to genomic data by using electronic communications. In fact, in the absence of WGS data, it would have been very difficult to identify the links between these isolates. Not only have we been able to use these tools to readily identify the problem but we also arguably achieved identification in a sufficiently timely manner as to enable countries to put in place interventions that can limit further the spread of this strain, including intensifying follow-up and contact tracing.

Differences in extraction and sequencing procedures among the 3 countries could introduce variations in DNA concentrations that might affect the quality of the sequencing, such as number of reads and depth of coverage. This limitation was minimized because downstream processing of the data, such as assembly and reference mapping software algorithms, standardizes input data before detailed analyses of the genomes are conducted. Laboratory and epidemiologic findings are critical for surveillance that closely tracks the dissemination and emergence of epidemic antimicrobial-resistant strains and for rapid recognition and implementation of control measures to limit the expansion of clones through sexual networks. We recommend that health departments in all countries be made aware of this spreading resistant strain and strengthen *N. gonorrhoeae* antimicrobial-resistance monitoring, including treatment failure identification, adequate follow-up and contact tracing of cases, and STI prevention programs.

In conclusion, international collaboration based on WGS typing methods revealed the dissemination of a ceftriaxone-resistant *N. gonorrhoeae* in Japan, Canada, and Australia. Sustained transmission spanning 2 years suggests unidentified cases are likely present in other locations. These findings warrant the intensification of surveillance strategies and establishment of collaborations with other countries to monitor spread and inform national and global policies and actions.

This study was funded by internal funds from the Public Health Agency of Canada and Forensic and Scientific Services, Queensland Department of Health (Queensland, Australia), the Australian Government Department of Health and Ageing, and was partly supported by the Research Program on Emerging and Re-emerging Infectious Diseases, Japan Agency for Medical Research and Development. D.W. is a recipient of an NHMRC fellowship.

D.W. reports research funding from SpeeDx Pty Ltd.

The study was approved by the South Eastern Sydney Local Health District Human Research Ethics Committee (HREC) and The University of Queensland HREC.

About the Author

Prof. Lahra is Medical Director, Division of Bacteriology, and Director of the World Health Organization Collaborating Centre for STD, Sydney, based in the Department of Microbiology, New South Wales Health Pathology, The Prince of Wales Hospital, Sydney. Her research interests include public health and antimicrobial resistance.

References

1. Ohnishi M, Saika T, Hoshina S, Iwasaku K, Nakayama S, Watanabe H, et al. Ceftriaxone-resistant *Neisseria gonorrhoeae*, Japan. Emerg Infect Dis. 2011;17:148–9. http://dx.doi.org/10.3201/eid1701.100397
2. Ohnishi M, Golparian D, Shimuta K, Saika T, Hoshina S, Iwasaku K, et al. Is *Neisseria gonorrhoeae* initiating a future era of untreatable *N. gonorrhoeae*?: detailed characterization of the first strain with high-level resistance to ceftriaxone. Antimicrob Agents Chemother. 2011;55:3538–45. http://dx.doi.org/10.1128/AAC.00325-11
3. Unemo M, Golparian D, Nicholas R, Ohnishi M, Gallay A, Sednaoui P. High-level cefixime- and ceftriaxone-resistant *Neisseria gonorrhoeae* in France: novel *penA* mosaic allele in a successful international clone causes treatment failure. Antimicrob Agents Chemother. 2012;56:1273–80. http://dx.doi.org/10.1128/AAC.05760-11
4. Cámara J, Serra J, Ayats J, Bastida T, Carnicer-Pont D, Andreu A, et al. Molecular characterization of two high-level ceftriaxone-resistant *Neisseria gonorrhoeae* isolates detected in Catalonia, Spain. J Antimicrob Chemother. 2012;67:1858–60. http://dx.doi.org/10.1093/jac/dks162
5. Lahra MM, Ryder N, Whiley DM. A new multidrug-resistant strain of *Neisseria gonorrhoeae* in Australia. N Engl J Med. 2014;371:1850–1. http://dx.doi.org/10.1056/NEJMc1408109
6. Deguchi T, Yasuda M, Hatazaki K, Kameyama K, Horie K, Kato T, et al. New clinical strain of *Neisseria gonorrhoeae* with decreased susceptibility to ceftriaxone, Japan. Emerg Infect Dis. 2016;22:142–4. http://dx.doi.org/10.3201/eid2201.150868
7. Nakayama S, Shimuta K, Furubayashi K, Kawahata T, Unemo M, Ohnishi M. New ceftriaxone- and multidrug-resistant *Neisseria gonorrhoeae* strain with a novel mosaic *penA* gene isolated in Japan. Antimicrob Agents Chemother. 2016;60:4339–41. http://dx.doi.org/10.1128/AAC.00504-16
8. Lefebvre B, Martin I, Demczuk W, Deshaies L, Michaud S, Labbe AC, et al. Ceftriaxone-resistant *Neisseria gonorrhoeae*, Canada, 2017. Emerg Infect Dis. 2018:24(2):381-383. https://dx.doi.org/10.3201/eid2402.171756
9. Terkelsen D, Tolstrup J, Hundahl Johnsen C, Lund O, Kiellberg Larsen H, Worning P, et al. Multidrug-resistant *Neisseria gonorrhoeae* infection with ceftriaxone resistance and intermediate resistance to azithromycin, Denmark, 2017. Euro Surveill. 2017;22:42. http://dx.doi.org/10.2807/1560-7917.ES.2017.22.42.17-00659
10. Unemo M, Golparian D, Sánchez-Busó L, Grad Y, Jacobsson S, Ohnishi M, et al. The novel 2016 WHO *Neisseria gonorrhoeae* reference strains for global quality assurance of laboratory investigations: phenotypic, genetic and reference genome characterization. J Antimicrob Chemother. 2016;71:3096–108. http://dx.doi.org/10.1093/jac/dkw288
11. Clinical and Laboratory Standards Institute. Methods for dilution antimicrobial susceptibility tests for bacteria that grow aerobically; approved standard, 10th edition (M07–A10). Wayne (PA): The Institute; 2015.

12. Clinical and Laboratory Standards Institute. Performance standards for antimicrobial susceptibility testing: twenty-seventh informational supplement (M100–S27). Wayne (PA): The Institute; 2017.
13. European Committee on Antimicrobial Susceptibility Testing. Breakpoint tables for the interpretation of MICs and zone diameters. 2017 [cited 2017 Oct 12]. http://www.eucast.org/clinical_breakpoints/
14. Demczuk W, Lynch T, Martin I, Van Domselaar G, Graham M, Bharat A, et al. Whole-genome phylogenomic heterogeneity of *Neisseria gonorrhoeae* isolates with decreased cephalosporin susceptibility collected in Canada between 1989 and 2013. J Clin Microbiol. 2015;53:191–200. http://dx.doi.org/10.1128/JCM.02589-14
15. Bankevich A, Nurk S, Antipov D, Gurevich AA, Dvorkin M, Kulikov AS, et al. 2012. SPAdes: A new genome assembly algorithm and its applications to single-cell sequencing. J Comp Biol 19:455-77. http://dx.doi.org/10.1089/cmb.2012.0021
16. Seemann T. 2014. Prokka: Rapid prokaryotic genome annotation. Bioinformatics 30:2068-2069. http://dx.doi.org/10.1093/bioinformatics/btu153
17. Petkau A, Mabon P, Sieffert C, Knox NC, Cabral J, Iskander M, et al. SNVPhyl: a single nucleotide variant phylogenomics pipeline for microbial genomic epidemiology. Microb Genom. 2017;3:e000116.
18. Martin IMC, Ison CA, Aanensen DM, Fenton KA, Spratt BG. Rapid sequence-based identification of gonococcal transmission clusters in a large metropolitan area. J Infect Dis. 2004;189:1497–505. http://dx.doi.org/10.1086/383047
19 Jolley KA, Maiden MCJ. BIGSdb: Scalable analysis of bacterial genome variation at the population level. BMC Bioinformatics. 2010;11:595. http://dx.doi.org/10.1186/1471-2105-11-595
20. Demczuk W, Sidhu S, Unemo M, Whiley DM, Allen VG, Dillon JR, et al. *Neisseria gonorrhoeae* sequence typing for antimicrobial resistance, a novel antimicrobial resistance multilocus typing scheme for tracking global dissemination of *N. gonorrhoeae* strains. J Clin Microbiol. 2017;55:1454–68. http://dx.doi.org/10.1128/JCM.00100-17
21. World Health Organization. Report on global sexually transmitted infection surveillance 2015 Geneva: The Organization. 2016 [cited 16 Jan 2018]. http://apps.who.int/iris/bitstream/10665/249553/1/9789241565301-eng.pdf?ua=1
22. Newman L, Rowley J, Hoorn SV, Wijesooriya NS, Unemo M, Low N, et al. Global estimates of the prevalence and incidence of four curable sexually transmitted infections in 2012 based on systematic review and global reporting. PLoS ONE. 2015; 10:e0143304.
23. Chisholm SA, Mouton JW, Lewis DA, Nichols T, Ison CA, Livermore DM. Cephalosporin MIC creep among gonococci: time for a pharmacodynamic rethink? J Antimicrob Chemother. 2010;65:2141–8. http://dx.doi.org/10.1093/jac/dkq289
24. Martin I, Sawatzky P, Liu G, Allen V, Lefebvre B, Hoang L, et al. Decline in decreased cephalosporin susceptibility and increase in azithromycin resistance in *Neisseria gonorrhoeae*, Canada. Emerg Infect Dis. 2016;22:65–7. http://dx.doi.org/10.3201/eid2201.151247
25. Wi T, Lahra MM, Ndowa F, Bala M, Dillon JR, Ramon-Pardo P, et al. Antimicrobial resistance in *Neisseria gonorrhoeae*: Global surveillance and a call for international collaborative action. PLoS Med. 2017;14:e1002344. http://dx.doi.org/10.1371/journal.pmed.1002344

Address for correspondence: David Whiley, The University of Queensland, Faculty of Medicine, Centre for Clinical Research, UQCCR, Herston, Brisbane, Queensland 4029, Australia; email: d.whiley@uq.edu.au

Imipenem Resistance in *Clostridium difficile* Ribotype 017, Portugal

Joana Isidro, Andrea Santos, Alexandra Nunes, Vítor Borges, Catarina Silva, Luís Vieira, Aristides L. Mendes, Mónica Serrano, Adriano O. Henriques, João Paulo Gomes, Mónica Oleastro

We describe imipenem-resistant and imipenem-susceptible clinical isolates of *Clostridium difficile* ribotype 017 in Portugal. All ribotype 017 isolates carried an extra penicillin-binding protein gene, *pbp5*, and the imipenem-resistant isolates had additional substitutions near the transpeptidase active sites of *pbp1* and *pbp3*. These clones could disseminate and contribute to imipenem resistance.

Clostridium difficile, a toxin-producing, spore-forming bacillus, is a main cause of nosocomial antimicrobial drug–associated diarrhea in industrialized countries (*1*). *C. difficile* infection (CDI) usually develops in previously hospitalized persons with a recent history of antimicrobial drug use and causes illness with symptoms ranging from mild diarrhea to potentially lethal pseudomembranous colitis (*2*). Antimicrobial drugs disrupt the protective gut microbiota, enabling ingested *C. difficile* spores to germinate in the colon and providing a selective advantage to nonsusceptible strains (*3*). CDI is mainly mediated by the TcdA and TcdB toxins, though some strains additionally produce a binary toxin. Multiple antimicrobial drugs can promote CDI, and cephalosporins and fluoroquinolones have been associated with a higher risk for CDI (*3*). Multidrug resistance is frequently found in epidemic *C. difficile* strains; determinants of resistance are often found in horizontally transferable mobile genetic elements (*4*). In past decades, CDI prominence has increased because of a sudden rise in outbreaks and an increase in disease severity and death (*5*). This shift was mainly associated with the dissemination of fluoroquinolone-resistant PCR ribotype (RT) 027, which has been responsible for hospital outbreaks worldwide. Strains of other ribotypes, including RT078 and RT017, which have enhanced virulence, have emerged (*6*). In particular, RT017, the most common toxin A–negative, toxin B–positive ribotype, is widespread in Asia and is common in Europe (*7*–*9*). In a pan-European study of ≈900 *C. difficile* strains, the overall rate of resistance to imipenem, an antimicrobial drug of the carbapenem class, currently widely used as a last-line drug to treat infections by gram-negative bacteria, was found to be 7.41%, and the geometric mean (GM) MIC of imipenem for RT017 strains was 5.91 mg/L (*8*). In another study, isolates collected in a South Korea hospital during 2000–2009 were analyzed, and a resistance rate to imipenem of 8% (12% among RT017 isolates) was found (*10*).

Author affiliations: National Institute of Health, Lisbon, Portugal (J. Isidro, A. Santos, A. Nunes, V. Borges, C. Silva, L. Vieira, J.P. Gomes, M. Oleastro); Instituto de Tecnologia Química e Biológica António Xavier, Oeiras, Portugal (A.L. Mendes, M. Serrano, A.O. Henriques)

DOI: https://doi.org/10.3201/eid2404.170095

The Study

We characterized 191 *C. difficile* isolates collected during September 2012–September 2015 from 15 hospitals in Portugal (online Technical Appendix, https://wwwnc.cdc.gov/EID/article/24/4/17-0095-Techapp1.pdf). We found 24 (12.6%) were resistant to imipenem. Of these 24 isolates, 22 were RT017, 1 was RT014, and 1 was RT477. The MIC for imipenem for RT017, the imipenem-resistant isolates, was >32 mg/L (Table 1); the MIC for the 2 non-RT017 isolates was 16 mg/L. The 22 imipenem-resistant RT017 isolates were found at hospital A throughout the study period, suggesting the existence of a persistent clone, a finding supported by whole-genome sequencing data (online Technical Appendix). Among the 25 RT017 isolates, 3 were imipenem-susceptible and from hospital B (MIC range 1.5–3 mg/L) (Table 1).

RT017 *C. difficile* strains are frequently resistant to clindamycin, erythromycin, moxifloxacin, tetracycline, or rifampin (individually or in combination) (*8*,*10*). In this study, the 22 RT017 imipenem-resistant isolates were also found to be resistant to all of these antimicrobial drugs and showed higher meropenem and ertapenem MICs than those of the RT017 imipenem-susceptible isolates (Table 1; online Technical Appendix; online Technical Appendix Figure). Multidrug resistance to noncarbapenem antimicrobial drugs correlated with the presence of several genetic determinants, many located in mobile genetic elements (Figure 1; online Technical Appendix), in line with the idea that multidrug-resistant strains have a selective advantage (*4*) and that horizontal gene transfer plays a major role in the evolution of this pathogen (*11*).

Table 1. Susceptibility of *Clostridium difficile* RT017 imipenem-resistant isolates from hospital A and imipenem-susceptible isolates from hospital B to 11 antimicrobial drugs, Portugal*

		Antimicrobial drug, MIC breakpoints, mg/L										
Hospital	Resistance breakpoint†	IMP‡ ≥16	ETP‡ ≥16	MRP‡ ≥16	MXF†§ >4	MTZ†§ >2	VAN†§ >2	CLI‡ ≥8	CHL‡ ≥32	RIF† >0.004	TGC† >0.25	TET‡ ≥16
A, 22 isolates	MIC range	>32	3–16	1.5–4	>32	<0.016–1	0.38–2	>256	2–6	>32	<0.016–0.094	16–32
	GM MIC	32	7.56	2.31	32	0.12	0.73	256	3.29	32	0.025	18.08
	MIC_{90}	32	12	3	>32	0.38	2	256	4	32	0.032	32
	MIC_{50}	32	6	2	>32	0.19	0.75	256	3	32	0.023	16
	% Resistant	100	4.5	0	100	0	0	100	0	100	0	100
B, 3 isolates	MIC range	1.5–3	1.5–2	0.5–1.5	1.5	<0.016–0.25	0.38–0.75	>256	3–4	>32	<0.016–0.023	16
	GM MIC	2.08	1.82	0.83	1.5	0.072	0.60	256	3.30	32	0.020	16
	MIC_{90}	3	2	1.5	1.5	0.25	0.75	256	4	32	0.023	16
	MIC_{50}	2	2	0.75	1.5	0.094	0.75	256	3	32	0.023	16
	% Resistant	0	0	0	0	0	0	100	0	100	0	100
p value		<0.0001	<0.0001	<0.0001	<0.0001	0.45	0.56	ND	0.98	ND	0.41	0.51

*CHL, chloramphenicol; CLI, clindamycin; ETP, ertapenem; GM, geometric mean; IMP, imipenem; MIC_{50}, minimal inhibitory concentration for 50% of strains; MIC_{90}, minimal inhibitory concentration for 90% of strains; MRP, meropenem; MTZ, metronidazole; MXF, moxifloxacin; ND, not done; RIF, rifampin; TGC, tigecycline; VAN, vancomycin.
†European Committee on Antimicrobial Susceptibility Testing breakpoint.
‡Clinical and Laboratory Standards Institute breakpoint.
§Previously determined (*9*).

Through whole-genome sequencing, we found 13 single-nucleotide polymorphisms (SNPs) that differentiated the imipenem-resistant and imipenem-susceptible RT017 isolates (Table 2; Figure 1; online Technical Appendix). We found 2 SNPs in the genes coding for 2 high molecular weight (HMW) penicillin-binding proteins (PBPs) (Figure 1). HMW PBPs, which are bifunctional enzymes containing transglycosylase and transpeptidase domains, are categorized into class A, and PBPs lacking the transglycosylase domain are categorized into class B. The transpeptidase domain harbors 3 functional motifs (SXXK, SXN, and KTG[T/S]) that comprise the active site. Carbapenems block cell wall synthesis by inhibiting transpeptidase activity (*12*). One of the mutations found in the imipenem-resistant isolates affected the gene coding for PBP1, the single class A bifunctional peptidoglycan synthase of *C. difficile*; the mutation resulted in the amino acid substitution Ala555Thr close to the SSN functional motif (Figure 2). The second mutation was found in the gene encoding for the PBP3 class B transpeptidase and caused the amino acid replacement Tyr721Ser between the SXN and KTGT motifs (Figure 2). Neither of these changes was found in the 3 imipenem-susceptible RT017 isolates (Figure 1). Moreover, the 2 non-RT017 imipenem-resistant isolates, with a MIC for imipenem lower than that of the RT017 isolates, revealed either the Ala555Thr change or a different substitution (Leu543His), both in PBP1, also close to the functional motif SXN (Table 2). Modified PBPs with reduced affinity for the antimicrobial drug have been associated with resistance to β-lactams and specifically to imipenem in several microorganisms (*12*). We found no differences between the imipenem-resistant and imipenem-susceptible RT017 isolates in genes encoding other peptidoglycan synthases (Figure 1). It is possible that the substitutions in PBP1 and PBP3 in RT017 confer high-level resistance to imipenem and reduced susceptibility to other carbapenems, and at least in the RT014 and RT477 isolates studied, the single Ala555Thr substitution (or other substitutions in the vicinity of the SXN motif) is sufficient for an intermediate level of resistance.

However, all RT017 isolates studied herein, as well as the previously annotated strains M68 (GenBank accession no. NC_017175) and BJ08 (accession no. CP003939), have a fifth HMW class B PBP, PBP5, encoded in a mobile element (online Technical Appendix). Whether PBP5 contributes to imipenem resistance remains to be determined. Moreover, in imipenem-resistant isolates, the key sporulation-specific gene *sigK*, which is contiguous to *pbp2*, is interrupted by the 17-kb *skin*^{cd} element (*13*), and the *pbp5* region is contiguous to a transposon-like element carrying the *ermB* gene (shown as PUBMLST allele 8; https://pubmlst.org/bigsdb?db=pubmlst_cdifficile_seqdef&page=alleleInfo&locus=ermB&allele_id=8). It is unknown whether these genetic differences contribute to imipenem resistance.

Conclusions

Imipenem resistance in *C. difficile* RT017 probably involves the acquisition of mutations in both *pbp1* and *pbp3* that lead to amino acid substitutions close to the functional motifs of their transpeptidase domains. These substitutions might decrease the affinity of PBP1 and PBP3 for imipenem, enabling peptidoglycan synthesis in the presence of the antimicrobial drug. Considering that the presence of an additional PBP (PBP5) is a characteristic of RT017 strains, we suggest that PBP5 facilitates the expression of imipenem resistance through acquisition of mutations in *pbp1* and *pbp3*. In strains of other ribotypes lacking PBP5, such as the RT014 and RT477 isolates herein described, mutations in *pbp1* might only lead to

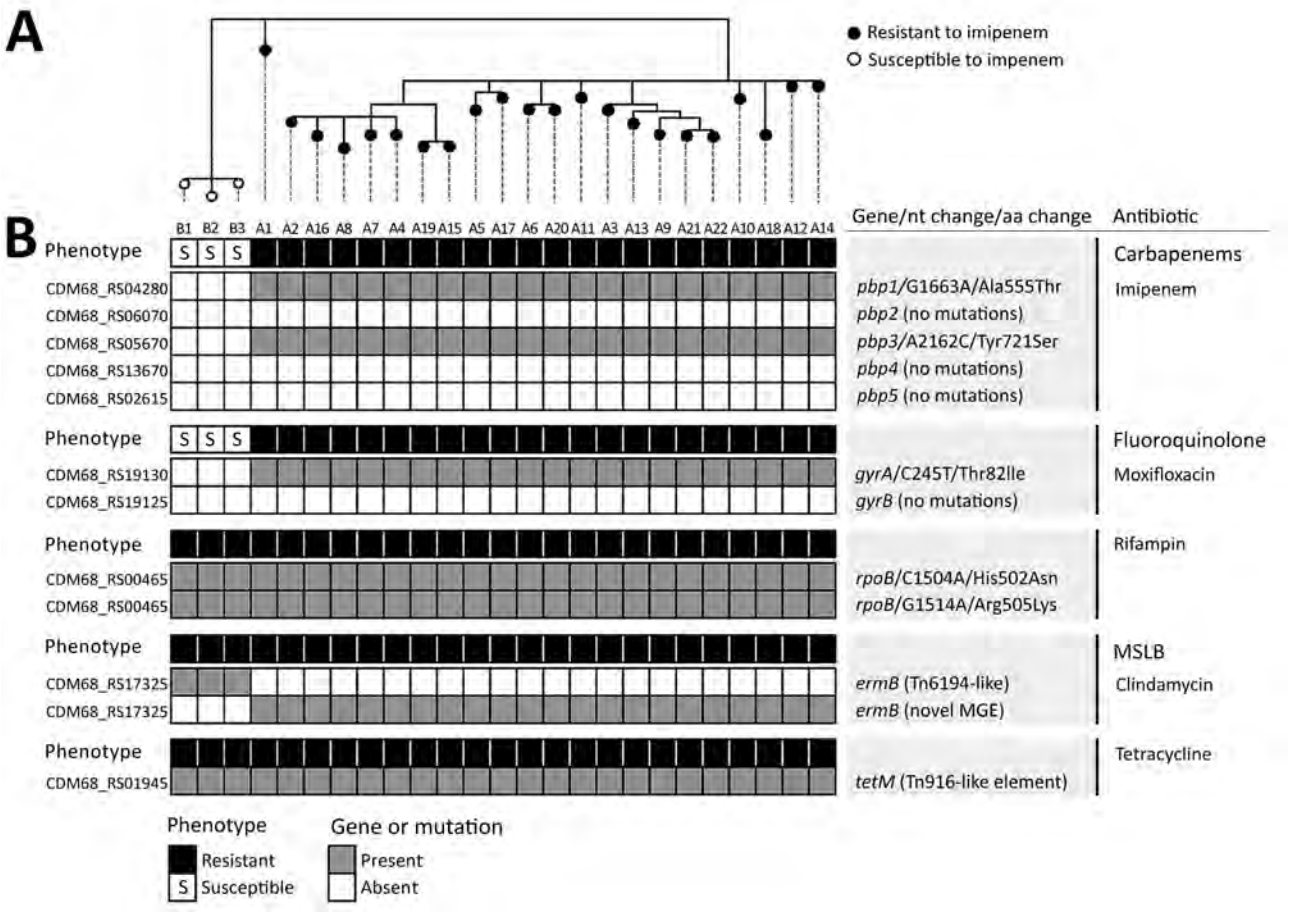

Figure 1. Phylogeny of *Clostridium difficile* RT017 isolates from hospitals A and B and genetic determinants of antimicrobial drug resistance, Portugal. A) Core genome single-nucleotide polymorphism–based neighbor-joining phylogeny of 25 RT017 *C. difficile* clinical isolates reconstructed by using 47 variant sites (outside MGEs) identified when mapping to either the corresponding genomic sequence of close relative *C. difficile* strain M68 (GenBank accession no. NC_017175) or a draft genome sequence of a representative clinical isolate. B) For each isolate, the profile of antimicrobial drug susceptibility is indicated together with respective potential genetic determinants of antimicrobial drug resistance. Only antimicrobial drugs for which a resistant phenotype was observed are displayed. Gene locus tags are relative to the *C. difficile* M68 genome annotation. Both nucleotide and amino acid replacements refer to mutations in the resistant isolates when comparing with susceptible isolates. No mutations means that no mutations are present differentiating resistant isolates of hospital A from susceptible isolates of hospital B, although mutations are present relative to M68. Both the *pbp5*-carrying region and the *ermB* gene (present in all isolates) were found to be inserted in distinct genomic contexts (online Technical Appendix, https://wwwnc.cdc.gov/EID/article/24/4/17-0095-Techapp1.pdf). MSLB, macrolide/lincosamide/streptogramin B; MGE, mobile genetic element.

intermediate levels of resistance. We further suggest that the spreading of *pbp5* might contribute to the dissemination of high-level imipenem resistance.

Portugal has a high rate of healthcare-associated infections and is a major consumer of carbapenems (*1*). Although carbapenem consumption has not been directly linked to *C. difficile* resistance, we speculate that the emergence of resistance and reduced susceptibility to these antimicrobial drugs might recapitulate the scenario observed with fluoroquinolone-resistant RT027 in the United States, where fluoroquinolones were the most prescribed antimicrobial drug (*14*). Our findings further reinforce the need for the responsible use of antimicrobial drugs; the emergence of carbapenem resistance in multidrug-resistant *C. difficile* clones might result in the dissemination of resistant strains.

Acknowledgments

We thank the participating hospitals for providing samples for the laboratory surveillance of CDI.

This work was supported by the National Institute of Health Dr. Ricardo Jorge (grant no. 2016DDI1284). We also acknowledge grant Pest-C/EQB/LA0006/2011 from Fundação para a Ciência e a Tecnologia (FCT; http://www.fct.pt) and program Investigador FCT (IF/00268/2013/CP1173/CT0006 to M.S.). A.L.M. was supported by a PhD fellowship (PD/BD/105738/2014) from the FCT.

Table 2. Mutations differentiating *Clostridium difficile* RT017 imipenem-resistant isolates found at hospital A from imipenem-susceptible isolates found at hospital B, Portugal

Gene in M68 genome*	Genome position*	Nucleotide in M68	Nucleotide change†	Amino acid change†	Gene product
RS02665	512416	C	C578T	Ala193Val‡	Multidrug ATP-binding cassette transporter permease, associated with antimicrobial drug resistance
RS04280/*pbp1*	905394	G	G1663A	Ala555Thr‡	Penicillin-binding transpeptidase
RS04935	1048151	C	T1010C	Ile337Thr‡	3-Isopropylmalate dehydratase large subunit
RS05670/*pbp3*	1221182	G	A2162C	Tyr721Ser‡	Penicillin-binding protein
RS07765	1666351	G	G214T	Gly72§	Hypothetical protein
RS07795/*hisB*	1671129	T	T209C	Ile70Thr‡	Imidazoleglycerol-phosphate dehydratase
RS07810	1673280	T	C474T	Ala158Ala	Imidazoleglycerol-phosphate synthase cyclase subunit
RS08415	1792079	G	A241G	Lys81Glu‡	Hypothetical protein (domain of MerR-like transcriptional regulators)
RS08810	1882950	C	C420T	Asp140Asp	Flavodoxin
RS14235	3083548	G	G421T	Gly141§	Haloacid dehalogenase
RS18530	4054525	C	C220T	Gln74§	S-adenosyl methionine–dependent methyltransferase
RS19130/*gyrA*	4174650	C	C245T	Thr82Ile‡	DNA gyrase subunit A
RS19545	4255124	C	C400T	His134Tyr‡	Phage portal, SPP1 Gp6-like family protein

*Relative to the annotation of the *C. difficile* M68 genome (GenBank accession no. NC_017175).
†Changes observed between imipenem-resistant and imipenem-susceptible isolates.
‡Nonsynonymous mutations.
§Mutations leading to putative protein truncation.

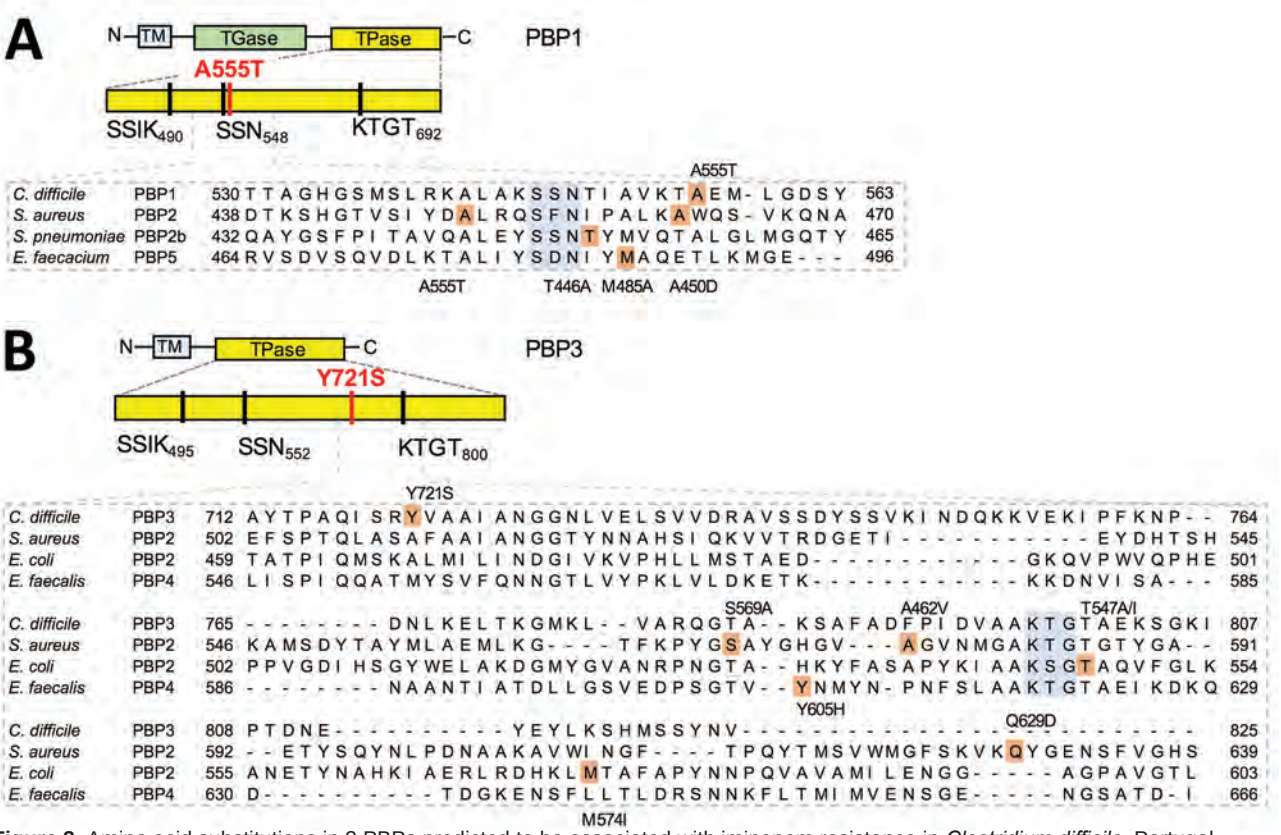

Figure 2. Amino acid substitutions in 2 PBPs predicted to be associated with imipenem resistance in *Clostridium difficile*, Portugal. The domains and conserved motifs SXXK, SXN, and KTG[T/S] are shown for the following proteins: PBP1 (A), homolog of CDM68_RS04280 of RT017 strain M68 (GenBank accession no. NC_017175) or CD630_07810 in the laboratory strain 630; and PBP3 (B), homolog of CDM68_RS05670 or CD630_11480. The mutations found in these resistant isolates are marked by red lines. The alignments below the 2 proteins show the position (shaded in pink) and nature of the amino acid substitutions observed in the imipenem-resistant RT017 isolates and select PBPs from microorganisms *Staphylococcus aureus* (GenBank accession no. AAA74375.1), *Streptococcus pneumoniae* (GenBank accession no. WP_001829432.1), *Escherichia coli* (GenBank accession no. AAB40835.1), *Enterococcus faecalis* (GenBank accession no. AAS77615.1), and *Enterococcus faecacium* (GenBank accession no. AIG13039.1). The conserved motifs in the vicinity of the substitutions are shaded in blue. PBP, penicillin-binding protein; TGase, transglycosylase; TM, transmembrane; TPase, transpeptidase.

About the Author

Dr. Isidro is a fellow in the Reference Laboratory for Gastrointestinal Infections at the National Institute of Health Dr. Ricardo Jorge in Lisbon, Portugal. Her primary research interests include CDI, antibiotic resistance, molecular typing, and whole-genome sequencing.

References

1. European Centre for Disease Prevention and Control. Point prevalence survey of healthcare-associated infections and antimicrobial use in European acute care hospitals, 2011–2012. Stockholm: The Centre; 2013.
2. Smits WK, Lyras D, Lacy DB, Wilcox MH, Kuijper EJ. *Clostridium difficile* infection. Nat Rev Dis Primers. 2016;2:201620.
3. Slimings C, Riley TV. Antibiotics and hospital-acquired *Clostridium difficile* infection: update of systematic review and meta-analysis. J Antimicrob Chemother. 2014;69:881–91. http://dx.doi.org/10.1093/jac/dkt477
4. Spigaglia P. Recent advances in the understanding of antibiotic resistance in *Clostridium difficile* infection. Ther Adv Infect Dis. 2016;3:23–42. http://dx.doi.org/10.1177/2049936115622891
5. Gerding DN, Lessa FC. The epidemiology of *Clostridium difficile* infection inside and outside health care institutions. Infect Dis Clin North Am. 2015;29:37–50. http://dx.doi.org/10.1016/j.idc.2014.11.004
6. Freeman J, Bauer MP, Baines SD, Corver J, Fawley WN, Goorhuis B, et al. The changing epidemiology of *Clostridium difficile* infections. Clin Microbiol Rev. 2010;23:529–49. http://dx.doi.org/10.1128/CMR.00082-09
7. King AM, Mackin KE, Lyras D. Emergence of toxin A-negative, toxin B-positive *Clostridium difficile* strains: epidemiological and clinical considerations. Future Microbiol. 2015;10:1–4. http://dx.doi.org/10.2217/fmb.14.115
8. Freeman J, Vernon J, Morris K, Nicholson S, Todhunter S, Longshaw C, et al.; Pan-European Longitudinal Surveillance of Antibiotic Resistance among Prevalent Clostridium difficile Ribotypes' Study Group. Pan-European longitudinal surveillance of antibiotic resistance among prevalent *Clostridium difficile* ribotypes. Clin Microbiol Infect. 2015;21:248.e9–16. http://dx.doi.org/10.1016/j.cmi.2014.09.017
9. Santos A, Isidro J, Silva C, Boaventura L, Diogo J, Faustino A, et al. Molecular and epidemiologic study of *Clostridium difficile* reveals unusual heterogeneity in clinical strains circulating in different regions in Portugal. Clin Microbiol Infect. 2016;22:695–700. http://dx.doi.org/10.1016/j.cmi.2016.04.002
10. Lee JH, Lee Y, Lee K, Riley TV, Kim H. The changes of PCR ribotype and antimicrobial resistance of *Clostridium difficile* in a tertiary care hospital over 10 years. J Med Microbiol. 2014;63:819–23. http://dx.doi.org/10.1099/jmm.0.072082-0
11. He M, Sebaihia M, Lawley TD, Stabler RA, Dawson LF, Martin MJ, et al. Evolutionary dynamics of *Clostridium difficile* over short and long time scales. Proc Natl Acad Sci U S A. 2010;107:7527–32. http://dx.doi.org/10.1073/pnas.0914322107
12. Zapun A, Contreras-Martel C, Vernet T. Penicillin-binding proteins and β-lactam resistance. FEMS Microbiol Rev. 2008;32:361–85. http://dx.doi.org/10.1111/j.1574-6976.2007.00095.x
13. Serrano M, Kint N, Pereira FC, Saujet L, Boudry P, Dupuy B, et al. A recombination directionality factor controls the cell type-specific activation of σ^K and the fidelity of spore development in *Clostridium difficile*. PLoS Genet. 2016;12:e1006312. http://dx.doi.org/10.1371/journal.pgen.1006312
14. He M, Miyajima F, Roberts P, Ellison L, Pickard DJ, Martin MJ, et al. Emergence and global spread of epidemic healthcare–associated *Clostridium difficile*. Nat Genet. 2013;45:109–13. http://dx.doi.org/10.1038/ng.2478

Address for correspondence: Mónica Oleastro, National Institute of Health Dr. Ricardo Jorge, National Reference Laboratory for Gastrointestinal Infections, Department of Infectious Diseases, Av Padre Cruz, 1649-016 Lisbon, Portugal; email: monica.oleastro@insa.min-saude.pt

Enhanced Replication of Highly Pathogenic Influenza A(H7N9) Virus in Humans

Seiya Yamayoshi,[1] Maki Kiso, Atsuhiro Yasuhara, Mutsumi Ito, Yuelong Shu, Yoshihiro Kawaoka[1]

To clarify the threat posed by emergence of highly pathogenic influenza A(H7N9) virus infection among humans, we characterized the viral polymerase complex. Polymerase basic 2–482R, polymerase basic 2–588V, and polymerase acidic–497R individually or additively enhanced virus polymerase activity, indicating that multiple replication-enhancing mutations in 1 isolate may contribute to virulence.

Highly pathogenic influenza A(H7N9) virus has infected humans every influenza season since 2013; the fifth epidemic wave occurred during the 2016–17 season (*1*,*2*). Since 2013, a total of 1,565 laboratory-confirmed human cases and 612 related deaths have been reported (http://www.who.int/influenza/human_animal_interface/Influenza_Summary_IRA_HA_interface_12_07_2017.pdf?ua = 1). During the fifth wave, H7N9 viruses possessing hemagglutinin with multibasic amino acids at the cleavage site were isolated from birds and humans (*2*–*4*). H7N9 isolates from humans possessed hemagglutinin with a preference for human-type receptors and neuraminidase with inhibitor resistance (*4*,*5*); one of those isolates transmitted among ferrets via respiratory droplets (*6*). Emergence of highly pathogenic H7N9 viruses with such properties is a serious threat to public health. Full comprehension of the extent of this threat requires detailed characterization of these viruses.

The Study

We attempted to identify the replication-enhancing amino acids in the polymerase complex of H7N9 virus A/Guangdong/17SF003/2016 (GD), which was isolated from the first reported H7N9-infected patient (*3*,*5*) and harbors polymerase basic (PB) 2 with 271T, 588V, 591Q, 627E, and 701D. Amino acids at these positions are known to alter viral polymerase activity in mammalian and avian cells at different temperatures (*7*–*11*).

Author affiliations: University of Tokyo, Tokyo, Japan (S. Yamayoshi, M. Kiso, A. Yasuhara, M. Ito, Y. Kawaoka); Sun Yat-Sen University, Shenzhen, China (Y. Shu); Chinese Centers for Disease Control and Prevention, Beijing, China (Y. Shu); University of Wisconsin–Madison, Madison, Wisconsin, USA, and Japan Science and Technology Agency, Saitama, Japan (Y. Kawaoka)

DOI: https://doi.org/10.3201/eid2404.171509

We compared the viral polymerase activity of wild-type GD with that of A/Anhui/1/2013(H7N9) virus (AN) in human A549 cells at 33°C or 37°C (temperatures of the human upper and lower respiratory tract) and in chicken DF-1 cells at 39°C (body temperature of birds). Although both viruses exhibited comparable activity in DF-1 cells, AN activity was higher than GD activity in A549 cells at both temperatures because wild-type AN/PB2 acquired polymerase activity–enhancing K at position 627 of PB2 during replication in the infected human (*8*). We therefore tested AN/PB2-627E, which possesses an avian ancestral amino acid in PB2-627, and AN/PB2-627E-701N, which possesses polymerase-enhancing PB2-701N (*8*). In human A549 cells, wild-type GD showed viral polymerase activity comparable to that of AN/PB2-627E-701N (online Technical Appendix Figure 1, panel A, https://wwwnc.cdc.gov/EID/article/24/4/17-1509-Techapp1.pdf). These results indicate that the viral polymerase activity of wild-type GD in mammalian cells has increased more than that of virus bearing avian-like ancestral AN/PB2–627E.

To determine which component of the viral replication complex (PB2, PB1, polymerase acidic [PA], or nucleoprotein) contributes to the activity of the GD polymerase complex, we tested the polymerase activity of GD replication complexes in which we had replaced each viral protein with its AN/PB2-627E counterpart. We found that the viral polymerase activity in A549 cells was remarkably decreased by AN/PB2-627E and moderately decreased by AN-PA (online Technical Appendix Figure 1, panel B). These results suggest that the PB2 and the PA of GD are involved in the relatively high polymerase activity of the GD replication complex.

When we compared the amino acid sequences of GD-PB2 and GD-PA with those of AN/PB2-627E and AN-PA, we found 8 and 6 differences, respectively (Table 1). To identify which substitutions contributed to the enhanced polymerase activity, we constructed a series of plasmids encoding GD-PB2 or GD-PA harboring single substitutions and examined polymerase activity. Of the 8 PB2 mutants, GD/PB2-482K and GD/PB2-588A drastically reduced viral polymerase activity in A549 cells, although this activity was slightly higher than that of AN/PB2-627E (Figure 1, panel A). Therefore, we tested the viral polymerase activity of GD-PB2 possessing both mutations (GD/PB2-482K-588A) and found a further decrease in the double mutant. Of the 6 PA mutants, GD/PA-497K showed reduced

[1]These senior authors contributed equally to this article.

Table 1. Amino acid differences between PB2 and PA in 2 influenza A(H7N9) viruses*

	PB2								PA					
Virus	191	340	482	559	560	584	588	702	100	262	387	394	465	497
GD wild-type	E	K	R	T	I	I	V	R	V	K	I	D	V	R
AN/PB2-627E†	K	R	K	N	V	V	A	K	A	R	V	N	I	K

*AN, A/Anhui/1/2013(H7N9); GD, A/Guangdong/17SF003/2016; PA, polymerase acidic; PB, polymerase basic.
†This mutant possessed a K to E substitution at position 627 of PB2, but the other residues of PB2 and PA were identical to those of wild-type AN.

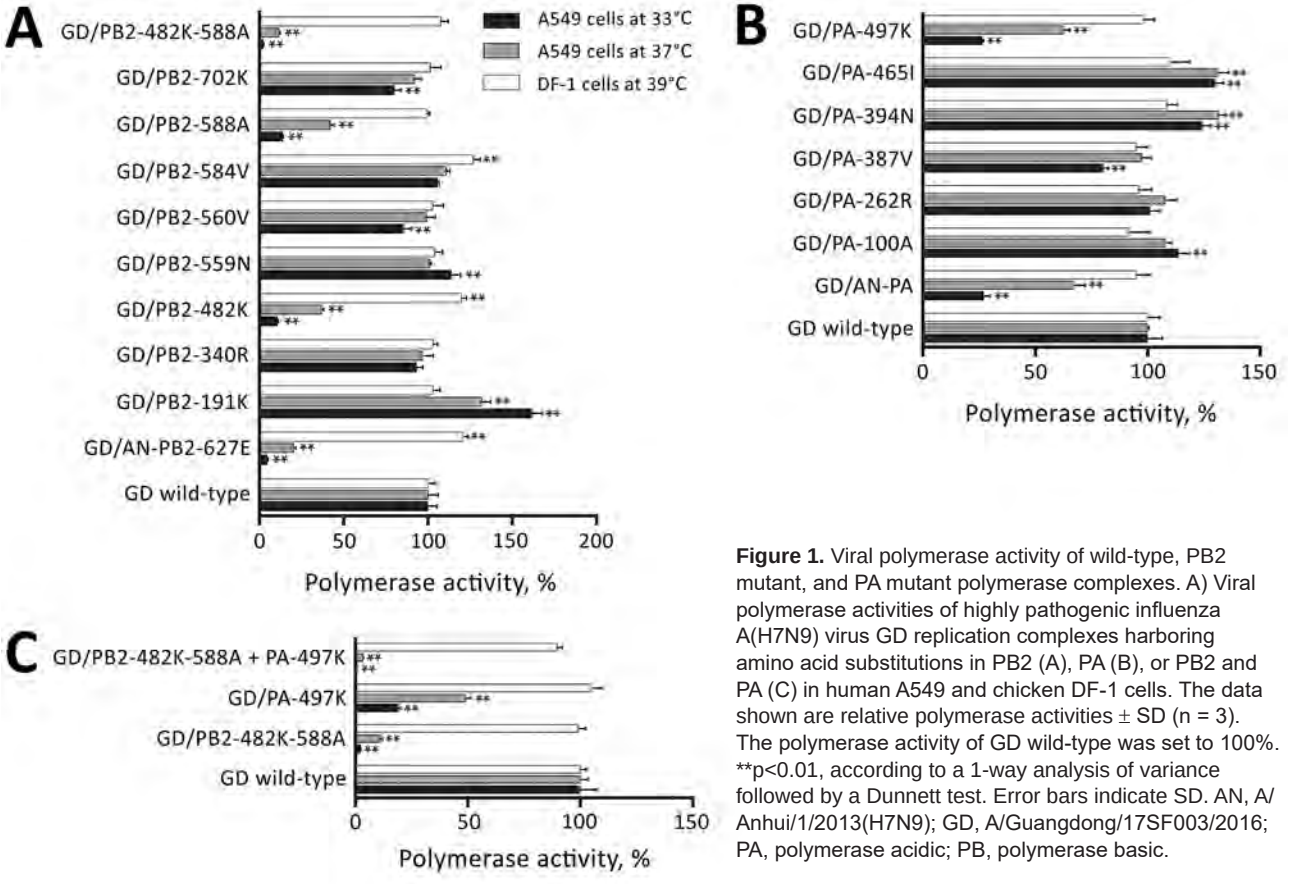

Figure 1. Viral polymerase activity of wild-type, PB2 mutant, and PA mutant polymerase complexes. A) Viral polymerase activities of highly pathogenic influenza A(H7N9) virus GD replication complexes harboring amino acid substitutions in PB2 (A), PA (B), or PB2 and PA (C) in human A549 and chicken DF-1 cells. The data shown are relative polymerase activities ± SD (n = 3). The polymerase activity of GD wild-type was set to 100%. **p<0.01, according to a 1-way analysis of variance followed by a Dunnett test. Error bars indicate SD. AN, A/Anhui/1/2013(H7N9); GD, A/Guangdong/17SF003/2016; PA, polymerase acidic; PB, polymerase basic.

viral polymerase activity in A549 cells (Figure 1, panel B). Compared with GD/PB2-482K-588A or GD/PA-497K alone, the polymerase activity of GD/PB2-482K-588A plus GD/PA-497K was further reduced (Figure 1, panel C). Collectively, these data demonstrate that PB-482R, PB2-588V, and PA-497R play crucial roles in the enhanced activity of the GD polymerase complex.

To examine the role of these amino acids on virus growth in human cells, we prepared wild-type and mutant viruses in the GD background by using reverse genetics. GD/PB2-482K and GD/PB2-588A viruses replicated less efficiently than wild-type GD virus in A549 cells (online Technical Appendix Figure 2, panels A, B). Replication of GD/PB2-482K-588A and GD/PB2-482K-588A+PA-497K

Table 2. Titers of influenza A(H7N9) GD virus in organs of experimentally infected mice*

	Postinfection day 3, mean $\log_{10}$ PFU ± SD/g			Postinfection day 6, mean $\log_{10}$ PFU ± SD/g		
Virus	Lung	NT	Brain	Lung	NT	Brain
GD wild-type	5.7 ± 0.2	4.2 ± 0.8	ND	5.8 ± 0.4	5.9 ± 0.7	3.2
GD/PB2-482K	ND, p<0.01	ND, p<0.01	ND	3.0, 3.4, p<0.01	2.6 ± 0.4, p<0.05	ND
GD/PB2-588A	3.3 ± 0.6, p<0.01	3.1, p<0.01	ND	4.6 ± 0.8	4.4 ± 2.5	ND
GD/PB2-482K-588A	ND, p<0.01	ND, p<0.01	ND	3.1 ± 0.3, p<0.05	ND, p<0.01	ND
GD/PA-497K	5.1 ± 0.2, p<0.05	2.9 ± 1.0	ND	4.6 ± 1.0	5.8 ± 0.4	ND
GD/PB2-482K-588A+PA-497K	ND, p<0.01	ND, p<0.01	ND	2.2, 2.7, p<0.01	ND, p<0.01	ND

*BALB/c mice were intranasally inoculated with 10^2 PFU of virus (in 50 μL). Three animals per group were euthanized on postinfection days 3 and 6. Statistically significant differences compared with GD wild-type–infected mice were determined by use of a 1-way analysis of variance followed by a Dunnett test. GD, A/Guangdong/17SF003/2016; ND, virus not detected (detection limit ≈2 $\log_{10}$ PFU/g); NT, nasal turbinates; PA, polymerase acidic; PB, polymerase basic.

viruses was less efficient than that of GD/PB2-482K and GD/PB2-588A viruses. GD/PA-497K virus showed growth comparable to that of the wild-type GD virus. In DF-1 cells, all tested viruses produced similar growth curves (online Technical Appendix Figure 2, panel C). These results indicate that PB2-482R and PB2-588V play a central role in enhancing virus replication in mammalian cells.

To assess the role of these amino acids in vivo, we compared virus titers in the lungs, nasal turbinates, and brains of mice infected intranasally with 10^2 PFU of each virus. On day 3 after infection, we did not detect GD/PB2-482K, GD/PB2-482K-588A, or GD/PB2-482K-588A+PA-497K viruses in the lungs or turbinates (Table 2). Replication of GD/PB2-588A or GD/PA-497K virus was significantly

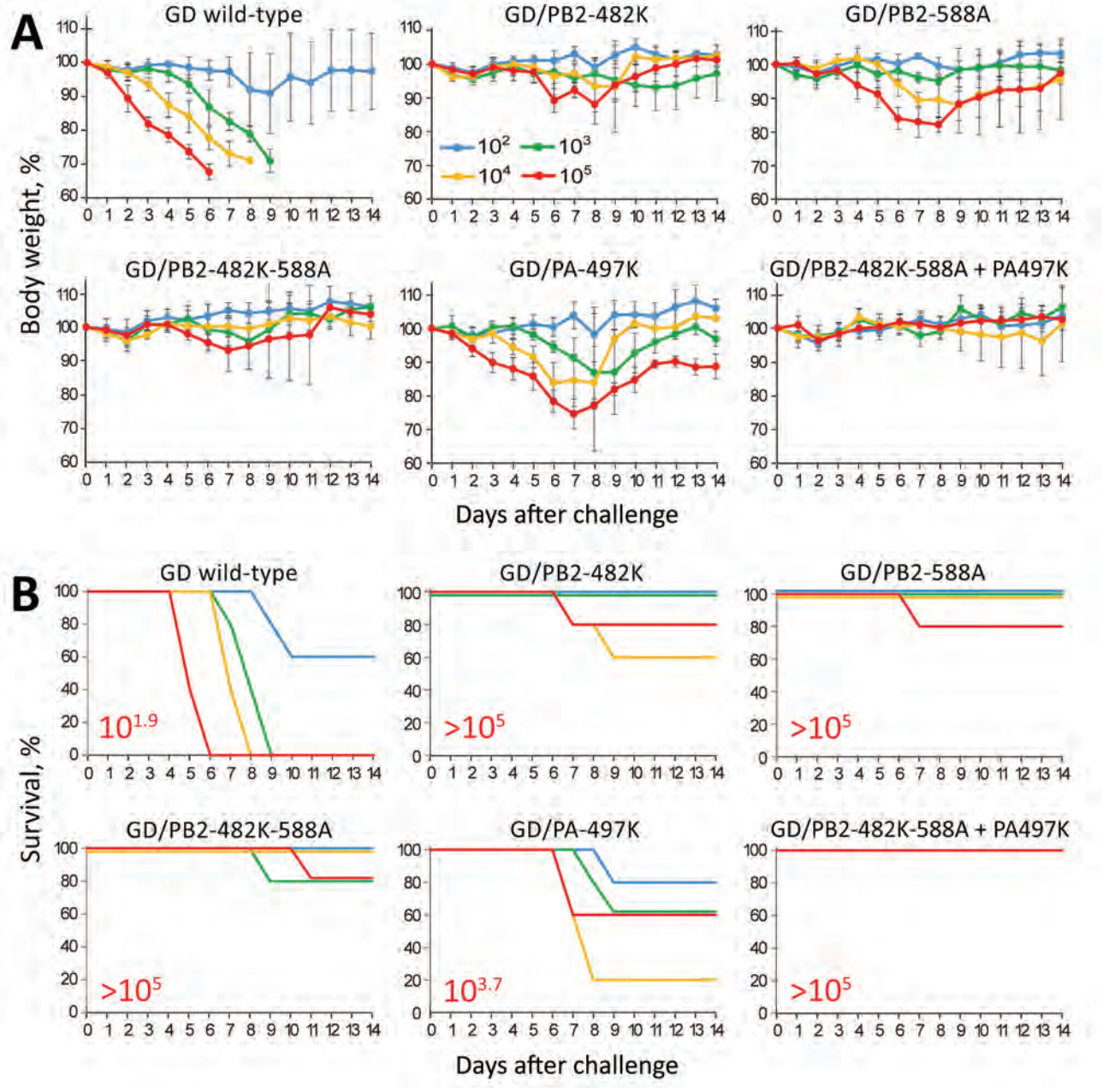

Figure 2. Virulence of wild-type and mutant highly pathogenic influenza A(H7N9) virus GD viruses in mice. Five mice per group were intranasally inoculated with 10^2, 10^3, 10^4, or 10^5 PFU (each in 50 μL) of the indicated viruses. Body weight (A) and survival (B) were monitored daily for 14 days. A) The values represent the average body weight ± SD compared with the baseline weight from 5 mice. Two-way analysis of variance followed by a Dunnett test revealed that the body weight loss of mice infected with each mutant virus at any dose was significantly reduced compared with that of mice infected with GD wild-type virus ($p<0.01$). B) The 50% lethal doses for mice (in red) were calculated according to the Spearman-Karber method. Error bars indicate SD. GD, A/Guangdong/17SF003/2016; PA, polymerase acidic; PB, polymerase basic.

decreased in the lungs and slightly decreased in the turbinates. On day 6 after infection, we found similar trends to those observed on day 3. Wild-type GD virus was detected in the brain of 1 of 3 mice.

Next, we evaluated virus pathogenicity in mice infected with 10^2–10^5 PFU of each virus by monitoring changes in body weight. When inoculated with wild-type GD virus, almost all mice had to be euthanized, resulting in a 50% mouse lethal dose (MLD_{50}) of $10^{1.9}$ PFU (Figure 2, panels A and B). Transient or severe weight loss was caused by GD/PB2-482K, GD/PB2-588A, and GD/PB2-482K-588A in 1–3 of 20 euthanized mice and by GD/PA-497K viruses in 9 of 20 euthanized mice; MLD_{50} values were higher than those for wild-type GD virus. The GD/PB2-482K-588A+PA-497K virus did not affect body weight (MLD_{50} >10^5 PFU). Virulence of GD/PB2-588A in mice was comparable to that of GD/PB2-482K and GD/PB2-482K-588A, although GD/PB2-588A replicated better in the lungs and turbinates than GD/PB2-482K and GD/PB2-482K-588A (Table 2); however, the levels of GD/PB2-588A replication in mice were lower than those of wild-type GD, resulting in reduced pathogenicity in mice. These results demonstrate that PB2-482R and PB2-588V contribute to high virulence in mice and that PA-497R is also involved.

Conclusions

We demonstrated that PB2-482R, PB2-588V, and PA-497R contribute to the enhanced polymerase activity of highly pathogenic H7N9 virus. These mutations additively increase viral polymerase activity and pathogenicity. PB2-482R is present in 0.79% (7/884) of human-derived H7N9 viruses, PB2-588V in 16.6% (147/883), and PA-497R in 0.81% (7/862) (online Technical Appendix Table). Of 31 highly pathogenic H7N9 viruses isolated from humans, 5 (16.1%) possessed PB2-482R and PA-497R, 12 (38.7%) PB2-627K, and 10 (32.3%) PB2-588V (online Technical Appendix Figure 3, panel A). Although conventional replication-enhancing amino acids (PB2-591R, PB2-627K, and PB2-701N) rarely coexist in 1 PB2 molecule, PB2-588V clearly permits acquisition of additional mutations, such as PB2-482R and PB2-627K (*12*). These double substitutions could have an additive effect on virulence enhancement, as also shown previously (*9*), suggesting that in mammalian hosts, these double-mutant viruses may be fitter than single-mutant viruses. Therefore, future H7N9 virus surveillance studies should take into consideration single markers and combinations of markers.

PB2-482R was located in 1 of 2 nuclear localization signals spanning amino acids 449 to 495 (*13*) within the cap-binding domain of the influenza A virus polymerase complex (online Technical Appendix Figure 3, panel B). PB2-588V was located near PB2-627K in the 627 domain. PA-497R was located at 1 of 2 binding sites for transcriptional activator hCLE (*14*) but was not exposed on the protein surface. PB2-588V is probably involved in ANP32A-dependent high polymerase activity in mammalian hosts (*15*), and the role of PB2-482R might differ from that of other polymerase-enhancing amino acids in PB2.

Acknowledgments

We thank Kohei Oishi for assistance with experiments and Susan Watson for editing the manuscript.

This work was supported by the Japan Initiative for Global Research Network on Infectious Diseases from the Japan Agency for Medical Research and Development (AMED); Leading Advanced Projects for Medical Innovation from AMED; the e-ASIA Joint Research Program from AMED; a Grant-in-Aid for Scientific Research on Innovative Areas from the Ministry of Education, Culture, Science, Sports, and Technology of Japan (nos. 16H06429, 16K21723, and 16H06434); and the Center for Research on Influenza Pathogenesis funded by US National Institutes of Health, National Institute of Allergy and Infectious Diseases contract no. HHSN272201400008C.

Y.K. has received speaker's honoraria from Toyama Chemical and Astellas Inc., and grant support from Chugai Pharmaceuticals, Daiichi Sankyo Pharmaceutical, Toyama Chemical, Tauns Laboratories, Inc., Tsumura & Co., and Denka Seiken Co., Ltd. Y.K. is a co-founder of FluGen.

About the Author

Dr. Yamayoshi is project associate professor of Division of Virology, Institute of Medical Science, University of Tokyo. His research interests are virus–host interactions at the community, individual, cellular, and molecular levels.

References

1. Gao R, Cao B, Hu Y, Feng Z, Wang D, Hu W, et al. Human infection with a novel avian-origin influenza A (H7N9) virus. N Engl J Med. 2013;368:1888–97. http://dx.doi.org/10.1056/NEJMoa1304459e
2. Su S, Gu M, Liu D, Cui J, Gao GF, Zhou J, et al. Epidemiology, evolution, and pathogenesis of H7N9 influenza viruses in five epidemic waves since 2013 in China. Trends Microbiol. 2017;25:713–28. http://dx.doi.org/10.1016/j.tim.2017.06.008
3. Zhang F, Bi Y, Wang J, Wong G, Shi W, Hu F, et al. Human infections with recently-emerging highly pathogenic H7N9 avian influenza virus in China. J Infect. 2017;75:71–5. http://dx.doi.org/10.1016/j.jinf.2017.04.001
4. Zhu W, Zhou J, Li Z, Yang L, Li X, Huang W, et al. Biological characterisation of the emerged highly pathogenic avian influenza (HPAI) A(H7N9) viruses in humans, in mainland China, 2016 to 2017. Euro Surveill. 2017;22:pii:30533. http://dx.doi.org/10.2807/1560-7917.ES.2017.22.19.30533

5. Ke C, Mok CKP, Zhu W, Zhou H, He J, Guan W, et al. Human infection with highly pathogenic avian influenza A(H7N9) virus, China. Emerg Infect Dis. 2017;23:1332–40. http://dx.doi.org/10.3201/eid2308.170600
6. Imai M, Watanabe T, Kiso M, Nakajima N, Yamayoshi S, Iwatsuki-Horimoto K, et al. A highly pathogenic avian H7N9 influenza virus isolated from a human is lethal in some ferrets infected via respiratory droplets. Cell Host Microbe. 2017;22:615–26.e8. http://dx.doi.org/10.1016/j.chom.2017.09.008
7. Yamayoshi S, Yamada S, Fukuyama S, Murakami S, Zhao D, Uraki R, et al. Virulence-affecting amino acid changes in the PA protein of H7N9 influenza A viruses. J Virol. 2014;88:3127–34. http://dx.doi.org/10.1128/JVI.03155-13
8. Yamayoshi S, Fukuyama S, Yamada S, Zhao D, Murakami S, Uraki R, et al. Amino acids substitutions in the PB2 protein of H7N9 influenza A viruses are important for virulence in mammalian hosts. Sci Rep. 2015;5:8039. http://dx.doi.org/10.1038/srep08039
9. Xiao C, Ma W, Sun N, Huang L, Li Y, Zeng Z, et al. PB2-588 V promotes the mammalian adaptation of H10N8, H7N9 and H9N2 avian influenza viruses. Sci Rep. 2016;6:19474. http://dx.doi.org/10.1038/srep19474
10. Mänz B, de Graaf M, Mögling R, Richard M, Bestebroer TM, Rimmelzwaan GF, et al. Multiple natural substitutions in avian influenza A virus PB2 facilitate efficient replication in human cells. J Virol. 2016;90:5928–38. http://dx.doi.org/10.1128/JVI.00130-16
11. Mok CK, Lee HH, Lestra M, Nicholls JM, Chan MC, Sia SF, et al. Amino acid substitutions in polymerase basic protein 2 gene contribute to the pathogenicity of the novel A/H7N9 influenza virus in mammalian hosts. J Virol. 2014;88:3568–76. http://dx.doi.org/10.1128/JVI.02740-13
12. Li Y, Qi W, Qiao J, Chen C, Liao M, Xiao C. Evolving HA and PB2 genes of influenza A (H7N9) viruses in the fifth wave–increasing threat to both birds and humans? J Infect. 2017;75:184–6. http://dx.doi.org/10.1016/j.jinf.2017.04.002
13. Mukaigawa J, Nayak DP. Two signals mediate nuclear localization of influenza virus (A/WSN/33) polymerase basic protein 2. J Virol. 1991;65:245–53.
14. Huarte M, Sanz-Ezquerro JJ, Roncal F, Ortín J, Nieto A. PA subunit from influenza virus polymerase complex interacts with a cellular protein with homology to a family of transcriptional activators. J Virol. 2001;75:8597–604. http://dx.doi.org/10.1128/JVI.75.18.8597-8604.2001
15. Long JS, Giotis ES, Moncorgé O, Frise R, Mistry B, James J, et al. Species difference in ANP32A underlies influenza A virus polymerase host restriction. Nature. 2016;529:101–4. http://dx.doi.org/10.1038/nature16474

Address for correspondence: Yoshihiro Kawaoka, Division of Virology, Department of Microbiology and Immunology, Institute of Medical Science, University of Tokyo, Minato-ku, Tokyo 108-8639, Japan; email: yoshihiro.kawaoka@wisc.edu or yamayo@ims.u-tokyo.ac.jp

Multidrug-Resistant *Salmonella enterica* 4,[5],12:i:- Sequence Type 34, New South Wales, Australia, 2016–2017

Alicia Arnott, Qinning Wang, Nathan Bachmann, Rosemarie Sadsad, Chayanika Biswas, Cristina Sotomayor, Peter Howard, Rebecca Rockett, Agnieszka Wiklendt, Jon R. Iredell, Vitali Sintchenko

Multidrug- and colistin-resistant *Salmonella enterica* serotype 4,[5],12:i:- sequence type 34 is present in Europe and Asia. Using genomic surveillance, we determined that this sequence type is also endemic to Australia. Our findings highlight the public health benefits of genome sequencing–guided surveillance for monitoring the spread of multidrug-resistant mobile genes and isolates.

Since the 1990s, the global incidence of infection with *Salmonella enterica* serotype 4,[5],12:i:- has increased sharply among humans, livestock, and poultry (*1*). This monophasic variant of *S. enterica* serovar Typhimurium ranges from pansusceptible to multidrug resistant. In 2015, an *S. enterica* strain displaying the plasmid-mediated colistin resistance *mcr-1* gene was discovered (*2*). In 2016, human and food isolates with *mcr-1* were identified in Portugal (*3*), China (*4*), and the United Kingdom (*5*). All *mcr*-1–harboring isolates were predominantly *Salmonella.* 4,[5],12:i:- multilocus sequence typing (MLST) sequence type (ST) 34. Before this study, the ST34 clone, already emerged in Europe and Asia, was yet to be detected in Australia as a drug-resistant pathogen of humans. We therefore investigated the circulation of drug-resistant *Salmonella* 4,[5],12:i:- ST34 in New South Wales (NSW), Australia.

The Study

Since October 2016, all *Salmonella* isolates referred to the NSW Enteric Reference Laboratory (Centre for Infectious Diseases and Microbiology Laboratory Services, Pathology West, Sydney, NSW, Australia) have undergone whole-genome sequencing in addition to serotyping and multilocus variable-number tandem-repeat analysis (MLVA) performed as described (*6*). Of the 971 isolates (96% from humans, 4% from food and animals) received from October 1, 2016, through March 17, 2017, a total of 80 (8.2%) were identified as *Salmonella* 4,[5],12:i:-, and 61 (76%) of these underwent whole-genome sequencing. Five duplicate isolates were excluded. In our retrospective study, we included 54 isolates from humans and 2 isolates from pork meat obtained from independent butchers during a routine survey conducted by the NSW Food Authority in 2016.

We extracted genomic DNA by using the chemagic Prepito-D (Perkin Elmer, Seer Green, UK) and prepared libraries by using Nextera XT kits and sequenced them on a NextSeq-500 (both by Illumina, San Diego, CA, USA) with at least 30-fold coverage. We assessed genomic similarity and STs by using the Nullarbor pipeline (*7*). We identified antimicrobial resistance (AMR) genes by screening contigs through ResFinder (*8*) and CARD (https://card.mcmaster.ca) by using ABRicate version 0.5 (https://github.com/tseemann/abricate). Markers of colistin resistance were examined by using CLC Genomics Workbench (QIAGEN, Valencia, CA, USA). We identified *Salmonella* 4,[5],12:i:- genomes recovered in Europe and Asia by using Enterobase (https://enterobase.warwick.ac.uk/). We confirmed phenotypic resistance on a randomly selected subset of isolates by using the BD Phoenix system (Becton Dickinson, Franklin Lakes, NJ, USA) or Etest (bioMérieux, Marcy L'Étoile, France).

We obtained 54 isolates from 53 case-patients who had a median age of 25 years (range <1 to 90 years). We detected 20 MLVA profiles; however, 2 profiles predominated: 3-13-10-NA-0211 (45%) and 3-13-11-NA-0211 (14%). All but 2 case-patients resided in areas of distinct postal codes distributed throughout NSW; we found no apparent temporal or geographic clustering. Recent overseas travel was reported by 5 case-patients: 2 to Cambodia and 1 each to Thailand, Vietnam, and Indonesia.

All 56 *Salmonella* 4,[5],12:i:- isolates were classified as ST34. The diversity between isolates was higher than that suggested by MLVA; we detected up to 112 single-nucleotide polymorphism (SNP) differences between isolates. The isolates from Australia clustered with each other and with isolates from the United Kingdom (Figure).

Author affiliations: Westmead Hospital, Sydney, New South Wales, Australia (A. Arnott, R. Sadsad, C. Biswas, C. Sotomayor, R. Rockett, J.R. Iredell, V. Sintchenko); The University of Sydney, Sydney (A. Arnott, R. Sadsad, C. Sotomayor, R. Rockett, J.R. Iredell, V. Sintchenko); NSW Health Pathology, Sydney (Q. Wang, P. Howard, A. Wiklendt, V. Sintchenko); Centenary Institute, Sydney (N. Bachmann)

DOI: https://doi.org/10.3201/eid2404.171619

Combined with the steady monthly incidence of infections, these findings suggest that local circulation of *Salmonella* 4,[5],12:i:- might play a larger role as the source of infection than independent importations from overseas. Of note, 1 isolate from pork differed from 1 isolate from a human by only 10 SNPs, indicating that pork may be a source of human infection (Figure, panel A).

We detected AMR genes in 95% of ST34 isolates from NSW. The number of AMR genes (up to 13) was equivalent to that reported for ST34 isolates from the United States and United Kingdom (Figure, panel B). Of the 53 AMR isolates from NSW, 48 (90%) were classified as multidrug resistant on the basis of containing >4 AMR genes conferring resistance to different classes of antimicrobial drugs. Among the AMR isolates, 39 (73.5%) displayed multidrug resistance patterns, all of which are associated with resistance to aminoglycosides, β-lactams, and sulfonamides. A total of 21 (40%) isolates, including 1 from pork, had the core resistance-type (R-type) ASSuT (resistant to ampicillin, streptomycin, sulfonamides, and tetracycline) conferred by the *strA-strB*, *blaTEM*-1b, *sul2*, and *tet*(B) genes (Figure, panel B). This multidrug resistance pattern is characteristic of the European clone (*9*), which has been reported in Europe and North America and is strongly associated with pork (*10*,*11*).

R-type ASSuTTmK was found for 12 (23%) isolates from humans: genes *strA-strB*, *aph*(3′)-Ia, *blaTEM*-1b, *tet*(A)-*tet*(B), *sul2*, and *dfr*A5 (which confers resistance against trimethoprim). Six isolates collected from case-patients who resided in the Sydney region over a 3-week period in 2017 shared R-type ASSuTmGK: genes *aac*

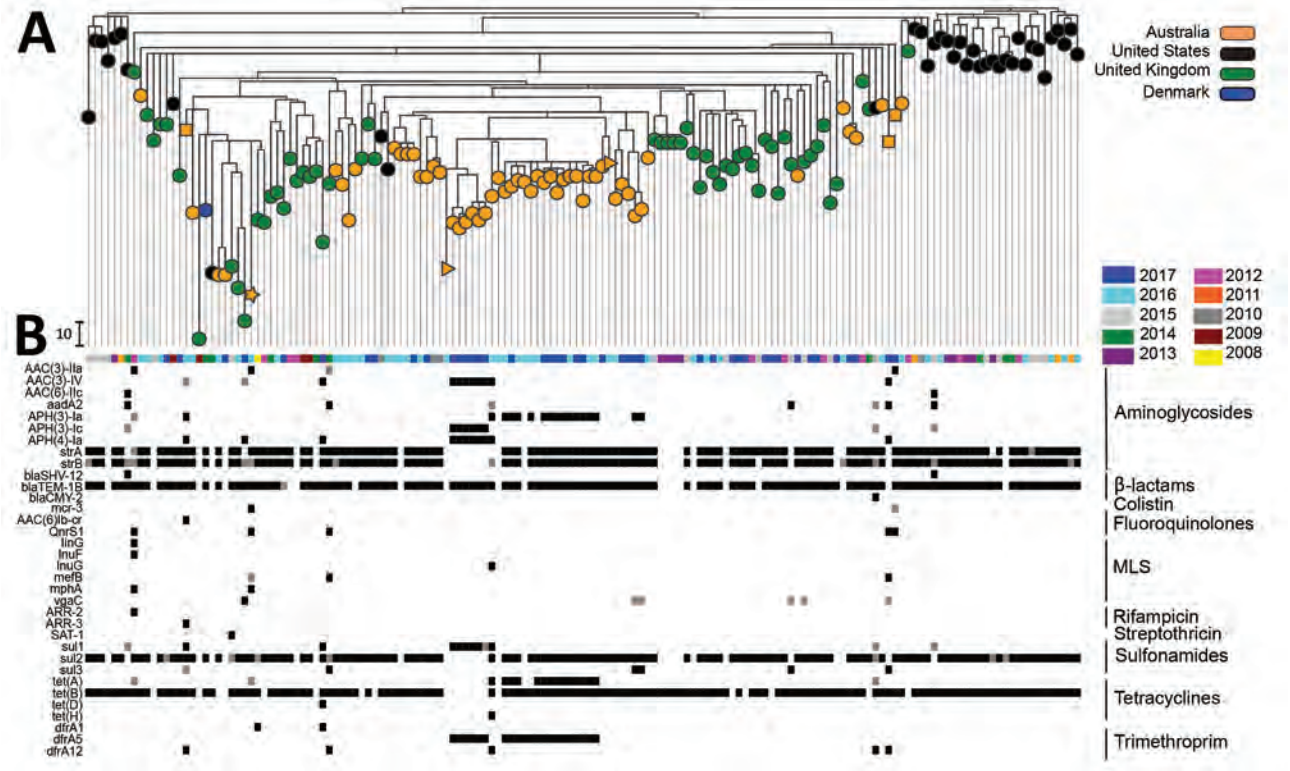

Figure. Maximum-likelihood phylogeny of whole-genome single-nucleotide polymorphisms (SNPs) of 153 *Salmonella enterica* 4,[5],12:i:- sequence type (ST) 34 isolates and acquired drug-resistance genes. A) SNP analysis was conducted by performing whole-genome alignment of ST34 isolates from New South Wales (NSW), Australia, and a selection of published ST34 isolates collected in the United Kingdom, United States, and Denmark by using Snippy Core (https://github.com/tseemann/snippy) (online Technical Appendix, https://wwwnc.cdc.gov/EID/article/24/4/17-1619-Techapp1.pdf). Regions of recombination were identified by using BratNextGen (www.helsinki.fi/bsg/software/BRAT-NextGen/) and removed. SNPs were identified by using SNP-sites (https://github.com/sanger-pathogens/snp-sites), and the phylogeny was generated by using FastTree (www.microbesonline.org/fasttree/). Phylogeny and antimicrobial resistance metadata were combined by using Microreact (https://microreact.org/showcase). The colistin-resistant ST34 isolate from NSW is denoted by an orange star, fluoroquinolone-resistant isolates from NSW by orange squares, and pork isolates from NSW by orange triangles. Scale bar indicates 10 SNPs. B) Year of isolation and acquisition of drug resistance. Acquired drug-resistance genes were identified by screening all isolate contigs through the ResFinder (*8*) and CARD (https://card.mcmaster.ca/*)* databases by using ABRicate version 0.5 (https://github.com/tseemann/abricate). Only genes with a 100% homology match in ≥1 isolate are shown. Columns depict the results for individual isolates; rows represent acquired drug-resistance genes. The antibiotic class that genes confer resistance against is indicated at right. White indicates that the specified gene was not detected, gray indicates that the specified gene was detected but sequence homology against the reference was <100%, black indicates a perfect match between the isolate and reference gene sequence. MLS, macrolide, lincosamide, and streptogramin B.

(3)-IV, *aph (4)*-Ia, *aph(3')*-Ic, *blaTEM*-1B, *sul1*, and *dfr*A5 (which also confers resistance against trimethoprim) (Figure, panel B). These 6 isolates differed by 1–18 SNPs (most by <10 SNPs), and associated cases were clustered in time and occurred in neighboring suburbs, suggesting a possible cluster with a common source.

Fluoroquinolone resistance–conferring genes *qnrS1* (from 3 case-patients) and *aac(6')lb-cr* (from 1 case-patient) were detected (Figure, panel B). As reported previously (*12*), the *aac(6')lb-cr* (aacA4-cr) gene was plasmid borne (IncHI2 plasmid) and was typically a class 1 integron–associated gene cassette (*13*). Of these 4 case-patients, 2 reported recent travel to Indonesia and Vietnam and the other 2 had no record of recent overseas travel; hence, we could not exclude the possibility of local acquisition. The isolate from the case-patient who traveled to Vietnam also displayed resistance to colistin (MIC 4 μg/mL). Neither the *mcr-1* or *mcr-2* genes nor mutations in the *pmrAB*, *phoPQ*, and *mgrB* genes were present (*14*). Rather, resistance was conferred by a recently identified third mobile colistin resistance gene, *mcr-3*, carried on a plasmid (*15*).

Conclusions

Using genomic surveillance, we identified the presence of novel colistin resistance gene *mcr-3* and indications that multidrug-resistant *Salmonella* 4,[5],12:i:- ST34 has established endemicity in Australia. Our findings highlight the public health benefits of genome sequencing–guided surveillance for monitoring the spread of multidrug-resistant mobile genes and isolates.

Acknowledgments

We thank the NSW Food Authority and the Health Protection Branch of the NSW Ministry of Health for expert advice.

This study was funded by the NSW Department of Health through the Translational Research Grants scheme. V.S. was funded by the Australian National Health and Medical Research Council Career Development Fellowship, and A.A. was funded by the National Health and Medical Research Council Centre of Research Excellence in Emerging Infectious Diseases.

About the Author

Dr. Arnott is a postdoctoral scientist with the Centre for Infectious Diseases and Microbiology–Public Health and Marie Bashir Institute for Infectious Diseases and Biosecurity, The University of Sydney. Her primary research interests are the molecular epidemiology and genomics of emerging and novel bacterial pathogens.

References

1. Switt AI, Soyer Y, Warnick LD, Wiedmann M. Emergence, distribution, and molecular and phenotypic characteristics of *Salmonella enterica* serotype 4,5,12:i:-. Foodborne Pathog Dis. 2009;6:407–15. http://dx.doi.org/10.1089/fpd.2008.0213
2. Hu Y, Liu F, Lin IY, Gao GF, Zhu B. Dissemination of the *mcr-1* colistin resistance gene. Lancet Infect Dis. 2016;16:146–7. http://dx.doi.org/10.1016/S1473-3099(15)00533-2
3. Campos J, Cristino L, Peixe L, Antunes P. MCR-1 in multidrug-resistant and copper-tolerant clinically relevant *Salmonella* 1,4,[5],12:i:- and *S.* Rissen clones in Portugal, 2011 to 2015. Euro Surveill. 2016;21:30270. http://dx.doi.org/10.2807/1560-7917.ES.2016.21.26.30270
4. Li XP, Fang LX, Song JQ, Xia J, Huo W, Fang JT, et al. Clonal spread of *mcr-1* in PMQR-carrying ST34 *Salmonella* isolates from animals in China. Sci Rep. 2016;6:38511. http://dx.doi.org/10.1038/srep38511
5. Doumith M, Godbole G, Ashton P, Larkin L, Dallman T, Day M, et al. Detection of the plasmid-mediated *mcr-1* gene conferring colistin resistance in human and food isolates of *Salmonella enterica* and *Escherichia coli* in England and Wales. J Antimicrob Chemother. 2016;71:2300–5. http://dx.doi.org/10.1093/jac/dkw093
6. Lindstedt BA, Vardund T, Aas L, Kapperud G. Multiple-locus variable-number tandem-repeats analysis of *Salmonella enterica* subsp. *enterica* serovar Typhimurium using PCR multiplexing and multicolor capillary electrophoresis. J Microbiol Methods. 2004;59:163–72. http://dx.doi.org/10.1016/j.mimet.2004.06.014
7. Seemann T, Goncalves da Silva A, Bulach DM, Schultz MB, Kwong JC, Howden BP. Nullarbor [cited 2018 Feb 12]. https://github.com/tseemann/nullarbor
8. Carattoli A, Zankari E, García-Fernández A, Voldby Larsen M, Lund O, Villa L, et al. In silico detection and typing of plasmids using PlasmidFinder and plasmid multilocus sequence typing. Antimicrob Agents Chemother. 2014;58:3895–903. http://dx.doi.org/10.1128/AAC.02412-14
9. Hopkins KL, Kirchner M, Guerra B, Granier SA, Lucarelli C, Porrero MC, et al. Multiresistant *Salmonella enterica* serovar 4,[5],12:i:- in Europe: a new pandemic strain? Euro Surveill. 2010; 15:19580.
10. Mulvey MR, Finley R, Allen V, Ang L, Bekal S, El Bailey S, et al. Emergence of multidrug-resistant *Salmonella enterica* serotype 4,[5],12:i:- involving human cases in Canada: results from the Canadian Integrated Program on Antimicrobial Resistance Surveillance (CIPARS), 2003-10. J Antimicrob Chemother. 2013;68:1982–6. http://dx.doi.org/10.1093/jac/dkt149
11. García P, Guerra B, Bances M, Mendoza MC, Rodicio MR. IncA/C plasmids mediate antimicrobial resistance linked to virulence genes in the Spanish clone of the emerging *Salmonella enterica* serotype 4,[5],12:i:-. J Antimicrob Chemother. 2011; 66:543–9. http://dx.doi.org/10.1093/jac/dkq481
12. Robicsek A, Strahilevitz J, Jacoby GA, Macielag M, Abbanat D, Park CH, et al. Fluoroquinolone-modifying enzyme: a new adaptation of a common aminoglycoside acetyltransferase. Nat Med. 2006;12:83–8. http://dx.doi.org/10.1038/nm1347
13. Partridge SR, Tsafnat G, Coiera E, Iredell JR. Gene cassettes and cassette arrays in mobile resistance integrons. FEMS Microbiol Rev. 2009;33:757–84. http://dx.doi.org/10.1111/j.1574-6976.2009.00175.x
14. Webb HE, Granier SA, Marault M, Millemann Y, den Bakker HC, Nightingale KK, et al. Dissemination of the *mcr-1* colistin resistance gene. Lancet Infect Dis. 2016;16:144–5. http://dx.doi.org/10.1016/S1473-3099(15)00538-1
15. Yin W, Li H, Shen Y, Liu Z, Wang S, Shen Z, et al. Novel plasmid-mediated colistin resistance gene *mcr-3* in *Escherichia coli.* MBio. 2017;8: e00543-17. http://dx.doi.org/10.1128/mBio.00543-17

Address for correspondence: Vitali Sintchenko, Centre for Infectious Diseases and Microbiology, Level 3, Institute of Clinical Pathology and Medical Research, Westmead Hospital, Westmead, Sydney, NSW, 2145, Australia; e-mail: vitali.sintchenko@sydney.edu.au

Genetic Characterization of Enterovirus A71 Circulating in Africa

Maria Dolores Fernandez-Garcia,[1] Romain Volle,[1] Marie-Line Joffret, Serge Alain Sadeuh-Mba, Ionela Gouandjika-Vasilache, Ousmane Kebe, Michael R. Wiley, Manasi Majumdar, Etienne Simon-Loriere, Anavaj Sakuntabhai, Gustavo Palacios, Javier Martin, Francis Delpeyroux, Kader Ndiaye,[2] Maël Bessaud[2]

We analyzed whole-genome sequences of 8 enterovirus A71 isolates (EV-A71). We confirm the circulation of genogroup C and the new genogroup E in West Africa. Our analysis demonstrates wide geographic circulation and describes genetic exchanges between EV-A71 and autochthonous EV-A that might contribute to the emergence of pathogenic lineages.

Enterovirus A71 (EV-A71; species *Enterovirus A*, genus *Enterovirus*, family *Picornaviridae*) is a common etiologic agent of hand, foot and mouth disease in young children. In addition, EV-A71 has been associated with severe and sometimes fatal neurologic diseases, including aseptic meningitis, encephalitis, and poliomyelitis-like acute flaccid paralysis (AFP) (*1*,*2*).

EV-A71 is classified into 7 genogroups (A–G). Genogroup A includes the prototype strain BrCr that was isolated in the United States in 1969 (*1*,*2*). Most EV-A71 isolates belong to genogroups B or C, which are each further divided into subgenogroups (*1*,*2*). Subgenogroups B4, B5, and C4 are mainly restricted to countries in Asia, whereas C1 and C2 circulate primarily in Europe and the Asia-Pacific region (*1*). Genogroup D and the newly proposed genogroup G appear to be indigenous to India, whereas genogroups E and F were recently discovered in Africa and Madagascar, respectively (*3*).

Although EV-A71 has been reported in many parts of the world, its epidemiology remains largely unexplored in Africa. An EV-A71 outbreak was documented in 2000 in Kenya, where HIV-infected orphans were infected by EV-A71 genogroup C (*4*). Several AFP cases have been associated with EV-A71 infection during 2000–2013 throughout Africa: in Democratic Republic of the Congo (*5*) (2000, n = 1); Nigeria (*6*) (2004, n = 1, genogroup E); Central African Republic (*7*) (2003, n = 1, genogroup E); Cameroon (*8*) (2008, n = 2, genogroup E); Niger (*9*) (2013, n = 1, genogroup E); and Senegal, Mauritania, and Guinea (*9*) (2013–2014, n = 3, subgenogroup C2). Four additional EV-A71 strains were obtained from captive gorillas in Cameroon during 2006–2008 (n = 2, genogroup E) (*10*) and from healthy children in Nigeria in 2014 (n = 2, genogroup E) (*11*). Molecular identification of all these isolates was based only on the analysis of sequences of the viral protein (VP) 1 capsid protein region.

Recombination events may be associated with the emergence and global expansion of new groups of EV-A71 that have induced large outbreaks of hand, foot and mouth disease with high rates of illness and death (*12*). For EV-A71, genetic exchanges have been described both within a given genogroup and with other types of enterovirus A (EV-A), usually in nonstructural genome regions P2 and P3 (*1*,*12*,*13*). However, before 2017, no complete genome sequence of EV-A71 detected in Africa has been reported, diminishing the power of such analysis. We examined the complete genome of most EV-A71 isolates reported to date in Africa to characterize the evolutionary mechanisms of genetic variability.

The Study

We sequenced the full genome of 8 EV-A71 isolates obtained from patients with AFP (Table): isolates 14-157, 14-250, 13-365, 13-194, and 15-355 from West Africa and isolates 08-041, 08-146, and 03-008 from Central Africa. We isolated and typed these isolates as previously described (*7*–*10*) and obtained nearly complete genomic sequences using degenerated primers (*13*) and additional primers designed for gene-walking (available on request) or unbiased

Author affiliations: Institut Pasteur, Dakar, Senegal (M.D. Fernandez-Garcia, O. Kebe, K. Ndiaye); Institut Pasteur, Paris, France (R. Volle, M.-L. Joffret, E. Simon-Loriere, A. Sakuntabhai, F. Delpeyroux, M. Bessaud); Institut National de la Santé et de la Recherche Médicale, U994, Paris (R. Volle, M.-L. Joffret, F. Delpeyroux); Centre Pasteur, Yaoundé, Cameroon (S.A. Sadeuh-Mba); Institut Pasteur, Bangui, Central African Republic (I. Gouandjika-Vasilache); University of Nebraska Medical Center, Omaha, Nebraska, USA (M.R. Wiley); US Army Medical Research Institute of Infectious Diseases, Frederick, Maryland, USA (M.R. Wiley, G. Palacios); National Institute for Biological Standards and Control, Hertfordshire, UK (M. Majumdar, J. Martin)

DOI: https://doi.org/10.3201/eid2404.171783

[1]These first authors contributed equally to this article.

[2]These senior authors contributed equally to this article.

Table. Description of enterovirus isolates from patients with acute flaccid paralysis in Africa that were sequenced for characterization of enterovirus A71*

Strain (reference)	Country of isolation	Patient age at diagnosis, y	Year	Virus	Genogroup or subgenogroup	Genbank accession no.
14-157 (*9*)	Senegal	3	2014	EV-A71	C2	MG672480
14-250 (*9*)	Mauritania	1.6	2014	EV-A71	C2	MG672481
13-365 (*9*)	Guinea	1.7	2013	EV-A71	C2	MG672479
15-355 (this study)	Senegal	2.4	2015	EV-A71	C2	MG013988
13-194 (*9*)	Niger	1.3	2013	EV-A71	E	MG672478
03-008 (*7*)	Central African Republic	1.9	2003	EV-A71	E	LT719068
08-146 (*8*)	Cameroon	2.6	2008	EV-A71	E	LT719066
08-041 (*8*)	Cameroon	1.7	2008	EV-A71	C1	LT719067
14-254 (*15*)	Senegal	3	2014	CV-A14	NA	MG672482

*NA, not available.

sequencing methods (*14*). We determined the 5′-terminal sequences by means of a RACE kit (Roche, Munich, Germany). We deposited viral genomes in GenBank (accession numbers in Table) and submitted sequence alignments under BioProject PRJNA422891. We aligned sequences using ClustalW software (http://www.clustal.org).

To investigate the genetic relationship between Africa and global EV-A71 isolates, we constructed subgenomic phylogenetic trees based on the P1, P2, and P3 regions of the genome (Figure 1). We identified viral isolates showing related sequences in 1 of these 3 regions by BLAST search (http://www.ncbi.nlm.nih.gov/BLAST) and included them in the corresponding datasets used for analyses. We completed these datasets with a representative global set of EV-A71 sequences available in GenBank and belonging to the different EV-A71 genogroups (https:///wwwnc.cdc.gov/EID/article/24/4/17-1783-Techapp1.pdf). As expected, in the structural P1 region, the 8 isolates we studied clustered within their respective genogroups (C1, C2, and E), previously established by VP1-based typing (Figure 1, panel A). In particular, the isolates of genogroup E consistently clustered together (bootstrap value 100%), confirming their belonging to the EV-A71 type and their divergence from the other isolates belonging to the common genogroups A, B, and C. Analysis of the nonstructural P2 and P3 genome regions were in agreement with these data. However, the genetic heterogeneity, ≤12%, observed among the complete genome of genogroup E sequences highly suggested that they have circulated and diverged for years in a large geographic area in Africa. The unique Africa EV-A71-C1 strain clustered with other C1 strains originating worldwide, regardless of which genome region we analyzed. In contrast, the nonstructural sequences of Africa EV-A71 isolates of subgenogroup C2 did not cluster with their non-Africa C2 counterparts or with any of the existing EV-A71 genogroups. The incongruent phylogenetic relationships of Africa C2 strains in the different regions of the genome suggested that recombination events have occurred during evolution.

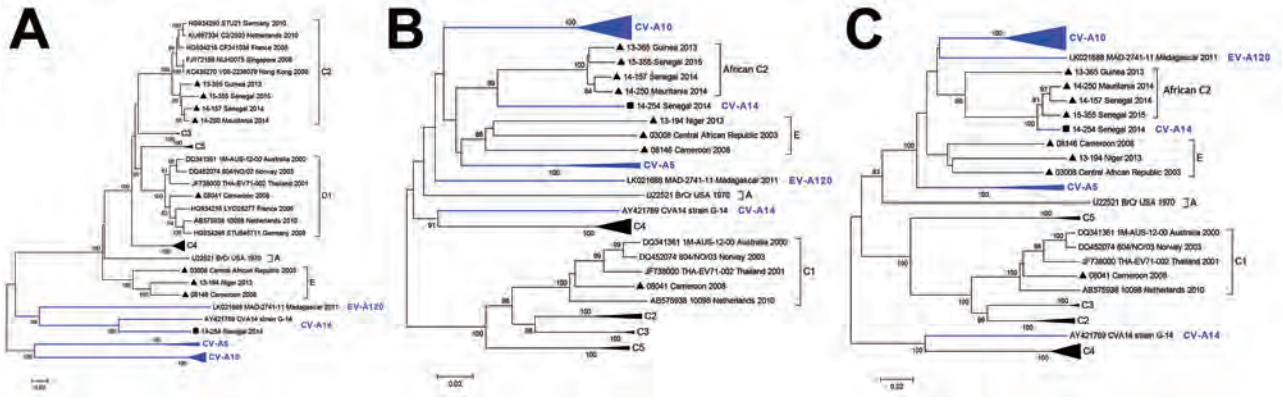

Figure 1. Phylogenetic relationships of EV-A71 isolates from patients with acute flaccid paralysis in Africa based on 3 coding regions: A) P1, B) P2, and C) P3. Apart from the studied sequences, subgenomic datasets included their best nucleotide sequence matches identified by NCBI BLAST search (http://www.ncbi.nlm.nih.gov/BLAST) as well as representative sequences of different EV-A71 genogroups and subgenogroups originating worldwide. Trees were constructed from the nucleotide sequence alignment using MEGA 5.0 software (http://megasoftware.net/) with the neighbor-joining method. Distances were computed using the Kimura 2-parameter model. The robustness of the nodes was tested by 1,000 bootstrap replications. Bootstrap support values ≥75 are shown in nodes and indicate a strong support for the tree topology. For clarity, CV-A10, CV-A5, and EV-A71 subgenogroups C3, C4, and C5 have been collapsed. Study strains are indicated by laboratory code, country of origin, and year of isolation; previously published strains are indicated by GenBank accession number, isolate code, country of origin, and year of isolation. Black triangles indicate EV-A71 strains from this study; black square indicates the CV-A14 strain from this study. Strains gathered in brackets belong to EV-A71 genogroups or subgenogroups; strains marked in blue color belong to other species of EV-A. Scale bars indicate nucleotide substitutions per site. CV, coxsackievirus; EV, enterovirus.

To examine further recombination events, we analyzed EV-A71-C2 study strains by similarity plot against potential parental genomes (Figure 2). This analysis showed that sequences 14-157, 14-250, and 15-355 had high similarity (≥95%). By contrast, 13-365 diverged from the other C2 isolates around nt 5600 in the P3 region, suggesting a recombination breakpoint. The analysis showed high sequence similarity (≥97%) between the studied EV-A71-C2 isolates and other subgenogroup C2 strains over the P1 capsid region. Conversely, in the noncapsid region, sequence similarity between Africa EV-A71-C2 isolates and classical subgenogroup C2 isolates (e.g., GenBank accession no. HQ647175) was much lower (66%–77%). This finding confirmed a recombination event of the Africa EV-A71 C2 lineage with an unknown enterovirus, the most likely breakpoint being located between nt 3596 and 3740, within the 2A gene. Sequence identity of EV-A71-C2 study strains with their closest related viruses (coxsackievirus A10 [CV-A10], CV-A5, EV-A120, and EV-A71 genogroup E strains) in the 3′ half of the genome was ≤87.7%. Of note, we found much higher sequence identity with the full-genome sequence of CV-A14 isolate in our database, obtained in 2014 from a patient with AFP in Senegal (*15*). This strain features a high similarity value (≥97%) with the 3′ half of the genomes of EV-A71-C2 West Africa strains (Figure 2), indicating that their P3 regions share a recent common ancestor. Because these strains belong to 2 different types, this finding strongly suggests that genetic exchanges occurred through intertypic recombination. This result cannot be a result of cross-contamination during the sequencing process because the CV-A14 and EV-A71 isolates were sequenced on 2 different platforms.

Conclusions

Genogroup E was previously identified and characterized only on the basis of VP1 analysis (*3*). This study confirms the circulation in West and Central Africa of EV-A71 isolates belonging to the new genogroup E on the basis of the characterization of whole genomes. The divergence among isolates indicates that this genogroup has been ex-

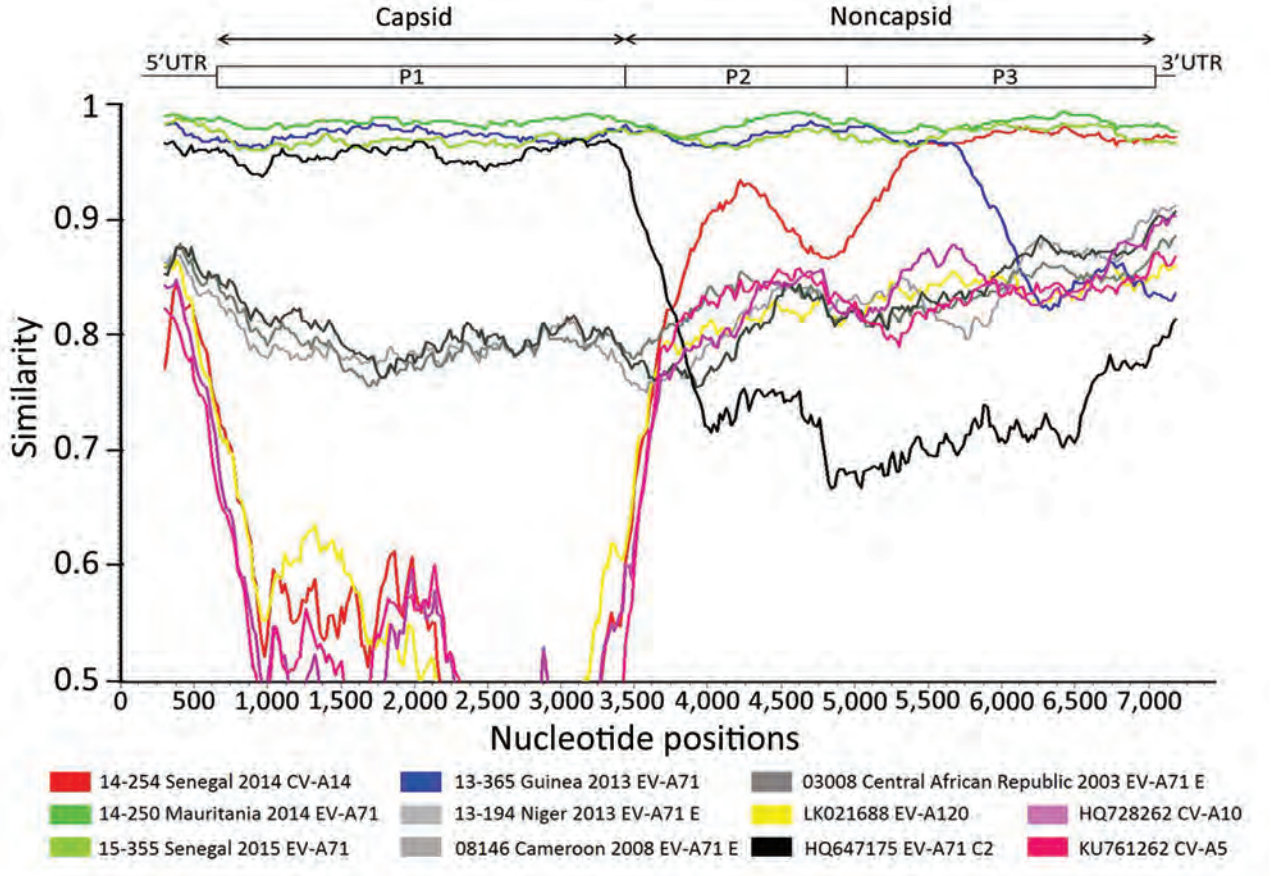

Figure 2. Identification of recombinant sequences in the genome of EV-A71 C2 isolates from patients with acute flaccid paralysis in Africa (14-157, 14-250, 13-365, 15-355) by similarity plot against potential parent genomes (CV-A14 strain 14-254; EV-A71 genogroup E strains 13-194, 08-146, and 03-008) and from GenBank (CV-A10, CV-A5, EV-A120). Similarity plot analysis was performed using SimPlot version 3.5.1 (http://sray.med.som.jhmi.edu/SCRoftware/simplot) on the basis of full-length genomes. For the analysis, we used a window of 600 nt moving in 20-nt steps. Approximate nt positions in the enterovirus genome are indicated. The enterovirus genetic map is shown in the top panel. We used the genome of EV-A71 study strain 14-157 as a query sequence. UTR, untranslated region.

tensively circulating in Africa. We also suggest that the common ancestor of EV-A71-C2 strains in West Africa has undergone recombination with ≥1 EV-A circulating in Africa. Genogroup E and recombinant C2 appear to be indigenous to Africa; they have not yet been detected elsewhere. Further exploration of environmental or clinical samples using deep sequencing technology would be of interest to determine the extent of EV-A71 circulation in Africa in the absence of AFP cases. Systematic surveillance based on full-genome sequencing could also serve to monitor these viruses for potential recombinations and to study their role in the emergence of new EV-A71 variants in Africa.

Acknowledgments

We thank Karla Prieto and Catherine Pratt, who assisted in obtaining nearly complete genomes of West Africa strains, and Joseph Chitty for analysis of the next-generation sequencing data.

The next-generation sequencing equipment at Institut Pasteur of Dakar was provided by the Defense Biological Product Assurance Office under the Targeted Acquisition of Reference Materials Augmenting Capabilities Initiative. This work was supported by the IPD, the Pasteur Institute's Transverse Research Program PTR484, Actions Concertées Inter-Pasteuriennes A22-16, Fondation Total Grant S-CM15010-05B, Roux Howard Cantarini postdoctoral fellowship, and Grant Calmette and Yersin from the International Directorate of the Institut Pasteur.

About the Author

Dr. Fernandez-Garcia is a scientist with a PhD degree in virology and is involved in research and surveillance of enterovirus infections at Institut Pasteur of Dakar, Senegal. Her research interests include infectious disease epidemiology and public health microbiology.

References

1. Solomon T, Lewthwaite P, Perera D, Cardosa MJ, McMinn P, Ooi MH. Virology, epidemiology, pathogenesis, and control of enterovirus 71. Lancet Infect Dis. 2010;10:778–90. http://dx.doi.org/10.1016/S1473-3099(10)70194-8
2. Chang P-C, Chen S-C, Chen K-T. The current status of the disease caused by enterovirus 71 infections: Epidemiology, pathogenesis, molecular epidemiology, and vaccine development. Vol. 13. Int J Environ Res Public Health. 2016;13:890. http://dx.doi.org/10.3390/ijerph13090890
3. Bessaud M, Razafindratsimandresy R, Nougairède A, Joffret ML, Deshpande JM, Dubot-Pérès A, et al. Molecular comparison and evolutionary analyses of VP1 nucleotide sequences of new African human enterovirus 71 isolates reveal a wide genetic diversity. PLoS One. 2014;9:e90624. http://dx.doi.org/10.1371/journal.pone.0090624
4. Chakraborty R, Iturriza-Gómara M, Musoke R, Palakudy T, D'Agostino A, Gray J. An epidemic of enterovirus 71 infection among HIV-1-infected orphans in Nairobi. AIDS. 2004;18:1968–70. http://dx.doi.org/10.1097/00002030-200409240-00018
5. Junttila N, Lévêque N, Kabue JP, Cartet G, Mushiya F, Muyembe-Tamfum JJ, et al. New enteroviruses, EV-93 and EV-94, associated with acute flaccid paralysis in the Democratic Republic of the Congo. J Med Virol. 2007;79:393–400. http://dx.doi.org/10.1002/jmv.20825
6. Oyero OG, Adu FD. Non-polio enteroviruses serotypes circulating in Nigeria. Afr J Med Med Sci. 2010;39(Suppl):201–8.
7. Bessaud M, Pillet S, Ibrahim W, Joffret ML, Pozzetto B, Delpeyroux F, et al. Molecular characterization of human enteroviruses in the Central African Republic: uncovering wide diversity and identification of a new human enterovirus A71 genogroup. J Clin Microbiol. 2012;50:1650–8. http://dx.doi.org/10.1128/JCM.06657-11
8. Sadeuh-Mba SA, Bessaud M, Massenet D, Joffret ML, Endegue MC, Njouom R, et al. High frequency and diversity of species C enteroviruses in Cameroon and neighboring countries. J Clin Microbiol. 2013;51:759–70. http://dx.doi.org/10.1128/JCM.02119-12
9. Fernandez-Garcia MD, Kebe O, Fall AD, Dia H, Diop OM, Delpeyroux F, et al. Enterovirus A71 genogroups C and E in children with acute flaccid paralysis, West Africa. Emerg Infect Dis. 2016;22:753–5. http://dx.doi.org/10.3201/eid2204.151588
10. Sadeuh-Mba SA, Bessaud M, Joffret ML, Endegue Zanga MC, Balanant J, Mpoudi Ngole E, et al. Characterization of Enteroviruses from non-human primates in cameroon revealed virus types widespread in humans along with candidate new types and species. PLoS Negl Trop Dis. 2014;8:e3052. http://dx.doi.org/10.1371/journal.pntd.0003052
11. Faleye TO, Adewumi MO, Coker BA, Nudamajo FY, Adeniji JA. Direct detection and identification of enteroviruses from faeces of healthy Nigerian children using a cell-culture independent RT-seminested PCR assay. Adv Virol. 2016;2016:1412838. http://dx.doi.org/10.1155/2016/1412838
12. McWilliam Leitch EC, Cabrerizo M, Cardosa J, Harvala H, Ivanova OE, Koike S, et al. The association of recombination events in the founding and emergence of subgenogroup evolutionary lineages of human enterovirus 71. J Virol. 2012; 86:2676–85. http://dx.doi.org/10.1128/JVI.06065-11
13. Yoke-Fun C, AbuBakar S. Phylogenetic evidence for inter-typic recombination in the emergence of human enterovirus 71 subgenotypes. BMC Microbiol. 2006;6:74. http://dx.doi.org/10.1186/1471-2180-6-74
14. Kugelman JR, Wiley MR, Mate S, Ladner JT, Beitzel B, Fakoli L, et al.; US Army Medical Research Institute of Infectious Diseases; National Institutes of Health; Integrated Research Facility–Frederick Ebola Response Team 2014–2015. Monitoring of Ebola virus Makona evolution through establishment of advanced genomic capability in Liberia. Emerg Infect Dis. 2015;21:1135–43. http://dx.doi.org/10.3201/eid2107.150522
15. Fernandez-Garcia MD, Kebe O, Fall AD, Ndiaye K. Identification and molecular characterization of non-polio enteroviruses from children with acute flaccid paralysis in West Africa, 2013-2014. Sci Rep. 2017;7:3808. http://dx.doi.org/10.1038/s41598-017-03835-1

Address for correspondence: Maria Dolores Fernandez-Garcia, Pôle de Virologie, Institut Pasteur, 36 Avenue Pasteur, BP220, Dakar, Senegal; email: dolores.fernandez@yahoo.es

Emergomyces canadensis, a Dimorphic Fungus Causing Fatal Systemic Human Disease in North America

Ilan S. Schwartz, Stephen Sanche, Nathan P. Wiederhold, Thomas F. Patterson, Lynne Sigler

We report 4 patients in North America with disease caused by *Emergomyces canadensis,* a newly proposed species of pathogenic dimorphic fungus. Affected persons were immunocompromised; lived in Saskatchewan, Colorado, and New Mexico; and had systemic disease involving blood, skin, cervix, lung, and lymph node. Two cases were fatal.

Members of the recently described fungal genus *Emergomyces* cause disseminated and often fatal disease in immunocompromised hosts (*1*,*2*). So named because of their recent global emergence (*1*), these dimorphic fungal pathogens have been reported from Africa, Asia, and Europe (*3*). Here we report from North America 4 cases of invasive fungal disease caused by a novel *Emergomyces* species, designated *Es. canadensis*.

The Study

In 2003, a 39-year-old man with a history of diabetes and a cadaveric renal transplantation 3 years prior visited a hospital in Saskatoon, Saskatchewan, Canada, reporting fever and throat pain. His medications included mycophenolate and prednisone (25 mg/d). The patient had no history of travel. He kept pet birds, none of which were ill, and had no other animal exposures.

On examination, the patient was cushingoid, normotensive, and afebrile. Results of oropharyngeal, chest, and abdominal examinations were unremarkable. Chest radiograph and computed tomography demonstrated diffuse micronodules, left upper lobe consolidation, and mediastinal lymphadenopathy. The patient was assessed by esophagoscopy, which indicated white, dry patches suspicious for esophageal candidiasis; consequently, we started him on oral fluconazole (200 mg/d). On day 5 postadmission, he had myalgias, arthralgias, and a fever of 38.9°C, prompting collection of mycobacterial and fungal blood cultures. Two days later, a bronchoscopy demonstrated white patches in the trachea and bronchi. On day 17 of admission, both the blood and bronchoalveolar lavage cultures grew a fungus. Repeated blood cultures subsequently grew the same fungus. We treated the patient with lipid complex amphotericin B for 3 weeks, with clinical improvement, and he was discharged after 7 weeks in the hospital.

Several days later, the patient returned, reporting weakness, postural dizziness, anorexia, and vomiting. Repeated chest radiograph and computed tomography showed patchy consolidation with increased right mediastinal lymphadenopathy. A mediastinoscopy with lymph node biopsy excluded lymphoma. No material was sent for culture, but histopathologic examination with fungal stains demonstrated small, round or oval yeasts (Figure 1). The patient remained afebrile, and he was managed expectantly without additional antifungal therapy. His symptoms resolved, and he was discharged. Serial chest radiographs demonstrated resolution of the mediastinal lymphadenopathy, and no clinical relapse occurred in 3 years of follow-up.

The clinical isolate was referred to the University of Alberta Microfungus Collection and Herbarium (UAMH) for characterization and identification. The fungus grew as a mold phase at 30°C and as a yeast at 35°C (Figure 2, panels A and B). Microscopic examination of mycelia demonstrated florets of 1 to 3 conidia borne at the ends of slightly swollen conidiophores (Figure 2, panel C), reminiscent of *Emmonsia*-like fungi (*1*,*2*). The yeast cells were small (2.5–5.0 μm) and round or oval, with 1 or occasionally 2 narrow-based buds (Figure 2, panel D).

DNA genetic analysis was performed by sequencing the internal transcribed spacer region and D1/D2 domain of the large subunit rDNA as previously described (*4*). The sequence of the case isolate was identical to one from another clinical isolate obtained in 1992 from another patient in Saskatchewan and thought to represent an

Author affiliations: Global Health Institute, University of Antwerp, Antwerp, Belgium (I.S. Schwartz); San Antonio Center for Medical Mycology, UT Health San Antonio, San Antonio, Texas, USA (I.S. Schwartz, N.P. Wiederhold, T.F. Patterson); University of Saskatchewan, Saskatoon, Saskatchewan, Canada (S. Sanche); UT Health San Antonio Fungus Testing Laboratory, San Antonio (N.P. Wiederhold); South Texas Veterans Health Care System, San Antonio (T.F. Patterson); University of Alberta Biological Sciences, Edmonton, Alberta, Canada (L. Sigler)

DOI: https://doi.org/10.3201/eid2404.171765

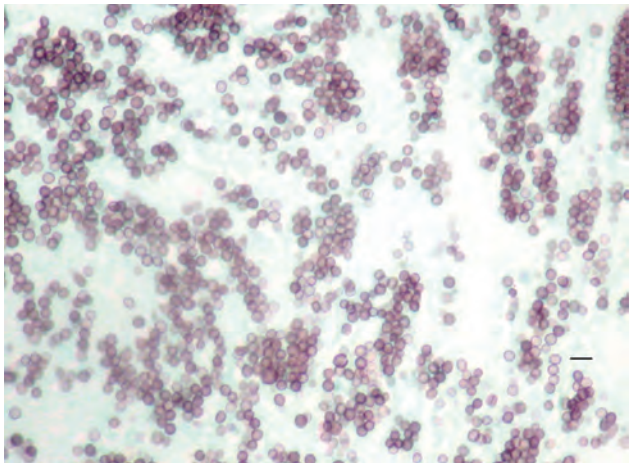

Figure 1. Methenamine silver stain of mediastinal lymph node biopsy, demonstrating small round or oval yeasts in tissue, from a patient infected with novel fungal species *Emergomyces canadensis* (case-patient 2), Saskatoon, Saskatchewan, Canada, 2003. Scale bar indicates 10 μm.

undescribed *Emmonsia* species (*4*,*5*). Recent phenotypic and phylogenetic analyses confirmed that these isolates represent a new species within the genus *Emergomyces* (*2*); the proposed name is *Es. canadensis* (Y. Jiang, S. de Hoog, pers. comm., 2018 Jan 19).

We searched for additional clinical isolates among those referred to the Fungus Testing Laboratory at UT Health San Antonio (San Antonio, TX, USA) during 2001–2016. We reviewed isolates previously identified as *Emmonsia* species or as *Blastomyces dermatitidis* based on low-positive (<400,000 relative light units) results on a *B. dermatitidis* DNA probe (AccuProbe, Hologic, Inc., San Diego, CA, USA). We confirmed identification by sequencing of the internal transcribed spacer and D1/D2 regions and thus identified 2 additional isolates of *Es. canadensis*.

We compiled and summarized epidemiologic and clinical data from submitting laboratories and clinicians for the 4 clinical *Es. canadensis* isolates (Table). Two isolates were referred from Saskatchewan, 1 from Colorado, and 1 from New Mexico. All 3 patients for whom medical histories could be ascertained were immunocompromised, 2 with advanced HIV infection and the third with a kidney transplantation. Histopathology results were available for 2 patients: in case 2, small yeasts were observed in tissue from mediastinal lymph node, and in case 3, in tissue from an endocervical mass. *Es. canadensis* was cultured from biopsied cutaneous lesions in 2 patients (in cases 1 and 4). For 2 remaining patients, *Es. canadensis* was cultured from blood, and additionally in 1 patient, from bronchoalveolar fluid. Two patients survived, and 2 died.

We performed limited antifungal susceptibility testing for 2 isolates (*6*). The MIC of UAMH 10370 was 0.125 μg/mL for amphotericin B. The MIC of UTHSCSA

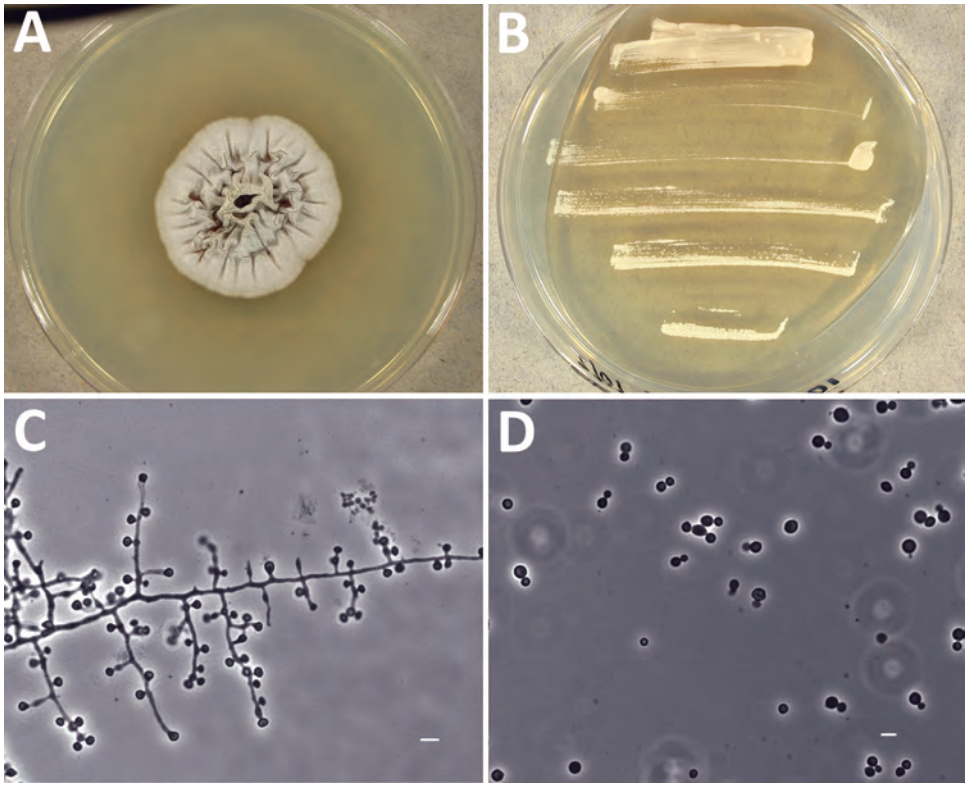

Figure 2. Morphologic features of novel fungal species *Emergomyces canadensis* isolated from case-patient 2, Saskatoon, Saskatchewan, Canada, 2003. A–B) Colonies grown on potato dextrose agar showing mold phase after 28 days at 30°C (A) and yeast phase after 9 days at 35°C (B). C) Mycelial phase showing 1–3 conidia borne at the ends of slightly swollen conidiophores or sessile on hyphae. D) Round to oval yeast cells with narrow-based budding produced at 35°C. Scale bars indicate 5 μm.

Table. Epidemiologic and clinical characteristics of 4 patients infected with *Emergomyces canadensis*, North America, 1992–2015*

Case no.	Year	Location	Patient age, y/sex	Medical history	Clinical syndrome	Specimen cultured	Treatment	Outcome	Strain ID†
1	1992	Regina, Saskatchewan	68/M	HIV	Sepsis, skin lesions	Skin biopsy	–	Died	UAMH 7172 (AF038322)
2	2003	Saskatoon, Saskatchewan	39/M	Kidney transplant, diabetes	Pneumonia, tracheitis, lymphadenopathy, esophagitis, sepsis	Blood, BAL fluid	Fluconazole, then amphotericin B	Survived	UAMH 10370 (EF592151)
3	2010	Colorado Springs, Colorado	75/F	–	Fungemia, endocervical lesion	Blood	–	Died	UTHSCSA DI17–85 (MG777526, MG777527)
4	2015	Santa Fe, New Mexico	40/M	HIV	Pneumonia, skin lesions, sepsis	Skin biopsy	–	Survived	UTHSCSA DI17–84 (MG777530, MG777528)

*BAL, bronchoalveolar; ID, identification; UAMH, UAMH Centre for Global Microfungal Biodiversity; UTHSCSA, University of Texas Health Science Center at San Antonio; –, data missing.
†GenBank accession numbers for relevant nucleotide sequences are given.

DI17–85 was 64 μg/mL for fluconazole and 0.125 μg/mL for itraconazole.

Conclusions

Es. canadensis is one of several newly recognized species within *Emergomyces* (*2*), and causes an endemic mycosis in North America, where it should be considered in immunocompromised hosts with systemic disease. *Es. africanus* causes the most common endemic mycosis in South Africa, primarily affecting HIV-infected persons (*7*); pulmonary and cutaneous disease are common, and the case-fatality rate is 50% (*8*). Invasive disease caused by *Es. pasteurianus* (previously *Emmonsia pasteuriana* [*2*,*9*]) has been reported from Italy, Spain, France, India, China, and South Africa (*3*). *Es. orientalis* was reported just once, from a man in China (*10*). Infection caused by another novel species, *Es. europaeus*, is known also from a single case from Germany (*11*).

Limited antifungal susceptibility testing of 2 *Es. canadensis* isolates found MICs elevated for fluconazole and low for itraconazole and amphotericin B. Dukik et al. (*12*) recently reported antifungal susceptibility results for 2 *Es. canadensis* isolates including UAMH 7172 (reported as CBS 139872) and UAMH 10370 (reported as CBS 139873). The authors similarly found that MICs were elevated for fluconazole and low for newer triazoles and amphotericin B (*12*). These findings are consistent with the antifungal susceptibility patterns reported for 50 *Es. africanus* isolates (*7*). The anecdotal observation in our study that a patient (in case 2) remained fungemic with *Es. canadensis* 2 weeks after initiating fluconazole but had rapid clinical improvement with amphotericin B is consistent with these in vitro results. Pending the availability of further data, treatment of disease caused by *Emergomyces* spp. infection should follow clinical practice guidelines for the management of other dimorphic fungal infections in immunocompromised hosts (*13*). Specifically, treatment should include amphotericin B (lipid formulation 3–5 mg/kg or deoxycholate 0.7–1.0 mg/kg) for 1–2 weeks, followed by itraconazole (or other newer triazole) for at least 12 months, depending on immune reconstitution (*13*).

This report raises many questions about the pathogenesis, distribution, and habitat of *Es. canadensis*. As is the case for other dimorphic fungi, inhalational infection by *Emergomyces* spp. is presumed to occur, followed by extrapulmonary dissemination and disease in susceptible hosts (*3*). Although limited by small numbers and the lack of travel histories, these cases suggest that the geographic range of *Es. canadensis* likely involves central and western regions of North America. An ecologic niche has only been investigated for *Es. africanus*, which has been detected from various soil habitats and in air samples from Cape Town, South Africa (*14*,*15*). Further investigations are required to better understand the epidemiology and prevalence of disease caused by *Emergomyces* spp. in North America and globally.

Acknowledgments

The authors acknowledge the laboratory technicians at the Fungus Testing Laboratory and Nancy Wengenack and Amy Gattis for help retrieving clinical data for isolates.

I.S.S. received the support of a Detweiler Travelling Fellowship award from the Royal College of Physicians and Surgeons of Canada.

About the Author

Dr. Schwartz is an infectious diseases clinician and researcher with interests in emerging fungal infections, immunocompromised hosts, and global health. He is currently a visiting scholar at the San Antonio Center for Medical Mycology at UT Health San Antonio.

References

1. Schwartz IS, Kenyon C, Feng P, Govender NP, Dukik K, Sigler L, et al. 50 years of *Emmonsia* disease in humans: the dramatic emergence of a cluster of novel fungal pathogens. PLoS Pathog. 2015;11:e1005198. http://dx.doi.org/10.1371/journal.ppat.1005198
2. Dukik K, Muñoz JF, Jiang Y, Feng P, Sigler L, Stielow JB, et al. Novel taxa of thermally dimorphic systemic pathogens in the *Ajellomycetaceae* (*Onygenales*). Mycoses. 2017;60:296–309. http://dx.doi.org/10.1111/myc.12601
3. Schwartz IS, Maphanga TG, Govender NP. *Emergomyces*: a new genus of dimorphic fungal pathogens causing disseminated disease among immunocompromised persons globally. Curr Fungal Infect Rep. 2018;12:44–50.
4. Peterson SW, Sigler L. Molecular genetic variation in *Emmonsia crescens* and *Emmonsia parva*, etiologic agents of adiaspiromycosis, and their phylogenetic relationship to *Blastomyces dermatitidis* (*Ajellomyces dermatitidis*) and other systemic fungal pathogens. J Clin Microbiol. 1998;36:2918–25.
5. Sigler L, Peterson SW. Molecular genetic analysis supports recognition of new species among *Emmonsia* and *Blastomyces* isolates. Int J Antimicrob Agents. 2009;34(s2):S93. http://dx.doi.org/10.1016/S0924-8579(09)70427-3
6. Clinical and Laboratory Standards Institute. Reference method for broth dilution antifungal susceptibility testing of filamentous fungi; approved standard, 2nd ed. (M38-A2). Wayne (PA): The Institute; 2008.
7. Maphanga TG, Britz E, Zulu TG, Mpembe RS, Naicker SD, Schwartz IS, et al. In vitro antifungal susceptibility of the yeast and mold phases of the dimorphic fungal pathogen, *Emergomyces africanus* (formerly *Emmonsia* sp.), from HIV-infected South African patients. J Clin Microbiol. 2017;55:1812–20. http://dx.doi.org/10.1128/JCM.02524-16
8. Schwartz IS, Govender NP, Corcoran C, Dlamini S, Prozesky H, Burton R, et al. Clinical characteristics, diagnosis, management, and outcomes of disseminated emmonsiosis: a retrospective case series. Clin Infect Dis. 2015;61:1004–12. http://dx.doi.org/10.1093/cid/civ439
9. Gori S, Drouhet E. Cutaneous disseminated mycosis in a patient with AIDS due to a new dimorphic fungus. J Mycol Med. 1998;8:57–63.
10. Wang P, Kenyon C, de Hoog S, Guo L, Fan H, Liu H, et al. A novel dimorphic pathogen, *Emergomyces orientalis* (*Onygenales*), agent of disseminated infection. Mycoses. 2017;60:310–9. http://dx.doi.org/10.1111/myc.12583
11. Wellinghausen N, Kern WV, Haase G, Rozdzinski E, Kern P, Marre R, et al. Chronic granulomatous lung infection caused by the dimorphic fungus *Emmonsia* sp. Int J Med Microbiol. 2003;293:441–5. http://dx.doi.org/10.1078/1438-4221-00281
12. Dukik K, Al-Hatmi AMS, Curfs-Breuker I, Faro D, de Hoog S, Meis JF. Antifungal susceptibility of emerging dimorphic pathogens in the family *Ajellomycetaceae.* Antimicrob Agents Chemother. 2017;62:e01886–17. http://dx.doi.org/10.1128/AAC.01886-17
13. Wheat LJ, Freifeld AG, Kleiman MB, Baddley JW, McKinsey DS, Loyd JE, et al.; Infectious Diseases Society of America. Clinical practice guidelines for the management of patients with histoplasmosis: 2007 update by the Infectious Diseases Society of America. Clin Infect Dis. 2007;45:807–25. http://dx.doi.org/10.1086/521259
14. Schwartz IS, Lerm B, Hoving JC, Kenyon C, Horsnell WG, Basson WJ, et al. *Emergomyces africanus* in Soil, South Africa. Emerg Infect Dis. 2018;24:377–80. http://dx.doi.org/10.3201/eid2402.171351
15. Schwartz IS, McLoud JD, Berman D, Botha A, Lerm B, Colebunders R, et al. Molecular detection of airborne *Emergomyces africanus*, a thermally dimorphic fungal pathogen, in Cape Town, South Africa. PLoS Negl Trop Dis. 2018; 12:e0006174. http://dx.doi.org/10.1371/journal.pntd.0006174

Address for correspondence: Ilan S. Schwartz, San Antonio Center for Medical Mycology, UT Health San Antonio, 7703 Floyd Curl Dr, San Antonio, TX 78229, USA; email: ilan.steven.schwartz@gmail.com

mcr-1 in Carbapenemase-Producing *Klebsiella pneumoniae* in Hospitalized Patients, Portugal, 2016–2017

Ana Constança Mendes,[1] Ângela Novais,[1] Joana Campos, Carla Rodrigues, Cláudia Santos, Patrícia Antunes, Helena Ramos, Luísa Peixe

We describe a hospital-based outbreak caused by multidrug-resistant, *Klebsiella pneumoniae* carbapenemase 3–producing, *mcr-1*–positive *K. pneumoniae* sequence type 45 in Portugal. *mcr-1* was located in an IncX4 plasmid. Our data highlight the urgent need for systematic surveillance of *mcr-1* to support adequate therapeutic choices in the nosocomial setting.

Infections with carbapenemase-producing *Enterobacteriaceae* (CPE), such as *Klebsiella pneumoniae*, have been increasing since 2011 in hospitalized patients in several countries in Europe, especially those with high resistance rates (https://ecdc.europa.eu/sites/portal/files/documents/antibiotics-EARS-Net-summary-2016_0.pdf; https://ecdc.europa.eu/sites/portal/files/documents/AMR-surveillance-Europe-2016.pdf). The emergence of mobilized colistin resistance (MCR) genes is particularly concerning because colistin is being intensively used as a last resource antimicrobial drug for treating CPE infections (*1*,*2*). In Europe, sporadic clinical CPE isolates with *mcr-1* have been reported (*3*,*4*). Because CPE has increased at an alarming pace in Portugal (*5*,*6*), we evaluated the occurrence of *mcr-1* among CPE isolated from patients admitted to Centro Hospitalar do Porto, a tertiary and university hospital in Porto, Portugal.

The Study

Using rectal swab specimens from 5,361 patients admitted to Centro Hospitalar do Porto during October 2015–July 2017, we screened for carbapenemase-positive isolates using Brilliance CRE Agar (Oxoid, Basingstoke, UK), Blue-carba test (*7*), and real-time PCR for carbapenemase genes (Xpert Carba-R; Cepheid, Sunnyvale, CA, USA) (Figure 1, panel A). We identified 283 patients with 359 CPE-positive samples available for further testing. Of the 359 isolates, 252 (75% *K. pneumoniae*–positive) were from patient fecal samples and 107 (86% *K. pneumoniae*-positive) were from other types of patient samples (e.g., blood, urine). We then screened these isolates for *mcr-1*, $bla_{\text{CTX-M-I}}$-like genes, and bla_{KPC} using PCR and sequencing (*5*,*8*,*9*). We determined the antimicrobial drug susceptibility profiles of the *mcr-1*–positive isolates by the broth microdilution method for colistin (http://www.eucast.org/fileadmin/src/media/PDFs/EUCAST_files/General_documents/Recommendations_for_MIC_determination_of_colistin_March_2016.pdf) and by disk diffusion for the other antimicrobial drugs using Clinical and Laboratory Standards Institute/European Committee on Antimicrobial Susceptibility Testing guidelines (http://www.eucast.org/). We evaluated clonal relatedness among *K. pneumoniae* isolates by multilocus sequence and *wzi* capsular typing (http://bigsdb.pasteur.fr/perl/bigsdb/bigsdb.pl?db = pubmlst_klebsiella_seqdef_public) and assessed plasmid replicon content using PCR (*5*). We performed whole-genome sequencing with 2 isolates of the predominant *K. pneumoniae* clones by Hi Seq 2500 Sequencing System (Illumina Inc., San Diego, CA, USA) (2 × 150 bp paired-ended reads, coverage 100×). We assembled reads de novo using SPAdes version 3.9.0 (http://cab.spbu.ru/software/spades/) and annotated contigs with Prokka (http://vicbioinformatics.com/). We used tools from the Center for Genomic Epidemiology (http://www.genomicepidemiology.org) to assess antimicrobial drug resistance genes and replicons and PLACNETw (https://castillo.dicom.unican.es/upload/) for plasmid reconstruction. We located *mcr-1* in the IncX4 plasmid near the replication (*pirF*) and maintenance (*parA*) conserved regions by PCR and sequencing (Figure 2).

We identified 24 carbapenemase-producing and MCR-1–producing *K. pneumoniae* isolates from samples collected during September 2016–February 2017 from 16 hospitalized patients (Figure 1, panel B). Seventeen isolates were colonizers (i.e., bacteria of the patients' gastrointestinal tract), and 7 were from other parts of the body (3 urine, 2 blood, 2 other biologic fluids) (Table). We recovered 1–4 isolates/patient; 10 colonizing isolates were from intensive care units. Patients (9 men, 7 women) were 50–87 years of age, and their clinical history included prolonged hospitalization (median 47 d, range 12–151 d); complicated conditions; and, for many, surgical interventions, immunosuppression, or previous antimicrobial drug

Author affiliations: Centro Hospitalar do Porto, Porto, Portugal (A.C. Mendes, C. Santos, H. Ramos); Faculdade de Farmácia, Universidade do Porto, Porto (Â. Novais, J. Campos, C. Rodrigues, P. Antunes, L. Peixe); Faculdade de Ciências da Nutrição e Alimentação, Universidade do Porto, Porto (P. Antunes)

DOI: https://doi.org/10.3201/eid2404.171787

[1]These authors contributed equally to this article.

use (usually β-lactams) favoring infection or colonization by multidrug-resistant (MDR) *mcr-1*–positive strains (*10*). Fecal samples were negative for CPE at admission (14/16 patients screened) and for a median of 15 (range 3–94) days after admission (Figure 1, panel B). Five patients had 1 or 2 extraintestinal infections with an MCR-1–producing isolate, sometimes with an isolate identical to one previously detected in their gastrointestinal tract.

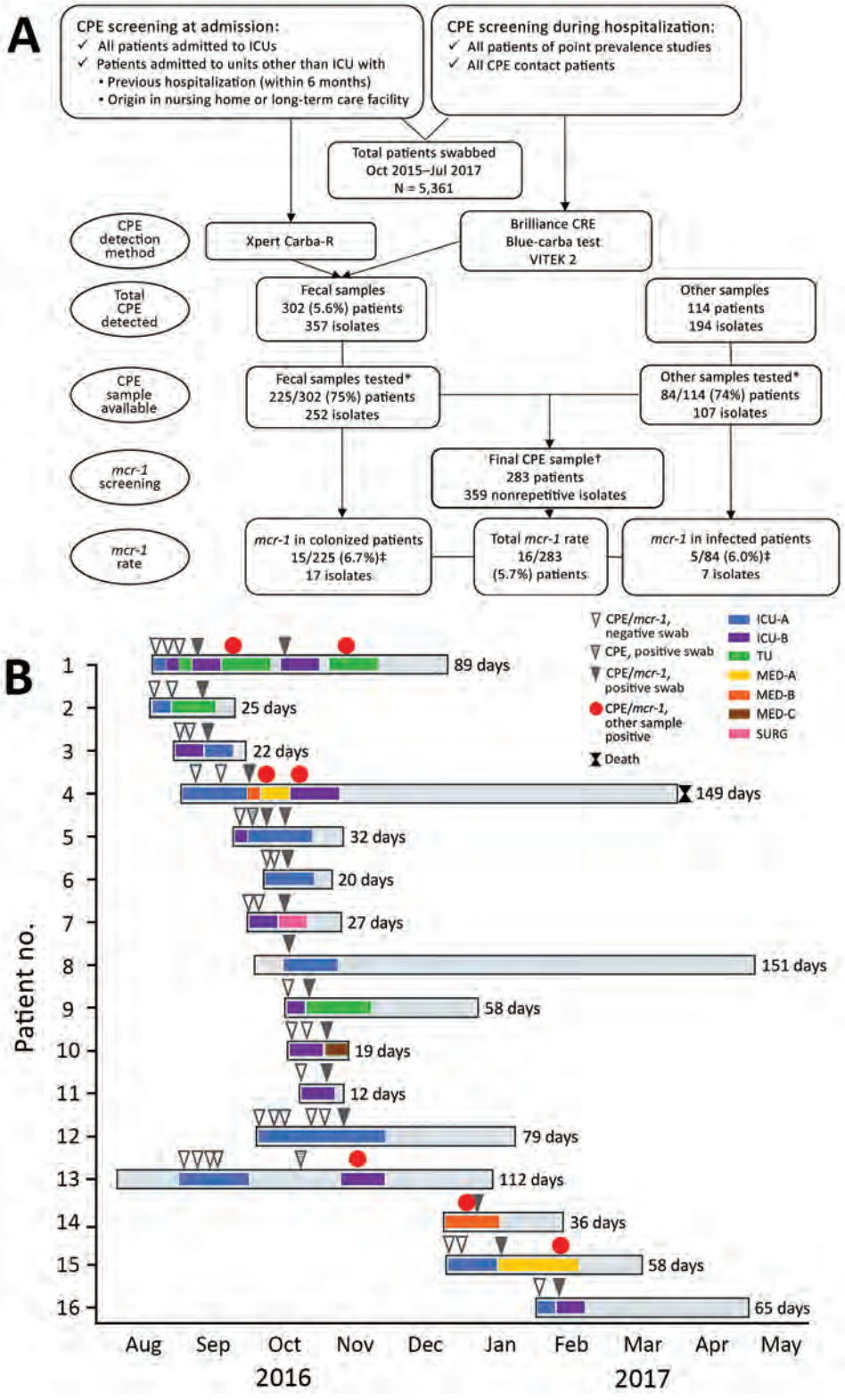

Figure 1. Selection for and testing of patients with *Klebsiella pneumoniae* carbapenemase 3–producing *mcr-1*–positive *Enterobacteriaceae*, Porto, Portugal, 2016–2017. A) Flowchart demonstrating rationale for sample selection. First, we screened for asymptomatic carriage of CPE in the gastrointestinal tract (i.e., colonization by CPE) by testing patient fecal samples with Brilliance CRE Agar (Oxoid, Basingstoke, UK); Xpert Carba-R (Cepheid, Sunnyvale, CA, USA); and VITEK 2 (bioMérieux, Marcy l'Etoile, France). Second, we tested for CPE with all patient samples available. Last, we screened the carbapenemase-producing isolates for *mcr-1* to identify the final sample. *CPE isolates and complete epidemiologic and clinical data were available for ≈75% of CPE patients. †The final sample screened for *mcr-1* included only nonrepetitive isolates. For fecal samples, we considered isolates repetitive when detected in the same patient in samples collected within 72 h from each other. For other types of samples, we considered isolates repetitive when detected in the same sample type collected at the same time point. ‡Four patients carried *mcr-1*–positive isolates either in the gastrointestinal tract or in other body sites. B) Timeline representing epidemiologic data of the 16 patients with *mcr-1*–positive CPE. CPE, carbapenemase-producing *Enterobacteriaceae*; ICU, intensive care unit; MED, medical unit; SURG, surgical unit; TU, transplant unit.

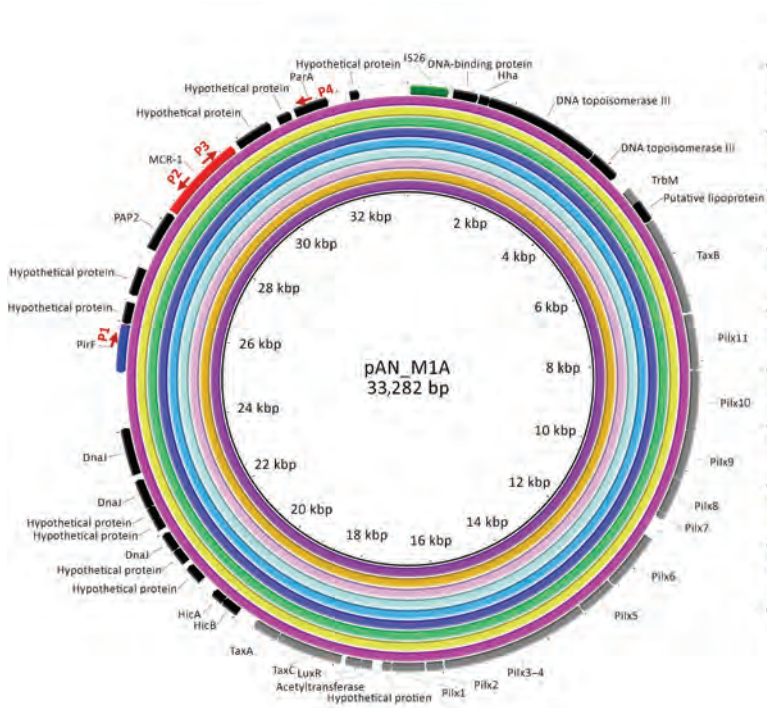

	Species	Source	Country	Genbank accession no.
pmcr1_IncX4	*Klebsiella pneumoniae*	Human (peritoneal fluid)	China	KU761327
pMCR1.2-IT	*K. pneumoniae*	Human (rectal swab)	Italy	KX236309
pMCR1-NJ-IncX4	*Escherichia coli*	Human (urine)	USA	KX447768
pICBEC72Hmcr	*E. coli*	Human	Brazil	CP015977
pNG14043	*Salmonella* Typhimurium	Human	Taiwan	KY120364
pMcp0271	*E. coli*	Chicken retail meat	Switzerland	KY565556
pESTMCR	*E. coli*	Pig slurry	Estonia	KU743383
pECGD-8-33	*E. coli*	Pig feces	China	KX254343
pIBMC_mcr1	*E. coli*	Environment	Italy	MF449287

Figure 2. Alignment of representative *mcr-1*–harboring IncX4 plasmids from different isolation sources and geographic regions. The *mcr-1*–harboring plasmid pAN_M1A was used as a reference plasmid. The outermost circle is an annotation of the reference plasmid and shows the direction of transcriptional open-reading frames. The *pil* loci and other genes (gray), replication-associated genes (dark blue), antimicrobial drug resistance gene (red), and insertion sequence (green) are indicated. The strategy for PCR mapping of *mcr-1*–carrying plasmids is indicated by red arrows. Primer P1 targets *pirF*, P2 *mcr-1* (3.3 kb), P3 *mcr-1*, and P4 *parA* (2.1 kb).

Colistin use and travel abroad were not recorded for any patient before *mcr-1* detection; however, 5 of the 16 patients had been hospitalized in the previous 6 months. Patients were treated for CPE infection with colistin and a carbapenem, which was supplemented with fosfomycin, tigecycline, or piperacillin/tazobactam depending on clinical criteria. We missed colistin resistance initially because we used conventional antimicrobial susceptibility tests VITEK 2 (bioMérieux, Marcy l'Etoile, France) and Etest (bioMérieux), which are unreliable at detecting colistin resistance. Adequate colistin resistance monitoring (http://www.eucast.org/fileadmin/src/media/PDFs/EUCAST_files/General_documents/Recommendations_for_MIC_determination_of_colistin_March_2016.pdf) and *mcr-1* screening for CPE isolates was implemented in July 2017.

Isolates carrying *mcr-1.1* were resistant to colistin (MIC 4–8 mg/L), produced *K. pneumoniae* carbapenemase 3 (KPC-3), and most (79%) produced CTX-M-15 β-lactamase. Besides 100% resistance to third and fourth generation cephalosporins and monobactams, *K. pneumoniae* isolates were also frequently resistant to nalidixic acid (100%), ciprofloxacin (96%), tigecycline (96%), tetracycline (92%), tobramycin (88%), gentamicin (88%), fosfomycin (83%), trimethoprim/sulfamethoxazole (79%), and chloramphenicol (67%) (Table). All isolates were susceptible to amikacin (which was contraindicated for some patients because of renal insufficiency) and ceftazidime/avibactam (which was not available).

All but 1 *K. pneumoniae* isolate belonged to sequence type (ST) 45 and carried *wzi*101/K24, a clone that has been infrequently detected among clinical MDR *K. pneumoniae* isolates in Portugal (*5*,*6*) but has circulated among KPC-3 producers (without *mcr-1*) during the same period (L. Peixe, unpub. data). We detected 1 *mcr-1*–positive *K. pneumoniae* (capsular type KL122) ST1112 isolate from the pus of an abdominal wall abscess in a patient having *mcr-1*–positive ST45 in previously collected fecal and urine samples (Table). The 2 whole-genome–sequenced *K. pneumoniae* ST45 isolates had genes encoding resistance to aminoglycosides [*aac(6')Ib-cr*,*aac(3)-IIa*]; β-lactams (bla_{KPC-3}, bla_{SHV-1}, bla_{OXA-1}), fluoroquinolones [*qnrB66*, *aac(6')Ib-cr*,*oqxAB*], and other antimicrobial drugs [*catB4*,*tet*(A)]; 1 of the 2 isolates possessed additional genes *aph(4)-Ib*, *strAB*, bla_{TEM-1B}, $bla_{CTX-M-15}$, *catA1*, *sul2*, and *dfrA14*.

In all *mcr-1*–positive isolates, the gene was located in an IncX4-type plasmid (Figure 2). Comparative genomics revealed that this plasmid (pAN_M1A) is circulating among diverse hosts (humans, pig, poultry) and the environment in many different countries, including Portugal (*11*). We identified bla_{KPC-3} in a Tn*4401d* isoform in an ≈58-kb

Table. Demographic and epidemiologic data for 16 patients with *Klebsiella pneumoniae* isolates producing KPC-3 and MCR-1, Porto, Portugal, 2016–2017*

Patient no.	Patient age, y/sex	MLST	Date of isolation	Unit	Specimen type	Antimicrobial drug resistance profile of non-β-lactams†
1	50/M	ST45	2016 Sep 10	ICU-B	Rectal swab	GEN, KAN, NET, TOB, STR, TET, MIN, TGC, FOT, TMP, SXT, NAL, CIP
		ST45	2016 Sep 23	TU	Peritoneal fluid	GEN, KAN, NET, TOB, STR, TET, MIN, TGC, FOT, TMP, SXT, CAM, NAL, CIP
		ST45	2016 Oct 14	ICU-B	Rectal swab	MIN, FOT, TET, TGC, SXT, CAM, NAL, CIP
		ST45	2016 Nov 8	TU	Urine	GEN, KAN, NET, TOB, STR, TET, MIN, TGC, FOT, TMP, SXT, NAL, CIP
2	55/M	ST45	2016 Sep 11	TU	Rectal swab	GEN, NET, TOB, STR, TET, MIN, TGC, FOT, TMP, SXT, CAM, NAL, CIP
3	58/F	ST45	2016 Sep 12	ICU-A	Rectal swab	GEN, KAN, NET, TOB, STR, TET, MIN, TGC, FOT, TMP, SXT, CAM, NAL, CIP
4	73/F	ST45	2016 Oct 1	MED-B	Rectal swab	GEN, KAN, NET, TOB, STR, TET, MIN, TGC, FOT, TMP, SXT, CAM, NAL, CIP
		ST45	2016 Oct 4	MED-A	Urine	GEN, KAN, NET, TOB, STR, TET, MIN, TGC, FOT, TMP, SXT, NAL, CIP
		ST1112	2016 Oct 22	ICU-B	Pus	TET, MIN, FOT, TMP, CAM, NAL, CIP
5	72/M	ST45	2016 Oct 10	ICU-A	Rectal swab	GEN, KAN, NET, TOB, TET, MIN, TGC, FOT, CAM, NAL, CIP
		ST45‡	2016 Oct 14	ICU-A	Rectal swab	GEN, KAN, NET, TOB, TET, MIN, TGC, FOT, CAM, NAL, CIP
6	75/M	ST45	2016 Oct 14	ICU-A	Rectal swab	GEN, KAN, NET, TOB, STR, TET, MIN, TGC, FOT, TMP, SXT, CAM, NAL, CIP
7	68/M	ST45	2016 Oct 14	SURG	Rectal swab	GEN, KAN, TOB, STR, TET, MIN, TGC, FOT, TMP, SXT, NAL, CIP
8	78/F	ST45	2016 Oct 15	ICU-A	Rectal swab	GEN, KAN, NET, TOB, STR, TET, MIN, TGC, FOT, TMP, SXT, CAM, NAL, CIP
9	58/M	ST45	2016 Oct 25	TU	Rectal swab	GEN, KAN, NET, TOB, STR, TET, MIN, TGC, FOT, TMP, SXT, CAM, NAL, CIP
10	51/M	ST45	2016 Nov 1	MED-C	Rectal swab	KAN, NET, TOB, STR, TET, MIN, TGC, TMP, SXT, CAM, NAL, CIP
11	87/F	ST45‡	2016 Nov 1	ICU-B	Rectal swab	GEN, KAN, STR, TET, MIN, TGC, FOT, TMP, SXT, NAL, CIP
12	67/F	ST45	2016 Nov 7	ICU-A	Rectal swab	GEN, TOB, STR, MIN, TGC, FOT, CAM, NAL, CIP
13	57/M	ST45	2016 Nov 7	ICU-B	Blood	GEN, NET, TOB, STR, TET, MIN, TGC, FOT, CAM, NA
14	76/M	ST45	2016 Dec 30	MED-B	Blood	GEN, KAN, NET, TOB, STR, TET, MIN, TGC, FOT, TMP, SXT, CAM, NAL, CIP
		ST45	2017 Jan 2	MED-B	Rectal swab	GEN, KAN, NET, TOB, STR, TET, MIN, TGC, TMP, SXT, NAL, CIP
15	85/F	ST45	2017 Jan 16	MED-A	Rectal swab	GEN, KAN, NET, TOB, STR, TET, MIN, TGC, FOT, TMP, SXT, CAM, NAL, CIP
		ST45	2017 Feb 7	MED-A	Urine	GEN, NET, TOB, STR, TGC, TMP, SXT, NAL, CIP
16	63/F	ST45	2017 Feb 7	ICU-B	Rectal swab	GEN, KAN, NET, TOB, STR, TET, MIN, TGC, TMP, SXT, NAL, CIP

*CAM, chloramphenicol; CIP, ciprofloxacin; FOT, fosfomycin; GEN, gentamicin; ICU, intensive care unit; KAN, kanamycin; KPC-3, *K. pneumoniae* carbapenemase 3; MCR-1, mobilized colistin resistance 1; MED, medical unit; MIN, minocycline; MLST, multilocus sequence type; NAL, nalidixic acid; NET, netilmicin; SURG, surgical unit; ST, sequence type; STR, streptomycin; SXT, trimethoprim/sulfamethoxazole; TET, tetracycline; TGC, tigecycline; TOB, tobramycin; TMP, trimethoprim; TU, transplant unit.
†We considered isolates with intermediate susceptibility profiles resistant.
‡Isolates selected for whole-genome sequencing.

IncN-ST15 plasmid, a minority platform in our previous survey (*5*); $bla_{\text{CTX-M-15}}$ was associated with multireplicon plasmid IncFII_{K}-FIA-FIB. We deposited this whole-genome shotgun project at DDBJ/European Nucleotide Archive/GenBank under accession no. PEHI00000000.

We found that 5.7% (16/283) of hospitalized patients had gastrointestinal tracts colonized with *mcr-1*–positive CPE, and in 1.8% (5/283) of these patients, an infection developed; these rates are comparable with those reported in China (up to 6.2% for fecal colonization, 1% for infections) (*10*,*12*). In China, only 1 outbreak involving *mcr-1*–carrying clinical isolates has been reported (*13*), and in Europe, a low occurrence (<1%) and sporadic clinical cases have been reported (*3*,*4*). Colistin is a critical last resource antimicrobial drug; prolonged carriage of *mcr-1*–positive MDR strains (especially by patients at discharge) represents a risk for subsequent infections and dissemination to other *Enterobacteriaceae* species. Of note, identifying CPE asymptomatic carriers at discharge is a practice recommended in Portugal, though not mandatory.

Considering the absence of CPE at admission, nosocomial acquisition and in-hospital dissemination of KPC-3–producing strains carrying *mcr-1* is plausible; however, we cannot rule out that other *K. pneumoniae* lineages or *Escherichia coli* might have been the source of *mcr-1*. Although the prevalence of colonization of humans by *mcr-1*–positive strains is unknown in Portugal, previous detection of *mcr-1* in livestock, such as *K. pneumoniae* ST45 in pigs, suggests transmission through the food chain and wider dispersion of MCR-1–producing *Enterobacteriaceae* (*8*,*11*,*14*,*15*).

Conclusions

We report the emergence of *mcr-1* in MDR KPC-3–producing *K. pneumoniae* associated with an unnoticed outbreak. High rates of CPE and colistin use (*2*,*5*,*6*) together with an ongoing community-based dissemination of *mcr* forebodes of future similar events. Our data stress the need for a concerted action involving different professionals and healthcare institutions to monitor and contain the spread of *mcr* across human and veterinary niches, the food chain, and the environment.

This work received financial support from the European Union (FEDER funds POCI/01/0145/FEDER/007728) and National Funds (Fundação para a Ciência e Tecnologia and Ministério da Educação e Ciência) under the partnership agreement PT2020 UID/MULTI/04378/2013. Fellowship support was provided by Fundação para a Ciência e Tecnologia through Programa Operacional Capital Humano to Â.N. (grant no. SFRH/BPD/104927/2014), to J.C. (grant no. SFRH/BD/93091/2013), and to C.R. (grant no. SFRH/BD/84341/2012).

About the Author

Ms. Mendes is a biomedical scientist in the Microbiology Service and Molecular Biology Unit at Centro Hospitalar do Porto (Porto, Portugal). She is currently pursuing her doctorate, with research interests in molecular epidemiology of multidrug-resistant *Enterobacteriaceae*.

References

1. Liu YY, Wang Y, Walsh TR, Yi LX, Zhang R, Spencer J, et al. Emergence of plasmid-mediated colistin resistance mechanism MCR-1 in animals and human beings in China: a microbiological and molecular biological study. Lancet Infect Dis. 2016;16:161–8. http://dx.doi.org/10.1016/S1473-3099(15)00424-7
2. European Centre for Disease Prevention and Control; European Food Safety Authority; European Medicines Agency. ECDC/EFSA/EMA second joint report on the integrated analysis of the consumption of antimicrobial agents and occurrence of antimicrobial resistance in bacteria from humans and food-producing animals—Joint Interagency Antimicrobial Consumption and Resistance Analysis (JIACRA) Report. EFSA Journal. 2017;15:4872.
3. Huang TD, Bogaerts P, Berhin C, Hoebeke M, Bauraing C, Glupczynski Y. Increasing proportion of carbapenemase-producing *Enterobacteriaceae* and emergence of a MCR-1 producer through a multicentric study among hospital-based and private laboratories in Belgium from September to November 2015. Euro Surveill. 2017;22:30530. http://dx.doi.org/10.2807/1560-7917.ES.2017.22.19.30530
4. Di Pilato V, Arena F, Tascini C, Cannatelli A, Henrici De Angelis L, Fortunato S, et al. *mcr-1.2*, a new *mcr* variant carried on a transferable plasmid from a colistin-resistant KPC carbapenemase-producing *Klebsiella pneumoniae* strain of sequence type 512. Antimicrob Agents Chemother. 2016;60:5612–5. http://dx.doi.org/10.1128/AAC.01075-16
5. Rodrigues C, Bavlovič J, Machado E, Amorim J, Peixe L, Novais Â. KPC-3-producing *Klebsiella pneumoniae* in Portugal linked to previously circulating non-CG258 lineages and uncommon genetic platforms (Tn*4401d*-IncFIA and Tn*4401d*-IncN). Front Microbiol. 2016;7:1000. http://dx.doi.org/10.3389/fmicb.2016.01000
6. Manageiro V, Ferreira E, Almeida J, Barbosa S, Simões C, Bonomo RA, et al.; Antibiotic Resistance Surveillance Program in Portugal. Predominance of KPC-3 in a survey for carbapenemase-producing *Enterobacteriaceae* in Portugal. Antimicrob Agents Chemother. 2015;59:3588–92. http://dx.doi.org/10.1128/AAC.05065-14
7. Pires J, Novais A, Peixe L. Blue-carba, an easy biochemical test for detection of diverse carbapenemase producers directly from bacterial cultures. J Clin Microbiol. 2013;51:4281–3. http://dx.doi.org/10.1128/JCM.01634-13
8. Campos J, Cristino L, Peixe L, Antunes P. MCR-1 in multidrug-resistant and copper-tolerant clinically relevant *Salmonella* 1,4,[5],12:i:- and *S.* Rissen clones in Portugal, 2011 to 2015. Euro Surveill. 2016;21:30270. http://dx.doi.org/10.2807/1560-7917.ES.2016.21.26.30270
9. Falgenhauer L, Waezsada S-E, Yao Y, Imirzalioglu C, Käsbohrer A, Roesler U, et al.; RESET consortium. Colistin resistance gene *mcr-1* in extended-spectrum β-lactamase-producing and carbapenemase-producing gram-negative bacteria in Germany. Lancet Infect Dis. 2016;16:282–3. http://dx.doi.org/10.1016/S1473-3099(16)00009-8
10. Wang Y, Tian GB, Zhang R, Shen Y, Tyrrell JM, Huang X, et al. Prevalence, risk factors, outcomes, and molecular epidemiology of *mcr-1*-positive *Enterobacteriaceae* in patients and healthy adults from China: an epidemiological and clinical study. Lancet Infect Dis. 2017;17:390–9. http://dx.doi.org/10.1016/S1473-3099(16)30527-8
11. Tacão M, Tavares RDS, Teixeira P, Roxo I, Ramalheira E, Ferreira S, et al. *mcr-1* and bla_{KPC-3} in *Escherichia coli* sequence type 744 after meropenem and colistin therapy, Portugal. Emerg Infect Dis. 2017;23:1419–21. http://dx.doi.org/10.3201/eid2308.170162
12. Zhong LL, Phan HTT, Shen C, Doris-Vihta K, Sheppard AE, Huang X, et al. High rates of human fecal carriage of *mcr-1*–positive multidrug-resistant *Enterobacteriaceae* emerge in China in association with successful plasmid families. Clin Infect Dis. 2017. http://dx.doi.org/10.1093/cid/cix885
13. Tian GB, Doi Y, Shen J, Walsh TR, Wang Y, Zhang R, et al. MCR-1-producing *Klebsiella pneumoniae* outbreak in China. Lancet Infect Dis. 2017;17:577. http://dx.doi.org/10.1016/S1473-3099(17)30266-9
14. Kieffer N, Aires-de-Sousa M, Nordmann P, Poirel L. High rate of MCR-1–producing *Escherichia coli* and *Klebsiella pneumoniae* among pigs, Portugal. Emerg Infect Dis. 2017;23:2023–9. http://dx.doi.org/10.3201/eid2312.170883
15. Manageiro V, Clemente L, Graça R, Correia I, Albuquerque T, Ferreira E, et al. New insights into resistance to colistin and third-generation cephalosporins of *Escherichia coli* in poultry, Portugal: novel $bla_{CTX-M-166}$ and bla_{ESAC} genes. Int J Food Microbiol. 2017;263:67–73. http://dx.doi.org/10.1016/j.ijfoodmicro.2017.10.007

Address for correspondence: Luísa Peixe, UCIBIO, Laboratório de Microbiologia, Faculdade de Farmácia, Universidade do Porto, Rua Jorge de Viterbo Ferreira, n. 228, 4050-313 Porto, Portugal; email: lpeixe@ff.up.pt

Bimodal Seasonality and Alternating Predominance of Norovirus GII.4 and Non-GII.4, Hong Kong, China, 2014–2017[1]

Martin Chi-Wai Chan, Kirsty Kwok, Lin-Yao Zhang, Kirran N. Mohammad, Nelson Lee,[2] Grace C.Y. Lui, E. Anthony S. Nelson, Raymond W.M. Lai, Ting F. Leung, Paul K.S. Chan

We report emerging subtropical bimodal seasonality and alternating predominance of norovirus GII.4 and non-GII.4 genotypes in Hong Kong. GII.4 predominated in summer and autumn months and affected young children, whereas emergent non-GII.4 genotypes predominated in winter months and affected all age groups. This highly dynamic epidemiology should inform vaccination strategies.

Human noroviruses are the leading cause of foodborne illnesses across all age groups (*1*) and account for nearly one fifth of all acute gastroenteritis (AGE) infections globally (*2*). Human noroviruses have started superseding rotavirus as the most common cause of AGE in children in regions where rotavirus vaccination has been widely and successfully deployed (*3*). This severe disease burden motivates the development of a norovirus vaccine, and children are an important target group because of high incidence (*4*). The norovirus pandemic GII.4 genotype has been associated with most AGE infections since the mid-1990s (*5*) and thus was an important genotype included and tested in norovirus vaccine clinical trials (*6*); however, this historical predominance of norovirus GII.4 was challenged by the recent emergence of epidemic non-GII.4 genotypes in Asia (*7*–*9*). A better understanding of the changing norovirus epidemiology in Asia might inform the current strategy on norovirus surveillance and vaccine development.

The Study

Hong Kong is a subtropical coastal city in southern China and has a temperate climate with hot summers and dry winters (Köppen-Geiger climate classification "Cwa"). Since March 2014, we have been monitoring virus genotypes in all hospitalized (i.e., severe) norovirus AGE case-patients of all ages diagnosed at the Prince of Wales Hospital of the Chinese University of Hong Kong and have reported the emergence and predominance of 2 previously less common non-GII.4 genotypes, GII.17 in 2014 and GII.2 in 2016 (*8*,*9*). Here we present further analysis of the seasonal dynamics of different norovirus genotypes during a 42-month period from March 2014 through August 2017. We identified norovirus genotypes in 1,100 (88.3%) of 1,246 case-patients by means of partial viral protein 1 Sanger sequencing and genotype assignment using a genotyping tool available through the National Institute of Public Health and the Environment of the Netherlands (http://www.rivm.nl/mpf/typingtool/norovirus). Seven case-patients were co-infected with >1 norovirus genotype. The proportion of GII.4 genotypes was 49.8% and that of non-GII.4 genotypes 50.2%. Overwhelmingly, most norovirus GII.4 belonged to the GII.Pe-GII.4 Sydney variant (512/544; 94.1%; online Technical Appendix Figure 1, https://wwwnc.cdc.gov/EID/article/24/4/17-1791-Techapp1.pdf). The recent recombinant GII.P16-GII.4 Sydney that emerged and predominated in the United States during 2016–2017 (*10*) was only detected sporadically in Hong Kong (online Technical Appendix Figure 1). The 2 most prevalent norovirus non-GII.4 genotypes were the recently emerged GII.17 (35.9%) and GII.2 (26.0%) (online Technical Appendix Figure 1).

We observed a bimodal seasonality of norovirus AGE requiring hospitalization, with periodic oscillation in the age group of admitted case-patients (Figure, panel A). Among the 19 months that norovirus preferentially affected young children <5 years old (as indicated by a monthly median age of case-patients <5 years), 17 (89%) were predominated by GII.4 genotype, whereas among the 23 months that preferentially affected older children and adults, 19 (83%) were predominated by non-GII.4 genotypes (Figure, panel B). By age groups, norovirus GII.4 accounted for most (68.5%) case-patients who were young children <5 years old, whereas norovirus non-GII.4 predominated in all other age groups: 5–17 years (75.7%), 18–40 years (87.0%), 41–65 years (78.6%), and >65 years (63.2%). The median age of case-patients infected with the recently emerged GII.17 and GII.2 was significantly higher than that for those infected with GII.4

Author affiliation: The Chinese University of Hong Kong, Hong Kong, China

DOI: https://doi.org/10.3201/eid2404.171791

[1]Preliminary results from this study were presented at the 1st International Workshop on Gastroenteritis Viruses, September 14–15, 2017, Shanghai, China.

[2]Current affiliation: Faculty of Medicine and Dentistry, University of Alberta, Edmonton, Alberta, Canada.

(GII.4, 2 years [interquartile range (IQR) 1–4 years]; GII.17, 49 years [IQR 10–72 years]; GII.2, 5 years [IQR 2–22 years]; p<0.0001, Kruskal-Wallis test) (online Technical Appendix Figure 2), as reported earlier over a shorter period (*8*,*9*). By season, late summer and autumn peaks were associated with norovirus GII.4, whereas winter peaks were associated with norovirus non-GII.4 (Figure, panel B). Norovirus infections have become equally common during summer and autumn months (52.3% of all infections during June–November) and during winter and spring months (47.7% of all infections during December–May).

Conclusions

We observed an influenza-like subtropical bimodal seasonality and alternating predominance of norovirus GII.4 and non-GII.4 genotypes, with each infecting different age groups. Norovirus GII.4 predominated in summer and autumn months and preferentially affected young children, who are also one of the age groups most affected by seasonal influenza. In contrast, emergent norovirus non-GII.4 predominated in winter months and affected wider age groups (e.g., all age groups were affected by GII.17 and older children and young adults by GII.2), a pattern which is reminiscent of pandemic influenza viruses. These findings illustrate a highly dynamic epidemiology of norovirus. A similar pattern of alternating epidemics has been observed among the 4 dengue virus serotypes and was shown to reflect moderate but not weak or strong interserotypic cross-protective immunity (*11*). The alternating predominance of norovirus GII.4 and non-GII.4 genotypes in severe infections might reflect an equally complex virus–human immunologic interaction on individual and population levels. This might be explained at least in part by the recently proposed concept that groups norovirus genotypes into so-called immunotypes (*12*).

The out-of-phase oscillation in the demographic characteristics of norovirus patients admitted to our hospitals

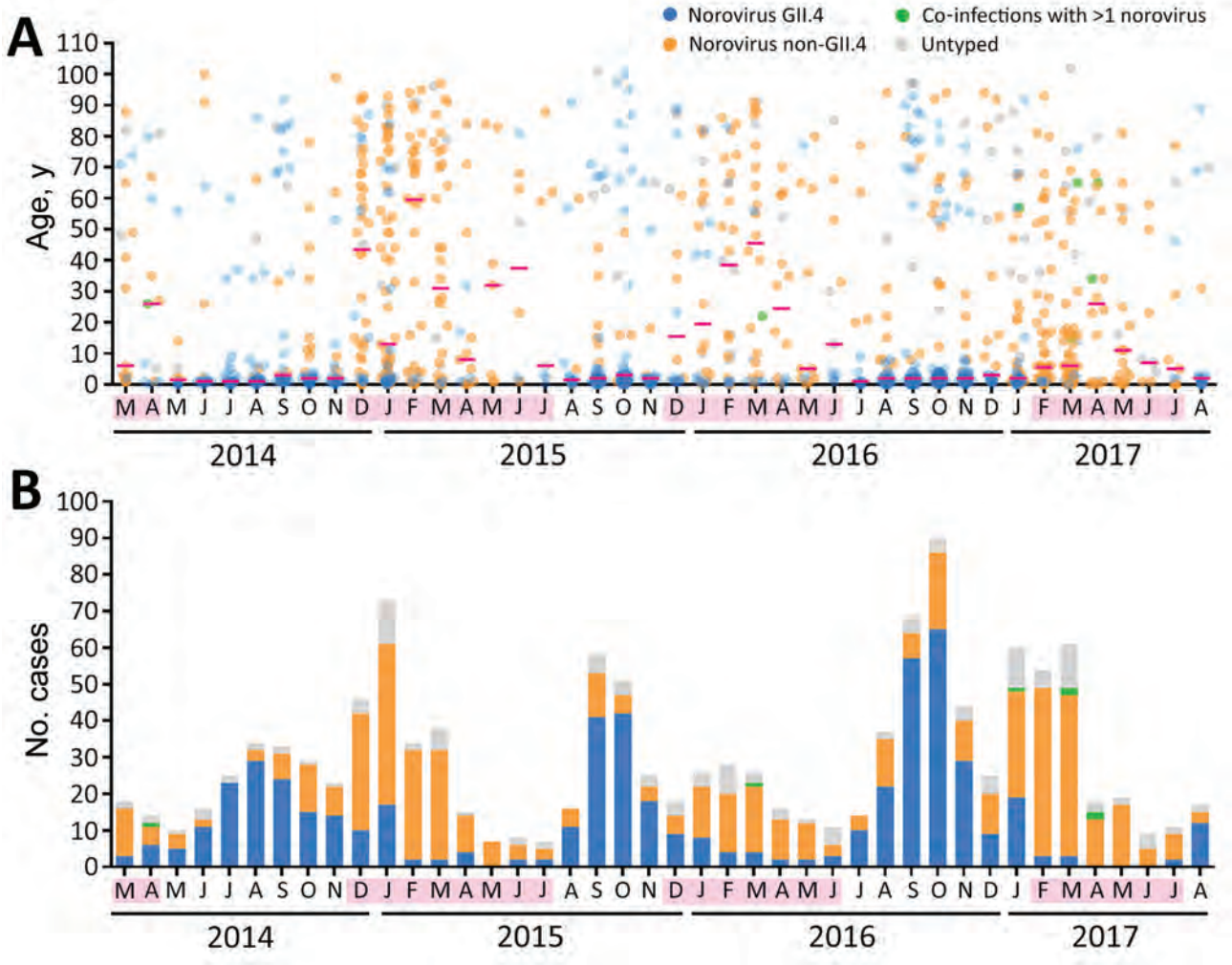

Figure. Bimodal seasonality and alternating predominance of norovirus GII.4 and non-GII.4 genotypes in Hong Kong, China, 2014–2017. A) Temporal distribution of ages of patients hospitalized for norovirus gastroenteritis. Each dot represents 1 patient. Red horizontal bars indicate medians. B) Epidemic curve during the study period. All cases shown are stratified by norovirus viral protein 1 genotype. Pink shading along baseline indicates months during which the median age of hospitalized case-patients was ≥5 years.

complicated clinical resource allocation such as bed management in pediatric and medical wards. High norovirus activity during late summer and autumn overlaps with the local summer peaks of seasonal influenza (*13*) and further increases the burden on the already strained hospital system. We speculate that the recent emergence of non-GII.4 viruses modified the seasonality of noroviruses because a summer peak of this bimodal seasonal pattern occurred only once in an outbreak setting during a 7-year period (2005–2011), during which GII.4 predominated in Hong Kong (http://www.chp.gov.hk/files/pdf/prevention_and_control_of_norovirus_infection_in_hong_kong_r.pdf).

Hong Kong was implicated as an epicenter in the spread of norovirus GII.17 in China during winter 2014–15 (*14*); whether or not the characteristic bimodal seasonality and alternating epidemic pattern we observed will favor the emergence of new noroviruses would be of public health importance. Of note, alternating predominance of 2 antigenic types of influenza B virus Yamagata lineage has been proposed as a mechanism to generate virus antigenic novelty (*15*). Continued and focused norovirus surveillance and genotyping in Southeast Asia are necessary to identify geographic hotspots of new noroviruses and thus guide vaccine strain selection. The variability of affected age populations among norovirus genotypes underscores the need to consider virus genotype in quantifying norovirus disease burden; this approach will provide more comprehensive evidence to advise future norovirus vaccination strategy.

This study was supported in part by grants from the commissioned Health and Medical Research Fund of the Hong Kong Special Administrative Region's Food and Health Bureau (CU-15-C2 to M.C-W.C.) and an institutional direct grant for research (2016.046 to M.C-W.C.).

Author contributions: M.C-W.C. and P.K.S.C. conceived the study; M.C-W.C. designed and coordinated the study; N.L., G.C.Y.L., E.A.S.N., T.F.L., and P.K.S.C. coordinated sample collection; K.K., L.-Y.Z., and M.K.N. performed experiments; M.C-W.C. analyzed data and drafted the manuscript. All authors critically reviewed and commented on the manuscript before submission.

About the Author

Dr. M.C.-W. Chan is an assistant professor in the Department of Microbiology of the Chinese University of Hong Kong. His research interest focuses on molecular epidemiology and pathogenesis of human noroviruses. Other research interests include use of metagenomic next-generation sequencing in clinical diagnosis, gut virome, and food virology.

References

1. Havelaar AH, Kirk MD, Torgerson PR, Gibb HJ, Hald T, Lake RJ, et al.; World Health Organization Foodborne Disease Burden Epidemiology Reference Group. World Health Organization global estimates and regional comparisons of the burden of foodborne disease in 2010. PLoS Med. 2015;12:e1001923. http://dx.doi.org/10.1371/journal.pmed.1001923
2. Ahmed SM, Hall AJ, Robinson AE, Verhoef L, Premkumar P, Parashar UD, et al. Global prevalence of norovirus in cases of gastroenteritis: a systematic review and meta-analysis. Lancet Infect Dis. 2014;14:725–30. http://dx.doi.org/10.1016/S1473-3099(14)70767-4
3. Payne DC, Vinjé J, Szilagyi PG, Edwards KM, Staat MA, Weinberg GA, et al. Norovirus and medically attended gastroenteritis in U.S. children. N Engl J Med. 2013;368:1121–30. http://dx.doi.org/10.1056/NEJMsa1206589
4. Lopman BA, Steele D, Kirkwood CD, Parashar UD. The vast and varied global burden of norovirus: prospects for prevention and control. PLoS Med. 2016;13:e1001999. http://dx.doi.org/10.1371/journal.pmed.1001999
5. Siebenga JJ, Vennema H, Zheng DP, Vinjé J, Lee BE, Pang XL, et al. Norovirus illness is a global problem: emergence and spread of norovirus GII.4 variants, 2001–2007. J Infect Dis. 2009;200:802–12. http://dx.doi.org/10.1086/605127
6. Bernstein DI, Atmar RL, Lyon GM, Treanor JJ, Chen WH, Jiang X, et al. Norovirus vaccine against experimental human GII.4 virus illness: a challenge study in healthy adults. J Infect Dis. 2015;211:870–8. http://dx.doi.org/10.1093/infdis/jiu497
7. de Graaf M, van Beek J, Vennema H, Podkolzin AT, Hewitt J, Bucardo F, et al. Emergence of a novel GII.17 norovirus—end of the GII.4 era? Euro Surveill. 2015;20:8–15. http://dx.doi.org/10.2807/1560-7917.ES2015.20.26.21178
8. Chan MC, Lee N, Hung TN, Kwok K, Cheung K, Tin EK, et al. Rapid emergence and predominance of a broadly recognizing and fast-evolving norovirus GII.17 variant in late 2014. Nat Commun. 2015;6:10061. http://dx.doi.org/10.1038/ncomms10061
9. Kwok K, Niendorf S, Lee N, Hung TN, Chan LY, Jacobsen S, et al. Increased detection of emergent recombinant norovirus GII.P16-GII.2 strains in young adults, Hong Kong, China, 2016–2017. Emerg Infect Dis. 2017;23:1852–5. http://dx.doi.org/10.3201/eid2311.170561
10. Cannon JL, Barclay L, Collins NR, Wikswo ME, Castro CJ, Magaña LC, et al. Genetic and epidemiologic trends of norovirus outbreaks in the United States from 2013 to 2016 demonstrated emergence of novel GII.4 recombinant viruses. J Clin Microbiol. 2017;55:2208–21. http://dx.doi.org/10.1128/JCM.00455-17
11. Adams B, Holmes EC, Zhang C, Mammen MP Jr, Nimmannitya S, Kalayanarooj S, et al. Cross-protective immunity can account for the alternating epidemic pattern of dengue virus serotypes circulating in Bangkok. Proc Natl Acad Sci U S A. 2006;103:14234–9. http://dx.doi.org/10.1073/pnas.0602768103
12. Parra GI, Squires RB, Karangwa CK, Johnson JA, Lepore CJ, Sosnovtsev SV, et al. Static and evolving norovirus genotypes: implications for epidemiology and immunity. PLoS Pathog. 2017;13:e1006136. http://dx.doi.org/10.1371/journal.ppat.1006136
13. Shu YL, Fang LQ, de Vlas SJ, Gao Y, Richardus JH, Cao WC. Dual seasonal patterns for influenza, China. Emerg Infect Dis. 2010;16:725–6. http://dx.doi.org/10.3201/eid1604.091578
14. Lu J, Fang L, Zheng H, Lao J, Yang F, Sun L, et al. The evolution and transmission of epidemic GII.17 noroviruses. J Infect Dis. 2016;214:556–64. http://dx.doi.org/10.1093/infdis/jiw208
15. Langat P, Raghwani J, Dudas G, Bowden TA, Edwards S, Gall A, et al. Genome-wide evolutionary dynamics of influenza B viruses on a global scale. PLoS Pathog. 2017;13:e1006749. http://dx.doi.org/10.1371/journal.ppat.1006749

Address for correspondence: Paul K.S. Chan, Department of Microbiology, 1/F Lui Che Woo Clinical Sciences Building, Prince of Wales Hospital, Shatin, Hong Kong, China; email: paulkschan@cuhk.edu.hk

Novel Highly Pathogenic Avian Influenza A(H5N6) Virus in the Netherlands, December 2017

Nancy Beerens, Guus Koch, Rene Heutink, Frank Harders, D.P. Edwin Vries, Cynthia Ho, Alex Bossers, Armin Elbers

A novel highly pathogenic avian influenza A(H5N6) virus affecting wild birds and commercial poultry was detected in the Netherlands in December 2017. Phylogenetic analysis demonstrated that the virus is a reassortant of H5N8 clade 2.3.4.4 viruses and not related to the Asian H5N6 viruses that caused human infections.

In 2014 and 2016, outbreaks of highly pathogenic avian influenza (HPAI) subtype H5N8 clade 2.3.4.4 were observed among wild birds and domestic poultry worldwide (*1*) and in the Netherlands (*2*–*4*). Transcontinental spread of these viruses, and that of the earlier HPAI H5N1 virus (goose/Guangdong lineage) (*5*), has been linked to dissemination by migratory wild birds (*6*). A novel group B HPAI H5N6 virus (*7*) was detected in wild birds and commercial poultry in the Netherlands in December 2017. On December 6–7, 2017, meat ducks on a 16,400-duck farm in the municipality of Biddinghuizen, the Netherlands, began dying at an exponentially increasing rate (Figure 1; online Technical Appendix Figure 1, https://wwwnc.cdc.gov/EID/article/24/4/17-2124-Techapp1.pdf). The duck farm consisted of 2 barns, each housing ≈8,200 ducks. One-day-old ducklings started production in barn 1 on November 9 and in barn 2 on December 7. Mean water intake of ducks in barn 1 dropped by 8.5% during December 4–5. Mean feed intake dropped by 4.3% during December 3–5. Recording ended on December 5. On December 7, the clinical signs observed in barn 1, in addition to sudden death, were watery diarrhea, conjunctivitis, and nervous disorders. The following clinical signs were checked, but absent: edema (of the neck, head, and eyes); cyanosis (in the comb, wattle, and feet); hemorrhagic conjunctivae; and respiratory problems. No clinical signs were observed in the ducklings in barn 2.

Author affiliations: Wageningen Bioveterinary Research, Lelystad, the Netherlands (N. Beerens, G. Koch, R. Heutink, F. Harders, C. Ho, A. Bossers, A. Elbers); Netherlands Food and Consumer Product Safety Authority, Utrecht, the Netherlands (D.P.E. Vries)

DOI: https://doi.org/10.3201/eid2404.172124

The Study

We collected swab samples from the trachea and cloaca of clinically affected ducks for diagnostic testing. The samples tested positive by real-time PCR on the matrix gene (*3*) and H5-PCR (*8*), demonstrating notifiable avian influenza A subtype H5 virus. We performed hemagglutinin (HA) and neuraminidase (NA) sequence analysis (*3*), which showed a HA cleavage site with polybasic properties PLREKRRKR*GLF, and subtyped the virus as HPAI subtype H5N6 on December 8. The intravenous pathogenicity index determined in 6-week-old chickens for the novel H5N6 virus was 2.99, similar to that of the 2016 H5N8 subtype, confirming the high pathogenicity of the H5N6 subtype.

The farm was located in a water-rich area, densely populated with wild waterbirds. Several mute swans (*Cygnus olor*) and a tufted duck (*Aythya fuligula*) were found dead in this area (online Technical Appendix Figure 1), and tested positive for HPAI H5N6 on December 11.

Since 2013, HPAI H5N6 viruses have emerged in poultry and caused sporadic infections in humans in Asia, raising global concerns regarding their potential as human pandemic threats. H5N6 viruses constitute ≥34 distinct genotypes, of which 4 were detected in humans (*9*). To genetically characterize the novel H5N6 subtype influenza virus detected in the Netherlands, we sequenced the full genome of the viruses found at the duck farm, and in the 2 mute swans and the tufted duck (GISAID [http://platform.gisaid.org] accession nos. EPI ISL 287907, EPI ISL 288409, EPI ISL 288410, and EPI ISL 288412), as described previously (*4*). Database searches (GISAID and GenBank) showed that these viruses are highly similar to the HPAI H5N8 clade 2.3.4.4 viruses, which were detected previously in wild birds at the Russia–Mongolia border in May 2016 (*10*), for the gene segments polymerase basic 1 (PB1), polymerase acidic (PA), HA, nucleoprotein (NP), matrix protein (MP), and nonstructural protein (NS) (Table). The polymerase basic 2 (PB2) and NA segments shared sequence similarity with Eurasian low pathogenicity avian influenza (LPAI) viruses. Moreover, the N6 gene of the H5N6 viruses found in the Netherlands showed high homology to those detected in Greece in February and in Japan and Taiwan in November–December 2017.

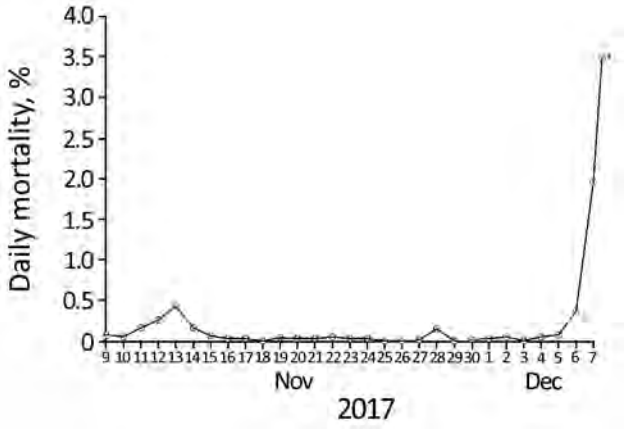

Figure 1. Daily mortality rate (% of ducks) in ≈8,000 ducks in barn 1 of the case flock during outbreak of highly pathogenic avian influenza A(H5N6) in the Netherlands, 2017. The farmer counted the dead ducks every morning. During clinical inspection on the last day, an additional number of dead ducks was counted (12 h after the farmer's morning count); the asterisk (*) indicates the total number of dead ducks at the end of the day on December 7 (farmer count + clinical inspection count).

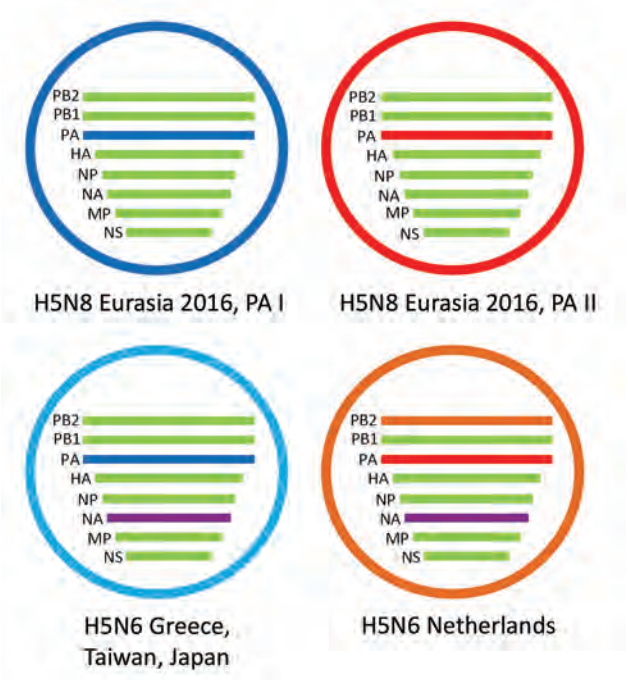

Figure 2. Schematic representation of the HPAI H5N6 reassortant virus detected in the Netherlands. Two variants of HPAI H5N8 were detected in 2016; they have different PA gene segments, called PA I and PA II. The novel virus evolved from H5N8 viruses having a PA II gene segment, but obtained both novel NA and PB2 gene segments. The H5N6 viruses detected in Greece, Japan, and Taiwan have evolved from H5N8 viruses that have a PA I gene segment and have an N6 segment similar to the virus detected in the Netherlands. HPAI, highly pathogenic avian influenza; PB, polymerase basic; PA, polymerase acidic; HA, hemagglutinin; NP, nucleoprotein; NA, neuraminidase; MP, matrix protein; NS, nonstructural protein.

To study the origin of the H5N6 virus detected in the Netherlands in December 2017, we performed a detailed phylogenetic analysis for all gene segments individually (online Technical Appendix Figure 2). This analysis shows that the novel H5N6 virus is genetically distinct from human H5N6 viruses found in China. The PB1, PA, HA, NP, MP, and NS gene segments are closely related to HPAI H5N8 viruses detected in Europe in 2016 (online Technical Appendix Figure 2, panels B–E, G, H). In contrast, the PB2 and NA genes are most closely related to Eurasian LPAI viruses (online Technical Appendix Figure 2, panels A, F). Of note, the N6 segment of the virus in the Netherlands is closely related to, but distinct from, that of the H5N6 viruses detected in Greece, Japan, and Taiwan in 2017. Furthermore, the virus in the Netherlands has PB2 and PA segments that are distinct from those found in the viruses from Greece, Japan, and Taiwan (Figure 2). These results indicate that H5N6 virus in the Netherlands is a reassortant of the HPAI H5N8 subtype that obtained novel PB2 and NA segments.

To explain the emergence of the novel H5N6 virus, we performed molecular dating using the Bayesian skyline coalescent model in BEAST version 1.8 software (http://beast.community/beast; online Technical Appendix Figure 3) and calculated the time to most recent common ancestor for the HA and NA gene segments (online Technical Appendix Table 1). For the H5 segment, the viruses in the Netherlands, Greece, Taiwan, and Japan share a common ancestor with HPAI H5N8, which was dated in January–September 2016 (online Technical Appendix Figure 3, panel A [node 1]). For the N6 segment, the common ancestor of the viruses in the Netherlands, Greece, Taiwan, and Japan was dated in December 2014–July 2016 (online Technical Appendix Figure 3, panel B [node 2]). The novel H5N6 virus probably arose by reassortment of HPAI H5N8 and descendants of LPAI A/barnacle goose/Netherlands/2014 (node 1), sometime in 2015–2016. These results suggest that the reassortment event that generated the novel HPAI H5N6 virus probably did not occur within the Netherlands in 2017.

Finally, we analyzed the genome of the novel H5N6 virus for potential zoonotic signatures associated with increased human risk (online Technical Appendix Table 2). We found that the virus has a typical avian receptor specificity and identified no sequence signatures associated with increased airborne transmission. In the MP and NS genes, we identified mutations that were associated with increased virulence, but similar mutations have been found in other H5 clade 2.3.4.4 viruses. Our analysis demonstrated that the virus may have reduced sensitivity to treatment with the antiviral drug oseltamivir.

Table 1. Genetic composition of the HPAI H5N6 virus isolated in the Netherlands, 2017*

Virus segment	GISAID no.†	Identity, %	Origin
Polymerase basic 2			
A/mallard duck/Netherlands/15/2011 (H6N8)	EPI889820	97	European LPAI
A/Eurasian teal/Netherlands/1/2011 (H3N8)	EPI889410	97	
A/mallard duck/Netherlands/20/2011 (H6N8)	EPI889594	97	
A/greater white-fronted goose/Netherlands/6/2011 (H6N8)	EPI1010712	97	
Polymerase basic 1			
A/chicken/Kalmykia/2643/2016 (H5N8)	EPI909458	99	H5N8 HPAI 2016
A/gadwall/Kurgan/2442/2016 (H5N8)	EPI961447	99	
A/T_Dk/NL-Werkendam/16014159–001/2016 (H5N5)	EPI1117251	98	
A/T_Dk/NL-Zeewolde/16013976–005/2016 (A/H5N8	EPI1019844	98	
Polymerase			
A/T_Dk/NL-Monnickendam/16013865–006–008/2016 (H5N8)	EPI1019770	99	H5N8 HPAI 2016
A/magpie/NL-Volendam/16014331–002/2016 (H5N8)	EPI1019722	99	
A/L-bl-ba-gull/NL-Sovon/16014324–014/2016 (H5N8)	EPI1019706	99	
A/G_c_grebe/NL-Monnickendam/16013865–009–010/2016 (H5N8)	EPI1019650	99	
Hemagglutinin			
A/Eur_Wig/NL-Zoeterwoude/16015702–010/2016 (H5N8)	EPI1019638	99	H5N8 HPAI 2016
A/Eur_Wig/NL-Reeuwijk/16015903–003/2016 (H5N8)	EPI1019590	99	
A/Eur_Wig/NL-Leidschendam/16015697–007/2016 (H5N8)	EPI1019582	99	
A/Eur_Wig/NL-Gouda/16015824–001/2016 (H5N8)	EPI1019550	99	
Nucleoprotein			
A/gadwall/Kurgan/2442/2016 (H5N8)	EPI961450	99	H5N8 HPAI 2016
A/wild duck/Tatarstan/3059/2016 (H5N8)	EPI909453	99	
A/T_Dk/NL-Werkendam/16014159–001/2016 (H5N5)	EPI1117254	99	
A/mute swan/Kaliningrad/132/2017 (H5N8)	EPI1044548	99	
Neuraminidase			
A/chicken/Greece/39_2017b/2017 (H5N6)	EPI1122895	98	H5N6 HPAI 2017
A/spoonbill/Taiwan/DB645/2017 (H5N6)	EPI1119073	97	
A/barnacle goose/Netherlands/2/2014 (H3N6)	EPI1011098	97	European LPAI
A/mute swan/Shimane/3211A001/2017 (H5N6)	LC335983	97	
Matrix protein			
A/mulard_duck/Hungary/59163/2016 (H5N8)	EPI1032553	99	H5N8 HPAI 2016
A/mulard_duck/Hungary/62902/2016 (H5N8)	EPI1032527	99	
A/mulard_duck/Hungary/60369/2016 (H5N8)	EPI1032519	99	
A/goose/Hungary/59763/2016 (H5N8)	EPI1032511	99	
Nonstructural protein			
A/duck/Hungary/60441/2016 (H5N8)	EPI866979	99	H5N8 HPAI 2016
A/goose/Italy/17VIR6358–3/2017 (H5N8)	EPI1081973	99	
A/swan/Italy/17VIR7064–1/2017 (H5N8)	EPI1081921	99	
A/mulard duck/Hungary/59163/2016 (H5N8)	EPI1032556	99	

*HPAI, highly pathogenic avian influenza; LPAI, low pathogenicity avian influenza.
†From GISAID EpiFlu database (http://platform.gisaid.org).

Conclusions

A novel reassortant HPAI H5N6 virus affected wild birds and commercial poultry in the Netherlands in December 2017. Phylogenetic analysis demonstrated that the virus is related to the HPAI H5N8 clade 2.3.4.4 viruses but contains novel PB2 and NA segments derived from Eurasian LPAI viruses. The N6 gene segment is related to that of HPAI H5N6 viruses found in Greece, Japan, and Taiwan, for which a common ancestor was estimated around November 2015. In addition, the H5N6 virus in the Netherlands differs from that in Greece by the PA and PB2 gene segments. This suggests that the H5N6 virus in the Netherlands did not result from continued circulation of the virus in Greece (or Europe) that was detected in February 2017 but likely represents a separate introduction related to wild bird migration in fall 2017. The reassortment events may have occurred on breeding grounds in Siberia, where large numbers of wild birds congregate, and the virus may have spread by long-distance flights of infected migratory birds (*6*).

Phylogenetic analysis demonstrated that the virus is not related to the zoonotic Asian H5N6 strains that cause infections in humans. Furthermore, genetic analysis identified no sequence features related to increased human risk. There are no indications that mammals (such as humans) can be infected by the novel reassortant HPAI H5N6 viruses detected in the Netherlands, Greece, Japan, and Taiwan. We recommend further studies in mammals (ferrets or mice) to provide experimental data on the virulence for mammals.

Acknowledgments

We thank Saskia Bergervoet, Sylvia Pritz-Verschuren, and Jayna Raghwani for technical assistance and the submitting laboratories for the sequences from the GISAID EpiFlu Database. This work was funded by the Dutch Ministry of Agriculture, Nature, and Food Quality.

About the Author

Dr. Beerens is a senior scientist and head of the National Reference Laboratory for Avian Influenza and Newcastle Disease in the Netherlands. Her research interests focus on molecular virology, genetics, and virus evolution.

References

1. Lee DH, Bertran K, Kwon JH, Swayne DE. Evolution, global spread, and pathogenicity of highly pathogenic avian influenza H5Nx clade 2.3.4.4. J Vet Sci. 2017;18(S1):269–80. http://dx.doi.org/10.4142/jvs.2017.18.S1.269
2. Bouwstra R, Heutink R, Bossers A, Harders F, Koch G, Elbers A. Full-genome sequence of influenza A(H5N8) virus in poultry linked to sequences of strains from Asia, the Netherlands, 2014. Emerg Infect Dis. 2015;21:872–4. http://dx.doi.org/10.3201/eid2105.141839
3. Bouwstra RJ, Koch G, Heutink R, Harders F, van der Spek A, Elbers AR, et al. Phylogenetic analysis of highly pathogenic avian influenza A(H5N8) virus outbreak strains provides evidence for four separate introductions and one between-poultry farm transmission in the Netherlands, November 2014. Euro Surveill. 2015;20:21174. https://doi.org/10.2807/1560-7917.ES2015.20.26.21174
4. Beerens N, Heutink R, Bergervoet SA, Harders F, Bossers A, Koch G. Multiple reassorted viruses as cause of highly pathogenic avian influenza A(H5N8) virus epidemic, the Netherlands, 2016. Emerg Infect Dis. 2017;23:1974–81. http://dx.doi.org/10.3201/eid2312.171062
5. Xu X, Subbarao, Cox NJ, Guo Y. Genetic characterization of the pathogenic influenza A/goose/Guangdong/1/96 (H5N1) virus: similarity of its hemagglutinin gene to those of H5N1 viruses from the 1997 outbreaks in Hong Kong. Virology. 1999;261:15–9. http://dx.doi.org/10.1006/viro.1999.9820
6. Global Consortium for H5N8 and Related Influenza Viruses. Role for migratory wild birds in the global spread of avian influenza H5N8. Science. 2016;354:213–7. http://dx.doi.org/10.1126/science.aaf8852
7. Lee DH, Bahl J, Torchetti MK, Killian ML, Ip HS, DeLiberto TJ, et al. Highly pathogenic avian influenza viruses and generation of novel reassortants, United States, 2014–2015. Emerg Infect Dis. 2016;22:1283–5. http://dx.doi.org/10.3201/eid2207.160048
8. Slomka MJ, Pavlidis T, Banks J, Shell W, McNally A, Essen S, et al. Validated H5 Eurasian real-time reverse transcriptase-polymerase chain reaction and its application in H5N1 outbreaks in 2005–2006. Avian Dis. 2007;51(Suppl):373–7. http://dx.doi.org/10.1637/7664-060906R1.1
9. Bi Y, Chen Q, Wang Q, Chen J, Jin T, Wong G, et al. Genesis, evolution, and prevalence of H5N6 Avian influenza viruses in China. Cell Host Microbe. 2016;20:810–21. http://dx.doi.org/10.1016/j.chom.2016.10.022
10. Lee DH, Sharshov K, Swayne DE, Kurskaya O, Sobolev I, Kabilov M, et al. Novel reassortant clade 2.3.4.4 avian influenza A(H5N8) virus in wild aquatic birds, Russia, 2016. Emerg Infect Dis. 2017;23:359–60. http://dx.doi.org/10.3201/eid2302.161252

Address for correspondence: Nancy Beerens, Wageningen Bioveterinary Research, Division of Virology, PO Box 65, 8200 AB, Lelystad, the Netherlands; email: nancy.beerens@wur.nl

Importation of Mumps Virus Genotype K to China from Vietnam

Wei Liu, Lili Deng, Xianyu Lin, Ximing Wang, Yuyan Ma, Qiuyun Deng, Xiaohua Xue, Ge Zhong, Li Jin

During May–August 2016, mumps virus genotype K was detected in 12 Vietnam citizens who entered China at the Shuikou border crossing and 1 girl from China. We provide evidence that mumps genotype K is circulating in Vietnam and was imported to China from Vietnam.

Mumps is an acute viral illness characterized by swelling of the parotid glands. The disease is highly contagious and shows nonspecific symptoms (e.g., headache and fever). However, in some cases complications, such as aseptic meningitis, orchitis, encephalitis, and deafness, might occur (*1*).

Mumps can be prevented by appropriate vaccination. Mumps virus–containing vaccine (e.g., MMR vaccines for measles, mumps, and rubella) has been given to children 18–24 months of age in China since 2008. However, this vaccine has not been included in immunization schedules in Vietnam (*2*). The Shuikou border crossing is located between TàLùng in CaoBằng Province, Vietnam, and Shuikou in Guangxi Province, China (online Technical Appendix Figure 1, https://wwwnc.cdc.gov/EID/article/24/4/17-0591-Techapp1.pdf). Approximately ≈1,500 persons/day cross the border between Vietnam and China to conduct business or receive healthcare. More than 90% of these persons are from Vietnam, many of whom visit clinics in Shuikou and return home the same day. We report importation of mumps virus genotype K to China from Vietnam.

The Study

On May 15, 2016, a 7-year-old boy from Vietnam with bilateral parotid gland swelling was observed at the border crossing and considered to have a suspected case of mumps. Over the next 4 months, 11 other patients from TàLùng (online Technical Appendix Figure 1) with suspected mumps were reported to the Longzhou County Center of Disease Prevention and Control (CDC) in China. None of these 12 patients had traveled outside CaoBằng Province, Vietnam, during the month before onset of infection. However, 7 patients reported contact with persons who had mumps-like illness.

On July 15, 2016, an 11-year-old girl from China with fever and unilateral parotid gland swelling was clinically confirmed as having mumps (Table). She was living in a village near the Shuikou border crossing, and her father and other villagers used this border crossing almost daily to conduct business, which suggested that she might be epidemiologically linked to the Vietnam patients. None of the 13 patients had received a mumps vaccine. We obtained data for all 13 patients (Table).

Throat swab specimens were collected from patients and immediately transported on icepacks to the Guangxi CDC. RNA was extracted from original samples and supernatants of Vero/hSLAM-cell cultures (*3*) by using the Viral RNA Mini Kit (QIAGEN, Valencia, CA, USA). We amplified extracted RNA by using the SuperScript-III Platinum One-Step Reverse Transcription PCR System (Invitrogen, Waltham, MA, USA) and primers for the small hydrophobic (SH) gene and hemagglutinin–neuraminidase (HN) gene as described (*4*,*5*). All throat swab specimens were positive for mumps virus by reverse transcription PCR. Mumps virus isolation was achieved for 8 (61.5%) of 13 specimens.

PCR products were sequenced by Life Technologies (Shanghai, China). We performed analyses of nucleotide sequences of SH and HN genes and deduced amino acid sequences by using BioEdit (*6*) and the neighbor-joining method in MEGA6 software (*7*). In accordance with World Health Organization mumps virus nomenclature (*8*), viruses were named and assigned a genotype on the basis of comparison with 12 reference strains and a high bootstrap score. Sequences formed 2 distinct clusters; both clusters had greatest homology with genotype K reference strains Stockholm.SWE/26.83/1[K] and RW154.USA/0.70s[K]. The SH gene homologies were 93.0%–94.3% with Stockholm.SWE/26.83/1[K] and 93.9%–95.8% with RW154.USA/0.70s[K]. Greatest heterogeneity was 15.6% with genotype A (online Technical Appendix Figure 2). A similar pattern was observed by additional phylogenetic

Author affiliations: Guangxi Zhuang Autonomous Region Center for Disease Prevention and Control, Nanning, China (W. Liu, L. Deng, Y. Ma, Q. Deng, G. Zhong); Shuikou Entry–Exit Inspection and Quarantine Bureau, Longzhou, China (X. Lin, X. Xue); Longzhou County Center for Disease Prevention and Control, Longzhou (X. Wang); Public Health England, London, UK (L. Jin)

DOI: https://doi.org/10.3201/eid2404.170591

Table. Characteristics of 13 mumps patients during importation of mumps virus genotype K to China from Vietnam, 2016*

Patient no.	Age, y/sex	Date of illness onset	Date of sample collection	Parotid gland swelling	Body temperature, °C	Virus isolation result	Mumps virus strain
1	7/M	May 15	May 15	Bilateral	37.3	+	MuVi/CaoBang.VNM/20.16/1[K]
2	9/F	May 16	May 21	Bilateral	36.8	–	MuVs/CaoBang.VNM/21.16/1[K]
3	4/M	May 16	May 22	Bilateral	37.5	–	MuVs/CaoBang.VNM/21.16/2[K]
4	5/M	Jun 4	Jun 4	Unilateral	37.5	+	MuVi/CaoBang.VNM/23.16/1[K]
5	4/M	Jun 6	Jun 6	Bilateral	37.0	+	MuVi/CaoBang.VNM/24.16/1[K]
6	5/M	Jun 13	Jun 14	Unilateral	37.5	+	MuVi/CaoBang.VNM/25.16/1[K]
7	6/M	Jun 13	Jun 14	Unilateral	38.0	+	MuVi/CaoBang.VNM/25.16/2[K]
8	5/F	Jun 17	Jun 19	Bilateral	37.0	+	MuVi/CaoBang.VNM/25.16/3[K]
9†	11/F	Jul 15	Jul 20	Unilateral	38.8	–	MuVs/Guangxi.CHN/29.16/1[K]
10	10/M	Jul 15	Jul 15	Unilateral	38.6	–	MuVs/CaoBang.VNM/29.16/1[K]
11	27/F	Aug 1	Aug 3	Unilateral	37.0	+	MuVi/CaoBang.VNM/32.16/1[K]
12	23/F	Aug 1	Aug 3	Bilateral	36.8	+	MuVi/CaoBang.VNM/32.16/2[K]
13	30/M	Aug 4	Aug 8	Bilateral	36.5	–	MuVs/CaoBang.VNM/32.16/3[K]

*All patients had positive results for mumps virus by PCR. +, positive; –, negative.
†Patient in China.

analysis with the HN gene (Figure 1), recommended by the World Health Organization (*8*). These analyses confirmed that all viruses had genotype K.

We performed further analysis of the SH gene to evaluate diversity of genotype K by construction of a phylogenetic tree that included 17 genotype K sequences from GenBank; 2 F strains detected in Guangxi Province during 2009–2012; reference strains of genotypes F, K, and A; and the mumps vaccine (S79/Jeryl Lynn, HQ416906) used in China. Homologies between the 2 clusters and other K strains ranged from 94.9% to 100% (Figure 2). Cluster 1, which contains the sequence obtained from the patient in China, is only 1 nt different from the K strain detected in the United States in 2012 (Washington.USA/4.12). This cluster is also closer to K strains detected more recently (2012–2016). Cluster 2 contains the remaining sequences from Vietnam, and this cluster is closely related to the K strain reported in 2009 in Canada (Alberta.CAN/19.09[K]). The genotype F virus identified in Guangxi (Guangxi.CHN/7.12[F]) showed a 9.5%–11.1% difference from the 2 K clusters. All sequences were submitted to GenBank (accession nos. KX622738–KX622745, KX671152, KX965999–KX966002, and KX966004–KX966016).

We compared amino acid sequences of the SH gene with sequences of other genotype K strains and found 5-aa differences between cluster 1 and cluster 2 isolates. The amino acid sequence of the Washington.USA/4.12 strain was identical to those in cluster 1, whereas strains in cluster 2 were unique for all amino acid sequences analyzed (online Technical Appendix Figure 3).

Conclusions

Laboratory investigations suggested an ongoing mumps outbreak in Vietnam. Further supportive information was obtained from the Official News Website of the government of Vietnam (*9*–*12*). During January–May 2016, >600 mumps cases were reported, which was 10 times higher than during the same period in 2015. The mumps outbreak occurred initially in southern Vietnam and quickly spread to northern provinces. In June, 1 hospital in the middle northern region had 50 patients with mumps, of whom 5 had encephalitis as a complication (*12*). The mumps epidemic became more severe in April in the northern region, which includes CaoBằng Province, where the Shuikou border crossing is located. TàLùng, Vietnam, and Shuikou, China, in this region are separated by the river Sông-băc-vọng/Shuikou (Vietnamese/Chinese name) River. Mumps vaccination is not part of the Vietnam national immunization program (*2*), and a shortage of the mumps vaccine has been confirmed by the government of Vietnam.

Because of lack of laboratory data for Vietnam, detection of mumps outbreaks by routine laboratory surveillance has not been established in this country. Patients identified in this report were probably linked to outbreaks described on the basis of timing and residence. We confirm that mumps virus genotype K is circulating in Vietnam, which is consistent with a report that genotype K is still circulating (*13*), and is supported by evidence that 2 recent genotype K strains, 1 from Canada (Ontario.CAN/52.12[K]) and 1 from the United States (Washington.USA/4.12[K]), were imported from Vietnam (R.J. McNall et al., pers. comm.).

The latest summary of global distribution of mumps genotypes (*8,13*) showed that genotype F has been circulating in China since 1995. Until now, genotype K was not identified in China. Mumps virus genotype K detected in the patient from China was identical to 1 of the Vietnam genotype K variants, suggesting that transmission of this genotype into China was caused by an importation from Vietnam. No further transmission has been identified in China, suggesting that vaccination coverage is high in the hometown of the child, although some cases might have been missed because up to 30% of mumps infections can be asymptomatic.

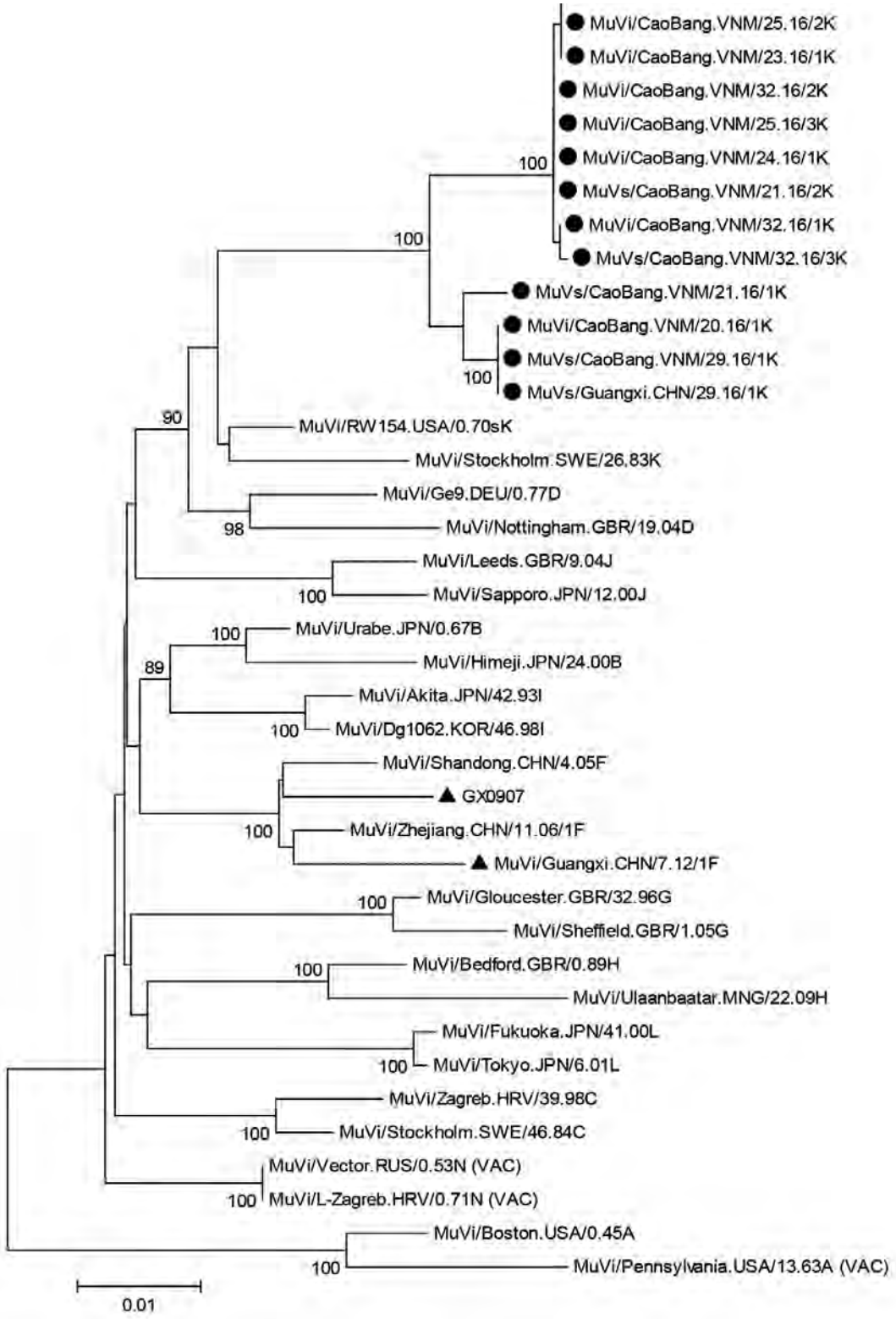

Figure 1. Phylogenetic tree of hemagglutinin–neuraminidase genes of 13 isolates of mumps virus genotype K from 1 patient from China and from 12 patients from Vietnam (solid black circles) compared with reference isolates. Solid black triangles indicate F strains isolated in Guangxi Province, China. The tree was constructed by using the neighbor-joining method in MEGA6 software (*7*). The Kimura-2 parameter model was used, and robustness of internal branches was determined by using 500 bootstrap replications. Numbers along branches are bootstrap values. Scale bar indicates nucleotide substitutions per site. MuV, mumps virus.

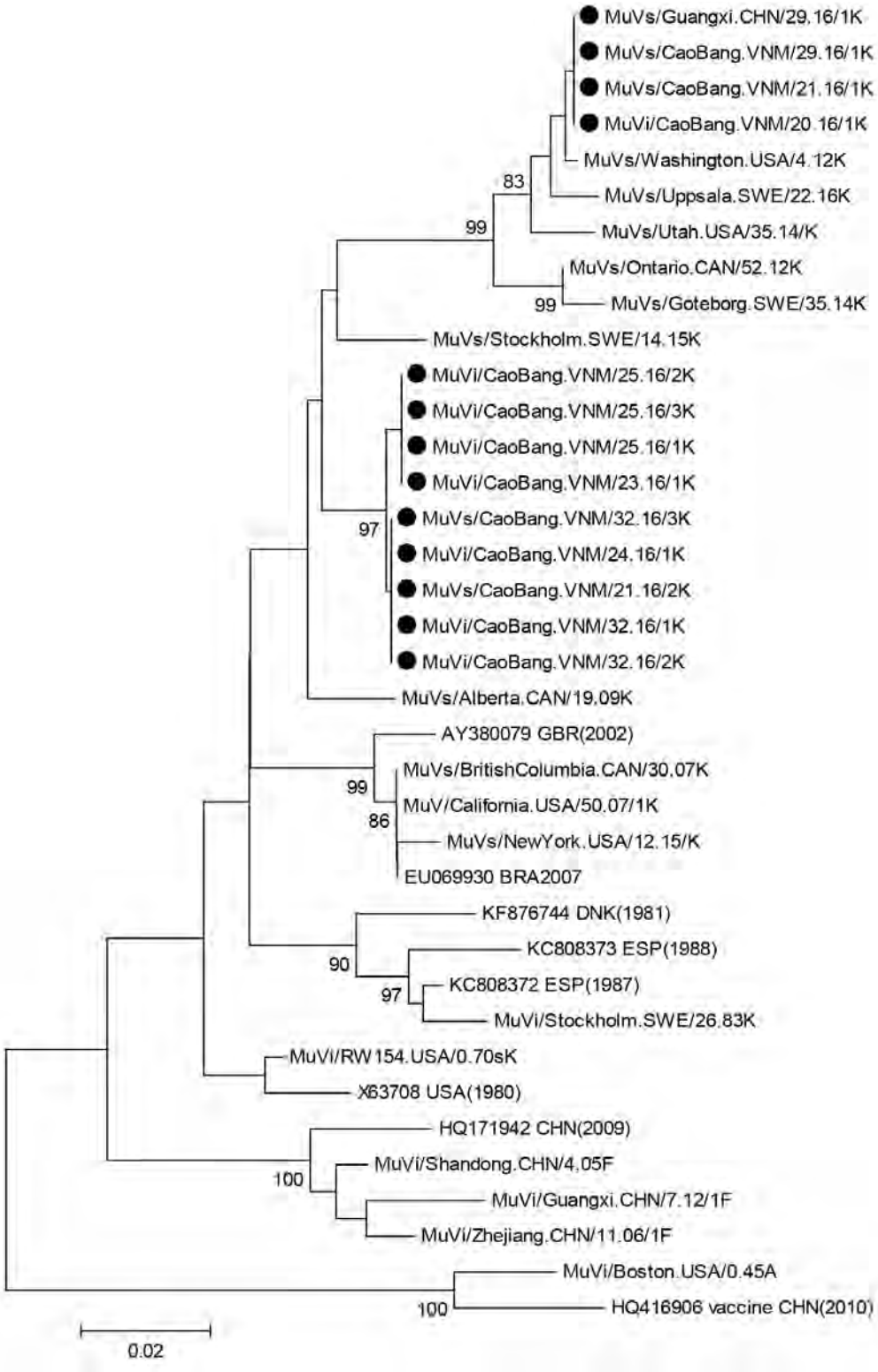

Figure 2. Phylogenetic tree of small hydrophobic genes of 13 isolates of mumps virus genotype K isolated in China from 1 patient from China and 12 patients from Vietnam (solid black circles) compared with reference isolates. The tree was constructed by using the neighbor-joining method in MEGA6 software (*7*). The Kimura-2 parameter model was used, and robustness of internal branches was determined by using 500 bootstrap replications. Numbers along branches are bootstrap values. Scale bar indicates nucleotide substitutions per site. MuV, mumps virus.

The lack of a strong global surveillance system makes understanding transmission patterns of mumps challenging. We provide evidence that mumps genotype K is circulating in Vietnam, and the sequence information presented confirms epidemiologic links between cases. These data increase understanding of the distribution of mumps virus genotypes and highlight the need for enhanced surveillance of infectious diseases at all border crossings between Vietnam and China.

Acknowledgments

We thank Rebecca J. McNall and Paul Rota for supportive input during preparation of the manuscript.

About the Author

Dr. Liu is a senior microbiologist and deputy director, Institute of Immunization and Prevention, Guangxi Zhuang Autonomous Region Center for Disease Prevention and Control, Nanning, China. His primary research interest is vaccine-preventable diseases (e.g., poliomyelitis, measles, rubella, mumps, meningitis, Japanese encephalitis, and hepatitis B).

References

1. Knowles WA, Jin L. Rubulavirus: mumps virus. In: Mahy BW, ter Meulen V, editors. Topley and Wilson's microbiology and microbial infections. 10th ed. New York: John Wiley and Sons, Ltd; 2005. p. 744–62.
2. World Health Organization—UNICEF. Don't be late! Follow the national immunization schedule and make sure your child's vaccinations are up-to-date; 2015 [cited 2018 Jan 24] http://www.wpro.who.int/vietnam/mediacentre/releases/2015/who_vietnam_2015_timely_immunization/en/
3. Ono N, Tatsuo H, Hidaka Y, Aoki T, Minagawa H, Yanagi Y. Measles viruses on throat swabs from measles patients use signaling lymphocytic activation molecule (CDw150) but not CD46 as a cellular receptor. J Virol. 2001;75:4399–401. http://dx.doi.org/10.1128/JVI.75.9.4399-4401.2001
4. Cui AL, Zhu Z, Wang CY, Wang Y, Zhou JH, Wu HW. Genetic characteristics of mumps virus in China from 2006 to 2008 [in Chinese]. Zhongguo Yi Miao He Mian Yi. 2009;15:8–13.
5. Ivancic-Jelecki J, Santak M, Forcic D. Variability of hemagglutinin-neuraminidase and nucleocapsid protein of vaccine and wild-type mumps virus strains. Infect Genet Evol. 2008;8:603–13. http://dx.doi.org/10.1016/j.meegid.2008.04.007
6. Hall TA. BioEdit: a user-friendly biological sequence alignment editor and analysis program for Windows 95/98/NT. Nucleic Acids Symp Ser. 1999;41:95–8.
7. Tamura K, Stecher G, Peterson D, Filipski A, Kumar S. MEGA6: Molecular Evolutionary Genetics Analysis version 6.0. Mol Biol Evol. 2013;30:2725–9. http://dx.doi.org/10.1093/molbev/mst197
8. World Health Organization. Mumps virus nomenclature update: 2012. Wkly Epidemiol Rec. 2012;87:217–24.
9. VTV24 News Center. A mumps outbreak occurred in Bac Lieu Province [cited 2018 Jan 24]. http://vtv.vn/chuyen-dong-24h/xuat-hien-o-dich-quai-bi-tai-bac-lieu-20160326123316491.htm
10. The Board of the Updated. Mumps outbreaks due to lack of vaccines [cited 2018 Jan 24]. http://vtv.vn/xa-hoi/gia-tang-cac-truong-hop-mac-quai-bi-o-hai-duong-20160406174208116.htm
11. The Board of the Updated. Cases of mumps in children increased in NgheAn Province [cited 2018 Jan 24]. http://vtv.vn/suc-khoe/benh-quai-bi-bung-phat-do-thieu-vaccine-20160508150127656.htm
12. VTV24 News Centre. Mumps cases rise in Hai Duong Province [cited 2018 Jan 24]. http://vtv.vn/chuyen-dong-24h/nghe-an-gia-tang-tre-mac-benh-quai-bi-20160617105652449.htm
13. Jin L, Örvell C, Myers R, Rota PA, Nakayama T, Forcic D, et al. Genomic diversity of mumps virus and global distribution of the 12 genotypes. Rev Med Virol. 2015;25:85–101. http://dx.doi.org/10.1002/rmv.1819

Address for correspondence: Li Jin, Virus Reference Department, Public Health England, 61 Colindale Ave, London NW9 5EQ, UK; email: li.jin@phe.gov.uk

Testing for Coccidioidomycosis among Community-Acquired Pneumonia Patients, Southern California, USA[1]

Sara Y. Tartof,[2] Kaitlin Benedict,[2] Fagen Xie, Gunter K. Rieg, Kalvin C. Yu, Richard Contreras, Jonathan Truong, Kimberlee Fong, Hung Fu Tseng, Steven J. Jacobsen, Rajal K. Mody

We conducted a cohort study to identify characteristics associated with testing for, and testing positive for, coccidioidomycosis among patients with community-acquired pneumonia in southern California, USA. Limited and delayed testing probably leads to underdiagnosis among non-Hispanic black, Filipino, or Hispanic patients and among high-risk groups, including persons in whom antimicrobial drug therapy has failed.

The public health impact of coccidioidomycosis (Valley fever) in the United States is increasing. The causative fungus, *Coccidioides*, is endemic to the southwestern and western United States. In 2015, California reported 3,015 cases, ≈25% of all US cases (*1*,*2*). In areas of Arizona where coccidioidomycosis is highly endemic, the disease might be responsible for 15%–29% of community-acquired pneumonia (CAP) cases; however, in some studies, <15% of CAP patients are tested, suggesting that the disease is underrecognized, even in endemic areas (*3*–*5*). Testing practices for CAP patients in southern California have not been well documented. Therefore, we determined the proportion of CAP patients who were tested, the proportion who tested positive, and clinical factors associated with being tested and having confirmed coccidioidomycosis among patients enrolled in the Kaiser Permanente Southern California (KPSC) healthcare system in 2011.

The Study

KPSC is an integrated healthcare organization with ≈4.4 million members who are representative of the socioeconomic and racial/ethnic diversity of the area's population (*6*). KPSC uses electronic health records (EHRs) to integrate medical information from all care and laboratory settings. We included all KPSC patients meeting membership criteria who had CAP diagnosed and received treatment for CAP as outpatients (online Technical Appendix Table 1, https://wwwnc.cdc.gov/EID/article/24/4/16-1658-Techapp1.pdf). Information about each patient's medical history during 2001–2011 was based on International Classification of Disease, Ninth Revision (ICD-9), codes retrieved from EHRs.

We searched CAP patient EHRs to identify coccidioidomycosis laboratory testing from all care settings (online Technical Appendix Table 1). We sought documentation of a coccidioidomycosis-related ICD-9 code (114.X) in any encounter type from 1 week before to 1 year after the sample collection date for patients with confirmed coccidioidomycosis cases. We excluded patients having received an ICD-9 coccidioidomycosis diagnosis before 2011 and those who had a hospitalization during the 2 weeks before CAP diagnosis.

To identify factors for multivariable modeling, we used χ^2 and *t*-tests (statistical significance defined as $p<0.2$), clinical knowledge, and a backward selection algorithm testing for interaction terms. We conducted analyses in SAS version 9.3 (SAS Institute, Cary, NC, USA).

After exclusions, the final cohort consisted of 33,756 patients (online Technical Appendix Table 2). Among patients with CAP, 2,061 (6%) were tested for coccidioidomycosis within 1 year of CAP diagnosis. A median of 6 (mean 46) days and a median of 2 (mean 5) clinic encounters elapsed between the index CAP date (i.e., the date the CAP ICD-9 code was first used) and the first order for a coccidioidomycosis test. Among patients who initially tested negative, 5% had a repeat test within 30 days and 8% within 90 days.

In adjusted analyses, testing for coccidioidomycosis was less likely among female patients and among Hispanic patients who survived 1 year after the index CAP date (compared with surviving non-Hispanic whites) (online Technical Appendix Table 2). Pulmonary clinics were most likely to test for coccidioidomycosis. Increasing

Author affiliations: Kaiser Permanente Southern California, Pasadena, California, USA (S.Y. Tartof, F. Xie, R. Contreras, H.F. Tseng, S.J. Jacobsen); Centers for Disease Control and Prevention, Atlanta, Georgia, USA (K. Benedict, R.K. Mody); Southern California Permanente Medical Group, Pasadena (G.K. Rieg, K.C. Yu, J. Truong, K. Fong)

DOI: https://doi.org/10.3201/eid2404.161568

[1]Preliminary results from this study were presented at the 60th Annual Coccidioidomycosis Study Group Meeting; Sacramento, California, USA; April 9, 2016.

[2]These authors contributed equally to this article.

numbers of healthcare encounters involving a CAP ICD-9 code, inpatient visits, chest radiograph orders, and antimicrobial drug prescriptions in the year after CAP diagnosis increased the odds of being tested for coccidioidomycosis. Patients whose race/ethnicity was Filipino, Hispanic, American Indian/Alaska Native multiple, other, or unknown who died (from any cause) had increased odds of being tested for coccidioidomycosis compared with surviving non-Hispanic whites.

Of the 2,061 CAP patients tested for coccidioidomycosis, 377 (18%) were positive by any test; of these, 45 (12%) had ≥1 previous negative test before testing positive, and 172 (46%) were confirmed by complement fixation or immunodiffusion. Among those who tested positive by both IgG and IgM enzyme immunoassay (EIA), 88% were confirmed by complement fixation or immunodiffusion; only 10% of IgG-positive results and 7% of IgM-positive results were confirmed (online Technical Appendix Table 3).

In adjusted analyses, female sex was associated with reduced odds of testing positive (adjusted odds ratio [aOR] 0.60 [95% CI 0.42–0.86]). Persons of Filipino ethnicity (aOR 3.56 [95% CI 1.57–8.08]), non-Hispanic black race (aOR 2.78 [95% CI 1.50–5.12]), and Hispanic ethnicity (aOR 1.83 [95% CI 1.23–2.73) were more likely to test positive than were non-Hispanic whites. Kern County residents were more likely to test positive than Los Angeles County residents (aOR 2.48 [95% CI 1.56–3.95]) (online Technical Appendix Table 4). Having antimicrobial drugs prescribed ≥2 times (in addition to the treatment-defining CAP diagnosis) from 1 week before the first CAP visit to the first coccidioidomycosis test (aOR 4.57 [95% CI 1.29–16.12]) and having chest radiographs within 1 year after CAP diagnosis (aOR 2.30 [95% CI 1.54–3.45]) were associated with increased odds of testing positive.

Conclusions

We assessed testing practices for coccidioidomycosis among patients with CAP in southern California and found that only 6% of CAP patients were tested, of whom 18% were coccidioidomycosis-positive by any test and 8% by confirmatory testing. Further, our data highlight delayed testing for some patients, low rates of retesting, and opportunities to reduce unnecessary antibiotic use.

In addition to low overall testing rates, we detected substantial testing delays, suggested by much higher estimated mean (compared with median) time to testing. We might underestimate delays because patients might have had CAP-related visits before the study period began. Delays in testing have been noted previously but were shorter among persons who knew about the disease before seeking healthcare, suggesting a benefit of community awareness (*7*).

Delays in testing affect healthcare use. CAP patients tested for coccidioidomycosis were more likely to have received multiple courses of antimicrobial drugs, experienced more inpatient admissions for CAP, and received more chest radiographs than CAP patients who were not tested, suggesting substantial resource utilization and possible worsening of symptoms before coccidioidomycosis was considered. Further, patients with confirmed coccidioidomycosis were more likely to have received ≥2 additional antimicrobial drug prescriptions between CAP diagnosis and their first coccidioidomycosis test. Other studies have described high rates of initial and subsequent antimicrobial treatment among coccidioidomycosis patients in Arizona (*5*,*7*).

Patients of Filipino, Hispanic, non-Hispanic black, and American Indian/Alaska Native or multiple, other, or unknown race/ethnicity who died had ≈8, 2, 2, and 3 times the odds of being tested for coccidioidomycosis, respectively, compared with surviving non-Hispanic whites. Although we could only capture all-cause mortality, the high probability for testing among patients who do not survive suggests possible progression of severe disease before consideration of coccidioidomycosis. Additionally, non-Hispanic black and Filipino patients with CAP had greater odds than non-Hispanic whites for having coccidioidomycosis. Historically, non-Hispanic black and Filipino patients have been identified as having increased risk for severe or disseminated coccidioidomycosis compared with other racial/ethnic groups (*8*–*11*). Unfortunately, we were unable to control for exposure-related factors, such as occupation, which might correlate with race/ethnicity.

Experts at the University of Arizona suggest that patients who initially have a negative serologic test should be retested within 2 months because serologic tests can be negative early in the course of infection (*12*). In our cohort, 12% of patients with any positive coccidioidomycosis test had previous negative tests. However, few CAP patients (8%) who tested negative were retested. Thus, increased awareness of repeat testing for those with persistent symptoms might be warranted. However, EIA testing has limitations; although it is widely used because it is faster and requires less technical expertise than complement fixation or immunodiffusion, the specificity is low. Having a positive EIA test result for IgG or IgM alone in our study correlated very poorly with positive confirmatory testing.

In conclusion, limited testing for coccidioidomycosis likely precludes accurate assessment of the overall frequency of the disease among CAP patients. Physician and community education might improve overall detection and result in earlier detection, which could be beneficial in decreasing overuse of antimicrobial drugs, reducing time and resources spent seeking other diagnoses, and improving monitoring for coccidioidomycosis complications.

Acknowledgments

We acknowledge Sekai Chideya-Chihota and Benjamin J. Park for early contributions to study design, Nicole Higashiyama for medical chart data support, Demosthenes Pappagianis for subject matter expertise on diagnostic methods, Lei Qian for statistical consulting, and Brendan Jackson and Tom Chiller for review and edits of the manuscript.

S.Y.T. had full access to all of the data in the study and takes responsibility for the integrity of the data and the accuracy of the data analysis. F.X. and R.C. conducted and are responsible for data analyses. R.K.M. and K.B. contributed to the design and conduct of the study; collection, management, analysis, and interpretation of the data; and preparation, review, or approval of the manuscript.

About the Author

Dr. Tartof is a research scientist at the Kaiser Permanente Southern California Department of Research and Evaluation. Her primary interests are in infectious disease epidemiology, with particular interest in antimicrobial resistance, antimicrobial stewardship, vaccine studies, hepatitis C infection, and hospital infections.

References

1. Marsden-Haug N, Goldoft M, Ralston C, Limaye AP, Chua J, Hill H, et al. Coccidioidomycosis acquired in Washington State. Clin Infect Dis. 2013;56:847–50. http://dx.doi.org/10.1093/cid/cis1028
2. CDC. Notice to readers: final 2015 reports of nationally notifiable infectious diseases and conditions. MMWR Morb Mortal Wkly Rep. 2016;65:1306–21. http://dx.doi.org/10.15585/mmwr.mm6546a9
3. Chang DC, Anderson S, Wannemuehler K, Engelthaler DM, Erhart L, Sunenshine RH, et al. Testing for coccidioidomycosis among patients with community-acquired pneumonia. Emerg Infect Dis. 2008;14:1053–9. http://dx.doi.org/10.3201/eid1407.070832
4. Kim MM, Blair JE, Carey EJ, Wu Q, Smilack JD. Coccidioidal pneumonia, Phoenix, Arizona, USA, 2000–2004. Emerg Infect Dis. 2009;15:397–401. http://dx.doi.org/10.3201/eid1563.081007
5. Valdivia L, Nix D, Wright M, Lindberg E, Fagan T, Lieberman D, et al. Coccidioidomycosis as a common cause of community-acquired pneumonia. Emerg Infect Dis. 2006;12:958–62. http://dx.doi.org/10.3201/eid1206.060028
6. Koebnick C, Langer-Gould AM, Gould MK, Chao CR, Iyer RL, Smith N, et al. Sociodemographic characteristics of members of a large, integrated health care system: comparison with US Census Bureau data. Perm J. 2012;16:37–41. http://dx.doi.org/10.7812/TPP/12-031
7. Tsang CA, Anderson SM, Imholte SB, Erhart LM, Chen S, Park BJ, et al. Enhanced surveillance of coccidioidomycosis, Arizona, USA, 2007–2008. Emerg Infect Dis. 2010;16:1738–44. http://dx.doi.org/10.3201/eid1611.100475
8. Crum NF, Lederman ER, Stafford CM, Parrish JS, Wallace MR. Coccidioidomycosis: a descriptive survey of a reemerging disease. Clinical characteristics and current controversies. Medicine (Baltimore). 2004;83:149–75. http://dx.doi.org/10.1097/01.md.0000126762.91040.fd
9. Rosenstein NE, Emery KW, Werner SB, Kao A, Johnson R, Rogers D, et al. Risk factors for severe pulmonary and disseminated coccidioidomycosis: Kern County, California, 1995–1996. Clin Infect Dis. 2001;32:708–15. http://dx.doi.org/10.1086/319203
10. Smith CE, Beard RR, Whiting EG, Rosenberger HG. Varieties of coccidioidal infection in relation to the epidemiology and control of the diseases. Am J Public Health Nations Health. 1946;36:1394–402. http://dx.doi.org/10.2105/AJPH.36.12.1394
11. Gifford M. Coccidioidomycosis, Kern County [cited 2016 Jul 12]. http://kerncountyvalleyfever.com/wp-content/uploads/2013/04/LibraryCocci-Article-1939.pdf
12. Valley Fever Center for Excellence. Valley fever (coccidioidomycosis) tutorial for primary care professionals [cited 2016 Jul 12]. http://vfce.arizona.edu/sites/vfce/files/tutorial_for_primary_care_professionals.pdf

Address for correspondence: Sara Y. Tartof, Kaiser Permanente Southern California, Department of Research and Evaluation, 100 S Los Robles, 2nd Fl, Pasadena, CA, 91101, USA; email: sara.y.tartof@kp.org

Lyssavirus in Japanese Pipistrelle, Taiwan

Shu-Chia Hu, Chao-Lung Hsu, Ming-Shiuh Lee, Yang-Chang Tu, Jen-Chieh Chang, Chieh-Hao Wu, Shu-Hwae Lee, Lu-Jen Ting, Kwok-Rong Tsai, Ming-Chu Cheng, Wen-Jane Tu, Wei-Cheng Hsu

A putative new lyssavirus was found in 2 Japanese pipistrelles (*Pipistrellus abramus*) in Taiwan in 2016 and 2017. The concatenated coding regions of the virus showed 62.9%–75.1% nucleotide identities to the other 16 species of lyssavirus, suggesting that it may be representative of a new species of this virus.

The *Lyssavirus* genus within the family *Rhabdoviridae* is composed of 14 species of lyssavirus: rabies lyssavirus (RABV), Lagos bat lyssavirus (LBV), Mokola lyssavirus (MOKV), Duvenhage lyssavirus (DUVV), European bat 1 lyssavirus (EBLV-1), European bat 2 lyssavirus (EBLV-2), Australian bat lyssavirus (ABLV), Aravan lyssavirus (ARAV), Khujand lyssavirus (KHUV), Irkut lyssavirus (IRKV), Shimoni bat lyssavirus (SHIBV), Bokeloh bat lyssavirus (BBLV), West Caucasian bat lyssavirus (WCBV), and Ikoma lyssavirus (IKOV) (*1*). In addition, Lleida bat lyssavirus (LLEBV) (*1,2*) and Gannoruwa bat lyssavirus (GBLV) (*3*) were recently identified in bats, but their taxonomic statuses have not been determined by the International Committee on the Taxonomy of Viruses. The genus *Lyssavirus* can be subdivided into phylogroup 1 (RABV, DUVV, EBLV-1, EBLV-2, ABLV, ARAV, KHUV, IRKV, BBLV, and GBLV) and phylogroup 2 (LBV, MOKV, and SHIBV) according to genetic distances and serologic cross-reactivity (*1*–*3*). The remaining species, WCBV, IKOV, and LLEBV, cannot be included in either of these phylogroups (*1,2*).

Bats are the natural hosts of most lyssaviruses, with the exceptions of MOKV and IKOV, which have not been identified in any bats (*1*–*4*). Information about lyssaviruses in bats in Asia is limited. In Central Asia, ARAV was identified in the lesser mouse-eared bat (*Myotis blythi*) in Kyrgyzstan in 1991, and KHUV was identified in the whiskered bat (*M. mystacinus*) in Tajikistan in 2001 (*5*). In South Asia, GBLV was identified in the Indian flying fox (*Pteropus medius*) in Sri Lanka in 2015 (*3*). Although IRKV was identified in the greater tube-nosed bat (*Murina leucogaster*) in China in 2012 (*6*), knowledge of the exact species and locations of lyssaviruses in East Asia bat populations remains limited.

In this article, we report a putative new lyssavirus isolated during our surveillance program in Taiwan. Our discovery suggests that this lyssavirus may be representative of a new species, based on genetic distance.

The Study

Specimens for this study were collected under a permit issued by the Forestry Bureau, Council of Agriculture, Executive Yuan, Taiwan (document no. 1055104969). From 2014 through the end of May 2017, a total of 332 bat carcasses from 13 species were collected for lyssavirus surveillance. Of the collected individuals, 2 tested positive for the virus by direct fluorescent antibody testing and reverse transcription PCR (*7*–*9*). The first bat showing loss of appetite without specific clinical signs was found in Tainan City and died on July 2, 2016. The second bat was found dead in Yunlin County on April 12, 2017, and the carcass was shipped to the Animal Health Research Institute (AHRI) in New Taipei City. We obtained two 428-bp amplicons (N113F/N304R, containing the partial nucleoprotein [N] gene and phosphoprotein [P] gene) from these cases using lyssavirus screen primers (Table 1); we then subjected their sequences to BLAST (https://www.ncbi.nlm.nih.gov/BLAST/), querying the GenBank database. Both sequences were similar to lyssaviruses, with nucleotide identities <79%.The 2 bats were identified as Japanese pipistrelle (*Pipistrellus abramus*), or Japanese house bat, by morphology (J.T. Wu, Taxonomic study of the genus *Pipistrellus* [chiroptera: vespertilionidae] in Taiwan. Master's thesis, Department of Biological Resources, National Chiayi University, Chiayi City, Taiwan, 2007 [in Chinese]) and DNA barcoding (based on subunit 1 of the mitochondrial protein NADH dehydrogenase [ND1] gene) (*10*). The 2 sequences of partial ND1 genes were then submitted to GenBank; the first had been designated as 2016-2300 (GenBank accession no. MG763889) and the second 2017-1502 (GenBank accession no. MG763890).

We isolated lyssavirus successfully from the 2 bats' brains; we confirmed the identity of lyssavirus

Author affiliations: Animal Health Research Institute, New Taipei City, Taiwan (S.-C. Hu, M.-S. Lee, Y.-C. Tu, J.-C. Chang, C.-H. Wu, L.-J. Ting, K.-R. Tsai, W.-J. Tu, W.-C. Hsu); National Taiwan University, Taipei City, Taiwan (C.-L. Hsu); Bat Conservation Society of Taipei, Taipei City (C.-L. Hsu); Animal Health Research Institute, Miaoli County, Taiwan (S.-H. Lee); National Pingtung University of Science and Technology, Neipu Township, Pingtung County, Taiwan (M.-C. Cheng)

DOI: https://doi.org/10.3201/eid2404.171696

Table 1. Lyssavirus screen primers and the 12 amplifying primer sets used to identify Taiwan bat lyssavirus, a putative new lyssavirus found in 2 Japanese pipistrelles (*Pipistrellus abramus*) in Taiwan in 2016 and 2017

Primer name	Sequence, 5′ → 3′	Position*
Lyssavirus screen		
JW12 (*7*)	ATGTAACACCYCTACAATG	
N165–146 (*7*)	GCAGGGTAYTTRTACTCATA	
N113F (*8*)	GTAGGATGCTATATGGG	
N304R (*9*)	TTGACGAAGATCTTGCTCAT	
Lyssavirus full genome		
TWBLV 1F	ACGCTTAACGACAAAAYC	1–18*
TWBLV 1R	TCTTGCATTTCTTTCTCATC	1154–1173
TWBLV 2F	TTCGTAGGATGTTACATGGG	1010–1029
TWBLV 2R	TAAAAATATCCCAGAAGATC	2174–2193
TWBLV 3F	AGARATAGCWCATCAGATWGC	2118–2138
TWBLV 3R	CTATTGTGTGGCACCATWAC	3205–3224
TWBLV 4F	GATGAGGATAAGAACACATC	3072–3091
TWBLV 4R	TCCTGAAGTGACTGAGTTTTC	4274–4294
TWBLV 5F	CTGATGGAYGGRTCATGGGT	4081–4100
TWBLV 5R	GAGACAGGAGCCGGAGTCTT	5280–5299
TWBLV 6F	AACAGGTAGCTCCCGAGTTTGTTC	4881–4904
TWBLV 6R	CTGAGTGAGACCCATGTATCCAAA	5767–5790
TWBLV 7F	ACTGAGGTTTATGATGACCC	5478–5497
TWBLV 7R	CCCCAGTGTCTATARCAWCC	6561–6580
TWBLV 8F	CATTCTTTGGGGGATTTCCC	6426–6445
TWBLV 8R	GTTTGTGATTCTCTRTCWATC	7595–7615
TWBLV 9F	CATGCTGGAACGGTCAGGAYG	7522–7542
TWBLV 9R	CTGAGTTAAAGAAAGATTCTT	8662–8682
TWBLV 10F	CTCAGTGAGTTRTTYAGCTC	8547–8566
TWBLV 10R	CAGATAGAAGAGCCTATT	9746–9763
TWBLV 11F	CATGATTCAGGGTAYAAYGA	9648–9667
TWBLV 11R	GTCTGTAACTTCTGCATCAC	10862–10871
TWBLV 12F	ATCTGGGAAAAGCCATCAGA	10755–10774
TWBLV 12R	ACGCTTAACAAAAAAAACAA	11961–11980

*Compared with reference genomic sequence, Irkut lyssavirus (GenBank accession no. NC020809). TWBLV, Taiwan bat lyssavirus.

morphologically by electron microscopy (*11*) and molecularly by nucleotide sequencing. In addition, after we isolated the viruses from the brain tissues, we performed reverse transcription PCR and virus isolation for visceral organs and salivary glands; both tests were positive for the salivary glands of both bats.

We determined nucleotide sequences of the genome of the isolated viruses, designated Taiwan bat lyssavirus (TWBLV). The first TWBLV isolate was designated TWBLV/TN/2016 (GenBank accession no. MF472710), and the second TWBLV/YL/2017 (GenBank accession no. MF472709). We amplified the nucleoprotein (N),

Table 2. Nucleotide identities for the N, P, M, G, L genes and the concatenated coding genes between Taiwan bat lyssavirus, a putative new lyssavirus found in 2 Japanese pipistrelles (*Pipistrellus abramus*) in Taiwan in 2016 and 2017, compared with other lyssaviruses*

	Identity, %					Concatenated coding genes
Lyssavirus species (GenBank accession no.)	N	P	M	G	L	(N+P+M+G+L)
Rabies lyssavirus (NC001542)	75.2	62.8–63.1	74.6–74.8	61.6–62.3	71.7	70.0–70.1
Lagos bat lyssavirus (NC020807)	73.5–73.7	53.8–54.1	73.6	55.0–55.6	71.3–71.4	67.8–67.9
Mokola lyssavirus (NC006429)	72.7–73.3	52.2–52.4	72.0–72.6	56.7–56.9	70.6–70.7	67.3 –67.4
Duvenhage lyssavirus (NC020810)	77.7–77.9	67.5–67.6	78.4–79.2	63.9–64.0	74.8–74.9	73.2
European bat 1 lyssavirus (NC009527)	78.8–79.4	69.6–69.7	80.9–81.1	66.1	76.7–76.8	75.1
European bat 2 lyssavirus (NC009528)	75.3–75.6	66.0–66.3	79.2–79.5	64.5–64.6	73.7	72.2–72.3
Australian bat lyssavirus (NC003243)	76.3–76.5	62.2	72.1	61.7–62.0	72.3–72.5	70.4
Aravan lyssavirus (NC020808)	76.5 –76.7	65.6–66	80.3–80.6	64.4–64.5	74.6–74.9	72.9–73.1
Khujand lyssavirus (NC025385)	74.6–74.7	67.0–67.1	78.6–78.7	64.5–64.9	74.2–74.3	72.4–72.5
Irkut lyssavirus (NC020809)	79.0–79.1	68.3–68.6	80.3	65.3–65.8	75.3–75.4	74
Irkut lyssavirus-THChina12 (JX442979)	80.5–80.6	68.7–69.0	79.8–80.0	64–64.6	75.1–75.4	74
West Caucasian bat lyssavirus (NC025377)	72.3–72.7	51.2–51.5	71.4	52.0	68.3–68.4	65–65.2
Shimoni bat lyssavirus (NC025365)	74.1–74.5	54.9–55.1	74.2–74.6	56.2–56.4	71.1–71.2	68.2
Ikoma lyssavirus (NC018629)	69.7–69.8	51.9–52.3	69.3–69.6	50.9–51.2	65.4–65.6	62.9
Bokeloh bat lyssavirus (NC025251)	75.0–75.2	66.0–66.3	78.2	64.4–64.5	74.1–74.2	72.3–72.4
Lleida bat lyssavirus (NC031955)	69.2–69.5	50.8–50.9	70.4–70.9	51.2	66.2	63.2–63.3
Gannoruwa bat lyssavirus (NC031988)	75.5–75.7	62.8–63.1	75.4–75.7	63.7–64.3	73.5–73.6	71.5–71.6

*G, glycoprotein; L, RNA-dependent RNA polymerase; M, matrix protein; N, nucleoprotein; P, phosphoprotein.

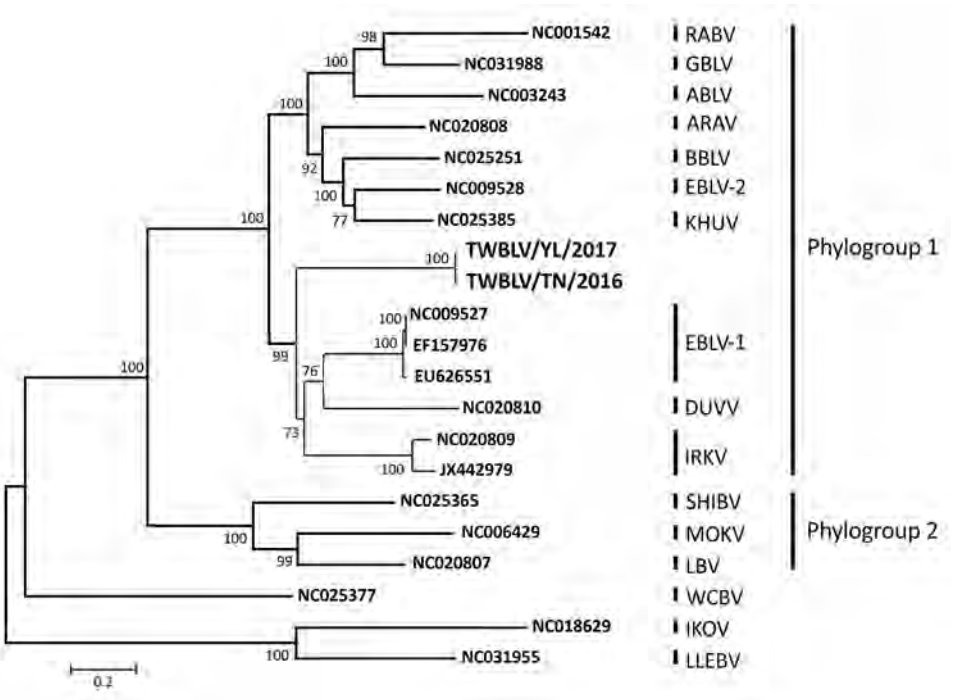

Figure. Phylogenetic relationship of TWBLV (boldface), a putative new lyssavirus found in 2 Japanese pipistrelles (*Pipistrellus abramus*) in Taiwan in 2016 and 2017, compared with other lyssaviruses. Using the concatenated coding genes, we constructed the phylogenetic tree by using the maximum-likelihood method with the general time reversible plus invariant sites plus gamma 4 model. Numbers at the nodes indicate bootstrap confidence values (1,000 replicates) for the groups being composed of virus genes at the right of the nodes. GenBank accession numbers are provided for reference viruses. Scale bar indicates nucleotide substitutions per site. ABLV, Australia bat lyssavirus; ARAV, Aravan lyssavirus; BBLV, Bokeloh bat lyssavirus; DUVV, Duvenhage lyssavirus; EBLV-1, European bat lyssavirus type 1; EBLV-2, European bat lyssavirus type 2; IKOV, Ikoma lyssavirus; IRKV, Irkut lyssavirus; KHUV, Khujand lyssavirus; LBV, Lagos bat lyssavirus; LLEBV, Lleida bat lyssavirus; MOKV, Mokola lyssavirus; SHIBV, Shimoni bat lyssavirus; RABV, rabies lyssavirus; TWBLV, Taiwan bat lyssavirus; WCBV, West Caucasian bat lyssavirus.

phosphoprotein (P), matrix protein (M), glycoprotein (G), and RNA-dependent RNA polymerase (L) genes of the 2 TWBLV isolates by 12 primer sets designed by the AHRI (Table 1). The genome length of the 2 TWBLV isolates was 11,988 bases, with G+C contents of 43.66% for TWBLV/TN/2016 and 43.83% for TWBLV/YL/2017. The genomic organization was similar to those of other lyssaviruses: 3′ untranslated region (UTR), 70 nt; N, 1356 nt; N-P UTR, 99 nt; P, 897 nt; P-M UTR, 82 nt; M, 609 nt; M-G UTR, 212 nt; G,1629 nt; G-L UTR, 518 nt; L, 6384 nt; and 5′ UTR, 132 nt. The 2 TWBLV isolates showed 98.7% nucleotide identity in the N gene and 98.6% nucleotide identity in the concatenated coding genes (N+P+M+G+L). Nucleotide identities of different genes between the TWBLVs and the other 16 lyssaviruses are listed in Table 2. For the N gene, the TWBLVs had the highest identities with IRKV (79.0%–80.6%), followed by EBLV-1 (78.8%–79.4%). The TWBLVs shared nucleotide identities with the concatenated coding genes of EBLV-1 (75.1%), followed by IRKV (74.0%). The phylogenetic analysis demonstrated that lyssaviruses were separated into 2 phylogroups; the TWBLVs were grouped into phylogroup 1 and clustered with the EBLV-1, IRKV, and DUVV (Figure).

Conclusions

We report a lyssavirus, TWBLV, that is closely related to EBLV-1, IRKV, and DUVV. The full-length nucleotide sequence of the concatenated coding genes of TWBLV showed 62.9%–75.1% nucleotide identities to the other 16 lyssaviruses (Table 2), and TWBLV was the most closely related to EBLV-1. The demarcation criteria of lyssavirus species, established by the International Committee on the Taxonomy of Viruses, include genetic distance, topology, antigenic patterns, and additional characteristics (*12*). Based on genetic distance, no similarity to the other lyssavirus species of more than 75.1% nucleotide identities of the concatenated coding genes of TWBLVs suggested that the isolated TWBLV was a new lyssavirus species.

The presence of TWBLV in the bats' salivary glands suggested that TWBLV may be shed through saliva. The study showed that the bat in East Asia could be infected with lyssavirus; however, because of the limited surveillance, the epidemiology of lyssavirus in Japanese pipistrelle and other bat species is still unclear. This uncertainty is likely to raise a public health concern in countries in Asia.

In conclusion, a lyssavirus, TWBLV, was identified in Japanese pipistrelle, and the infected bats may shed the virus through saliva. Japanese pipistrelle is a common insectivorous bat of low-altitude urban areas in East Asia (*13,14*). Persons in countries in Asia should be aware to seek proper prophylaxis immediately if bitten by a bat. Studies on the epidemiology and pathogenicity of TWBLV are necessary to further characterize the virus.

Acknowledgments

We thank Fan Lee for his help in improving the manuscript. We also thank Tien-Cheng Li, Yi-Tang Lin, Chia-Jung Tsai, and Ya-Lan Li for their assistance during this study.

This study was supported by grant no. 106AS-9.9.1-BQ-B2(1) from the Bureau of Animal and Plant Health Inspection and Quarantine, Council of Agriculture, Executive Yuan, Taiwan.

About the Author

Dr. Hu is an assistant research fellow at Epidemiology Division, Animal Health Research Institute, New Taipei City, Taiwan. Her main research interests are in the molecular epidemiology of lyssaviruses.

References

1. Kuzmin IV. Basic facts about lyssavirus. In: Rupprecht CE, Nagarajan T, editor. Current laboratory techniques in rabies diagnosis, research, and prevention, volume 1. Laguna Hills (CA): Elsevier; 2014. p. 3–17.
2. Aréchiga Ceballos N, Vázquez Morón S, Berciano JM, Nicolás O, Aznar López C, Juste J, et al. Novel lyssavirus in bat, Spain. Emerg Infect Dis. 2013;19:793–5. http://dx.doi.org/10.3201/eid1905.121071
3. Gunawardena PS, Marston DA, Ellis RJ, Wise EL, Karawita AC, Breed AC, et al. Lyssavirus in Indian flying foxes, Sri Lanka. Emerg Infect Dis. 2016;22:1456–9. http://dx.doi.org/10.3201/eid2208.151986
4. Banyard AC, Evans JS, Luo TR, Fooks AR. Lyssaviruses and bats: emergence and zoonotic threat. Viruses. 2014;6:2974–90. http://dx.doi.org/10.3390/v6082974
5. Kuzmin IV, Orciari LA, Arai YT, Smith JS, Hanlon CA, Kameoka Y, et al. Bat lyssaviruses (Aravan and Khujand) from Central Asia: phylogenetic relationships according to N, P and G gene sequences. Virus Res. 2003;97:65–79. http://dx.doi.org/10.1016/S0168-1702(03)00217-X
6. Liu Y, Zhang S, Zhao J, Zhang F, Hu R. Isolation of Irkut virus from a *Murina leucogaster* bat in China. PLoS Negl Trop Dis. 2013;7:e2097. http://dx.doi.org/10.1371/journal.pntd.0002097
7. Hayman DT, Banyard AC, Wakeley PR, Harkess G, Marston D, Wood JL, et al. A universal real-time assay for the detection of lyssaviruses. J Virol Methods. 2011;177:87–93. 10.1016/j.jviromet.2011.07.002 http://dx.doi.org/10.1016/j.jviromet.2011.07.002
8. Franka R, Constantine DG, Kuzmin I, Velasco-Villa A, Reeder SA, Streicker D, et al. A new phylogenetic lineage of rabies virus associated with western pipistrelle bats (*Pipistrellus hesperus*). J Gen Virol. 2006;87:2309–21. http://dx.doi.org/10.1099/vir.0.81822-0
9. Trimarchi CV, Smith JS. Diagnostic evaluation. In: Press A, Jackson AC, Wunner WH, editors. Rabies. 1st ed. San Diego (CA): Academic Press; 2002. p. 308–44.
10. Mayer F, von Helversen O. Cryptic diversity in European bats. Proc Biol Sci. 2001;268:1825–32. http://dx.doi.org/10.1098/rspb.2001.1744
11. Bozzola JJ, Russell LD. Electron microscopy: principles and techniques for biologists. Burlington (MA): Jones & Bartlett Learning; 1992. p. 130–134.
12. World Health Organization. WHO Expert Consultation on Rabies. Second report. World Health Organ Tech Rep Ser. 2013;982:1–139.
13. Francis CM. Chiroptera In: Mayer K, editor. A field guide to the mammals of South-East Asia, 1st ed. London: New Holland; 2008. p. 238.
14. Srinivasulu B, Srinivasulu C, Kaur H, Srinivasulu A. A new distribution record of the Japanese pipistrelle (*Pipistrellus abramus* (Temminck, 1840); Mammalia, Chiroptera) in India. Acta Zoologica Lituanica. 2011;21:268–72. http://dx.doi.org/10.2478/v10043-011-0029-8

Address for correspondence: Wei-Cheng Hsu, Animal Health Research Institute, Council of Agriculture, Executive Yuan, No. 376, Chung-Cheng Rd., Tamsui District, New Taipei City 25158, Taiwan; email: wchsu@mail.nvri.gov.tw

Direct Whole-Genome Sequencing of Cutaneous Strains of *Haemophilus ducreyi*

Michael Marks,[1] Maria Fookes,[1] Josef Wagner, Rosanna Ghinai, Oliver Sokana, Yaw-Adu Sarkodie, Anthony W. Solomon, David C.W. Mabey, Nicholas R. Thomson

Haemophilus ducreyi, which causes chancroid, has emerged as a cause of pediatric skin disease. Isolation of *H. ducreyi* in low-income settings is challenging, limiting phylogenetic investigation. Next-generation sequencing demonstrates that cutaneous strains arise from class I and II *H. ducreyi* clades and that class II may represent a distinct subspecies.

Since 2000, the global prevalence of chancroid, caused by *Haemophilus ducreyi*, has declined (*1*). *H. ducreyi* is an emerging cause of cutaneous ulcers in tropical countries (*1*–*4*). Cutaneous lesions of *H. ducreyi* are difficult to distinguish from other common causes of ulcerative skin disease, such as yaws (*3*,*4*), which presents problems in diagnosing yaws and has resulted in the World Health Organization recommending molecular testing of yaws-like lesions (*5*).

Culturing *H. ducreyi* is challenging. PCR is usually used for diagnosis (*6*). Culture requirements limit sequencing and phylogenetic analyses. Traditional phylogenies divide genital strains of *H. ducreyi* into class I and II clades. Most studies suggest that cutaneous strains of *H. ducreyi* have diversified from within the class I clade (*7*,*8*), and a recent study reported cutaneous strains that appear to arise from class II strains (*9*). These studies have been limited by the number and geographic spread of samples included.

Next-generation sequencing enables whole-genome sequencing from clinical samples without prior culture, bypassing the culture requirements of *H. ducreyi* and enabling more detailed phylogenetic analysis. We performed next-generation sequencing on samples collected in previous surveys conducted in the Solomon Islands (in 2013) and Ghana (in 2014) (*2*,*4*). In both surveys, skin swab specimens had been collected from persons with chronic ulcerative lesions believed, at the time, to be clinically consistent with yaws. DNA was prepared for the current study from samples with residual material from those original surveys. The London School of Hygiene & Tropical Medicine, Solomon Islands National Health Research, and Kwame Nkrumah University of Science and Technology ethics committees approved these studies.

The Study

We tested 72 samples from 63 persons (Figure 1). Twenty-five persons (27 samples) had been recruited in Ghana and 38 persons (45 samples) in the Solomon Islands. Median age of participants in the original studies was 9 years (interquartile range 7–11 years); 36 (57.1%) were male. In the original studies, 24 samples had tested positive for *H. ducreyi* using a 16S rRNA-targeted PCR (*2*,*4*): 15 from the Solomon Islands and 9 from Ghana.

In Ghana, samples were collected directly onto dry Dacron swabs. In the Solomon Islands, swab exudate was placed into transport medium (AssayAssure; Sierra Molecular, Incline Village, NV, USA) or onto an FTA Elute Card (Thermo-Fisher Scientific, Waltham, MA, USA). Samples were frozen at –20°C and shipped to the Centers for Disease Control and Prevention (Atlanta, GA, USA) on dry ice for the original laboratory analyses, which included real-time PCR for *Trepomema pallidum* subspecies *pertenue* (*7*) and a real-time 16S rRNA-targeted PCR for *H. ducreyi* (*2*,*4*). After testing, samples were shipped on dry ice to the London School of Hygiene & Tropical Medicine (London, UK) and frozen at –20°C before analysis.

We extracted DNA from residual sample material using QIAamp Mini kits (QIAGEN, Hilden, Germany) (online Technical Appendix 1, https://wwwnc.cdc.gov/EID/article/24/4/17-1726-Techapp1.pdf). We screened DNA using a quantitative PCR (qPCR) targeting the *hhdA* gene and 16S rRNA gene sequencing for *H. ducreyi* (*6*,*10*). From samples that tested positive, we selected those with genomic DNA concentration ≥10 copies/μL for direct (non–culture-based) sequencing.

Genomic DNA was fragmented to an average size of 150 bp and subjected to DNA library creation using

Author affiliations: London School of Hygiene & Tropical Medicine, London, UK (M. Marks, R. Ghinai, A.W. Solomon, D.C.W. Mabey, N.R. Thomson); Hospital for Tropical Diseases, London (M. Marks, A.W. Solomon, D.C.W. Mabey); Wellcome Trust Sanger Centre, Cambridge, UK (M. Fookes, J. Wagner, N.R. Thomson); Solomon Islands Ministry of Health and Medical Services, Honiara, Solomon Islands (O. Sokana); Kwame Nkrumah University of Science and Technology, Kumasi, Ghana (Y.-A. Sarkodie)

DOI: https://doi.org/10.3201/eid2404.171726

[1]These authors contributed equally to this article.

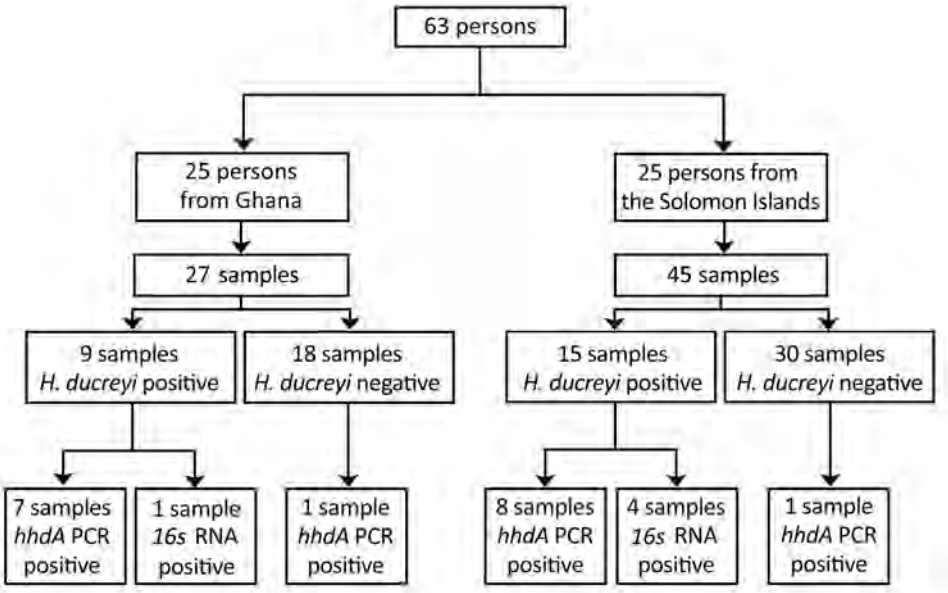

Figure. Flowchart of whole-genome sequencing of *Haemophilus ducreyi*. Samples were originally collected in 2 studies conducted in Ghana (2014) and the Solomon Islands (2013) (*2*,*4*). Results of the *H. ducreyi* PCR conducted in the original studies and of the 2 *H. ducreyi* PCRs performed in this study are shown.

established Illumina paired-end protocols (*11*). We amplified adaptor-ligated libraries and indexed them by PCR. We used a portion of each library to create an equimolar pool and hybridized each pool to custom-made SureSelect RNA baits (Agilent Technologies, Santa Clara, CA, USA; baits based on published sequences of *H. ducreyi* [*12*]) (online Technical Appendix 1). Targets were captured and amplified in accordance with manufacturer's recommendations. We subjected enriched libraries to standard 75-bp end sequencing (HiSeq 2000; Illumina, San Diego, CA, USA). Samples' public accession numbers are listed in online Technical Appendix 2 Table 1 (https://wwwnc.cdc.gov/EID/article/24/4/17-1726-Techapp2.xlsx). We used whole-genome sequence data to estimate phylogenies for *H. ducreyi* (online Technical Appendix 1), including publicly available *H. ducreyi* genomes alongside those obtained in this study.

We identified *H. ducreyi* in 17 samples by *hhdA*-targeted qPCR and in 5 additional samples using an assay targeting the rRNA gene. From these 22 positive samples, we obtained 21 (95.5%) complete genomes from 13 persons from the Solomon Islands and 8 from Ghana. Mean coverage of *H. ducreyi* genomes was 91% (online Technical Appendix 2 Table 1). We found no evidence of sequence heterozygosity that would indicate any participant was infected with multiple distinct strains of *H. ducreyi*.

H. ducreyi sequences fell into both previously defined *H. ducreyi* clades: class I and class II (Figure 2). To estimate genetic distance between strains, we determined the number of single-nucleotide polymorphisms (SNPs) in pairwise whole-genome comparisons. The average distance between class I and class II sequences was 21,238 SNPs, compared with a maximum pairwise distance of 641 SNPs between class I sequences. We detected 4 major recombination blocks within class I genomes. These regions included the *dsrA, tad,* and *flp* loci, associated with serum resistance, tight adhesion, and production of fimbriae, respectively, functions important in micro-colony formation and potentially associated with virulence (online Technical Appendix 1 Figure 1; online Technical Appendix 2 Table 2) (*13*). The other regions of likely recombination were related to integrated prophage elements, implying *H. ducreyi* has an actively exchanging bacteriophage repertoire in its genome (online Technical Appendix 1 Figure 1). These prophage elements included the region coding for the ctdABC genes, which have been associated with virulence (*14*). The class I prophage elements were absent from class II genomes but intermittently present in class I genomes(online Technical Appendix 1 Figure 2). The presence or absence of the ctdABC coding region was not associated with cutaneous or genital ulcer disease. Another recombination region spanned the *hhdA* specific qPCR primer binding site. Samples with high sequence variation in this region tested negative for *H. ducreyi* by qPCR but gave high numbers of reads by 16S rRNA gene sequencing.

Conclusions

We obtained whole-genome sequences of *H. ducreyi* without prior culture. Most earlier studies have suggested that cutaneous strains emerged by diversification from within the class I clade (*7*,*8*), although 1 study found, in keeping with our findings, cutaneous strains emerging from class II (*9*). We found genital and cutaneous strains are represented in all lineages of the expanded phylogenetic tree (*7*). We found considerable genetic variation between class I and

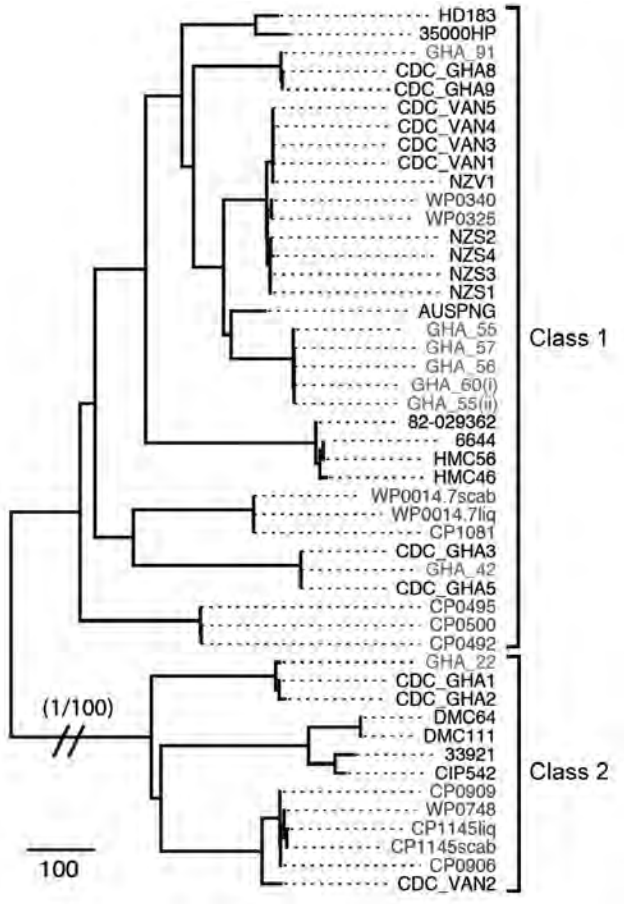

Figure 2. Phylogenetic tree of *Haemophilus ducreyi* genome sequences inferred from mapping using the *H. ducreyi* 35000HP strain as reference and after removing high-density single-nucleotide polymorphisms regions with Gubbins (3). Included are published genomes (black text), Ghanaian strains (gray text, GHA designations), and Solomon Islands strains (gray text, CP/WP designations). Sequences from cutaneous ulcers in Ghana and the Solomon Islands were found within both previously described clades of *H. ducreyi* class I and class II. Scale bar indicates nucleotide substitutions per site. An expanded version of this figure providing complete phylogeny details, including countries of origin, years, ulcer types, and genome region designations, is provided in online Technical Appendix 1 Figure 1 (https://wwwnc.cdc.gov/EID/article/24/4/17-1726-Techapp1.pdf).

class II *H. ducreyi* sequences. Together with existing 16S rRNA data and multilocus sequence typing data (*12*) these findings suggest class II strains might represent a discrete subspecies of *H. ducreyi*.

We identified 2 samples that had been negative in the original studies but were found to contain *H. ducreyi* DNA in the current study. Repeated freeze–thaw cycles and limited residual DNA volumes might have contributed to our lack of detection of *H. ducreyi* DNA in 4 samples that tested positive in the original studies (Figure 1). Five samples that returned a weak signal by *hhdA* qPCR contained class II clade *H. ducreyi* genomes. The failure of qPCR to detect *H. ducreyi* in these samples was most likely explained by variation in the sequence of the *hhdA* pPCR primer binding sites (*13*) between class I and II genomes (online Technical Appendix 1 Figure 1), demonstrating our limited understanding of the diversity of these pathogens.

Culture for *H. ducreyi* is not practical in the low-income settings where cutaneous strains of this organism are endemic. Next-generation sequencing circumvents this problem by enabling whole-genome sequencing direct from clinical samples. This approach considerably strengthens our ability to sequence *H. ducreyi* and broaden knowledge of this emerging pathogen.

M.M. is supported by the Wellcome Trust (102807). N.R.T. and M.F. were supported by the Wellcome Trust (098051). Funding for the fieldwork in Ghana was additionally supported by a grant from the Royal Society of Tropical Medicine & Hygiene to M.M.

About the Author

Dr. Marks is an assistant professor at the London School of Hygiene & Tropical Medicine. His primary research interests are the control of neglected tropical diseases, particularly yaws and scabies.

References

1. González-Beiras C, Marks M, Chen CY, Roberts S, Mitjà O. Epidemiology of *Haemophilus ducreyi* infections. Emerg Infect Dis. 2016;22:1–8. http://dx.doi.org/10.3201/eid2201.150425
2. Ghinai R, El-Duah P, Chi K-H, Pillay A, Solomon AW, Bailey RL, et al. A cross-sectional study of 'yaws' in districts of Ghana which have previously undertaken azithromycin mass drug administration for trachoma control. PLoS Negl Trop Dis. 2015;9:e0003496. http://dx.doi.org/10.1371/journal.pntd.0003496
3. Mitjà O, Lukehart SA, Pokowas G, Moses P, Kapa A, Godornes C, et al. *Haemophilus ducreyi* as a cause of skin ulcers in children from a yaws-endemic area of Papua New Guinea: a prospective cohort study. Lancet Glob Health. 2014;2:e235–41. http://dx.doi.org/10.1016/S2214-109X(14)70019-1
4. Marks M, Chi K-H, Vahi V, Pillay A, Sokana O, Pavluck A, et al. *Haemophilus ducreyi* associated with skin ulcers among children, Solomon Islands. Emerg Infect Dis. 2014;20:1705–7. http://dx.doi.org/10.3201/eid2010.140573
5. Marks M, Mitjà O, Vestergaard LS, Pillay A, Knauf S, Chen C-Y, et al. Challenges and key research questions for yaws eradication. Lancet Infect Dis. 2015;15:1220–5. http://dx.doi.org/10.1016/S1473-3099(15)00136-X
6. Chen C-Y, Ballard RC. The molecular diagnosis of sexually transmitted genital ulcer disease. In: MacKenzie CR, Henrich, editors. Diagnosis of sexually transmitted diseases—methods and protocols. New York: Springer-Verlag; 2012. p. 103–12.
7. Gangaiah D, Webb KM, Humphreys TL, Fortney KR, Toh E, Tai A, et al. *Haemophilus ducreyi* cutaneous ulcer strains are nearly identical to Class I genital ylcer strains. PLoS Negl Trop Dis. 2015;9:e0003918. http://dx.doi.org/10.1371/journal.pntd.0003918
8. Gangaiah D, Marinov GK, Roberts SA, Robson J, Spinola SM. Draft whole-genome sequence of *Haemophilus ducreyi* strain AUSPNG1, isolated from a cutaneous ulcer of a child from

Papua New Guinea. Genome Announc. 2016;4:e01661–15. http://dx.doi.org/10.1128/genomeA.01661-15
9. Gangaiah D, Spinola SM. *Haemophilus ducreyi* cutaneous ulcer strains diverged from both Class I and Class II genital ulcer strains: implications for epidemiological studies. PLoS Negl Trop Dis. 2016;10:e0005259. http://dx.doi.org/10.1371/journal.pntd.0005259
10. Marks M, Vahi V, Sokana O, Puiahi E, Pavluck A, Zhang Z, et al. Mapping the epidemiology of yaws in the Solomon Islands: a cluster randomized survey. Am J Trop Med Hyg. 2015;92:129–33. http://dx.doi.org/10.4269/ajtmh.14-0438
11. Orle KA, Gates CA, Martin DH, Body BA, Weiss JB. Simultaneous PCR detection of *Haemophilus ducreyi, Treponema pallidum*, and herpes simplex virus types 1 and 2 from genital ulcers. J Clin Microbiol. 1996;34:49–54.
12. Quail MA, Kozarewa I, Smith F, Scally A, Stephens PJ, Durbin R, et al. A large genome center's improvements to the Illumina sequencing system. Nat Methods. 2008;5:1005–10. http://dx.doi.org/10.1038/nmeth.1270
13. Ricotta EE, Wang N, Cutler R, Lawrence JG, Humphreys TL. Rapid divergence of two classes of *Haemophilus ducreyi*. J Bacteriol. 2011;193:2941–7. http://dx.doi.org/10.1128/JB.01400-10
14. Janowicz DM, Cooney SA, Walsh J, Baker B, Katz BP, Fortney KR, et al. Expression of the Flp proteins by *Haemophilus ducreyi* is necessary for virulence in human volunteers. BMC Microbiol. 2011;11:208. http://dx.doi.org/10.1186/1471-2180-11-208

Address for correspondence: Michael Marks, Clinical Research Department, London School of Hygie ne & Tropical Medicine, Keppel Street, London WC1E 7HT, UK; email: michael.marks@lshtm.ac.uk; Nicholas Thomson, Wellcome Trust Sanger Centre, Hinxton CB10 1SA, UK; email: nrt@sanger.ac.uk

Region-Specific, Life-Threatening Diseases among International Travelers from Israel, 2004–2015

Chen Avni, Shmuel Stienlauf, Eyal Meltzer, Yechezkel Sidi, Eli Schwartz, Eyal Leshem

We characterized posttravel hospitalizations of citizens returning to Israel by summarizing the returning traveler hospitalization dataset of the national referral Center for Travel Medicine and Tropical Diseases at Sheba Medical Center in Israel. Of 722 hospitalizations, 181 (25%) infections were life-threatening; most would have been preventable by chemoprophylaxis and pretravel vaccination.

International travel, particularly to tropical regions and low-income countries, may be associated with the risk for acute illness and hospitalization (*1*). The Center for Travel Medicine and Tropical Diseases at Sheba Medical Center (SMC; Tel Hashomer, Israel) is the national referral center for travel-associated illness in Israel. We characterized posttravel hospitalizations of citizens returning to Israel by summarizing the SMC returning traveler hospitalization dataset.

The Study

We investigated all international travel–associated hospitalizations of citizens of Israel at SMC during 2004–2015. We excluded case-patients for whom the time interval between return from travel and symptom onset exceeded the known incubation period for the cause of hospitalization. When identified illness after travel leading to hospitalization was nonendemic to Israel and caused symptoms after a long incubation (e.g., leishmaniasis, schistosomiasis), patients were included regardless of the time interval since return. We defined nonspecified febrile illness as a febrile illness with an undetermined cause (*2*). We excluded hospitalized persons who had unspecified febrile illness when the interval between return from travel and disease onset exceeded 2 weeks, because of the lower certainty of association between travel and illness. We defined acute and potentially life-threatening tropical diseases as infectious diseases largely confined to tropical and subtropical areas of the world that had an incubation period of >4 weeks and an estimated risk for death >5% within 4 weeks after symptom onset if left untreated (*3*).

We determined the country of disease acquisition by a history of travel to a single country or exposure to a single country during the incubation period for the cause of hospitalization. To put the number of hospitalizations for illness acquired in each destination country in context of the estimated number of Israelis traveling to that country, we extracted the number of Israeli citizen entries by country from the United Nations World Tourism Organization dataset (*4*). We compared continuous variables by using the Student *t*-test and compared categorical variables by using the χ^2 test. Statistical significance was set at $p<0.05$. The SMC Institutional Review Board approved this study.

During 2004–2015, a total of 722 travelers returning to Israel were hospitalized (Table 1; online Technical Appendix Table 1, https://wwwnc.cdc.gov/EID/article/24/4/17-1542-Techapp1.pdf). The median patient age was 33 years (interquartile range 26–50 years); 530 (73%) were male. By continent, 330 (46%) patients had traveled to Asia; 267 (37%) to Africa; and 73 (10%) to South America, Central America, and the Caribbean. The travel destination countries from which the highest number of travelers were hospitalized were India (116 [16%]), Thailand (106 [15%]), and Ethiopia (48 [7%]). In relative terms, several countries, mostly in Africa, had a high number of hospitalizations respective to the estimated number of entries by Israeli citizens (Figure; online Technical Appendix Table 2).

Overall, the most common causes of hospitalization were malaria (145 [20%]), dengue (74 [10%]), and enteric fever (59 [8%]). Among 145 hospitalized malaria patients, 86 (59%) tested positive for *Plasmodium falciparum*. For Asia, the most common causes of admission were dengue fever, enteric fever, and unspecified febrile illnesses; for Africa, the most common were malaria, unspecified febrile illnesses, and acute schistosomiasis; and for South America, Central America, and the Caribbean, the most common were dengue fever and leptospirosis.

Patients hospitalized for *P. falciparum* malaria (n = 86) were older than those positive for *P. vivax* (n = 36) (43 ± 14 y vs. 34 ± 12 y; $p<0.01$) and were more likely to be business travelers (39 [45%]

Author affiliations: The Center for Travel Medicine and Tropical Diseases, The Chaim Sheba Medical Center, Tel Hashomer, Israel; Sackler School of Medicine, Tel Aviv University, Tel Aviv, Israel

DOI: https://doi.org/10.3201/eid2404.171542

Table 1. Characteristics of travel-associated hospitalizations of citizens of Israel at Sheba Medical Center, Israel, 2004–2015*

Category	Africa, n = 267	Asia, n = 330	South America, n = 43	Central America/ Caribbean, n = 30	North America/ Europe, n = 26	Other,† n = 26	Total, n = 722
Patient characteristics							
Sex							
M	226 (85)	219 (66)	28 (65)	20 (67)	21 (81)	16 (62)	530 (73)
F	41 (15)	111 (34)	15 (35)	10 (33)	5 (19)	10 (38)	192 (27)
Age, median (IQR)	41 (29–53)	29 (24–43)	24 (23–43)	29 (27–46)	55 (39–64)	27 (23–41)	33 (26–50)
Age ≥60 y	37 (14)	27 (8)	4 (9)	3 (10)	8 (31)	4 (15)	83 (11)
Category of travelers							
Tourism	154 (58)	313 (95)	41 (95)	29 (97)	23 (88)	26 (100)	586 (81)
Business travelers	93 (35)	17 (5)	2 (5)	1 (3)	3 (12)	0	116 (16)
Visiting friends or relatives	19 (7)	1 (<1)	0	0	0	0	20 (3)
Type of illness							
Potentially preventable	85 (32)	25 (8)	0	1 (3)	0	1 (4)	112 (16)
Febrile conditions							
Malaria							
Plasmodium falciparum‡	82 (30)	4 (1)	0	0	0	0	86 (12)
P. vivax	23 (9)	7 (2)	3 (7)	0	0	3 (12)	36 (5)
P. ovale	8 (3)	0	0	0	0	0	8 (1)
P. malariae	7 (3)	0	0	0	0	0	7 (<1)
Unidentified malaria	6 (2)	2 (<1)	0	0	0	0	8 (1)
Dengue fever	4 (1)	59 (18)	2 (5)	8 (27)	0	1 (4)	74 (10)
Enteric fever							
Salmonella enterica serovar Typhi	2 (<1)	19 (6)	0	1 (3)	0	1 (4)	23 (3)
S. enterica ser. Paratyphi	0	36 (11)	0	0	0	0	36 (5)
Leptospirosis	1 (<1)	18 (5)	0	7 (23)	1 (4)	2 (8)	29 (4)
Pneumonia	10 (4)	11 (3)	0	1 (3)	5 (19)	1 (4)	28 (4)
Febrile diarrheal diseases	10 (4)	5 (2)	1 (2)	0	2 (8)	1 (4)	19 (3)
Acute schistosomiasis	16 (6)	3 (<1)	0	0	0	0	19 (3)
Influenza	0	7 (2)	0	0	0	1 (4)	8 (1)
Epstein–Barr virus	1 (<1)	6 (2)	1 (2)	0	0	0	8 (1)
Cytomegalovirus	4 (1)	2 (<1)	2 (5)	0	0	0	8 (1)
Amebic liver abscess	0	5 (2)	0	0	0	2 (8)	7 (<1)
Rickettsial diseases	3 (1)	3 (<1)	0	0	0	0	6 (<1)
Upper respiratory tract infection	4 (1)	1 (<1)	0	0	0	0	5 (<1)
Unspecified febrile illness	34 (13)	55 (17)	7 (16)	3 (10)	6 (23)	4 (15)	109 (15)
Other febrile conditions	15 (6)	29 (9)	8 (19)	2 (7)	3 (12)	2 (8)	59 (8)
Afebrile conditions							
Afebrile diarrheal diseases	5 (2)	7 (2)	2 (5)	0	4 (15)	0	18 (2)
Afebrile eosinophilia	4 (1)	6 (2)	2 (5)	1 (3)	1 (4)	2 (8)	16 (2)
Skin disease	7 (3)	4 (1)	2 (5)	1 (3)	0	0	14 (2)
Afebrile nondiarrheal GI illness	3 (1)	8 (2)	2 (5)	0	0	0	13 (2)
Viral hepatitis	2 (<1)	8 (2)	0	2 (7)	0	0	12 (2)
Leishmaniasis	2 (<1)	0	9 (21)	0	0	0	11 (2)
Giardiasis	0	4 (1)	0	1 (3)	0	0	5 (<1)
Other afebrile	14 (5)	21 (6)	2 (5)	3 (10)	4 (15)	6 (23)	50 (7)
Outcome							
Intensive care unit hospitalization	4 (1)	4 (1)	0	0	2 (8)	1 (4)	11 (2)
Death	1 (<1)	1 (<1)	0	0	0	0	2 (<1)

*Values are no. (%) patients except as indicated. Further details are available in online Technical Appendix Table 1 (https://wwwnc.cdc.gov/EID/article/24/4/17-1542-Techapp1.pdf). GI, gastrointestinal; IQR, interquartile range.
†Other comprises case-patients in Oceania (n = 6) and those for whom exact region of infection was undetermined (n = 26).
‡One patient returning from Asia with malaria had a coinfection with *P. falciparum* and *P. vivax*. In this table, we listed the patient under *P. falciparum*.

vs. 1 [3%]); p<0.01); male (81 [94%] vs. 26 [72%]; p<0.01); and to have traveled to middle and western Africa (64 [74%] vs. 0; p<0.01). The annual number of *P. vivax* malaria hospitalizations declined during the study period from an average of 7.3 hospitalizations per year during 2004–2006 to <1 hospitalization per year during 2013–2015 ($R^2 = 0.62$).

Of the 181 acute life-threatening tropical diseases, 86 (48%) were acquired in Africa and 83 (46%) in Asia (Table 2). Male sex, business travel, and travel to Africa characterized travelers hospitalized for treatment of life-threatening diseases. The most common causes of life-threatening illness requiring hospitalization were *P. falciparum* malaria (86 [48%]) and enteric fever (59 [33%]). Of the 74 cases of dengue fever, none were dengue hemorrhagic fever or dengue shock syndrome; therefore, no dengue cases were considered life-threatening. Eleven (2%) hospitalized travelers required admission to

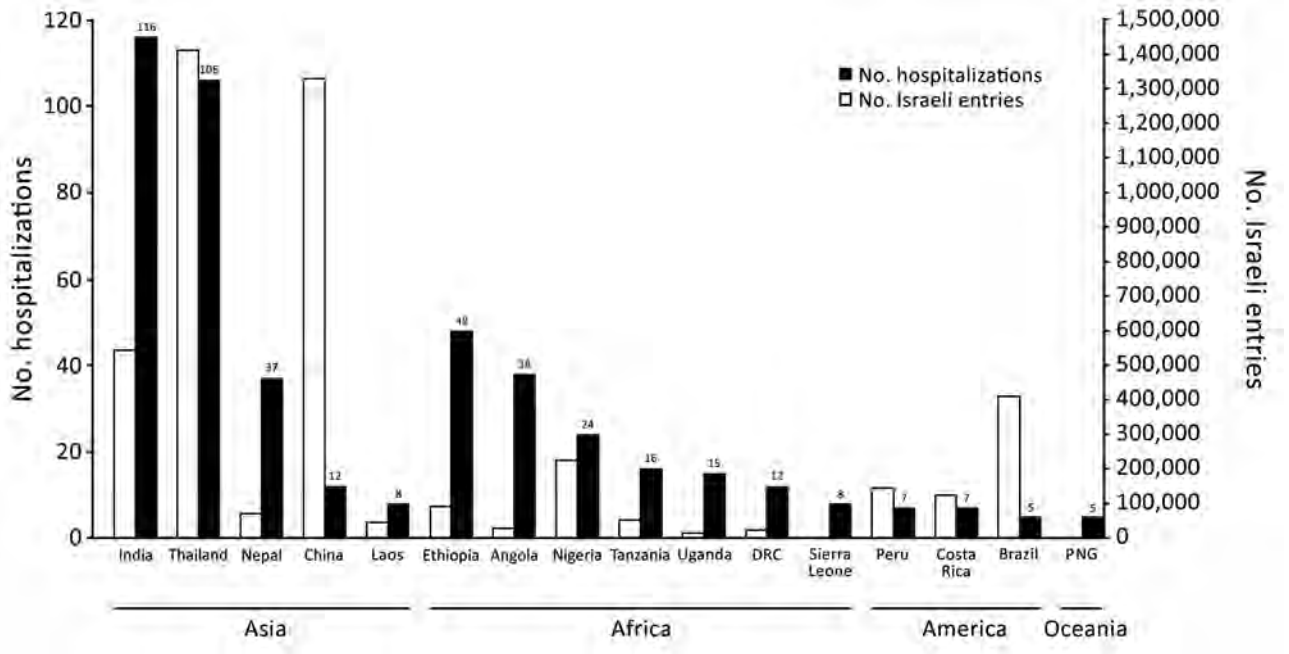

Figure. Travel-associated hospitalizations of citizens of Israel at Sheba Medical Center, Israel, by country of disease acquisition (A), and estimated number of Israeli citizen entries to each country (B), 2004–2005. Data on Israeli citizen entries from the United Nations World Tourism Organization (*4*). DRC, Democratic Republic of the Congo; PNG, Papua New Guinea.

an intensive care unit, and 2 of these patients died during their hospitalization. One patient died from endocarditis caused by *Staphylococcus aureus* and 1 from necrotizing fasciitis in a surgical wound while hospitalized for eosinophilia and abdominal mass.

A total of 112 (16%) hospitalizations were potentially preventable by chemoprophylaxis or pretravel vaccination: *P. falciparum* malaria (86, 12%); *Salmonella enterica* serovar Typhi (23, 3%); hepatitis A (2, <1%); and acute hepatitis B (1, <1%). Most of the life-threatening diseases acquired in Africa were potentially preventable (84, 98%); significantly fewer (25, 30%) from Asia were potentially preventable (p<0.01).

Conclusions

We reviewed >700 posttravel hospitalizations of citizens in Israel during 2004–2015. Acute, life-threatening illnesses necessitated 25% of admissions, most of which were potentially preventable by malaria chemoprophylaxis or pretravel vaccination. Compared with other regions,

Table 2. Comparison of characteristics of travelers hospitalized for treatment of acute life-threatening tropical diseases and those with non–life-threatening illnesses, Sheba Medical Center, Israel, 2004–2015*

Patient characteristics	Life-threatening illness,† n = 181	Non–life-threatening illness, n = 541	p value
Male sex	145 (81)	385 (71)	0.02
Age, median (IQR)	33 (25–49)	33 (25–50)	0.62
Elderly, age ≥60 y	15 (8)	68 (13)	0.12
Category of travelers			
Tourism	138 (76)	448 (83)	0.05
Business travelers	43 (24)	73 (13)	<0.01
Visiting friends or relatives	0 (0)	20 (3)	<0.01
Continent of travel			
Africa	86 (48)	181 (33)	<0.01
Asia	83 (46)	247 (46)	0.98
South America	0	43 (8)	<0.01
Central America and Caribbean	8 (4)	22 (4)	0.83
North America and Europe	1 (<1)	25 (5)	<0.01
Other‡	3 (2)	23 (4)	0.11

*Values are no. (%) patients except as indicated. IQR, interquartile range.
†Life-threatening diseases (n = 181): *P. falciparum* (86), *S. enterica* ser. Paratyphi (36), leptospirosis (29), *S. enterica* ser. Typhi (23), rickettsial diseases (3), melioidosis (2), hantavirus (1), trypanosomiasis (1).
‡Other comprises Oceania (n = 6) and cases whose exact region of infection was undetermined (n = 26).

nearly all life-threatening diseases in travelers returning from Africa were preventable.

Most travelers who were admitted to hospitals to treat preventable life-threatening diseases after returning from Africa were diagnosed with *P. falciparum* malaria. The number of *P. vivax* malaria hospitalizations declined during the study years, possibly related to discontinuation of rafting trips to the Omo River in Ethiopia, which had resulted a high number of infections in earlier years. In travelers returning from Asia, enteric fever was the second most common cause of hospitalization, after dengue fever; *S. enterica* ser. Paratyphi, for which an effective vaccine is not available, caused most of those illnesses. An outbreak of *Salmonella* Paratyphi A enteric fever in Nepal (*5*) may have contributed to this trend.

Our study has several limitations. SMC is the national referral center for travel-related illness; therefore, an unusually high number of severe or complicated illnesses may have affected our results. Because of the relatively small number of hospitalizations related to individual destination countries, singular events or large outbreaks may have biased the country-specific data (*5*). The Israeli traveler population is generally characterized by a low rate of travelers visiting friends and relatives, except travelers to Ethiopia. Approximately one third of the patients hospitalized after travel to Ethiopia were born in Ethiopia or born to parents from Ethiopia who immigrated to Israel. This relationship may have resulted in a higher posttravel hospitalization number among citizens of Israel returning from Ethiopia, because travelers visiting friends and relatives may be at a higher risk (*6*). Because of the different methods of traveler data capture used by different countries reporting to the United Nations World Tourism Organization, our use of the reported number of Israeli citizen entries from this dataset was limited to contextualize the number of hospitalizations from specific countries in relative terms, rather than to calculate country-specific rates of hospitalization.

In conclusion, Israeli citizens hospitalized to treat life-threatening diseases after returning from travel to Africa were likely to suffer from preventable illnesses. Knowledge of region-specific hospitalization causes and impact should be used to identify at-risk travelers, enhance pretravel preparation, and advocate adherence to recommended vaccines and malaria prophylaxis.

About the Author

Dr. Avni is a medical intern at The Chaim Sheba Medical Center, Tel Hashomer, Israel. His research interests include infectious diseases, tropical diseases, travel medicine, and epidemiology.

References

1. Ryan ET, Wilson ME, Kain KC. Illness after international travel. N Engl J Med. 2002;347:505–16. http://dx.doi.org/10.1056/NEJMra020118
2. Leder K, Torresi J, Libman MD, Cramer JP, Castelli F, Schlagenhauf P, et al.; GeoSentinel Surveillance Network. GeoSentinel surveillance of illness in returned travelers, 2007–2011. Ann Intern Med. 2013;158:456–68. http://dx.doi.org/10.7326/0003-4819-158-6-201303190-00005
3. Jensenius M, Han PV, Schlagenhauf P, Schwartz E, Parola P, Castelli F, et al.; GeoSentinel Surveillance Network. Acute and potentially life-threatening tropical diseases in western travelers—a GeoSentinel multicenter study, 1996-2011. Am J Trop Med Hyg. 2013;88:397–404. http://dx.doi.org/10.4269/ajtmh.12-0551
4. United Nations World Tourism Organization. Israel: country-specific: outbound tourism 1995–2016 (12.2017). Tourism statistics. 2017 [cited 2018 Mar 12]. http://www.e-unwto.org/doi/abs/10.5555/unwtotfb037625011995201620171 2
5. Meltzer E, Stienlauf S, Leshem E, Sidi Y, Schwartz E. A large outbreak of *Salmonella paratyphi* A infection among israeli travelers to Nepal. Clin Infect Dis. 2014;58:359–64. http://dx.doi.org/10.1093/cid/cit723
6. Ericsson CD, Hatz C, Leder K, Tong S, Weld L, Kain KC, et al. Illness in travelers visiting friends and relatives: a review of the GeoSentinel Surveillance Network. Clin Infect Dis. 2006;43:1185–93. http://dx.doi.org/10.1086/507893

Address for correspondence: Eli Schwartz, Center of Geographic Medicine, The Chaim Sheba Medical Center, Tel Hashomer 52621, Israel; email: elischwa@post.tau.ac.il; Eyal Leshem, Infectious Diseases Unit, The Chaim Sheba Medical Center, Tel Hashomer 52621, Israel; email: leshem@gmail.com

Intensive Care Admissions for Severe Chikungunya Virus Infection, French Polynesia

Adrien Koeltz, Stephane Lastere, Sylvain Jean-Baptiste

Author affiliations: Taaone Hospital, Papeete, French Polynesia (A. Koeltz, S. Lastere); Bichat Hospital, Paris, France (S. Jean-Baptiste)

DOI: https://doi.org/10.3201/eid2404.161536

During the 2014–2015 chikungunya outbreak in French Polynesia, 64 patients with confirmed chikungunya virus infection were admitted into intensive care. Sixty-three were nonpregnant adults; 11 had an atypical form, 21 had severe sepsis or septic shock, and 18 died. These findings indicate that critical illness frequently complicates the course of chikungunya virus infection.

The first case of chikungunya virus (CHIKV) infection in French Polynesia (Tahiti) was diagnosed in May 2014; it was imported from Guadeloupe Island in the Caribbean (*1*). During the outbreak that developed during October 2014–March 2015, ≈25% of the local population (272,000 residents) became infected with CHIKV (*2*). French Polynesia has 2 potential mosquito vectors for CHIKV: *Aedes aegypti* and *A. polynesiensis.* Phylogenic analysis showed that the French Polynesia strain of CHIKV belongs to the Asian lineage and is closely related to the strain collected in Guadeloupe and the British Virgin Islands in 2014, showing 99.9% homology with that strain (*3*). To describe patient characteristics and clinical courses of chikungunya patients in French Polynesia during 2014–2015, we retrospectively reviewed the medical files of all patients with documented CHIKV infection.

CHIKV infection was defined by the association of compatible symptoms of fever and arthralgia and positive IgM serology or positive blood reverse transcription PCR (RT-PCR). We defined types of CHIKV infection as follows: 1) common form (i.e., only fever or arthralgia); 2) atypical form (i.e., involvement of ≥1 organ systems); and 3) severe form (i.e., failure of ≥1 organ systems or admission to an intensive care unit [ICU]).

We used standard definitions for organ system failures and severe sepsis shock (*4*). Organ failures were defined by a Sequential Organ Failure Assessment score ≥3 for each organ. Encephalitis was defined in accordance with Position Consensus Statement of the International Encephalitis Consortium criteria (*5*) and myocarditis in accordance with Consensus Statement of the European Society of Cardiology criteria (*6*).

During the outbreak, CHIKV was confirmed in 63 adults and one 11-year-old girl (Table). Forty-two patients had positive results for blood RT-PCR, and 22 had positive results for IgM serology. Virus load in serum was high; median load was 7.52 $\log_{10}$ copies/mL (interquartile range 3.47–9.39 $\log_{10}$ copies/mL). Of 5 patients with encephalitis symptoms, 3 had positive results for cerebrospinal fluid RT-PCR.

Forty-nine (76%) patients had a preexisting disease, 33 (51%) required invasive mechanical ventilation, 40 (62%) were in shock and needed vasoactive drugs, and 30 (46%) required renal replacement therapy. The ICU death rate for chikungunya was 28%, slightly higher than the usual 22% ICU death rate (A. Koeltz, unpub. data). Five patients had encephalitis, 2 had myocarditis, and 4 had Guillain-Barré syndrome (GBS). Fifty-five patients had a severe form of chikungunya, and 21 had illness consistent with the case definition for severe sepsis; for 2 patients, no other cause for GBS than CHIKV was identified. Two patients had CHIKV–leptospirosis co-infection, and 1 had CHIKV–dengue virus co-infection. Among the 55 patients who had the severe form of chikungunya, 17 had exacerbations of a chronic condition.

Chikungunya can be complicated by severe multiple organ failure and lead to death either from exacerbation of a preexisting disease or by severe atypical infection. Severe septic shock directly attributable to CHIKV was reported during the 2014 outbreak (*7*,*8*), and these reports seem consistent with our study (2 cases). This finding could be explained by the fact that chikungunya induces lymphopenia.

Neurologic complications of arbovirus infections are well documented, as illustrated by the high incidence of GBS reported during French Polynesia's outbreak of Zika virus (42 cases) (*9*). In our study, we observed 4 severe cases of GBS, and 10 GBS cases were managed in the hospital during the outbreak; GBS incidence was 4 times higher than usually observed in this hospital.

The most severe atypical complication in our study was myocarditis (2 cases), which had a 100% case-fatality rate. These deaths included an 11-year-old child and a 56-year-old woman without preexisting disease.

Our findings indicate that critical illness frequently complicates the course of CHIKV infection. Hospitals in chikungunya-endemic areas should be aware of the potential for increases in the number of ICU admissions during outbreaks.

Acknowledgment

We thank Thomas Koeltz for his review.

About the Author

Dr. Koeltz is a cardiac anesthesiologist at Bichat Claude-Bernard University Hospital in Paris. His research interests include infectious diseases in tropical areas.

Table. Clinical and laboratory characteristics of 64 patients with chikungunya virus infection admitted into the intensive care department, French Polynesia, 2014–2015*

Characteristic	Result
Baseline	
Median age, y (IQR)	62 (49–71)
Sex, no. (%)	
M	37 (58)
F	27 (42)
Preexisting disease, no. (%)	
Hypertension	37 (58)
Diabetes mellitus	22 (34)
Chronic renal failure	15 (23)
Chronic heart failure	12 (19)
Chronic liver disease	3 (5)
None	15 (23)
Simplified Acute Physiology Score (IQR)	48 (28.5–68.5)
Chikungunya diagnosis, no. (%)	
By reverse transcription PCR	42 (66)
By IgM	26 (41)
By reverse transcription PCR and IgM	4 (6)
Finding at admission	
Organ failure,† no. (%)	
Hemodynamic	40 (63)
Renal	30 (47)
Neurologic	20 (31)
Respiratory	33 (52)
Hepatic	16 (25)
Hematologic	9 (14)
Laboratory‡	
Leukocyte count, cells/m^3, median (IQR)	11,600 (7,200–15,200)
Lymphocyte count, cells/m^3, median (IQR)	1,000 (600–1,500)
Lymphopenia, <1,000 cells/m^3 (% of patients)	36 (56)
Platelet count, cells/m^3, median (IQR)	155,000 (79–208)
Platelet count, <150,000 cells/m^3 (% of patients)	34,000 (53)
Creatinine, μmol/L, median (IQR)	132 (79–184)
Creatine phosphokinase, mmol/L, median (IQR)	222 (124–1,160)
Alanine aminotransferase, UI/L, median (IQR)	35 (19–76)
C-reactive protein, mg/L, median (IQR)	10.6 (2.8–18.3)
Procalcitonin, μg/L, median (IQR)	1.72 (0.42–18.3)
Lactate, mmol/L, median (IQR)	2.6 (1.1–5.4)
Chikungunya reverse transcription PCR‡	
Viral load in serum, log_{10} copies/mL (IQR)	7.52 (3.47–9.39)
Viral load in cerebrospinal fluid,§ log_{10} copies/mL (IQR)	4.18 (3.86–4.26)
Outcome variable	
ICU length of stay, d, median (IQR)	3 (2–7)
Crude intensive care unit deaths, no (%)	18 (28)

*IQR, interquartile range.
†Organ failure is defined according to a Sequential Organ Failure Assessment score ≥3 for each organ.
‡Blood samples during the first 24 h. Reference values are as follows: leukocytes, 4.0–10.0 × 10^3 cells/mm^3; lymphocytes, 1.5–3.4 × 10^3 cells/mm^3; platelets, 150–400 × 10^3/mm^3; creatinine, 0.56–1.0 mg/dL; creatine phosphokinase, 0–130 U/L; alanine aminotransferase, 0–35 U/L; C-reactive protein, <5 mg/L; procalcitonin, <0.5 ng/mL; lactate, 5–15 mg/dL.
§Virus load was positive for 5 of the 9 cerebrospinal fluid samples.

References

1. Nhan T-X, Claverie A, Roche C, Teissier A, Colleuil M, Baudet J-M, et al. Chikungunya virus imported into French Polynesia, 2014. Emerg Infect Dis. 2014;20:1773–4. http://dx.doi.org/10.3201/eid2010.141060
2. Nhan TX, Musso D. The burden of chikungunya in the Pacific. Clin Microbiol Infect. 2015;21:e47–8. http://dx.doi.org/10.1016/j.cmi.2015.02.018
3. Aubry M, Teissier A, Roche C, Richard V, Yan AS, Zisou K, et al. Chikungunya outbreak, French Polynesia, 2014. Emerg Infect Dis. 2015;21:724–6. http://dx.doi.org/10.3201/eid2104.141741
4. Dellinger RP, Carlet JM, Masur H, Gerlach H, Calandra T, Cohen J, et al.; Surviving Sepsis Campaign Management Guidelines Committee. Surviving Sepsis Campaign guidelines for management of severe sepsis and septic shock. Crit Care Med. 2004;32:858–73. Erratum in Crit Care Med. 2004;32:2169-70. Erratum in Crit Care Med. 2004; 32:1448. http://dx.doi.org/ 10.1097/01.CCM.0000117317.18092.E4
5. Venkatesan A, Tunkel AR, Bloch KC, Lauring AS, Sejvar J, Bitnun A, et al.; International Encephalitis Consortium. Case definitions, diagnostic algorithms, and priorities in encephalitis: consensus statement of the International Encephalitis Consortium. Clin Infect Dis. 2013;57:1114–28. http://dx.doi.org/10.1093/cid/cit458
6. Caforio AL, Pankuweit S, Arbustini E, Basso C, Gimeno-Blanes J, Felix SB, et al. Current state of knowledge on aetiology, diagnosis, management, and therapy of myocarditis: a position statement of the European Society of Cardiology Working Group on Myocardial

and Pericardial Diseases. Eur Heart J. 2013;34:2636–48, 2648a–2648d.
7. Torres JR, Castro JS, Rodríguez L, Saravia V, Arvelaez J, Ríos-Fabra A, et al. Chikungunya fever: ftypical and lethal cases in the Western Hemisphere: A Venezuelan experience. IDCases. 2014;2:6–10. http://dx.doi.org/10.1016/j.idcr.2014.12.002
8. Rollé A, Schepers K, Cassadou S, Curlier E, Madeux B, Hermann-Storck C, et al. Severe sepsis and septic shock associated with chikungunya virus infection, Guadeloupe, 2014. Emerg Infect Dis. 2016;22:891–4. http://dx.doi.org/10.3201/eid2205.151449
9. Cao-Lormeau V-M, Blake A, Mons S, Lastère S, Roche C, Vanhomwegen J, et al. Guillain-Barré syndrome outbreak associated with Zika virus infection in French Polynesia: a case–control study. Lancet. 2016;387:1531–9. http://dx.doi.org/10.1016/S0140-6736(16)00562-6

Address for correspondence: Adrien Koeltz, Department of Anesthesiology and Intensive Care, Centre Hospitalier Universitaire Bichat Claude-Bernard, 46 Rue Henri Huchard, 75018 Paris, France; email: adrien.koeltz@aphp.fr

African Swine Fever Virus, Siberia, Russia, 2017

Denis Kolbasov, Ilya Titov, Sodnom Tsybanov, Andrey Gogin, Alexander Malogolovkin

Author affiliation: Federal Research Center for Virology and Microbiology, Pokrov, Russia

DOI: https://doi.org/10.3201/eid2404.171238

African swine fever (ASF) is arguably the most dangerous and emerging swine disease worldwide. ASF is a serious problem for the swine industry. The first case of ASF in Russia was reported in 2007. We report an outbreak of ASF in Siberia, Russia, in 2017.

African swine fever (ASF) is arguably the most dangerous swine disease worldwide. ASF virus (ASFV) is highly virulent for domestic swine and remains a global threat because no effective vaccine is available to eradicate the disease. The emergent potential of ASF has been demonstrated by its spread into Russia. In the 10 years since ASF was first diagnosed in the Caucasian region of Russia (*1*), the disease has reached Palearctic regions and is spreading into western Europe (*2*,*3*).

In 2017, the Federal Service for Veterinary and Phytosanitary Surveillance (Rosselkhoznadzor) reported that, during 2007–2017, >1,000 ASF outbreaks resulted in deaths of ≈800,000 pigs in 46 regions across Russia (*4*). Production of backyard swine industry decreased by almost half, from 1,119 tons of pork in 2007 to 608 tons of pork in 2017 (*5*). However, highly industrialized pig farms showed increased production every year during this same period, despite the ASF epidemic.

ASF has seriously affected and is actively spread by wild boar populations in Russia, but accurate numbers of boar killed by ASF or culling attempts are difficult to estimate. In June 2017, ASF was detected in the Czech Republic in 2 wild boar (*6*), demonstrating disease spread toward western Europe. In 2017, ASFV cases among backyard domestic pigs were detected in July in Romania (*7*), and later in October 2017 in Moldova (*8*). We report an outbreak of ASF in Far Eastern Russia.

Early in March 2017, an ASF outbreak was reported on 1 backyard farm in the Irkutsk region near the border with Mongolia (Figure) (*5*). All pigs had clinical signs typical of acute ASF, and 40 pigs died within 6 days of the appearance of the first clinical signs. In a 5-km risk zone established around the affected farm, 1,327 pigs were slaughtered within 3 days. Epidemiologic analysis showed that the farmer used table leftovers to feed pigs.

ASFV DNA was identified by real-time PCR in the frozen pork products found on the farm. The origin of contaminated pork products is still under investigation. It is likely that ASFV-contaminated pork products provided a source of infection because these products are the most common source of ASF infection on backyard farms (*9*). ASF outbreaks nearest to the outbreak in Irkutsk occurred >4,000 km away in European Russia. Such a long geographic distance between ASF outbreaks within the country demonstrates that ASFV has a tremendous capacity for transboundary and transcontinental spread.

We identified the ASFV isolate from Irkutsk (ASFV/Irkutsk/dom/2017) by using nucleotide sequencing and molecular analysis. This isolate has capsid protein P72 genotype II and central variable region I and is an intergenic region (IGR) I variant (GenBank accession nos. KY963545, KY938010, and KY982843, respectively) according to the nomenclature of Gallardo et al. (*10*). The intergenic region between the *I73R* and *I329L* genes at the right end of the ASFV/Irkutsk/dom/2017 genome contains no additional tandem-repeat sequences. The ASFV IGRI variant is identical to the ASFV/Georgia/wb/2007 index isolate of the epidemic in Georgia in 2007 but represents an ASFV variant that is rare among recent ASFV isolates in Russia. In comparison, all recent ASF outbreaks in European Russia and eastern Europe have been caused by ASFV of the IGRII variant, which has an insertion of a tandem-repeat sequence in the intergenic region between the I173R and the I329L protein genes.

Figure. African swine fever outbreaks in Russia and countries in eastern Europe, 2017. Black box indicates outbreak in the Irkutsk region in Siberia, Russia.

Our results indicate that an ASF outbreak in Siberia in 2017 was caused by the pan-Russian strain of ASFV (genotype II, central variable region I, and IGRI) that contains B646L (P72), B602L, and intergenic region I173–I329L sequences identical to those of ASFV index isolate ASFV/Georgia/wb/2007 (GenBank accession no. FR682468.1). ASFV-contaminated pork products still pose a major risk for transboundary emergence and spread of ASF. ASFV/Irkutsk/dom/2017 is a highly virulent strain and causes acute ASF in domestic swine. Since the outbreak in Irkutsk, subsequent ASF outbreaks have occurred in Siberia (March–October 2017) and near the border with China, raising concerns that ASF might be introduced into a population of 500 million pigs. This continued and far-reaching spread of ASF in Russia demonstrates the threat of disease emergence and increased spread worldwide.

Acknowledgment

We thank Edan R. Tuman for reviewing the manuscript and providing useful comments.

This study was supported by the Federal Agency of Scientific Organizations (agreement no. 0615-2017-0001).

About the Author

Dr. Kolbasov is director of the Molecular Virology Unit, Federal Research Center for Virology and Microbiology, Pokrov, Russia. His research interests are epidemiology of emerging animal diseases, diagnostics, and vaccine development.

References

1. Gogin A, Gerasimov V, Malogolovkin A, Kolbasov D. African swine fever in the North Caucasus region and the Russian Federation in years 2007-2012. Virus Res. 2013;173:198–203. http://dx.doi.org/10.1016/j.virusres.2012.12.007
2. Śmietanka K, Woźniakowski G, Kozak E, Niemczuk K, Frączyk M, Bocian Ł, et al. African swine fever epidemic, Poland, 2014-2015. Emerg Infect Dis. 2016;22:1201–7. http://dx.doi.org/10.3201/eid2207.151708
3. Sánchez-Vizcaíno JM, Mur L, Martínez-López B. African swine fever (ASF): five years around Europe. Vet Microbiol. 2013;165:45–50. http://dx.doi.org/10.1016/j.vetmic.2012.11.030
4. The Federal Service for Veterinary and Phytosanitary Supervision [in Russian] [cited 2018 Feb 5]. http://www.fsvps.ru
5. Kovalev YI. Veterinary medicine and pigs. Swine production in Russia 2015–2020: current challenges, risks and solutions. Novosibirsk, May 18–19, 2017 [cited 2018 Feb 5]. http://www.pigproducer.net/uploads/media/3_Jurij-Kovalev_.pdf
6. World Organisation for Animal Health. World Animal Health Information Database. Exceptional epidemiological events [cited 2018 Feb 5]. http://www.oie.int/wahis_2/public/wahid.php/Countryinformation/Countryreports
7. World Organisation for Animal Health. World Animal Health Information Database, African swine fever, Romania [cited 2018 Feb 5]. http://www.oie.int/wahis_2/public/wahid.php/Reviewreport/Review?reportid=24456
8. World Organisation for Animal Health. World Animal Health Information Database. African swine fever, Moldava [cited 2018 Feb 5]. https://www.oie.int/wahis_2/public/wahid.php/Reviewreport/Review?page_refer=MapFullEventReport&reportid=25134
9. Food and Agricultural Organization of the United Nations. African swine fever in the Russian Federation: risk factors for Europe and beyond. Rome: The Organization; 2013.
10. Gallardo C, Fernández-Pinero J, Pelayo V, Gazaev I, Markowska-Daniel I, Pridotkas G, et al. Genetic variation among African swine fever genotype II viruses, eastern and central

Europe. Emerg Infect Dis. 2014;20:1544–7. http://dx.doi.org/10.3201/eid2009.140554

Address for correspondence: Alexander Malogolovkin, Federal Research Center for Virology and Microbiology, 601125, Vladimirskaya Oblast', Pokrov, Russia; email: malogolovkin@inbox.ru

Classical Swine Fever Outbreak after Modified Live LOM Strain Vaccination in Naive Pigs, South Korea

Sang H. Je,[1] Taeyong Kwon,[1] Sung J. Yoo, Dong-Uk Lee, SeungYoon Lee, Juergen A. Richt, Young S. Lyoo

Author affiliations: Konkuk University, Seoul, South Korea (S.H. Je, T. Kwon, S.J. Yoo, D.-U. Lee, Y.S. Lyoo); HanByol Farm Tech, Namyangju, South Korea (S. Lee); Kansas State University, Manhattan, Kansas, USA (J.A. Richt)

DOI: https://doi.org/10.3201/eid2404.171319

We report classical swine fever outbreaks occurring in naive pig herds on Jeju Island, South Korea, after the introduction of the LOM vaccine strain. Two isolates from sick pigs had >99% identity with the vaccine stain. LOM strain does not appear safe; its use in the vaccine should be reconsidered.

Classical swine fever is a highly contagious disease of pigs that tremendously affects the swine industry. Although several countries have become free from classical swine fever after eradication programs, sporadic outbreaks continue to occur in most major pig-producing countries, and classical swine fever is endemic to some countries in Asia. Vaccination is regarded as one of the most effective tools to prevent and control classical swine fever. Modified live vaccines (MLVs) mainly containing C-strain have been used widely because of their safety and provide complete protection against virus challenge (*1*,*2*).

Since 1974, the LOM strain has been the MLV strain for classical swine fever in South Korea. As a result of the government's classical swine fever eradication program, Jeju Island, South Korea, became a classical swine fever virus (CSFV)–free area, and vaccination efforts ceased there in 1999 (*3*). Strong prohibition of live pig trade has also contributed to the maintenance of CSFV-naive herds on Jeju Island for over a decade, although sporadic classical swine fever outbreaks have occurred in mainland South Korea, despite mandatory vaccination with the LOM strain (*4*). This study describes classical swine fever outbreaks in naive pig herds on Jeju Island caused by the MLV.

Since 2014, multiple classical swine fever outbreaks have occurred on Jeju Island (online Technical Appendix Figure 1, https://wwwnc.cdc.gov/EID/article/24/4/17-1319-Techapp1.pdf). Clinical manifestation is characterized by reproductive problems (including stillbirth and fetus mummification), lethargy, cutaneous hyperemia, and cyanosis of the ear in young pigs. Pathologic examination showed typical classical swine fever lesions (Figure). Clinical samples from 2 nonvaccinated herds in 2016 were submitted for laboratory analysis.

PCR showed that these samples were positive for CSFV. Other viral pathogens involved in abortions (e.g., porcine reproductive and respiratory syndrome virus, Aujeszky disease virus, porcine parvovirus, Japanese encephalitis virus, and encephalomyocarditis virus) were not detected in any samples; however, lymph node, tonsil, lung, and brain fetal specimens and placenta specimens from farm A and lung specimens from farm B were weakly positive for porcine circovirus type 2, which is ubiquitous in South Korea (*5*). At farm B, serum samples from 20% of suckling piglets and 30% of weaned pigs were positive for CSFV. Although blood samples from growing and finishing pigs were not positive for CSFV, fecal samples were positive, indicating possible horizontal transmission in the field.

LOM isolates JJ-1601 (identified in a placenta sample from farm A) and JJ-1602 (in a spleen sample from farm B) shared 99.0% nucleotide identity with each other; and JJ-1601 shared 99.1% and JJ-1602 shared 99.5% nucleotide identity with the LOM strain. However, they shared low nucleotide identity (84%) with PC11WB, a virus isolated from a wild boar in South Korea (*6*). Phylogenetic analysis indicated that both viruses were classified within subgroup 1.1 (online Technical Appendix Figure 2). Compared with LOM, JJ-1601 contained 5 aa and JJ-1602 10 aa substitutions in the N^{pro}-E2 region; these substituions are not critical for acquisition of pathogenicity (online Technical Appendix Table 2) (*7*).

In this study, we observed residual virulence of the LOM strain in naive herds. Since CSFV vaccine was accidentally introduced onto Jeju Island in 2014, continuous LOM outbreaks have occurred (online Technical Appendix Table 3), resulting in tremendous damage to pig farms on the island. In addition, the virus has persistently circulated and caused repeated problems within the infected herds. Given that accidental vaccination was limited in 2014, the

[1]These authors contributed equally to this article.

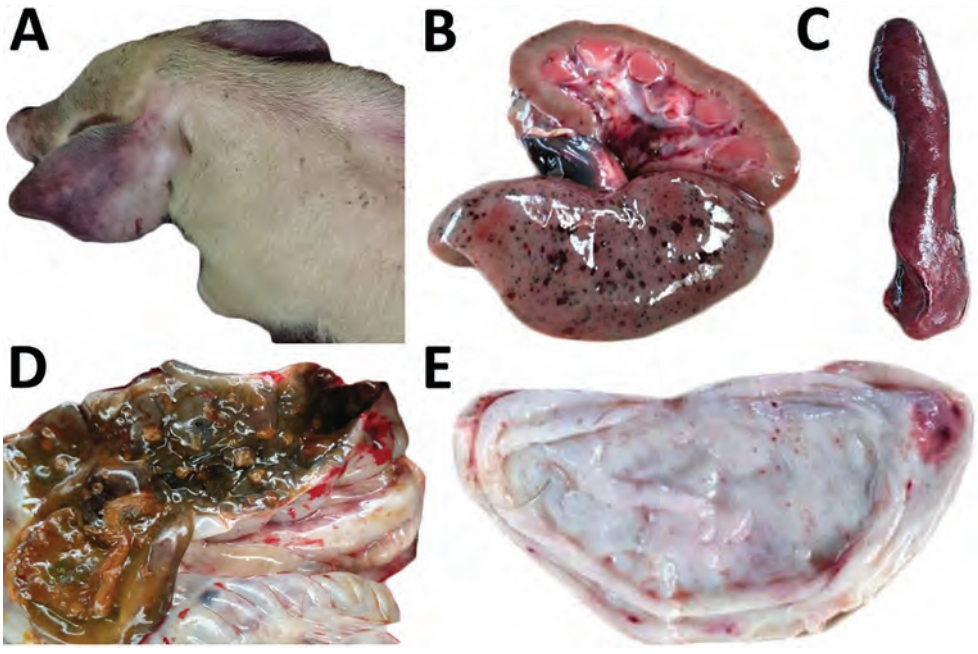

Figure. Clinical signs and pathologic lesions in naive pig infected with classical swine fever virus LOM vaccine strain, Jeju Island, South Korea. A) Cyanosis of ear. B) Hemorrhages in kidney. C) Marginal infarction of spleen. D) Button ulcers in large intestine. E) Hemorrhages in bladder.

continuous classical swine fever outbreaks, including those occurring on farms A and B, resulted from farm-to-farm transmission of the vaccine virus strain.

CSFV live vaccination should guarantee safety to host animals: safety in young pigs, safety in pregnant sows, non-transmissibility, and no reversion to virulence (*8*). The first problem with the LOM vaccine was that the virus spread beyond initially introduced herds. Our results indirectly support horizontal transmissibility of the LOM vaccine within the infected herd. Another factor is the capacity of LOM to cause clinical signs in both young pigs and pregnant sows. Although we could not make observations in 2014 when the vaccine strain was first introduced, viruses with 99% nucleotide identity with LOM were found in CSFV-infected pigs that exhibited clinical signs and typical pathologic lesions of classical swine fever. This virulence could have occurred because of insufficient attenuation or reversion to virulence (*7*,*9*). In a previous study, vaccination of naive pregnant sows with LOM induced stillbirth and fetus mummification (*10*). These results suggested that transplacental transmission and fetal death might be inherent features of the vaccine, which indicates insufficient attenuation during virus adaption in vitro. Further study is needed to determine the basis for the virulence of the LOM strain in young pigs.

In conclusion, we must reconsider the use of LOM in the classical swine fever MLV and use a strain with experimental results satisfying safety requirements. Furthermore, control methods, including a marker vaccine for differentiating infected from vaccinated animals, are needed to stop the continuous damage and spread of LOM on Jeju Island.

Acknowledgments

We thank Hyekyung Yoo and Kyungsu Yang for providing data and critical information about the current status of classical swine fever on Jeju Island, South Korea.

This work was partially supported by a grant from the Department of Homeland Security Center of Excellence for Emerging and Zoonotic Animal Diseases at Kansas State University (Manhattan, Kansas, USA).

About the Author

Mr. Je is a pig veterinarian who previously completed his master's degree at Konkuk University, Seoul, South Korea. His primary research interests include highly contagious diseases of pigs. Mr. Kwon is a graduate student at Konkuk University. His research interests are viral and contagious diseases of pigs.

References

1. van Oirschot JT. Vaccinology of classical swine fever: from lab to field. Vet Microbiol. 2003;96:367–84. http://dx.doi.org/10.1016/j.vetmic.2003.09.008
2. Graham SP, Everett HE, Haines FJ, Johns HL, Sosan OA, Salguero FJ, et al. Challenge of pigs with classical swine fever viruses after C-strain vaccination reveals remarkably rapid protection and insights into early immunity. PLoS One. 2012;7:e29310. http://dx.doi.org/10.1371/journal.pone.0029310
3. Song JY, Lim SI, Jeoung HY, Choi EJ, Hyun BH, Kim B, et al. Prevalence of classical swine fever virus in domestic pigs in South Korea: 1999–2011. Transbound Emerg Dis. 2013;60:546–51. http://dx.doi.org/10.1111/j.1865-1682.2012.01371.x
4. Yoo SJ, Kwon T, Kang K, Kim H, Kang SC, Richt JA, et al. Genetic evolution of classical swine fever virus under immune environments conditioned by genotype 1-based modified live virus vaccine. Transbound Emerg Dis. 2018 Jan 10; [Epub ahead of print]. http://dx.doi.org/10.1111/tbed.12798

5. Kwon T, Lee D-U, Yoo SJ, Je SH, Shin JY, Lyoo YS. Genotypic diversity of porcine circovirus type 2 (PCV2) and genotype shift to PCV2d in Korean pig population. Virus Res. 2017;228:24–9. http://dx.doi.org/10.1016/j.virusres.2016.11.015
6. Jeoung HY, Lim JA, Lim SI, Kim JJ, Song JY, Hyun BH, et al. Complete genome sequences of classical swine fever virus strains isolated from wild boars in South Korea. Genome Announc. 2013;1:e0014713. http://dx.doi.org/10.1128/genomeA.00147-13
7. Tamura T, Sakoda Y, Yoshino F, Nomura T, Yamamoto N, Sato Y, et al. Selection of classical swine fever virus with enhanced pathogenicity reveals synergistic virulence determinants in E2 and NS4B. J Virol. 2012;86:8602–13. http://dx.doi.org/10.1128/JVI.00551-12
8. World Organisation for Animal Health. Classical swine fever (hog cholera). In: OIE terrestrial manual. Paris: The Organisation; 2014. p. 1–26.
9. Terpstra C. Epizootiology of swine fever. Vet Q. 1987;9(sup1):50–60. http://dx.doi.org/10.1080/01652176.1987.9694138
10. Lim SI, Song JY, Kim J, Hyun BH, Kim HY, Cho IS, et al. Safety of classical swine fever virus vaccine strain LOM in pregnant sows and their offspring. Vaccine. 2016;34:2021–6. http://dx.doi.org/10.1016/j.vaccine.2016.02.062

Address for correspondence: Young S. Lyoo, Konkuk University, College of Veterinary Medicine, 120 Neungdong-ro Gwangjin-gu, Seoul 05029, South Korea; email: lyoo@konkuk.ac.kr

Imported Congenital Rubella Syndrome, United States, 2017

Roukaya Al Hammoud, James R. Murphy, Norma Pérez[1]

Author affiliation: The University of Texas Health Science Center, Houston, Texas, USA

DOI: https://doi.org/10.3201/eid2404.171540

Although transmission of rubella virus within the United States is rare, the risk for imported cases persists. We describe a rubella case in a newborn, conceived in Saudi Arabia, in Texas during 2017, highlighting the importance of active surveillance and early diagnosis of this disease.

A full-term male infant was born in Houston, Texas, USA, in early 2017 to a 29-year-old woman from Pakistan; this pregnancy was her first. Delivery was by emergent cesarean section because of fetal cardiac decelerations. The mother had lived in Saudi Arabia for 3 years before traveling to the United States in her third trimester of pregnancy. Early in pregnancy, while in Saudi Arabia, she had acute onset of fever and rash, then arthralgia. Symptoms resolved within a week without medical treatment. She reported prenatal care in Saudi Arabia but had no records with her; she knew of no ill contacts during pregnancy. At delivery, she had negative results for HIV and negative rapid plasma reagin but positive rubella IgG titers (>500 IU/Ml; reference, positive >10 IU/mL).

The infant was transferred to The University of Texas Health Science Center (Houston, Texas, USA). Birthweight and head circumference were below the third percentile. Symptoms were respiratory distress, left leucocoria (Figure), systolic heart murmur, and depressed neonatal reflexes. Laboratory evaluation showed normal peripheral leukocyte count, hemoglobin, and liver enzymes and platelet count of 93,000/mm^3. Because of suspected congenital rubella infection, we placed the patient on contact isolation. Tests for cytomegalovirus and toxoplasma were negative. We considered congenital Zika syndrome, but no testing was done. An ophthalmologic exam confirmed left cataract without retinal involvement. Chest radiograph showed clear lungs; echocardiogram showed supravalvular pulmonary stenosis and patent ductus arteriosus. Cerebrospinal spinal fluid (CSF) analysis showed normal leukocyte, glucose, and protein levels. Blood and CSF cultures were negative. On the fourth day of life, blood rubella IgG was >500 IU/mL (reference, immune ≥10 IU/mL), and blood rubella IgM was >400 AU/mL (reference range 20–24.9 AU/mL). Ultrasound examination of the brain was unremarkable. Radiographic evaluation of long bones showed diffuse coarse trabecular pattern, striated appearance of the metaphysis, and lucent linear areas. Audiometry brainstem response testing failed in the left ear. Thrombocytopenia self-resolved.

We reported the case to the local health department. We sent no clinical specimens for rubella virus detection. The patient was discharged on his tenth day of life and had uncomplicated pulmonary valvuloplasty and cataract removal surgery by 6 weeks of age. The infectious disease team last saw the patient at 2 months of age; at that time, he was developing well, but his growth was borderline. The patient and his family traveled to Pakistan 3 months after birth.

Figure. Left eye cataract (arrow) in case-patient with congenital rubella syndrome, Texas, USA, 2017. Patient was 4 weeks of age.

[1]All authors contributed equally to this article.

Rubella is of global public health concern; >100,000 cases of congenital rubella syndrome (CRS) are reported annually worldwide (*1*). An immunization program resulted in rubella elimination in the United States during 2004 (*2*). Currently, the Centers for Disease Control and Prevention (CDC) estimates that <10 persons are reported to have rubella annually in the United States (*2*). During the 8 years after rubella was eliminated (2004–2012), 79 of rubella cases were reported, including in case-patients with no travel history (*3*). For the same period, 6 CRS cases were reported to CDC, 5 of which were likely imported (*3*). The sixth case was the infant of a US-born vaccinated mother without known risk factors (*4*). During the next 4 years (2013–2016), 5 confirmed CRS cases were reported to CDC, indicating a relative increase in the total number of new cases in the United States. The 5 cases were reported by three states, Illinois (2 cases), New York (2 cases), and Maryland (1 case); infections were likely acquired in Algeria, Pakistan, Yemen, and Nigeria (US Centers for Disease Control and Prevention, pers. comm, March 2017) (*5*).

During early pregnancy, the mother of the case-patient likely acquired acute rubella infection in Saudi Arabia, which increased its rubella vaccine program in July 2017 to meet control needs (*6*). Maternal immunization records and rubella titers were not available. The infant had positive rubella IgM, cataract, congenital heart disease, microcephaly, unilateral hearing loss, and radiolucent bone disease, meeting criteria for CRS. Screening for rubella titers in early pregnancy is standard in the United States. The presence of positive maternal rubella serology at delivery does not always reflect maternal immunization but can be the result of a rubella infection in early pregnancy. A similar scenario was misleading in a case that was recently reported and resulted in late diagnosis of CRS and subsequent multiple exposures (*6*).

Rubella-like illness in early pregnancy warrants testing for acute rubella infection, which offers parents an opportunity to decide about pregnancy outcome. For confirmed cases, maternal counseling and pregnancy termination may be considered. Testing for CRS is critical for early disease confirmation, implementation of appropriate infection control, timely reporting, and possible epidemiologic investigation. Infants with CRS shed large quantities of virus from bodily secretions for up to 1 year and can transmit rubella virus to susceptible persons (*7*). The presence of unimmunized persons in the United States (for age, personal, or medical reasons) and entry of persons from rubella-endemic countries enable potential circulation of the virus. Despite rubella elimination in the United States, the presence of birth defects compatible with CRS warrants consideration of rubella in addition to other congenital infections.

Acknowledgments

We thank the parents of the reported patient for providing the photograph that is included in this manuscript and consent to publish the case.

About the Author

Dr. Al Hammoud is an instructor in the Pediatric Infectious Diseases division at UT Health, McGovern Medical School. Her research interests include general pediatric infectious diseases and immunization response in pediatric HIV patients.

References

1. Rubella—fact sheet (updated March 2017) [cited 2018 Feb 10]. http://www.who.int/mediacentre/factsheets/fs367/en/
2. Centers for Disease Control and Prevention. Rubella [cited 2018 Feb 10]. https://www.cdc.gov/rubella/about/in-the-us.html
3. Three Cases of Congenital Rubella Syndrome in the Postelimination Era—Maryland, Alabama, and Illinois, 2012. MMWR Morb Mortal Wkly Rep. 2013;62:226–9 [cited 2018 Feb 10]. https://www.cdc.gov/mmwr/preview/mmwrhtml/mm6212a3.htm
4. Pitts SI, Wallace GS, Montana B, Handschur EF, Meislich D, Sampson AC, et al. Congenital rubella syndrome in child of woman without known risk factors, New Jersey, USA. Emerg Infect Dis. 2014;20:307–9. http://dx.doi.org/10.3201/eid2002.131233
5. Robyn M, Dufort E, Rosen JB, Southwick K, Bryant PW, Greenko J, et al. Two imported cases of congenital rubella syndrome and infection-control challenges in New York State, 2013–2015. J Pediatric Infect Dis Soc. 2017. http://dx.doi.org/10.1093/jpids/pix028/3828486
6. Rasooldeen M. Vaccination of children in Saudi Arabia now available daily. 2017 Jul 23 [cited 2018 Feb 10]. http://www.arabnews.com/node/1133506/saudi-arabia
7. Epidemiology and prevention of vaccine-preventable diseases [cited 2018 Feb 10]. https://www.cdc.gov/vaccines/pubs/pinkbook/rubella.html

Address for correspondence: Roukaya Al Hammoud, UT Health, McGovern Medical School, Pediatric Infectious Diseases Division, 6431 Fannin St, Ste 3.126, Houston, TX 77030, USA; email: Roukaya.AlHammoud@uth.tmc.edu

Candida auris Infection Leading to Nosocomial Transmission, Israel, 2017

Ana Belkin, Zeala Gazit, Nathan Keller, Ronen Ben-Ami, Anat Wieder-Finesod, Ana Novikov, Galia Rahav, Tal Brosh-Nissimov

Author affiliations: Sheba Medical Center, Tel Hashomer, Israel (A. Belkin, Z. Gazit, N. Keller, A. Wieder-Finesod, G. Rahav,

T. Brosh-Nissimov); Sackler Medical School, Tel Aviv University, Tel Aviv, Israel (A. Belkin, R. Ben-Ami, A. Wieder-Finesod, G. Rahav, T. Brosh-Nissimov); Ariel University, Ariel, Israel (N. Keller); Tel Aviv Sourasky Medical Center, Tel Aviv (R. Ben-Ami, A. Novikov)

DOI: https://doi.org/10.3201/eid2404.171715

A patient transferred from South Africa to Israel acquired a *Candida auris* infection. Phylogenetic analysis showed resemblance of *C. auris* to isolates from South Africa but not Israel, suggesting travel-associated infection. *C. auris* infection occurred weeks later in another patient at the same hospital, suggesting prolonged environmental persistence.

Candida auris is a multidrug-resistant yeast that has emerged over the past 3 years to cause nosocomial outbreaks in multiple countries. *C. auris* can cause serious invasive infections, may spread between patients, and can survive for months on hospital room surfaces (*1*). Whole-genome sequencing has determined the presence of country-specific clades, which differ from one another by thousands of single-nucleotide polymorphisms (*2*). The mode of spread between countries remains unclear. We present a case of international *C. auris* transmission related to a medically repatriated patient.

A previously healthy 25-year-old Israeli man (patient A) was admitted to a hospital in Johannesburg, South Africa, after a motor vehicle accident on July 24, 2016. He had severe limb injury and underwent open reduction and internal fixation on both femurs, complicated by fat emboli, acute respiratory distress syndrome requiring mechanical ventilation, and ventilator-associated pneumonia. He was empirically treated with broad-spectrum antimicrobial drugs and caspofungin. Three weeks after the accident, he was transferred to the intensive care unit (ICU) of Sheba Medical Center, Tel Hashomer, Israel. Ten days after his arrival, a deep surgical-site infection developed in his left thigh. We initiated debridement and broad-spectrum antimicrobial drugs. After cultures obtained during surgery grew extended-spectrum β-lactamase–producing *Klebsiella pneumoniae* and meropenem-resistant *Pseudomonas aeruginosa,* we initiated contact isolation. Two of 3 deep-wound cultures grew *C. auris*. Two days later, 1 blood culture grew *C. parapsilosis*. We administered amphotericin B and appropriate antibacterial drugs, discontinuing amphotericin B after 10 days due to increased creatinine. The surgical site healed, and the patient was transferred to a rehabilitation unit. Rectal and skin surveillance cultures obtained 4 weeks after the first isolation of *Candida* were negative for *C. auris*. Routine ICU environmental disinfection included daily bleach cleaning of surfaces and quaternary ammonium wipes of sensitive medical equipment.

In January 2017, we isolated *C. auris* from a urine culture obtained through a catheter of a 70-year-old patient (patient B) who was admitted to the Sheba Medical Center ICU 6 weeks after the discharge of patient A. Patient B had not traveled abroad recently. Surveillance cultures (urine, axilla, perineum) of patients in the ICU at the time of *C. auris* isolation of either patient A or B were negative for *C. auris*. One environmental sample from the floor next to patient B's bed in proximity to the urinary catheter bag was positive for *C. auris*. All other environmental samples were negative. We removed the urinary catheter without further antimicrobial therapy. Strict environmental cleaning was performed in the ICU.

We performed drug susceptibility testing using broth microdilution in accordance with Clinical Laboratory Standards Institute methods (https://clsi.org/standards/products/microbiology/documents/m27/) and reported results with preliminary breakpoints as published by the US Centers for Disease Control and Prevention (*3*). The study was approved by the Sheba Medical Center institutional review board.

We identified isolates as *C. auris* by matrix-assisted laser desorption/ionization time-of-flight mass spectrometry (Bruker Daltonik, Bremen, Germany) and as *C. parapsilosis* by the Phoenix system (Becton Dickinson, Franklin Lakes, NJ, USA). Sequence alignment with *C. auris* type strain CBS10913T produced similarity scores of 98% for internal transcribed spacer and 100% for large subunit ribosomal DNA segments for all 4 strains. Internal transcribed spacer and large subunit sequences of isolates from both patients were 100% identical to strains for MRL293 and MRL208 from South Africa (*4*) and distinct from sequences of strains previously isolated in our hospital and in Tel Aviv (Figure) (*5*).

C. auris isolates from patients A and B were resistant to fluconazole and susceptible to anidulafungin and had high MICs to voriconazole (≥8 μg/mL). One isolate was resistant to amphotericin B (MIC 2 μg/mL) (*3*), although a recent study suggested a higher epidemiologic cutoff that defines the isolate as susceptible (*6*).

Nosocomial outbreaks associated with *C. auris* were reported from several countries and continents including India, South Africa, Venezuela, Pakistan, and the United States (*2*,*7*,*8*). Sporadic cases were reported from Israel (*5*). Echinocandin exposure, which preceded *C. auris* infection in patient A, was also reported in South Africa (*2*). Environmental contamination appears to be a common mode of *C. auris* spread within medical facilities (*1*); it is the suspected cause for the 2 cases reported here, despite the time between them. The use of quaternary ammonium compounds, which are less effective than bleach, for disinfecting equipment might contribute to persistence of *Candida* (*9*).

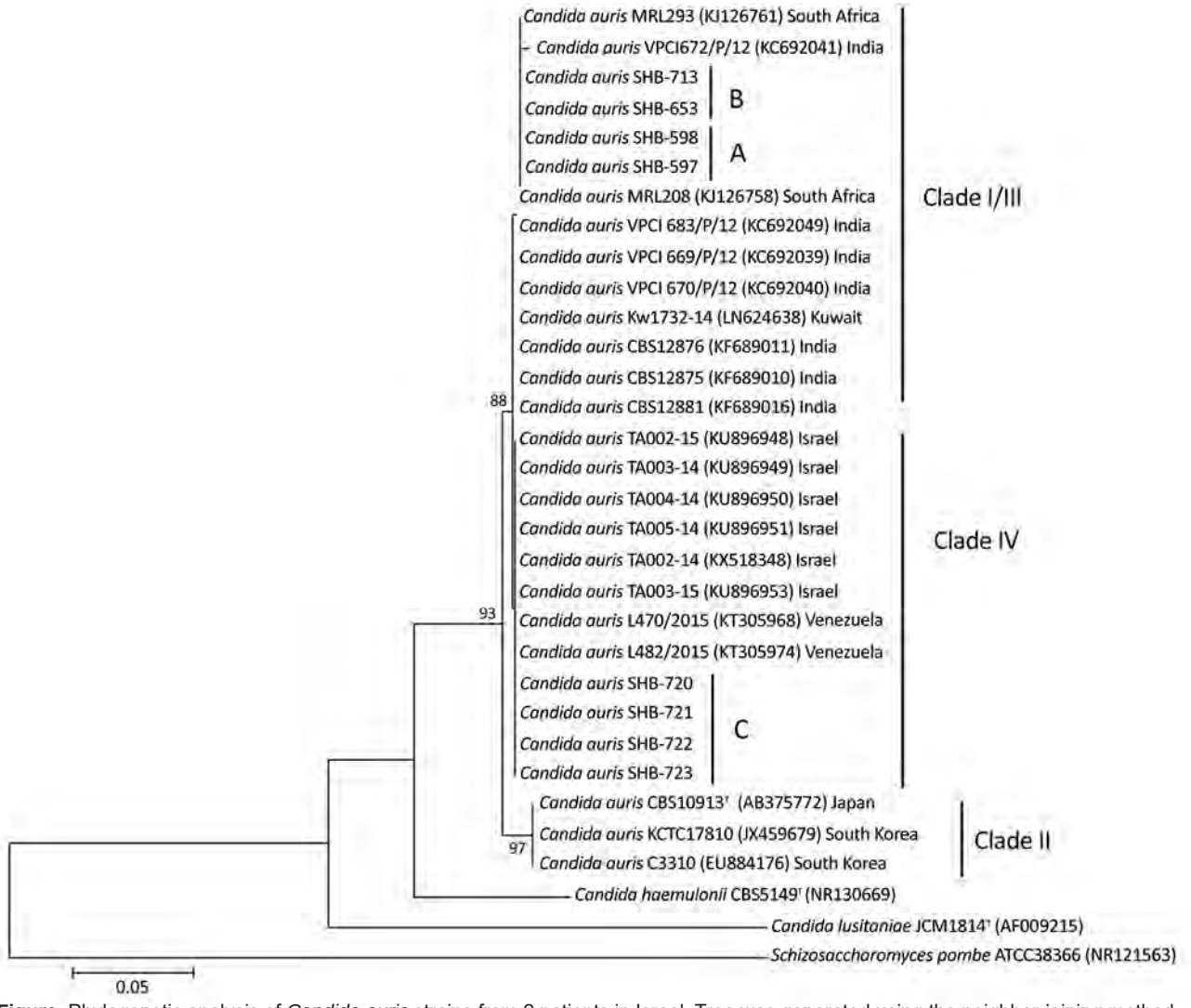

Figure. Phylogenetic analysis of *Candida auris* strains from 2 patients in Israel. Tree was generated using the neighbor-joining method. Internal transcribed spacer sequences of *C. auris* strains were aligned with the *C. auris* type strain CBS5149^T, strains previously isolated in Tel Aviv (TA002-TA005), and additional clinical strains available from GenBank. A indicates isolates from patient A, who was transferred from South Africa to Sheba Medical Center in Israel in late 2016. B indicates isolates from patient B, who was admitted to the same unit 6 weeks after the discharge of patient A, in January 2017; SHB-713 is an environmental sample from the floor near patient B's bed. C indicates isolates from sputum and urine from 2 different patients infected with *C. auris* in Sheba Medical Center during 2017 (SHB-720–723). The percentages of replicate trees in which the associated taxa clustered together in the bootstrap test (500 replicates) are shown next to the branches. GenBank accession numbers are given in parentheses, and countries of origin are listed. *C. lusitaniae* JCM1814^T and *Schizosaccharomyces pombe* ATCC38366 were used as outgroups. Scale bar indicates nucleotide substitutions per site.

International travel is an increasingly recognized risk factor for infection with drug-resistant pathogens. Our investigation underscores the potential role of international travel and especially the transportation of patients between countries as a mode of *C. auris* dissemination. The wide genetic gap between country-specific clades allows the use of ribosomal DNA typing as a tool for identifying the geographic origin of specific isolates (*2*,*5*). A similar approach was used to demonstrate multiple transmission events into the United Kingdom (*10*).

About the Author

Dr. Belkin is an internal medicine specialist and an infectious diseases fellow at the Infectious Disease Unit, Sheba Medical Center, Israel. Her primary research interests include infectious disease medicine and hospital-acquired infections.

References

1. Tsay S, Welsh RM, Adams EH, Chow NA, Gade L, Berkow EL, et al.; MSD. Notes from the field: ongoing transmission of *Candida auris* in healthcare facilities—United States, June 2016–May 2017. MMWR Morb Mortal Wkly Rep. 2017;66:514–5. http://dx.doi.org/10.15585/mmwr.mm6619a7

2. Lockh art SR, Etienne KA, Vallabhaneni S, Farooqi J, Chowdhary A, Govender NP, et al. Simultaneous emergence of multidrug-resistant *Candida auris* on 3 continents confirmed by whole-genome sequencing and epidemiological analyses. Clin Infect Dis. 2017;64:134–40. http://dx.doi.org/10.1093/cid/ciw691
3. Centers for Disease Control and Prevention (CDC). Recommendations for identification of *Candida auris*. 2017 [cited 2017 Nov 17]. https://www.cdc.gov/fungal/diseases/candidiasis/recommendations.html
4. Magobo RE, Corcoran C, Seetharam S, Govender NP. *Candida auris*–associated candidemia, South Africa. Emerg Infect Dis. 2014;20:1250–1. http://dx.doi.org/10.3201/eid2007.131765
5. Ben-Ami R, Berman J, Novikov A, Bash E, Shachor-Meyouhas Y, Zakin S, et al. Multidrug-resistant *Candida haemulonii* and *C. auris*, Tel Aviv, Israel. Emerg Infect Dis. 2017;23. http://dx.doi.org/10.3201/eid2302.161486
6. Arendrup MC, Prakash A, Meletiadis J, Sharma C, Chowdhary A. Comparison of EUCAST and CLSI reference microdilution MICs of eight antifungal compounds for *Candida auris* and associated tentative epidemiological cutoff values. Antimicrob Agents Chemother. 2017;61:e00485–17. http://dx.doi.org/10.1128/AAC.00485-17
7. Vallabhaneni S, Kallen A, Tsay S, Chow N, Welsh R, Kerins J, et al.; MSD. Investigation of the first seven reported cases of *Candida auris*, a globally emerging invasive, multidrug-resistant fungus—United States, May 2013–August 2016. MMWR Morb Mortal Wkly Rep. 2016;65:1234–7. http://dx.doi.org/10.15585/mmwr.mm6544e1
8. Centers for Disease Control and Prevention (CDC). Healthcare professionals *Candida auris* clinical update—September 2017. 2017 [cited 2017 Sep 30]. https://www.cdc.gov/fungal/diseases/candidiasis/c-auris-alert-09-17.html
9. Cadnum JL, Shaikh AA, Piedrahita CT, Sankar T, Jencson AL, Larkin EL, et al. Effectiveness of disinfectants against *Candida auris* and other *Candida* species. Infect Control Hosp Epidemiol. 2017;38:1240–3. http://dx.doi.org/10.1017/ice.2017.162
10. Borman AM, Szekely A, Johnson EM. Isolates of the emerging pathogen *Candida auris* present in the UK have several geographic origins. Med Mycol. 2017;55:563–7. http://dx.doi.org/10.1093/mmy/myw147

Address for correspondence: Tal Brosh-Nissimov, Infectious Diseases Unit, Sheba Medical Center, Emek Ha'Ela St. 1, Tel Hashomer, Israel; email: tbrosh@gmail.com

Cephalosporin-Resistant *Neisseria gonorrhoeae* Clone, China

Shao-Chun Chen, Yue-Ping Yin, Xiang-Sheng Chen

Author affiliations: Chinese Academy of Medical Sciences and Peking Union Medical College, Nanjing, China (S.-C. Chen, Y.-P. Yin, X.-S. Chen); Chinese Center for Disease Control and Prevention, Nanjing (S.-C. Chen, Y.-P. Yin, X.-S. Chen)

DOI: https://doi.org/10.3201/eid2404.171817

Cephalosporin-resistant *Neisseria gonorrhoeae* is a major public health concern. *N. gonorrhoeae* of multiantigen sequence type G1407 and multilocus sequence type 1901 is an internationally spreading cephalosporin-resistant clone. We detected 4 cases of infection with this clone in China and analyzed resistance determinants by using *N. gonorrhoeae* sequence typing for antimicrobial resistance.

Gonorrhea, the second most prevalent sexually transmitted infection (STI) globally, remains a major public health concern in China. From 2015 to 2016, the reported cases of gonorrhea in China increased by 14.7% (100,245 to 115,024) (*1*). The extended-spectrum cephalosporin ceftriaxone has been recommended as monotherapy to treat gonorrhea in China since 2007 (*2*), but resistance to this drug emerged almost at the same time (*3*). Presently, the transmission of internationally spread cephalosporin-resistant clones in China has become a threat to effectively controlling gonorrhea (*4*). Strains with *N. gonorrhoeae* multiantigen sequence type (NG-MAST) G1407 and multilocus sequence type (MLST) 1901 have been successful clones associated with cephalosporin resistance and have caused clinical treatment failures in France and Spain (*5*,*6*); these strains have also became the predominant clones in the United Kingdom (*7*) and Japan (*8*) and among US men who have sex with men (*9*). Here we report 4 cephalosporin-resistant NG-MAST G1407/MLST 1901 clones identified out of 2,038 isolates collected through China's Gonococcal Resistance Surveillance Program during 2015–2016.

Demographic and clinical information for the 4 case-patients are summarized in online Technical Appendix Table 1 (https://wwwnc.cdc.gov/EID/article/24/4/17-1817-Techapp1.xlsx). All case-patients were adult men; gonococcal isolates were obtained from urethral swab samples. The 4 men had obvious urethral discharge and were diagnosed with acute urethritis. Gram staining and culture of the urethral swabs were positive for gonococcal infection. One of the 4 patients self-reported being a man who has sex with men. One of the infections, occurring in Zhejiang Province, was treated with a single-dose regimen of spectinomycin (4 g); the other 3 infections, occurring in the municipality of Chongqing, were treated with a 2-dose regimen of ceftriaxone (1 g) administered over 2 days. Test-of-cure follow-ups were not performed.

All strains were transferred to the reference laboratory at the National Center for Sexually Transmitted Disease Control, Chinese Center for Disease Control and Prevention. Gram staining, a rapid oxidase reaction test, and a carbohydrate utilization test confirmed the identification of *N. gonorrhoeae*. We determined antimicrobial susceptibility to ceftriaxone (CRO), cefixime (CFM), spectinomycin (SPT), azithromycin (AZM), ciprofloxacin (CIP), and

Table. MICs of antimicrobial drugs for *Neisseria gonorrhoeae* isolates from 4 case-patients with cephalosporin-resistant NG-MAST G1407/MLST 1901 infections identified through the national Gonococcal Resistance Surveillance Program, China, 2015–2016*

Case-patient no.	MIC, mg/L						
	CRO	CFM	CIP	PEN	SPT	AZM	PPNG
1	0.5/R	0.5/R	8/R	16/R	16/S	1/S	No
2	0.5/R	1/R	32/R	16/R	32/S	0.5/S	No
3	0.5/R	0.5/R	32/R	16/R	32/S	1/S	No
4	0.25/R	0.5/R	32/R	16/R	64/S	1/S	No

*AZM, azithromycin; CFM, cefixime; CIP, ciprofloxacin; CRO, ceftriaxone; MLST, multilocus sequence type; NG-MAST, *N. gonorrhoeae* multiantigen sequence type; PEN, penicillin; PPNG, penicillinase-producing *N. gonorrhoeae*; R, resistant; S, susceptible; SPT, spectinomycin.

penicillin (PEN) by using the agar dilution method. We detected β-lactamase (penicillinase)–producing *N. gonorrhoeae* isolates by using a nitrocefin solution filter paper test. These strains were resistant to CRO, CFM, PEN, and CIP but susceptible to AZM and SPT based on susceptibility and resistance breakpoints from the European Committee on Antimicrobial Susceptibility Testing (http://www.eucast.org/clinical_breakpoints) (Table). MICs of ceftriaxone ranged from 0.25 to 0.50 mg/L, and MICs of cefixime ranged from 0.5 to 1.0 mg/L.

We performed NG-MAST and MLST genotyping to identify the sequence types (*10*). MLST showed all 4 strains to be type 1901, and NG-MAST showed the Zhejiang strain to be sequence type (ST) 10332 and the Chongqing strains to be ST1407. ST10332 has a 2-basepair difference in the *porB* (*porB*6067) gene from that of ST1407 (*porB*908) and belongs to genogroup G1407. We used *N. gonorrhoeae* sequence typing for antimicrobial resistance (NG-STAR) to identify the characteristics of resistance determinants (*11*). NG-STAR showed 2 of the Chongqing strains to be ST90; the third Chongqing strain was ST194. The strain isolated in Zhejiang was ST507. All 4 strains had type XXXIV mosaic *penA* (*penA* 34.001), –35A Del in the *mtrR* promoter (*mtrR*1), G120K-A121N/D in PorB (PorB8/11), L421P in PonA (PonA1), S91F-D95A/G in GyrA (GyrA1/7), S87R in ParC (ParC3), and wild-type 23srRNA (23 srRNA0) (online Technical Appendix Table 2).

We conclude that the internationally reported cephalosporin-resistant NG-MAST G1407/MLST 1901 *N. gonorrhoeae* clone has spread into China. Genotyping and resistance determinants analysis showed similarity to the predominant G1407/MLST 1901 clone reported in other regions (*7*–*9*), indicating that importation into and transmission within China has occurred. Our findings suggest that increased monitoring of this clone by China's Gonococcal Resistance Surveillance Program will be vital for monitoring trends in antimicrobial resistance.

Acknowledgments

We are grateful to the members of China's Gonococcal Resistance Surveillance Program for providing the isolates and making this study possible. We thank William Shafer for his valuable comments.

The study was supported by grants from the Chinese Academy of Medical Sciences Initiative for Innovative Medicine (2016-I2M-3-021) and the Jiangsu Natural Science Foundation (BK20171133).

About the Author

Dr. S.-C. Chen received his PhD in microbiology and is an associate professor at the National Center for STD Control, Chinese Center for Disease Control and Prevention. His primary research interests include molecular epidemiology and the antimicrobial resistance mechanism of *N. gonorrhoeae*.

References

1. Chinese Center for Disease Control and Prevention. Epidemic of infectious diseases in China, 2016 [2018 Jan 12]. http://www.nhfpc.gov.cn/jkj/s3578/201702/38ca5990f8a54ddf9ca6308fec406157.shtml
2. Wang QQ, Zhang GC. Guidelines for diagnosis and treatment of sexually transmitted diseases [in Chinese]. Shanghai: Shanghai Science and Technology Press; 2007.
3. Chen SC, Yin YP, Dai XQ, Unemo M, Chen XS. Antimicrobial resistance, genetic resistance determinants for ceftriaxone and molecular epidemiology of *Neisseria gonorrhoeae* isolates in Nanjing, China. J Antimicrob Chemother. 2014;69:2959–65. http://dx.doi.org/10.1093/jac/dku245
4. Chen SC, Yin YP, Dai XQ, Unemo M, Chen XS. First nationwide study regarding ceftriaxone resistance and molecular epidemiology of *Neisseria gonorrhoeae* in China. J Antimicrob Chemother. 2016;71:92–9. http://dx.doi.org/10.1093/jac/dkv321
5. Unemo M, Golparian D, Nicholas R, Ohnishi M, Gallay A, Sednaoui P. High-level cefixime- and ceftriaxone-resistant *Neisseria gonorrhoeae* in France: novel *penA* mosaic allele in a successful international clone causes treatment failure. Antimicrob Agents Chemother. 2012;56:1273–80. http://dx.doi.org/10.1128/AAC.05760-11
6. Cámara J, Serra J, Ayats J, Bastida T, Carnicer-Pont D, Andreu A, et al. Molecular characterization of two high-level ceftriaxone-resistant *Neisseria gonorrhoeae* isolates detected in Catalonia, Spain. J Antimicrob Chemother. 2012;67:1858–60. http://dx.doi.org/10.1093/jac/dks162
7. Ison CA, Town K, Obi C, Chisholm S, Hughes G, Livermore DM, et al.; GRASP collaborative group. Decreased susceptibility to cephalosporins among gonococci: data from the Gonococcal Resistance to Antimicrobials Surveillance Programme (GRASP) in England and Wales, 2007–2011. Lancet Infect Dis. 2013;13:762–8. http://dx.doi.org/10.1016/S1473-3099(13)70143-9
8. Shimuta K, Watanabe Y, Nakayama S, Morita-Ishihara T, Kuroki T, Unemo M, et al. Emergence and evolution of internationally disseminated cephalosporin-resistant *Neisseria gonorrhoeae* clones from 1995 to 2005 in Japan. BMC Infect Dis. 2015;15:378. http://dx.doi.org/10.1186/s12879-015-1110-x

9. Grad YH, Kirkcaldy RD, Trees D, Dordel J, Harris SR, Goldstein E, et al. Genomic epidemiology of *Neisseria gonorrhoeae* with reduced susceptibility to cefixime in the USA: a retrospective observational study. Lancet Infect Dis. 2014; 14:220–6. http://dx.doi.org/10.1016/S1473-3099(13)70693-5
10. Martin IM, Ison CA, Aanensen DM, Fenton KA, Spratt BG. Rapid sequence-based identification of gonococcal transmission clusters in a large metropolitan area. J Infect Dis. 2004;189:1497–505. http://dx.doi.org/10.1086/383047
11. Demczuk W, Sidhu S, Unemo M, Whiley DM, Allen VG, Dillon JR, et al. *Neisseria gonorrhoeae* sequence typing for antimicrobial resistance, a novel antimicrobial resistance multilocus typing scheme for tracking global dissemination of *N. gonorrhoeae* strains. J Clin Microbiol. 2017;55:1454–68. http://dx.doi.org/10.1128/JCM.00100-17

Address for correspondence: Yue-Ping Yin, National Center for STD Control, Chinese CDC, Institute of Dermatology, Chinese Academy of Medical Sciences and Peking Union Medical College. 12 Jiangwangmiao St, Nanjing 210042, China; email: yinyp@ncstdlc.org

Chlamydia trachomatis in Cervical Lymph Node of Man with Lymphogranuloma Venereum, Croatia, 2014[1]

Branimir Gjurašin, Snježana Židovec Lepej, Michelle J. Cole, Rachel Pitt, Josip Begovac

Author affiliations: University Hospital for Infectious Diseases Dr. Fran Mihaljević, Zagreb, Croatia (B. Gjurašin, S.Ž. Lepej, J. Begovac); Public Health England, London, UK (M.J. Cole, R. Pitt); University of Zagreb School of Medicine, Zagreb (J. Begovac)

DOI: https://doi.org/10.3201/eid2404.171872

We report an HIV-infected person who was treated for lymphogranuloma venereum cervical lymphadenopathy and proctitis in Croatia in 2014. Infection with a variant L2b genovar of *Chlamydia trachomatis* was detected in a cervical lymph node aspirate. A prolonged course of doxycycline was required to cure the infection.

[1]Results from this study were presented as a poster at the IDWEEK 2017 Conference, October 4–8, 2017, San Diego, CA, USA. Abstracts of the IDWEEK 2017 Conference have been published in a supplement issue of Open Forum Infectious Diseases (https://idsa.confex.com/idsa/2017/webprogram/POSTER.html).

Lymphogranuloma venereum (LGV) is a sexually transmitted infection caused by serovars L1, L2, and L3 of the bacterium *Chlamydia trachomatis*. The infection typically causes genital ulcers, proctitis, or femoral/inguinal lymphadenopathy with or without constitutional symptoms. In the past decade, outbreaks of LGV have been reported in North America, Australia, and Europe, mainly as proctitis among HIV-infected men who have sex with men (MSM) (*1*). We report a patient with pharyngitis, proctitis, and cervical lymphadenitis in whom LGV-specific DNA was detected by real-time reverse transcription PCR (RT-PCR) in a cervical lymph node fine-needle aspirate.

The patient was a 48-year-old, HIV-positive man in Croatia who came to an outpatient HIV clinic in August 2014 with perianal pain for 10 days and bloody rectal discharge with normal stool consistency. He also reported a painful, enlarged cervical lymph node but did not have a sore throat. On the first day of the illness, he had fever, which subsided the next day. He reported having unprotected receptive anal and oral sex with other men while visiting Berlin, Germany, 2 weeks earlier. Clinical examination demonstrated exudate on the right tonsil, a painful and enlarged right cervical lymph node (5 × 2 cm) (online Technical Appendix Figure, https://wwwnc.cdc.gov/EID/article/24/4/17-1872-Techapp1.pdf), perianal pain on palpation, and a purulent rectal discharge.

The patient was given a diagnosis of HIV infection in 2002 and had been receiving antiretroviral therapy since July 2002. Plasma viremia had been undetectable since October 2002, and his CD4+ T-cell count before this illness was 2,082 cells/mm^3. His clinical history included treatment for neurosyphilis, epilepsy, and diarrhea caused by *Microsporidiae* spp., *Blastocystis hominis*, and *Entamoeba histolytica*.

During examination at the HIV clinic, specimens were obtained from the pharynx, rectum, and urine for culture and a nucleic acid amplification test (NAAT). During fine-needle aspiration of a cervical lymph node, ≈1 mL of pus was removed and analyzed. The lymph node aspirate and a rectal swab specimen were positive for *C. trachomatis* DNA by the *C. trachomatis*/*Neisseria gonorrhoeae* RT-PCR (Abbott Laboratories, Abbott Park, IL, USA).

Cytologic examination of the fine-needle aspirate of the affected lymph node predominantly showed elements of granulomatous inflammation. An indirect immunofluorescence assay serum test result for *C. trachomatis* antibodies was positive (IgG titer >1:512, IgA titer 1:256). Test results for *N. gonorrhoeae* were negative (culture of the rectal swab and NAAT for urine and rectum). Results of a throat culture for *Streptococcus pyogenes* and routine lymph node aspirate culture for bacteria were also negative. Serum serologic test results were negative for acute infection with *Treponema pallidum, Bartonella* spp., and *Toxoplasma gondii*.

Table. Characteristics of 8 patients with lymphogranuloma venereum and cervical lymphadenopathy*

Reference	Patient age, y/sex	Clinical presentation	Method of laboratory confirmation	Therapy/duration
Andrada et al. (*7*)	30/M	Mouth ulcer, weight loss, cervical lymphadenopathy	Serologic analysis	Tetracycline/5 wk
Thorsteinsson et al. (*3*)	31/M	Fever, supraclavicular, axillar, retroperitoneal, and cervical lymphadenopathy	Serologic analysis	Tetracycline/4 wk
Watson et al. (*6*)	19/F	Sore throat, tonsillitis, arthritis, erythema nodosum, cervical lymphadenopathy	Serologic analysis	Phenoxymethylpenicillin, indomethacin, erythromycin†
Albay and Mathisen (*5*)	18/F	Fever, cervical lymphadenopathy	Serologic analysis	Ampicillin/sulbactam, doxycycline†
Tchernev et al. (*8*)	36/M	Facial skin lesions, cervical and axillary lymphadenopathy	NAAT: *Chlamydia trachomatis* DNA in skin lesions and serologic analysis	Surgical excision of cervical lymph nodes; pentamidine and doxycycline/3 wk
Dosekun et al. (*4*)	32/M	Sore throat, cervical lymphadenopathy, odynophagia, mouth ulcer, proctitis, cervical lymphadenopathy	NAAT: LGV-specific DNA in pharyngeal swab specimen	Amoxicillin/1 wk, doxycycline/1 wk
Dosekun et al. (*4*)	27/M	Sore throat, cervical lymphadenopathy, odynophagia, mouth ulcer, proctitis, cervical lymphadenopathy	NAAT: LGV-specific DNA in pharyngeal and rectal swab specimens	Azithromycin/1 g, doxycycline/2 wk
This study	48/M	Fever, cervical lymphadenopathy, proctitis	NAAT: LGV-specific DNA in cervical lymph node sample obtained by fine-needle aspirate; serologic analysis	Ceftriaxone/5 d, doxycycline/6 wk

*LGV, lymphogranuloma venereum; NAAT, nucleic acid amplification test.
†Duration of therapy not reported.

DNA from the lymph node specimen was frozen and sent to Public Health England (London, UK) in February 2017. LGV-specific DNA was detected by using an in-house TaqMan RT-PCR. The sequence of the outer membrane protein gene from lymph node punctate was identical to that of the *C. trachomatis* L2 reference strain L2/434/Bu.

At the initial visit, the patient was treated with intravenous ceftriaxone (2 g) and oral doxycycline (2 × 100 mg). After NAATs showed *C. trachomatis* infection, only doxycycline therapy was continued. Symptoms of proctitis subsided in 2 days. However, because cervical lymphadenitis persisted, we treated the patient with a prolonged course (6 weeks) of doxycycline. Eventually, the patient showed a full recovery.

Our report indicates that LGV might be present in MSM in Croatia. The first NAAT-confirmed case of LGV in southeastern Europe was reported in Slovenia and described an HIV-negative MSM who was ill in 2015 (*2*). LGV is probably underdiagnosed in southeastern Europe because of lack of diagnostics and awareness of the infection.

There have been only a few case reports of LGV with associated cervical lymphadenopathy (*3*–*8*) (Table). Some cases had generalized lymphadenopathy (axillar, supraclavicular, and retroperitoneal) with constitutional symptoms (*3*); pharyngitis/odynophagia/proctitis/tongue soreness (*4*,*7*); constitutional symptoms (*5*,*7*); tonsillitis (*6*); or skin lesions (*8*). Case reports have also been described of LGV with supraclavicular and mediastinal lymphadenopathy without cervical involvement (*9*). In all of these cases, infection with LGV caused by *C. trachomatis* was established by serologic testing or an NAAT for a pharyngeal specimen. It is essential to maintain a high level of clinical suspicion for LGV in MSM even if noninguinal/femoral lymph nodes are affected.

The recommended treatment for LGV is doxycycline for 21 days. However, several clinical observations have suggested that a 21-day course of doxycycline therapy is insufficient for treating inguinal bubonic LGV (*2*,*10*), Recommendations have been given to carefully follow up with patients and continue doxycycline treatment until symptoms resolve (*10*). We followed these recommendations for our patient who had bubonic cervical lymph node LGV.

Acknowledgment

We thank the patient for providing permission to publish the case.

This study was partially supported by the Croatian Science Foundation (project no. IP-2014-09-4461) and the European Centre for Disease Prevention and Control (service contract no. ECD.6300).

Dr. Gjurašin is a fourth-year resident in infectious diseases at the University Hospital for Infectious Diseases Dr. Fran Mihaljević, Zagreb, Croatia. His primary research interests are infectious diseases of the central nervous system, sexually transmitted infections, zoonoses, and implementation of antimicrobial drug stewardship in Croatia.

References

1. de Vrieze NH, de Vries HJ. Lymphogranuloma venereum among men who have sex with men. An epidemiological and clinical review. Expert Rev Anti Infect Ther. 2014;12:697–704. http://dx.doi.org/10.1586/14787210.2014.901169
2. Matičič M, Klavs I, Videčnik Zorman J, Vidmar Vovko D, Kogoj R, Keše D. Confirmed inguinal lymphogranuloma venereum genovar L2c in a man who had sex with men, Slovenia, 2015. Euro Surveill. 2016;21:2–5. http://dx.doi.org/10.2807/1560-7917.ES.2016.21.5.30129
3. Thorsteinsson SB, Musher DM, Min KW, Gyorkey F. Lymphogranuloma venereum. A cause of cervical lymphadenopathy. JAMA. 1976;235:1882. http://dx.doi.org/10.1001/jama.1976.03260430052029
4. Dosekun O, Edmonds S, Stockwell S, French P, White JA. Lymphogranuloma venereum detected from the pharynx in four London men who have sex with men. Int J STD AIDS. 2013;24:495–6. http://dx.doi.org/10.1177/0956462412472830
5. Albay DT, Mathisen GE. Head and neck manifestations of lymphogranuloma venereum. Ear Nose Throat J. 2008;87:478–80.
6. Watson DJ, Parker AJ, Macleod TI. Lymphogranuloma venereum of the tonsil. J Laryngol Otol. 1990;104:331–2. http://dx.doi.org/10.1017/S0022215100112629
7. Andrada MT, Dhar JK, Wilde H. Oral lymphogranuloma venereum and cervical lymphadenopathy. Case report. Mil Med. 1974;139:99–101.
8. Tchernev G, Salaro C, Costa MC, Patterson JW, Nenoff P. Lymphogranuloma venereum: "a clinical and histopathological chameleon?" An Bras Dermatol. 2010;85:525–30. http://dx.doi.org/10.1590/S0365-05962010000400015
9. Bernstein DI, Hubbard T, Wenman WM, Johnson BL Jr, Holmes KK, Liebhaber H, et al. Mediastinal and supraclavicular lymphadenitis and pneumonitis due to *Chlamydia trachomatis* serovars L1 and L2. N Engl J Med. 1984;311:1543–6. http://dx.doi.org/10.1056/NEJM198412133112405
10. Oud EV, de Vrieze NH, de Meij A, de Vries HJ. Pitfalls in the diagnosis and management of inguinal lymphogranuloma venereum: important lessons from a case series. Sex Transm Infect. 2014;90:279–82. http://dx.doi.org/10.1136/sextrans-2013-051427

Address for correspondence: Branimir Gjurašin, University Hospital for Infectious Diseases Dr. Fran Mihaljević, Mirogojska Cesta 8, 10000 Zagreb, Croatia; email: brangjur@gmail.com

Letters

Letters commenting on recent articles as well as letters reporting cases, outbreaks, or original research are welcome. Letters commenting on articles should contain no more than 300 words and 5 references; they are more likely to be published if submitted within 4 weeks of the original article's publication. Letters reporting cases, outbreaks, or original research should contain no more than 800 words and 10 references. They may have 1 Figure or Table and should not be divided into sections. All letters should contain material not previously published and include a word count.

Zika Virus MB16-23 in Mosquitoes, Miami-Dade County, Florida, USA, 2016

John-Paul Mutebi, Holly R. Hughes, Kristen L. Burkhalter, Linda Kothera, Chalmers Vasquez, Joan L. Kenney

Author affiliations: Centers for Disease Control and Prevention, Fort Collins, Colorado, USA (J.-P. Mutebi, H.R. Hughes, K.L. Burkhalter, L. Kothera, J.L. Kenney); Miami-Dade County Mosquito Control, Miami, Florida, USA (C. Vasquez)

DOI: https://doi.org/10.3201/eid2404.171919

We isolated a strain of Zika virus, MB16-23, from *Aedes aegypti* mosquitoes collected in Miami Beach, Florida, USA, on September 2, 2016. Phylogenetic analysis suggests that MB16-23 most likely originated from the Caribbean region.

In 2016, outbreaks of locally transmitted Zika virus occurred in Miami (Wynwood neighborhood) and Miami Beach, in Miami-Dade County, Florida, USA (*1*). During these outbreaks, a Centers for Disease Control and Prevention (CDC) emergency response team was deployed to assist Miami-Dade County disease surveillance and control efforts. CDC entomologists within the CDC emergency response team worked with Miami-Dade County Mosquito Control and sampled mosquito populations using BG-Sentinel type-2 traps (Biogents AG, Regensburg, Germany) to determine basic entomological parameters. Routinely, mosquitoes were collected, identified to species on the basis of the morphologic characteristics described by Darsie and Ward (*2*), and shipped inactivated and preserved in RNAlater (Ambion Inc., Austin, TX, USA) to the Bronson Animal Disease Diagnostic Laboratory (Kissimmee, FL, USA) for Zika virus testing.

In addition to the routine outbreak protocol, 2 BG-Sentinel type-2 traps were placed at a construction site near the intersection of James Avenue and Lincoln Road (25°47′25.68″N, 80°07′50.24″W) in Miami Beach on September 1, 2016. This site was selected because it was adjacent to a site where Zika cases had been detected. On September 2, 2016, the mosquitoes captured were frozen and shipped on dry ice to the CDC laboratory in Fort Collins, Colorado, USA. In the laboratory, the mosquitoes were identified to species on chill tables; female *Aedes aegypti* mosquitoes were separated into pools of 50 mosquitoes or less. A total of 293 female *Ae. aegypti* mosquitoes were collected (146.5/trap/day), grouped into 7 pools, and processed for presence of arboviral agents by cytopathic effect (CPE) assay.

We triturated pools of mosquitoes in 500 μL of Dulbecco's modified Eagle medium complete with penicillin

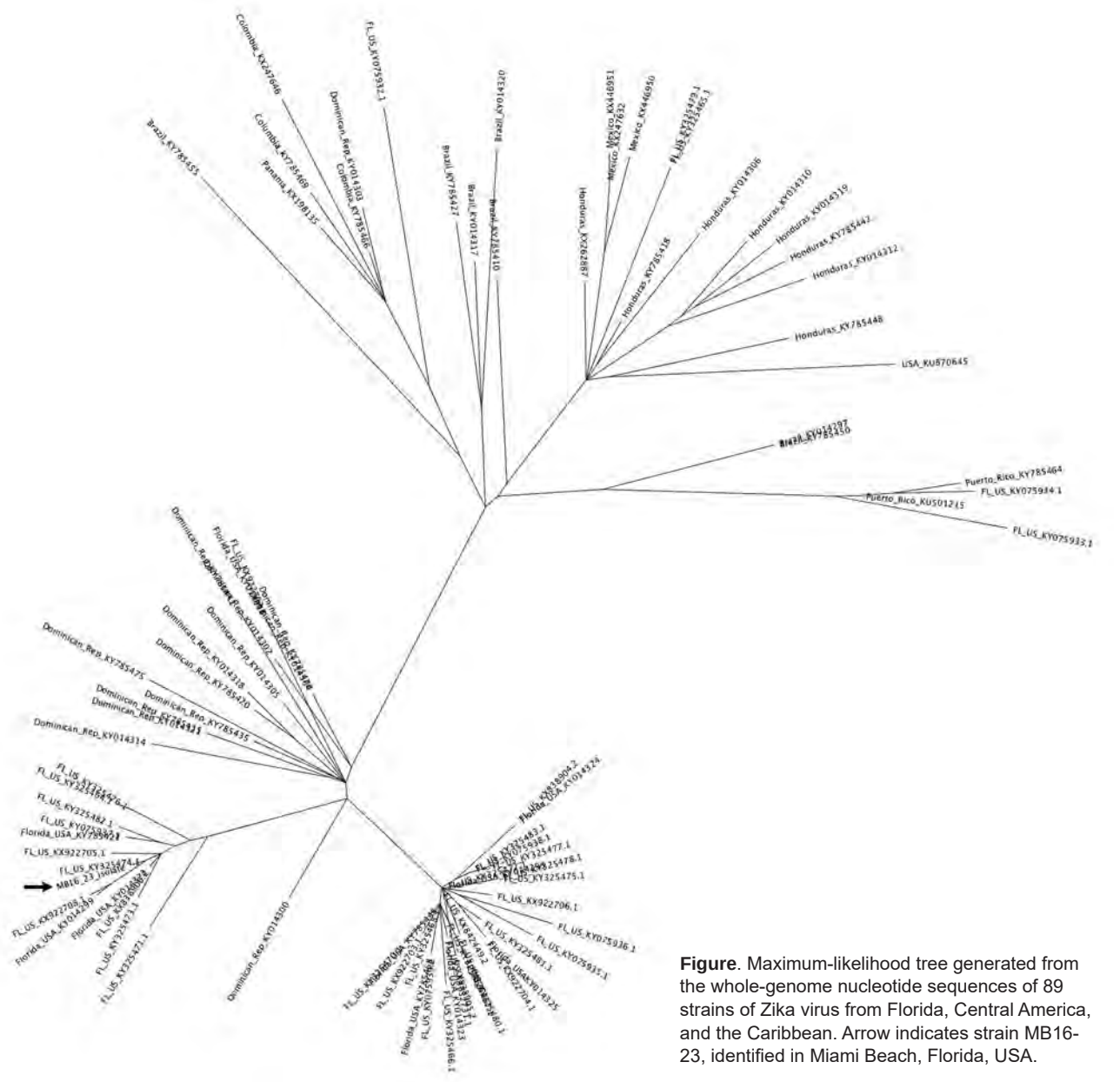

Figure. Maximum-likelihood tree generated from the whole-genome nucleotide sequences of 89 strains of Zika virus from Florida, Central America, and the Caribbean. Arrow indicates strain MB16-23, identified in Miami Beach, Florida, USA.

(100 U/mL), streptomycin (100 mg/mL), 20% fetal bovine serum, and 50 μg/mL amphotericin B. We used the clarified supernatants from triturated mosquito pools to inoculate Vero (mammalian) cells in 24-well plates. We observed the inoculated cells daily and harvested them upon the appearance of CPE. Of the mosquito pools processed, only 1 pool of 50 female *Ae. aegypti* mosquitoes caused CPE. Final titration of the Vero passage was 7.02 $\log_{10}$ PFU/mL. We reinoculated the harvested supernatant onto *Ae. albopictus* C6/36 cells; these cell cultures were maintained at 28°C with complete Dulbecco's modified Eagle medium supplemented with 2% fetal bovine serum and penicillin/streptomycin. We extracted viral RNA from 140 μL of the supernatant harvested from the C6/36 cell cultures using a QIAamp RNA Mini Kit (QIAGEN, Valencia, CA, USA). We performed reverse transcription PCR confirmation on the extracted RNA using flavivirus-specific primers, as described previously (*3*).

We performed all procedures using commercial products according to the manufacturer's protocols unless otherwise noted. We generated cDNA from extracted RNA using the NuGEN Ovation RNA-seq system V2 (NuGEN Technologies, San Carlos, CA, USA). Libraries were constructed using the Ion Xpress Plus gDNA Fragment Library preparation kit (Life Technologies, Carlsbad, CA, USA) by fragmenting cDNA for 1.5 min, generating fragments of

250 bp on average; we quantified the libraries using the Ion Library TaqMan Quantitation kit (Life Technologies).

We performed whole-genome sequencing on the Ion Torrent Personal Genome Machine system (Life Technologies) and completed preparation of template-positive ion sphere particles using the Ion OneTouch 2 system and Ion PGM Hi-Q OT2 Kit (Life Technologies). We loaded Ion spheres into an Ion 316 Chip v2 (Life Technologies) and sequenced them on the Ion Torrent Personal Genomics Machine instrument using the Ion PGM Hi-Q sequencing kit (Life Technologies). We generated full genome sequences using a templated assembly in SeqMan NGen (DNASTAR, Madison, WI, USA) and using Zika virus strain PRVABC-59 (GenBank accession no. KX377337) as a reference. We subjected consensus genomes generated by templated assemblies to BLAST analysis (http://www.ncbi.nlm.nih.gov/BLAST) and determined that they were >98% similar to the respective reference sequences.

We aligned the full genome sequence of MB16-23 (GenBank accession no. MF988743) with available sequences in the National Center for Biotechnology Information database (NCBI Bioprojects PRJNA342539 [*4*] and PRJNA344504 [*5*]) using MUSCLE (*6*) on the Cipres Science Gateway (*7*). We performed maximum-likelihood inference with GTRCAT majority rule criterion bootstrapping using RAxML-HPC2 on XSEDE of the Cipres Science Gateway (*8*). We edited output trees with FigTree version 1.4 (http://tree.bio.ed.ac.uk/software).

Phylogenetic analysis showed that MB16-23 was closely related to 9 other sequences from Miami, suggesting a common origin to all these sequences (Figure), and was also closely related to the sequence DominicanRepublic_KY014300, from Santo Domingo, Dominican Republic. This finding suggests that MB16-23 and the 9 related sequences originated from a strain or strains introduced from the Caribbean region. Our results support previous observations that genomes collected in Miami-Dade County during July 2016–November 2016 share a common ancestor with genomes localized to the Caribbean area, particularly the Dominican Republic (*4*,*5*).

In summary, we report an isolate of Zika virus, strain MB16-23, from a pool of 50 *Ae. aegypti* mosquitoes collected in Miami Beach, Florida. Phylogenetic analysis suggests that MB16-23 shares a common ancestor with other Florida Zika virus genomes as well as genomes localized to the Caribbean region.

About the Author

Dr. Mutebi is a research entomologist with the Division of Vector-Borne Diseases, National Center for Emerging and Zoonotic Infectious Diseases, Centers for Disease Control and Prevention, Fort Collins, Colorado, USA. His research interests include mosquito surveillance and control methods, mosquito–virus interactions, and mosquito genetics and population genetics.

References

1. Likos A, Griffin I, Bingham AM, Stanek D, Fischer M, White S, et al. Local mosquito-borne transmission of Zika virus—Miami-Dade and Broward Counties, Florida, June–August 2016. MMWR Morb Mortal Wkly Rep. 2016;65:1032–8. http://dx.doi.org/10.15585/mmwr.mm6538e1
2. Darsie RF Jr, Ward RA. Identification and geographical distribution of the mosquitoes of North America, north of Mexico. Gainesville (FL): University Press of Florida. 2005.
3. Kuno G, Chang GJ, Tsuchiya KR, Karabatsos N, Cropp CB. Phylogeny of the genus Flavivirus. J Virol. 1998;72:73–83.
4. Grubaugh ND, Ladner JT, Kraemer MUG, Dudas G, Tan AL, Gangavarapu K, et al. Genomic epidemiology reveals multiple introductions of Zika virus into the United States. Nature. 2017;546:401–5. http://dx.doi.org/10.1038/nature22400
5. Metsky HC, Matranga CB, Wohl S, Schaffner SF, Freije CA, Winnicki SM, et al. Zika virus evolution and spread in the Americas. Nature. 2017;546:411–5. http://dx.doi.org/10.1038/nature22402
6. Edgar RC. MUSCLE: multiple sequence alignment with high accuracy and high throughput. Nucleic Acids Res. 2004;32:1792–7. http://dx.doi.org/10.1093/nar/gkh340
7. Miller MA, Pfeiffer W, Schwartz T. Creating the CIPRES Science Gateway for inference of large phylogenetic trees. Paper presented at: Gateway Computing Environments Workshop, November 14, 2010, New Orleans, LA.
8. Stamatakis A. RAxML version 8: a tool for phylogenetic analysis and post-analysis of large phylogenies. Bioinformatics. 2014;30:1312–3. http://dx.doi.org/10.1093/bioinformatics/btu033

Address for correspondence: John-Paul Mutebi, Centers for Disease Control and Prevention, 3150 Rampart Rd, Fort Collins, CO 80521, USA; email: grv0@cdc.gov

Identification of Wild Boar–Habitat Epidemiologic Cycle in African Swine Fever Epizootic

Erika Chenais, Karl Ståhl, Vittorio Guberti, Klaus Depner

Author affiliations: National Veterinary Institute, Uppsala, Sweden (E. Chenais, K. Ståhl); National Institute for Environmental Protection and Research, Rome, Italy (V. Guberti); Friedrich Loeffler Institute, Greifswald-Insel Riems, Germany (K. Depner)

DOI: https://doi.org/10.3201/eid2404.172127

The African swine fever epizootic in central and eastern European Union member states has a newly identified component involving virus transmission by wild boar and virus

survival in the environment. Insights led to an update of the 3 accepted African swine fever transmission models to include a fourth cycle: wild boar–habitat.

The main components in the epidemiology of African swine fever (ASF) have been known since the first description of the disease: soft *Ornithodoros* spp. ticks, warthogs, domestic pigs, and pig-derived products such as pork. Three independent epidemiologic cycles (sylvatic, tick–pig, and domestic) have been described (*1*) (Figure). In the sylvatic cycle, ASF virus circulates between the natural reservoirs of the virus (i.e., warthogs and soft ticks), without causing disease in the warthogs. This ancient cycle is the origin of the tick–pig cycle and the domestic cycle and thus the origin of ASF as a disease. In the tick–pig cycle, the virus circulates between soft ticks and domestic pigs. This cycle has mainly been described in sub-Saharan Africa, but also played an important role during the epizootic on the Iberian Peninsula. In the domestic cycle, the virus is transmitted among domestic pigs, or from pig products to domestic pigs. This cycle does not involve the natural reservoirs.

In 2007, ASF was introduced into Georgia in Eurasia. The epizootic was not brought under control, and the disease spread to the surrounding countries, including the Russian Federation, and further to Belarus and Ukraine (*2*). In 2014, ASF reached the European Union (EU) member states of Estonia, Latvia, Lithuania, and Poland; in 2016, Moldova; and in 2017, the Czech Republic and Romania. In the ongoing epizootic in the Caucasus, Moldova, Romania, the Russian Federation, and Ukraine, the epidemiology seems to follow the common domestic cycle: the infection circulates among small pig farms, affecting few commercial farms, and somewhat frequently spills over to wild boar (*3*). A similar cycle has been present in Sardinia since 1978 (*1*). Since 2014, the affected EU member states have applied a common reporting framework and shared outbreak data. From these data, a previously undescribed epidemiologic pattern became evident: a cycle that focuses on the wild boar population and its habitat as a virus reservoir (*4*) (Figure). We suggest naming this cycle the wild boar–habitat cycle.

In the ongoing epizootic, ASF disease dynamics have proven to be complex and difficult to control (*5*). ASF prevalence remains <5%, and a pattern of local persistence with slower than expected dynamic spatial spread is evident, estimated at an average of 1–2 km/month (*6*). During

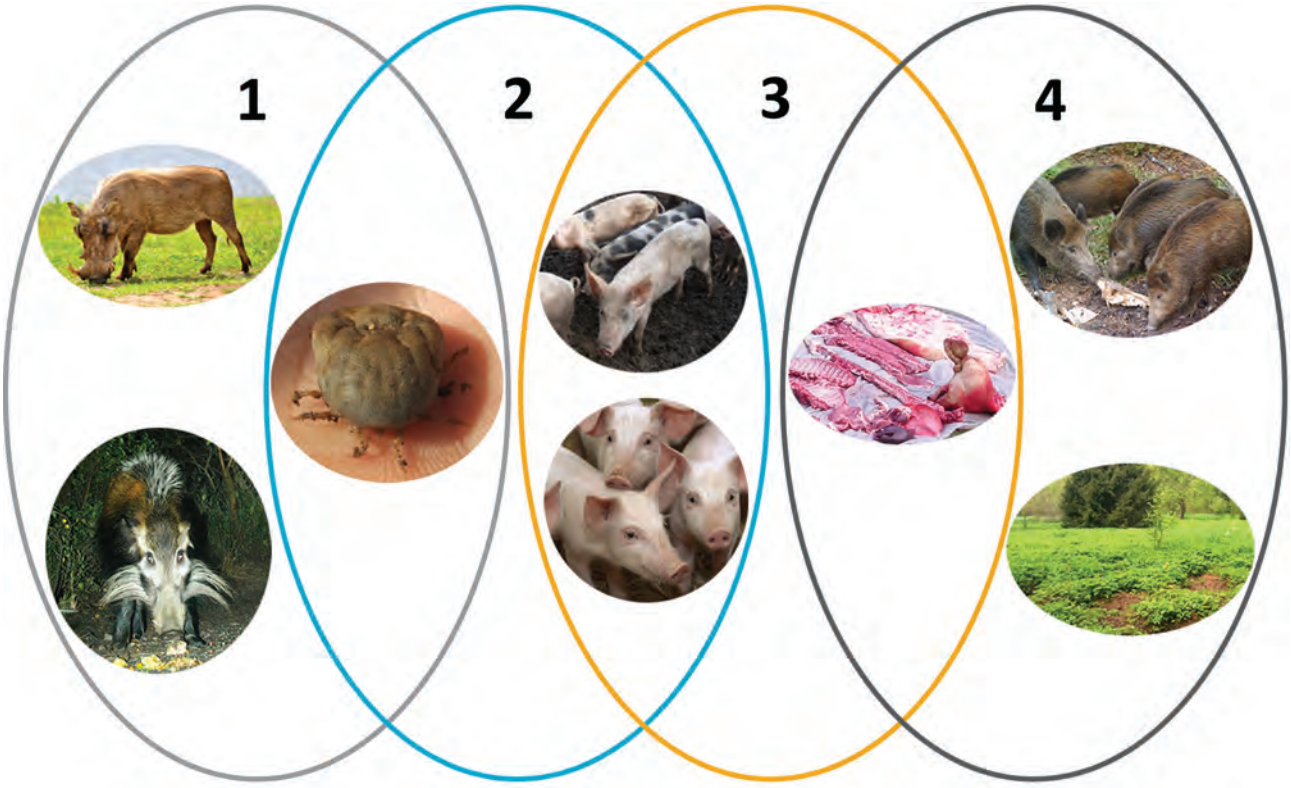

Figure. The 4 epidemiologic cycles of African swine fever and main transmission agents. 1) Sylvatic cycle: the common warthog (*Phacochoerus africanuus*), bushpig (*Potamochoerus larvatus*), and soft ticks of *Ornithodoros* spp. The role of the bushpig in the sylvatic cycle remains unclear. 2) The tick–pig cycle: soft ticks and domestic pigs (*Sus scrofa domesticus*). 3) The domestic cycle: domestic pigs and pig-derived products (pork, blood, fat, lard, bones, bone marrow, hides). 4) The wild boar–habitat cycle: wild boar (*S. scrofa*), pig- and wild boar–derived products and carcasses, and the habitat.

2016 in the Baltic states, ≤85% of wild boar found dead were ASF virus–positive, although virus prevalence in hunted wild boar was very low (0.5%–3%) (*6*). Currently, a standardized approach for estimating prevalence is lacking, and depending on which areas (infected, surveillance, or unrestricted zones) and categories (found dead, killed in car accidents, or hunted) of wild boar that are included, the reported figures can underestimate or overestimate the true prevalence. The prevalence of antibody-positive hunted wild boar is lower than the virus prevalence for all infected countries and has no clear temporal trend. The low prevalence in hunted wild boar is to be expected, because this group represents an apparently healthy population, considering the nature of the disease and its high case-fatality rate among wild boar (*7*).

The wild boar–habitat cycle is characterized by both direct transmission between infected and susceptible wild boar and indirect transmission through carcasses in the habitat. The habitat contamination from ASF virus–positive wild boar carcasses, and the possible subsequent intraspecies scavenging (*8*), offer possibilities for both low-dose and high-dose infections, depending on landscape, time, season, and carcass decomposition. These epidemiologic drivers of disease intermingle with wild boar population determinants such as wild boar demography, including fertility; management factors such as winter feeding to avoid wild boar population crashes associated with cold weather and feed scarcity; hunting rates; hunting techniques; and hunting bag composition. Positive associations between wild boar population density and ASF have been found (*4*), but contrary to earlier predictions, wild boar density does not seem to be a strictly limiting factor for persistence (*9*). The long-term availability of the virus in infected carcasses overtakes the expected density-dependent transmission pattern and enables the virus to persist despite any wild boar depopulation effort and the high mortality rate (*10*). Environmental persistence of the virus is favored by a cold and moist climate. In the ongoing outbreak, geography, ecology, meteorology, and wild boar demography all affect the epidemiology, and each contributes to the viability of the wild boar–habitat cycle. This association further suggests that ASF may persist in the habitat despite low availability of susceptible hosts.

Despite each epidemiologic cycle being independent, intercycle disease transmission will occasionally occur. Just as the intracycle spread in the domestic transmission cycle, such spread can be anthropogenic. Anthropogenic factors and intercycle spread from the domestic cycle to the wild boar–habitat transmission cycle seem to be causative factors for long-distance spread of ASF, thus contributing to sustaining and enlarging the geographic range of the wild boar–habitat transmission cycle in the ongoing epizootic.

This research received support from the *CA COST Action CA15116* "Understanding and Combating African Swine Fever in Europe (ASF-STOP)," funded by the EU Framework Programme Horizon 2020.

About the Author

Dr. Chenais is a veterinary epidemiologist at the National Veterinary Institute in Sweden. Her main research interests are African swine fever epidemiology, animal disease impact in low-income countries, and the role that humans play in infectious disease epidemiology.

References

1. Costard S, Mur L, Lubroth J, Sanchez-Vizcaino JM, Pfeiffer DU. Epidemiology of African swine fever virus. Virus Res. 2013;173:191–7. http://dx.doi.org/10.1016/j.virusres.2012.10.030
2. Gavier-Widén D, Ståhl K, Neimanis AS, Hård av Segerstad C, Gortázar C, Rossi S et al. African swine fever in wild boar in Europe: a notable challenge. [Editorial]. Vet Rec. 2015;176:199–200. http://dx.doi.org/10.1136/vr.h699
3. EFSA Panel on Animal Health and Welfare. Scientific opinion on African swine fever. EFSA Journal- 2014;12:3628. http://dx.doi.org/10.2903/j.efsa.2014.3628
4. Beltrán-Alcrudo D, Arias M, Gallardo C, Kramer S, Penrith ML. African swine fever: detection and diagnosis—a manual for veterinarians. Rome: Food and Agriculture Organization of the United Nations; 2017 [cited 2017 Dec 21]. https://www.researchgate.net/publication/318347207_African_swine_fever_detection_and_diagnosis_-_A_manual_for_veterinarians
5. Nurmoja I, Schulz K, Staubach C, Sauter-Louis C, Depner K, Conraths FJ, et al. Development of African swine fever epidemic among wild boar in Estonia—two different areas in the epidemiological focus. Sci Rep. 2017;7:12562. http://dx.doi.org/10.1038/s41598-017-12952-w
6. European Food Safety Authority (EFSA), Cortiñas Abrahantes J, Gogin A, Richardson J, Gervelmeyer A. Epidemiological analyses on African swine fever in the Baltic countries and Poland. EFSA Journal. 2017;15:4732. http://dx.doi.org/10.2903/j.efsa.2017.5068
7. Blome S, Gabriel C, Beer M. Pathogenesis of African swine fever in domestic pigs and European wild boar. Virus Res. 2013;173:122–30. http://dx.doi.org/10.1016/j.virusres.2012.10.026
8. Probst C, Globig A, Knoll B, Conraths FJ, Depner K. Behaviour of free ranging wild boar towards their dead fellows: potential implications for the transmission of African swine fever. R Soc Open Sci. 2017;4:170054. http://dx.doi.org/10.1098/rsos.170054
9. European Food Safety Authority. Evaluation of possible mitigation measures to prevent introduction and spread of African swine fever virus through wild boar. EFSA Journal. 2014;12:3616. http://dx.doi.org/10.2903/j.efsa.2014.3616
10. European Food Safety Authority, Depner K, Gortazar C, Guberti V, Masiulis M, More S, Oļševskis E, et al. Epidemiological analyses of African swine fever in the Baltic States and Poland. EFSA Journal. 2017;15(11):5068. http://dx.doi.org/10.2903/j.efsa.2017.5068

Address for correspondence: Erika Chenais, National Veterinary Institute (SVA), Department of Disease Control and Epidemiology, Uppsala 75189, Sweden; email: erika.chenais@sva.se

Two Cases of Dengue Fever Imported from Egypt to Russia, 2017

Muhammad A. Saifullin, Victor P. Laritchev, Yana E. Grigorieva, Nadezhda N. Zvereva, Anna M. Domkina, Ruslan F. Saifullin, Marina V. Bazarova, Yulia A. Akinshina, Ludmila S. Karan, Aleksandr M. Butenko

Author affiliations: Research Institute of Epidemiology and Microbiology n.a. N.F. Gamalei, Moscow, Russian Federation (M.A. Saifullin, V.P. Laritchev, Y.A. Akinshina, A.M. Butenko); Municipal Infectious Diseases Hospital No. 1, Moscow (M.A. Saifullin, R.F. Saifullin, M.V. Bazarova); Central Scientific Research Institute of Epidemiology, Moscow (Y.E. Grigorieva, L.S. Karan); Pirogov Russian National Research Medical University, Moscow (N.N. Zvereva, R.F. Saifullin); Municipal Infectious Diseases Hospital No. 2, Moscow (A.M. Domkina)

DOI: https://doi.org/10.3201/eid2404.172131

In 2017, two cases of dengue fever were imported from Hurghada, Egypt, where dengue fever was not considered endemic, to Moscow. These cases show how emergence of dengue fever in popular resort regions on the coast of the Red Sea can spread infection to countries where it is not endemic.

From 2012, when registration of dengue fever cases became official in the Russian Federation, through December 2017, ≈700 cases of imported dengue fever have been registered in Russia (*1*). Of these, ≈90% of cases were associated with travel to southern and Southeast Asia, mainly Thailand. In 2015, almost 2.5 million Russian citizens visited Egypt (the fifth most popular destination for tourists from Russia) (*2*). After a plane crash caused by a terrorist attack on October 31, 2015, air connections and tours to Egypt were stopped; however, many Russian citizens with relatives or real estate in resort areas of Egypt still travel there.

In Africa, dengue fever is endemic to 34 countries, including Egypt. During 1960–2010, a total of 20 confirmed outbreaks in 15 countries were registered (*3*). For the past 7 years, outbreaks in East Africa have been registered in Somalia (2011, 2013), Kenya (2011, 2013, 2014), Tanzania (2013, 2014), and Mozambique (2014). In 2017, outbreaks were registered in 8 countries, 6 in West Africa and 2 in East Africa (Kenya, Seychelles). In Sudan, which is bordered on the north by Egypt, outbreaks were registered in 2010, 2011, and 2014 (*4*,*5*).

Dengue fever cases have been registered earlier in Egypt; the last outbreak was in 2015 in Dairut, but there are no data about outbreaks in cities on the coast of the Red Sea (e.g., Hurghada, Sharm El-Sheikh, and Dahab), which have become resort destinations for Russian citizens (*6*). In October 2017, the health department of the Red Sea governorate reported cases of dengue fever in El Qoseir, a city 145 km south of Hurghada, with a population of ≈50,000. Preliminary results indicated that 1,200–2,500 persons were infected (*7*,*8*). Since November 2017, six cases of dengue among tourists returning from Hurghada (*9*,*10*) were reported in Belgium (*1*), Austria (*1*), and Germany (*4*). Until 2017, to our knowledge, no cases of dengue fever had been imported from Egypt to Russia. We report 2 cases in persons returning to Russia after visiting Hurghada.

Patient 1 was a 63-year-old female Moscow resident. During October 12–28, 2017, she had visited relatives in Hurghada, stayed in their apartment, and noted multiple insect bites. On October 18, she experienced acute onset of chills, fever, and aches. She did not seek medical care and did not measure her temperature. She took acetaminophen to control her symptoms. Over 10 days, her health gradually improved, but the fatigue remained. After returning to Moscow, she noted low-grade fever (up to 37.0°C) and was hospitalized in Infectious Clinical Hospital No. 1 with a diagnosis of fever of unknown origin. At admission, she complained of fatigue, restless sleep, dizziness, and tinnitus. Her general condition was stable and her temperature was 37.5°C; physical examination revealed no significant abnormalities. Complete blood count, urinalysis, and biochemical test results were within normal limits. On day 32 after symptom onset, serum testing by IgM antibody capture (MAC)–ELISA (in-house kit) detected IgM (titer 1:1,600) and IgG ELISA detected IgG (titer 1:12,800) against dengue virus (DENV). On day 34, real-time PCR (Dengue Real-TM Genotype; Sacace Biotechnologies, Como, Italy), used according to the manufacturer's instructions, detected DENV type 2 RNA in urine (detected on 35th amplification cycle). Patient 1 received symptomatic treatment and was discharged after improvement with no complications.

Patient 2 was a 49-year-old male Moscow resident. During October 28–November 17, 2017, he had vacationed in Hurghada, stayed in a hotel, and noted insect bites. He denied having had contact with ill persons. On November 15, he experienced acute onset of chills, fatigue, and fever (39.0°C). He did not seek medical care and did not measure his temperature again. He took nonsteroidal antiinflammatory medications to control his symptoms. After returning to Moscow (via Istanbul), he was taken by emergency ambulance to Municipal Infectious Diseases Hospital No. 2, where he was hospitalized for suspected malaria. At admission, he had fever and rash. His general condition was stable and his temperature was 39.0°C. Physical examination revealed mild macular rash and liver enlargement 3 cm below the edge of the costal arch. Complete blood count indicated thrombocytopenia (106×10^9 thrombocytes/L) and

leukopenia (1.8×10^9 cells/L); urinalysis and biochemical test results were within normal limits. On day 7 after symptom onset, real-time PCR (Dengue Real-TM Genotype) detected DENV type 2 RNA in blood (25th cycle) and urine (30th cycle). Patient 2 received symptomatic treatment and was discharged after improvement with no complications.

The emergence of dengue fever on the coast of the Red Sea, a popular resort region for tourists from many countries, can lead to increased importation to countries where it is not endemic. Considering these 2 cases of dengue fever imported from Hurghada, Egypt, tourists should be informed about the risk for DENV infection before they travel, preventive measures should be explained, and tourists should be advised to seek medical care early if they experience symptoms.

Dr. M.A. Saifullin is a chief of the Isolation Department in the Municipal Infectious Diseases Hospital No.1, Moscow, Russian Federation, and a researcher in the arboviruses biology laboratory of the Research Institute of Epidemiology and Microbiology n.a. N.F. Gamalei, Moscow. His research interests include arboviral infections, tropical diseases, and travel medicine.

References

1. Rospotrebnadzor. About situation with dengue fever [in Russian] [cited 2017 Dec 21]. http://rospotrebnadzor.ru/about/info/news/news_details.php?ELEMENT_ID=7015
2. Rosturizm. Statistical indicators of mutual trips of citizens of the Russian Federation and citizens of foreign states [in Russian] [cited 2017 Dec 11]. https://www.russiatourism.ru/contents/statistika/
3. Were F. The dengue situation in Africa. Paediatr Int Child Health. 2012;32(Suppl 1):18–21. PubMed http://dx.doi.org/10.1179/2046904712Z.00000000048
4. World Health Organization. Weekly bulletins on outbreaks and other emergencies [cited 2018 Jan 3]. http://www.afro.who.int/health-topics/disease-outbreaks/outbreaks-and-other-emergencies-updates?page=0
5. Baba M, Villinger J, Masiga DK. Repetitive dengue outbreaks in East Africa: a proposed phased mitigation approach may reduce its impact. Rev Med Virol. 2016;26:183–96. PubMed http://dx.doi.org/10.1002/rmv.1877
6. World Health Organization. Dengue fever—Egypt [cited 2017 Dec 11]. http://www.who.int/csr/don/12-november-2015-dengue/en/
7. El-Sheikh S. Only 5% of Al-Qoseir citizens infected with dengue fever: Health Minister [cited 2017 Dec 11]. https://dailynewsegypt.com/2017/10/12/5-al-qoseir-citizens-infected-dengue-fever-health-minister
8. Mahmoud M. NGOs: 1,200 infected with dengue fever in Red Sea governorate [cited 2017 Dec 11]. https://www.egypttoday.com/Article/1/25517/NGOs-1-200-infected-with-dengue-fever-in-Red-Sea
9. Vandecasteele S, Marton S. Dengue/DHF update. ProMed. 2017 Dec 2 [cited 2018 Jan 3]. http://www.promedmail.org, archive no. 20171202.5478708.
10. Frank C. Dengue/DHF update. ProMed. 2018 Jan 1 [cited 2018 Jan 3]. http://www.promedmail.org, archive no. 20180101.5531177.

Address for correspondence: Muhammad A. Saifullin, Municipal Infectious Diseases Hospital No.1, Volokolamskoye Shosse, 63, 125310, Moscow, Russian Federation; email: dr_saifullin@mail.ru

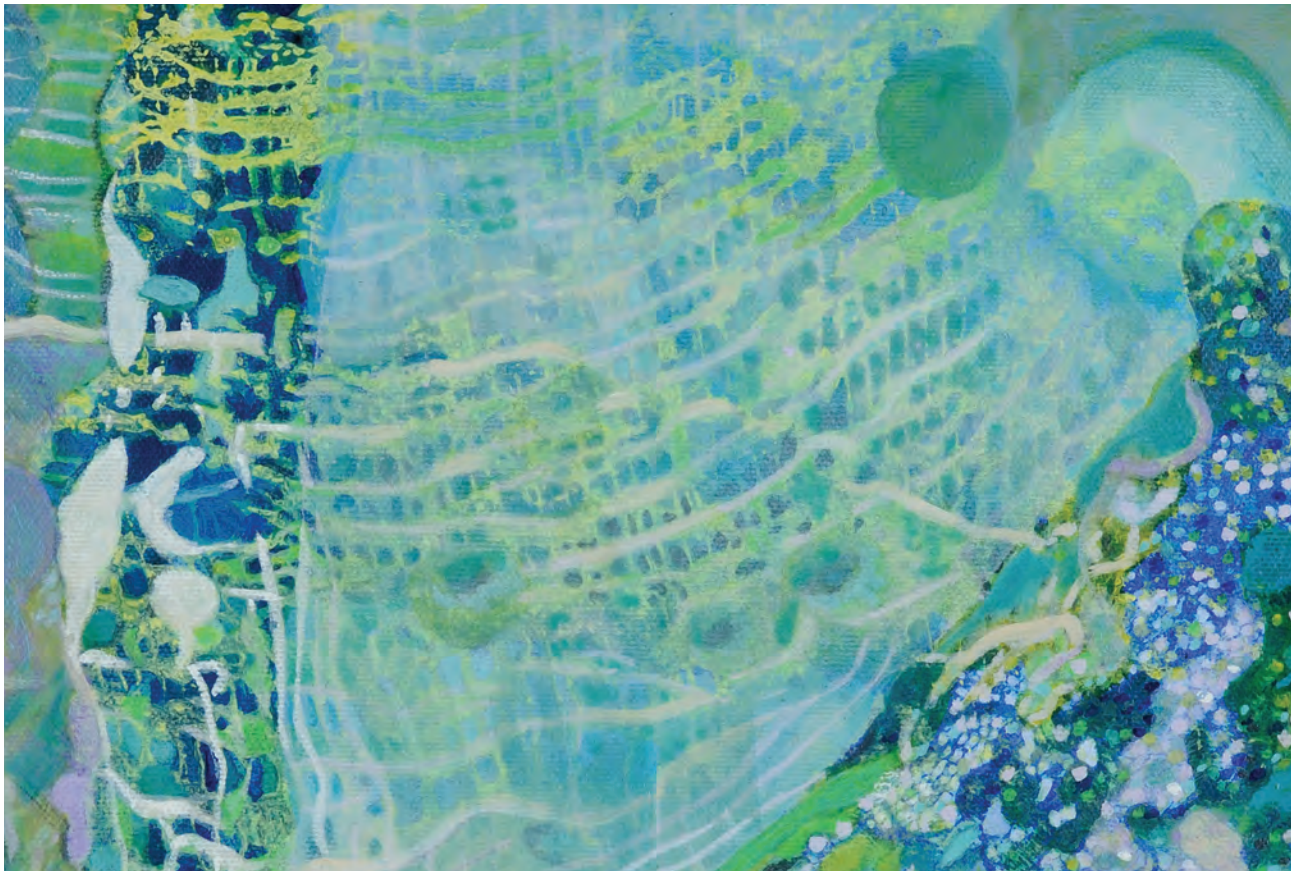

Patricia Goslee, (b. 1960), Water Prayer I, 2005 (detail). Acrylic on canvas, 11 in × 17 in/28 cm × 43 cm. Digital image courtesy of the artist. Washington, DC, United States.

"No Water, No Life. No Blue, No Green"

Byron Breedlove and J. Todd Weber

"Thousands have lived without love,
not one without water."

—W. H. Auden, "First Things First"

Water is the most precious and essential natural resource. If unadulterated and at room temperature, it is tasteless, odorless (to humans), and transparent. Water sustains life, reshapes topography, provides passage and conveyance, and delineates and destroys geopolitical boundaries. Water comprises ≈71% of Earth's surface, and the United States Geological Survey estimates that Earth is covered by more than 332,500,000 cubic miles (mi^3) of water. Archaeology, history, and anthropology corroborate that most civilizations originated near water. American marine biologist Sylvia Earl offers this perspective: "No water, no life. No blue, no green."

Vivid blues and greens interspersed with layers of white splash across this month's cover art, "Water Prayer I," one of a series of water-related pieces from the portfolio of artist Patricia Goslee, who lives in Washington, DC, United States. Her abstract work points to the possibility of mutability and transformation in water. A hazy hatchwork sweeps across the top of the painting and repeats in the lower right. Green and pale blue spheres of color float above the patterns. Dominating the image, a dense V-shaped amalgamation of speckled shapes—some uniform

Author affiliation: Centers for Disease Control and Prevention, Atlanta, Georgia, USA

DOI: https://doi.org/10.3201/eid2404.AC2404

and others elongated—streaks diagonally across the center of the canvas while a column of undulating forms juts up along the left side.

Goslee's water-themed painting can be viewed from divergent perspectives. It might be perceived as capturing a teeming collection of microorganisms inhabiting a drop of water. Conversely, it could suggest the proverbial 10,000-foot view, the stretched convergence of a city and river delta, interlaced with roads, canals, and lakes and dotted with buildings, fields, forests, and towns as viewed from an airplane window.

It may be a viewer's choice, because Goslee, who favors a style that is colorful and intuitive, approaches her painting without a preconceived plan. In her words, "It's a blank slate every time I start. I make marks, move and pour paint on the canvas. Sometimes I use spray paint, and sometimes I draw on the surface of the paintings. It all evolves and is ultimately a practice that allows me to process my experience of the world." (P. Goslee, pers. comm., 2018 Feb 11.)

"Flow" was an exhibition of Goslee's works displayed at the District of Columbia Arts Center in 2009–2010. Notes from this exhibition also offer perspective into her style of painting, "The most obvious unifying element in Goslee's mixed media work is pattern: layers of color and form operate as a visual metaphor for layers of awareness. The results achieved often depict isolated moments, visualizations."

Water is essential for life and for preserving health, but under certain circumstances, it can be the reservoir and conduit for pathogens that can lead to disease and death. Water is used in myriad ways to maintain hygiene, arguably handwashing being most critical for preventing the spread of organisms responsible for diseases as diverse as influenza and other respiratory infections, diarrheal disease, and healthcare-associated infections in hospitals. Water is critical for sterilization: steam under pressure has a long history of use for sterilization to prevent the spread of infections by reusable surgical instruments.

Water has been the source for infections of international and local importance. *Vibrio cholerae*, which preys on areas without adequate access to clean water and sanitation systems, has been responsible for 7 pandemics since the 19th century, killing millions of people across the globe. This organism remains endemic to many countries. *Legionella pneumophila* is transmitted by inhalation of contaminated aerosols from cooling towers, decorative fountains, hot water tanks, large plumbing systems, and the like. More recently, complex devices that use water and water drains have been identified as the site of biofilms harboring pathogens. Biofilms may form on a variety of water-associated surfaces, including living tissues, indwelling medical devices, industrial or potable water system piping, and natural aquatic systems. Surgical site infections caused by nontuberculous mycobacteria associated with the heater–cooler devices used during cardiac surgery have been reported internationally. *Pseudomonas aeruginosa* and other highly resistant organisms have been responsible for outbreaks associated with the waste and tap water systems in healthcare institutions.

Antibiotics themselves can contaminate water. A group of researchers discovered concentrations of pharmaceuticals, including levels of ciprofloxacin greater than those found in the blood of humans taking this antibiotic, in effluent from a water treatment plant that served around 90 drug manufacturers in India. They studied bacteria in river sediments and found genetic materials that could potentially confer resistance to ciprofloxacin and other antibiotics.

One of the most abundant and indispensable compounds, water courses through art, literature, history, and science. A multitude of different names exist for water, and cataloguing these would prove an arduous, complicated endeavor. Spending a few minutes reflecting on Goslee's "Water Prayer I" enables us to move beyond words and simply appreciate how important water is to life and health.

Bibliography

1. Centers for Disease Control and Prevention. Healthy water [cited 2018 Feb 20]. https://www.cdc.gov/healthywater/
2. Decker BK, Palmore TN. The role of water in healthcare-associated infections. Curr Opin Infect Dis. 2013;26:345–51. http://dx.doi.org/10.1097/QCO.0b013e3283630adf
3. District of Columbia Arts Center. Pat Goslee: Flow. Mixed media works by Pat Goslee [cited 2018 Feb 16]. https://dcartscenter.org/2009/11/21/pat-goslee-flow-november-21-january-4/
4. Donlan RM. Biofilms: microbial life on surfaces. Emerg Infect Dis. 2002;8:881–90. http://dx.doi.org/10.3201/eid0809.020063
5. Earle S. My wish: protect our oceans [cited 2018 Feb 16]. https://www.ted.com/talks/sylvia_earle_s_ted_prize_wish_to_protect_our_oceans/transcript
6. Jahren P, Tongbo S. How water influences our lives. Bejing (China): Chemical Industry Press/Springer; 2017. p. 19–37.
7. Larsson DG, de Pedro C, Paxeus N. Effluent from drug manufactures contains extremely high levels of pharmaceuticals. J Hazard Mater. 2007;148:751–5. http://dx.doi.org/10.1016/j.jhazmat.2007.07.008
8. Lubick N. Tools for tracking antibiotic resistance. Environ Health Perspect. 2011;119:A214–7. http://dx.doi.org/10.1289/ehp.119-a214
9. Lyman MM, Grigg C, Kinsey CB, Keckler MS, Moulton-Meissner H, Cooper E, et al. Invasive nontuberculous mycobacterial infections among cardiothoracic surgical patients exposed to heater–cooler devices. Emerg Infect Dis. 2017; 23:796–805. http://dx.doi.org/10.3201/eid2305.161899
10. National Oceanic and Atmospheric Administration, National Ocean Service. How much water is in the ocean? [cited 2018 Feb 20] https://oceanservice.noaa.gov/facts/oceanwater.html

Address for correspondence: Byron Breedlove, EID Journal, Centers for Disease Control and Prevention, 1600 Clifton Rd NE, Mailstop C19, Atlanta, GA 30329-4027, USA; email: wbb1@cdc.gov

EMERGING INFECTIOUS DISEASES®

Upcoming Issue

- History of Mosquitoborne Diseases in the United States and Implications for New Pathogens
- Surveillance for Mosquitoborne Transmission of Zika Virus, New York City, NY, USA
- Two Cases of Israeli Spotted Fever with Purpura Fulminans, Sharon District, Israel
- Dynamics of Spirochetemia and PCR Detection of *Borrelia miyamotoi* Disease
- Epidemic Dynamics of *Vibrio parahaemolyticus* K17 Illness in a Hotspot of Disease Emergence
- Human Usutu Virus Infection with Atypical Neurologic Presentation, Montpellier, France, 2016
- Heartland Bunyavirus and Hemophagocytic Lymphohistiocytosis in an Immunocompromised Patient
- Epizootic Hemorrhagic Disease Virus Serotype 6 Infection in Cattle, Japan, 2015
- External Quality Assessment for Zika Virus Molecular Diagnostic Testing, Brazil
- Seroprevalence of Severe Fever with Thrombocytopenia Syndrome Virus in Rural Areas, South Korea
- Equine Encephalosis Virus in India, 2008
- Foodborne Outbreaks Caused by Human Norovirus GII.P17-GII.17–Contaminated Dried Shredded Seaweed (Nori), Japan, 2017
- Fatal Visceral Leishmaniasis Caused by *Leishmania infantum*, Lebanon
- *Borrelia miyamotoi* sensu lato in Highly Endangered Père David Deer and *Haemaphysalis longicornis* Ticks
- Multiple Introductions of Influenza A(H5N8) Virus into Poultry, Egypt, 2017
- Fatal Tickborne Encephalitis Virus Infections Caused by Siberian and European Subtypes, Finland, 2015
- Middle East Respiratory Syndrome Coronavirus Antibodies in Dromedary Camels, Bangladesh, 2015
- Potentially Same Novel *Ehrlichia* Species in Horses in Nicaragua and Brazil

Complete list of articles in the May issue at http://www.cdc.gov/eid/upcoming.htm

Upcoming Infectious Disease Activities

April 18–20, 2018
ISIRV
International Society for Influenza and Other Respiratory Virus Diseases Neglected Influenza Viruses Group
Brighton, UK
https://science.vla.gov.uk/flu-lab-net/index.html

April 18–20, 2018
SHEA
Society for Healthcare Epidemiology of America Spring 2018 Conference
Portland, OR, USA
http://sheaspring.org/

April 23–25, 2018
2018 Annual Conference on Vaccinology Research
Bethesda, MD, USA
www.nfid.org/acvr

May 6–9, 2018
ASM Clinical Virology Symposium
West Palm Beach, FL, USA
https://www.asm.org/index.php/2018-clinical-virology-symposium

June 7–11, 2018
ASM Microbe
Atlanta, GA, USA
https://www.asm.org/index.php/asm-microbe-2018

August 26–29, 2018
ICEID
International Conference on Emerging Infectious Diseases
Atlanta, GA, USA
https://www.cdc.gov/iceid/index.html

October 28–30, 2018
2018 Annual Congress
International Society for Vaccines
Atlanta, GA, USA

Announcements
Email announcements to EID Editor (eideditor@cdc.gov). Include the event's date, location, sponsoring organization, and a website. Some events may appear only on EID's website, depending on their dates.

Earning CME Credit

To obtain credit, you should first read the journal article. After reading the article, you should be able to answer the following, related, multiple-choice questions. To complete the questions (with a minimum 75% passing score) and earn continuing medical education (CME) credit, please go to http://www.medscape.org/journal/eid. Credit cannot be obtained for tests completed on paper, although you may use the worksheet below to keep a record of your answers.

You must be a registered user on http://www.medscape.org. If you are not registered on http://www.medscape.org, please click on the "Register" link on the right hand side of the website.

Only one answer is correct for each question. Once you successfully answer all post-test questions, you will be able to view and/or print your certificate. For questions regarding this activity, contact the accredited provider, CME@medscape.net. For technical assistance, contact CME@medscape.net. American Medical Association's Physician's Recognition Award (AMA PRA) credits are accepted in the US as evidence of participation in CME activities. For further information on this award, please go to https://www.ama-assn.org. The AMA has determined that physicians not licensed in the US who participate in this CME activity are eligible for AMA PRA Category 1 Credits™. Through agreements that the AMA has made with agencies in some countries, AMA PRA credit may be acceptable as evidence of participation in CME activities. If you are not licensed in the US, please complete the questions online, print the AMA PRA CME credit certificate, and present it to your national medical association for review.

Article Title

Reemergence of Intravenous Drug Use as Risk Factor for Candidemia, Massachusetts, USA

CME Questions

1. Your patient is a 32-year-old man with a history of intravenous drug use (IVDU) who was admitted to the intensive care unit for an invasive infectious illness. Based on the case series by Poowanawittayakom and colleagues, which of the following statements about the clinical features of candidemia in patients with a history of IVDU vs. those without such a history is correct?

A. Patients with vs. those without a history of IVDU were significantly more likely to be coinfected with HIV
B. Patients with vs. those without a history of IVDU were more likely to have end-organ involvement, suggesting a reemergence of IVDU as a risk factor for invasive candidiasis
C. Mortality rate was higher in patients with IVDU than in patients without IVDU
D. The percentage of patients with a prosthetic valve did not differ significantly between groups

2. Based on the case series by Poowanawittayakom and colleagues, which of the following statements about the microbiological features of candidemia in patients with vs. those without a history of IVDU is correct?

A. *Candida albicans* was isolated from the bloodstream in a significantly higher percentage of patients with IVDU than in patients without IVDU
B. The percentage of *Candida* isolates identified as *C. parapsilosis* was significantly higher in the non-IVDU group than in the IVDU group
C. *C. glabrata* and *C. tropicalis* were significantly more common in the non-IVDU group
D. The finding of different species of *Candida* in the IVDU group argues against a common source of infection

3. Based on the case series by Poowanawittayakom and colleagues, which of the following statements about the clinical implications of findings from this case series of patients with candidemia associated or not associated with IVDU is correct?

A. IVDU-associated candidemia cases declined during the 7-year study
B. IVDU-associated candidemia cases in this study were very similar to previously reported cases associated with injection of brown heroin
C. Infections are a significant cause of morbidity/mortality in IVDU, and invasive candidiasis should be considered in the differential diagnosis of infectious sequelae of IVDU
D. Fluconazole is the treatment of choice for IVDU-associated candidemia

Earning CME Credit

To obtain credit, you should first read the journal article. After reading the article, you should be able to answer the following, related, multiple-choice questions. To complete the questions (with a minimum 75% passing score) and earn continuing medical education (CME) credit, please go to http://www.medscape.org/journal/eid. Credit cannot be obtained for tests completed on paper, although you may use the worksheet below to keep a record of your answers.

You must be a registered user on http://www.medscape.org. If you are not registered on http://www.medscape.org, please click on the "Register" link on the right hand side of the website.

Only one answer is correct for each question. Once you successfully answer all post-test questions, you will be able to view and/or print your certificate. For questions regarding this activity, contact the accredited provider, CME@medscape.net. For technical assistance, contact CME@medscape.net. American Medical Association's Physician's Recognition Award (AMA PRA) credits are accepted in the US as evidence of participation in CME activities. For further information on this award, please go to https://www.ama-assn.org. The AMA has determined that physicians not licensed in the US who participate in this CME activity are eligible for AMA PRA Category 1 Credits™. Through agreements that the AMA has made with agencies in some countries, AMA PRA credit may be acceptable as evidence of participation in CME activities. If you are not licensed in the US, please complete the questions online, print the AMA PRA CME credit certificate, and present it to your national medical association for review.

Article Title

Rickettsial Illnesses as Important Causes of Febrile Illness in Chittagong, Bangladesh

CME Questions

1. You are asked to evaluate a patient with a 2-week history of fever and malaise. Which one of the following symptoms was least common in cases of rickettsial illness in the current study?

A. Headache
B. Skin lesions
C. Myalgia
D. Anorexia

2. What does the current study describe regarding the epidemiology of rickettsial illness in Bangladesh?

A. 23% of cases of fever were attributable to rickettsial infection
B. Murine typhus was more common than scrub typhus overall
C. Murine typhus and scrub typhus occurred at equal rates
D. Most patients with scrub typhus came from rural areas

3. The prevalence of scrub typhus peaked during which of the following months in the current study?

A. February/March
B. June/July
C. September/October
D. November/December

4. Which one of the following strains of *Orientia tsutsugamushi* was most prevalent during the observation year in the current study?

A. Karp
B. Gilliam
C. TA763
D. Kato

Join CDC's Laboratory Leadership Service (LLS)

Training the next generation of laboratory leaders

CDC's Laboratory Leadership Service (LLS) prepares high caliber scientists to become public health leaders through experiential training in laboratory quality management and the science of biosafety.

Application Period for Class of 2019: April 16-July 11, 2018

LLS fellows

- Conduct cutting-edge laboratory research
- Conduct comprehensive laboratory safety and risk assessments
- Evaluate laboratory quality management systems
- Collaborate with CDC Epidemic Intelligence Service (EIS) officers during outbreak investigations
- Participate in public health field investigations
- Present findings from laboratory research, investigations, and studies

Learn more at cdc.gov/LLS.

Who can apply?

1. Early-career laboratory scientists with a PhD in a laboratory related discipline
2. Two years post-graduate experience and
3. American citizenship or United States permanent residency

"LLS is a great investment in my future career and I feel confident that I will be able to successfully integrate leadership, quality and safety in any position I may take."

Atanaska Marinova-Petkova
Class of 2017

Centers for Disease Control and Prevention
Center for Center for Surveillance, Epidemiology, and Laboratory Services
Division of Scientific Education and Professional Development

Emerging Infectious Diseases is a peer-reviewed journal established expressly to promote the recognition of new and reemerging infectious diseases around the world and improve the understanding of factors involved in disease emergence, prevention, and elimination.

The journal is intended for professionals in infectious diseases and related sciences. We welcome contributions from infectious disease specialists in academia, industry, clinical practice, and public health, as well as from specialists in economics, social sciences, and other disciplines. Manuscripts in all categories should explain the contents in public health terms. For information on manuscript categories and suitability of proposed articles, see below and visit http://wwwnc.cdc.gov/eid/pages/author-resource-center.htm.

Summary of Authors' Instructions

Authors' Instructions. For a complete list of EID's manuscript guidelines, see the author resource page: http://wwwnc.cdc.gov/eid/page/author-resource-center.

Manuscript Submission. To submit a manuscript, access Manuscript Central from the Emerging Infectious Diseases web page (www.cdc.gov/eid). Include a cover letter indicating the proposed category of the article (e.g., Research, Dispatch), verifying the word and reference counts, and confirming that the final manuscript has been seen and approved by all authors. Complete provided Authors Checklist.

Manuscript Preparation. For word processing, use MS Word. Set the document to show continuous line numbers. List the following information in this order: title page, article summary line, keywords, abstract, text, acknowledgments, biographical sketch, references, tables, and figure legends. Appendix materials and figures should be in separate files.

Title Page. Give complete information about each author (i.e., full name, graduate degree(s), affiliation, and the name of the institution in which the work was done). Clearly identify the corresponding author and provide that author's mailing address (include phone number, fax number, and email address). Include separate word counts for abstract and text.

Keywords. Use terms as listed in the National Library of Medicine Medical Subject Headings index (www.ncbi.nlm.nih.gov/mesh).

Text. Double-space everything, including the title page, abstract, references, tables, and figure legends. Indent paragraphs; leave no extra space between paragraphs. After a period, leave only one space before beginning the next sentence. Use 12-point Times New Roman font and format with ragged right margins (left align). Italicize (rather than underline) scientific names when needed.

Biographical Sketch. Include a short biographical sketch of the first author—both authors if only two. Include affiliations and the author's primary research interests.

References. Follow Uniform Requirements (www.icmje.org/index.html). Do not use endnotes for references. Place reference numbers in parentheses, not superscripts. Number citations in order of appearance (including in text, figures, and tables). Cite personal communications, unpublished data, and manuscripts in preparation or submitted for publication in parentheses in text. Consult List of Journals Indexed in Index Medicus for accepted journal abbreviations; if a journal is not listed, spell out the journal title. List the first six authors followed by "et al." Do not cite references in the abstract.

Tables. Provide tables within the manuscript file, not as separate files. Use the MS Word table tool, no columns, tabs, spaces, or other programs. Footnote any use of boldface. Tables should be no wider than 17 cm. Condense or divide larger tables. Extensive tables may be made available online only.

Figures. Submit editable figures as separate files (e.g., Microsoft Excel, PowerPoint). Photographs should be submitted as high-resolution (600 dpi) .tif or .jpg files. Do not embed figures in the manuscript file. Use Arial 10 pt. or 12 pt. font for lettering so that figures, symbols, lettering, and numbering can remain legible when reduced to print size. Place figure keys within the figure. Figure legends should be placed at the end of the manuscript file.

Videos. Submit as AVI, MOV, MPG, MPEG, or WMV. Videos should not exceed 5 minutes and should include an audio description and complete captioning. If audio is not available, provide a description of the action in the video as a separate Word file. Published or copyrighted material (e.g., music) is discouraged and must be accompanied by written release. If video is part of a manuscript, files must be uploaded with manuscript submission. When uploading, choose "Video" file. Include a brief video legend in the manuscript file.

Types of Articles

Perspectives. Articles should not exceed 3,500 words and 50 references. Use of subheadings in the main body of the text is recommended. Photographs and illustrations are encouraged. Provide a short abstract (150 words), 1-sentence summary, and biographical sketch. Articles should provide insightful analysis and commentary about new and reemerging infectious diseases and related issues. Perspectives may address factors known to influence the emergence of diseases, including microbial adaptation and change, human demographics and behavior, technology and industry, economic development and land use, international travel and commerce, and the breakdown of public health measures.

Synopses. Articles should not exceed 3,500 words in the main body of the text or include more than 50 references. Use of subheadings in the main body of the text is recommended. Photographs and illustrations are encouraged. Provide a short abstract (not to exceed 150 words), a 1-line summary of the conclusions, and a brief biographical sketch of first author or of both authors if only 2 authors. This section comprises case series papers and concise reviews of infectious diseases or closely related topics. Preference is given to reviews of new and emerging diseases; however, timely updates of other diseases or topics are also welcome. If detailed methods are included, a separate section on experimental procedures should immediately follow the body of the text.

Research. Articles should not exceed 3,500 words and 50 references. Use of subheadings in the main body of the text is recommended. Photographs and illustrations are encouraged. Provide a short abstract (150 words), 1-sentence summary, and biographical sketch. Report laboratory and epidemiologic results within a public health perspective. Explain the value of the research in public health terms and place the findings in a larger perspective (i.e., "Here is what we found, and here is what the findings mean").

Policy and Historical Reviews. Articles should not exceed 3,500 words and 50 references. Use of subheadings in the main body of the text is recommended. Photographs and illustrations are encouraged. Provide a short abstract (150 words), 1-sentence summary, and biographical sketch. Articles in this section include public health policy or historical reports that are based on research and analysis of emerging disease issues.

Dispatches. Articles should be no more than 1,200 words and need not be divided into sections. If subheadings are used, they should be general, e.g., "The Study" and "Conclusions." Provide a brief abstract (50 words); references (not to exceed 15); figures or illustrations (not to exceed 2); tables (not to exceed 2); and biographical sketch. Dispatches are updates on infectious disease trends and research that include descriptions of new methods for detecting, characterizing, or subtyping new or reemerging pathogens. Developments in antimicrobial drugs, vaccines, or infectious disease prevention or elimination programs are appropriate. Case reports are also welcome.

Research Letters Reporting Cases, Outbreaks, or Original Research. EID publishes letters that report cases, outbreaks, or original research as Research Letters. Authors should provide a short abstract (50-word maximum), references (not to exceed 10), and a short biographical sketch. These letters should not exceed 800 words in the main body of the text and may include either 1 figure or 1 table. Do not divide Research Letters into sections.

Letters Commenting on Articles. Letters commenting on articles should contain a maximum of 300 words and 5 references; they are more likely to be published if submitted within 4 weeks of the original article's publication.

Commentaries. Thoughtful discussions (500–1,000 words) of current topics. Commentaries may contain references (not to exceed 15) but no abstract, figures, or tables. Include biographical sketch.

Another Dimension. Thoughtful essays, short stories, or poems on philosophical issues related to science, medical practice, and human health. Topics may include science and the human condition, the unanticipated side of epidemic investigations, or how people perceive and cope with infection and illness. This section is intended to evoke compassion for human suffering and to expand the science reader's literary scope. Manuscripts are selected for publication as much for their content (the experiences they describe) as for their literary merit. Include biographical sketch.

Books, Other Media. Reviews (250–500 words) of new books or other media on emerging disease issues are welcome. Title, author(s), publisher, number of pages, and other pertinent details should be included.

Conference Summaries. Summaries of emerging infectious disease conference activities (500–1,000 words) are published online only. They should be submitted no later than 6 months after the conference and focus on content rather than process. Provide illustrations, references, and links to full reports of conference activities.

Online Reports. Reports on consensus group meetings, workshops, and other activities in which suggestions for diagnostic, treatment, or reporting methods related to infectious disease topics are formulated may be published online only. These should not exceed 3,500 words and should be authored by the group. We do not publish official guidelines or policy recommendations.

Photo Quiz. The photo quiz (1,200 words) highlights a person who made notable contributions to public health and medicine. Provide a photo of the subject, a brief clue to the person's identity, and five possible answers, followed by an essay describing the person's life and his or her significance to public health, science, and infectious disease.

Etymologia. Etymologia (100 words, 5 references). We welcome thoroughly researched derivations of emerging disease terms. Historical and other context could be included.

Announcements. We welcome brief announcements of timely events of interest to our readers. Announcements may be posted online only, depending on the event date. Email to eideditor@cdc.gov.

In This Issue

Synopses

Research

Dispatches

ISSN 1080-6040